

**UNIVERSIDAD DE CANTABRIA
SAPIENZA- UNIVERSITÀ DI ROMA
UNIVERSITAT AUTÒNOMA DE BARCELONA**

PROGRAMA DE DOCTORADO DE ARQUEOLOGÍA PREHISTÓRICA



SAPIENZA
UNIVERSITÀ DI ROMA

TESIS DOCTORAL

**La Prehistoria del color: función y significado del
ocre en el Paleolítico Superior y Mesolítico del
suroeste de Europa**

PHD THESIS

**The Prehistory of colour: function and meaning
of ochre in the Upper Palaeolithic and Mesolithic
of south-western Europe**

Realizada por: ELIANA CATELLI

Dirigida por: Prof. PABLO ARIAS CABAL, Prof.^a MARGHERITA MUSSI

Escuela de Doctorado de la Universidad de Cantabria

Santander, septiembre de 2018

To my parents Nicola and Giovanna, and
my brother Gianni

Acknowledgments

I thank Prof. Margherita Mussi (Sapienza-University of Rome) and Prof. Pablo Arias Cabal (University of Cantabria) for their guidance and support during this work.

I thank Prof. Margherita Mussi for the provision of ochre samples from the site of Grotta di Pozzo.

I thank Prof. Pablo Arias Cabal for the provision of ochre samples from the site of Los Canes, Arangas and La Garma A.

I thank Prof. Rita Teresa Melis (University of Cagliari) for the provision of ochre samples from the site of S'Ormu e S'Orku.

I thank Prof. Fabio Martini (University of Florence) for the provision of ochre samples from the site of Grotta del Romito and Grotta San Teodoro.

I thank Prof. Delia Gazzoli for the analysis by Raman at Dep. Of Chemistry of Sapienza-University of Rome

David Hernández Manrique and SERCAMAT (University of Cantabria) are thanked for the analysis by X-Ray Fluorescence

Manuel De Pedro Del Valle and CITIMAC (University of Cantabria) are thanked for the analysis by X-Ray Diffractometry.

Estela Ruiz Martínez and LADICIM (University of Cantabria) are thanked for the analysis by SEM-EDS.

Miguel Angel Sanchez Carro (University of Cantabria) is thanked for supporting me in ochre provenance researches.

Luis César Teira Mayolini (University of Cantabria) is thanked for providing me archaeological maps and valuable commentary for the spatial analysis.

Patricia Fernández Sánchez and Jorge Vallejo Llano are thanked for the assistance during a geological survey of the Asturian sources.

I acknowledge financial support accessed via my supervisor Pablo Arias Cabal with the project "Coastal societies in a changing world: A diachronic and comparative approach to the Prehistory of SW Europe from the late Palaeolithic to the Neolithic". Funding Body: Ministerio de Economía y Competitividad.

Gobierno de España. Call: Plan Estatal de Investigación Científica y Técnica y de Innovación 2013-2016; Programa Estatal de Fomento de la Investigación Científica y Técnica de Excelencia; Subprograma Estatal de Generación de Conocimiento. Reference: HAR2014-51830-P.

I acknowledge financial support accessed via my supervisor Margherita Mussi with the project "Comparative studies and methodological developments for the characterization of ocher from archaeological contexts: the case of Grotta di Pozzo (Aq , Italy)". Funding body: Sapienza-University of Rome. Call: Progetto Avvio alla Ricerca.

In addition thanks to the people who are always by my side.

INDEX OF CONTENTS

Abstract of thesis

Resumen de la tesis

Riassunto della tesi

Introduction	p.1
Chapter 1. Ochre: state of knowledge	p.3
I.1. Definitions of ochre	p.4
I.2. Iron ores	p.6
I.2.1. Genesis of ochre	p.9
I.2.3. Cinnabar: HgS	p.12
I.2.4. Jarosite: $\text{KFe}_3(\text{SO}_4)_2(\text{OH})_6$	p.13
I.2.5. Properties of iron ores	p.13
I.3. Ochre in Prehistory	p.15
I.3.1. Potential use of ochre	p.20
I.4. Synthesis	p.30
Chapter II. Studying ochre from archaeological contexts	p.33
II.1. Ochre in archaeological contexts	p.33

II.2. Objectives of study	p.43
II.3. Evaluating methodological protocols	p.45
II.3.1. Identification of raw materials	p.46
II.3.2. Provenance researches	p.52
II.3.4. Treatments and transformations	p.55
II.3.5. Balance of methods	p.57
II.4. Assessing a methodological protocol	p.58
II.4.1. Selection of materials	p.59
II.4.2. Application of analytical techniques and data collection	p.62
II.4.3. Data processing and evaluation of the methods	p.81
II.4.4. Definition of methodological protocol	p.83
II.5. Spatial analysis	p.85

Chapter III. General framework: sites and sampling conditions	p.87
III.1. The Cantabrian region	p.88
III.1.1. Solutrean	p.88
III.1.2. Magdalenian	p.89
III.1.3. Azilian	p.91

III.1.4. Mesolithic	p.92
III.2. The Italian Peninsula	p.94
III.2.1. Epigravettian	p.94
III.2.2. Mesolithic	p.96
III.3. The Iberian sites	p.99
III.3.1. La Garma A	p.99
III.3.1.1. Stratigraphy and chronology	p.103
III.3.1.2. Ochre recovery strategies and sampling conditions	p.105
III.3.2. Los Canes	p.108
III.3.2.1. Stratigraphy and chronology	p.114
III.3.2.2. Ochre recovery strategies and sampling conditions	p.122
III.3.3. Arangas	p.123
III.3.3.1. Stratigraphy and chronology	p.125
III.3.3.2. Ochre recovery strategies and sampling conditions	p.127
III.4. The Italian sites	p.127
III.4.1. Grotta del Romito	p.128
III.4.1.1. Stratigraphy and chronology	p.133

III.4.1.2. Ochre recovery strategies and sampling conditions	p.134
III.4.2. Grotta San Teodoro	p.137
III.4.2.1. Stratigraphy and chronology	p.142
III.4.2.2. Ochre recovery strategies and sampling conditions	p.143
III.4.3. Grotta di Pozzo	p.143
III.4.3.1. Stratigraphy and chronology	p.145
III.4.3.2. Ochre recovery strategies and sampling conditions	p.148
III.4.4. S'Orku e S'Orku	p.150
III.4.4.1. Stratigraphy and chronology	p.153
III.4.4.2. Ochre recovery strategies and sampling conditions	p.155
Chapter IV. General evaluation of materials	p.157
IV.1. Los Canes	p.162
IV.1.1. Colour	p.163
IV.1.2. Mass and dimensions	p.164
IV.1.3. State of conservation	p.172

IV.2. Arangas	p.180
IV.2.1. Colour	p.180
IV.2.2. Mass and dimensions	p.183
IV.2.3. State of conservation	p.187
IV.3. La Garma A	p.193
IV.3.1. Colour	p.193
IV.3.2. Mass and dimensions	p.194
IV.3.3. State of conservation	p.202
IV.4. Grotta di Pozzo	p.207
IV.4.1. Colour	p.209
IV.4.2. Mass and dimensions	p.210
IV.4.3. State of conservation	p.213

Chapter V. Identification and characterization

of raw materials	p.217
V.1. Classification criteria	p.218
V.1.1. Characterization of raw materials	p.219
V.2. Los Canes	p.220
V.2.1. Iron ores and colour	p. 220
V.2.2. Geochemical composition	p.222

V.2.3. Proportion of raw materials	p.226
V.2.4. Evaluation of identification and characterization factors of raw materials	p.232
V.3. Arangas	p.235
V.3.1. Iron ores and colour	p.235
V.3.2. Geochemical composition	p.237
V.3.3. Proportion of raw materials	p.239
V.3.4. Evaluation of identification and characterization factors of raw materials	p.243
V.4. La Garma A	p.244
V.4.1. Iron ores and colour	p.244
V.4.2. Geochemical composition	p.246
V.4.3. Proportion of raw materials	p.247
V.4.4. Evaluation of identification and characterization factors of raw materials	p.251
V.5. Grotta di Pozzo	p.252
V.5.1. Iron ores and colour	p.252
V.5.2. Geochemical composition	p.253
V.5.3. Proportion of raw materials	p.254

V.5.4. Evaluation of identification and characterization factors of raw materials	p.256
V.6. Comparative analysis	p.258
V.6.1. Iron ores and colour	p.260
V.6.2. Geochemical composition	p.263
V.6.3. Evaluation of comparison factors	p.267
Chapter VI. Ochre procurement strategies and supplying areas	p.269
VI.1. Provenance research and archaeological contexts	p.273
VI.1.1. Geological setting	p.275
VI.2. Iron ores sources	p.278
VI.2.1. Geological mapping	p.278
VI.2.2. Geological survey	p.283
VI.2.3 Geological samples	p.284
VI.3. Sourcing raw materials	p.287
VI.3.1. Comparative analysis	p.300
VI.4. Summary of results	p.302

Chapter VII. Ochre exploitation and mechanical transformations	p.307
VII.1. Mechanical transformations	p.309
VII.1.1. Archaeological indices	p.309
VII.1.1.1. Upper Palaeolithic	p.310
VII.1.1.2. Mesolithic	p.322
VII.2. Ochre processing from domestic contexts	p.331
VII.3. Ochre processing from funerary contexts	p.333
VII.4. Ochre processing tools	p.334
VII.5. Reconstructing the <i>chaîne opératoire</i>	p.344
Chapter VIII. Spatial distribution	p.345
VIII.1. Los Canes	p.346
VIII.1.1. Evaluation of results	p.357
VIII.2. Arangas	p.363
VIII.2.1. Evaluation of results	p.367
VIII.3. La Garma A	p.368
VIII.3.1. Evaluation of results	p.374
VIII.4. Grotta di Pozzo	p.378
VIII.4.1. Evaluation of results	p.381

VIII.5 Synthesis of data analysis	p.382
Chapter IX. Final considerations	p.385
IX.1. Procurement strategies and exploitation of raw materials	p.385
IX.2. The <i>chaîne opératoire</i>	p.391
IX.3. Management of ochre in the archaeological sites	p.394
IX.4. Hypotheses on ochre function	p.396
Conclusions	p.403
Conclusiones	p.405
Conclusioni	p.407
References	p.409
List of figures	p.469
List of tables	p.487
Annex I	p.491
Annex II	p.499

ABSTRACT

The colouring minerals are widespread in the Palaeolithic and Mesolithic European contexts, although the information available on their use is still few. The interest in this category of materials is increasing as their study can provide new knowledge on technologies and symbolism of past human groups given their intense colouring power and the peculiarities of iron oxides as primary constituents.

In a phase of transition such as that from Late Glacial to Holocene marked by climatic and environmental changes, of which human cultures are the reflection, the analysis of ochre vestiges can support the reconstruction of the life-styles of Upper Palaeolithic and Mesolithic hunter-gatherers.

Archaeological fieldworks brought to light a series of ochre assemblages in two key areas for the prehistoric European population: the Cantabrian region and the Italian peninsula. The discovery of ochre pieces, ochre processing tools and ochre residues on ornaments and lithic artefacts supposes utilitarian and symbolic functions.

To investigate these aspects, this thesis has been organized into nine chapters that can be summarized in three main parts.

Specifically, the introduction exposes the problems still unresolved on the role of ochre in the evolution of prehistoric human culture, introducing the methods and materials.

In chapter I it is defined the main object of this work, ochre, in all its aspects with a focus on its use in Prehistory.

The first part of chapter II refers a catalogue of ochre vestiges that can be found in the archaeological contexts with the aim to provide essential data to discriminate the anthropic origin of the assemblages. In the second part, the methodological protocol elaborated starting from the execution of a preliminary test is presented to verify the efficacy of the investigated techniques that are preliminary reviewed.

The chapter III is dedicated to the exposition of the sites from which the studied materials were collected. Furthermore, ochre recovery strategies and sampling conditions are discussed.

Chapter IV opens the part dedicated to the study of archaeological materials. In this chapter the data obtained from the evaluation of the materials are described according to specific criteria (colour, mass, dimensions, state of conservation) to estimate the representativeness of ochre remains in the site and the intensity of anthropic exploitation.

Chapter V shows the data obtained from the physical-chemical characterization of raw materials. The results of a comparative analysis are presented to search indexes of peculiar transformations and intentional mixtures on continental scale.

This is followed by chapter VI in which the results of the statistical data processing obtained from the geochemical characterization of archaeological and geological samples are reported. The main objective of this study is to recognize archaeological sources to reconstruct human mobility patterns and to investigate the geographical range explored by human groups, starting from the resources potentially available.

The chapter VII focuses on what way ochre was processed investigating the mechanical transformations of raw materials.

The chapter VIII closes the part dedicated to the study of archaeological materials. In this chapter it is assess the link between ochre remains of sites by analysing their distribution on the archaeological surface. The main purpose is to define the relationship between the materials and the context according to the anthropic organization of the space.

Lastly, the chapter IX offers a general discussion of the results obtained defining the innovative contributions made by this work on procurement and treatment of colouring minerals, their management in the site and potential uses of ochre.

The work ends with final considerations in which the key role played by ochre in human cultures of Upper Palaeolithic and Mesolithic is highlighted.

Therefore, this research attempts to update the knowledge on the exploitation of ochre, red or yellow iron ores, during the Late Glacial and Early and Middle Holocene, in south-western Europe.

Starting from the combination of data obtained through an integrated approach crossing the results of the archaeological study and the physical-chemical analyses and the contextualization of ochre vestiges in the site, it was possible to investigate the supply strategies and the selective criteria of the raw materials, as well as reconstruct the main stages of their processing to formulate hypothesis of use.

This work highlights the intentional provision to the site of large quantities of ferruginous rocks selected for their intense red colour. The supply of these raw materials was continuous from the Upper Palaeolithic to the Mesolithic. The blocks or nodules was partially fragmented and powdering, while another part

was used to realize objects to directly transfer the colour on the surfaces (*crayons*). These objects could be exploited both within domestic space as part of daily activities, and in spaces designed to host human burials, as part of funeral rituals.

Moreover, the study of ochre assemblages made it possible to detect the continuity of technological practices over time, attesting to a transfer of technical knowledge related to the exploitation of the same raw materials for their functionality during the Late Glacial and the Early and Middle Holocene. Its use in diversified contexts attests both the utilitarian and the symbolic value of ochre. Its meaning is not fixed, but it depends on the function for which it is used.

RESUMEN

Los minerales colorantes están ampliamente representados en los contextos Paleolíticos y del Mesolíticos europeos, aunque la información disponible sobre su uso es aún escasa. El interés en esta categoría de materiales está aumentando en la medida que su estudio puede ampliar el conocimiento sobre las tecnologías y el simbolismo de los grupos humanos del pasado por su intenso poder colorante y las peculiaridades de los óxidos de hierro como componentes primarios. En una fase de transición como la de Tardiglacial al Holoceno marcada por los cambios climáticos y ambientales, con su consiguiente reflejo en las culturas humanas, el análisis de los restos de ocre puede apoyar la reconstrucción de los estilos de vida de los grupos humanos del Paleolítico Superior y del Mesolítico.

Los trabajos de campo han sacado a la luz una serie de evidencias en dos áreas clave para la ocupación prehistórica europea: la región cantábrica y la península italiana. El descubrimiento de restos de ocre, objetos para su procesamiento y residuos de color sobre ornamentos y artefactos líticos tanto en contextos residenciales como funerarios presupone una función tanto utilitaria como simbólica de este material.

Para investigar estos aspectos, esta tesis se ha organizado en nueve capítulos que se pueden resumir en tres partes fundamentales.

Primero, la introducción expone los problemas aún no resueltos sobre la posición ocupada por el ocre respecto a la evolución de las culturas humanas prehistóricas mediante la exposición preliminar de objetivos de la investigación, métodos y materiales.

En el capítulo I se define la materia central de este trabajo, el ocre, en todos sus aspectos, con un enfoque sobre su uso en la Prehistoria.

La primera parte del capítulo II presenta una catalogación de los restos de ocre hallados en contextos arqueológicos con el fin de proporcionar datos esenciales para reconocer el origen antrópico de los conjuntos. En la segunda parte se presenta el protocolo metodológico elaborado a partir de la ejecución de una prueba preliminar para comprobar la eficacia de las técnicas de investigación previamente discutidas.

Sigue el capítulo III, que está dedicado a la descripción de los contextos arqueológicos de los cuales provienen los materiales estudiados y las estrategias de recolección y muestreo del ocre.

El capítulo IV abre la parte dedicada al estudio de los materiales. Este capítulo proporciona los datos obtenidos de la evaluación de los materiales en función de criterios específicos (color, peso, tamaño, estado de conservación) para estimar la representatividad de los restos de ocre en el depósito y para evaluar el grado de explotación antrópica.

En el capítulo V, se refieren los datos obtenidos de la caracterización fisicoquímica de las materias primas. Además, para definir un cuadro de los comportamientos humanos a una escala continental, se presentan los resultados de análisis comparativos llevados a cabo para determinar índices de mezclas intencionales y transformaciones específicas.

En el capítulo VI se discuten los resultados del procesamiento estadístico de los datos obtenidos de la caracterización geoquímica de muestras arqueológicas y geológicas. El objetivo principal de esta parte del estudio es investigar el origen de las muestras arqueológicas identificando las fuentes geológicas originales

para reconstruir los modelos de movilidad humana e definir el rango geográfico explorado por los grupos humanos, a partir del análisis de las fuentes geológicas potencialmente explotables.

Sigue el capítulo VII enfocado al estudio del procesamiento del ocre a través del examen de las huellas de transformaciones mecánicas de las materias primas para comprender mejor su función en la vida de los grupos paleolíticos y mesolíticos.

El capítulo VIII cierra la parte dedicada al estudio del material arqueológico. En este capítulo se evalúa la relación entre los restos de ocre y los sitios a través del análisis de su distribución en la superficie arqueológica. El objetivo es definir la relación entre los materiales y el contexto de acuerdo con la organización antrópica del espacio.

Por último, el capítulo IX presenta una discusión general de los datos obtenidos al definir las contribuciones innovadoras hechas por este trabajo sobre la adquisición y el tratamiento de minerales colorantes, su gestión en el sitio y los usos potenciales del ocre.

El trabajo finaliza con unas reflexiones finales en las que se destaca el rol clave del ocre por las culturas humanas del Paleolítico Superior y el Mesolítico.

Por lo tanto, este proyecto de investigación tiene como objetivo ofrecer nuevos conocimientos sobre la explotación del ocre, en el Tardiglacial y en el Holoceno Antiguo y Medio, en el suroeste de Europa.

A partir de la combinación de los datos obtenidos a través de un enfoque integrado, cruzando los resultados del estudio arqueológico y los análisis fisicoquímicos, y la contextualización de los restos de ocre dentro del yacimiento, ha sido posible investigar las estrategias de aprovechamiento y los

criterios selectivos de las materias primas, así como 'reconstruir las etapas de su procesamiento y formular hipótesis de uso. Este trabajo destaca el abastecimiento intencional de grandes cantidades de rocas ferruginosas. Este proceso fue continuo desde el Paleolítico Superior hasta el Mesolítico. Una parte de los bloques o nódulos de ocre se fragmentaban o pulverizaban, mientras que otra parte se usaba para crear objetos para transferir directamente el color en las superficies (crayones). Estos objetos podrían ser explotados tanto dentro del espacio doméstico como parte de las actividades diarias, como en espacios diseñados para alojar enterramientos humanos, como parte de los rituales funerarios.

Por otra parte, el estudio de las colecciones de ocre hace posible la detección de una continuidad en las prácticas tecnológicas, lo que demuestra una transferencia de conocimientos técnicos relacionados con la explotación de las mismas materias primas para su funcionalidad durante el Tardiglacial y el Holoceno Antiguo y Medio. Su uso en contextos diferentes documenta el valor tanto utilitario como simbólico del ocre. Su significado no es constante, sino que depende de la función para la que se utiliza.

RIASSUNTO

I minerali coloranti sono ampiamente diffusi nei contesti europei paleolitici e mesolitici, sebbene le informazioni disponibili sul loro uso sono ancora poche. L'interesse verso questa categoria di reperti è crescente in quanto il loro studio può ampliare le conoscenze sulle tecnologie e sul simbolismo dei gruppi umani del passato dato il loro intenso potere colorante e le peculiarità degli ossidi di ferro quali costituenti primari. In una fase di passaggio come quella dal Tardiglaciale all'Olocene segnata da mutamenti climatici e ambientali, di cui sono il riflesso le culture umane, l'analisi delle vestigia di ocra può supportare la ricostruzione degli stili di vita dei gruppi umani del Paleolitico Superiore e del Mesolitico.

Le indagini di campo hanno riportato alla luce una serie di assemblaggi di ocra in due aree chiave per il popolamento preistorico europeo: la regione Cantabrica e la Penisola Italiana. Il rinvenimento di resti di ocra, strumenti per la sua lavorazione e residui di colore su ornamenti e manufatti litici sia in contesti abitativi che funerari presuppone una funzione tanto utilitaristica quanto simbolica di questo materiale.

Per indagare questi aspetti, questa tesi è stata organizzata in nove capitoli che possono essere riassunti in tre parti fondamentali.

L'introduzione espone le problematiche ancora irrisolti riguardanti il ruolo dell'ocra nell'evoluzione della cultura umana preistorica, introducendo metodi e materiali.

Nel capitolo I viene definito l'oggetto principale di questo lavoro, l'ocra, in tutti i suoi aspetti con un focus specifico sul suo uso nella Preistoria.

La prima parte del capitolo II fa riferimento a un catalogo delle evidenze che possono essere trovate nei contesti archeologici allo scopo di fornire dati essenziali per discriminare l'origine antropica dei materiali. Nella seconda parte viene presentato il protocollo metodologico elaborato a partire dall'esecuzione di un test preliminare per verificare l'efficacia delle tecniche investigate che vengono preliminarmente discusse.

Il capitolo III è dedicato all'esposizione dei siti da cui sono stati raccolti i materiali studiati. Inoltre, vengono esposte le strategie di recupero dei materiali archeologici e le condizioni del campionamento del corpus di studio.

Il capitolo IV apre la parte dedicata allo studio dei materiali archeologici. In questo capitolo i dati ottenuti dalla valutazione dei reperti sono descritti a partire da criteri specifici (colore, massa, dimensioni, stato di conservazione) per stimare la rappresentatività dei resti ocra nel sito e l'intensità dello sfruttamento antropico.

Il capitolo V mostra i dati ottenuti dalla caratterizzazione fisico-chimica delle materie prime. I risultati di un'analisi comparativa vengono presentati allo scopo di ricercare indici delle trasformazioni antropiche e della creazione di miscele intenzionali su scala continentale.

Segue il capitolo VI in cui sono riportati i risultati dell'elaborazione dei dati statistici ottenuti dalla caratterizzazione geochimica di campioni archeologici e geologici. L'obiettivo principale di questo studio è riconoscere le fonti archeologiche per ricostruire i modelli di mobilità umana e indagare il range

geografico esplorato dai gruppi umani, partendo dalle risorse potenzialmente disponibili.

Il capitolo VII si concentra sul modo in cui l'ocra è stata elaborata investigando le trasformazioni meccaniche delle materie prime.

Il capitolo VIII chiude la parte dedicata allo studio dei materiali archeologici. In questo capitolo si valuta il legame tra i resti di ocra e la loro distribuzione sulla superficie archeologica. Lo scopo principale è definire la relazione tra i materiali e il contesto secondo l'organizzazione antropica dello spazio.

Infine, il capitolo IX offre una discussione generale dei risultati ottenuti definendo i contributi innovativi apportati da questo lavoro sull'approvvigionamento e il trattamento dei minerali coloranti, la loro gestione nel sito e i potenziali usi dell'ocra.

Il lavoro termina con considerazioni finali in cui viene evidenziato il ruolo chiave dell'ocra nelle culture umane del Paleolitico Superiore e del Mesolitico.

Pertanto, questa ricerca tenta di aggiungere nuove conoscenze sullo sfruttamento dell'ocra, minerale ferruginoso rosso o giallo, durante il Tardiglaciale e l'Olocene Iniziale e Medio, nell'Europa sud-occidentale.

A partire dalla combinazione dei dati ottenuti mediante un approccio integrato, incrociando i risultati dello studio archeologico e delle analisi fisico-chimiche, e dalla contestualizzazione delle vestigia di ocra all'interno del sito, e' stato possibile indagare le strategie di approvvigionamento e i criteri selettivi delle materie prime, nonché ricostruire le fasi del loro processamento e formulare ipotesi d'uso.

Il lavoro svolto ha messo in luce l'apporto intenzionale nel sito di cospicue quantità di rocce ferruginose selezionate per l'intenso colore rosso.

L'approvvigionamento di queste materie prime e' stato continuo dal Paleolitico Superiore al Mesolitico ed era rivolta alla raccolta di blocchi o noduli di cui una parte veniva frammentata e polverizzata, mentre un'altra parte era usata per fare oggetti per trasferire direttamente il colore sulle superfici (crayons). Questi prodotti potevano essere sfruttati sia all'interno dello spazio domestico nell'ambito di attivita' quotidiane, sia in spazi destinati ad ospitare delle sepolture, nell'ambito di rituali funerari.

Inoltre, lo studio delle collezioni di ocra ha permesso di rilevare il perdurare nel tempo di pratiche tecnologiche attestando un passaggio di conoscenze tecniche legate allo sfruttamento delle stesse materie prime per le loro funzionalita', sia nel Paleolitico Superiore che nel Mesolitico. L'uso in contesti diversificati attesta il valore sia utilitaristico che simbolico dell'ocra. Il suo significato non e' fisso, ma dipende dal posto che va ad occupare nella vita umana a seconda della funzione per cui viene sfruttata.

Introduction

This work aims to offer new contributes on the study of ochre exploitation in Prehistory, with a specific focus on human groups that during Late Glacial and Early and Middle Holocene occupied the south-west of Europe.

The word ochre comes from the Greek ὤχρως and means “pale yellow”. This term is used to indicate rocks or earths rich in iron with shades of colour from deep red, red, reddish-brown to brownish-yellow and yellow due to the presence of iron oxide and hydroxide ores: hematite, goethite, lepidocrocite, maghemite, magnetite, ferrihydrite (Cornell & Schwertmann, 2004).

Although it is well known that ochre has been used since Prehistory, in archaeology there is not yet an exact and shared definition of the term “ochre”. This word is used to indicate any type of ferrous rock that produces red or yellow signs. The archaeological record confirms a full knowledge of ochre potentialities by *Homo* sp. since Upper Pleistocene that was used not only for its colouring properties but also to abrade and dry materials (Allard *et al.* 1997, Salomon 2009), to protect the human skin (Rifkin, 2015; Rifkin *et al.*, 2015; Tributsch, 2016), to prepare adhesive agents (Becker & Wendorf 1993; Bocquentin & Bar-Yosef 2004; Gibson *et al.* 2004, Lombard, 2006) and for medical purposes (Velo, 1984; Salomon, 2009).

In the last few decades, the study progress and several new discoveries contribute to formulate theories that currently interpret the ochre use as tangible evidence of the emergence of Modern Human Behaviour, as well as a

proxy for the articulated language and symbolism (d'Errico *et al.* 2001; Rifkin, 2012; Seawright, 2014).

The objective of this research is to define raw materials, procurement and supply strategies, treatments and transformations of ochre, as well as its use to better understand the role played by this material in the life of Palaeolithic and Mesolithic hunter-gatherers. In order to increase knowledges on this phenomenon, some ochre assemblages from European sites will be analysed by a global approach that integrates archaeological methodologies and analytical techniques (physical-chemical analysis). It will be explored the sequence of human gestures and technical processes implemented to process colouring raw materials by observing the traces that will be interpreted based on archaeological comparisons and experimental references. Furthermore, the spatial distribution of ochre remains in the sites will be analysed to investigate the management of colouring materials in the space occupied by human groups to recognize potential areas of activity.

In light of the above, this thesis is structured in three parts. In the first part, will be presented what is ochre (general definitions, theoretical framework, use in Prehistory). A sort of catalogue of ochre remains in archaeological contexts will be reported to recognize anthropic evidences. Then the methods of investigation will be discussed. The methodological protocol will be presented based on the execution of a preliminary test to validate tools and techniques. Then, sites and strategies for collecting and sampling ochre will be described. In the second part will be described the data obtain from the study of materials. Finally, the results will be discussed to emphasize the contributions offered by this work on knowledge of ochre exploitation in Prehistory.

Chapter I.

Ochre: state of knowledge

“Définir l’ocre, ou les ocres, est un exercice de style difficile. Pour aborder le problème, quelques citations relevées dans de vieux ouvrages, dans des dictionnaires, montrent que, depuis des siècles, l’imprécision demeure”

(Triat, 2010).

It is complicated to give a single definition of what ochre is. In this section we will try to approach this theme by reporting important archaeological notions and testimonies to offer a good basic knowledge better to understand ochre exploitation and its use among Palaeolithic and Mesolithic hunter-gatherers.

Geological and archaeological knowledges on ochre will be reported. However, these notices may appear quite heterogeneous and unrelated to each other, it will be necessary to acquire basic skills to make significative reflections on data proposing interpretative hypotheses.

Moreover, these aspects here reported constitute an important reference for setting the main objectives of this research without the danger of wandering towards other features.

In any case, the vastness of this topic and the debates yet in progress make the approach to ochre phenomenon not immediate. In this section it will try to explain it. It will start from the definition of raw materials to the genesis and properties of iron ores, as well as to the most ancient archaeological evidences retracing the most important interpretative theories about the use of ochre by prehistoric humans.

I.1. Definitions of ochre

From a geochemical perspective, there are no doubts that the word “*ochre*” defines rocks and earths rich in Iron (oxide, hydroxide, oxy-hydroxide) with shades of colour from deep red to reddish brown-purple, to orange and yellow. It is thus more difficult to give a definition from an archaeological perspective:

- “Ochre is a general term for any ferruginous earth, clay, mineral or rock containing sufficient hematite (an iron oxide) or iron hydroxide (e.g. goethite) to produce, respectively, either a red or yellow streak” (Watts, 2002).
- “Ochre is typically a product of chemical weathering which has been sufficiently enriched in iron oxide (generally hematite) or iron hydroxide (typically goethite) to produce (respectively) a reddish or yellowish mark when drawn over a surface” (Henshilwood *et al.*, 2009).
- “Ochre is a general term that is used, archaeologically, to describe a variety of iron-rich or ferruginous minerals that produce a reddish or streak, including hematite, limonite, goethite, specularite, shale, snuffbox shale, mudstone and sandstone” (Hodgskiss, 2010).

- “Ferruginous rocks that contain iron oxide or iron hydroxide are colloquially called *ochre*” (Wadley, 2009).
- “*Sensu stricto*, ochre is coloured earth, composed of a mixture of clay, quartz, and iron oxides or oxy-hydroxides, such as hematite or goethite. The meaning of this term has been extended to archaeology to refer to any category of rocks containing iron oxides (or oxy-hydroxides), with a reddish or yellowish streak” (Dayet, 2013).

In his *Naturalis Historia* (vol. XXXV, par.35), Pliny the Elder wrote:

*“E reliquis rubricae generibus fabris utilissima Aegyptia et Africana, quoniam maxime sorbentur tectoriis. *rubrica* autem nascitur et in ferrariis metallis. ea et fit ochra exusta * in ollis novis luto circumlitis. quo magis arsit in caminis, hoc melior. omnis autem rubrica siccatur ideoque ex emplastris conveniet igni etiam sacro”.*

In this version, Pliny describes two types of red Egyptian and African ochres used in buildings. Furthermore, he affirms that this material could be obtained from both iron mines, and from heat treatment through the baking of new pots sprinkled with mud. In the following steps, Pliny describes the *sinopia*. This material, like red ochre, was available in three variants and obtained from sources in Egypt, Balearic Islands, Africa, Lemnos and Cappadocia. The *sinopia* was also used as a pigment to cure ulcers, herpes, intestinal problems, roughness of the eyes, and when mixed with *minium*, it was also used like a medicine against lacrimation, blood loss, pains in the spleen and liver as well as an antidote for poisons. On the other hand, archaeological evidence

demonstrated the ubiquity of this material in several contexts (domestic, funerary, artistic) from Prehistory.

I.2. Iron ores

The main constituents of ochre are iron ores in form of oxide, hydroxide and oxy-hydroxide, but there are two main compounds that are the major constituent: red hematite (Fe_2O_3) and yellow goethite ($\text{FeO}(\text{OH})$). Despite hematite and goethite being the main iron ores used due to their properties and colouring power, other minerals such as lepidocrocite and ferrihydrite can be exploited to obtain dark yellow, brown and orange pigments. In addition, black and brownish-black pigments can also be derived from iron ores such as magnetite and maghemite.

Hematite: Fe_2O_3

Hematite derives its name from the Greek: $\alpha\mu\alpha$, "blood" for the blood-red colour of its powder. Chemically known with the formula $\alpha\text{-Fe}_2\text{O}_3$ (iron sesquioxide), this mineral contains about 69,9% of iron and 30% of oxygen. In nature, it can be found in crystal form or granular aggregates. The crystals can have a rhombohedral, pyramidal, tabular or lamellar structure, isolated or in parallel-helical groupings like a "rose" (Eisenrosen "iron roses") with metallic and iridescent colours from dark grey-steel to black-iron (Cornell & Schwertmann, 2004; <http://www.handbookofmineralogy.org/>). The granular aggregates can constitute masses or concretions in soils, sedimentary rocks or their metamorphosed equivalents. The hematite may also be present in weathering products of iron-bearing minerals (Deer *et al.*, 2013).

Goethite: $\alpha\text{-FeO}(\text{OH})$

The term “goethite” is related to the poet J. W. Von Goethe who was interested in mineralogy and geology. The goethite, α - FeO-OH (sesquioxide of iron hydrate), is an iron hydroxide composed of about 63% of iron and, in varying percentages, manganese (Cornell & Schwertmann, 2004) In nature, it is present as a weathering product of iron-bearing minerals in acicular form or tabulated aggregate, botryoidal stalactites or incoherent masses with a blackish-brown or yellowish-reddish-brown colour in massive aggregates.

In powder form, the goethite has a colour from brownish-yellow, yellow to yellowish-orange. Usually, this mineral is associated with materials commonly identified as limonite (Deer *et al.*, 2013; <http://www.handbookofmineralogy.org/>).

Lepidocrocite: γ -Fe O(OH)

From the greek λεπις, “scale”, and κροκος, “fibers”, the lepidocrocite also called emeraldine or hydro-hematite, is an iron oxy-hydroxide with the chemical formula γ -Fe O(OH). For its orthorhombic crystalline structure, this mineral is like the boehmite contained in the bauxite deposits (Cornell & Schwertmann, 2004). The lepidocrocite appears in flattened crystal form, isolated or aggregated into plumose or rosette-like groups. The crystals, with a submetallic lustre, have a ruby red/reddish-brown colour, but they may provide a dull orange powder (<http://www.handbookofmineralogy.org/>).

Ferrihydrite: $2(\text{Fe}_2\text{O}_3) \text{H}_2\text{O}$

The ferrihydrite, *ferr*i for the ferric composition and *hydrite* a hydrated mineral, is an oxy-hydroxide ore chemically identified with the formula $2(\text{Fe}_2\text{O}_3) \text{H}_2\text{O}$.

This mineral has a hexagonal structure and it crystalizes into globular micro-aggregates which are not easy to recognize (Cornell & Schwertmann, 2004). The ferrihydrite appears in soils and weathered rocks, in acid mine and around cold and hot springs as fine grains with a yellow-brown colour. It is commonly associated with goethite, lepidocrocite, hematite and manganese oxide (Deer *et al.*, 2013; <http://www.handbookofmineralogy.org/>)

Magnetite: Fe₃O₄

The name comes from *Magnesia ad Sipylum*, in Asia Minor, near Mount Sipylus where this mineral was present in abundance. The magnetite, composed by approximately 72,4% of iron and 27,6% of oxygen, is part of the isomorphic group of spinels and is known with the formula Fe₃O₄ (Cornell & Schwertmann, 2004; Deer *et al.*, 2013). This is the mineral with the highest percentage of iron and the element with the most intense magnetic susceptibility. Commonly, the magnetite is present as octahedral crystals, rarely rhomb-dodecahedral, but it can also be found in granular or massive aggregates.

Maghemite: γ-Fe₂O₃

The name maghemite comes from the combination of magnetite and hematite because this iron oxide has a similar structure to the magnetite, but the composition is like hematite. The maghemite is part of the isomorphic group of the spinels and it is known for its intense ferromagnetic properties. In chemistry, the maghemite is identified with this formula: γ-Fe₂O₃. It is close to ferric oxide in its composition: Fe₂O₃. This iron oxide is present in nature with

cubic crystals, typically with a tetragonal supercell, but rarely as minute octahedral crystals, or acicular overgrowths with a brown, bluish black colour. In nature, the maghemite appears like a widespread yellow pigment in soils, rocks or continental sediments for processes of weathering or low-temperature oxidation of spinels containing ferrous iron such as magnetite or titanomagnetite (Cornell & Schwertmann, 2004; <http://www.handbookofmineralogy.org/>).

I.2.1. Genesis of ochres

Ochre is a native compound of Fe. The most usual form of iron ores are the oxides, hydroxides and oxy-hydroxide. The combination of Fe with O (oxygen) and OH (hydroxide), during the processes of enrichment, precipitation, dissolution, re-precipitation, for the interaction of stimulator factors such as PH, temperature, and weathering agents, it generates sixteen iron compounds: hematite, magnetite, maghemite, β -Fe₂O₃, ϵ -Fe₂O₃, wüstite, goethite, lepidocrocite, akaganeite, schwertmannite, δ' -FeO(OH), feroxyhyte, high pressure FeOOH, ferrihydrite, bernalite, Fe(OH)₂ (Cornell & Schwertmann, 2004).

Iron ores in magmatic and metamorphic rocks

Titanomagnetite, ilmenite and, rarely, hematite are the main iron ores in magmatic rocks. The abundance of titanomagnetite and ilmenite in basalts, and to a lesser extent, in trachites, liparites, phonolites and rhyolites is due to the processes of oxidation, decomposition and/or exsolution influenced by several factors such as the composition of the melting, rate of cooling and oxygen

fugacity. In regards the metamorphic rocks, magnetite, ilmenite and hematite are the most abundant iron ores, mainly for metamorphic processes. Magnetite is usually found in metaperidotites, metabasites, iron-formations, gneiss and metapelites. Ilmenite occurs in metapelitic, metabasic and metaperidotites rocks, instead hematite in metamorphized iron-formations, metabasites, aerobic clay rocks and metamorphosed manganiferous rocks (Cornell & Schwertmann, 2004).

Iron ores in sediments and sedimentary rocks

Iron is a mineral commonly present in sediments and sedimentary rocks. Sandstones, claystones and carbonatic rocks contain Fe in different percentages, but two groups of iron-enriched sediments and rocks are the most evocative: the red beds and the sedimentary iron ores.

The red beds are reddish coloured rocks and are widespread all over the continents from the Proterozoic (1.500 million years) to Miocene (6 million years). The attractive red colour is due to the presence of hematite in the form of fine grains of clays, silts, sands and conglomerates and limestones in the rock formations (Cornell and Schwertmann, 2004).

The sedimentary iron ores are sedimentary rocks rich in Fe (>15%), preferably in the form of Fe oxides, that can be distinguished into two groups: the sedimentary iron formation and the sedimentary iron stones. The sedimentary iron formation or BIF (banded iron formations) or itabirites are millimetre layers of hematite or magnetite interbedded with quartz and chert formed during Precambrian Aeon (Trendall & Morris, 1983). The sedimentary iron stones are Phanerozoic rocks rich in Fe mainly for supergene enrichment

(enrichment of ores in metal components for the circulation of meteoric waters that trigger chemical processes) or cementation of sediments, with iron oxide (Cornell & Schwertmann, 2004).

Iron biominerals

The biominerals are products of biomineralization, the creation of inorganic solids by living organisms. All the major iron ores, except hematite, may be generated by biomineralization (Cornell & Schwertmann, 2004). The biological environment, in fact, has the ideal condition to favour the accumulation of iron used by the organism during metabolic processes (Frankel & Blakemore, 1991).

Iron ores in weathering zones of rocks

“Relative” or “Absolute” concentrations of iron oxide may be found in weathering zones of rocks. The first type, “relatives”, are due to the precipitation of Fe oxides during weathering where they are deposited in the weathering zones of rocks due to high stability and low solubility.

The second type, “absolutes”, typical of the low-lying regions of the landscape that mostly originate from the Tertiary to the Pleistocene, consists of Fe-oxide crusts: ferricretes. However, the category of weathering zones enriched in Fe oxides includes the bauxite deposits mainly formed from the weathering of Aluminium. Generally, they contain iron oxides (Anand *et al.*, 1991; Cornell & Schwertmann, 2004).

Iron ores in recent geological environments

The recent formation of iron can exist in various environments of the Earth such as soils, spring and ground water, deep sea, continental shelves, lakes and streams.

On the terrestrial surface, the debris products of iron formations as red beds, iron stones or detrital hematite can accumulate forming red dune sands. In the case of aquatic environments, accumulations of ferrihydrite may characterize (initial stage in the formation of the iron oxides) the areas with spring and ground waters. Also, scabs or nodules of FeIII oxides can be widespread on the ocean floors or in the fresh water lakes: lake iron ores. (Cornell & Schwertmann, 2004).

I.2.3. Cinnabar: HgS

The cinnabar, in ancient Greek Κιννάβαρι and in Latin *cinnàbaris*, would derive its name from the Persian word *zinjifrah* (dragon blood) for its characteristic red bright colour. Technically a mercury sulphide, cinnabar is derived from an association of sulphur and mercury and is therefore considered to be toxic. This mineral present in massive form or granular deposits, in hydrothermal deposits near volcanic areas, appear as tabular or prismatic crystals. Being a polymorph, it is found with two distinct crystalline forms: α -HgS with trigonal structure (resulting from red pigment) and β -HgS with cubic structure (<http://www.handbookofmineralogy.org/>).

I.2.4. Jarosite: $\text{KFe}_3(\text{SO}_4)_2(\text{OH})_6$

Jarosite, a basic sulphate of iron and potassium ($\text{KFe}_3(\text{SO}_4)_2(\text{OH})_6$), is part of the group of the alunite and derives its name from the place where it was discovered in 1852 by the German mineralogist J.F.A. Breithaupt, Barranco Jaroso (Spain). Jarosite, with its yellow coloration, has a hexagonal crystalline system with rhomboid or tabular pseudo-cubic crystals. Generally recognizable as minute crystalline crusts, it can be found also as fibrous or nodular agglomerates. Regarding the genesis, it originates from the oxidation of rocks containing sulphide or from pyrite alteration. It may rarely have a hydrothermal genesis (<http://www.handbookofmineralogy.org/>).

I.2.5. Properties of iron ores

The properties of a material depend largely on its structure. Ochre is chemically formed from a set of iron ores (oxides, hydroxides and oxy-hydroxides or iron) which are the product of different combinations of iron with oxygen and/or water. This chemical ambiguity gives ochre its several properties which makes it a versatile and largely used material. In the work "*The Iron Oxides: Structure, Properties, Reactions, Occurrences and Uses*" the authors Cornell and Schwertmann (2004) summarized the main common uses of iron ores which will be briefly summed up below.

Iron ores as pigments

Iron ores make up the basic components of inorganic natural and synthetic pigments due to their extreme stability and high resistance to acids and

alkalines. Additionally, since they are insoluble and UV absorbent, they can be used as binders for paints because they protect the surface from degrading processes caused by outside and atmospheric agents. The natural iron ore based inorganic pigments (ochre) range from deep red to yellow to reddish brown depending on the main constituents and if there are added organic materials or other mineral components (silicates or micas), they can vary from greenish-brown to grey hues of umbers or burnt sienna, burnt umber, metallic browns due to calcination processes. On the other hand, the synthetic inorganic pigments based on iron ores are mainly produced through three processes: precipitation from soluble Fe salts through hydrolysis/oxidation processes, the transformation to solid state and the reduction of nitrobenzene by scrap of iron. The most commonly synthesized pigments are red (hematite), yellow (goethite), orange (lepidocrocite), brown (maghemite) and black magnetite).

Iron ores to produce ferrites

Ferrite is a chemical compound with excellent magnetic and electrical insulation properties that can be synthetically produced by heating iron oxides (hematite) at high temperatures (1100^o-1400^o) in a nitrogen atmosphere or in the air. Thanks to its properties, this material is used as a permanent magnet or in the field of electro-technologies to build inductors, transformers or magnetic strips on cards.

Iron ores as catalysts

Iron ores are often either used as catalysts to produce hydrogen or for the desulphurisation of natural gas. The ones that are predominantly used are

magnetite and hematite which can also be exploited in the oxidation/reduction processes or acid/base catalysts.

Iron ores as abrasive or polishing agents

One of the properties of magnetite and hematite is their robustness. Since ancient times, this property of magnetite and hematite have been used as abrasive agents, for the polishing of some metals like gold, silver, brass and aluminium or for the shining of porcelains.

Iron ores for thermite welding

Thermite welding is a welding technique for the heating of thermite. This reaction occurs when mixing aluminium and hematite powder amongst themselves. The compound which is placed in a melting pot is quickly heated to around 3000°. This heating leads to the formation of aluminium oxide (Al_2O_3) and metallic iron (Fe^0).

I.3. Ochre in Prehistory

The earliest claims of ochre exploitation are dated to about 1,2 million and 790,000 years ago at Olduvai Gorge in Tanzania (Leaky, 1958, Sagona 1994) and Wonderwerk Cave, South Africa (Beaumont & Vogel, 2006). Doubts and uncertainties surround these finds, among which there are some ochre remains of Kathu Pan and Kathu Townlands I, South Africa (Beaumont & Vogel, 2006). So, the first clear evidences of anthropic exploitation of ochre are 176 remains from Twin Rivers in Zambia dated to 260-400,000 years ago. The fragments, with a wide range in colour, from red to yellow, to purple to black, suggest the

existence of an assorted palette with varied shades of colour in Africa during the Middle Stone Age (Barham, 1998, 2002). These materials find comparisons with several discoveries:

- Red ochre lumps from Garba I-Melka Kunture, Ethiopia; dated around 500,000 years ago (Chavaillon & Berthelet, 2004);
- Worked ochre fragments from Olorgesailie, Kenya, dated to 340-490,000 years ago (Tryon & Mc Brearty, 2002b);
- Stone balls with black and red pigments residues from Kabwe, Kenya, dated to 300,000 years ago (Barham, 2002);
- More than 70 ochre pieces from Kapthurin Formation, Kenya, associated with Early MSA artefacts dated to about 285,000 years ago (McBrearty, 2001; McBrearty & Tryon, 2006);
- Red hematite remains from Duinefontein 2, South Africa, around 270-290,000 years ago (Cruz-Uribe *et al.*, 2003);
- Ochre pieces (111) from Border Cave, South Africa, around 170-277,000 years ago (Grün & Beaumont, 2001);
- Red ochre remains from Sai Island, Sudan, 200,000 years ago (Van Peer *et al.*, 2004);
- Potential pieces of ochre (1,032) from Pinnacle Point Cave, South Africa, dated to 164,000 years ago (Marean *et al.*, 2007).
- Ochre remains (9,000 specimens), most of them (600 specimens) with anthropic traces at Blombos Cave, South Africa 120,000 years ago (Henshilwood *et al.*, 2009; Watts, 2009).

Analysis of remains confirm high percentages of red pigments (Watts, 2002; Power, 2004) suggesting intentional choice in the exploitation of red ochre, but not allow to determine an exclusive way of use during these phases.

Also, in Europe remains of colouring materials are found starting from the Lower Palaeolithic. Several red ochre lumps and pebbles with red ochre residues were found at Isernia-La Pineta (Italy), 610,000 years ago approx. (Cremaschi & Peretto, 1988). The information of the discovery does not provide precise data on use of these objects, while at Terra Amata blocks with striations dated to 380,000 years ago approx. seems to refer to an anthropic use (de Lumley, 1969). At Ambrona, a worked plaquette dated to >350,000 years ago confirm anthropic transformations (Howell, 1966). Use wear traces were also recognized on an ochre fragment from Acheneim while at the site of Maastricht-Belvédère traces of red ochre in soil were noted. Both the evidences are dated to 250,000 years ago approx. (Roebroeks *et al.*, 2012; Wernert, 1957). Soil with ochre lenses and raw blocks were also found at Becov Ia, 200,000 years ago approx. (Fridrich, 1976; Marshack, 1981). Ochred tools and pieces of colouring materials appeared in the layer 58 of Combe Grenal, >133,000 years ago (Demars, 1992). These findings focused the scientific interest on the use of pigments by Neanderthals as a proxy of symbolism. In this sense, one of the most attractive sites for the quantity of blocks of dioxide manganese discovered in Mousterian of Acheulian tradition layers was Pech de l'Azé (France). This site was excavated since the early 60' of the XIX century by F. Bordes and recently by F. Soressi in 2004-2005 (Soressi & d'Errico, 2007).

During the fieldworks were found more than 450 remains of manganese dioxide at Pech de l'Azé I and about 26 remains of manganese dioxide at Pech de l'Azé IV (McPherron *et al.*, 2001, d'Errico, 2008). Initially, these remains were

related to an exclusive use of black manganese as a pigment. Recent analysis show that blocks of manganese dioxide were used in fire-making activities. Anyway, the same research does not exclude the possibility of using manganese as a pigment by Neanderthals (Heyes *et al.*, 2016).

According to published notices, black and red pigment lumps in association with Neanderthal evidences were also found in Châtelperronian contexts (Bailleau, 1869; Bouyssonie, 1923; Peyrony, 1934; Chauchat, 1968; Delporte *et al.*, 1999; de Sonneville-Bordes, 2002; David *et al.*, 2005; Salomon *et al.*, 2008; Rios-Garaizar, 2008; Scandiuzzi, 2008; Caron *et al.*, 2011; Rios-Garaizar *et al.*, 2012). In the specific, fragments of black manganese oxides and mainly red hematite and reddish-yellow goethite from Châtelperronian layers were systematically exploited to obtain powdered colouring compounds used as pigment at Grotte du Renne, Roc-de Combe and Le Basté and Bidart (Dayet *et al.*, 2014).

In light of above, the archaeological evidences testify the exploitation of colouring materials both in Africa and Europe involving different human species. However, the exploitation of ochre is systematic with *Homo sapiens* who use ochre to trace graphic signs organized in articulated figurative representations and to realize hand-stencils, two-dimensional figures, signs, lines or points on rock fixed surfaces and to decorate portable supports or personal objects manipulating and admixture organic and inorganic materials to obtain pigments and compounds. The symbolic dimension of *Homo sapiens* takes shape by colouring materials representing natural images adapting natural morphologies for its purposes profiting by protrusions and clefts of rocks and using red, black and yellow pigments in a dynamic and polychrome style. The red and yellow colorants were obtained by oxide and oxy-hydroxide iron ores such as hematite, goethite, lepidocrocite. Black was obtained from

charcoal or manganese oxides as reported by several studies on cave painted (Cabrera Garrido, 1978; Clottes *et al.*, 1990; Baffier *et al.*, 1990; Pepe *et al.*, 1991; Menu & Walter, 1992; Labeau, 1993; Lorblanchet, 1996; Pomiès *et al.*, 1999; García Díez, 2001; Smith *et al.*, 2001; Chalmin *et al.*, 2002; Navarro Gascón, 2002; Arias *et al.*, 2011; Beck *et al.*, 2012; Gay *et al.*, 2015, 2016). One of the European regions in which this phenomenon seems to explode during Upper Palaeolithic, is the Franco-Cantabrian region where are located most of the painted caves that have been discovered up until now. The phenomenon of cave art marks the Upper Palaeolithic, although recent dates back the appearance of rock paintings at about 64,8 thousand years (Hoffmann *et al.*, 2018). However, doubts on this date persist (Pierce & Bonneau, 2018; Aubert *et al.*, 2018).

Surely the amplitude of the archaeological documentation reported here defines a complex and intricate framework in which a very interesting topic for the human symbolism is the use of ochre in funerary contexts. The consciousness of death is one of the main human hallmarks and the abundance of Upper Palaeolithic burials confirm that ritualization of funeral gestures by *Homo sapiens*. Also, Neanderthals remains (Solecki, 1960, 1961; Bar Yosef *et al.*, 1992; Turq *et al.*, 2012) suggest intentional human bone accumulation (Valladas *et al.*, 1987; Schwarcz *et al.*, 1988; Stewart *et al.*, 1977; Guérin *et al.*, 2015). With *Homo sapiens* the bodies, buried in caves or open-air places, could be wrapped in shrouds or clothes and accompanied with grave goods (Pettitt, 2013). Red ochre remains were found in several Upper Palaeolithic and Mesolithic human burials such as the "Red Lady" of Paviland-England, (Stringer & Gamble, 1996), Dolní-Věstonice and Brno II in Moravia, Krems Watchberg-Austria, Kostenki, Sungir and Oleniy Ostrov (Pettitt, 2003; Mussi, 2009; Ravdonikas, 1956; Gurina, 1956) in Russia, the "Prince" of Arene Candide (Cardini, 1942), Grotta Continenza, Grotta del Romito, Grotta di San Teodoro, S'Ormu e S'Orku,

Mezzocorona, Vatte de Zambana, Mondeval de Sora in Italy (Martini, 2006; Fontana, 2016; Melis & Mussi, 2016), Tévéc, Hoedic and La Vergne in France (Péquart & Péquart, 1929, 1934; Duda & Courtaud, 1998), Morín I (González Echegaray, Freeman, 1971, 1973, 1978), El Mirón (Straus *et al.*, 2015), La Braña Arintero 1-2 (Vidal *et al.*, 2008; Vidal & Prada, 2010), Cueva de Los Azules I (Arias, *et al.*, 2009; Fernández-Tresguerres, 1976, 1979), Cueva de Tito Bustillo (Arias *et al.*, 2009; Balbín & Alcolea, 2005; Drak *et al.*, 2008) and Cueva de Los Canes (Arias *et al.*, 2009, Arias & Pérez, 1990) in Spain, Lagar Velho (Zilhao & Trinkaus, 2002) and Moita do Sebastião-Portugal (Roche, 1956), Ofnet (Schmidt, 1909) and Bad Dürrenberg (Geupel, 1977) in Germany, Spiginas and Duonkalnis (Česnyš & Butrimas, 2009) in Latvia, Zvejnieki-Letonia (Zagorskis, 2004), Valma-Estonia (Jaanits, 1965). The non-randomness of data and the diffusion of this practice on large scale confirm the rituality of ochre use during Upper Palaeolithic with continuity during Mesolithic in Europe.

I.3.1. Potential use of ochre

Ochre is a material that has been used since ancient times in different contexts. Start from the first findings in the XIX century the attention was focused on the use of ochre as pigment in rock art. In 1902, the chemist H. Moissan (1902; 1903) analysed the paintings in two French caves: Font de Gaume and La Mouthe. confirming the nature of pigments (red hematite). Start from this study, the increase of discoveries improved the application of physical-chemical methods to characterize ochre (Clottes *et al.*, 1990; Menu & Walter, 1992; Hernanz *et al.*, 2009; Iriarte *et al.*, 2009; Menu, 2009; Seva Romàn *et al.*, 2009; Beck *et al.*, 2011; Jezequel *et al.*, 2011; Olivares *et al.*, 2013; Gay *et al.*, 2016). Furthermore, techno-functional studies developed on the construct of *chaine-opératoire* conceptualized

by Leroi-Gourhan in 1964, establish the exploitation of ochre not only as pigment but also to abrade and dry materials (Allard *et al.*, 1997; Salomon, 2009), to protect the human skin from the sun (Rifkin *et al.*, 2015), to prepare adhesive agents (Becker & Wendorf, 1993; Bocquentin & Bar-Yosef, 2004; Gibson *et al.*, 2004; Lombard, 2006) as well as medicines (Velo 1984).

In the last years, new studies following a multidisciplinary analytical approach (Salomon, 2009, Dayet, 2013, Pradeau, 2014, Rosso, 2017) allowed to reconstruct the *chaîne opératoire* of colouring materials in Prehistory. According to the construct of Leroi-Gourhan (1964) the main phases were identified: procurement, treatments, transformations and use.

The reconstruction of ochre procurement strategies appears focus on mobility patterns (shorter or longer distance) and selection criteria (needs, accessibility of sources; social organization) to acquire the raw materials (Binford 1980, Inizan *et al.* 1995). As well as for lithic resources, the procurement on short, medium or long distances may be related to the quality and value of geological sources, or to human exchanges (García Borja *et al.*, 2004). Comparative studies between archaeological ochre samples and geomaterials show local (Salomon, 2009) and non-local raw materials selection (d'Errico *et al.*, 2010, Roebroeks 2011, Dayet *et al.*, 2015). Exchanges are suggested by ethnography. This is the case of ochre from the mines of Pukardu Hill and Wilga Mia (Australia) that are used as element of economic exchanges between aboriginal groups (Paterson & Lampert 1985, Dayet 2012).

Regarding treatments of ochre, mechanical (fragmentation, powder reduction, faceting) and chemical (heat treatment) transformations were recognized. In the specific, the mechanical reduction of the volume of blocks of raw materials could be carried out mainly by *débitage* or *crushing* (Dayet, 2012). *Débitage*

implied chipping of blocks that left detachments negatives on surfaces, percussion bulbs or lancets like in lithic tools, in case of direct percussion (Henshilwood *et al* 2009, Salomon 2009, Watts 2010). The *crushing* leaves irregular fractures on blocks or indirect traces on ochre processing tools such as residues or wear traces (Dayet, 2013). Also, the powder reduction of ochre could be made by *grinding* and *scoring* (Hodgskiss, 2010; Hodgskiss & Wadley, 2017; Hayes *et al.*, 2017). The *grinding* implied the use of an active tool (pestle) and a passive tool (slab). The pieces of ochre were placed on a slab and grinded by a pestle. In the *scoring*, an ochre piece was scored on an abrasion surface (for example a tablet) producing striations and, rarely, metallic lustre, smoothing, polish or edge modification on surface. Furthermore, *rubbing*, the use of an ochre pieces on soft surfaces such as animal hide, human skin and hair, wooden branches, produced single parallel grooves or grouped parallel striations, with external micro-striations (Hodgskiss, 2010). The engraving presupposed the use, as in the *scoring*, of a tool to engrave the surface. Diagnostic traces of *engraving* are deep incisions on worked surface (Henshilwood, 2009). Furthermore, a series of mechanical gestures and actions could produce ochre pieces with a predetermined morphology such as faceted pieces or *crayons* (Henshilwood *et al.*, 2001; Hivers *et al.*, 2003; Wadley 2005; Watts, 2009; Rifkin 2012). Among the chemical treatments, the *thermal treatment* provided hematite by heating yellow ochre at high temperature (260°-300°) producing intrinsic modifications in the materials as the rearrangement of crystals of iron oxides and hydroxides in ochres. This is a rare practice according to the available archaeological evidence of which some well-documented examples are Arcy-sur-Cure and Riparo Dalmeri (Giallanella *et al.*, 2011, Salomon, 2009). At any way, ethnographic evidence shows that among African groups in Lesotho, it was a widespread practice the thermal treatments during rituals (How, 1962).

The potential use of ochre by prehistoric hunter-gatherers is one of the key issues of ongoing debate on the emergence of cognitive complexity and human symbolism and focuses on two lines of thought interpreting the value of ochre to its use:

- utilitarian value related to a functional use as a manifestation of an advanced and complex human thought (Wadley et al., 2003; Lombard, 2005, 2006; Hodgskiss, 2010; Hodgskiss & Wadley, 2017);
- symbolic value related to a ritual use as a manifestation of self-consciousness (McBrearty & Brooks, 2000; Power, 2004; Barham & Mitchell, 2008; Jacobs & Roberts, 2009; Henshilwood, D'Errico & Watts 2009; Watts, 2009, 2010).

Starting from the archaeological evidences, it is by no means obvious an exclusive use of ochre and colouring materials for artistic purposes and, therefore, exclusively as pigments. As already mentioned several hypotheses suggest a use as pigment, adhesive, abrasive, medicinal agent, hide-tanning ingredient, to preserve food and to manipulate defuncts in burial practices.

Ochre as pigment

The use of ochre as pigment is highlighted by the archaeological evidence: painted caves, as well as painted shells, plaquettes and pebbles, of this practice during Prehistory. The exploitation of colouring ores as means of graphic expression is attested since the Early Upper Palaeolithic in some caves of the Franco-Iberian region such as El Castillo, Chauvet, Altamira, Tito Bustillo (Pike *et al.*, 2012) from about 64,8 thousand years (Hoffmann *et al.*, 2018), even if doubts and uncertainties persist on the beginning of the phenomenon (Pierce &

Bonneau, 2018; Aubert *et al.*, 2018). At any way, geochemical characterization confirms the presence of ochre (hematite and goethite) in parietal pigments (Chalmin *et al.*, 2003; Hernanz *et al.*, 2009; Iriarte *et al.*, 2009; Arias *et al.*, 2011; Beck *et al.*, 2011; Jezequel *et al.*, 2011; Olivares *et al.*, 2013; Gay *et al.*, 2015). Ochre pigment residues were found on Middle Palaeolithic shells from Iberian contexts (Zilhão *et al.*, 2009). In this sense, pigments can be interpreted as a proof of human symbolism (d’Errico *et al.* 2003; Hovers, 2003; Watts, 2009). There are no clear and generally valid criteria for establishing a symbolic use of ochre as pigment. In this sense, it is possible to recognize a purely *decorative* or *aesthetic* use both for art (parietal and portable) and for body painting. About this, the archaeologist P. Pettitt writes (in Henshilwood & d’Errico, 2011):

“I suggest, for example, that one or several of the following could be in operation at any one time or place:

Decoration: the employment of colouring/ornamentation for visual effect with no associated symbolic meaning, or the uninformed reading of an otherwise symbolic code (‘I wear red because I like red’).

Enhancement: the use of colouring/ornamentation/modification to bring out a simple (symbolic) message by enhancing existing clues (‘I wear red as I know you will read it as a sign of my strength or be impressed by it’).

Accessorization: the use of colouring/ornamentation/modification to make a more subtle or specific statement than enhancement by acting as a material cultural accessory to message (‘I wear red as I know you will recognise it as the regalia of our clan and infer from it that we are culturally the same’).

Full symbolism: the use of colouring/ornamentation/modification to make an explicit statement by acting as a full material cultural symbol from which a reader can decode

complex messages from ('I wear red as, like you, I am a successful hunter and have killed an adult eland; it is my right to wear this colour and I therefore command respect from all').

Time/space-factored symbolism: the incorporation of temporal and spatial dimensions into full symbolism, e.g. beliefs, myths and stories, object biographies and histories ('I wear red only at a specific time, marking the time of the year when the ancestors created this land, in honour of the creation myths and to mark out that I am the bearer of this knowledge')".

Pettit, therefore, proposes a series of criteria adaptable to each situation starting from the reflection that the archaeological evidence shows discontinuity and regional variables in the use of ochre. Assuming the use of ochre to decorate the body as for the ornaments, he combines different uses that schematizes from the simplest to the most complex.

Regarding ochre as a pigment for body painting, it is archaeologically problematic to demonstrate. Archaeological evidence attests the use of personal ornaments as a widespread and general practice among human groups starting from the Middle Pleistocene (Henshilwood *et al.*, 2004; d'Errico *et al.*, 2005, 2008; 2009; Millard, 2006; Vanhaeren *et al.*, 2006; Bouzouggar *et al.*, 2007; Bar-Yosef Mayer *et al.*, 2009; Zilhão *et al.*, 2010) is therefore conceivable that ochre pigments were also applied on human skin. This hypothesis was already suggested by the first studies on prehistoric pigments (Peyrony, 1921; Bordes, 1952; Le-Roi Gourhan, 1976).

Experimental researches and ethnographic evidence support the application on human skin attributing to this practice both a symbolic and a utilitarian value. The Female Cosmetic Coalitions Hypothesis (FCCH) associates the use of red ochre to female fertility. According to this model (Knight *et al.*, 1995; Power,

1999, 2009; Power & Aiello, 1997; Power *et al.*, 2013) ochre is used as cosmetic, applied on body, to simulate the menstrual cycle, a strong fertility signal and attraction for the male. Within the group, menstruating and non-menstruating women are coalescing using red ochre on their bodies to create "false menstruation". The man, therefore, receives continuous fertility inputs and the women thus assume the control of sexuality assuring of continuous male care because he is always attracted.

The cosmetic use of ochre associated with female menstruation finds ethnographic comparisons between sub-Saharan African groups (Knight 1991, Watts 1999, Power 1999). Body painting practices were already reported by first explorers. In the report of his third expedition towards the mid 1700's, captain James Cook described the common use of applying a mixture of fat and red ochre on the hair of Australian aboriginal men (Noetling, 1909). A similar practice was also recognized among the Himba, nomadic shepherds, in the region of Kunene in north Namibia. The Himba women sprinkle their body and hair with a creamy mixture made of butter and red ochre powder: *otjize*, which according to ethnographic sources, was also used by men for the initiation of rituals or to treat defuncts. (Galton, 1853; Tönjes, 1911). Further examples are the corporal painting of Mursi and Surmi, in the Omo Valley (Ethiopia). These groups are known to adorn their body with natural elements like plants and flowers as well as red, white and orange mineral powders which are applied on the skin to compose geometric and abstract figures.

At the same time, ochre on human skin can assumed a utilitarian function. Experimental studies assessed the efficacy of red ochre on human skin as photoprotector and insect-repellent suggesting the hypothesis that the habitual

exploitation of red ochre during MSA in Africa had a positive impact in human adaptive strategies (Rifkin 2014; 2015).

Ochre as adhesive agent

The ochre use as adhesive agent is attested by the presence of red residues on hafted lithic tools and projectile weapons from Middle/Late Pleistocene contexts (Audouin & Plisson, 1982; Beyries & Inizan, 1982; Gibson *et al.*, 2004; Wadley *et al.*, 2004; Lombard, 2005, 2006; Villa *et al.*, 2005; Lombard & Wadley, 2007; Dayet *et al.*, 2013; Helwig *et al.*, 2014). Optical observation, physical-chemical analysis and blind tests (Allain & Rigaud, 1986; Williamson, 1997; Wadley, 2005; Zipkin *et al.*, 2014) support the role of ochre as ingredient of adhesive mixtures or mastics to haft artefacts.

Ochre as abrasive agent

The presence of small quartz crystals within hematite and the hardness of mineral (5.5–6.5 Moss scale) allow the use of ochre as abrasive agent. Indirect archaeological evidences are polishing traces (micro-striations) and red residues also inside the striations on bone antler beads (Allard *et al.*, 1997) and on portable art objects such as the Venus of Brassempouy, the Venus of Lespugue (Walter, 1995) and the Venus of Savignano (Mussi, 2005). Well known is the *Jeweller's Rouge* (Fe_2O_3) used to polishing the surfaces of metallic jewellery and small glass lenses that attest this current practice and support the hypothesis on a Prehistoric use.

Ochre as hide tanning ingredient

Ochre and all iron oxides allow to dry organic substances because the particles of the oxides tend to absorb the organic molecules as water and fatty acids (Mandl, 1961). Several studies show antibacterial properties of iron ores (Velo, 1984, 1986; Ellis *et al.*, 1997) allowing to suggest the role of ochre as a prehistoric hide-tanning ingredient (Beyries & Walter 1996, Rifkin, 2011). Ethnographic notices confirm that the Tehuelche of Patagonia use a mixture of animal fat, ochre and/or rock alum to preserve animal skins (Laloy, 1906), and Indian tribes in South America treat hides for the construction of housing structures with animal fat and red paint, probably ochre (Cooper 1946).

Ochre as food preservative

Regarding this use, direct evidence available from ethnographic reports attest this practice among Australian aborigines that preserve food in ochre bowls (Basedow, 1925; Flood, 1983).

Ochre as medicine

The use of ochre as medicine is conceivable if it reflects on the well attested through History. Usually, ancient Romans locally applied red ochre to calm herpes, watery eyes and various pains. As a basic ingredient of drinks, it was given to those who spit blood, for female bleeding and as an antidote against poisons (Pliny the Elder, vol. XXXV). Among the aborigines, ochre-based compresses are applied on lesions to cicatrise and calm burnings (Velo 1984).

Ochre in mortuary practices

The presence of red ochre in prehistoric human burials is attested as a widespread practice starting from the Gravettian period. Ochre fragments and powder in funerary structures and ochre residues on skeletal remains suggest the use of ochre to manipulate defuncts. The richness of archaeological record confirms the recurrence of this practice, allowing to recognize repeated and generalized mortuary practices. The Palaeolithic and Mesolithic hunter-gatherers who occupied the European continent developed a system of symbolic behaviours to face death. This rituality of death is displayed by symbolic gestures of bodies manipulation ritually repeated such as ornamentation, ochre use and grave goods. Since the first discoveries, human skeletons with red ochre at Cro-Magnon rock-shelter (Lartet, 1868) and Caviglione Cave (Rivière, 1887) in Italy, assumed the key role of ochre in ritual dimension of prehistoric societies confirmed by successive discoveries of Palaeolithic and Mesolithic ochred burials (Schmidt 1909; Péquart & Péquart 1929; Gurina, 1956; Ravdonikas, 1956; Roche 1956; Jaanits 1965; González Echegaray, Freeman, 1971, 1973, 1978; Fernández, 1976, 1979; Geupel 1977; Arias & Pérez, 1990a, 1990b; Stringer & Gamble, 1996; Duday and Courtaud 1998; Zilhao & Trinkaus, 2002; Pettitt, 2003; Zagorskis 2004; Balbín & Alcolea, 2005; Martini, 2006; Vidal *et al.*, 2008; Arias, *et al.*, 2009; Česnys & Butrimas 2009; Mussi, 2009; Vidal & Prada, 2010). Red ochre for funeral purposes leads to reflect on the association of red ochre with red-blood. Red colour has an attractive power on humans. In this sense, therefore, the non-random choice of the red colour is undeniable. Ethnographic data attest both a ritual and functional use of iron ores. Among Australian aborigines of Lower River

Murray, a mixture of ochre is used with a partial mummification of the deceased with a conservative and antibacterial function to odour control and to reduce putrefaction (Berndt & Berndt, 1964); while among the Ovahimba of Namibia, Africa, the *otjize* (mixture of animal fat and red ochre) as well as applied on women skin with aesthetic function, as reported before, it is also used for the ritual treatment of defuncts (Galton, 1853; Tönjes, 1911)

I.4. Synthesis

The information reported in this chapter confirms the versatility of the ochre, a material with multiple properties and widely exploited by humans since Lower Palaeolithic, and systematically from the Upper Palaeolithic.

The archaeological evidence confirms the abundance of red ochre used both for functional and symbolic purposes. Although the use of ochre is not a prerogative of *Homo sapiens*, it is with this species that ochre is used for diversified activities.

For this reason, it is legitimate to wonder about the role of ochre for hunter-gatherers who exploit this mineral resource with an intense colouring power during Upper Palaeolithic and Mesolithic. In a context such as the south-western Europe in which the human events of Palaeolithic and Mesolithic hunter-gatherers are intertwined, the sites are abundant and offer numerous and interesting perspectives of study to always offer new contributions on the knowledge of Prehistory.

From here arises a precise question: What is the meaning and function of ochre for human groups that occupied south-western Europe during Upper Palaeolithic and Mesolithic?

To answer this question, it is advisable to start from the study of archaeological remains in different European. The possibility of evaluating several archaeological assemblages offers an exceptional opportunity to discover several forms of ochre remains in archaeological deposits. Furthermore, this aspect is significative to appreciate technical skills and economic management of raw materials among synchronic culture in different geographic regions, in order to evaluate the impact of human adaptation to the environmental context in which the same groups live. Moreover, the opportunity of accessing materials ascribable to distinct cultural phases allows a diachronic study to evaluate elements of continuity and discontinuity in the phenomenon of anthropic ochre exploitation during the Late Glacial and Early and Middle Holocene.

Chapter II.

Studying ochre from archaeological contexts

Ochre is a versatile and ubiquitous material. But, how does it appear in archaeological contexts? Ochre appears in a variety of forms. So, the discrimination of an anthropic origin in prehistoric sites cannot be immediate and easy. An investigation of the archaeological context and taphonomical processes involved in the formation of deposits is necessary, as well as a good knowledge of the different evidences of ochre remains that are potentially recognizable in an archaeological site. A general assessment of physical traits such as colour, mass and dimensions, state of conservation of specimens, as well as diversity and fragmentation of specimens can provide essential data to discriminate the origin of materials and the degree of anthropic contribution on the formation of the assemblage.

II.1. Ochre in archaeological contexts

Knowing the form in which ochre can be found is a crucial aspect to reflect on materials. The progress of archaeological studies and the increase in discoveries of ochre remains from prehistoric contexts make it possible to have a broad reference in order to develop a sort of catalogue of vestiges that can be found in

archaeological contexts. This catalogue constitutes a guide to typologically define ochre vestiges during this study.

Raw ochre pieces

Raw ochre pieces are not uncommon in prehistoric sites. These objects can appear as compact masses of mixtures of quartz, clay and iron minerals (oxides, hydroxides, oxyhydroxides) with red, orange and yellow colour, variable in size and tendentially with an irregular morphology which have not suffered modifications. For this reason, the anthropic origin can be doubtful. Specifically, they are found as raw blocks or fragments, as well as plaquettes without any sort of use wear traces or diagnostic signs.

Ochre pieces with anthropic modifications

Each compact mass of mixture of quartz, clay and iron minerals (oxides, hydroxides, oxo-hydroxides) with red, orange and yellow shades of colour modified by anthropic actions can be enclosed into this category.

A typological model elaborated by C. Couraud (1983) supports the identification of these objects. This model is based on the presence of diagnostic traces corresponding to specific human actions: *lustrage* (polish), *frottage* (rubbing), *raclage* (scraping), *cupules* (cups), *perforation* (drilling), *gravure* (engraving), *entaille* (carving), *modelage* (modelling).

Lustrage (polish) - striations unnoticeable upon touch, with a shiny and/or bright aspect produced using the piece on a soft surface. Hypothesis: use of a colouring block on organic soft surfaces (animal or human skin).

Frottage (rubbing) - striations noticeable upon touch due to the rubbing of the piece on a hard object. Hypothesis: use of the block on a stone. The rubbed part is rather convex.

Raclage (scoring) - striations due to the scoring of the block by a hard object. Hypothesis: block scored with a flint artefact. The scored part is rather concave.

Cupule (cups) – small depression obtained by scraping or perforating with a sharp object the surface or by dissolution of the raw material with a moistened brush in a way to obtain a coloured powder or liquid.

Perforation (perforation) – small cavity obtained with a sharp object. The block can be partially or totally perforated.

Gravure (engraving) – lines of different shapes obtained with a sheared or sharp object.

Entaille (carving) – very short carving obtained by a sheared object.

Modelage (modeling) – particularly coloured clay or mixtures of various elements, sometimes with fingerprints. These hand modelled blocks can also have traces of *frottage*.

Furthermore, experimental comparisons (Hodgskiss, 2010) allow to interpret use wear traces with experimental creations by *grinding*, *scoring*, *rubbing*, as well as *trampling* and *soaking* (post-depositional traces).

Grinding: single or grouped unidirectional and parallel striations with a U-shaped profile and internal micro-striations.

Scoring: multiple striations with a varied internal profile (U, V, \ _ /) and fringed at the end, on ground and unground ochre pieces. They are often

associated with internal micro-striations, but also other elements that modify the surface of the pieces such as lustrations, polishing and edge modifications.

Rubbing: grooves with external micro-striations, smoothing, rounded edges and modification of slightly convex to flat surfaces as a faceted.

Trampling and *Soaking*: irregular striations, scratches and scuffmarks (trampling) or polishing and lustration of surfaces (soaking) can be affect ochre modified pieces.

Based on the archaeological evidence, it is possible to add fragments with use wear traces, faceted pieces, crayons, pieces with engraved motifs or perforations into this category.

Ochre fragments with diagnostic traces as striations, lustrations, chipping, polishing, etc....produced by mechanical fragmentation actions and reduction of larger pieces. However, faceted pieces are small to medium sized ochre pieces in which a reduction in volume is due to anthropic modifications by *crushing* (Hodgskiss, 2010; Salomon, 2009; Dayet, 2012).

Crayons are compact pieces of ochre of centimetric dimensions in which the volume is defined by a certain number of faces converging in one point (Henshilwood *et al.*, 2001). Although rare in archaeological contexts, it is important to specify that the archaeological value of these elements is essential to better understand the use of ochre implicitly related to the term defining these pieces. The term "*crayon*" is used in its modern meaning indicating pieces of compact ochre and with a well-defined form that are exploited to colour surfaces (organic/inorganic).

Crayons were defined by a systematic study of ochre pieces from African Middle Stone Age sites (Watts, 1998; Henshilwood *et al.*, 2001) such as Apollo

11, Boomplaas, Hollow Rock Shelter, Klasies River Cave 1, Shelter 1A, Shelter 1B, Border Cave, Umhlatuzana, Rose Cottage Cave, Bushman Rock Shelter, Olieboomspoort, Mwulu's Cave, Linksfield, Primrose Ridge and Blombos Cave (Wadley, 2005).

A rarer case of *crayons* is represented by globular or polygonal compact masses of ochre with a suspension hole. In the classification of Couraud (1983), it is specified that if the object shows decorations, it falls into the category of artistic supports, on the other hand, if it shows traces of use, it falls into the category of modified pieces, even if it is a decorative element or an amulet.

The definition of perforated ochre pieces is exposed by Salomon (2009), who highlights the potential utilitarian nature of these "*pearls-outil*" or "*pendeloque-outil*".

It is pliable to admit that the presence of a perforation with a diameter smaller than a finger of an infant allows to establish the function of these objects as pendants (Alarashi, 2014) regardless of the symbolic value (ornament) or utilitarian (colouring instrument). However, due to their rarity, the pieces of ochre perforated by some sites of the Franco-Cantabrian region deserve to be cited as a necklace made of perforated atrophic canines of red deer with a triangular ochre pendant with a hole from the Solutrean levels of La Lluera I, Spain (Rodríguez Asensio, *et al.*, 2012). Furthermore, a very rare globular perforated piece of ochre comes from the Solutrean levels of Fourneau Du Diable, France (San Juan, 1990).

Another group of objects as *compact masses of ochre with variable dimensions and motifs engraved with parallel, oblique or crossed lines* appear in prehistoric sites. These very rare pieces, but significant in the appearance of human symbolic behaviour, come from Klasies River Cave 1, dating back to between 100,000-

85,000 ky (d'Errico *et al.*, 2011) and Blombos Cave, in levels dating back to around 70,000 years ago (Henshilwood *et al.*, 2009).

Blocks of engraved ochre defined as artistic supports in the typology of Couraud (1983) are also found in some European Palaeolithic contexts such as a horse engraved on a block of hematite from Lumentxa, Spain, (Aranzadi & Barandiarán, 1935), a "*bâton d'ocre*" with horizontal and parallel lines engraved from the Abri Blanchard, France (Didon, 1911).

Ochre lenses on soils

Thin layers or spots of red ochre in soils can be found in sites such as the evidence from Maastricht-Belvédère, Netherlands, (Roebroeks *et al.* 2012) or Pincevent, France, where red ochre lens extends over a large domestic area in association with flint artefacts and hearth remains described by Leroi-Gourhan and Brézillon (1966):

"Une mince pellicule d'ocre rouge revêtait le sol d'habitat, répartie avec netteté dans zones vides VII, VIII et IX et de l'abord immédiat des foyers. Cette pellicule avait manifestement couvert le sol dès le début de l'occupation... (...) ..."

(A thin film of red ochre coated the floor of habitat, sharply distributed in empty zones VII, VIII and IX and the immediate approach of the hearths. This film had obviously covered the ground from the beginning of the occupation).

More common are ochre lenses in funerary contexts. Layers of red ochre are identified in one of the earliest discoveries of prehistoric burials at the beginning of the XX century as reported by Cardini (1980) in an article on burials of the Arene Candide (Liguria). The burials were preliminary dating

back to a Mesolithic phase, then were attributed to the Upper Palaeolithic (Maggi *et al.*, 1996).

Cardini writes:

"...Mesolitico: 6A, paleosuolo rossastro impregnato d'ocra, con sepolture...(....)..."

(Mesolithic: 6A, reddish paleo-soil impregnated with ochre, with burials).

In any case, it is worth pointing out that ochre in funerary contexts, in addition to thin layers of red ochre in burials, gives the possibility of recognizing the red residues directly on the deceased depending on practices of body manipulation or by the presence of shrouds or ochred clothing that enveloped the body (Mussi, 1986; Martini, 2006; Pettitt, 2010).

Ochre residues on objects

What remains of a substance (ochre) on a surface (fixed or mobile) after its use is defined as residual. In an archaeological context, residues (patches, lumps, macro-microscopic traces) of ochre can be recognized on diversified surfaces through the naked eye or with a high-magnification optical microscope.

In this sense, it needs to distinguish between residues on objects to contain or process ochre, residues on lithic artefacts, residues on ornaments or portable art objects.

Ochre residues on containers and processing tools can be recognized as patches or microscopic traces. Ochre-stained artefacts and ochre containers were found in several archaeological sites. Grindstones with ochre residues, were found in Africa from MSA layers (500-284 ky) of GnJh-15, in the Kapthurin formation,

Kenya. In order of time, going on to quartzite cobble ochre-stained at Twin Rivers-Zambia, sandstone mortars with red and yellow residues associated with use wear traces dating back to 180,000 years ago, and two ochre toolkits made by two abalone shells with inside pigment residues (McBrearty & Brooks, 2000; Barham, 2002; Henshilwood *et al.*, 2011).

In Europe, the oldest evidence date back to about 250-200,000 years ago. From the Mousterian levels of Bečov I, Czech Republic (Šajnerová-Dušková *et al.*, 2009), grindstones potentially used to powder mineral pigments were discovered. However, most clear evidences were found at Cioarei-Boroșteni Cave, Romania (Cârciumaru & Tuțuianu-Cârciumaru, 2009). In this site, eight concave pieces of stalagmites with red pigment residues attributed to around 52-45 / 48 ky were discovered.

A limestone modified block was also reported from the Late Mousterian levels of Grotte de Néron (Comber, 1989). Shells with iron ores residues interpreted as potential ochre containers were collected from two Iberian sites dating back to 50 Ky (Zilhão *et al.*, 2010): Cueva Antón (*Pecten maximus*) and Cueva de Los Aviones (*Spondylus gaederopus*). An ochred marine shell of *Aspa marginata* also were discovered at the Mousterian site of Fumane, Italy (47,6-45,0 Ky cal BP).

Starting from the Upper Palaeolithic, processing tools (lithic, bone, shell, tools) appear widespread in European contexts confirming the technological innovation of this period and the systematic use of ochre in human activities. Some examples are shell tools in Magdalenian rock art (Cuenca-Solana, *et al.*, 2013, 2016) and slabs, pestles and pebbles to process ochre from Epigravettian layers of Arene Candide (Granato, 2011).

Ochre residues can be found on hafted objects used as an ingredient for mastics and adhesive agents (Gibson et al., 2004; Wadley et al., 2004, 2009; Lombard, 2006; Pargeter, 2007; Soriano et al., 2009; Wadley, 2013).

At the same time, residues of ochre can also be observed on tools such as scrapers, burins, blades, on the active parts of these artefacts suggesting interpretations regarding a functional use of ochre. As for Combe-Grenal Mousterian scrapers (Beyries & Walter, 1996), from the Epigravettian site of Grotta Polesini (Venditti et al., 2016) or the ochre blades of the Capsian (Beyries, 1983).

*Personal ornaments on shells or organic hard materials (bones and teeth) with traces of red ochre are frequent. A category of findings that is emblematic of the emergence of human symbolism and that already appear towards the Middle Palaeolithic. Ochred shell beads of *Nassarius gibbolosus* were collected from the Middle Palaeolithic layers of Pigeon's Cave. Further, specimens of *Nassarius krassanius* from Blombos Cave were found in layers dating back to 75,600 uncal BP (Taborin 2003, d'Errico et al., 2005; Bouzouggar et al., 2007).*

The perforated teeth of deer, such as those from Grotte de l'Abbé in France, (Langley et al., 2015) and chamois, such as those from Praileaitz I, Basque Country-Spain (Sims, 2016), or even carp like those from Vlasac, Serbia (Cristiani et al., 2014) are particularly interesting for the category of ochre ornaments.

Red ochre residues can also be found on portable art objects like rounded anthropomorphic statuettes. Precious objects of an expressive phenomenon of prehistoric art such as the "*Figurine en ivoire à l'ocre rouge*" from the Grotta del Principe, Balzi Rossi, Italy (White & Bisson, 1998), the "*Dame à la capuche*" at Brassempouy, France, (Piette, 1894; White, 2006), the "*Venere di Savignano*" at

Savignano sul Panaro, Italy, (Mussi, 1996) or the “*Venus de Laussel*”, France (Lalanne, 1913) can be found.

In regards the presence of these residues, there are several interpretations: hematite to clean and refine the surfaces (Peyrony, 1930; White, 1992) or in Laussel’s case ochre with a symbolic-ritual value (Marshack, 1991, Petru, 2010).

Ochre pigments

Pigments are the most recurrent forms of ochre in archaeological contexts, especially in Upper Palaeolithic sites. Pigments proposed as ochre vestige are of some doubt when placing it in our inventory, but due to the importance and recurrence in the prehistoric record, it needs to be mentioned in this catalogue.

To better define ochre pigments, it needs to start from the presupposition that the iron-based pigments are inorganic and insoluble and highly stable. In most cases, it deals with more or less liquid solutions of pulverized ochre dispersed in a medium (liquid) to be laid out on a surface and coloured by overlapping and not penetrating. Thus, what is found in an archaeological context is a colourful surface.

By ignoring the expressive-figurative aspect of the applicative practice of ochre as a pigment, this category surely appears to be the most pleasant to the eye as well as the most attested in European context with a high concentration in Magdalenian sites in the Franco-Cantabrian region. More than 300 painted caves which not only represent a clear form of ochre but highlights the stylistic technology of Upper Palaeolithic human groups. In order to have a clearer idea, it need to think about the impressive paintings of Altamira (Cartailhac & Breuil, 1906) and Lascaux (Breuil, 1940), such beautiful treasures of humanity.

II.2. Objectives of study

The inventory of archaeological vestiges proposed here highlights the ubiquity of ochre by leading us to reflect on the fact that among the colouring materials available in nature, red ochre was the most exploited by prehistoric groups.

For sure, the most immediate response to this reflection could be the one that in nature, man spontaneously attributes a symbolic value to the red colour. Red is the colour of blood, love, passion, strength, life and rebirth. It is enough to consider the fact that the word *rubens* (red), in Latin, is synonymous of colour. But, what is the colour?

Generally, a colour appears like a physical trait of any element observed by the human eye, even if in a Newtonian perspective, colour is the product of a complex perceptive process of light between the eye and mind in which the first colour to be perceived is the red colour. This could explain the high recurrence of the red colour right from Prehistory. An intrinsic predilection to the human species right from his beginnings would have led man to the intense use of this colour which is available in nature, and as it has seen in the first chapter, under the form of iron ores.

However, the archaeological evidences not only attest the omnipresence of red ores but allows us to better understand how these make up a category of archaeological vestige that are potentially rich in value for past human cultures, and therefore worth studying to better understand the behaviours of humans that used them and the activities in which these pigments were used.

Based on current knowledge, thanks to those researchers who have dedicated themselves until today to the examination of ochre vestiges in Prehistoric sites, some unanalysed materials coming from Upper Palaeolithic and Mesolithic

sites can be taken into consideration and for which there is still a lot to investigate.

Thus, this work starts from the study of ochre specimens found in several sites located between the North of the Iberian Peninsula and the South of the Italian Peninsula with the aim of defining these materials and the human groups who produced them by trying to demonstrate the role and function of ochre for Palaeolithic and Mesolithic hunters-gatherers.

With the aim of constructing a valid reasoning in order to launch this research and to understand the key role of ochre reconstructing uses of this material, it will first clarify the motives which pushed them to elaborate this project.

The first objective of this work is that of determining the anthropic origin of the archaeological ochre remains in Prehistoric contexts chosen for this work and which will be described later. This aspect, as demonstrated by the previously information, reminds us that ochre can be used in several situations and contexts just like caves and shelters with archaeological deposits in which its presence could be accidental and not due to an anthropic approach.

After having established whether there is an anthropic origin of the materials, the second objective is that of establishing which raw colouring materials were exploited by Palaeolithic and Mesolithic hunters-gatherers and in what measure trying to recognize the human activities which pushed towards the symbolic use and in the daily life.

In addition, by taking the several properties of ochre into account such as its physical-chemical components which allows, even today, for a broad and diversified use, a further important aim is to better understand why such

colouring materials were chosen above others and how they were recovered, or rather according to which selective criteria and strategies.

The exploitation of raw materials is inevitably linked to another crucial objective of the research, in other words, identifying the supply sources and search for the provenance of raw materials.

Lastly, by supporting the hypothesis of the anthropic origin of vestiges in archaeological deposits, and thus the intentional human exploitation of ochre, the objective to achieve is to define the role played in the life of human groups of Upper Palaeolithic and Mesolithic through the study of its treatments and transformations to describe the use, economic management and cultural meaning.

In this sense, it therefore appears necessary to reflect on a methodological protocol which allows us to achieve these objectives through the study of ochre remains from sites of two different European regions, the Iberian and Italian peninsulas, which during the second Pleniglacial and the deep paleogeography changes were separated by natural barriers. This separation limited the contacts between human groups determining different adaptations and cultural local phenomena. To this end, a comparative study in a synchronic perspective is desirable to recognize cultural regionalization which involved south-western Europe about 20,000 years ago.

II.3. Evaluating methodological protocols

By starting from the presupposition that the archaeological remains provide concrete evidence of the anthropic exploitation of ochre, which, in light of the current research, appears to be a complex and diversified phenomenon, the

only knowledge of contexts and raw materials is not enough. It is fundamental to also investigate the technologies and working processes to better understand human behaviours involved in the ochre exploitation.

There are several aspects to evaluate. An analytical approach is needed that is both *integral* (overall evaluation of the phenomenon) and *integrated* (punctual investigation of the phenomenon in each of its aspect through the integration of methods and different techniques, but complementary between them).

To this end, a review of methods and techniques to study ochre is significant to choose a suitable methodology to pursue the main aims of this scientific research. A brief methodological discussion will be done to exploring “potentiality” and “limits” of analytical procedures.

II.3.1. Identification of raw materials

The identification of raw materials is based on visual criteria which evaluates colour, dimensions, mass, state of conservation allowing to determine the type of ochre.

Although it is not heavily emphasized among the analytical methods for a preliminary identification of raw materials, optical microscope allows to assess the main physical traits (colour, granulometry, mineral inclusions, superficial conditions) of ochres. Among the most traditional and easiest analytical tools, it provides a view in reflected light which produces a three-dimensional image just like in a direct view. An artificial light located at the bottom of the microscope makes it function based on reflection and refraction principles.

Through a condenser placed under the specimen, the beam of light is focused on the sample, into the lens, through the optic tube, up to the eyepiece. An adjustable dual lens system in the eyepiece allows for the zooming of the observed image.

The most recent applications of the optical microscope in the field of prehistoric archaeology (Wadley, 2005; Watts, 2010; Hodgskiss, 2010, 2013; Rosso *et al.*, 2014; Hayes *et al.*, 2017) demonstrate the efficacy of this tool alongside more modern and sophisticated analytical techniques.

Being a non-invasive and non-destructive technique, it is one of the most applied tools to preliminary investigate archaeological materials. Furthermore, it returns colour images, easy to use with immediate results and is also relatively inexpensive.

For a more accurate identification, the determination of the elemental composition (larger, smaller, traced chemical elements) through a geochemical characterization is fundamental. Analytical techniques such as SEM-EDS, X-Ray Fluorescence (XRF), X-Ray Diffractometry (XRD), Raman Spectroscopy and FT-IR allow to define the nature of materials by giving precise information on crystalline structure, chemical composition (qualitative-quantitative), as well as mineralogical properties (Clottes *et al.*, 1990; Menu & Walter, 1992; Hernanz *et al.*, 2009; Iriarte *et al.*, 2009; Menu, 2009; Seva Romàn *et al.*, 2009; Beck *et al.*, 2011; Jezequel *et al.*, 2011; Olivares *et al.*, 2013; Gay *et al.*, 2016).

The Scanning Electron Microscope (SEM) connected to an Energy Dispersive system (EDS) is a versatile and reliable technique to investigate the main chemical composition of ochres. This tool uses electrons as a source of radiation. In the Scanning Electron Microscope, the electron beam is not fixed, but is made to pass row by row in sequence on the sample in a rectangular area.

From the surface of the sample, the particles are emitted, and secondary electrons are captured by a special detector and converted into electrical impulses.

Therefore, the chemical analysis (microanalysis) is accomplished by measuring the energy and distribution of X ray intensity generated from the electronic beam on the sample by using Energy-dispersive X-ray Spectroscopy.

SEM-EDS systems combine morphological information captured from the Scanning Electron Microscope (SEM) with quantitative and qualitative data of the mineralogical composition through the X-ray spectrophotometer. In this way, it is possible to observe the distribution of elements present in the sample in function to the distance of the surface.

This technique is one of the largely used for compositional analyses (Hodgskiss, 2012; Dayet *et al.*, 2013, 2014) given the ease of sample preparation, as well as the non-destruction of materials, high level of zoom, high resolution power, broad field depth and immediate results on morphology samples and compositional structure. However, this tool provides just monochrome images detecting only major chemical elements.

The X-ray Fluorescence (XRF) is a non-destructive technique which determines the atomic species characterizing a surface. The interior electron orbitals of the atoms composing the elements are excited by X-ray and, when it returns to its fundamental state, it re-emits radiations with wave lengths which are characteristic for each element.

XRF also allow to detect minor chemical elements but does not provide indications on chemical compounds. The introduction of versatile and compact tools around the 1990's favoured the application of this technique in the study

of archaeological materials (Jercher *et al.*, 1998; Young, 2000; Popelka-Filcoff, *et al.*, 2007; d'Errico *et al.*, 2012; Moyo *et al.*, 2015, Seva Román *et al.*, 2015; Gay *et al.*, 2016). Portable XRF perform non-invasive and non-destructive analysis through direct tests on materials which returns reliable results in a few seconds detecting up to about 40 chemical elements.

X-Ray Diffraction (XRD) is a technique used for the qualitative and quantitative analysis of materials in crystalline, powder and solid forms. The instrumental set-up allows to register the X-radiations diffracted from crystalline materials with an ordered structure. Each material produces a diffraction spectrum which constitutes a “finger print” and thus makes it possible to identify an unknown material and compare it to the spectrum of other well-known materials.

X-Ray Diffraction is basically obtained like a “reflection” of an X-Ray beam from a family of parallel and equidistant atomic planes by following Bragg's law: when a beam of monochrome x-ray wavelengths (the wavelength of the radiation that is produced by an x-ray tube) is incident on a lattice plain with an angle, a diffraction is created if the path of the reflected rays from the following plains (with distance d) is a multiple of the wavelength. The study of the diffraction intensity at the various angles identifies the symmetries of crystal and the dimensions of its unitary cell. The use of this technique for the ochre study is fundamental given the possibility of recognizing specific chemical compositions and, at the same time, investigating the changes of the molecular structure following the exposure of the sample at elevated temperatures.

In recent years, XRD has been used on archaeological samples to test the hypotheses of heating transformations of yellow goethite into red hematite (Dayet, 2012; Cavallo *et al.*, 2015).

Raman spectroscopy is a technique used to determine the vibration frequencies of a molecule based on the interactions between the molecule itself and the radiation emitted from a laser beam. It is a non-invasive and non-destructive technique and requires small sample portions which do not need any preparation.

The sample is illuminated by a monochrome beam of photons with frequency ν_0 that can be partly absorbed and partly diffused. In case of absorption, a spectrum of infrared absorption will be obtained, while in the case of diffusion, a Raman spectrum will be obtained. From the interaction between the beam of photons and the vibrational motions of the irradiated molecules, it is possible to have the re-emission of a portion of the photons with a different wavelength from the incident one (greater or smaller). This process is defined as the “anelastic diffusion” and it is based on the so-called “Raman effect”.

In Raman spectroscopy, the quantitative aspect of the samples is scarcely considered. The most relevant will be given by the qualitative component of the sample. In recent years, this technique which is widely used for the study of pigment in general, has also been applied for the analysis of ferruginous pigments from prehistoric art contexts (Tournié *et al.*, 2010; Hernanz *et al.*, 2008, 2010; Goodall *et al.*, 2009; Erdogu & Ulubey, 2011).

The Fourier-Transform Infrared Spectroscopy (FT-IR) is a technique based on the absorption by organic and inorganic materials of infrared radiation. A component (spectrometry) focuses the infrared radiation on the sample to measure both the wavelengths absorbed from the material and the absorption intensity. A spectrum through a mathematical operation called Fourier-Transform is therefore produced. Spectra can give both qualitative and quantitative information. The wavelengths absorbed by the sample are

characteristic of the chemical groups present in the sample. The absorption intensity to a defined wavelength indicates the concentration of the chemical group responsible for the absorption.

One of the main disadvantages of this technique is the need to prepare the sample. The solid samples must be pulverized with a sterile agate mortar and mixed with potassium chloride powder (KCl) or Potassium bromide (KBr). Afterwards, the obtained compound is pressed with a suitable press to obtain tablets. The tablets are positioned into sample holders and placed inside the machine in which the light beam is conveyed onto the tablets. Generally, FT-IR is used for the analysis of organic materials, but it can also be used for inorganic materials. In regards ochres, this technique is often preferred to Raman for the more reliable results in the analysis of clay fractions (Cavalcante *et al.*, 2011; Hodgskiss, 2012; Moyo *et al.*, 2015).

The classification and characterization of colouring raw materials is essential to investigate cognitive capacities, or rather, to know processes and mental activities which allow prehistoric human groups to satisfy their physical and social needs in relation to the surrounding environment, as it allows us to know exactly which resources (raw materials) have been anthropically exploited and to provide the basis for distinguishing any selective human choices according to specific criteria. Furthermore, the identification of raw materials allows us to recognize any intentional mixtures by the presence of additives and inclusions in ochres compounds.

II.3.2. Provenance researches

Searching the original sources of archaeological ochres is another essential topic to better understand its anthropic exploitation. Researches that try to find original sources of archaeological ochres (Iriarte *et al.*, 2009; Attard Montalto *et al.*, 2012; Bonneau *et al.*, 2012; Mathis *et al.*, 2014; Cavallo *et al.*, 2015; Dayet *et al.*, 2015; Goemaere *et al.*, 2016) start with the application of analytical protocols validated by Glascock & Neff (2003), Popelka-Filcoff *et al.*, (2007) and Erlandson *et al.*, (1999) based on the measurement of major and minor chemical elements, as well as in traces, of archaeological ochres as opposed to geomaterials collected from geological sources to recognize intra/inter source variations establishing chemical patterns or “fingerprints” of ochres.

These methodological approaches involve the use of invasive techniques such as INAA (Instrumental Neutron Activation Analysis), XRF (X-Ray Fluorescence), PIXE (Particle-Induced X-Ray Emission or Proton-Induced X-Ray Emission), ICP-MS (Inductively Coupled Plasma Mass Spectrometry) that offer clear and certain data.

However, the mineralogical variability inside the same geological formation have a considerable reach and can make it impossible, or almost impossible, to find correspondence with the archaeological materials. This condition can be further limited if it considers the potential variation, over time, of the geological formations and the lack of punctual mineralogical references for ochre deposits. It is desirable to focus these types of studies on well know and geologically defined areas.

In any case, provenance studies are based on the principle of comparing physical-chemical traits of archaeological ochre with geological samples taken from quarries which are identified as potential ancient supply sources.

There are not fixed criteria to recognize original geological sources, but it is necessary to satisfy the postulate of provenance.

In the field of archaeological sciences, it is possible to recognize the origin of an archaeological material based on its geochemical traits (fingerprints) that are specific to each source from which the raw materials were taken. In this sense, it is important that the geological samples have not suffered any type of contamination after being extracted, to conserve the original traits of geological provenance.

Regarding provenance research of archaeological ochres and the leading role taken by the solid and valid methodologies of Glascock & Neff (2013) and Popelka-Filcoff *et al.* (2007) and Erlandson *et al.*, (1999), the analytical techniques used are PIXE, INAA, ICP-MS and XRF. Although, these are invasive and destructive, and they can limit the application on archaeological materials.

The PIXE technique which was introduced around 1970 (Johansson *et al.*, 1970), uses a proton beam with an intensity equal to a few MeV. From the clash of protons with atoms that compose the sample, indirectly X-Ray waves with typical wavelengths of elements composing the bombed sample area are emitted with a proportional intensity to the concentration of chemical elements. This non-invasive and non-destructive technique for samples allows to recognize major and minor elements, even if it is only applicable on a very thin sample. For this reason, PIXE analysis is often applied in association with other techniques:

- PIGE (Proton Induced Gamma-Ray Emission) uses a protonic beam which directly hits the nucleus of the atoms of the sample in the investigated area and thus determines reactions which bring about the emission of γ rays, which when analysed, give the elemental composition of the sample.
- RBS (Rutherford Backscattering Spectroscopy) uses a He⁺ ion beam in which a small portion is backscattered due to the ion-nucleus smashing of the atoms of the sample. By analysing the energy of the backscattered ions, it is possible to determine the elemental composition of the sample.
- Nevertheless, the PIXE technique is largely applied in archaeometric studies for the analysis of ochres and pigments (Erlandson *et al.*, 1999; Popelka-Filcoff, 2006; Beck *et al.*, 2011, 2012; Lebon *et al.*, 2014).

The Neutron Activation Analysis (NAA), introduced in 1936 by G.C. de Hevesey and H. Levi is a technique where the induced radioactivity allows us to have qualitative and quantitative information on the chemical composition of a sample. The NAA uses a source of thermal neutrons which bombard the sample thus causing the formation of radioactive isotopes. Knowing the radioactive emissions and the forms of radioactive decay of elements and analysing the radiation emitted by the sample, it is possible to determine the specific concentration of the elements. This technique does not require the destruction of the sample and it is generally use for provenance studies (Glascock & Neff, 2003; Popelka-Filcoff *et al.*, 2007).

The Inductively Coupled Plasma Mass Spectrometry (ICP-MS) and the Inductively Coupled Plasma–Optical Emission Spectrometry are two very similar techniques in that they both use a plasma as a source of atomization and excitement, even if the ICP-MS is more sensitive. These techniques provide

elemental and isotopic analysis of the samples and are currently under experimentation for provenance studies coupled to NAA and XRF (Desaulty *et al.*, 2008; Iriarte *et al.*, 2009; Attard Montalto *et al.*, 2012; Dayet *et al.*, 2015).

Over the years, provenance studies increased in this sense. Experiments on non-invasive and non-destructive techniques are preferred in order to reduce the loss of archaeological materials as much as possible which, for ethical reasons, must be preserved. An example worth mentioning is the study conducted by Beck *et al.*, (2011) regarding the provenance research of prehistoric pigments from Grotte du Renne, in Arcy-sur-Cure, France (38,000–34,000 BP) by external PIXE technique.

Searching the provenance of archaeological ochres and investigating potential original sources, may allow us to evaluate human mobility patterns for the procurement of raw materials and, at the same time, selection criteria of sources and the degree of accessibility to the resources. Furthermore, the identification of original sources allows us to reflect on possible symbolic-ritual choices of geological formations considering the "landscape" not as a physical place or pure container, but as a space in continuous construction, an "open construction site" in which cultural identities are defined (Dei, 2004; Ceccarini, 2014) and which reflects the social structure of prehistoric groups.

II.3.4. Treatments and transformations

Another fundamental step of the research is reconstructing anthropic treatments and transformation of ochres. In this sense, the interpretation of use wear traces and signs and the morphological analysis of the materials, as well as the study of the intrinsic changes to materials like the crystalline structure

and chemical composition, represents the main point to start off to recognize potential modification by humans.

Generally, ochres can be susceptible to two main types of anthropic transformations: *mechanical* and *chemical*. The mechanical ones determine changes in the morphology and the surfaces of the pieces while the chemical ones, like heat treatment, determine the alterations of the crystalline structure.

In regards the mechanical transformation, the macro-microscopic observation of the surfaces represents a means to recognize superficial diagnostic traces to distinguish an anthropic transformation from taphonomical modification.

However, knowledge does not pass only from the direct observation of archaeological vestiges but, also from the full comprehension of technological and symbolic variables that may influence this phenomenon. For this reason, an accurate evaluation of the relations between the ochre vestiges and the other archaeological materials in the deposit can complete the study in this sense.

In regards the chemical transformations, the heat treatment, or simply put, the heating of the yellow ochre (goethite) to a temperature beyond 300° brings about the creation of hematite (red ochre). The same is true if goethite is exposed to high temperatures as it recrystallizes into hematite (Cornell & Schwertmann, 2004). The detection of the structural anomalies in archaeological ochre with specific methods like X-Ray Diffractometry, Raman Spectroscopy and Transmission Electron Microscope (TEM) can help us understand whether red ochre found in one site is the product of heating of goethite (Pomiès, 1997, 2000; Pomiès *et al.*, 1998; Baffier *et al.*, 1999; Salomon, 2009; d'Errico *et al.*, 2010; Gialanella *et al.*, 2011).

X-Ray Diffractometry, one of the first methods used to detect thermal treatments, is based on the evaluation of the thickness of some significant peaks in the spectrum on the detection of maghemite that is an indicator of heating (Onoratini, 1985; Pomiès, 1997). This tool can be joined to the Transmission Electron Microscope (TEM) to evaluate the porosity of the crystalline structure. Hematite obtained by heating goethite has pores among the crystals (Pomiès, 1997, 2000; Pomiès *et al.*, 1998; Baffier *et al.*, 1999; San Juan, 2005; Salomon, 2009; d'Errico *et al.*, 2010).

On the other hand, the Raman spectroscopy is based on the evaluation of bands. Hematite deriving from heating at high temperatures has a spectrum with very broad bands and an accessory band positioned at 657 cm^{-1} (de Faria & Lopes, 2007). This technique can be used in addition to the previous ones used to give a more complete picture (Gialanella *et al.*, 2011). In any case, heating of ochre can be intentional or accidental and even though these methods offer reliable data on heat transformation, they do not confirm the human intentions of this transformation.

II.3.5. Balance of methods

The methodological review carried out here allows us to reflect on the methods and techniques to choose for this study to develop a valid methodological protocol. In this sense, based on materials and available resources, a preliminary test will be conducted with a set of objectives in mind: test the generally used techniques for ochre analysis establishing what are the most suitable ones to satisfy the objectives of this research; evaluate the feasibility of

the analyses based on the instrumental set-up, timing and coating; determine statistical methods for data processing to provenance studies.

II.4. Assessing a methodological protocol

The lack of a unique methodological approach accepted by the scientific community requires evaluating the most suitable techniques to investigate archaeological ochres through a preliminary test. During the general assessment of materials, several reflections were made on the better ways of studying ochres.

After estimating a series of possible methodologies, it was decided to test some analytical techniques on a small sample in order to explore their efficacy. Several tools such as the binocular optical microscope, SEM-EDS, XRF, XRD, FT-IR and Raman Spectroscopy were chosen to investigate morphometrical and morphological traits (superficial physical features), crystalline structure, elemental (major and minor elements) and molecular composition (chemical compounds) of samples.

This test is developed in five steps:

1. selection of materials;
2. application of analytical techniques and data collection;
3. statistical processing of data;
4. evaluation of results;
5. definition of the methodological protocol.

This test is particularly important for establishing the right investigative path to follow, especially in view of the numerous methods for characterizing raw materials and search their origin.

II.4.1. Selection of materials

The first step is the selection of samples to test. By keeping in mind, one of main objectives of this work, it was decided to use specimens from two prehistoric sites of Los Canes and Arangas (Asturias, Spain) that returned considerable materials. A total of 12 samples from Los Canes and 13 samples from Arangas were selected.

Additionally, 16 geological samples which were extracted from geological sources around the sites were chosen as comparative materials for provenance purposes (Tab.II.1).

The sampling of geomaterials involved two distinct areas, one about 200 m from the caves (*Arangas-source 1* and *Arangas-source-2*) and another on the coast, about 20 km (*Acantilado*). The samples were preliminarily tested to verify the geochemical reliability.

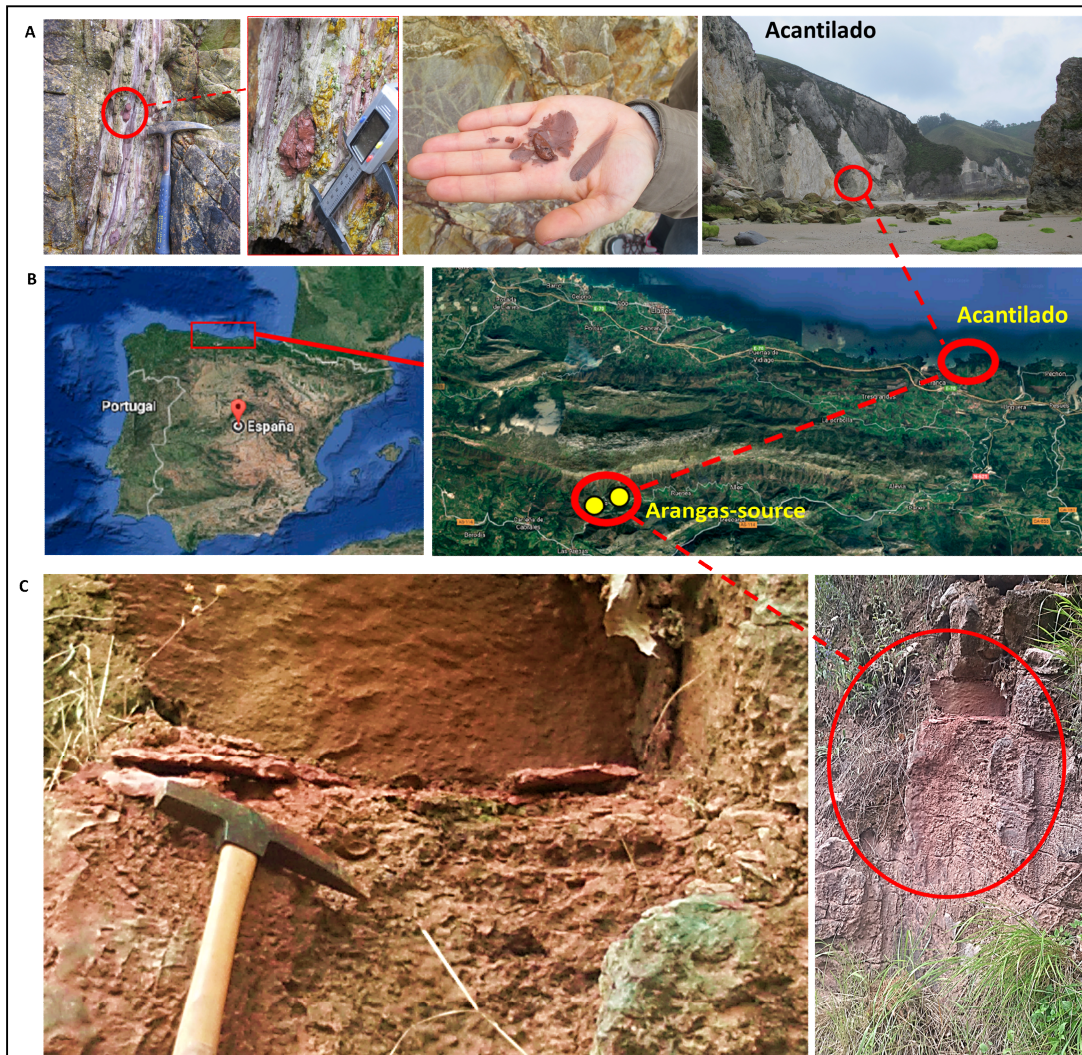


Fig.II.1.: Geographical position of geological samples (b) near the coast (a) and near the archaeological sites (c).

Site	ID Sample	Cultural Attribution	Colour (Munsell Soil Color Chart)
Los Canes	5p	Solutrean	2.5Y 6/8
Los Canes	3b	Solutrean	10R 4/4
Los Canes	14a	Upper Magdalenian	10R 4/4
Los Canes	35e	Upper Magdalenian	10R 4/6
Los Canes	20a	Upper Magdalenian	2.5Y 6/8
Los Canes	80b	Azilian	10R 4/3
Los Canes	79b	Azilian	10YR 7/8
Los Canes	76b	Azilian	7.5YR 5/8
Los Canes	133a	Mesolithic	2.5YR 6/8
Los Canes	464a	Mesolithic	10R 4/6
Los Canes	469d	Mesolithic	10R 4/8
Los Canes	326b	Mesolithic	10YR 8/8
Arangas	1a	Magdalenian	10R 3/4
Arangas	119a	Magdalenian	10R 4/6
Arangas	83a	Magdalenian	10R 3/6
Arangas	47d	Lower Magdalenian	10R 4/8
Arangas	20a	Lower Magdalenian	10R 4/4
Arangas	147a	Azilian	10R 4/6
Arangas	98d	Azilian	10R 4/4
Arangas	104a	Azilian	10R 4/3
Arangas	106b I	Azilian	10R 4/2
Arangas	133c	Mesolithic	10R 4/8
Arangas	122b	Mesolithic	2.5YR 4/3
Arangas	133b	Mesolithic	10R 4/4
Arangas	124a	Mesolithic	2.5YR 4/1

Tab.II.1.: List of archaeological samples from Palaeolithic and Mesolithic units of Los Canes and Arangas used for the preliminary test.

II.4.2. Application of analytical techniques and data collection

The second step consists on testing the techniques chosen after the previous review. In this way, the following methodological approach was carried out:

- Surface analysis by binocular optical microscope and SEM-EDS;
- Powder analysis by FT-IR, XRF and XRD.

Regarding the characterization of raw materials, the use of binocular optical microscope and SEM-EDS has been chosen for their non-invasive application. These techniques are complementary amongst them in that they allow us to obtain valid data on morphological features (binocular optical microscope), elemental composition and crystalline structure (SEM-EDS). However, the binocular optical microscope is also a useful tool for micro-topographical analysis to investigate signs and traces which may suggest specific anthropic treatments and transformations of ochre.

For what concern Fourier-transform infrared spectroscopy (FT-IR), a series of probes was executed to verify the effectiveness of the instrumental set-up on inorganic materials. The disappointing results from the measurements carried out on red and yellow ochres left no choice to abandon this technique.

The XRD was chosen to detect chemical compounds. This technique provides detailed and accurate information, but the available instrumentation brought about a partial destruction of the sample, pulverized. So, the XRD was used just for a minimum of representative samples.

The XRF was fundamental for this research. As previously mentioned, it is difficult to accurately establish an effective method for provenance studies. Based on the available resources and the accessibility of instruments, XRF was

used for provenance purposes. Although fully aware that there are some limits relating to detection of trace elements, this tool was chosen for practical issues as well as for the readiness of data and for the easy interpretation of results. It is therefore worth highlighting that the obtained results are part of a preliminary framework of research that will be the subject of a continuous study in the future.

In summary, the following methodological protocol for the preliminary test was applied.

Binocular optical microscope

Superficial observation by optical microscope was developed by taking notes of the general state of conservation, colour, dimensions and mass of samples and evaluating the physical structure (mineral inclusions) in order to classify raw materials. A stereoZoom Leica S8 APO, fully apochromatic stereomicroscope with 8:1 zoom, 300 Lp/mm resolution and peerless 70 μm depth of field, was used to observe physical traits.

All information obtained by microscopic analysis were annotated in a specific database that will be described in the chapter dedicated to the evaluation of materials. Concerning the colour recognized by optical observation of surfaces, it was preliminary codified by *Munsell Soil Color Chart*, even if the use of these tables posed some problems for our materials that show a different colour on the surface compared to the one internally visible through fractures. For this reason, the colours of the materials were indicated on the basis of a visual perception approximating all the nuances for large categories of colour: red and yellow.

Los Canes samples appear like small pieces and a wide range of colour from deep red to yellow. Optical observation reveals the presence of quartz grains and black shining plaquette of mica in a compact structure.

For Arangas samples, the superficial observation revealed a heterogeneous surface with quartz (grains) and mica (black shining plaquette) typically associated with ochres (Fig.II.2).

Scanning Electron Microscope

The Scanning Electron Microscope with an energy dispersive X-ray microanalysis (SEM-EDS) was carried out to inspect the crystalline structure and to determine the major element content of each sample. A Carl Zeiss, EVO MA15, microscope with an electronic probe for microanalysis has been used to analyse the quantitative and qualitative composition of archaeological samples. The Scanning Electron Microscope provided backscattered images where areas with intense brightness (light grey) correspond to Fe concentrations,

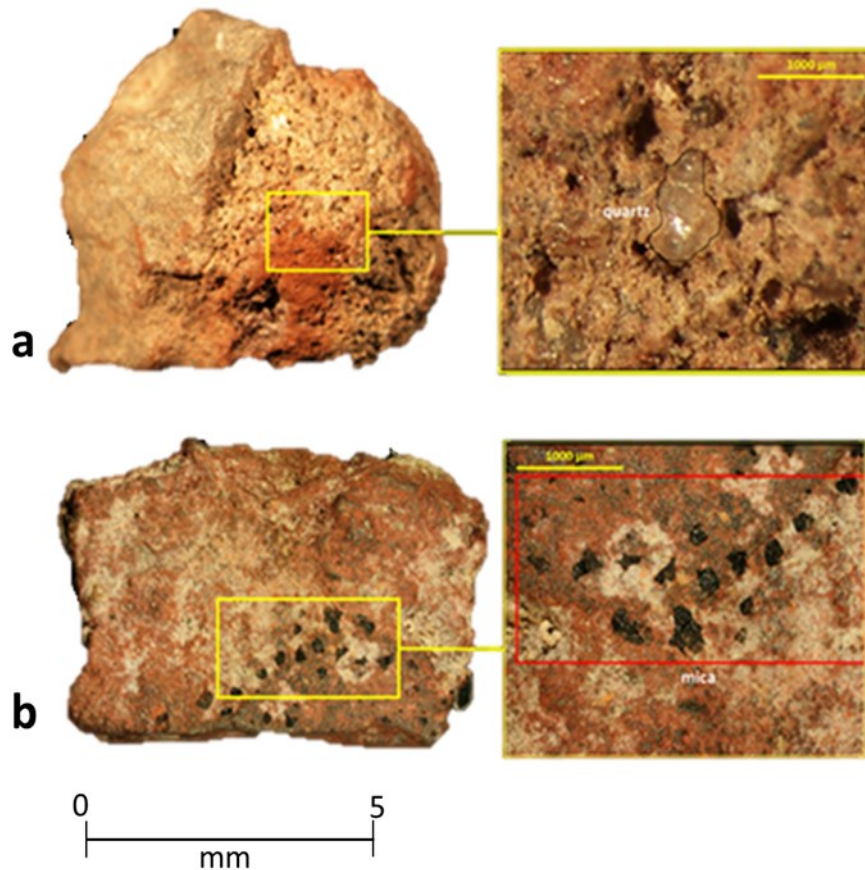


Fig.II.2.: Image of mineral inclusions in Arangas ochre samples: a) n.119a-grain quartz; b) n.133b-mica.

while areas with less intense brightness (dark grey) correspond to significant percentages of Si, with quite high percentages of Al and Ca, and smaller percentages of P, Mg, K (Fig.II.3).

The analysis shows a peculiar micro-structure depending on the raw material: yellow and red ochres.

The Scanning Electron Microscope (SEM) highlights two distinct types of micro-structures, depending on the arrangement of crystals: finely grained structure with nanocrystals organized in micro granular accumulation and laminar

oriented structure with pseudo-hexagonal laminar nanocrystals arranged according to the typical iron oxide structure.

The red ochres are characterized by crystals in thin tablet form arranged in a fine clayey fraction, representative of typical Iron oxides crystalline aggregations. The primary constituents identify are Fe-Al-Si follow by small percentages of K, P, Mg, Mn (Fig.II.4).

The yellow ochres (Fig.II.4) have small acicular particles organized in overlapped fibrous agglomerates on quartz grains, a common mineral habitus of goethite. Semi-quantitative analysis with EDS of yellow ochres confirm the presence in similar percentages of Si-Al-Fe-Ca-K-P for Los Canes. The association of these elements suggest that the yellow pigmentation is mainly due to the presence of iron hydroxides (goethite: α -FeO(OH)). Even if, the detection of S (Sulphur) in association with O-Fe-K-S refers to the presence of sulfates of potassium and iron such as yellow Jarosite ($\text{KFe}_3\text{3(OH)}_6(\text{SO}_4)_2$).

X-Ray Powder Diffraction (XRD)

Mineral compounds were detected by X-Ray Powder Diffraction. The spectra were obtained on a Bruker D8 Advance X-ray Diffractometer, with $\text{CuK}\alpha$ radiation (40 kV, 40 mA). The configuration used is a set of fixed windows with 1 min of divergence and 1 min of anti-divergence with a scintillation counter. Previously, two samples were powdered in an agate mortar and put into a conventional sample holder in an elevated temperature chamber.

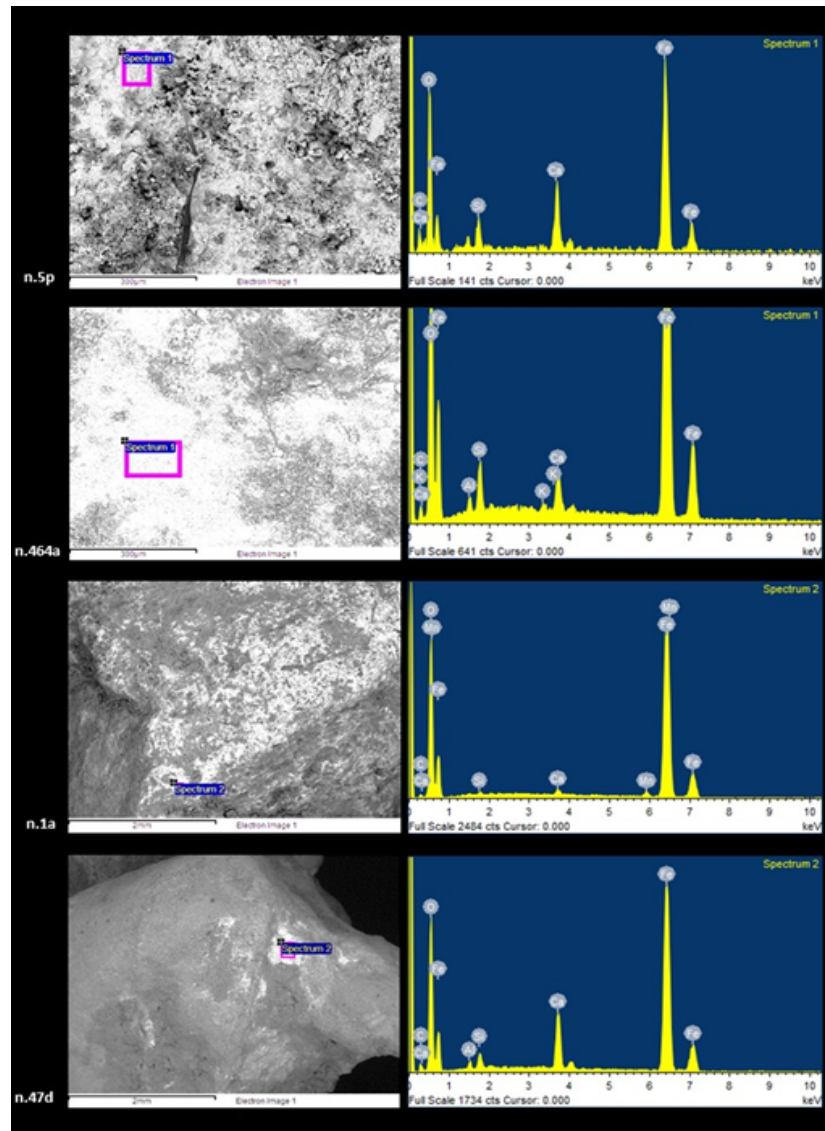


Fig.II.3.: Backscattered images of ochre from Los Canes and Arangas obtained by SEM-EDS: the collected spectra on more intense light grey areas report Fe high concentrations

The spectrum was collected with angles 2Θ between 10° and 70° ($\Delta 2\Theta = 0.02^\circ$) at room temperature, with an integration time of 10s per step. Spectrum analysis was performed by visual inspection by comparing the spectra of the JPDFS tables (simultaneous position and relative intensities of the peaks), using the EVA program supplied by Bruker. This program gives simple corrections of

experimental data and briefly estimates the percentage of each phase in the sample

The XRD data confirm that the most recognized mineral phase is the goethite (Fig.II.6). In one sample (N.326B), jarosite and potassium oxide were detected. These results justify the presence of Sulphur and potassium detected by EDS (N.79B).

What should be noted is that not all categories of pigments (yellow-red) was analysed by XRD. Due to the complete destruction of the archaeological sample and the execution costs and times, it was decided to analyse four yellow fragments with the aim of recognizing specific mineral phases responsible for this coloration and, at the same time, to investigate the nature of Sulphur traces in association with potassium and iron detected by EDS system.

The XRD spectra of two Arangas samples (Fig.II.5) confirm the presence of hematite as the main reason behind the red shades of ochres. Hematite is the main mineral phase detected and in one case, it has been associated with larnite, a calcium silicate, (N.1A) while in another case, with magnetite, an iron oxide (N.20A).

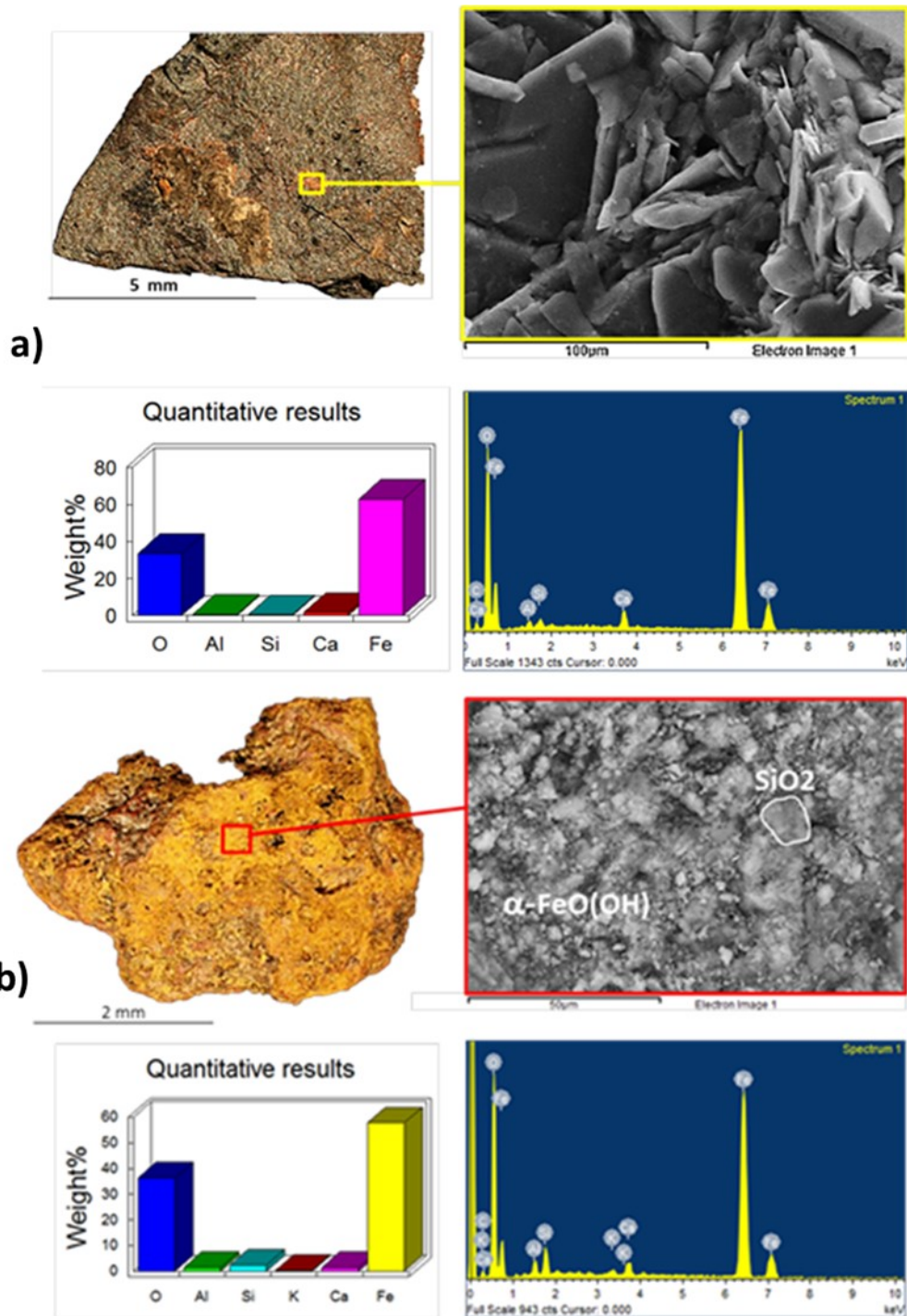


Fig.II.4.: Red ochre a) and yellow ochre b) samples from Los Canes analysed by SEM-EDS showing the crystalline structure and quantitative composition with major elements.

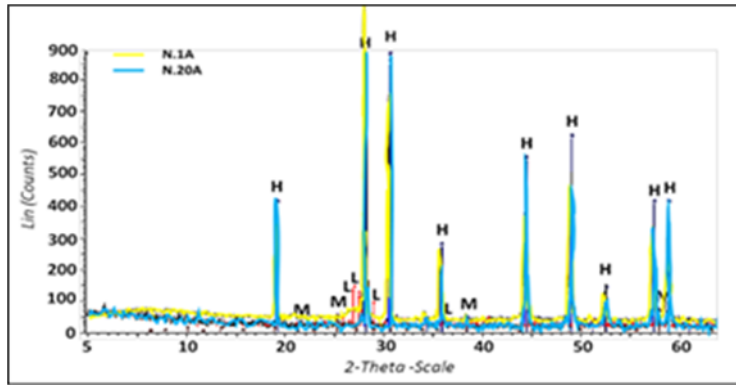


Fig.II.5.: Overlapped XRD spectra of red ochres from Arangas (n.1a-n.20a): H (hematite); L (larnite); M (magnetite).

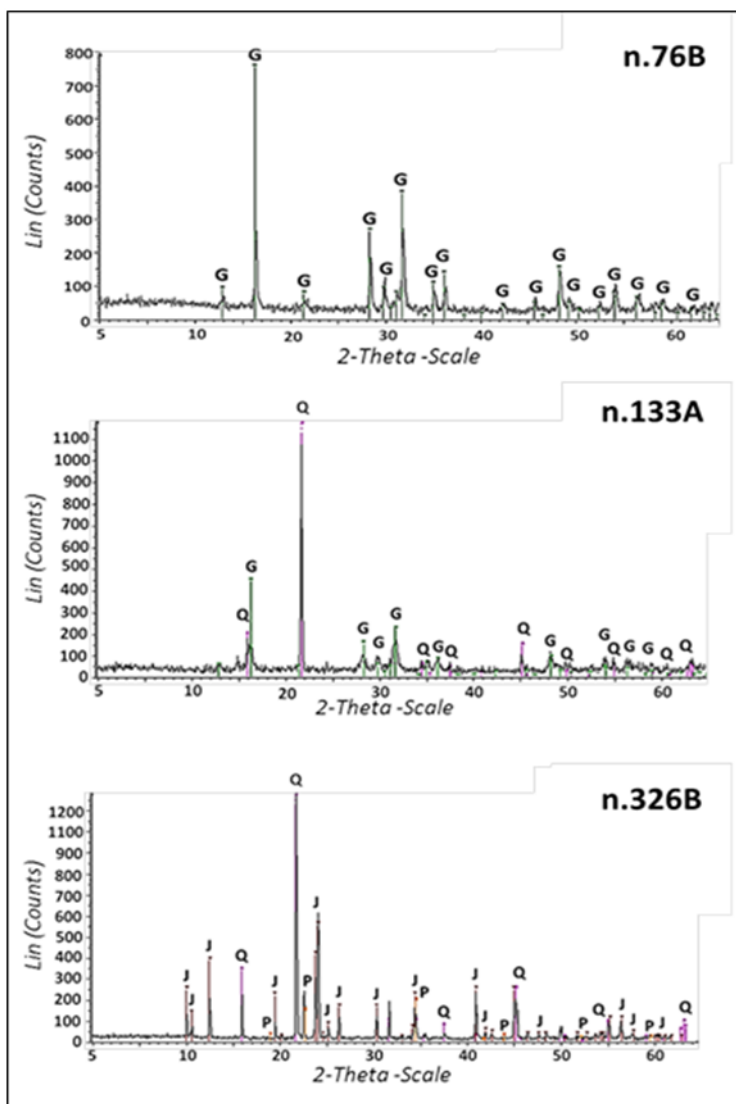


Fig.II.6.: XRD spectra of Los Canes yellow ochres reporting the main chemical compounds: Q (quartz); G (goethite); J (jarosite); P (potassium oxide).

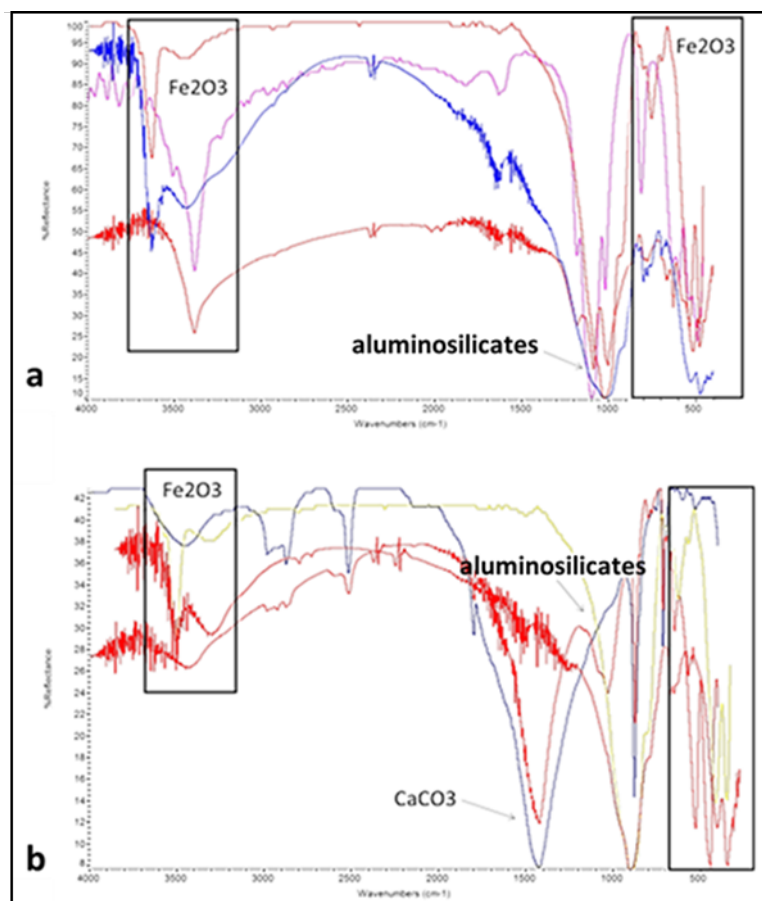


Fig.II.7.: FT-IR spectra of yellow ochres (a) and red ochres (b) from Arangas.

Fourier Transformed IR Spectroscopy (FT-IR)

Some powdered samples previously analysed by XRD and XRF have been used for Fourier Transformed IR Spectroscopy (FT-IR). The ochre powder has been mixed with potassium bromide and then pressed into tablets. The tablets have been analysed into a THERMO-NICOLET-670. The spectra have been captured with a resolution of 0.09 cm⁻¹ and 32 scans per spectrum. The FT-IR has been preliminarily tested on 4 Arangas ochre samples, two yellow ones and two red ones.

The spectrum of yellow ochres (N.10E; N.33A) reports intense peaks around ~500 cm⁻¹ and at ~3.500 cm⁻¹ representative of iron oxides (Fe₂O₃). Intense peaks also appear in the region of aluminosilicates, at ~1000 cm⁻¹. The peaks around ~1500 cm⁻¹ are attributable to carbonate calcium (CaO₃). For the red ochres (N.130; N.33A), it is possible to recognize weak peaks at ~3.500 cm⁻¹ and intense peaks at ~500 cm⁻¹ of the iron oxides and peaks at ~1000 cm⁻¹ of aluminosilicates.

Correlation with Fe	All samples	Los Canes	Acantilado	Arangas	source	Arangas
<i>Si</i>	-0,79485	-0,51151	-0,86805	-0,67628		-0,36538
<i>Al</i>	-0,62447	-0,3879	-0,53349	0,58315		-0,36332
<i>Fe</i>	1	1	1	1		1
<i>K</i>	-0,63453	-0,39134	-0,57806	0,89086		-0,26134
<i>Mg</i>	-0,51256	0,03465	-0,42697	0,91433		-0,55576
<i>Ti</i>	-0,70044	-0,48639	-0,62314	0,79177		-0,17487
<i>Ca</i>	-0,16857	-0,47996	0,73807	0,09277		-0,92723
<i>P</i>	0,14252	-0,28307	0,05077	0,87491		0,04283
<i>Cu</i>	0,45453	0,25334	0,46841	-0,70504		0,01114
<i>Mn</i>	-0,15288	-0,40553	0,0159	-0,12832		-0,27802
<i>V</i>	0,22351	0,07783	0,93961	0,73265		0,37857
<i>Zn</i>	0,40352	0,2597	0,68972	0,497		0,10118
<i>Rb</i>	-0,59132	-0,51455	-0,65967	0,99383		--
<i>Cl</i>	-0,03957	0,09973	0,66737	-0,79119		0,39974
<i>Zr</i>	-0,51313	-0,50546	-0,50275	0,2829		0,98198
<i>Cr</i>	0,03295	-0,25202	0,15029	0,45162		--
<i>La</i>	-0,34307	-0,62358	-0,4115	0,82301		-0,94424
<i>Sr</i>	-0,38665	-0,41319	-0,59617	0,89191		-0,11623
<i>Ar</i>	0,13019	-0,03268	-0,3876	-0,98686		0,09356
<i>Sn</i>	0,57089	0,33787	0,34549	-0,40122		0,17248
<i>S</i>	-0,03277	-0,20339	-0,09671	-0,411		-0,73353
<i>Ba</i>	-0,4649	-0,23656	-0,98593	0,10127		--
<i>Ga</i>	-0,66771	-0,96841	-0,89867	0,07801		--
<i>Pb</i>	0,46006	0,56678	0,86495	-0,76907		0,32597
<i>Co</i>	0,70145	0,73122	0,8512	0,83163		0,08748

Ni	0,42491	0,34853	0,8705	0,83971	0,16503
Ir	0,8701	0,98858	0,29878	0,69053	--
As	0,32476	-0,07085	0,94714	0,87075	--
Pu	0,76392	-0,00376	1	--	--
Se	0,44977	0,88839	0,74562	-1	--
Y	0,26149	-0,6307	0,55053	0,52576	1
Sc	-0,1822	-0,4249	0,23814	-0,60772	--
Nd	-0,05177	--	0,35943	0,78012	--
Ce	-0,66086	0,12428	-0,76029	1	--
Sb	0,55546	0,60369	0,91293	1	0,38628
Rh	0,68966	0,93971	--	--	--
Br	0,54746	-0,7017	0,55727	--	1
U	1	--	--	--	--
Ta	0,57288	0,28146	0,87259	-0,97043	1
W	0,34114	0,37173	0,2998	-0,59528	--
Ge	0,29779	0,35236	0,14918	-0,9384	--
Os	0,05709	-0,64835	1	-1	--
Mo	0,43948	0,60241	-0,65443	--	--
Pt	0,40174	0,2325	-0,35784	--	--
Hg	0,56464	0,312	0,86866	-1	--
Hf	-1	-0,45249	--	1	--
Bi	-0,19954	-1	0,19826	--	--
Nb	-0,65411	-0,04593	-0,77686	0,49569	--
Re	0,20374	0,51572	0,68773	1	--
Au	0,41997	0,52296	-1	--	--
Tl	0,52966	1	0,14639	--	--
Am	0,40007	0,19027	0,21137	1	--
I	0,31302	--	0,76754	--	--
Cs	1	0,53276	--	--	--
Th	0,52231	--	--	1	--
Yb	0,63089	--	0,55015	1	--

Tab.II.2.: Pearson correlation coefficients calculated on the samples selected to perform a preliminary test (correlation is significant at the 0,05 level).

XRF and statistical data treatments

X-Ray Fluorescence was chosen for the elemental analysis of archaeological ochres and comparative geological samples. This technique was tested on the previously selected ochre archaeological samples, as opposed to the 16 geological samples (tot.4-*Arangas-source I*, tot.1-*Arangas-source II*; tot.5-*Acantilado I*; tot.5-*Acantilado II*; tot.1-*Acantilado III*¹). The choice to use only red ochre samples for provenance purposes is due to the richness in red ochre of the archaeological assemblages and for the geological formations found during our surveys that revealed the presence of hematite quarry sites near the sites and in the coastal areas at a maximum distance of about 30 km. Not one goethite ochre source was recognized.

The analysis was carried out with the instruments provided by SERCAMAT laboratory at the University of Cantabria, Santander (Spain). Data was statistically processed to recognize significant elemental concentrations among the archaeological samples and geomaterials. Using multivariate statistical analysis, according to the criteria established by Popelka-Filcoff *et al.* (2007; 2008), it is possible to reflect on percentages of major and minor elements in samples, investigating which elements guide the variance in comparison to the others. Based on the significant relationships between the elements, it was possible to observe the distribution of samples on a plot graph to discriminate intra-source and inter-source variations. Therefore, the preliminary test was carried out to verify the validity of the criteria established in literature, given the assumption that inter-source and intra-source variations can be defined by

¹ The names *Acantilado I*; *Acantilado II* and *Acantilado III* are used in this preliminary phase to distinguish the samples collected from three different points in the same geological formation.

the correlation of minor elements with a dominant element which is Fe (iron) in ochres. Positive and negative correlations are estimating through the Pearson's test. All those elements that correlate to Fe have been selected as these elements are associated to the mineral phases of ochres which depend on the provenance geological sources. The element ratio values, plotted in log-10, were considered for statistical purposes.

As Iron is the most representative chemical element in ochres and the element with the most content detected in archaeological samples, the comparison of Fe with other major elements usually associated in archaeological ochres such as Si, Al, Ca with those of geological samples, allow us to appreciate significant trends that show preliminary inter-group variations. The most different trends are noted by the percentages related to Fe. High archaeological Fe values do not correspond to those from the *Arangas-source* (1-2) and *Acantilado*. Fe is always the most representative element, but with a lower percentage. In this case, a comparable situation occurs with Ca-Si-Al, just like for Fe, which report lower values.

A Pearson's test (Tab.II.2) was conducted on selected samples for the preliminary test. This statistical test calculates the correlation coefficient that ranges between -1 (negative correlation) and 1 (positive correlation). Based on this assumption, Pearson's test confirms that significant elements correlated with Fe are: Si, Al, K, Mg, Ti, Ca, Cu, V, Zn, Rb, Cl, Zr, La, Ar, S, Sn, Pb, Co, Ni, Ir, As, Sb, Br, Ta, Hg, Nb, Ba, Ce. A preliminary Principal Component Analysis (PCA) was carried out to determine which variables guide the variance but due to the high number of missing values of minor elements, a new PCA was conducted.

This Principal Component Analysis was performed by using those elements highly correlated with Fe: Al, Si, Fe, K, Mg, Mn, Ca, Cu, V, Zn, Cl, Sn, Pb, Sb, Ni, As. PCA excluding those elements that, even if they show strong correlations with Fe, they report a high number of missing values which invalidate the result.

From a total of 16 variables, the main components from 1 to 6 explain 100% of the variance, but as is known in literature, there are some specific elements that substitute Fe III oxide in the ochres characterizing single sources, despite the weathering and several potential contamination phenomena (Cornell and Schwertmann, 2004; Popelka-Filcoff *et al.*, 2008). Based on the results of this first PCA, another PCA test was carried out to extract significant variables that may well-identify an intra-source variation. The analysis was repeated using these variables: Al, Fe, K, V, Mn, As, Cu, Zn, Ti, Sb. The second PCA shows that all components 1-10 achieve 100%, with a higher incidence of components 1-4 that describe the 75.28% of the variance. The PCA graph shows that the elements with the longest vectors drive the samples into the space with a preliminary distribution per source. These elements were plotted in several combinations in a bivariate graph to recognize specific groups of samples per source.

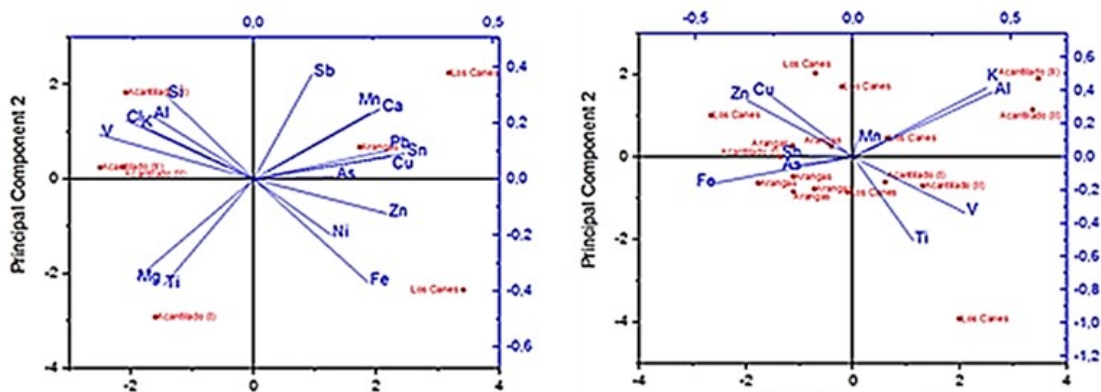


Fig.II.8.: Bivariate loading plots of Principal Component Analysis performed with sample of Los Canes, Arangas, Acantilado (I-II-III) and Arangas source (1-2).

It was decided to start with two elements commonly used in intra-sources discriminations, As and Sb to test the samples (Smith *et al.*, 1998; Popelka-Filcoff *et al.*, 2007; Attard Montalto, 2012; Dayet *et al.*, 2015).

In this plot, Los Canes and Arangas ellipses intersect between them, including all samples of both sites except in one case. Within this intersected part, it is possible to distinguish *Acantilado I* samples that are grouped into a single smallest ellipse inside the Los Canes-Arangas intersection.

The $\log_{10} (\text{Sb}/\text{Fe})$ vs. $\log_{10} (\text{As}/\text{Fe})$ exclude samples of *Arangas-source 2* and *Acantilado II* because they do not have antimony (Sb) and arsenic (As) respectively. In addition, the Sb and As relationship with Fe does not allow for a clear separation of *Acantilado III* and *Arangas-source I*, both represented by a single sample (Fig.II.9).

Arangas-source I and *Acantilado I* appear well distinguished in $\log_{10} (\text{Mn}/\text{Fe})$ vs. $\log_{10} (\text{As}/\text{Fe})$. In this bivariate plot, it is possible to clearly appreciate samples of grouping per source. The samples of Los Canes and Arangas are distributed in the same confidence ellipse where one sample of *Acantilado II* is also present (Fig.II.10).

On the other hand, the bivariate plot of As and Al with Fe shows a greater dispersion of the archaeological samples that can be partially associated with the *Acantilado I* group, which is distinguishable in the overall context. (Fig.II.11).

Outside each confident ellipse, the *Arangas-source I* in $\log_{10} (\text{K}/\text{Fe})$ vs. $\log_{10} (\text{As}/\text{Fe})$ is confirmed like the first two examples of the bivariate plot. In addition, the Los Canes and Arangas intersection, with a slight variation from previous attempts, is characterized by the presence of some samples of both archaeological sites.

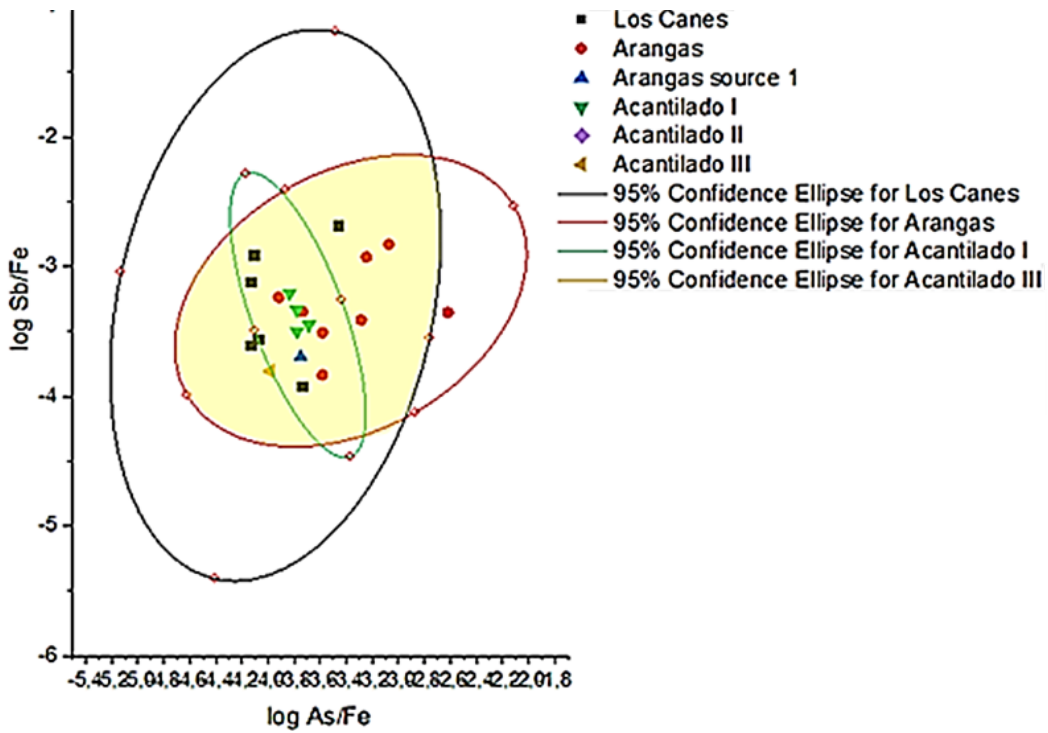


Fig.II.9.: $\log_{10}(\text{Sb}/\text{Fe})$ vs. $\log_{10}(\text{As}/\text{Fe})$ with confidence ellipse of 95%.

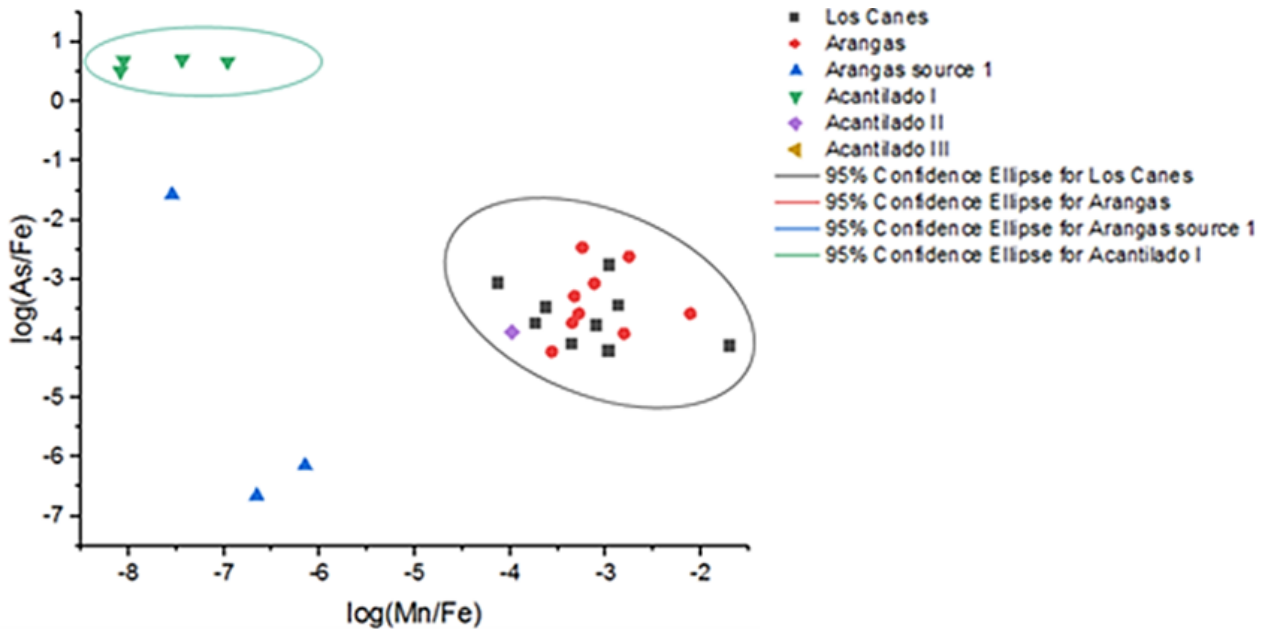


Fig.II.10.: $\log_{10}(\text{Mn}/\text{Fe})$ vs. $\log_{10}(\text{As}/\text{Fe})$ with confidence ellipse of 95%.

A separated portion of Los Canes samples are not part of the intersection area with Arangas and are embedded into *Acantilado I* confidence ellipse that extends externally to Los Canes-Arangas area, but still inside Los Canes ellipse which also includes the *Arangas-source II* and *Acantilado III* (Fig.II.12).

However, plotting As and V with Fe, the Los Canes-Arangas intersection is confirmed and *Acantilado I* appears partially included in this area with just one sample. On the outside of the intersection, but always inside the *Acantilado I*, are located *Arangas-source II* and *Acantilado III*. Outside the *Acantilado I* ellipse there is represented *Arangas-source I*, which is part of the Los Canes ellipse (Fig.II.13).

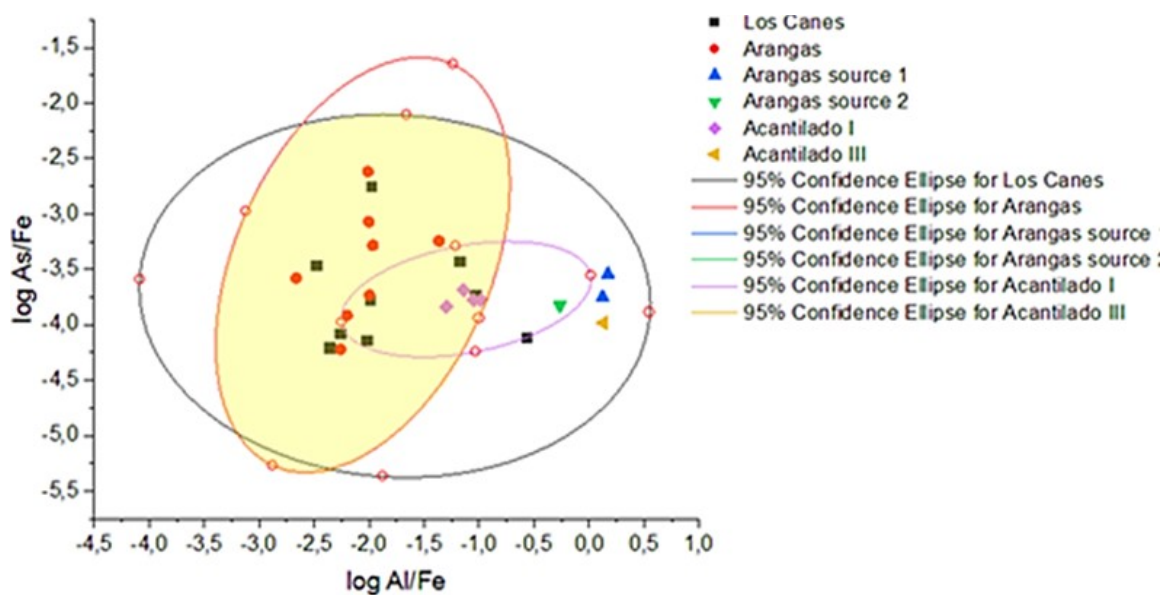


Fig.II.11.: $\log_{10}(As/Fe)$ vs. $\log_{10}(Al/Fe)$ with confidence ellipse of 95%.

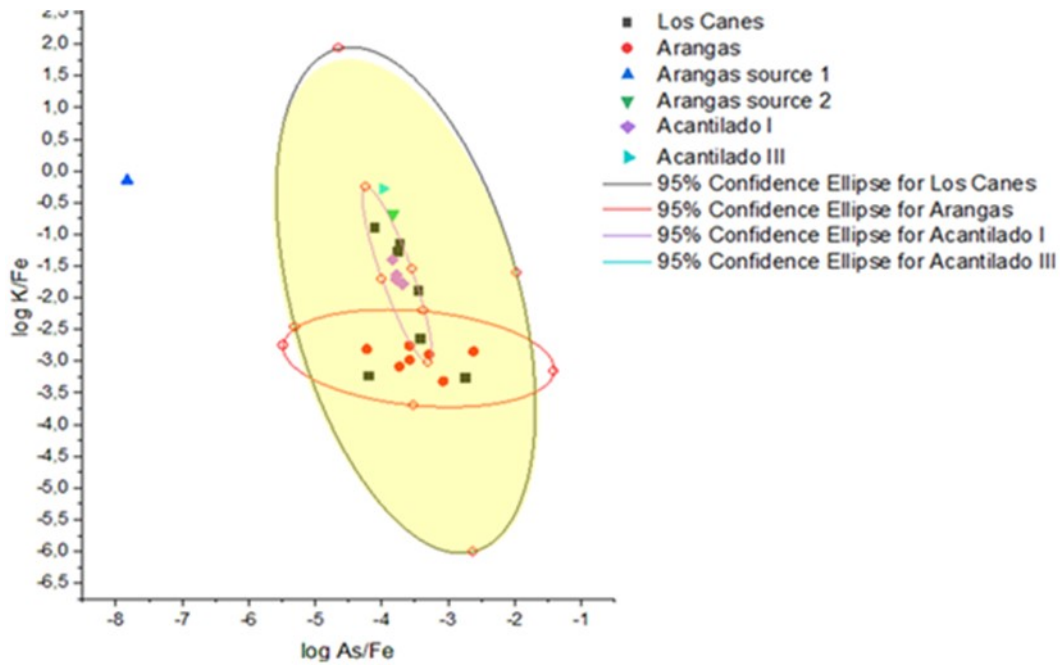


Fig.II.12.: $\log_{10}(K/Fe)$ vs. $\log_{10}(As/Fe)$ with confidence ellipse of 95%.

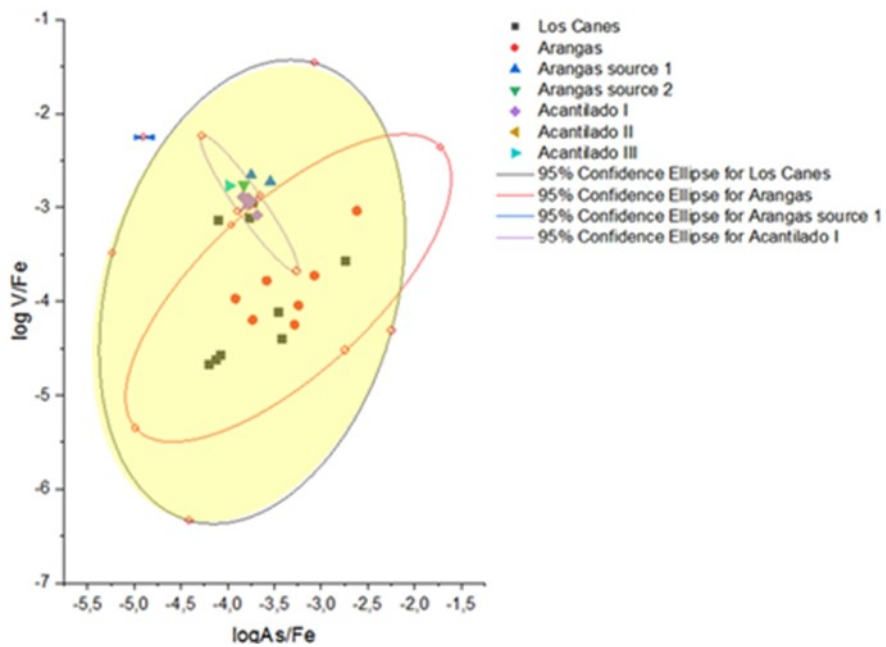


Fig.II.13.: $\log_{10}(V/Fe)$ vs. $\log_{10}(Al/Fe)$ with confidence ellipse of 95%.

II.4.3. Data processing and evaluation of the methods

Performing a preliminary test proved to be fundamental in correctly assessing the extent of estimating the analytical conditions and to choose the most appropriate methods to characterize archaeological raw materials. In this regard, it is necessary to discuss the techniques implemented, as well as the analysis conditions.

Raw materials and treatments

Macro-microscopic observation with naked eye and Binocular Optical Microscope (StereoZoom Leica S8 APO) allow us to investigate colour, mineral inclusions and surfaces of samples. The estimation of colour, and mineral inclusions seem to be crucial criteria to classify ochres. Furthermore, the use of the binocular optical microscope has been fundamental to catalogue diagnostic signs and traces on surfaces.

The SEM-EDS system tested to investigate the chemical composition of ochres, confirms the usefulness of this technique to analyze crystalline structure, mineral inclusions and major mineral phases. In fact, SEM-EDS yields digital images in which the different intensity of colors, in grayscale, corresponds to the X-Ray intensity of each chemical element directly proportional to the quantity of the same element present in the sample. These “digital maps” are the result of the presence of specific elements, in percentage. By analyzing these major chemical elements that constituent the archaeological ochres, it is possible to recognize the main mineral phases such as aluminosilicates, oxides and hydroxides.

X-Ray Diffractometry performed on representative ochre samples, confirms the presence of hematite, as the main compound of red ochre, and goethite with traces of jarosite for yellow ochres. At this stage of research, this technique is complementary to Optical Microscope and SEM-EDS system. However, XRD is a useful technique to investigate mineral phases, above all, to detect mineral phases in trace.

Data obtained with FT-IR is not satisfactory for characterizing inorganic pigments. The response of archaeological ochres to infrared radiation is weak and the spectra are not easy to interpret. In this case, the FT-IR did not give further information to XRD. As shown by the spectra, significant peaks appear in the region of aluminosilicates and iron oxides, but it is not easy to discriminate specific mineral phases to discriminate yellow ochres from red ones. It is possible to observe the same values when comparing the spectra of yellow with the red specimens. It appears that the FT-IR technique does not seem to distinguish between the mineral phases of hematite and goethite which are well identified by XRD.

Provenance Research

XRF data processing by statistical tests such as Pearson's test, Principal Component Analysis and bivariate plots have been used to verify the degree of correspondences between archaeological ochres and geomaterials. Pearson's test demonstrates that several elements correlate with Fe. Some of these elements are fundamental to the ion exchange processes of ochre formation, such as: Al, K, Mn, Cu, V, Pb, Sb, As.

PCA confirms that these elements, including Fe, drive the covariance in the ochre groups and highlights a preliminary distribution of samples in the space of graph. These trends in PCA plots give data on geochemical fingerprints of ochres and on provenance sources. As expected, the elements with the longest vectors that pull the samples with a similar chemical composition in the same direction are: Fe, As (*Arangas*); Sb (*Acantilado I*); Zn, Cu, Mn, Ti (*Los Canes*); K, Al, V (*Acantilado II, Acantilado III*). As was previously described, these elements, plotted in pairs in log₁₀, reveal a potential matching between Los Canes and Arangas in all combinations. The scatter plots of log₁₀(Sb/Fe) vs. log₁₀(As/Fe), log₁₀(As/Fe) vs. log₁₀(Al/Fe) log₁₀(K/Fe) vs. log₁₀(As/Fe) show that archaeological ochres exhibit a clear correspondence. However, these ratios do not allow to geochemically discriminate ochre sources (geological and archaeological). Therefore, the log₁₀(Mn/Fe) vs. log₁₀ (As/Fe) appear to be the key ratio to distinguish intra-source variations. A high discrimination of samples for mineral groups is highlighted when plotting Mn and As with Fe.

II.4.4. Definition of methodological protocol

Based on the obtained data by the preliminary test, the following methodological protocol was elaborated:

- Identification of raw materials: Binocular optical microscope, SEM-EDS, XRD;
- Provenance research: XRF and statistical methods (PCA, Pearson's test, Biplot and Scatter plot);
- Treatment and transformations: Macroscopic observation by naked eye and microscopic observation through the binocular optical microscope.

The use of binocular optical microscope allows us to discriminate raw materials by physical traits such as colour recognizing two main classes: red ochre and yellow ochre. Also, the presence of inclusion and the evaluation of the degree of compactness of the mass can be used as distinctive criteria. Furthermore, the inspection of surfaces by binocular optical microscope allows us to recognize diagnostic traces and to reason on the study of use wear traces. The chemical characterization by SEM-EDS confirms the preliminary distinction made through the microscopic observation on surfaces. Regarding the use of SEM-EDS, this technique not only recognizes the major chemical elements, but also allows us to investigate the arrangement and the morphology of crystals which constitute the microstructure of ochres. Regarding XRF, this technique establishes the percentage content of chemical elements from Magnesium to Uranium. The statistical processing of data allows us to recognize intra and inter source variations discriminating archaeological ochres and geological samples by the ratios in log₁₀ of pair elements.

To sum up, the execution of a preliminary test was fundamental in setting up the methodological protocol for this study. By starting from the methods and techniques already validated by others and tested on our materials to view the efficacy based on the prefixed objectives, it has been decided to utilize these tools:

- Binocular optical microscope;
- SEM-EDS;
- XRD;
- XRF.

The variety of methods chosen reflects the multiplicity of the aspects to investigate as well as the complexity of the anthropic exploitation phenomenon of ochre in prehistoric times.

II.5. Spatial analysis

The spatial analysis of materials was carried out to obtain further information starting from the distribution of ochre vestiges *in situ* in association with significant elements in the archaeological context (ochre lenses in soil, hearths, burials and other structures, concentration of archaeological remains, etc....).

The main purpose of spatial analysis is to interpret the spatial distribution of a series of points plotted in a space. The points represent the archaeological vestiges and the space is the archaeological site.

The objects can have a random distribution or regular and uniform distribution. Also, they can show a specific concentration such as a clustered distribution (Renfrew & Bahn, 1995).

In order to verify the spatial distribution of ochre vestiges studied for this research, a reflection on the spatial distribution of objects in site was carried out starting from the information collected by the general assessment of the materials.

In general, most of the objects have not the specific coordinates X, Y, Z. But, these objects just have the indication of the square and, in some cases of the sector of recovery.

The absence of detailed coordinates is due to the fact that most of the materials were collected by sieving the sediment and not from an exact point of the

archaeological surface. For this reason, the spatial analysis will be realized by constructing concentration maps of the total mass (gr) of ochre collected from squares of each stratigraphic unit. The quantitative distribution will be indicated on a site-map using a colour scale, according to mass of ochre graphically represented.

For this purpose, the excavation grid will be used in which the dimensions of each square are 1m x 1m in all sites analysed. Each square, in turn, is divided into 4 quadrants (north, south, east, west), each of 50 cm x 50 cm.

The ochre mass was considered through horizontal spatial distribution, so the quantities will be indicated with shades of colours on the background plan. The obtained maps will be reported to highlight concentrations in relation to any areas of the archaeological surface.

Chapter III.

General framework: sites and sampling conditions

The richness of the archaeological record for the Upper Palaeolithic and Mesolithic draws the attention on two main scenarios of the cultural fragmentation that Europe experienced during the geographical changes after the climatic phenomena of the second Würmian Pleniglacial.

Approximately 22,000 years ago, an intense freeze caused the geographical isolation of human groups breaking the cultural unit which characterized the previous phase, the Gravettian. Natural barriers hindered the relations among human groups. The Alpine arc became insurmountable impeding human networks between Central and Southern Europe. A progressive regionalization brought about the formation of two distinct cultural areas in the Franco-Iberian region and the Mediterranean one. In the Franco-Iberian region, the Gravettian culture was followed by Solutrean and Magdalenian which enclosed the Upper Palaeolithic. In the Mediterranean region (from Provence to the Black sea, including the Italian Peninsula) the Epigravettian culture was developed which lasted throughout the Late Glacial phase. Around 11,700 cal BP, the beginning of the Holocene and the progressive changing of climatic and environmental conditions favoured the adaptation of human groups who went towards a new European cultural phase, the Mesolithic (Mussi, 2002; Martini, 2008).

III.1. The Cantabrian region

III.1.1. Solutrean

Around 22,000 cal BP, a sudden climatic deterioration corresponding to the II Pleniglacial undermined the Gravettian *koiné*, which characterized whole Europe between 28-23,000 cal BP.

Generally, the mean density of the European population decreased, and some groups disappeared totally, while others remained confined in refuged areas like the Franco-Cantabrian region. This area persisted isolated experiencing a peculiar human culture: the Solutrean.

The Solutrean which was later the Gravettian in the chrono-cultural periodization of the Upper Palaeolithic, was characterized by characteristic “foliate” lithic tools. These artefacts were obtained through face plane retouching executed with pressure on lithic surfaces. The term Solutrean was coined by G. De Mortillet (1873) based on the findings in the *Solutré* site (Bourgogne, France) and was generally divided into:

1. *Proto-Solutrean*: points à *face plane* retouched only in dorsal part;
2. *Lower Solutrean*: points à *face plane* retouched in dorsal and ventral part;
3. *Middle Solutrean*: Solutrean laurel-leaf points with a flat bifacial retouch;
4. *Upper Solutrean*: Solutrean willow-leaf points with a flat bifacial retouch.

The origin of the Solutrean still needs to be clarified. In any case, during its middle phase, the Solutrean penetrated in the Iberian territories. There, the human groups carriers of this culture adapted to the steppe environments developing local tendencies.

The archaeological evidence in the sites of Las Caldas, Cueto de La Mina and Cueva del Castillo (Jordá Cerdá, 1960, 1963; Smith 1966, Corchón, 1971, 1981; Straus, 1975, 1983, 2000; Aura, 2012) testify:

- Production of medium-large sized flint artefacts and the presence of typical laurel-leaf points (Middle Solutrean);
- Production of smaller sized quartzite artefacts with the presence of backed blades/bladelets, laurel-leaf points, concave base points and shoulders (Upper Solutrean);
- Progressive reduction of typical Solutrean industries and increase in the use of quartzite (Final Solutrean).

In the Cantabrian region, the Solutrean hunter-gatherers progressively integrated themselves within the environment living in caves and hunting medium and large sized herbivores like oxen, reindeers, horses, ibexes, chamois, roe deer, deer, wild boar (Andres-Herrero *et al.*, 2017) with retouched flint artefacts and, then, in quartzite from local sources.

Regarding the symbolic dimension, the use of colouring materials is attested (red ochre) to paint signs and points, animal silhouettes and hand-stencils on cave walls like La Riera, El Chufín, Altamira, El Castillo (Bicho *et al.*, 2007; Pike *et al.*, 2012). A phenomenon that was largely expressed in the Magdalenian culture (González Sainz & Utrilla, 2005; Aura *et al.*, 2012).

III.1.2. Magdalenian

The progressive climatic improvements which alternated between the deep freeze of the Ancient Dryas are reflected in a new human expansion in Central-

Western Europe. The progressive abandonment of the Solutrean practices was followed by an innovative culture: the Magdalenian. The term Magdalenian is related to the discoveries in the French site of La Madeleine (Perigord, France) excavated by E. Lartet in 1863.

The Magdalenian hunter-gatherers adapted themselves to different environmental and climatic conditions by developing new strategies of subsistence and supplying of resources. Combined with the hunt of medium sized herbivores, the hunt of small mammals appeared. Fishing activities were intensified.

Lithic and bone tools were produced for these activities like geometrics, spears, toothed harpoons, propellers and perforated batons decorated with animal motifs. The typing of these objects initially allowed to recognize the evolution from Magdalenian I to Magdalenian VI in the French areas (Breuil, 1912).

In the Northern Iberian Peninsula, some regional phenomena defined variations of the Magdalenian culture, the so called "Cantabrico" (Utrilla, 1996; González Sainz & Utrilla, 2005):

- *Initial/Lower Magdalenian* (20,000/19,000 cal BP): large flakes, denticules, notches, sidescrapers, choppers, ("archaic" tool types) on local raw materials such as mudstone, quartzite, limestone and poor-quality chert, few backed bladelets, bone and antler artefacts (needles);
- *Middle Magdalenian* (17,500/16,200 cal BP): portable art objects such as proto-harpoons and *contours découpés* which attested connections to the French Pyrenees;
- *Upper/Final Magdalenian* (16,200/16,000 cal BP-14,800 cal BP): backed blades/bladelets, backed micro-points, end-scrapers, knives, perforators

and burins, “archaic” tool types on locally non-flint raw materials, harpoons (mainly unilateral), needles and decorated bone/antler tools (wands, spatulas, *bâtons de commandement*).

Nevertheless, this regional specialization in the first half of the Cantabrian Magdalenian (Early and Lower Magdalenian) seems like a “local” phenomenon while in the second half (Middle and Upper Magdalenian), it appears like a broader phenomenon where cultural contacts are recognized inside the Franco-Iberian region.

The Magdalenian is characterized by the abundance of artistic productions (painted caves and portable art) in which the use of colouring materials (red/yellow ochre, black manganese, black charcoal) takes on a key role in the symbolism of hunter-gatherers in both the artistic and funerary dimension (Bicho *et al.*, 2007; Straus & González Morales, 2012; Pérez Iglesias, 2012-2013).

III.1.3. Azilian

Approximately 13,700 cal BP, during the climatic improvement (Alleröd) after the deep freeze of the Younger Dryas, a change in lifestyles of human groups were reflected in the progressive reduction of the Magdalenian phenomenon and in the appearance of a new cultural system, the Azilian.

This new cultural system characterized western Europe until the end of the Pleistocene.

The Azilian was identified by E. Piette at the site of Mas d’Azil (France) in 1889 and is distinguished by the definition of the new economic-social order;

technological changes, reduced communication among human groups and greater variability and specialization of subsistence activities.

In the Cantabrian region, the Azilian experienced an initial phase (Ancient Azilian) during the microlithic artefacts, already attested in the Final Magdalenian, increased. Also, flat bone antler with carved teeth directly from the same part of the piece appeared. In full Azilian phase, (Classic Azilian) acquired an oval hole in the central part. Such artefacts were functional for hunting deer, boars and birds, fishing and gathering molluscs.

A huge reduction in the artistic manifestations marked this stage. Cave art became a rare phenomenon and the artistic production appeared to be limited to the creation of harpoons with geometric decorations.

Decorated pebbles spread with decorative patterns made with points and lines in red and black pigments, start from the Classic Azilian (Straus, 2005; Fernández-Tresguerres, 2006).

III.1.4. Mesolithic

The end of the Pleistocene determined the progressive closure with the Palaeolithic dimension and the beginning of new cultural systems. The Holocene warming transformed the Cantabrian region in terms of environment and climate conditions (11,700-7,400 cal BP).

Mixed deciduous woods (Harrison & Digerfeldt, 1993) inhabited by animal species like small mammals, rodents, birds and small and medium sized herbivores (roe deer, chamois, deer, wild boar) replaced the steppes and open areas in the previous phases.

The new faunistic assemblage involves the construction of innovative hunting equipment in which the projectile points disappear and geometric microliths appear on rods for light and functional weapons to hunt animals of smaller size. This renewal also covers other aspects of subsistence such as fishing.

The progressive abandonment of harpoons in bone and horn suitable for fishing in impetuous rivers, allowed the production of slightly arched and thin weapons for fishing. Nevertheless, the exploitation of malacological resources (molluscs and terrestrial and aquatic gastropods) marked an essential change in the subsistence of Mesolithic groups.

This change was an essential trait of the human groups which occupied the Cantabrian region in this phase, and especially those in the western part (Asturias) which is also distinguished by technologies. In fact, the presence of picks in the Asturian territory at the beginning of the Cantabrian Mesolithic is peculiar and thus would identify the Asturian (Vega del Sella, 1923) between the human cultures of the Initial Holocene. The *picos asturienses* are unifacial artefacts on flattened pebbles with a rounded cortical base and a pointed apical part and would have been used for the supply of molluscs (Vega del Sella, 1923) to open the sea urchins (Madariaga, 1976) or to dig the land superficially in order to look for edible roots (Jordá Cerdá, 1970; Pérez Pérez, 1999). These interpretations are still doubtful, but it is also true that the presence of these artefact identifies a precise space-temporal dimension by configuring itself as one of the main features of the Cantabrian Mesolithic.

Several practices of manipulating the body defuncts marked the Mesolithic. Caves and rock-shelters were perfect location to made burials in oval pits where the dead were positioned with several ornamental elements which expressed the artistic dimension of the Mesolithic hunter-gatherers.

The phenomenon of parietal art that characterized the Upper Palaeolithic was almost finished. The artistic sense of human groups was expressed by personal ornaments mostly on shells.

The internal circulation of these objects attested a social interaction at short distance and a high territoriality of the Mesolithic groups as opposed to the high Palaeolithic mobility (Fano, 2004, Arias *et al.*, 2009).

III.2. The Italian Peninsula

III.2.1. Epigravettian

In parallel with the Solutrean in central-western Europe, Mediterranean Europe experienced the development of an emblematic cultural phenomenon of the human groups which persisted on the southern part of the alpine arc during the II Pleniglacial phase.

After the break of the Gravettian *koiné*, the Italian Peninsula persisted geographically and culturally isolated. The alpine arc was impenetrable, and the only possible contacts were on the west side with Provence (France), and on the east side with the Balkans.

So, the human groups in this part of the European continent moved towards a different cultural dimension which took the name of Epigravettian.

The Epigravettian was conventionally divided according to the classification of G. Laplace (1964, 1966) in:

- *Ancient Epigravettian* (21,000-16,000 cal BP) characterized by elements deriving from the Gravettian due to the lack of burins of Noailles and the presence of *pointe à face plane* and *cran* points in the final phase;
- *Advanced Epigravettian* (16,000-14,500 cal BP) as a transitional phase marked by truncations, backed points, longed scrapers, tendency towards a certain microlithism, progressive disappearance of *cran* points and diffusion of geometrics only in Tyrrhenian territories;
- *Final Epigravettian* (14,500-10,500 cal BP), a phase characterized by regionalization of lithics complexes.

Nevertheless, several issues persist in the taxonomy of this human culture. After the studies conducted by A. Palma di Cesnola (1983), as far as the Italic Epigravettian is concerned, the Laplacian periodization was further studied by A. Broglio (1997, 1998) who, based on the chrono-climatic elements, divided the Epigravettian into:

- *Ancient Epigravettian*: lithic complexes of the II Pleniglacial within two cultural *facies*, one with *pointe à face plane* and another one with *cran* points which were already spread all over Liguria (Cave of the Arene Candide), Veneto (Grotta di Paina) and later in the Southern territories of the Peninsula (Broglio, 1997, 1998). The origins of the two *facies* would need to be searched in central-eastern Europe where similar elements were found towards 23,000 cal BP;
- *Recent Epigravettian*: lithic complexes of the Late Glacial correlated to the Azilian phenomena to the end of the Late Palaeolithic in north-eastern Europe and Atlantic-western Europe. There were several innovative elements like the increase in curved backed blade knives, the decrease of *gravettes* and

microgravettes, the spread of backed bladelets, shorter scrapers and microburins for geometric productions.

Although the problem in defining the chrono-cultural limits of the Italic Epigravettian persist, generally it is possible to note that this phenomenon embraced the whole of Mediterranean Europe from Provence to the Balkans, with evident local specializations in the lithic production, but a certain homogeneity in the funerary rituals (burial bodies in a supine position, in a closed pit with blocks of stone and grave goods as personal ornaments and red ochre) and in the visual art with zoomorphic profiles, phytomorphic and geometric motifs both engraved and painted with red ochre (Martini, 2006, 2008, 2016).

III.2.2. Mesolithic

Generally, the Italian Peninsula between 11,700 cal BP (end of the Würm III) and 7,400 cal BP experienced a deep change which largely affected the European territory after the improvement in climate and the variation of the environmental conditions.

The human groups reacted implementing innovative economic-social and cultural behaviours. In this framework, the main cultural *facies* were the Sauveterrian and Castelnovian.

The Sauveterrian (Pre-Boreal/Boral: 10,300-7,765 cal BP) was identified by Coulonges (1930) based on microlithic tools (triangles, segments, backed bladelets, relatively circular scrapers, *sauveterrian points* with one or double backed bladelets) is the cultural expression of the hunter-gatherers who occupied these territories after the retreating of the glaciers.

The Sauveterrian groups of Northern Italy occupied the piedmont areas with a seasonal nomadism based on the availability of the resources (Broglia & Lanzinger, 1990). This settlement was also reflected near the Tuscan-Emilian Apennines where not only was there seasonal nomadism, but human groups tended to live continuously in camps in the plains near sources of water (Martini & Tozzi, 1996; Martini, 2008).

In central-southern Italy, the use of caves and shelters next to open sites was also a strategy adopted by hunter-gatherers in the internal territories. Compared to the intense exploitation of malacological resources which identified the Mesolithic groups of the Cantabrian region, in the Italian Peninsula the hunt for small and medium sized herbivores like deer, ibex, chamois, roe deer, wild boar, birds and small mammals was the main subsistence strategy (Martini, 2008) integrated by fish and collection of molluscs (Wierer & Boscato, 2006; Bisegna *et al.*, 2011). The production of triangular microlithics, especially scalene, segments, backed bladelets, relatively circular scrapers, *sauveterrian* blades (micro lithic, symmetrical armor, with one or two backs worked by retouching) increased as functional tools to hunt medium and large sized animals.

The Castelnovian (Atlantic: 7,960-6,500 cal BP), recognized by M. Escalon de Fonton (1966, 1967, 1968) was based on the production of trapezium microliths, especially rectangles, isosceles and scalene in the site of Châteauneuf-Les-Martigues (Bouches-du-Rhône) in France.

Next to the alpine arc, the Castelnovian groups continued to go down towards the valleys due to the progressive expansion of the forested area in the highlands (Fontana, 1997), while they continued to occupy hilly areas in the Venetian plains (Broglia & Lanzinger, 1990) and mountainous areas in the

Apennine arc (Martini, 2008). Generally, the lifestyles of the Castelnovian groups was not so different by the Sauveterrian, but peculiarities appear in the lithic production, as the replacement of triangular with trapezoidal armour (Dalmeri *et al.*, 2002).

Nevertheless, the cultural framework of the Mesolithic in the Italian Peninsula appears just as complex and diversified. Next to the *facies* of the Sauveterrian and Castelnovian, an undifferentiated Epipaleolithic deriving from the evolution of the latest cultural complexes of the Final Epigravettian was found in Sicily and the Tyrrhenian part (Martini, 1993) with evident comparisons between Northern Sardinia and Southern Corsica.

Although Sicily remained fully in the Epigravettian phenomenon during the Upper Palaeolithic, towards the end of the Pleistocene, the local specializations determined the disappearance of geometric microliths in the Final Sicilian Epigravettian and the evolution of cultural local complexes (Aranguren & Revedin, 1996). The Mesolithic hunter-gatherers that occupied Sicily during the Initial Holocene followed the typical adaptations of the European Mesolithic with local ones: on the western side, Sauveterrian influxes were found while at the same time on the eastern part emerged an undifferentiated Epipaleolithic (Martini, 1993) that arrive up to the area which includes northern Sardinia and southern Corsica. The Holocene population of these territories is connected to the presence of the Mesolithic groups who favoured coastal areas and short-term occupations. The extension of the sites and archaeological evidences confirm the presence of small groups who exploited local resources over short distances to produce lithic objects similar to the lithic productions of the undifferentiated Epipaleolithic (Martini, 1993).

In regards the symbolic sphere, the funerary practices (Gagnière *et al.*, 1969; Floris *et al.*, 2009) of the Corsica-Sardinian area is in harmony with the European Mesolithic contexts. Therefore, a large part of the sites characterizes the Corsica-Sardinian area and the finding of funerary burials with typical Mesolithic traits (burial in a grave, use of red ochre and shelled ornaments as funerary decoration) in central western Sardinia refer to a very ancient inhabitancy of this part of the island.

Mesolithic groups occupied south-western Sardinia towards 7,860-7,127 bp (Melis & Mussi, 2016) thus enriching the Mesolithic population of Europe.

III.3. The Iberian sites

The Iberian Peninsula is rich in contexts which can be dated back to the Upper Palaeolithic and Mesolithic. As explained in the previous chapter, for this thesis, it was only possible to have access to the collections from three sites in the Cantabrian region: La Garma A, Los Canes and Arangas (Fig.III.1).

It will proceed to the description of these sites in a chronological way, from the oldest to the most recent in order of human occupation.

III.3.1. La Garma A

The archaeological site of La Garma A is part of a wide complex karst system on a hill at about 186 m a.s.l., in the Cantabrian coast, and about 12 km from the city of Santander.

The archaeological investigations developed from 1995 onwards under the direction of Pablo Arias Cabal and Roberto Ontañón allowed to highlight a set of archaeological sites with stratigraphic sequences which go from the Lower Palaeolithic to the Middle Ages.

Among these sites, La Garma A and the Galería Inferior are the most important ones in terms of prehistoric occupation of the area: the first with an archaeological sequence from the Aurignacian to the Middle Ages; the second contains an important deposit dating back to Middle Magdalenian with exceptional examples of rock art (Arias, 1999; Arias & Ontañón, 2012; González Sainz *et al.*, 2003).

Currently, La Garma A is the only entrance to the karst through a tunnel of around 7 m high connected to the Galería Intermedia, at around 70 m a.s.l. The entrance of this floor corresponds to another Bronze Age deposit, the Garma B. At about 59 m a.s.l. there is the Galería Inferior where currently it is possible to have access only through the Galería Intermedia, but until the end of the Pleistocene, it was directly accessible to the alluvial plain of Omoño from an opening at around 25 m a.s.l. (Arias & Ontañón, 2012).

Accessing to La Garma A through an opening with south-west direction, it is possible to arrive in a small vestibule (4 m x 2 m). By going through the vestibule along a narrow corridor on the right, it arrives to a larger room (6,5 m x 2m). In the right corner of this room towards the back wall, it is possible to find a set of limestone blocks which close a corner of the wall by forming a small oval setting (2,4 m x 1,7 m). The structure dates to the Middle Magdalenian and is contemporary to the occupation of the Galería Inferior (Arias *et al.*, 2005).



Fig.III.1.: Geographical localization of the Iberian sites: La Garma A; Los Canes; Arangas (map elaborated from Google Earth).

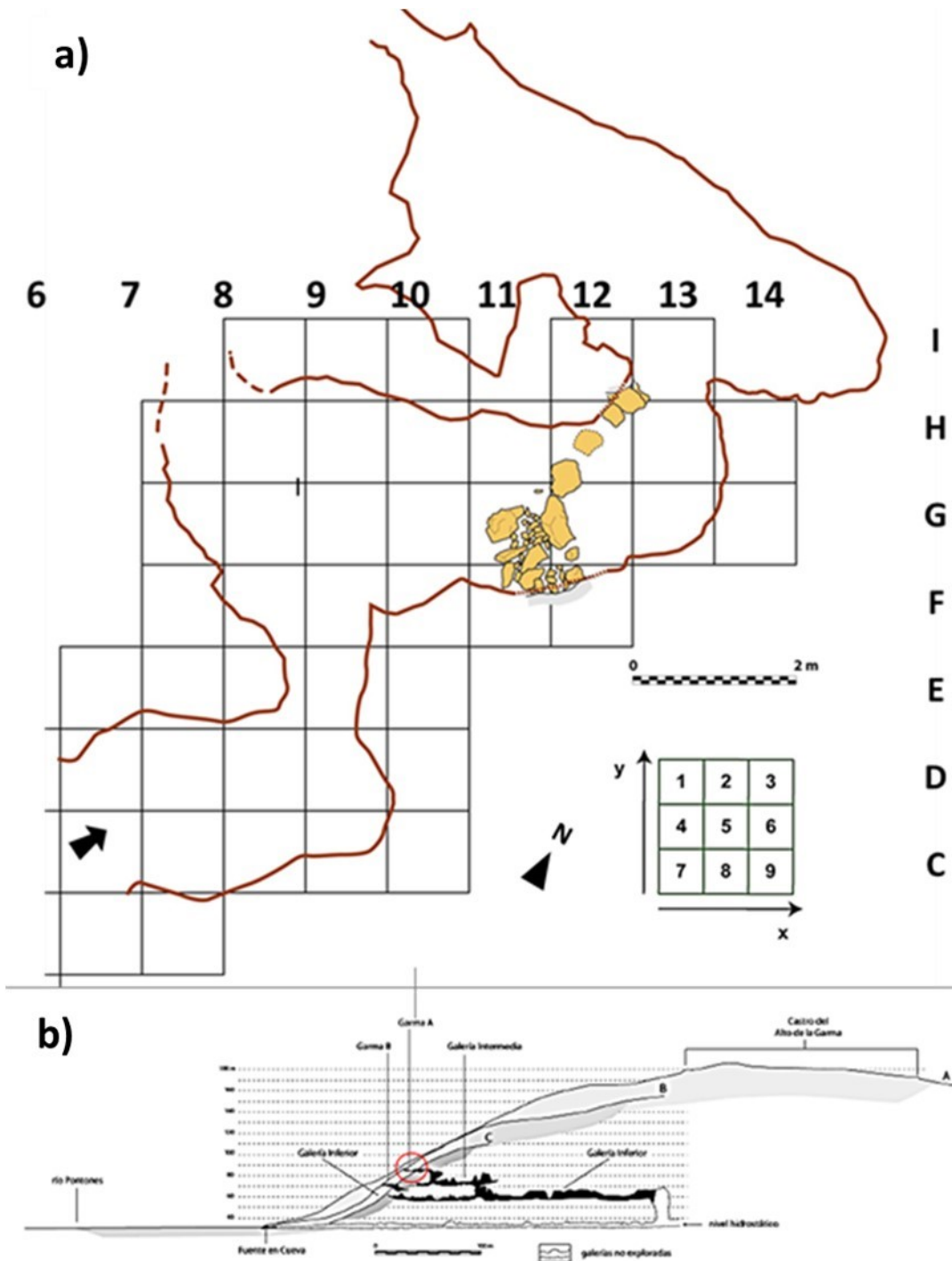


Fig.III.2.: La Garma A: (a) archaeological surface and (b) section of the hill (Peñalver et al., 2007).

III.3.1.1. Stratigraphy and chronology

The archaeological investigations highlighted two related stratigraphic sequences deposited in two distinct zones: one is deposited in a vertical conduit that connects La Garma A to the Galería Intermedia, another inside the cave. Currently, it is possible to recognize distinct stratigraphic units: cemented unit formed by clayey silts with abundant faunal remains and lithic tools which fills a large part of the tunnel connecting the two cavities; rubble unit formed by horizontal laminar concretions and sporadic clasts rich of faunal remains and lithic artefacts. This unit fills the whole of the vertical conduits by being the foundation at the deposit of La Garma A; clay mixture made up of reddish clays that are connected to the Upper Palaeolithic levels (layer C and E) of La Garma A. As far as the internal sequence of the cave is concerned, the excavations of the vestibule (bands 1-5) and the internal room highlight a similar sequence.

- Layer C (Aurignacian) represents the lower one and was deposited towards 31,950 cal BP below layer D (Aurignacian) and characterized by an abundant deposit of locally laminated clayey silt and fine sand.
- Layer E (Gravettian) darker and full of materials dating back to approximately 25,000 cal BP.
- Layer F (Gravettian) thin sterile layer where there is a perforated and engraved metapodium of *Capra pyrenaica*.
- Layers G-H-I that constituted the Solutrean unit corresponding to about 24,600 cal BP.
- Layer J (Magdalenian) full of faunal remains, lithic industries and hearth remains which can be seen in sections dating back to approximately 16,650 cal BP.

- Layer L (Magdalenian) dating back to 16,450- 14,350 cal BP, can be divided into four sublevels (Arias *et al.*, 2005): L1 (yellowish silty layer with few inclusions); L2 (greyish silty layer for the presence of carbonaceous remains; L3 (yellowish silty layer with abundant limestone and stalagmite fragments of Anthropoc origin); L4 (yellowish silty layer with few inclusions).
- Layer N (Magdalenian) dark, almost blackish with many clasts deriving from gelifraction processes and separated from the lower layer by a thin crust. The dating obtained at C14 links it towards 14,350 cal BP;
- Layer O (Magdalenian) slightly behind layer N and dating back to around 14,090 cal BP. It appears like a very clear layer where the malacological remains attest the passage from *Littorina littorea* to *Osilinus lineatus*.
- Layer P (Azilian) dating back to around 11,150 cal BP and is the darkest layer compared to the previous one which is well detached.
- Layer Q (Mesolithic) composed of clear soil and rich in typically Mesolithic industries and marine gastropods that match the dates between 8,450 and 7,650 cal BP.

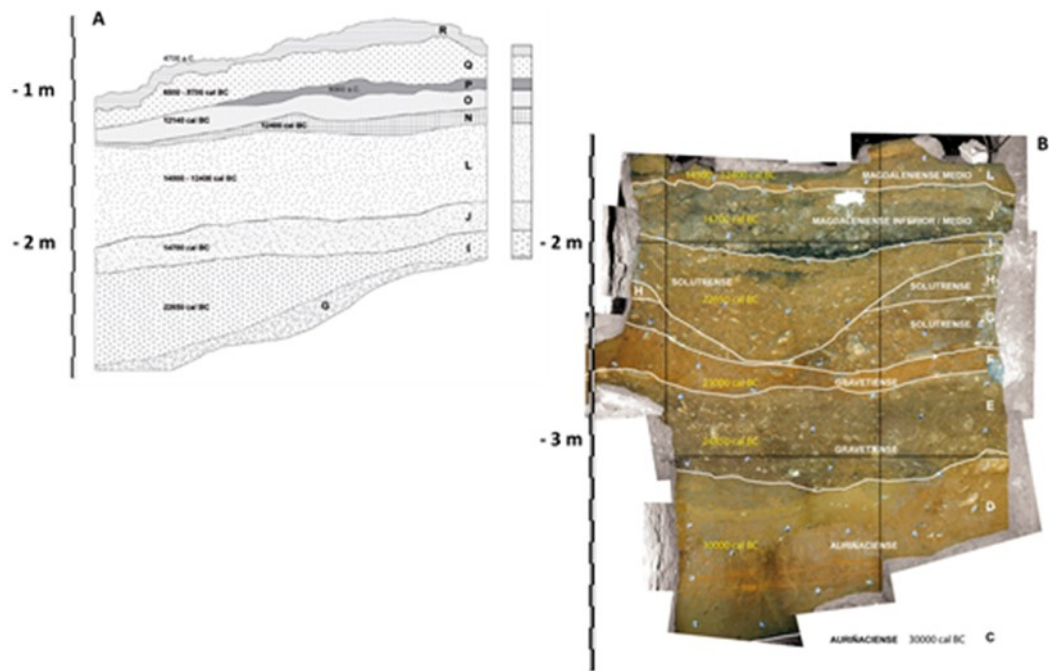


Fig.III.3.: La Garma A: a) stratigraphic sequence visible on the Southern profile (quadrants 9 and 10); b) photogrammetric return of the stratigraphic sequence from the Northern profile of the vestibule (quadrants F and G).

III.3.1.2. Ochre recovery strategies and sampling conditions

The recovery of ochre remains from the archaeological deposit of La Garma A occurred by an accurate methodology of fieldwork. The archaeological surface was divided into quadrants of 1 m x 1 m within the Cartesian plan. The plan was formed by the crossing of intersected orthogonal lines (X, Y, Z) starting from point 0 from which a progressive number and letters from A to Z began. Each quadrant was indicated according to a combination of a letter and a number and was delimited by a pair of semi-axes X and Y. The Z indicated the depth. In turn, each quadrant was divided into nine sectors of 10 cm x 10 cm. By starting from this organization of the archaeological surface, only the pieces ≥ 5

cm was punctually collected and placed in the archaeological plan based on the quadrant and provenance sector.

The recovery of the remains below this size and not identified during the excavation were sieved. Dry sieving of the sediment was realized by meshes of 0,2 cm in order to collect smaller objects. Successively, the sediment was sieved with water and the 30% was floated. Later, the sediment was left to dry to open air and examined in the laboratory to recover more little elements of archaeological interest. Each piece of ochre acquired by this methodology was identified with a progressive number per square and stored in transparent plastic and sterile bags to avoid contaminations. Each bag had a label placed on it with the following information: year of excavation, site, quadrant, sector, recovery strategy (*in situ* or sieving), type of material. This recovery strategy allowed us to position *in situ* by X, Y, Z coordinates about 2% of the ochre pieces (n.17 pieces) while the remaining 98% were recovered through sieving.

The systemic wash of sediments allowed us to collect a large part of the materials as well as smaller ones. Nevertheless, the passage with water eroded the ochre surfaces and thus limiting the readability eliminating, partially or totally, diagnostic traces and signs.

Furthermore, the use of sieves with meshes of 0,2 cm determined an involuntary selection allowing to recover only those pieces with dimensions ≥ 2 mm. All pieces of ochre together with the other materials collected were inserted in a big database. The materials collected *in situ* within a system of spatial coordinates X, Y, Z and those recovered through sieving from 1993 to 2005, were sampled for this study. The ochre remains are partly conserved in the deposits of MUPAC (Museum of Prehistory and Archaeology of Cantabria)

and partly at the deposits of Universidad de Cantabria – IIPC (*Instituto Internacional de Investigaciones Prehistóricas*).

A total of 840 elements coming from Palaeolithic (Solutrean-Magdalenian) and Mesolithic units were viewed. A total of 667 were selected from levels: G, G1, G2 (Solutrean); I (Solutrean); J1, J1b, J2, J2c (Middle/Lower Magdalenian); L1, L2, L3, L4 (Middle Magdalenian); N (Upper Magdalenian); O (Final Magdalenian); Q (Mesolithic). The poor representativeness of the material from some of these levels gave problems from a statistical point of view. For this reason, it was convenient to group some stratigraphic units to obtain a reasonable number of pieces statistically significant.

The materials were organized by grouping the following stratigraphic units according to a chrono-cultural coherence:

- Unit G includes S.U. G, S.U. G1 and S.U. G2 formed during the Solutrean between 26,259±413 cal BP/26,304±390 cal BP;
- Unit I includes S.U. I1 and S.U. I2 formed during the Solutrean dating back to 25,463±345 cal BP (I2);
- Unit J includes S.U. J1, S.U. J1b, S.U. J2, S.U. J2c formed during the Middle/Lower Magdalenian dating back to 19,537±284 cal BP- 17,125±205 cal BP;
- Unit L includes the S.U. L1, S.U. L2, S.U. L3, S.U. L4 formed during the Medium Magdalenian dating back to 16,371±445 cal BP- 16,425±428 cal BP;
- Unit N dating back to 14,656±431 cal BP;
- Unit O dating back to 14,090±260 cal BP;
- Unit Q dating back to 8,486±57 cal BP e 7,717±51 cal BP.

S.U.	Laboratory	Dated material	Date BP	Date cal BP CalPal2007_HULU	Range 2σ (a.C./cal BC) INTCAL 04
G	OxA-X-2261-42	Bone	21,160 ± 130	25,319±362	-----
I	TO-11698	Bone	21,320±140	25,463±345	-----
L1	AA-45562	Bone	13,450±140	16,371±445	14,561-13,526
L2	AA-45559	Bone	13,780±150	16,913±271	14,993-13,971
L3	AA-45577	Bone	13,810±180	16,965±322	15,087-13,939
L4	AA-45571	Charcoal	12,377±60	14,585±337	12,835-12,144
N/L	AA-45560	Charcoal	12,241±68	14,314±266	12,509-11,941
N	AA-45558	Bone	12,420±180	14,656±431	13,136-12,012
O	OxA-7203	Bone	12,070±100	14,090±260	12,198-11,786
P	MAD-644	Carbonate	11,002±1,106	12,899±1566	11,214-6,790
Q	OxA-7284	Bone	7,685±65	8,486±57	6,641-6,439
Q	OxA-7150	Bone	6,870±50	7,717±51	5,878-5,661

Tab.III.1.: Radiocarbon dates of La Garma A (Arias Cabal, pers.comm.).

III.3.2. Los Canes

The site of Los Canes, a small cave in Cibrales (Asturias), was discovered in 1972 by D. Gregorio Gil Álvarez. During a survey in the valley of Cares, D. Gregorio Gil Álvarez with his collaborator M. Gutiérrez, noted a series of digital engraved traits inside the cave (Arias *et al.*, 1981). Some years later (1981-1985) prehistoric remains in the vestibule of the cave were found and it was decided to develop a stratigraphic test pit that revealed a detailed Holocene sequence highlighting a funerary structure. For this reason, a team under the

direction of Pablo Arias Cabal and Carlos Pérez Suárez decided to carry out systematic excavations from 1986 to 1993 that brought to light a complex Late Pleistocene/Early Holocene sequence (Arias, 2002; Arias, 2013) with human burials. The skeletal remains were discovered in three main oval structures (6-III, 6-II, 6-I) ascribable to Mesolithic period (Arias & Garralda 1996a, 1996b; Drak *et al.*, 2010).

Funerary structure 6-III

The structure identified as 6-III is in the vestibule of the cave and contains the remains of an adult male in anatomical connection with some faunal remains and shell ornaments as grave goods. Human remains of a second non-anatomically connected individual (infant of 1-2 years old) were also found in the same structure. The structure is an oval pit of 120 cm x 83 cm with a depth of 54 cm with three levels of filling: 6-IIIA, 6-IIIB, 6-IIIC. Radiocarbon dating refer the 6-IIIA to 7,781±92 cal BP.

A total of 290 ochre pieces were collected from the three levels that fill the burial among which the most attractive are two crayons from the stratigraphical unit 6-IIIA (Fig.III.5).

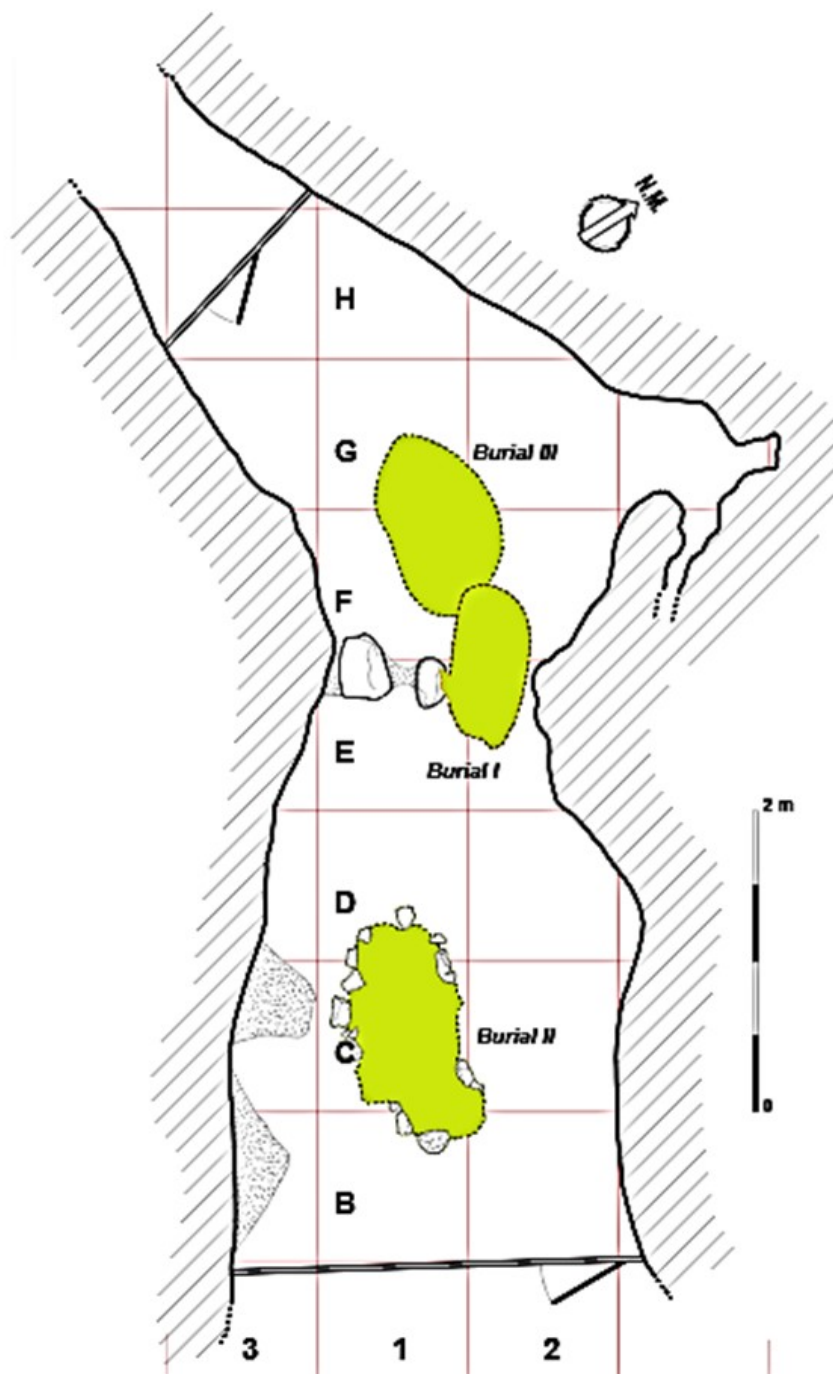


Fig.III.4.: Planimetry of the archaeological surface (elaborated from Arias, 2002).

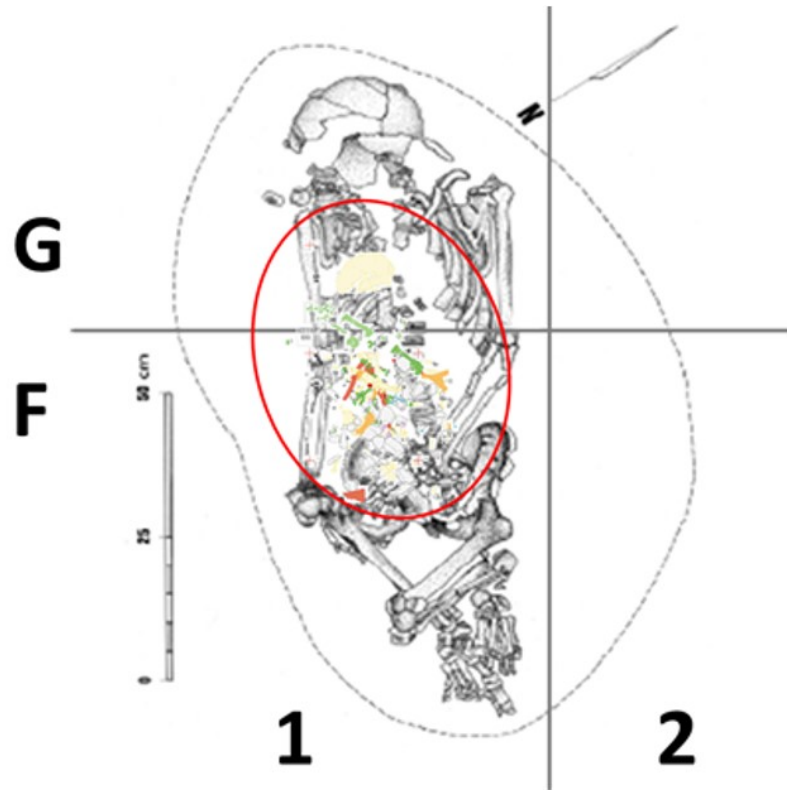


Fig.III.5.: Los Canes: image of funerary structure 6-III with the skeletal of the male adult individual. In the circle are enclosed the faunal remains and the infant bones (adapted from Arias, 2002).

Funerary structure 6-II

The funerary structure 6-II, in the final part of the cave, is a 110 cm x 75 cm oval pit with a depth of 40 cm with the remains of a fully anatomically connected skeleton of a sub-adult male dating back to around 8,032±46 cal BP and 7,628 ± 43 cal BP. Furthermore, part of some anatomically connected lower limbs of another individual adult was found in the same burial. Radiocarbon dating refer it to 7,942±35 cal BP/7,709±67 cal BP.

In total, 65 pieces of ochre were collected from the burial in association with two skulls of *Capra pyrenaica* on the pelvis, an oblong pebble with round edges

and residues on the surface near the right forearm, a perforated baton, a bone awl and a rounded pebble with use wear traces at the height of the right shoulder. In addition, several shells beads on *Trivia* sp. were also found above the back of the deceased and a pendant of *Callista chione* above the skull (Fig.III.6). A total of 45 pieces of ochre in association to 10 retouched lithic tools and several grave elements were collected from this structure. A red deer scapula near the right foot and three atrophic red deer canines below the left foot and some shells of *Cepaea nemoralis*, a terrestrial gastropod, and marine molluscs were found in the structure scattered on the skeleton (Fig.III.7).

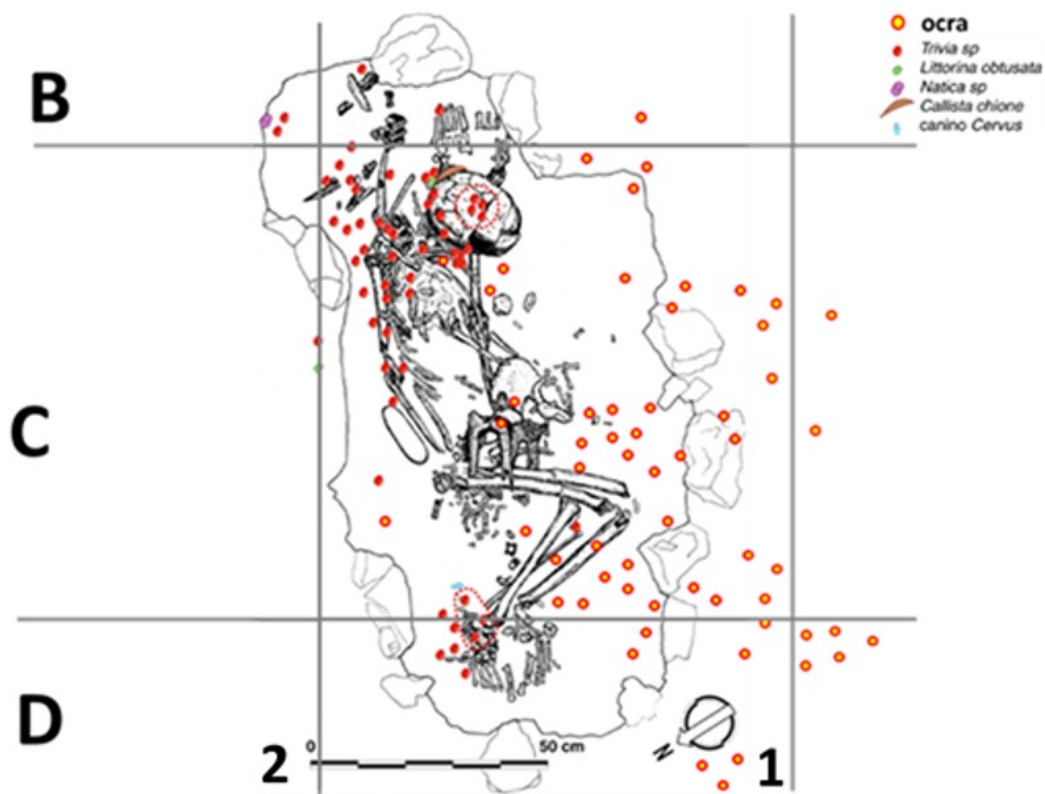


Fig.III.6.: Los Canes: image of funerary structure 6-II (adapted from Arias, 2002).

Funerary structure 6-I

Structure 6-I (108 cm x 50 cm), in the central part of the cave vestibule, is a burial of a female adult individual in a supine position without the lower limbs which were damaged during the excavation of another Mesolithic structure (6C). The lower limbs of the deceased were destroyed by the excavation of another Mesolithic pit called 6A.

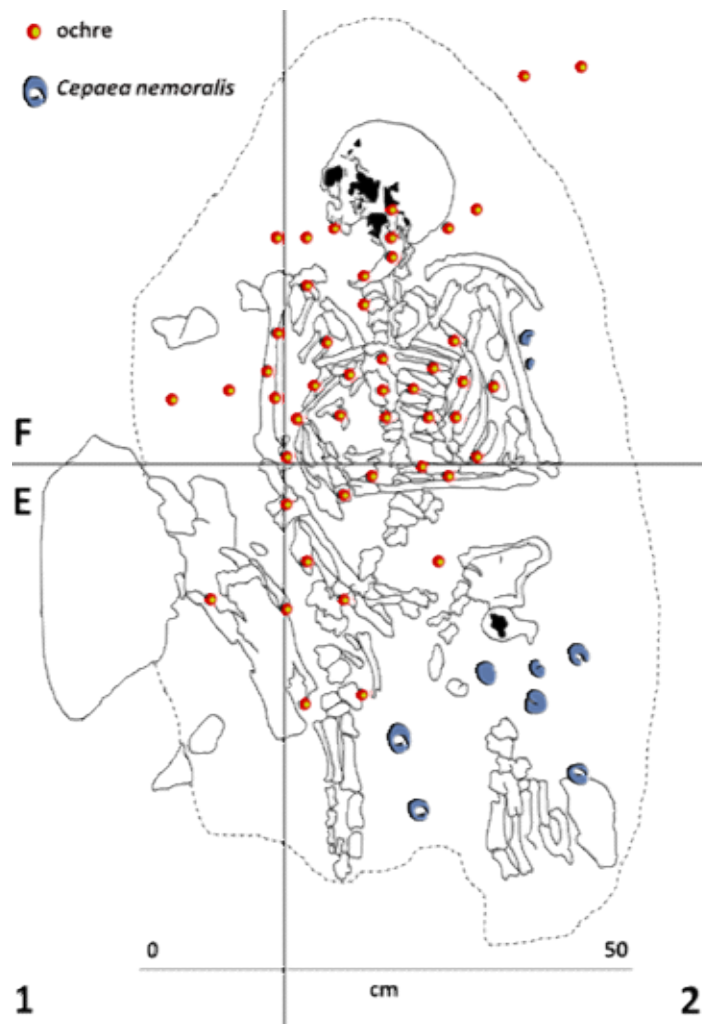


Fig.III.7.: Los Canes: image of funerary structure 6-I (adapted from Arias, 2002).

III.3.2.1. Stratigraphy and chronology

The stratigraphical sequence of Los Canes is a reference to better understand the prehistoric occupation of Asturias. The archaeological deposit provides valid information on the exploitation of mountainous areas during Late Pleistocene and Early Holocene in Northern Spain.

The fieldworks highlighted eleven stratigraphic units from the Solutrean to the Bronze Age that are summarized here below (Arias, 2002; Arias, 2013).

- *Unit 1*
- Unit 1 (about 60 cm of thickness) is composed mainly of sterile accumulation of light yellowish clay interspersed, in some areas, with large calcareous blocks fallen from the roof of the cave. Sediment analysis reveals a cold and humid stage before the human occupation of the cave.
- *Unit 2:*
- Unit 2 is formed of three different clayey units: 2A (10 cm approx. of thickness of reddish-brown clays), 2B (from about 5 cm to maximum 15 cm of thickness of light reddish-brown clays), 2C (about 10-15 cm of thickness of yellowish-light brown clays with pebble).
- Stratigraphical unit 2A testifies the first anthropic occupation of the site around $19,949 \pm 340$ cal BP when Solutrean hunter-gatherers occupied the cave during a cold and humid phase.
- Human presence increased during $19,850 \pm 345$ cal BP/ $19,062 \pm 244$ cal BP. The lithic artefacts from S.U. 2B confirm a Lower Magdalenian occupation, when lowest temperatures with colder oscillations

characterized a steppe landscape with *Artemisia* and *Poaceae* vegetal species.

- A general warming, suggested by the malacological remains collected from S.U. 2C, occurred around 17,153±224 cal BP (2C-Upper Magdalenian)
- *Unit 3:*
- Unit 3 is formed by S.U. 3A (stratum of about 2-3 cm of thickness formed by reddish sediments), S.U. 3B (layer of about 7 cm of average thickness with large calcareous pebbles in a dark matrix), S.U. 3C (layer with a thickness between 7-10 cm characterised by a black matrix with few calcareous pebbles).
- Sedimentological analysis reveals that S.U. 3A is a thin layer that was formed during an interstadial stage due its composition and fossil content. The archaeological materials such as a few stone tools show intermediate characters between the Upper Magdalenian (2C) and Azilian (3B) cultures, confirming the transitional phase.
- The upper S.U. 3B raises several doubts for the discrepancies between the micro-faunal remains and the content in terrestrial gastropods. The disappearance of a cold climate indicator, *Microtus oeconomus*, shows that it does not match an increase in terrestrial gastropods typical of warm and humid conditions.
- According to the radiocarbon date (13,702±146 cal BP) and the available paleo-climatic data for the northern Iberian Peninsula (Lotter *et al.*, 1992; González-Sampériz *et al.*, 2010), it is possible to ascribe the S.U. 3B to a climatic fluctuation during the Tardiglacial period. Unit 3C confirms an

interstadial phase with the increase of terrestrial gastropods and the presence of a dark soil with some small stones testifying the formation of this stratum during a warmer phase, after 13,400 cal BP. The study of the lithic tools assigns units 3C to the Azilian culture.

- *Unit 4:*
- Unit 4 marks the beginning of the Holocene period. The layer is characterized by the accumulation of dark-brown clays and terrestrial gastropods as diagnostic element of a progressive climate improvement. Archaeological evidence confirms an Azilian occupation of the site
- *Unit 5:*
- The heterogeneous organization of this unit denotes karst phenomena during Early Holocene. The circulation of water impacted on sediments deposited during the earlier stages. Therefore, unit 5 is formed by an accumulation of pebbles and fragments of stalagmite crust in a dark clay matrix with lenses of yellowish clays and areas of incoherent light-grey materials.
- *Units 6:*
- This unit is characterized by the presence of Mesolithic burials as previously described, and structures. The structure 6-III is formed by three filling phases (Fig.II.8): S.U. 6-IIIA (clayey level of 12 cm of thickness of dark-brown colour with rare clasts); S.U. 6-IIIB (matrix like 6-III-A rich in blocks of medium size between 5-10 cm. Its thickness is about 12 cm); S.U. 6-IIIC (clayey light brown stratum quite homogeneous, with abundant not very large stones oriented in all

directions. In some areas it is quite compacted by the action of dripping. It has about 30-35 cm of thickness).

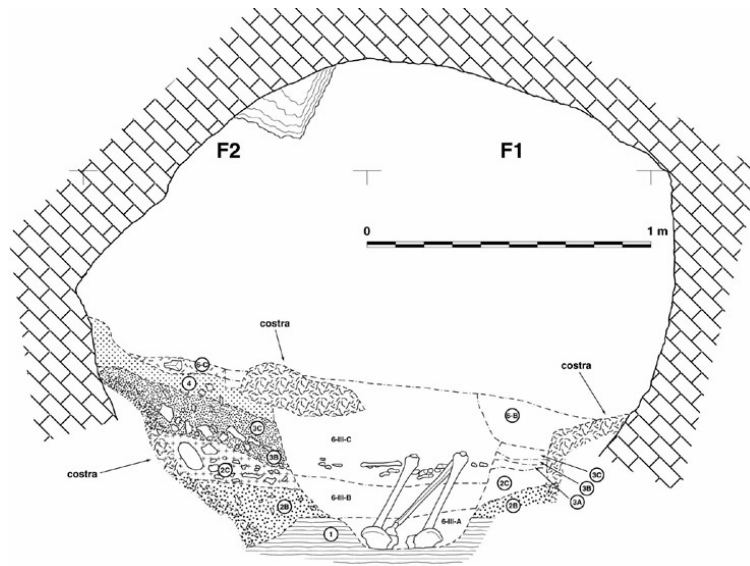


Fig.III.8.: Transversal section of the central portion of the funerary structure 6-III (Arias, 2002).

The structure 6-II (Fig.II.9) is characterized by very compact reddish-brown earth with few angular pebbles. The sediments fill a pit excavated until the S.U. 1 (compact and stony layer).

The structure 6-I is a pit around 27 cm deep filled by clayey dark-brown earth with abundant angular pebbles, fragments of stalagmitic crust and shells.

The unit from 6A to 6G consist in Mesolithic structure probably with a funeral function. The archaeological content is quite rare, but in some cases as for the structure 6A, it indicates a probable funerary function as for the 6-III; 6-II; 6-I. The unit 6A is an oval pit (115 cm x 83 cm) with a heterogeneous deposit made by some dark-brown areas and some clayey yellowish areas. The unit is rich in little angular pebbles, fragments of stalagmitic crust and rare archaeological

remains. The structure is probably another Mesolithic funerary structure dating back to $7,977 \pm 23$ cal BP.

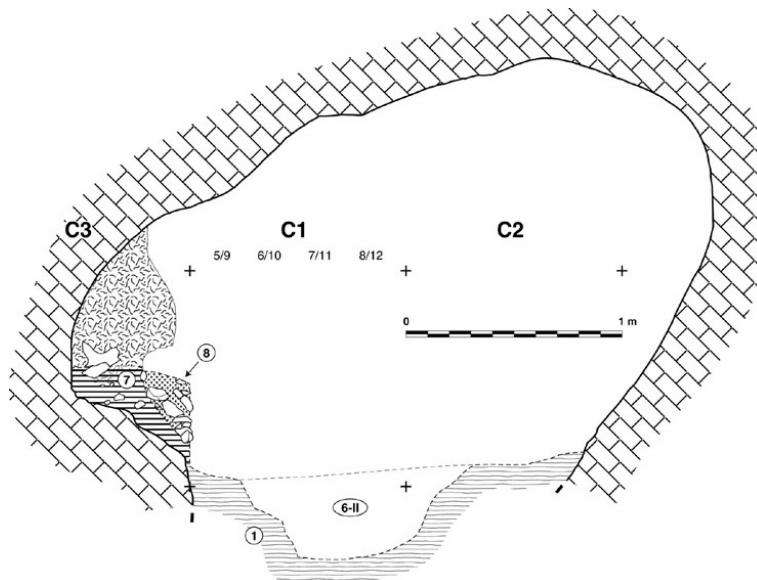


Fig.III.9.: Transversal profile of the entrance to the cave with the view of the section of the funerary structure 6-II (Arias, 2002).

Unit 6B is a pit 25 cm deep and probably a Mesolithic funerary structure filled by greyish sediments and abundant stones and crusty fragments dropped in different directions.

Unit 6C is a thin layer of 7-8 cm of thickness slightly clayey and sandy, quite compact, with some small stones.

Unit 6D is a pit of 6 cm of thickness filled by loose sandy sediments of light grey colour.

Unit 6E is a thin sandy dark-brown layer of 1 cm of thickness.

Unit 6F (2 cm of thickness) is sandy level of light grey colour rich of sands formed by the crushing of a stalagmite crust.

Unit 6G is characterized by a light brown deposit too homogeneous and sandy with some concretion blocks and remains of terrestrial molluscs.

- *Unit 7:*
- S.U. 7 is characterized by another large pit that cuts the lower units. This unit is filled with mostly remixed ancient materials, even if it is possible to recognize the remains of Neolithic pottery. The radiocarbon date indicates $6,828 \pm 84$ cal BP/ $6,678 \pm 89$ cal BP.
- *Unit 8:*
- Unit 8 looks like a big depression in the vestibule of the cave. This structure, filled by large angular pebbles with a chaotic orientation, cut the lower levels. The exiguous quantity of archaeological materials confirms sporadic anthropic occupations of the cave during the Bronze Age, a cross-cultural attribution obtained by the discovery of a bronze plate fragment in the stratum. Absolut chronology date this unit to $3,747 \pm 60$ cal BP.
- *Unit 9:*
- Unit 9 is a circular pit of about 125 cm in diameter and 25 cm in depth. The pit is filled with loose clayey sediments with a range in colour from brown to dark grey with abundant small disorganized pebbles and fragments of stalagmite crust. This unit is probably a Mesolithic funerary structure even if the archaeological remains are scarce and not clear.
- *Unit 10*
- Unit 10 corresponds to a confused and heterogeneous deposit with a dark-brown colour. The unit is characterized by the presence of pebbles

and some fragments of stalagmite crust. The materials appear in a chaotic way and in different directions.

- *Unit 11:*
- The stratigraphic sequence finishes with the S.U. 11, a small depression of uncertain origin located on the northern wall of the cave. The unit dates to $3,766\pm 48$ cal BP.

S.U	Laboratory	Dated material	Date BP	Date cal BP	
				CalPal2007_HULU	Range 2σ (a.C./cal BC) INTCAL 04
2 A	AA-12166	Bone	16,700 \pm 210	19,949 \pm 340	18,323-17,514
2 B	AA-12165	Bone	16,560 \pm 200	19,850 \pm 345	18,196-17,396
2 C	AA-18020	Charcoal	13,009 \pm 105	15,876 \pm 429	13,837-13,083
3 B	AA-18019	Charcoal	11,795 \pm 84	13,702 \pm 146	11,866-11,486
6-III	AA-6071	Human bone	6930 \pm 95	7,781 \pm 92	5,995-5,660
6-II	AA-5295	Human bone	6,860 \pm 65	7,709 \pm 67	5,886-5,637
6-II	AA-11744	Human bone	7,025 \pm 80	7,849 \pm 82	6,032-5,736
6-II	AA-5296	Human bone	6,770 \pm 65	7,628 \pm 43	5,789-5,558
6-I	AA-5294	Human bone	6,265 \pm 75	7,162 \pm 100	5,464-5,021
6-I	OxA-7148	Human bone	6,160 \pm 55	7,067 \pm 78	5,292-4,950
7	AA-5788	Charcoal	5,865 \pm 70	6,678 \pm 89	4,906-4,546

Tab.III.2.: Radiocarbon dates of Los Canes re-calibrated from re-calibrated from raw dates in Arias (2002).

From this description, the stratigraphic sequence of Los Canes is rather complex and presents problems related to the formation of the Holocene deposit.

Regarding Pleistocenic deposit, the stratigraphic and sedimentary studies (Arias, 2002) did not highlight any important post-depositional alterations. Hideouts for small mammals were detected which partially affected units 2C and 2B and some movements of land due to the growth of roots.

The Holocenic deposit however had an intricate and heterogeneous situation.

Unit 5 has an unordered deposit characterized by materials with a chaotic arrangement which in some cases are placed vertically. Additionally, the presence of Pleistocene micromammal remains (*Ptyomys lenki*), heavily coated Palaeolithic industries and a high density of faunal remains confirm post-depositional movements. Stratigraphic studies and sedimentological analyses confirm that unit 5 was affected by the circulation of water inside the cave towards the beginning of the Holocene. This natural agent determined the mixing of sediments and the inclusion of archaeological materials from the lower Palaeolithic units (2A, 2B, 2C, 3, 4).

Nevertheless, some clues confirm that despite the rearrangement phenomena, unit 5 was formed during the Initial Holocene: the presence of Mesolithic industries; the prevalence of grey flint compared to other units; minimum density of some materials like lithic artefacts, micro mammal remains, and shell ornaments compared to the lower units (4, 2C, 2A).

The inclusion of Pleistocenic materials is certain for the Holocene units 6-9-10. It deals with graves in which the excavation brought about the removal of portions of sediment of the lower units. The removed sediment was then used by the Mesolithic groups who excavated the graves to fill them. This explains the presence of some heavily mineralized faunal elements like those of the Palaeolithic units which justifies the date $19,062 \pm 244$ cal BP obtained on a fragment of bone recovered in the Mesolithic structure 6-III.

In any case, the presence of Mesolithic lithic industries, the variation density of the marine molluscs between the funerary structures 6-III, 6-II, 6-I in accordance with the radiometric dating obtained from the human remains confirm the Mesolithic origin of these units and the Holocene attribution of a part of the pit.

III.3.2.2. Ochre recovery strategies and sampling conditions

The recovery of ochre occurred according to a conventional methodology applied for systematic excavations in caves, in the Cantabrian region (Arias, 2011). The collection of materials with dimensions ≥ 5 cm was realized in relation to a grid of 25 cm x 25 cm in relation to a plan formed by the crossing of orthogonal lines (X, Y) starting from a point 0, for the entire superficial of the cave.

Around 4% of ochre pieces were horizontally localized in the plane with X-Y coordinates and vertically with the measurement of the depth (Z) calculated starting from point 0.

About the 97% of ochre pieces observed for this study, were recovered by dry and water sieving. The sediments were initially dry sieved in front of the cave with meshes of 0,2 cm to recover the more fragile fragments. Later, the sediment was further water sieved in an installation positioned in an ancient washbasin in the small town of Arangas. Even water sieving was realized with meshes of 0,2cm. The sediment that was sieved was dried to open air and later scrutinized in the laboratory to recover the smaller objects which escaped from the previous sieving. All the recovered materials were identified with an inventory number assigned per quadrant of provenance. The ochre pieces were preserved in transparent plastic bags and a label was placed on them with the

year of excavation, quadrant, X-Y-Z coordinates and type of material. The material was transported at Universidad de Cantabria in closed boxes. The boxes are made of opaque plastic materials in which the findings were stored in dark and constant temperature condition, to favour the stability of iron ores avoiding physical alterations. The materials were exposed once again for this research with the aim of selecting the elements collected in the Palaeolithic and Mesolithic levels.

III.3.3. Arangas

During the archaeological fieldworks which started in 1985, P. Arias Cabal (Universidad de Cantabria) and C. Pérez Suarez decided to carry out a trial excavation in a cave adjacent to Los Canes: the cave of Arangas. The two cavities are part of the same karst system formed by two levels: one at about 335 m a.s.l. with the caves of Los Canes and Tiu Llines, and another one at about 345 m a.s.l. with the cave of Arangas.

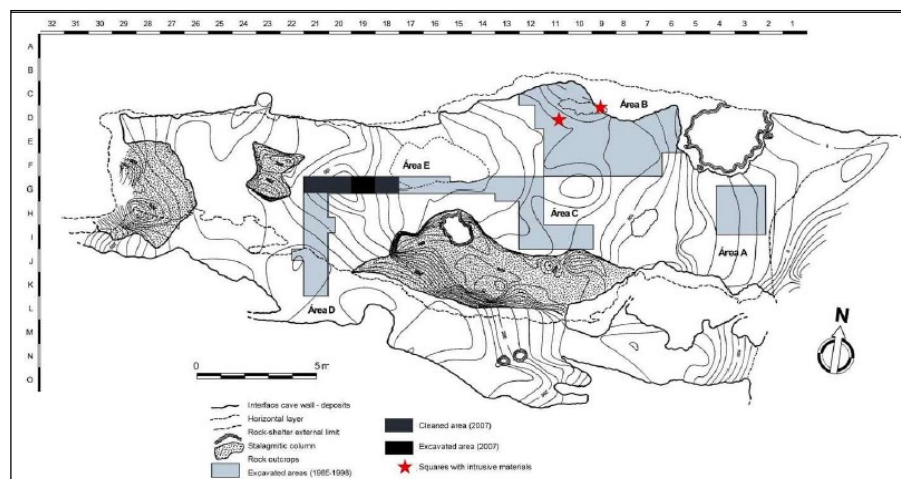


Fig.III.10.: Planimetry of the archaeological surfaces of Arangas.

The site (25 m long × 6-7 m wide), oriented to the north-east and about 10 m above Los Canes and Tiu Lines, consists of a large cavity with a long stratigraphic sequence investigated between 1992-1998. In 2007, with a subsequent general revision by E. Álvarez and M. Cubas, sector E was excavated to clarify some doubts about Late-Glacial/Early Holocene sequence and to collect samples for sedimentological and archaeobotanical analysis (Arias *et al.*, 2007).

Little is known about the Upper Palaeolithic of Arangas. On the contrary, the Mesolithic and Neolithic phases are well documented thanks to the publications by Arias *et al.*, (2013) and to PHD researches developed by P. Fernández Sánchez (PHD thesis, 2016) and I. López Dóriga (PHD thesis, 2016).

The studies allow us to recognize main raw materials exploited during Mesolithic phase of the site (layers 4-3): radiolarite, flint, flysch, quartz and quartzite.

Bone industry is represented by a unique element (S.U. 3), a red deer stag with a double deep mark, which suggests a flake extraction.

Archaeobotanical analysis was conducted by I. López Dóriga to better understand plants exploitation in the Atlantic Iberia with a focus on Mesolithic and Neolithic phases. The carpological studies revealed a variety of taxa such as *Corylus avellana* L., *Quercus* sp., *Hordeum vulgare* L. var. *nudum*, *Sorbus* sp.

Regarding the archaeozoological investigation, 976 faunal remains in total (443 determinable; 533 not determinable) were collected from Mesolithic units. The general well-preserved state allows for the identification of specimens of *Capra pyrenaica*, *Rupicapra pyrenaica*, *Cervus elaphus*, *Capreolus capreolus*, *Sus scrofa*.

Taphonomical analysis shows cut marks and impact marks on bones, confirming the slaughter of the animal carcasses and recovery of marrow. Furthermore, the discovery of ungulate foetal remains among faunal assemblages, denote hunting pregnant females.

III.3.3.1. Stratigraphy and chronology

The fieldworks of 1992-1998 focused on 5 areas: Area A (rock-shelter), Areas B-C (vestibule), Area D (bottom cave), Area E (centre) providing preliminary information on the stratigraphic sequence from Magdalenian to Chalcolithic with a Mesolithic stage related to Los Canes (Arias & Pérez, 1995).

In 2007, a last excavation was conducted to clarify depositional processes interspersed in the archaeological deposit formation. It was decided to investigate Area E. A surface of about 4 cm x 0.67 cm was refreshed and a sector of about 1 m² was excavated in square G19.

The survey clarified some stratigraphic uncertainties and made it possible to outline a more complete sequence (Arias *et al.*, 2007):

- *Base level*: sterile level of light-yellow sandy clays, very compact with numerous calcareous blocks;
- *Unit 5D*: calcareous pebbles in black matrix with reddish thin lenses. The level, clearly visible in the areas C-B (squares I1O-E7), are moderately rich in faunal remains with a low content of lithic tools.
- *Unit 5C*: black clayey matrix including medium sized calcareous shaped pebbles. The layer, clearly visible in squares I10 and F8, appear poor of

lithic industries, like level 5D. On the contrary, faunal remains are abundant. Radiocarbon date refer this unit to 18,251±238 cal BP.

- *Unit 5B*: blackish matrix with large calcareous inclusions and faunal remains dating back to 12,118±202 cal BP.
- *Unit 5A*: matrix of incoherent orange sands with few archaeological remains with the same date of unit 5B.
- *Unit 4*: brownish-orange matrix with calcareous pebbles. This unit separates the precedent (Unit 3) for the low content of archaeological materials and dates back to 9,310±89 cal BP.
- *Unit 3*: clayey black matrix with calcareous shaped pebbles rich in faunal remains dated to 7,162±100/9,166±97 cal BP.
- *Unit 2B*: light yellow clayey layer with few clasts and less faunal remains than the upper level. Radiocarbon date refers this unit to 8,879±127/8,879±127 cal BP.

S. U.	Dated material	Date BP	Date cal BP CalPal2007_HULU	Range 2σ (a.C./cal BC) INTCAL 04
5D	Bone	15,000	18,250±242	16,683-16,058
5C	Bone	12,500	14,806±329	1,3067-12,222
5B	Bone	10,300	12,137 ± 269	10,661-9,759
5A	Bone	10,300	12,137 ± 269	10,661-9,759
4	Charcoal	8,300	9,281±133	7,534-7,082
3	Charcoal	8,200	7,162±100	7,519-6,848
2B	Human bone	8,000	8,853±145	7246-6638

Tab.III.3.: Radiocarbon dates of Arangas calibrated from raw dates unpublished (standard error not received).

III.3.3.2. Ochre recovery strategies and sampling condition

The materials were recovered with a dual strategy implemented by the excavators during the fieldworks carried out to the site. The excavation area was divided into 9 sub-quadrants of 33 cm² starting from the orthogonal semi axes starting from point 0 for the whole cave. All ochre pieces were recovered by dry sieving the sediment before and then with water with meshes of 0,2 cm. No pieces with coordinates X, Y, Z which indicated the horizontal and vertical localization of the plane were found. In the years 1992-1997, all the sediments of the sub-segments named below after being sieved were floated (55% of the area squared).

During the next years, all the sediment from a diagonal row of three sub-quadrants were floated (33%). The ochre pieces were identified with an inventory number based on the quadrant of provenance. The number was assigned in a progressive way starting from 1. Later, all materials were stored in transparent plastic bags with a label reporting year of excavation, quadrant, sector, type of material. The material is still conserved in the Universidad de Cantabria storage in closed dark boxes to avoid the passage of light that can bring about alterations in the material. The materials were placed in the same location as the materials of Los Canes with the same temperature and lighting conditions. The exposition occurred with this research.

III.4. The Italian sites

As previously reported, the contacts between the Iberian and Italian spheres faded after the Gravettian phase. The geographical isolation of human groups favoured the emergence of contemporary and distinct cultures. While, in the

Franco-Cantabrian region there is the chrono-cultural sequence of Solutrean-Magdalenian-Azilian, in the Italian Peninsula, the environmental dynamics brought about a regionalization with the development of the Epigravettian cultures. Both in the Franco-Cantabrian region and the Italian Peninsula, humans continued to exploit colouring raw materials.

However, it is possible to appreciate substantial differences. In the northern Iberian Peninsula, red and yellow ochre was intensively used to create figurative representations on cave walls. On the other hand, in the Italian Peninsula the parietal rock art did not reach the abundance of the Atlantic repertoire even if ochre also was intensively exploited for funerary purposes. By beginning with these presuppositions and with the aim of obtaining valid comparisons, it was possible to have access to the collection of colouring materials of Grotta di Pozzo as well as taking some samples from the sites of Grotta del Romito, Grotta San Teodoro and S'Orku e S'Orku.

By keeping the chronological order also used for the Iberian sites, the contexts of Grotta del Romito, Grotta San Teodoro, Grotta di Pozzo and S'Orku e S'Orku will be described.

III.4.1. Grotta del Romito

The cave-shelter of Romito complex, in Papasidero (Calabria, Italy), is a horizontal karstic cavity among the Apennines at around 275 m a.s.l. with one of the most important stratigraphic sequences for the Italian Peninsula, with archaeological evidences from Upper Palaeolithic to Neolithic periods. Currently, the cave and the shelter are two areas separated by an artificial modern wall and are almost surrounded by calcite castings. Even if, during the

Palaeolithic period, the two areas constituted a single large communicating room.



Fig.III.11.: Geographical position of Italian sites: Grotta del Romito, Grotta San Teodoro, Grotta di Pozzo, S'Ormu e S'Orku.

The systematic excavation started with P. Graziosi (1961) and successively by the University of Florence under the supervision of the Professor F. Martini, contributed to the discovery of two double burials in the shelter, and four single burials in the cave with grave goods and ochre remains as well as lithic and bone artefacts, faunal remains, personal ornaments and portable art objects.

Furthermore, the importance of the complex is also due to the presence of bovid figures engraved on an imposing rock to the exterior of the shelter (Martini, 2000-2001).

Starting from Graziosi's research between 1961 and 1968 (Graziosi, 1961, 1963, 1964, 1965, 1968; Messeri, 1966) and with the systemic excavations of the last

few years (Fabbri *et al.*, 1988; Mallegni *et al.*, 1995; Martini *et al.*, 2004; Martini & Lo Vetro, 2005; Martini, 2006a), the following burials were brought to light.

Romito 1-2: double burial from Epigravettian layer (4) of the shelter not too far from a large rock engraved with the figure of a *Bos primigenus*. The burials contain the remains of a probable adult female individual (Martini & Lo Vetro, 2011) and a young male individual suffering from dwarfism, in a supine position lying next to each other. An intact horn of *Bos primigenus* and one fragment are found respectively between the legs and on the woman's right. These elements were interpreted by P. Graziosi as grave goods.

Romito 3 and Romito 4: two single burials localized in level C3 (Final Epigravettian) of the internal deposit of the cave.

The lying supine remains are of an adult male (*Romito 3*) and a young female individual (*Romito 4*) discovered in an oval pit covered by stone blocks removed by successive and clandestine excavations.

Romito 5-6: a double burial localized at the top of cut 7 in the shelter. The two supine burials with flexed legs were disposed into a single pit covered by stones. During the discovery, the bones of *Romito 6* were not anatomically connected. This data suggests a successive re-opening of the pit with the purpose of introducing the body of *Romito 5*. Genetic studies confirm a direct maternal relationship.

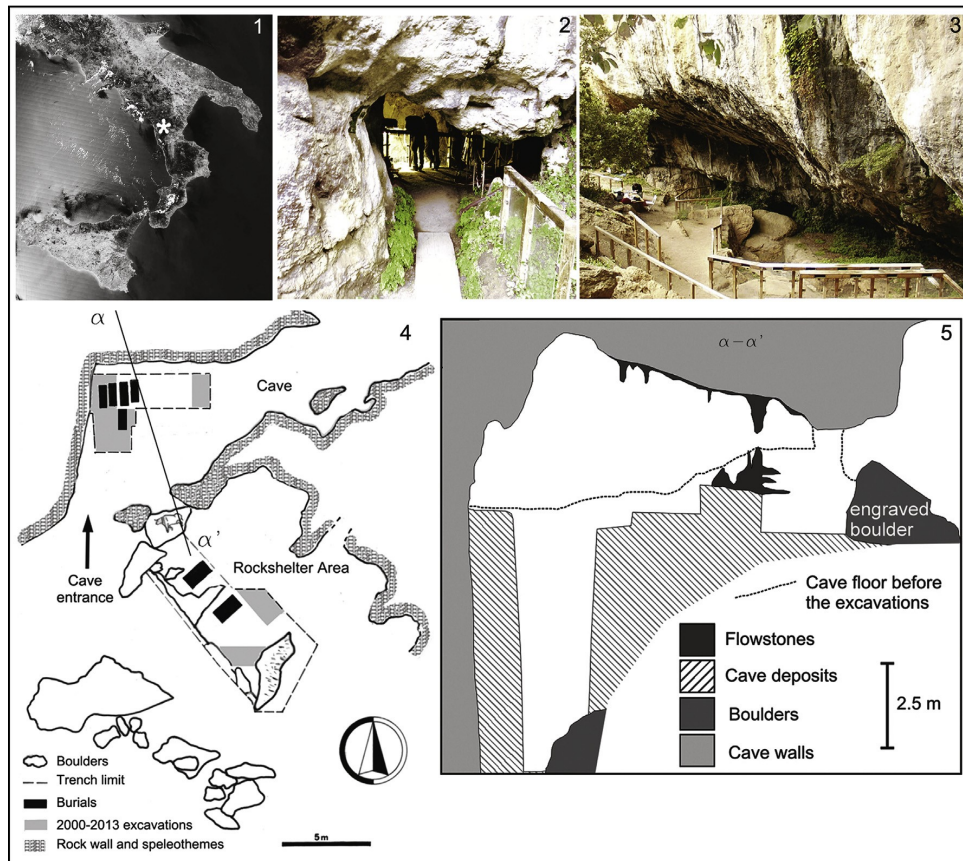


Fig.III.12.: Geographical localization of Grotta del Romito (1) and the cave entrance (2-3). Planimetry of the archaeological surface showing the distribution of trenches and burials (4). Cross-section of the site and of the excavated area along the axis a-a' indicated in the plan (5) (Martini & Lo Vetro, 2011; Blockley et al., 2017).

Romito 7: a single burial of an approximately 18-20-year-old male individual supinely deposited with hands crossed on the pubis in a pit protected by blocks in correspondence to the pelvis. Few elements of grave goods are found: a blade made of flint and a backed blade (Bisconti et al., 2005; Martini, 2006a). A considerable quantity of red ochre was found above and below the pelvis up to the IV vertebrae.

Romito 8: a burial of an adult individual in a supine position covered by stone slabs. The signs on the skeleton confirm that, when alive, the individual suffered physical trauma which brought about a paralysis in the left upper

limb. Dental wear suggests that he used his teeth to help him with everyday tasks in order to overcome this disability.

Romito 9: burial of an adult male placed in a pit and accompanied with several objects of grave goods. This is the earliest burial of the site (Ancient Epigravettian). As well as the antiquity compared to the others, the singularity of the burial is in the richness of grave goods formed by of a headpiece, a necklace, a bracelet and an anklet of marine shells. Furthermore, the deceased was wrapped in a shroud decorated by marine shells and atrophic canines of red deer. Red ochre covers the whole body.

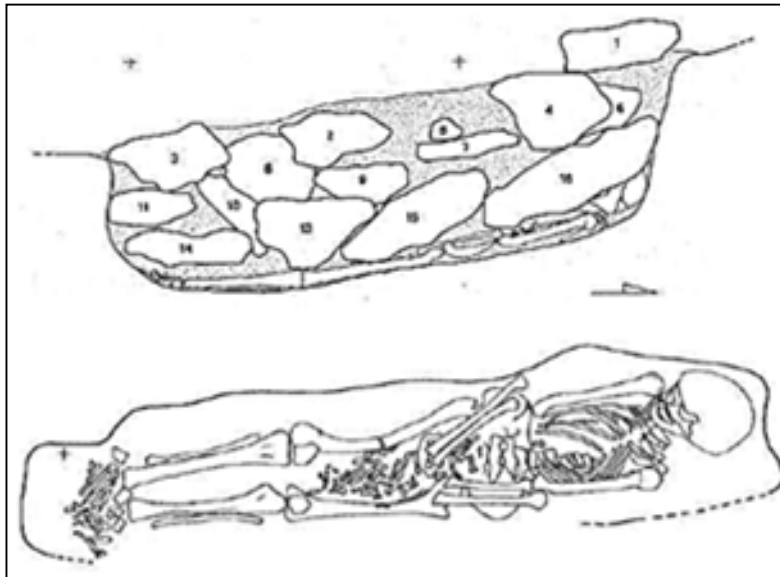


Fig.III.13.: Image of human burial Romito 7 (Martini, 2002).

The magnificence of the shelter-cave complex of Romito is attributed not only to the presence of the burials but also to the imposing rock with bovidae engravings. An imposing *Bos promigenus* figure rises among the other figures and is defined by features which give a detailed profile of a bull. Under the bull,

among the legs, there is the figure of another smaller sized bovidae, linear marks and a small unfinished bovidae head

III.4.1.1. Stratigraphy and chronology

The stratigraphic series of shelter-cave reveal human presence from the Gravettian phase to the Late Upper Palaeolithic with Neolithic presence (24,000-10,000 years ago).

It is possible to recognize two large blocks of stratigraphic cuts:

- cut 1-12, dating back to about 6,500 years ago;
- cut 13-44, dating back to between 11,000 (cut 13bis) and 18,750 years ago (cut 34).

The fieldworks of P. Graziosi interested the exterior of the shelter with a test pit between the two large rocks at the entrance. The investigation brought to light a sequence of 12 cuts. The two-stratigraphic series investigated by Graziosi were re-excavated in 2000 by the team of the University of Florence and are still ongoing. These investigations had the aim of verifying the Palaeolithic stratigraphy obtained by P. Graziosi collecting new samples for dating. Up to now, the new fieldworks in the cave highlight the following stratigraphy (Fig.III.14):

- Layer A: Final Epigravettian with Neolithic contaminations from the most superficial layer;
- Layer B: Final Epigravettian with few anthropic evidences;

- Layer C: Final Epigravettian with anthropic evidence, artefacts and hearth remains;
- Layer D: Final Epigravettian with abundant artefacts and hearth remains;
- Layer E: Final and Recent Epigravettian;
- Layer F: Ancient Epigravettian;
- Layer G: Final Gravettian with transitional levels from Final Gravettian to Ancient Epigravettian;
- Layer H: Final Gravettian;
- Layer I-M: Recent Gravettian.
- According to the stratigraphical investigation and radiocarbon dates, from the stratigraphy here below it is possible to appreciate the association between stratigraphy and chronology according to the dates reported in Table.III.4 (Bockley *et al.*, 2017).

III.4.1.2. Ochre recovery strategies and sampling conditions

The samples from this state were collected for this project by the author of this thesis with the aim of recovering ochre remains from prehistoric context with burials for comparative analysis. With the concession of Prof. F. Martini, it was possible to look at the collection of coloring materials collected during the new excavation campaigns (2005) from the Epigravettian levels of the site.

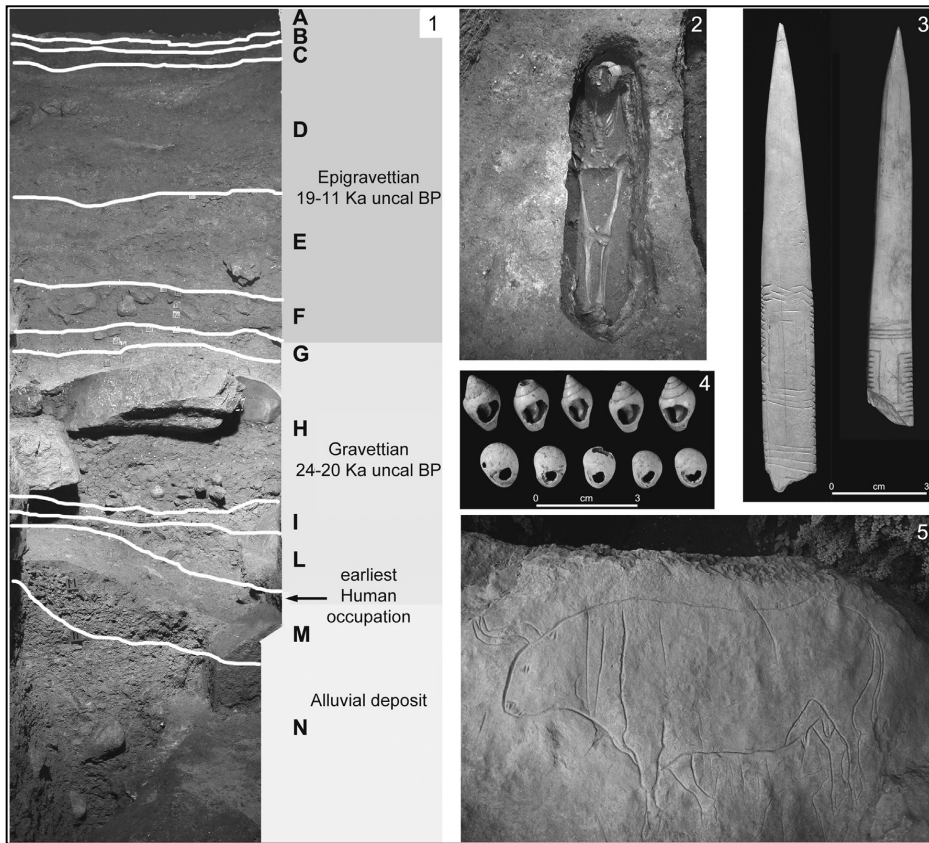


Fig.III.14.: Stratigraphical sequence of Grotta del Romito (Bockley et al., 2017).

The materials were conserved in plastic bags and wrapped with paper to avoid alterations and stored at Florentine Museum of Prehistory of Florence-“P.Graziosi”. A total of 14 fragments and about 1 gr of red ochre powder were sampled from levels D, E, F with the aim of carrying out comparative studies. They were sampled with the use of gloves and wrapped with white paper and placed in transparent sterile plastic bags to avoid contaminations for chemical analyses.

S.U.	Sample code	Date BP	Date cal BP CalPal2007_HULU	Range 2σ (a.C./cal BC) INTCAL 04
B	ROM 2	10,115±45	11,719±193	10,032- 9,458
B	ROM 1	11,000±45	12,913±100	11,094-10,913
B	ROM 1a	11,035±45	12,933±103	11,119-10,932
C	Beta-160,295	11,060±100	12,962±127	11,209-10,904
C2	Beta-160,296	11,060±100	12,962±127	11,209-10,904
C3	ROM 3-1	11,090±70	12,985±117	11,182-10,937
C3	ROM 3-2	11,075±50	12,964±102	11,145-10,951
C3	Beta-160,297	11,060±40	12,951±99	11,126-10,951
C4	Beta-160,298	11,380±70	13,279±135	11,426-11,170
C4	ROM 4	11,250±70	13,151±109	11,317-11,037
D	Beta-160,299	14,305±65	17,490±252	15,571-14,716
D1	Beta-160,300	11,580±70	13,462±120	11,668-11,329
D1	ROM 5-1	11,765±50	13,656±119	11,801-11,511
D1	ROM 5-2b	12,415±50	14,645±332	12,874-12,203
D5a	Beta-160,302	12,060±90	14,077±253	12,164-11,796
D5b	Beta-160,303	12,160±50	14,193±229	12,199-11,917
D8	LTL234A	12,170±60	14,204±232	12,224-11,908
D11	LTL238A	12,334±75	14,505±355	12,800-12,066
D13	LTL607A	12,258±75	14,355±291	12,642-11,972
D14	LTL603A	12,377±95	14,588±358	12,926-12,102
D15	LTL608A	12,331±55	14,495±344	12,714-12,087
D16	LTL601A	12,369±100	14,573±364	12,928-12,087
D20	LTL602A	12,438±85	14,689±346	12,972-12,188

D23	ROM 6-1	12,650±50	15,020±301	13,218-12,717
D23	ROM 6-2	12,545±50	14,884±290	13,086-12,354
D29	LTL1050A	12,494±75	14,802±311	13,024-12,253
D33	LTL14264A	13,300±100	16,227±429	14,280-13,404
D35	LTL1052A	12,970±150	15,806±478	13,910-12,972
E2	LTL1046A	13,650±120	16,676±324	14,786-13,841
E5	ROM 7	15,230±70	18,350±275	16,861-16,540
E5	LTL1047A	13,646±120	16,667±330	14,781-13,834
E8	LTL1590A	14,373±90	17,531±257	15,783-14,790
E10	LTL1591A	15,273±150	18,383±298	1,6937-16,156
E16	LTL1592A	16,129±100	19,254±253	17,527-17,118
F1	LTL1593A	17,376±90	20,830±300	18,939-18,286
F2	LTL239A	18,978±130	22,854±307	20,897-20,281
F31	LTL606A	18,483±95	22,093±319	20,377-19,569
G1	LTL236A	19,351±180	23,126±321	21,685-20,564
G2	LTL237A	19,373±90	23,135±275	21,501-20,686
H4	LTL604A	20,210±245	24,136±383	23,013-21,561
I	LTL1048A	23,475±190	28,387±354	25,977-25,408

Tab.III.4.: Radiocarbon dates of Grotta del Romito re-calibrated from raw dates in Bockley et al. (2017).

III.4.2. Grotta San Teodoro

The cave of San Teodoro, known since 1859 from Baron Anca's reports (Anca, 1860) is a large cavity at about 144 m a.s.l. at the foot of a cliff in the municipality of Acquadolci (Messina).

The cave is located on the Northern slope of a Jurassic limestone massif formed by a large room (60 m x 20 m) occupied by blocks fallen from the vault. The construction of a wall to defend the island from the Saracen raids totally closes the entrance to the cave and forms a type of small tower on the right side (Fig.III.15).

Following the discovery of Anca, systemic research was undertaken at the site: Gemmellaro (1867), de Gregorio (1925), Vaufrey (1928). However, since the 1940's human remains were brought to light by the excavations of Bonafede (1937), Maviglia (1942) and Graziosi (1943, 1947). The site of San Teodoro plays a key role in the reconstruction of the prehistoric population of Sicily (Graziosi, 1943, 1947; Graziosi & Maviglia, 1946).

The deposit returned several archaeological evidences relating to the Palaeolithic human occupation of the site. The study of the lithic industry confirms the typological attribution of the artefacts in flint and quartzite to the Final Epigravettian (Maviglia, 1942; Vigliardi, 1968, 1989).

Regarding the faunal remains, these are heterogeneous and offer key data to reconstruct paleoenvironments and paleoclimates during the Pleistocene in Sicily.

The faunal remains from the lower levels (sandy-clay) are: *Crocuta crocuta spelaea*, *Canis lupus*, *Vulpes vulpes*, *Sus scrofa*, *Elephas mnaidriensis*, *Cervus elaphus siciliae*, *Equus hydruntinus*, *Bos primigenius*, *Terricola savii*. Given the presence of hyena coprolite and traces of carnivore chewing on large mammals, the researchers suggest that the cave was used as hyena burrows about 40,000 years ago. Faunal assemblages from upper anthropic levels consist in remains of *Cervidae*, *Bovidae* and *Suidae*.

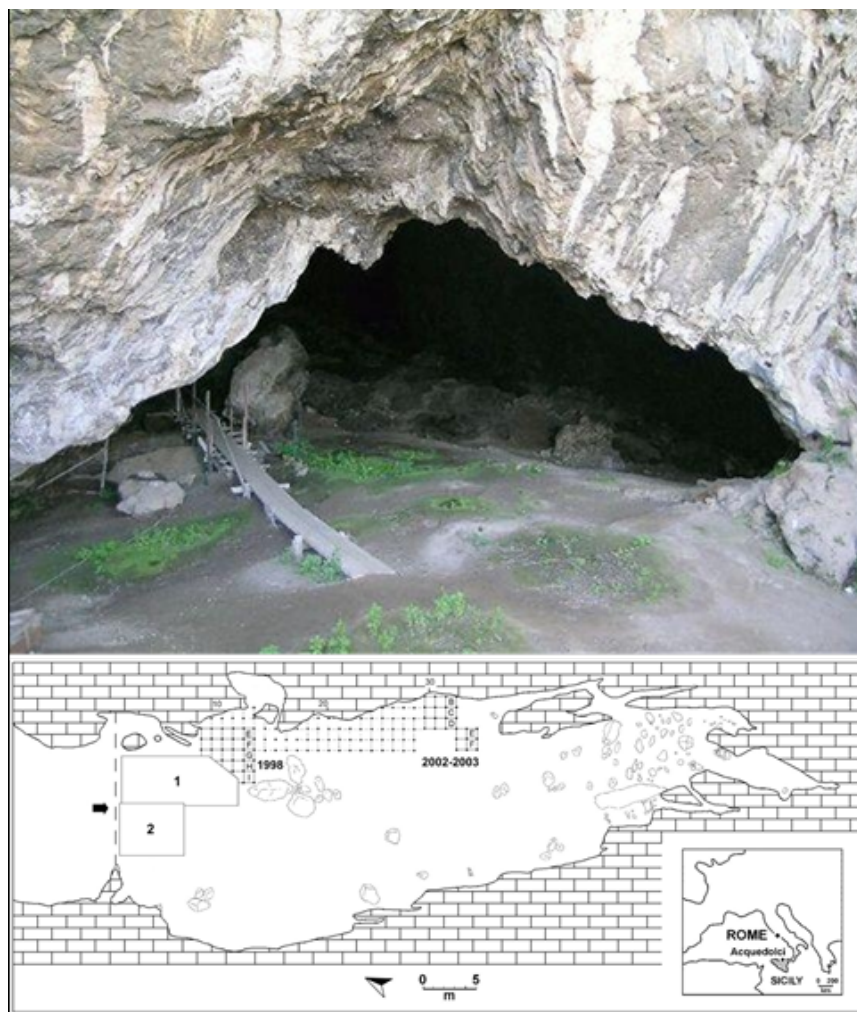


Fig.III.15.: Image of the cave's vestibule and planimetry of the archaeological surface of San Teodoro (Mangano & Bonfiglio, 2005).

Terrestrial gastropods, fresh water molluscs and bivalves were also collected from the archaeological deposit. The malacofauna is represented by endemic species of Sicily that were typical of late Pleistocene: *Mercuria similis*, *Pseudamnicola moussonii*, *Galba truncatula*, *Palorbis planorbis*, *Nacylus fluviatilis*, *Oxyloma elegans*, *Pyramidula pusilla*, *Chondrina avenacea*, *Chondrula pupa*, *Daudebardia rufa*, *Papillifera papillaris*, *papillifera solida*, *Cernuella cisaplina*, *Cernuella virgata*, *Cernuella* sp., *caracollina lenticula*, *Trochoidea pyramidata*, *Monacha cartusiana*, *Cochlicella acuta*, *Chilostoma planospira*, *Marmorana*

fuscolabiata, *Unio* sp., *Pisidium casertanum*. The systemic analysis of the remains suggests that the presence of these species in the cave is to be attributed partly to human action, and partly to carnivores (Esu *et al.*, 2007).

In any case, the relevance of the site is also attributed to human burials. In total, 7 individuals, 3 males and 4 females were discovered, mainly from layer E (Epigravettian) underneath a diffused ochre layer of 5 cm of thickness (Graziosi, 1947).

San Teodoro 1: a burial of a female individual lying on the left side who suffered from thalassemia (Correnti, 1967) (Maviglia, 1941; Graziosi, 1947). Traces of red ochre can be seen on the skull which is probably due to the contact with layer β . In total, 12 atrophic red deer canines were found inside the burial.

San Teodoro 2: a burial of an individual adult. Maviglia (1938) was only able to recover a part of skull remains.

San Teodoro 3: a burial of an adult male individual where only a part of the skull and some fragments of long bones are found due to dripping in the cave.

San Teodoro 4: a burial of an adult female individual where only bones anatomically connected in the upper part of the skeleton until the waist and some phalanxes of toes were found. Clandestine excavations in modern times devastated a large part of the skeleton which was, in any case, lacking feet. Graziosi's hypothesis (1943) is that the feet were found at a higher level from the head when buried and thus, it was only covered by a thin layer of sediments that disappeared before modern works. Compared to previous burials mentioned beforehand, the layer of ochre in this case was extended only on the higher area until the femurs. Some grave goods need to be highlighted: a small fluvial pebble at the height of the wrist, part of a deer antler on the left-

hand side and some bones spread around the animal itself. From Graziosi's conclusions, a hyena skull found not too distant from the skeleton would have been included in the grave goods.

San Teodoro 5: the only burial coming from layer B. It is characterized by few skulls remains, fragments of humerus and vertebrae. The gender of the defunct cannot be determined. An important aspect is the finding of skeletal remains inside a hearth in association with animal remains and lithic artefacts. Even this burial appears below the layer of red ochre.

San Teodoro 6: dubious burial location but probably originates from the same layer as the previous ones, it is represented more than likely from skeletal remains of an individual female (Pardini, 1975; Fabbri, 1995).

San Teodoro 7: even this burial, like ST6 is of dubious provenance. Nevertheless, the remains of an incomplete skull would be those of an individual adult, albeit with the sex unknown. Residues of red ochre of layer β , have been observed on the cranial bones.

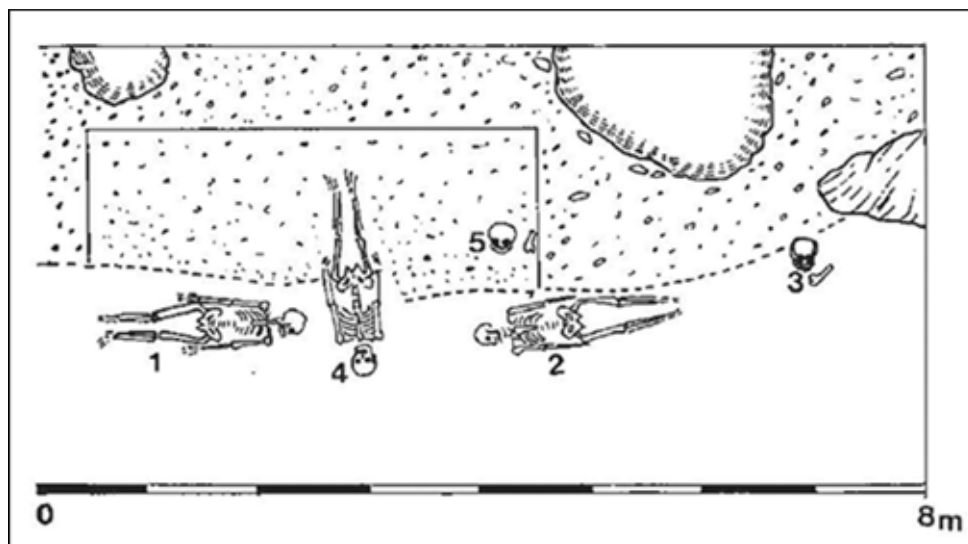


Fig.III.16.: Planimetry of archaeological surface with human remains from Grotta San Teodoro (da Palma di Cesnola, 1993 in Gazzoni, 2011).

III.4.2.1. Stratigraphy and chronology

The research at Grotta San Teodoro brought to light a Pleistocene deposit with Palaeolithic layers. The base level (layer G) is made of sand and clay (layer F-E) without anthropic evidence but characterized by abundant remains of faunal species living in Sicily during the Late Pleistocene.

Above these levels, there is layer D rich in anthropic evidence such as hearth remains and lithic artefacts typologically attributable to the Upper Palaeolithic and a thin red ochre lens (layer β) of anthropic origin too.

The upper layer, layer C, is formed by dark organic material rich in lithic industries. The successive layer B is composed of brown-reddish sediments of fine grain granulometry and little archaeological evidence (Graziosi, 1943, 1947; Bonfiglio, 1983; Mangano & Bonfiglio, 2005). The only available dates are obtained by U/Pa on human remains: ST1-10,000 \pm 3,000 years; ST2-20,000 \pm 6,000 years (Sineo *et al.*, 2002).

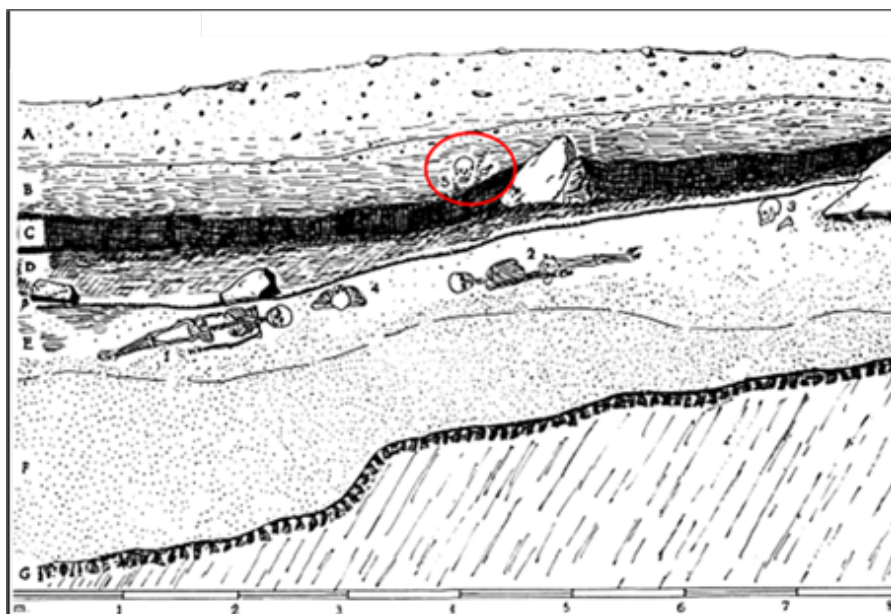


Fig.III.17.: Stratigraphy of Grotta San Teodoro (da Graziosi in Bonfiglio et al., 2005) with the highlighted area from which two of the ochre samples used for this research were collected.

III.4.2.2. Ochre recovery strategies and sampling conditions

The materials, also stored at the Florentine Museum of Prehistory of Florence for Grotta del Romito, have been viewed thanks to Prof. F. Martini. A total of 5 samples of red ochre were sampled with the same strategy and conditions of Grotta del Romito, among the colouring materials collected during the excavations conducted by P. Graziosi and C. Mavaglia in 1942.

A total of 2 samples were sampled from the sediment that filled skull 5. On the other hand, the other 3 samples were sampled as comparative materials for characterization purposes because they do not have a clear stratigraphic attribution.

III.4.3. Grotta di Pozzo

Grotta di Pozzo (Abruzzo, Italy) is a site at about 720 m a.s.l. located in the heart of the central-Southern Apennines, around the Fucino plain which was once occupied by a big lake.

The shelter was discovered in 1992 and systematically excavated from 1993 to 2014. In total, more than 24 m² of surface was excavated and 30 m³ of sediments was removed (Mussi *et al.* 2011). A survey of about 7 m² of extension and 15 m³ of depth was carried out in the external area of the shelter. The fieldworks brought to light one of the most completed Late glacial sequence of South-Central Italy.

The lithic artefacts found at the site identify different chrono-cultural horizons, from Ancient Epigravettian to the Sauveterrian phase.

Traces of domestic activities are recognizable for the presence of combustion structures, hearths and masses of ashes deriving from the cleaning of the hearths, combusted vegetable residues and pits interpreted as oval cooking structures covered in animal skin and filled with water heated to boiling point using burning rocks (Piarulli, 2015).

Bone artefacts are rare and only an awl, two fragments of points/awls and some artefacts from Final Epigravettian units were found.

On the contrary, several ornamental elements were noted: perforated deer canines and shells (with ochre residues in some cases) of *Cyclope neritea*, *Cyclope donovani* and *Mitra* sp. (Final Epigravettian), and *Columbella rustica* and *Antalis dentalis* (Sauveterrian). A worthy element is also a semilunar valve of *Glycimeris* sp. with engraved parallel notches filled with red ochre.

Faunal remains largely attributable to typical mountainous species have been collected from Palaeolithic and Mesolithic units of the site. The remains of the more ancient levels which are rather poorly and badly conserved, attest the presence of *Rupicapra rupicapra* and *Capra ibex*. The numerous and easily identifiable bone remains from levels attributable to the Final Epigravettian, in addition to chamois and ibex, confirm the presence of *Cervus elaphus* and *Sus scrofa*.

The remains of *Equus hydruntinus*, *Capreolus capreolus* and *Bos Primigenus* are rare, but identifiable. Among the carnivores, only the fox is present, *Vulpes vulpes*. It is possible to also recognize some elements attributable to *Lepus* sp., *Marmota marmota* and *Erinaceus europaeus* (Mussi *et al.*, 2003). The microscopic observations on some bone elements show cut marks that attest hunting activities oriented mainly towards medium sized ungulates such as chamois and ibex. Of note is a distal humerus of a marmot where traces of carcass

disarticulation have been observed. The age of death, established from the tooth eruption stage, shows the high percentages of young adults and the scarcity of adult-senile individuals. This element indicates a seasonal occupation of the site during summer-autumn period.

It is also possible to identify the remains of fish such as *Salmo trutta* (Russ, 2008; Russ & Jones, 2009) and birds such as *Tetrao tetrix*.

For the Holocene units, next to the few and in some cases combusted fragmented remains of *Cervus elaphus*, *Sus scrofa*, *Capra ibex* and *Rupicapra rupicapra*, it is possible to notice remarkable accumulations of endemic terrestrial gastropods, the *Helix delpretiana* (Giusti, 1971). Of particularly importance which needs highlighting, is the finding of carapace fragments of *Testudo* sp. (Mussi *et al.*, 2008).

Lastly, the parietal art in the limestone wall at the bottom of the cave. It is possible to observe four engravings: a horizontal notch, a vulva in low relief (about 90 mm high), a vulva obtained from a small slit in the wall (50 mm long and up to 20 mm wide) and a female profile about 27 mm long of Gönnesdorf-Lalinde type (Mussi *et al.*, 2011).

III.4.3.1. Stratigraphy and chronology

The stratigraphic sequence (Tab.III.5) is characterised by seven lithostratigraphical units (Mussi *et al.* 2003).

Unit I in the Northern-Eastern part of the cave, is set on rounded limestone blocks and formed by two alternating pebbled levels on two sandy levels deposited towards 23,000-21,000 cal BP. The confirmed dating is based on

chronostratigraphic correlations with a high level of fluvial-lacustrine sediments of the Fucino lake attributable to the Last Glacial Maximum (Giraudi *et al.*, 1995, 1997, 1999).

Unit II, which can also be found in the north-east of the cave, is formed from a deposit of large sharp-edged blocks collapsed by the vault, with a diameter of more than 50 cm and an unclassified heteromeric deposit with angular pebbles between 2 cm and 20 cm of diameter.

Following on from Unit I and Unit II, Unit III is made up of layered debris, *éboulis*, in which poor levels of matrix with coarse and angular clasts alternate with richer levels of matrix with angular but smaller sized clasts. This alternation is due to the processes of sliding fragments on icy surfaces and the runoff phenomena. Thin anthropic levels of organic material and archaeological evidence are intercalated at these levels. The nature of the levels of this unit show an improvement of climatic conditions compared to the lower levels.

Unit IV follows Unit III which is separated by an erosion surface attributed to the Bølling-Allerød interstadial stage. Even Unit IV like Unit III is made up of *éboulis* layered deposit which is less cemented and coarse and in which scree and anthropic levels alternate with fragments of charcoals and reddish-brown organic materials.

Unit V, which concludes the Pleistocene succession, confirms a climatic deterioration because it is made up of fine colluvial sediments with a coarse fraction of fine gravel and sub angular limestone.

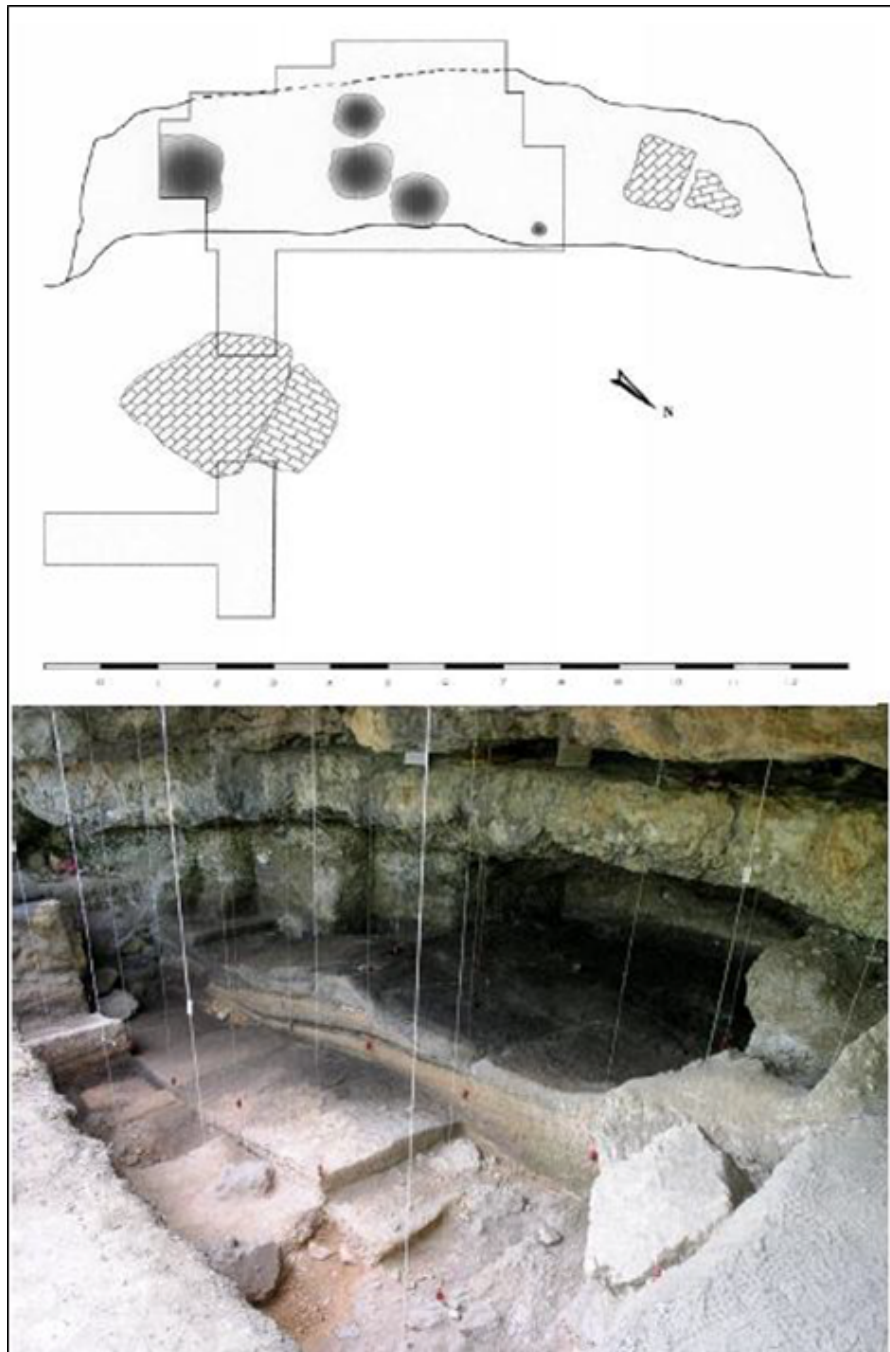


Fig. III.18.: Planimetry of the archaeological excavated surface and picture of the interior cave of Grotta di Pozzo (Catelli, 2014).

The last two units, *Unit VI* and *Unit VII* initiate the Holocene sequence.

Unit VI, on the eastern side of the cave which was formed during Early Holocene, is separated by the *Unit V* from another erosion surface with lime

scale deposits of other medium-fine material that intercalate with accumulations of shells of terrestrial gastropods on cinerite lenses of anthropic origin. Circular pits attributable to the Neolithic period cut these levels. The *Unit VII*, which closes the sequences, has a very heterogeneous composition given the presence of gastropod shells, ashes, limestone pebbles and ceramic fragments. In the northern sector of the cave, the Unit VII was removed by post-Neolithic erosive processes (Mussi *et al.* 2008).

III.4.3.2. Ochre recovery strategies and sampling conditions

The recovery of ochre pieces was carried out with a strategy set up during the fieldworks director Prof. M. Mussi, according to a dual modality: *in situ* recovery with localization of the pieces in the squared plane (quadrants 1m x 1m identified by the intersection of letters and numbers) with X, Y, Z coordinates; sieving recovery of sediments.

About 12% of the ochre pieces were recovered with localization in the horizontal plane and listed in a system of orthogonal axes generated by point 0 of the caves. The remaining 88% of the elements were recovered through dry sieving in front of the cave with meshes of 0,2cm to recover the more delicate fragments.

The sediment taken from the quadrants at the bottom of the cave (band 6) was water sieved being rich in ichthyofaunal remains.

S. U.	Dated material	Date BP	Date cal BP CalPal2007_HULU	Range 2 σ (a.C./cal BC) INTCAL 04
PS 19	Bone	18,910 \pm 260	22,725 \pm 429	21,472-20,013
PS 15	Bone	18,550 \pm 250	22,163 \pm 412	20,633-19,312
PS β	Charcoal	15,790 \pm 90	19,014 \pm 228	17,264-16,896
PS α	Bone	14,100 \pm 70	17,339 \pm 229	15245-14421
PS6e	Bone	12,820 \pm 130	15,381 \pm 400	13,656-12,734
PS6c	Bone	11,120 \pm 60	13,020 \pm 126	11,195-10,961
PS5	Bone	12,590 \pm 40	14,944 \pm 289	16,877-15,249
PS1	Fish vertebra	12,320 \pm 50	14,473 \pm 339	12,669-12,085
Shell-midden	<i>Helix delpeiriana</i>	10,290 \pm 80	12,123 \pm 243	10,614-9,806
Shell-midden	Charcoal	9,370 \pm 80	10,588\pm106	9,112-8,344
Shell-midden	Charcoal	9,140 \pm 70	10,335\pm82	8,548-8,249
Shell-midden	Charcoal	9,110 \pm 80	10,314\pm88	8,566-8,020
Shell-midden	Charcoal	8,840 \pm 100	9,921\pm184	8,247-7,653
Shell-midden	Charcoal	8,790 \pm 110	9,873\pm202	8,213-7606
Shell-midden	Charcoal	8,110 \pm 90	9,035\pm166	7,446-6,711

Tab.III.5.: Radiocarbon dates of Grotta di Pozzo.

Water sieving was done in a lower area of the cave where a tank was positioned. The sediment was sieved and left to dry in the open air.

Once dried, they were taken directly to a station set up in front of the cave. All the recovered elements from sieving of the sediments from each quadrant was wrapped in aluminium involucre and conserved in a transparent and sterile plastic bags, which were used to collect materials taken with sieving. During the general organization for this thesis in the laboratories of the Sapienza-University of Rome, each element was extracted from a common bag and progressively numbered starting from 1. For this occasion and as was described in the previous chapter, a database was created in order to insert all

the information and broaden the computerized archive of the site. The general organization of all ochre pieces collected from 1995 to 2014 was carried out by the author of this thesis for this project according to the criteria described in the chap. II of this work.

III.4.4. S'Omu e S'Orku

S'Omu e S'Orku is located along the western coast of Sardinia near Arbus (Cagliari, Italy). The site was identified in 1982 by some tourists who, by chance, found skeletal remains of an individual adult near the shoreline, totally covered by red ochre. In association, a shell of *Charonia lampas* was also found. The name S'Omu e S'Orku derive from the Sardinian language and literary means "the ogre's home".



Fig.III.19.: Panoramic view of S'Omu e S'Orku and localization of the archaeological deposit (Melis & Mussi, 2016)

The human remains were transferred and conserved in a small museum in the village of Guspini (Medio Campidano, Sardinia) under the supervision of "Neapolis Archaeological Association".

Systematic research was carried out in 2002 due to the interest shown by Prof. R. T. Melis (University of Cagliari) and Prof. M. Mussi (Sapienza, University of Rome). The fieldworks brought to light the identification of the area where was found the reddish skeletal remains. Skeletal samples were taken for dating with C14. The absence of collagen did not provide any data.

During the fieldworks conducted in 2007, a part of another skeletal remains was recovered which belonged to another individual adult (SOMK2). Several human remains of a third individual adult were found in 2011 (SOMK3). During the excavation, another specimen of *Charonia lampas*, shells and micromammals remains, rare lithic artefacts and ochre fragments were recovered. Since 2011, systemic investigations have been conducted yearly and the archaeological materials are being studied.

The investigations realized by Prof. R.T. Melis and Prof M. Mussi have not only brought to light human remains, but also fundamentally important archaeological materials to understand the role of the site. The systemic excavations returned lithic artefacts, several faunal remains of micro mammals (*Prolagus sardus* and *Tyrrhenicola henseli*), sea shells of *Charonia lampas*, *Cyprea* sp., *Columbella rustica*. The lithic assemblage shows few elements in flint and obsidian such as small flakes, blades and bladelets which does not give specific tecno-typological information. Non-marginal data is the presence of obsidian that is abundant in the nearby isle of Carlo Forte (Sardinia). Human remains of three individual adults certainly constitutes the most important archaeological evidence of the site and allows us to hypothesize the main funerary function of the shelter during Mesolithic period.

SOMK1: skeletal remains of an individual adult covered by red ochre (Floris *et al.*, 2012). A notable accumulation of pigment is observed near the skull and

long bones. There is also a shell of *Charonia lampas* with red ochre traces (Melis & Mussi, 2016). The bones, as previously reported, were fortuitously found and for this reason little scientific information was recovered when they were discovered and there are no photos or graphical representations. There is some data thanks to the recognition of the exact location of the finding during recent excavations. Systemic fieldworks of the area showed traces of burrow of *Prolagus sardus*.



Fig.III.20.: Human skeletal remains with red ochre residues of burial SOMK 1 (Melis & Mussi, 2016).

SOMK2: lower portion of the skeleton of an individual adult dating back to 8,596-8,373 cal BP (Melis *et al.*, 2012). The grave which is strongly eroded, returned pelvic bones, lower limbs and the feet of an individual. Chest remnants and upper limbs found not too far away would seem to belong to the same individual (Floris *et al.*, 2012). This might be due to the falling of blocks on the buried individual. Fragments of red ochre have been collected from the sediment around the skeletal remains of SOMK2 (Melis *et al.*, 2012).

SOMK3: a partially intact individual adult was found among the higher part of the refuge on the rocky surface and level F. Flexed lower limbs and part of an upper limb remains of the skeleton were found in association to a *Charonia lampas* with traces of red pigment and other shells with ochre of *Cypraea* sp. and *Columbella rustica* as grave goods (Melis & Mussi, 2016). Different sized fragments of red ochre and crayons (Melis & Mussi, 2016) were collected from the archaeological deposit during the most recent fieldworks.

III.4.4.1. Stratigraphy and chronology

The complex stratigraphy sequence was brought to light by the rock shelter area between Quaternary dunes and Palaeozoic reliefs. Differing from the current one on the beach, the original opening was connected internally by an aeolianite wall, sedimentary rocks which originated from the diagenesis of limestone sands and aeolian deposits

Stratigraphic studies reveal a lithostratigraphy strongly damaged by collapses, aeolian erosion processes and weathering (Melis *et al.*, 2012; Melis & Mussi, 2016). An irregular layer of Late Pleistocene aeolianites is at the base of this sequence and is covered by a sandy layer (layer F) formed by detrital and cinerite accumulations and dating back to 8,950-8,850 cal BP.

Layer F, with a height of about 20 cm filling some depressions in the Aeolianites, is characterized by a sediment of dark grey colour which is rich in charcoal remains and micro-mammal bone fragments such as *Prolagus sardus* and *Tyrrhenicola henseli*.

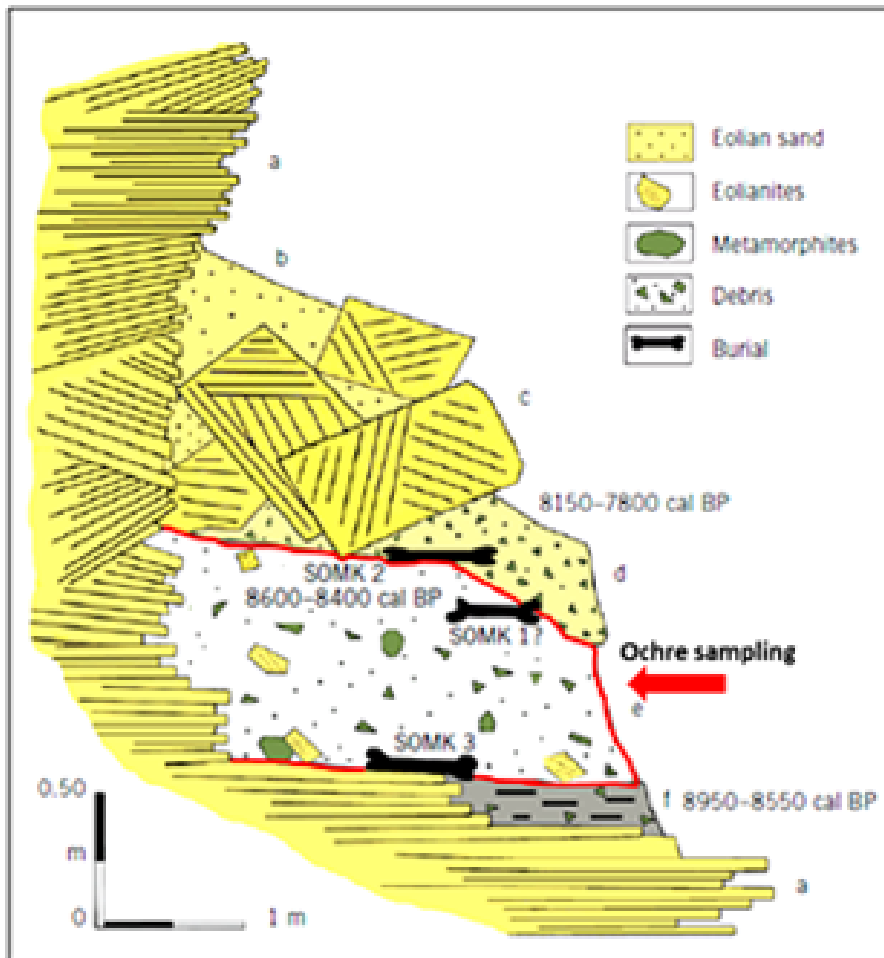


Fig.III.21.: Lithostratigraphic sequence of S'Orku e S'Orku: a) Pleistocenic aeolianites; b) aeolian deposits; c) rock fall; d) debris slope with sand matrix and ashes; e) sandy loam slope deposits with metamorphic and aeolianite debris and blocks; f) sandy gravel deposit rich in charcoal fragments (Melis & Mussi, 2016).

Layer E, which follows layer F, is more than 1 m thick with a dark grey colour and is composed of sloping deposits: aeolianite and metamorphic pebbles and blocks accumulate through runoff processes of the rocky slopes and weathering. Plentiful charcoal remains are attributed to probable natural fires in which it is possible to see traces of micro faunal remains too.

Layer D covers layer E with sloping deposit accumulations. Radiometric dating places this layer between 8,150 and 7,800 cal BP.

Layer B, which follows on from the previous one is formed by aeolianites from the collapse of the sheltered roof.

The sandy layer of Aeolian origin, layer A, closes the sequence.

Laboratory	Dated material	Date cal BP
AA-79862	Charcoal	7.944±56
AA-76545	Human bone (SOMK2)	8.484±61
AA-76546	Charcoal	8.675±65

Tab.III.6.: Radiocarbon dates of S'Ormu e S'Orku (Melis & Mussi, 2016).

III.4.4.2. Ochre recovery strategies and sampling conditions

The site was sampled in the excavation campaign of 2014. The sampling strategy was set during the excavation of an archaeological surface divided by 1 m x 1 m quadrants from a point 0. The sediment taken from each quadrant was sieved in proximity to the archaeological field where a specific area was set up for this operation. Dry sieving of the sediment was realized with meshes of around 0,2 cm which is typically used for the recovery of remains that were non-localizable during the excavation. A total of 4 samples were recovered by the sediment excavated from the same level in which SOMK1 was presumably found and from the level in which SOMK2 was found in a punctual and systemic way. After the collection of the samples, the ochres were wrapped in aluminium involucres and preserved in small sterile plastic bags containing a label with the information about year of excavation, progressive number of the finding and the material.

Site	Type of context	Cultural attribution	Recovery strategy and sampling conditions	N. of samples
La Garma A	Domestic	Palaeolithic/Mesolithic	Identification <i>in situ</i> by spatial coordinates (x,y,z)/Sieving	840
Los Canes	Funerary	Palaeolithic/Mesolithic	Identification <i>in situ</i> by spatial coordinates (x,y,z)/Sieving	1222
Arangas	Domestic	Palaeolithic/Mesolithic	Identification <i>in situ</i> by spatial coordinates (x,y,z)/Sieving	373
Grotta del Romito	Domestic/Funerary	Palaeolithic	Representative sampling from ochre collections	14 and 1 gr of powder
Grotta San Teodoro	Funerary	Palaeolithic	Representative sampling from ochre collections	5
Grotta di Pozzo	Domestic	Palaeolithic/Mesolithic	Identification <i>in situ</i> by spatial coordinates (x,y,z)/Sieving	140
S'Orku e S'Orku	Funerary	Mesolithic	Sieving	4

Tab.III.7.: Summary table of total of ochre samples and sampling conditions.

Chapter IV.

General evaluation of materials

The corpus study appears well-assorted and heterogeneous consisting in raw and modified pieces. The selection of materials was decided after a long work of inventory with the aim in mind to offer new contributions to the knowledge of ochre exploitation in Prehistory. At the beginning of this research, it was possible to assess the materials that were collected in several archaeological sites of the Cantabria region. This region is a key area for the development of Upper Palaeolithic cultures that intensively exploited ochre as pigment in parietal paintings on rock surfaces.

The access to the materials of Los Canes and Arangas represented an exceptional opportunity of study both the importance of sites regarding the prehistoric peopling of Asturias, and for the presence of human burials in Los Canes dating back to the Mesolithic. The materials inventoried as "ochre" were various and came from both Palaeolithic and Mesolithic levels of the two sites. In order to manage the information that would derive from the study of the finds, it was decided to set up a database in Excel format.

Name and *type* of the site are the first items of the database followed by *year* (about the year of the fieldworks, when the remains were collected), *materials*, *inventory ID*, *level*, *stratigraphic unit*, *square*, *sector*, *X*, *Y*, *Z coordinates*. All this information was indicated on the label of each piece of ochre placed in a single transparent plastic bag, divided into containers for each stratigraphy unit.

Starting from the stratigraphical position, it was possible to chronologically frame the object also with radiocarbon dating available for Los Canes (Arias, 2002) and Arangas (unpublished) provided by Prof. Arias Cabal, director of the fieldworks.

Cultural attribution and absolute dating are the following items. The second part of the database collects all data taken from the organization and preliminary observation of the pieces. For this reason, the following items are insert for each finding: *length, width, thickness, mass, colour, raw material, superficial alterations, observations.*

Firstly, the materials of Los Canes were observed. The pieces were extracted from the plastic bags where were deposited and they were weighed, measured and divided by the external colour.

The measurement of dimensions (length, width and thickness) brought about some problems in that there were many small and easily damageable pieces. For this reason, an electronic calibre was used, and the ends of this tools were covered by a transparent film to avoid alterations of the surfaces.

Another problem occurred to define the colour. Starting with the idea of following the procedures already applied for the study of colouring materials, the Munsell Soil Colour Charts were chosen.

The reliability of the detection, however, involved the estimation of the colour starting from the trace left by the mineral on a white porcelain tile (Watts, 1998, 2002) and observed in a natural light using the Munsell Code to define the colour.

This detection was a destructive procedure and for this reason it was decided to avoid it. Therefore, the problem of how to obtain an objective colour definition remained.

By starting with the assumption that the primary constituents of ochre are iron oxides and hydroxides which have a range of well-defined colours (Cornell & Schwertman, 2004), it was decided to estimate the visible colour in fractured points using a magnifying glass. In case fractured points were not well visible, the colour was detected observing some areas of the surface that were clear and clean, without signs, concretions or other elements that could have impeded its reading.

In regards the light, an artificial white cold light was used that was not susceptible to variations like sunlight. The colour was coded according to the Munsell Soil Color Charts which in any case offered a standardized system to define the dyes based on three fundamental parameters: tonality, brightness and saturation.

During the general organization, it was decided to replace the used and damaged plastic bags and to equip each element with an additional new label which had a new inventory number (sample ID) as well as the one assigned during the recovery *in situ* for the insertion in the database created for this research.

A number starting from 1 was progressively assigned to each piece. In the case where the same bag contained various elements, a letter was added to the Arab number.

This procedure of general organization of the material was also applied for the materials of the Arangas site.

At the end of the work on the findings of Los Canes and Arangas, and with the aim of obtaining valid comparisons for the European continent, it was decided to add samples from sites in another key region for the development of Palaeolithic human cultures: the Italian Peninsula.

With the objective of evaluating the anthropic exploitation of ochre in function to the local adaptation of hunter-gatherers occupying these two European areas, there was necessary to search contexts within the Italian Peninsula with accessible ochre collections from Palaeolithic and Mesolithic deposits.

The materials from Grotta di Pozzo were chosen. The lithic ochred artefacts from the Epigravettian and Sauveterrian levels as well as ochre residues on shell ornaments were already studied for the master's thesis of the author (Catelli, 2014). A collection of about one hundred pieces were prepared according to the validated procedure for Los Canes. The presence of ochre from the Mesolithic burials of Los Canes led us towards the research of ochre samples from other European funerary contexts for a synchronous and diachronous study.

It was decided to request the accessibility of materials from the Mesolithic sites of S'Orku and S'Orku in Sardinia (Italy). During the fieldworks in June 2014, which the author of this thesis participated in, the site returned some ochre fragments from the same levels in which human remains of two individuals were found.

As already mentioned previously, the site is known for ochred skeletal remains of a male individual dated to Mesolithic. Furthermore, S'Orku e S'Orku is a key site in the prehistoric occupation of Sardinia.

There were few samples available in comparison to the quantities from Los Canes and Arangas. However, these ochres are unique for the key role of the site and value of its burials. In total, 4 pieces of red ochre were sampled. Furthermore, it was possible to collect some red ochre samples from Grotta del Romito (Calabria, Italy) and Grotta San Teodoro (Sicily, Italy) which are two main sites for the presence of prehistoric burials. The samples were extracted for physical-chemical analysis to search variability of raw colouring materials in prehistoric funerary contexts.

The availability of ochre samples from Palaeolithic and Mesolithic sites in the Cantabria region and in Southern Italy provided both a diachronic analysis over time, and a synchronic analysis over space, from a comparative research. Furthermore, the possibility of viewing the materials of La Garma A was allowable. Even though the study was already well assorted, due to issues of time, it was decided to view all materials available and stored in the University of Cantabria and at the Museum of Prehistory and Archaeology of Cantabria where a specific permit was required.

The main goal is to estimate the representativeness of the raw materials in the site and the intensity of anthropic exploitation according to the following criteria:

- *Colour*: identification of the main tints to estimate the representativeness of the classes of ochres in the archaeological deposit as an indicator of anthropic selection;
- *Mass*: evaluation of the distribution of pieces by colour, in function of the mass in a diachronic sense;

- *Dimensions*: evaluation of the general distribution of the materials for dimensional classes in function to each stratigraphical unit to estimate the compositional variability of the assemblage. Calculation of the Pearson correlation coefficient between the average total mass of the materials and the average values of the maximum lengths per level to verify the ratio between dimension and mass;
- *State of conservation*: typological differentiation of the materials to establish the agent (natural/anthropic) responsible of its morphology, to estimate the level of anthropic exploitation to the site;
- *Shannon-Weaver diversity index (H)*: calculation of the Shannon-Weaver diversity index to assess the richness of ochre assemblage in a diachronic way and to define the probability that an element falls within one of the established categories based on the researcher's subjectivity;
- *Evenness*: calculation of evenness to define the degree of homogeneity according to the distribution of elements in the same categories used for the diversity index;
- *Fragmentation index*: calculation of the fragmentation index to evaluate the fragmentation of the archaeological collection for each unit of the deposit.

IV.1. Los Canes

Los Canes is a narrow and long cavity that opens inside carboniferous rocks (*Barcaliente-Valdeteja*) excavated by karst phenomena. It is known that the circulation of water underground can favour residual accumulations of iron

ores in the cave, even if ferruginous crusts can be generated by precipitations of Fe-oxides due to variations in PH or microbiological activities in the cave, like the Soplao cave in Cantabria, Northern Spain (Gázquez & Calaforra, *et al.*, 2011). For Los Canes cannot be excluded ferrous deposits in karst environment for internal circulation of water, changes in PH or microbiological activities as the impossibility of a direct exploration of the cave for current logistical impediments to access, does not allow to refute this hired. The macroscopic observation of the materials does not show the presence of inclusions or impurities as indicators of genetic processes. For this reason, this aspect will be studied further through provenance research with the aim of recognizing the geological sources of raw materials. The evaluation of the materials according to the established criteria allows us to define the anthropic origin of the materials present in the archaeological deposit.

IV.1.1. Colour

The colour evaluation allowed us to detect the tints in a range from red to yellow. To simplify the presentation of data, all tints that have been coded through the Munsell Soil Color Charts will be grouped into two large colour classes (red and yellow) in this chapter. (Tab.IV.1) Red is the predominant colour. About 97% (n.1180) of the elements fall within this collection while only 3% (n.42) falls within the yellow one. A general distribution of pieces by colour in a diachronic way highlights a larger concentration of red elements in the 2C level that falls drastically in units 3A, 3B, 3C and 4. A new increase is observed in units 5 and 6III (Fig. IV. 1).

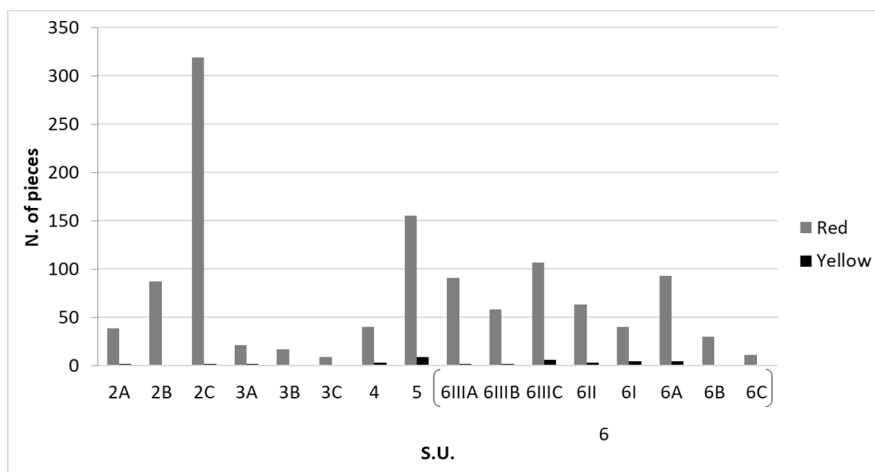


Fig.IV.1.: Los Canes: distribution of number of red and yellow ochre pieces collected from each stratigraphic unit of the archaeological deposit.

IV.1.2. Mass and dimensions

By evaluating the distribution of elements based on mass (Fig.IV.2), the 2A unit (Solutrean) returns a total of 7,05 gr (41 pieces) of which 7,3 gr of red material (39 elements) and 0,02 gr (2 elements) of yellow materials. An increase is registered for unit 2B where 25,69 gr of red ochre is present (87 elements). This quantity almost doubles in unit 2C 45,81gr (319 red elements) and 0,51 gr (4 yellow elements).

In the passage from Magdalenian to Azilian, it is interesting to notice the comparison between the number of pieces (319) of unit 2C and unit 3A (21). Despite the conspicuous number of elements counted at unit 2C, the mass of red ochre is greater at unit 3A even if there are fewer elements, which are evidently heavier. For the yellow ones, it can only count 2 pieces for a total of 0,25gr.

Unit 3B approximately refers to the same number of red vestiges (n.17) that have a lower mass when compared to S.U. 3A (21,67 gr). The unit did not return yellow ochres.

The continuous decrease in level 3C with a total mass of 7,44 gr for 9 red pieces. An increase is observed in S.U. 4 with 17,6gr of red ochre and only 0,12 gr of yellow ochre.

A noticeable increase characterizes unit 5 with several counted elements (n.155) less than half of S.U. 2C, but with a mass of 138,57 gr. A total of 3,18 gr of yellow ochre was collected from this unit.

Units 6IIIA (54,25 gr) and 6IIIB (58,28 gr) have similar quantities of red material. Yellow material is very scarce in both units at 6IIIA (2,3 gr) and 6IIIB (0,02 gr).

List of tints in the Munsell Soil Color Charts	
Red	Yellow
10R 3/2 dusky red	10YR 5/8 yellowish brown
10R 3/4 dusky red	10YR 6/6 brownish yellow
10R 3/6 dark red	10YR 6/8 brownish yellow
10R 4/2 weak red	10YR 7/6 yellow
10R 4/3 weak red	10YR 7/8 yellow
10R 4/4 weak red	10YR 8/8 yellow
10R 4/6 red	7.5YR 4/6 strong brown
10R 4/8 red	7.5YR 5/6 strong brown
10R 5/3 reddish brown	7.5YR 5/8 strong brown
10R 5/6 red	2.5Y 6/8 olive yellow
1R 5/8 red	
2.5YR 3/4 dark reddish brown	
2.5YR 4/2 weak red	

2.5YR 4/3 reddish brown
2.5YR 4/4 reddish brown
2.5YR 4/6 red
2.5YR 4/8 red
2.5YR 5/4 reddish brown
2.5YR 5/6 red
2.5YR 5/8 red
2.5YR 6/8 light red
5YR 4/4 reddish brown
5YR 4/6 yellowish red

Tab.IV.1.: Los Canes: list of tints in Munsell Soil Color Charts approximate in two set of colours: red and yellow.

An increase is seen in S.U. 6IIIC with a mass of 103,35 gr of red ochre. There is also a very scarce quantity of yellow ochre: 1,13gr. In regards 6II and 6I, the mass of red material is almost the same; 6II (30,17 gr) and 6I (35,5 gr). The yellow ochre collected is 0,79 gr (6II) and 2,65 gr (6I) respectively. An increase in red ochre is registered for unit 6A with 51,66 gr. The quantity falls progressively in the S.U. 6B (20,86 gr) and 6C (8,44 gr). Even if in these units, the quantities of yellow ochre are lacking: 6A (2,8 gr), 6B (0,18 gr) and 6C (0,02 gr).

As previously shown, the archaeological deposit of Los Canes has taphonomical problems which concern the origin of S.U. 5 and the units of the IV millennium A.D. (6III-6II-6I-6A-6B-6C) with excavated pits for the deposition of defuncts. Nevertheless, the abundance of very small pieces could be due to the fragmentation of more voluminous blocks (Salomon, 2009, Dayet, 2013). This element highlights a problem of representativeness for the ochre quantities that effectively arrived at the site.

The evaluation of the density of mass in each stratigraphic unit in function to m^3 of sediment excavated is required to evaluate the distribution of materials in a diachronic way and deal with the taphonomical aspects of the deposit. As is shown in the graph (Fig.IV.3), the density of red ochre for units 2A, 2B and 2C is very low.

A remarkable increase is seen in S.U. 3A which returns the highest value compared to the other units. This high density is associable with a red lens highlighted in the same stratigraphic unit. The red ochre lens in the soil allowed to distinguish S.U. 3A from S.U. 3B inside the block 3. The S.U. 3A in the central-southern section of the western part of the vestibule appears to be characterized by a red ochre lens of around 1-2 cm thick under which a layer of about 2-3 cm of black soil is present with abundant small sized clasts like unit 3B (Arias, 2002). From S.U. 3B and S.U. 3C, the density of red ochre gets smaller. A new increase is registered for S.U. 4 while the density at S.U. 5 is poor. In regards the units 6IIIA, 6IIIB and 6IIIC, it was possible to calculate the density of ochre for the whole 6III block in that it did not have the excavated m^3 for the single S.U. The 6IIIA, 6IIIB and 6IIIC consist in the filling of structure 6III and thus, the data is useful considering a quantitative evaluation. In the S.U. 6III, the density is noticeable compared to the previous units.

The density decreases in S. U. 6II to then increase once again in S.U. 6I and 6A. In S.U. 6B and 6C, the density decreases with concentrations quite similar to each other.

As far as density of yellow ochre in concerned, the material concentration is similarly quite low in all stratigraphic units except S.U. 2B, S.U. 3B and S.U. 3C which are totally absent.

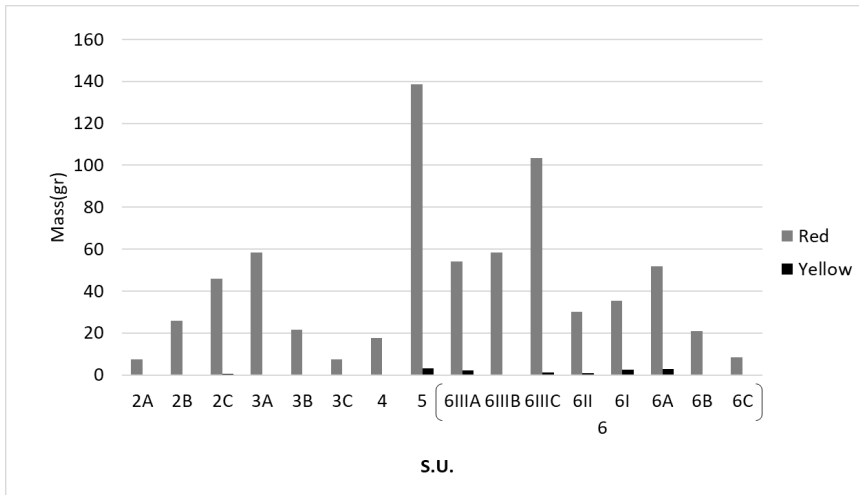


Fig.IV.2.: Los Canes: distribution of red and yellow ochre specimens in function of the mass in grams.

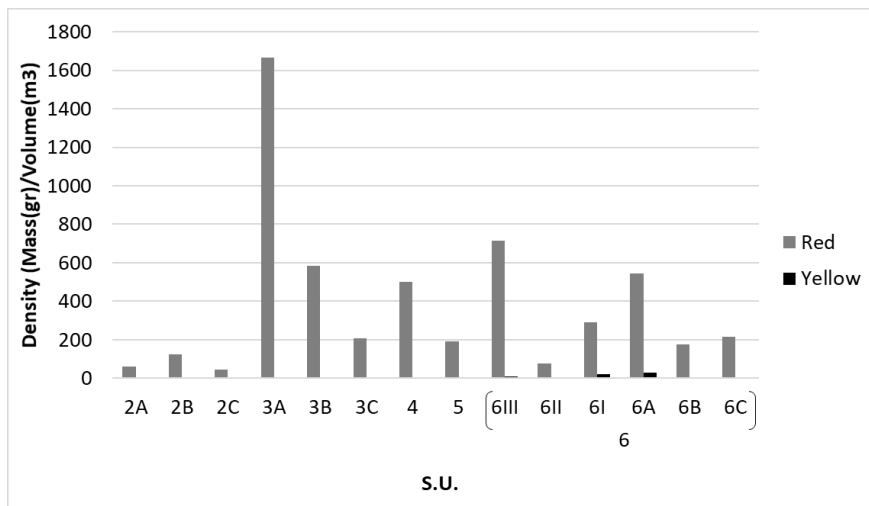


Fig.IV.3.: Los Canes: distribution of ochre specimens in function of the density $M(\text{gr})/V(\text{m}^3)$.

The size of the pieces is in a well-defined dimensional range of 2-32,50 mm (Fig.IV.4). It is worth highlighting that the excavation methodology adopted in Los Canes foresaw the recovery of materials below 5 cm with dry sieving. Sieving was carried out with 2 mm wide meshes. This intervention determined an indirect selection of collected materials. In a preliminary observation, there are no pieces with maximum dimensions (length, width and thickness) <2 mm. By establishing the dimensional classes to evaluate the dimensional distribution

of the materials in each stratigraphic unit, it is worth using the following dimensional classes: 0-2 mm; 2-10 mm; >10 mm. The dimensional distribution highlights a predominance of very small pieces with dimensions between 2 and 10 mm. The minimum value observed for both red and yellow pieces was around 2 mm. About 88% of all red elements (n. 1044 pieces) had a maximum length between 2-10mm while only 12% (n. 136 pieces) had a maximum length >10 mm. As far as the set of yellow elements is concerned, they are scarce in the whole archaeological deposit. A total of 37 pieces (88%) have dimensions between 2-10 mm and only 5 pieces (12%) are over 10 mm (Fig.IV.5). By evaluating the relation between the average values of the maximum lengths and the mass of the S.U., there is a high correlation ($r^2 = 0,8$). The two variables show a linear relationship in which the increase in the maximum length corresponds to an increase in mass. A very strong relation characterizes the points which intersect the line highlighted in the graph.

For the yellow elements, the data shown needs to be evaluated considering the quantity of pieces counted. From the graph, a very good correlation with $r^2 = 0,9$ (Fig.IV.6) can be seen.

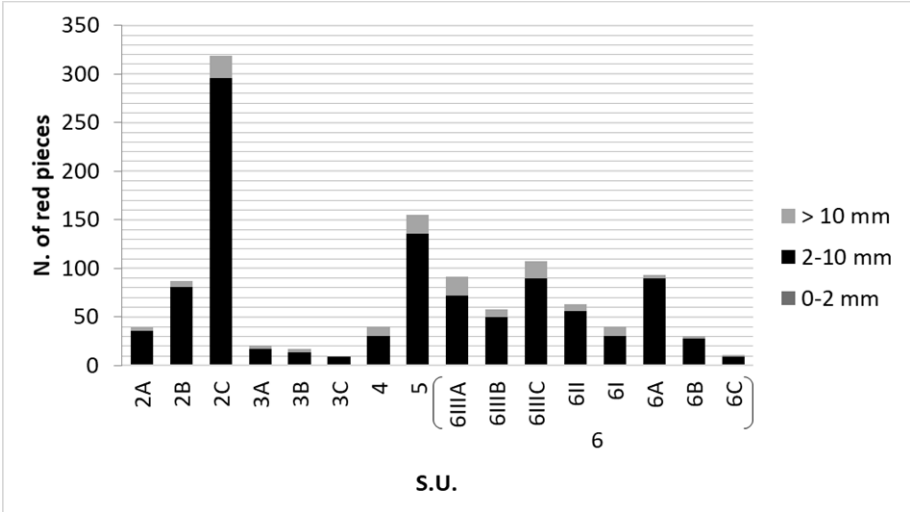


Fig.IV.4.: Dimensional distribution of red pieces from Los Canes.

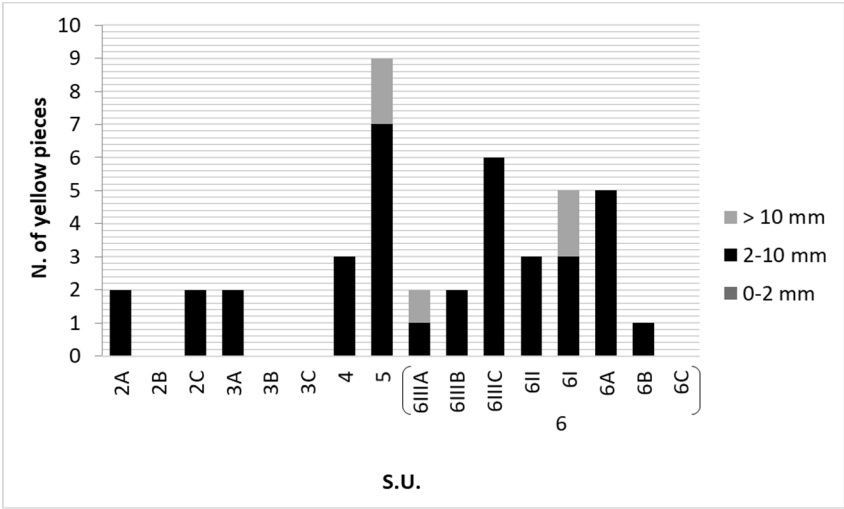


Fig.IV.5.: Dimensional distribution of yellow pieces from Los Canes

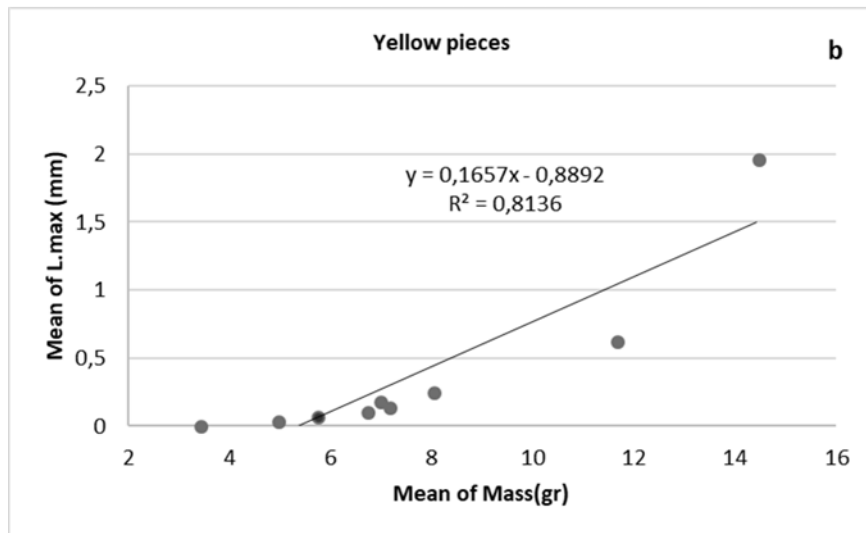
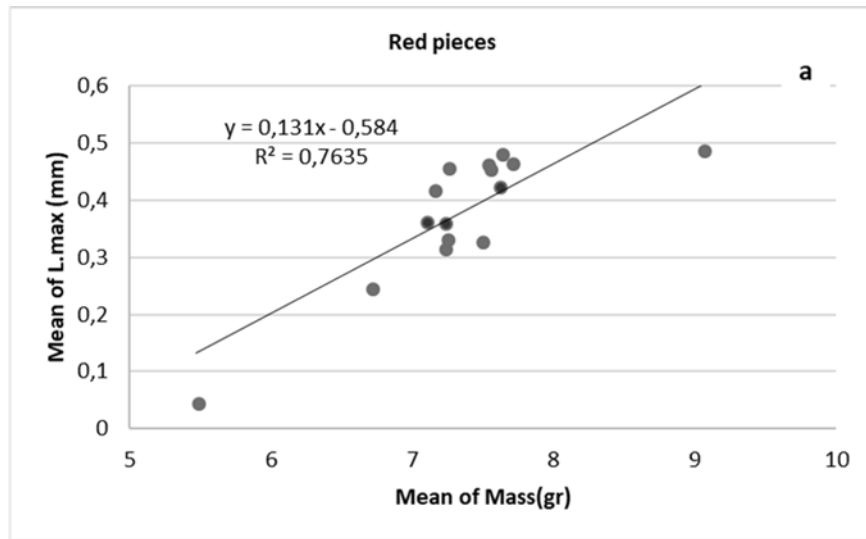


Fig.IV.6: Los Canes: correlation graph of mean values of Length max. (mm) and Mass(gr) of red (a) and yellow (b) pieces.

IV.1.3. State of conservation

The state of conservation of both red and yellow elements appear similar in all the units. The surface is fairly conserved despite the water sieving. The high number of very small pieces with dimensions between 2-10 mm indicates a high fragmentation of the assembly and therefore suggesting a fragmentation of more voluminous blocks that are not found in the assemblages of both red and yellow materials.

Index of Shannon-Weaver (H) and Evenness (J)

For the red group, the conspicuous presence of very small pieces (2-10 mm) and small pieces (>10 mm) without any superficial traces and signs next to pieces with diagnostic traces and *crayons* allow us for the evaluation of the compositional variability with the Shannon-Weaver diversity index (H). By measuring the ratio between the number of elements per category and the total number of elements, it is possible to obtain a value $H=0,9$. By keeping in mind that the total number of categories are five, the diversity is not too high. By presupposing that each category could have an infinite number of elements, the ratio between observed diversity ($H = 0,9$) and maximum possible diversity ($H_{max}= 2$) allows us to obtain a mean value. Evenness ($J= 0,4$) about a scale of values between 0 and 1 indicates that the distribution of the red objects in the recognized categories is homogeneous (Tab.IV.2).

Red pieces				
Categories	Quantity	Relative abundance (Pi)	Log2(Pi)	Pi * Log2(Pi)
Raw pieces (2-10 mm)	969	0,821186441	-0,284218288834123	-0,233396205
Raw pieces (>10 mm)	122	0,103389831	-3,27383380668632	-0,338481122
Modified pieces (2-10 mm)	63	0,053389831	-4,22729122074929	-0,225694362
Modified pieces (>10 mm)	18	0,015254237	-6,03464614280689	-0,092053924
Crayons	8	0,006779661	-7,20457114424921	-0,04884455
			H	0,938470163
			J	0,469235082
Yellow pieces				
Categories	Quantity	Relative abundance (Pi)	Log2(Pi)	Pi * Log2(Pi)
Raw fragments (2-10 mm)	50	0,877192982	-0,189033824390017	-0,165819144
Raw fragments (>10 mm)	6	0,105263158	-3,24792751344359	-0,341887107
Modified pieces (2-10 mm)	1	0,01754386	-5,83289001416474	-0,102331404
			H	0,610037655
			J	0,384890907

Tab.IV.2.: Los Canes: Index of Shannon-Weaver (H) and Evenness (J) of red and yellow pieces.

The yellow elements are classified into three categories. No modified pieces with dimensions greater than 10 mm or *crayons* were detected. Furthermore, the calculation of the Shannon-Weaver diversity index shows a middle diversity ($H=0,6$) when considering that the maximum possible diversity ($H(\max)$) is equal to 1,5. The single elements are distributed in a rather non-homogeneous way between the distinct categories as is confirmed by the value of $J=0,3$ in relation to a scale of reference from 0 to 1.

Index of fragmentation

The Shannon-Weaver index certifies the presence of small elements (>10 mm) and very small ones (2-10 mm). By calculating the fragmentation index of the red pieces in function to the dimensional classes established for each stratigraphic unit, a high fragmentation is registered in unit 4 for modified pieces (2-10 mm). This category is attested in the lower units: 2B and 2C with lower and similar values. In regards the modified pieces >10 mm, the indexes are extremely scarce and characterize only these units.: 2B, 2C, 3A, 5, 6IIIC, 6II, 6B, 6C. The category of raw pieces (2-10 mm) follows. The fragmentation indexes are higher and similar for units: 2A, 2B, 2C. The indexes for the other units are evidently lower with almost the same or rather low values (Fig.IV.7; Tab.IV.3).

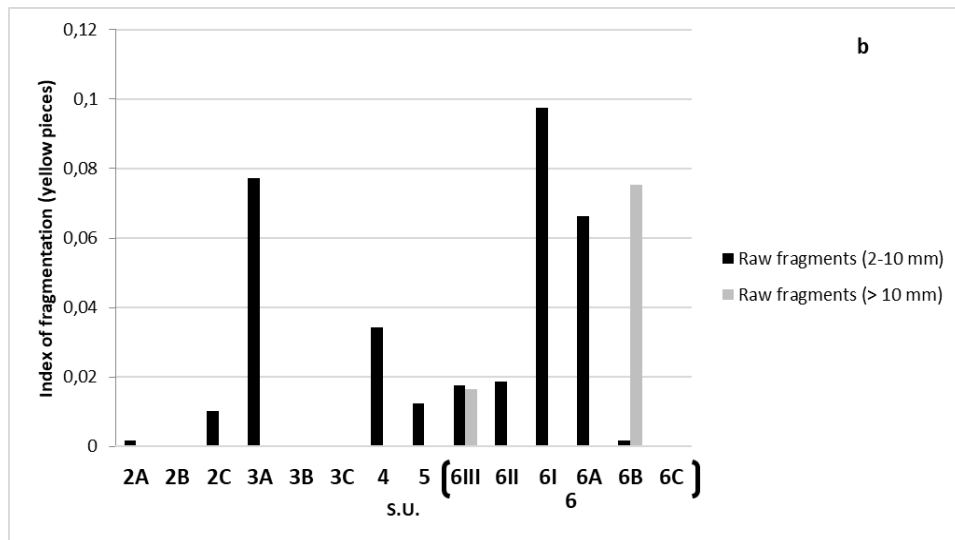
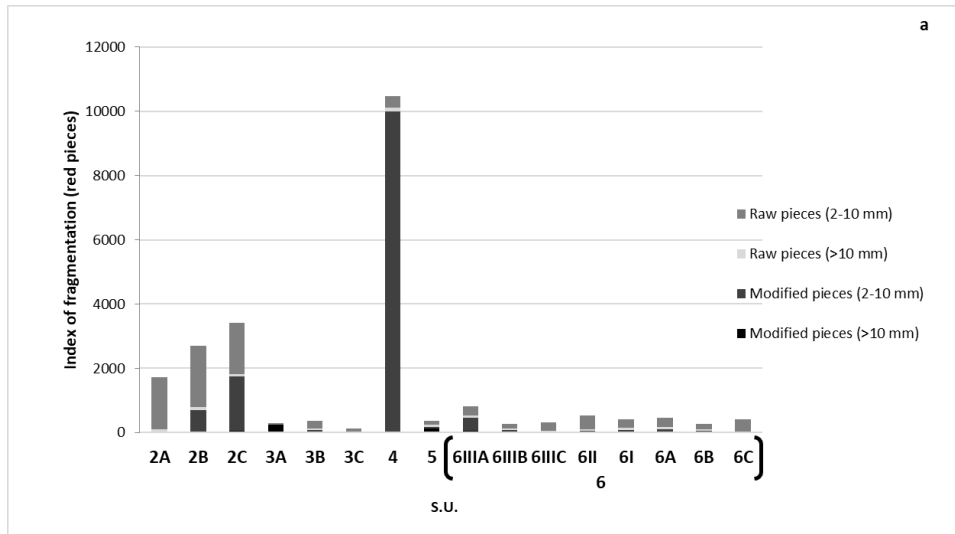


Fig.IV.7.: Los Canes: distribution of the fragmentation indices according to the established categories for the red (a) and yellow (b) pieces.

Red pieces				
	Raw pieces (2-10 mm)	Raw pieces (>10 mm)	Modified pieces (2-10 mm)	Modified pieces (>10 mm)
2A	1634,6	95,6	n.c.*	nick
2B	1896,1	102,5	672,2	17,9
2C	1583,2	86,7	1691,1	48,6
3°	38,6	21,6	n.c.	232,5
3B	247,2	31,2	85,4	n.c.
3C	120,9		n.c.	n.c.
4	358	105,3	10.000	n.c.
5	136,8	52,7	60	120
6IIIA	287,2	70,7	400	53,8
6IIIB	158,4	50,5	47	21,4
6IIIC	267	26,3	20,6	n.c.
6II	432,6	39,3	58,8	n.c.
6I	268,9	62,8	61,8	20,5
6A	283,1	80,8	82,4	11,7
6B	182,8	47,7	48	n.c.

**n.c. (not calculable)*

Tab.IV.3a.: Values of Indices of fragmentation: red pieces from Los Canes.

Yellow pieces		
	Raw fragments (2-10 mm)	Raw fragments (> 10 mm)
2°	10.000	n.c.
2B	n.c.	n.c.
2C	2.000	n.c.
3°	740,7	n.c.
3B	n.c.	n.c.
3C	n.c.	n.c.
4	2.500	n.c.
5	989	n.c.
6IIIA	10.000	200
6IIIB	10.000	n.c.
6IIIC	1.200	n.c.
6II	422,5	n.c.
6I	252,1	224,7
6°	793,6	n.c.
6B	5.000	n.c.
6C		

**n.c. (not calculable)*

Tab.IV.3b.: Values of Indices of fragmentation of yellow pieces from Los Canes.

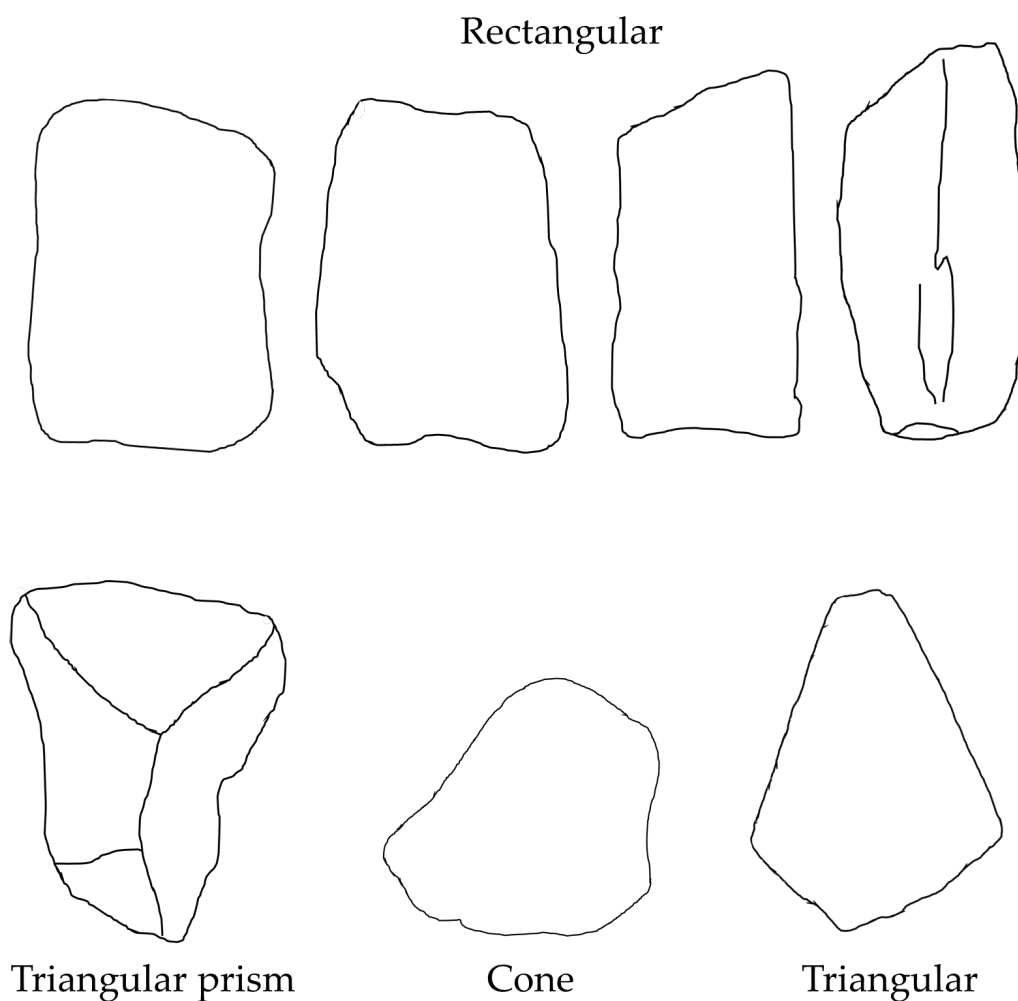


Fig.IV.8.: Main identifying morphologies of crayons by inscribing the forms in a two-dimensional plane.

Crayons

The elements defined as *crayon* consist in solid polyhedral pieces with a finite number of flat faces that are polygonal and connected between them. In some cases, the faces have use-wear traces. A total of 8 red ochre specimens fall in this category. No yellow elements were recorded.

The dimensions are remarkable and less variable in comparison to the fragments. The length values are between 8,97 mm and 22,92 mm and a mass between 0,4 gr and 3,38 gr.

The pieces can be enclosed into three main geometric solids: cone, rectangular, triangular and triangular prism. By cutting the solids with an imaginary plane perpendicular to the axis that indicates greater lengthening, it is possible to obtain two parts in equilibrium amongst themselves. The rectangular and the triangular prism are the most recurrent morphologies.

Only one element is cone shaped. In two cases, well defined and oblique parallel striae were observed at the large axis of the piece evidently produced in contact with another surface.

ID sample	S.U.	Length	Width	Thickness	Weight	Morphology
27b	2C	9,71	7,72	4,03	0,45	triangular prism
22	2C	10,1	7,41	3,93	0,4	rectangular
23a	2C	22,92	16,85	5,96	2,5	rectangular
61b	3A	8,97	7,86	7,92	0,72	cone
121a	5	17,33	9,18	6,72	0,88	rectangular
214	6 IIIA	15,47	8,74	7,96	1,4	rectangular
241a	6 IIIA	12	8,4	2,09	3,38	triangular

Tab.IV.4.: Summary table of main physical traits of crayons.

IV.2. Arangas

The Arangas site is a wide cavity (25 m x 7 m) of karst origin which is part of the same fossil complex of the cave of Los Canes. Direct explorations did not show any presence of iron minerals formations inside the cave.

The ochre remains collected from the archaeological deposit cannot be the result of the desegregation of ferrous deposits in the cave. Reviewing stratigraphic data, there are no taphonomical problems even if the layers have post depositional alterations due to modern visits which have damaged the higher units of the deposit which is classified between the Neolithic and the Bronze age. In any case, these units are not included in this study.

The systemic excavation of the surfaces has highlighted the presence of micromammal burrows as well as movements due to clandestine excavations which have only damaged the upper units in the NW part of the cave (square G and F, S.U. 14). In the explanation that follows, some units divided into excavation stages were grouped based on a chrono-cultural coherence. In the meantime, the evolutionary tendencies of the materials will be shown in function to the following stratigraphic organization: 5D (Lower Magdalenian); 5C (Upper Magdalenian); 5B and 5A (Azilian); 3-4-2B (Mesolithic). It is important to specify that the general organization of the materials did not return ochre elements from the units 3 and 4.

IV.2.1. Colour

The observation of materials allowed us to ascertain a series of tints which are grouped into two classes: red and yellow. The tints have been coded in the

Munsell Soil Color Charts and listed in the table below to facilitate data exposition (Tab.IV.5). By plotting the distribution of the counted materials by colour class in each stratigraphic unit on a graph, it is possible to count 32 red pieces and no yellow elements in the S.U. 5D and S.U. 5C. A noticeable increase was registered for S.U. 5B and S.U. 5A in which n.269 red pieces and n.17 yellow pieces were counted. A decrease is seen in unit 2B in which n.40 red and n.2 yellow elements are counted. The poor presence of yellow material allowed us to make general qualitative considerations, but which are statistically unreliable (Fig.IV.9).

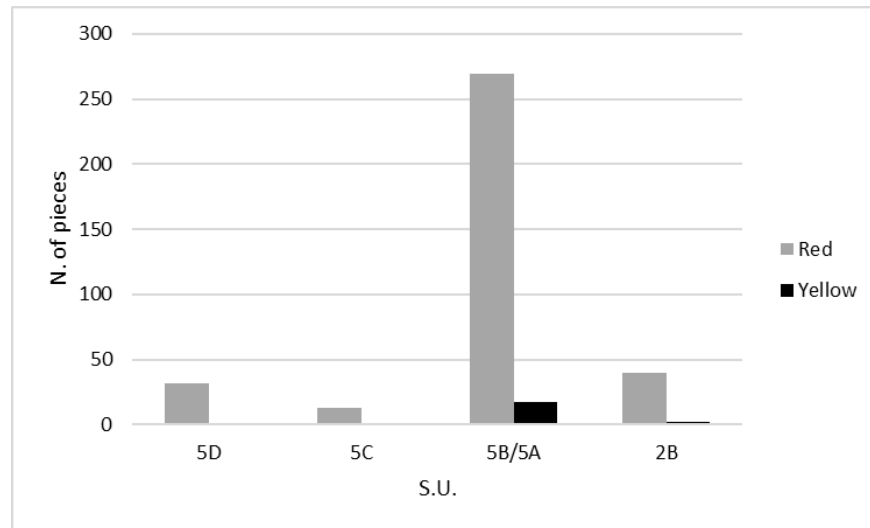


Fig.IV.9.: Arangas: distribution of red and yellow ochre specimens in each stratigraphic unit of the archaeological deposit.

List of tints in the Munsell Soil Color Charts

Red	Yellow
<i>10R 3/1 dark reddish grey</i>	<i>10YR 7/4 very pale brown</i>
<i>10R 3/2 dusky red</i>	<i>10YR 7/6 yellow</i>
<i>10R 3/3 dusky red</i>	<i>10YR 7/8 yellow</i>
<i>10R 3/4 dusky red</i>	<i>10YR 8/8 yellow</i>
<i>10R 3/6 dark red</i>	<i>2.5Y 6/8 olive yellow</i>
<i>10R 4/1 dark reddish grey</i>	<i>2.5Y 7/6 yellow</i>
<i>10R 4/2 weak red</i>	<i>2.5Y 7/8 yellow</i>
<i>10R 4/3 weak red</i>	<i>7.5YR 5/6 strong brown</i>
<i>10R 4/4 weak red</i>	<i>7.5YR 5/8 strong brown</i>
<i>10R 4/6 red</i>	<i>10YR 7/4 very pale brown</i>
<i>10R 4/8 red</i>	
<i>10R 5/4 weak red</i>	
<i>10R 5/6 red</i>	
<i>1R 5/8 red</i>	
<i>2.5YR 3/3 dusky red</i>	
<i>2.5YR 3/4 dusky red</i>	
<i>2.5YR 3/6 dark red</i>	
<i>2.5YR 4/1 dark reddish grey</i>	
<i>2.5YR 4/3 dusky red</i>	
<i>2.5YR 4/4 dusky red</i>	
<i>2.5YR 4/6 red</i>	

<i>2.5YR 4/8 red</i>
<i>2.5YR 5/4 reddish brown</i>
<i>2.5YR 5/6 red</i>
<i>2.5YR 5/8 red</i>
<i>2.5YR 6/6 red</i>
<i>2.5YR 6/8 red</i>
<i>5YR 4/6 yellowish red</i>
<i>5YR 5/6 yellowish red</i>
<i>5YR 5/8 yellowish red</i>
<i>5YR 6/6 reddish yellow</i>
<i>5YR 6/8 reddish yellow</i>
<i>5YR 7/8 reddish yellow</i>

Tab.IV.5.: Arangas: list of tints in Munsell Soil Color Charts approximate in two set of colours: red and yellow.

IV.2.2. Mass and dimensions

The diachronic distribution in function to the total mass of ochre collected from the deposit highlights quantities which range between 14,52 gr and 268,5 gr. From the graph (Fig.IV.10), it possible to appreciate a progressive increase from the S.U. 5D and S.U. 5C with an exponential rise for units S.U. 5B and S.U. 5A where a total of 525,13 gr were collected. In unit 2B, the quantities of material are rather scarce. (14,52 gr).

As far as mass of yellow ochre is concerned, this is directly proportional to the number of counted pieces. In units 5B and 5A, about 7,68 gr of yellow ochre was quantified. For the S. U. 2B just 0,02 gr is quantified.

In regards the dimensions and considering the values of the maximum lengths of each element, from an initial observation, it is possible to notice that the minimum dimensions are approximately <2 mm. Knowing that the dimensions of the meshes are like the ones used in Los Canes, the minimum dimensions detected are placed in relation to the width of the meshes.

In consideration of this element, it is opportune to turn to the same dimensional classes used to evaluate the distribution of the red and yellow elements in function to the maximum length. The dimensional class of red pieces between 2-10 mm is well represented with similar values for S.U. 5D, S.U. 5C, S.U. 5A and S.U. 2B. While in line with what is attested for the number of counted pieces by colour and total mass of red material quantified by stratigraphic unit, the Azilian units 5B/5A return higher values with n.224 pieces with dimensions between 2 and 10 mm were counted.

In regards the dimensional class >10 mm, n.2 elements are attested in S. U. 5D and only one piece in S.U. 5C. For units 5B/5A are n.45 elements are counted. Unit 2B had 6 elements with dimensions >10mm. The dimensional distribution confirms the absence of red and yellow elements with dimensions <2 mm (Fig.IV.11).

The yellow vestiges which were generally few, were mainly very small elements (2-10 mm) and attested in units 5B/5A and 2B with a progressively decreasing trend.

The dimensional class >10 mm appears to be underestimated. A total of n.3 yellow pieces greater than 10 mm from unit 5B were counted. The dimensional class 0-2 mm was also absent for yellow ochres (Fig.IV.12). A high correlation emerges between the means of the mean values of length and mass in each stratigraphic unit for red elements ($r^2= 0,9$). By increasing the dimensions, the mass of the material increases too.

For the yellow ones, it is not possible to estimate the same correlation of mean values of L(max) and mass for each stratigraphic unit. By calculating the ration between the maximum lengths and mass of the yellow elements available in the set of materials, it is possible to see a very strong linear correlation.

The value of the correlation coefficients $r^2=0$, is too high and attests the increase in maximum length in function to the mass.

This result needs to be evaluated considering the total number of samples, n.8 elements out of a total n.19 yellow elements (Fig.IV.13).

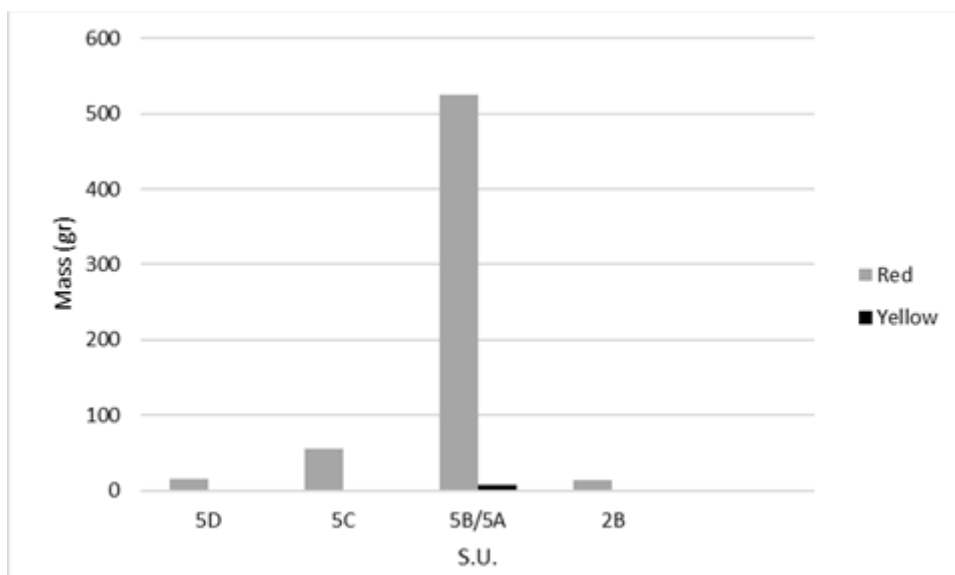


Fig.IV.10.: Arangas: distribution of red and yellow ochre specimens in function of the mass(gr).

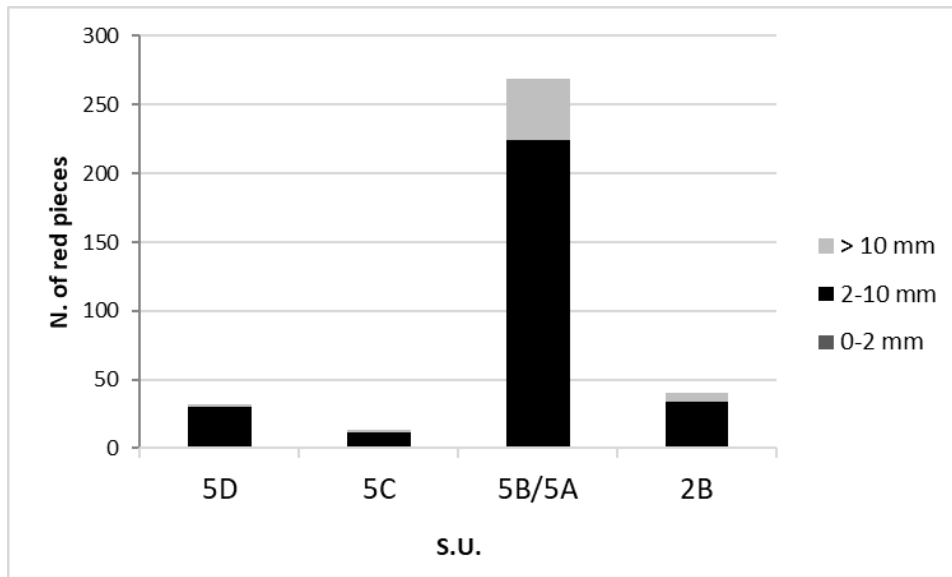


Fig.IV.11.: Dimensional distribution of red pieces from Arangas.

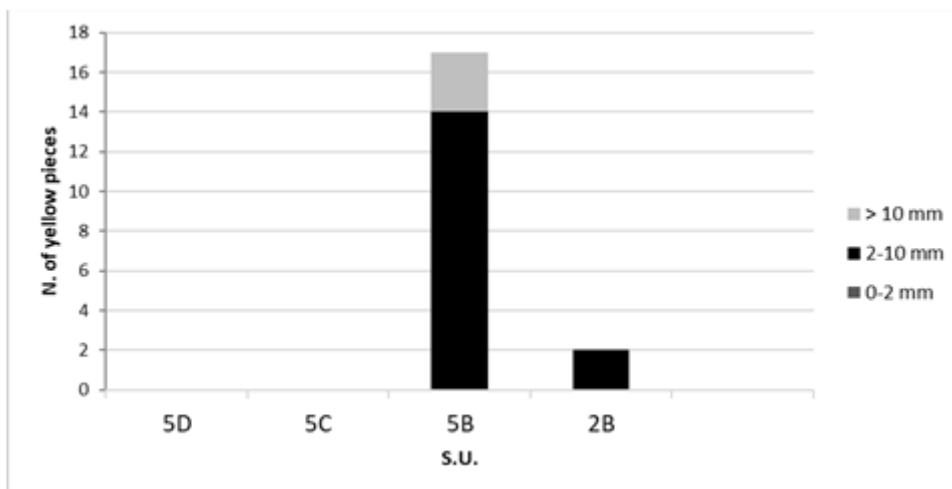


Fig.IV.12.: Dimensional distribution of yellow pieces from Arangas.

IV.2.3. State of conservation

The conservation state appears to be rather good. Nevertheless, the recovery methodology of the materials *in situ* could have created some problems. The materials were recovered through systemic wet sieving of sediments as for Los Canes. This operation certainly provided for the recovery of many red and yellow ochre vestiges, although the use of meshed sieving with 2 mm determined the indirect selection of materials. In addition, the washing of sediments with water could have remarkably compromised the readability of the surfaces by partially or totally deleting diagnostic use wear traces of ochre and other important signs to understand anthropic transformations and functions of ochre by traceological analysis.

Diagnostic traces (striae, lustrations and chipping) were recognized on 6% of the elements (n.25) out of a total of 373 objects. Even if this percentage is low, it demonstrates that despite washing with water, some traces were preserved.

The evaluation of the degree of diversity and the estimation of the distribution of elements for categories provides useful data in order to understand whether the origin of the materials depend on anthropic or natural factors. Furthermore, the estimation of the fragmentation of the assemblage allows us to obtain important data to research mechanical transformations.

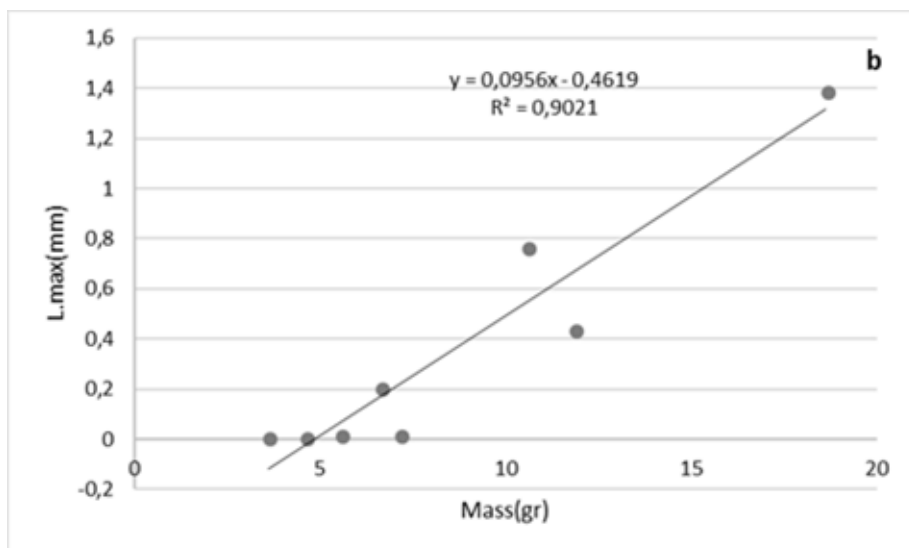
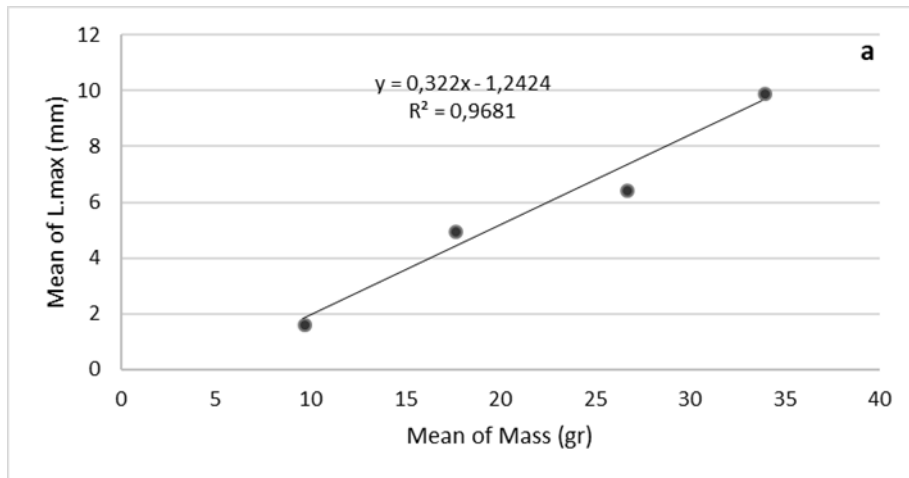


Fig.IV.13: Arangas: correlation graph of mean values of Length max. (mm) and mass(gr) of red (a) pieces and correlation graph of values of Length max. (mm) and mass(gr) (b) of individual yellow pieces.

Index of Shannon-Weaver (H) and Evenness (J)

From a global assessment of the assembly, a total of four categories can be identified in which the individual objects comprising it can be included. The recognized categories are the following: raw fragments (2-10 mm); raw fragments (>10 mm); modified fragments (2-10 mm); modified fragments (>10 mm); faceted pieces (Tab.IV.6). The Shannon-Weaver index attests a middle degree of diversity ($H=0,9$) by considering that the maximum diversity possible $H(\max)$ is equal to 2. Dividing this value (H) by the maximum diversity indicated as $H(\max)$, it is possible to obtain the value $J=0,4$ which indicates a degree of distribution of the individual objects in the distinct categories discretely homogeneous. The diversity index was also calculated for yellow pieces. The small number of pieces (n.19) has a rather doubtful valence from a statistical point of view but allows us to highlight some aspects:

- Absence of modified elements or with superficial traces or signs;
- Majority of elements between 2 and 10 mm;

Based on these statements, the yellow elements were included into two categories: raw pieces (2-10 mm) and raw pieces (>10 mm). The value of the diversity index is equal to $H= 0,6$ which corresponds to about a 60% probability that each element could be included in one of the two categories.

By calculating the Evenness value, with $H(\max)=1$, the same value is obtained for $J=0,6$ and thus confirms a rather good homogeneity of the distribution.

Red pieces				
Categories	Quantity	Relative abundance (Pi)	Log2(Pi)	Pi * Log2(Pi)
Raw pieces (2-10 mm)	293	0,827683616	-0,27284869566075	-0,225832395
Raw pieces (> 10 mm)	31	0,087570621	-3,51340923969612	-0,307671431
Modified pieces (2-10 mm)	18	0,050847458	-4,29768054864069	-0,21852613
Modified pieces (> 10 mm)	12	0,033898305	-4,88264304936184	-0,165513324
			H	0,917543279
			J	0,458771639
Yellow pieces				
Categories	Quantity	Relative abundance (Pi)	Log2(Pi)	Pi * Log2(Pi)
Raw pieces (2-10 mm)	16	0,842105263	-0,247927513443586	-0,208781064
Raw pieces (> 10 mm)	3	0,157894737	-2,66296501272243	-0,42046816
			H	0,629249224
			J	0,629249224

Tab.IV.6.: Arangas: Index of Shannon-Weaver (H) and Evenness (J) of red and yellow pieces.

Index of fragmentation

The evaluation of the diversity of the categories identified within the materials confirms the abundance of very small (2-10 mm) and small (>10 mm) pieces. This presence could lead us to the reduction of the more voluminous mass of ochre. The calculation of the index of fragmentation highlights a high fragmentation for the raw pieces class (2-10 mm). The highest values correspond to units 5B and 5A. The indexes of units 5D and 2B take on similar values. The index of fragmentation is extremely low for the class (2-10 mm) in unit 5C. The indexes of fragmentation of raw pieces (>10 mm) and modified pieces (2-10 mm) are lower and in each case, it is just attested in the Azilian and Mesolithic units. It is clearly shown in the graph that in unit 2B, the index of fragmentation for raw pieces >10 mm is higher if compared to the other units. For the yellow elements also, the sample is extremely low to make reliable statistical considerations in a diachronic sense. Generally, it is necessary to have a bigger sample to have more valid data, but in this case, the counted pieces for each stratigraphic unit are very small. To overcome this problem, the elements coming from different stratigraphic units (S.U. 5B; S.U. 5A; S.U. 2B) were grouped to have a more conspicuous sample and which allows us to achieve relatively reliable indexes. The index of fragmentation obtained refers to the set of all the yellow elements collected from the deposit. The value is 0,04 which is rather low when comparing it with the indexes obtained for the red elements (Fig.IV.14; Tab.IV.7).

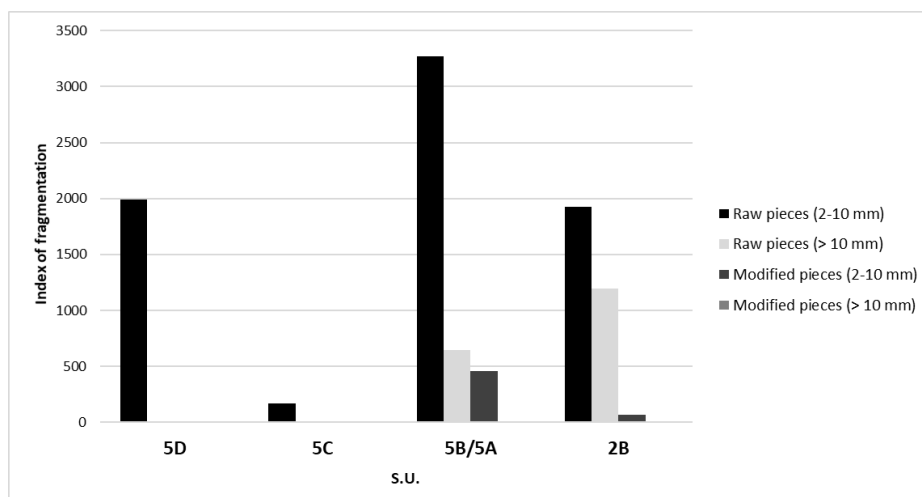


Fig.IV.14.: Arangas: distribution of the fragmentation indices according to the established categories for the red pieces.

Red pieces				
	Raw pieces (2-10 mm)	Raw pieces (> 10 mm)	Modified pieces (2-10 mm)	Modified pieces (> 10 mm)
5D	1989,4	n.c.*	n.c.	n.c.
5C	166,6	n.c.	n.c.	n.c.
5B/5A	3271,7	642,9	455,7	n.c.
2B	1927,5	1192	70,9	n.c.
Yellow pieces				
Tot. 19	Index of fragmentation 0,4			

*n.c. (not calculable)

Tab.IV.7.: Values of Indices of fragmentation: red pieces and yellow pieces from Arangas.

IV.3. La Garma A

The site of La Garma A is part of a complex of cavities that are opened within La Garma mount in a karst system excavated in limestone of middle Albian and Lower Bedoulian (Arias *et al.* 1997, 2000a, 2001) for the dissolution of calcium carbonates. This genesis does not exclude the formation of superficial ferrous encrustations for precipitations of ferrous materials in water, which brings us to reflect on the potential contamination of the archaeological deposit.

Nevertheless, the presence of parietal paintings with iron-based pigments (hematite, goethite, manganese oxide) in the lower levels of La Galería Inferior (Arias *et al.*, 2011), a cavity that is part of the same rocky formation and that could have had direct access to Mid-Magdalenian attests the use of ochre in the complex of La Garma during Palaeolithic period. An evaluation of the materials according to the criteria shown at the start of this chapter provides data to discuss about the anthropic provision of ochre in the site.

IV.3.1. Colour

The mostly attested colour based on the number of pieces counted is red (n. 603), followed by yellow (n. 64). Several tonalities of red and yellow are seen which have been coded with the Munsell Soil Color Charts and listed in the table below (Tab.IV.8). Just like the assemblages of Los Canes and Arangas, the site of La Garma A also follows the same procedure. The pieces are counted and divided into two classes of main colours: red and yellow.

Red vestiges are counted in each stratigraphic unit of the deposit in variable quantities while the yellow vestiges were absent in S.U. 1 (Fig.IV.16). By starting from the lower units of the archaeological deposit, S.U. G has a total of

63 objects in which 50 are red and 13 are yellow. The following unit I, has a noticeable decrease of the red vestiges (n. 3) and a total disappearance of the yellow vestiges. A new increase is attested in unit J which has 61 red objects and 8 yellow ones. The following unit L is the one full of materials. This unit returned a total of 268 objects of which 251 were red and 17 were yellow. The number of pieces falls in the following S. U. N which in any case has several red pieces (n. 85) and few yellow pieces (n. 10). The number of pieces continues to decrease also in unit O in which 56 red pieces are counted and only 5 yellow ones. Lastly, unit O which closes the studied sequence and is characterized by a minor increase if it is compared to the previous units S.U. O and S.U. N. This unit returned a total of 108 objects divided between 97 red ones and 11 yellow ones.

IV.3.2. Mass and dimensions

A total of 426,23 gr of ochre was collected from the Palaeolithic and Mesolithic levels of the archaeological deposit of the La Garma A site. In the material mass, red ochre is in abundance with a total of 375,16 gr. It is possible to quantify a total of about 51 gr for the yellow ochre. An increase of ochre mass is visible in unit J with a total of 54,25 gr of which 36,94 gr is red ochre and 17,31 is yellow. Ochre is abundant in unit P. Due to the richness of objects at this level (n. 268) the total mass corresponds to 271,78 gr of ochre which is largely characterized by red ochre (252,77 gr). Approximately 20 gr of yellow ochre is quantified.

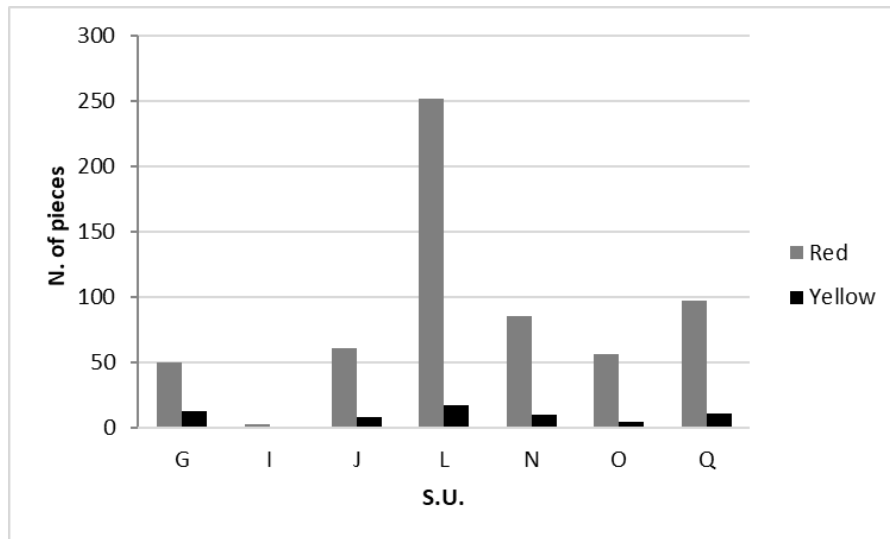


Fig.IV.15.: La Garma A: distribution of number of red and yellow ochre pieces collected from each stratigraphic unit of the archaeological deposit.

List of tints in the Munsell Soil Color Charts

Red	Yellow
10R 3/2 dusky red	10YR 5/6 yellowish brown
10R 3/3 dusky red	10YR 5/8 yellowish brown
10R 3/4 dusky red	10YR 6/6 brownish yellow
10R 3/6 dark red	10YR 6/8 brownish yellow
10R 4/2 weak red	10YR 7/6 yellow
10R 4/3 weak red	10YR 7/8 yellow
10R 4/4 weak red	2.5Y 6/8 olive yellow
10R 4/6 red	2.5Y 7/3 pale yellow
10R 4/8 red	2.5Y 7/8 yellow
10R 5/3 weak red	2.5Y 8/8 yellow
10R 5/6 red	

10R 5/8 red
2.5YR 3/4 dusky red
2.5YR 4/4 dusky red
2.5YR 4/6 dark red
2.5YR 4/8 dark red
2.5YR 5/6 red
2.5YR 5/8 red
5YR 4/4 reddish brown
5YR 4/6 yellowish red
5YR 5/3 reddish brown
5YR 5/8 yellowish red
5YR 6/8 reddish yellow

Tab.IV.8.: *La Garma A: list of tints in Munsell Soil Color Charts approximate in two set of colours: red and yellow.*

By analysing the mass distribution of red and yellow ochre in a diachronic way, it possible to observe that the mass of ochre in unit G is rather scarce with a total of 14,44 gr in which 13,16 is red ochre and 1,28 is yellow ochre.

The mass decreases further in the next unit, S.U. I from which less than one gram of red material is collected (0,03 gr).

In accordance with the number of objects counted per unit, a progressive reduction follows in S. U. N with around 28,75 gr of ochre in which 26,61gr is red ochre while 2 gr is yellow.

In S. U. O the mass falls further. About 15 gr of material comes from this unit of which only 0,12 gr are yellow ochre and the remaining mass is red. An increase in ochre mass is attested in unit Q with 31,35 gr of red ochre and 11,21 gr of yellow ochre.

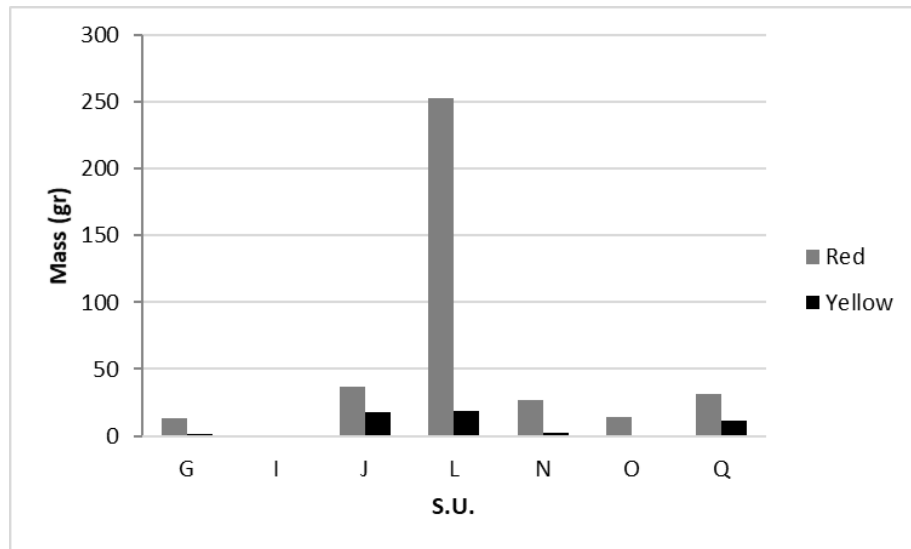


Fig.IV.17.: La Garma A: distribution of red and yellow ochre specimens in function of the mass in grams

By observing the values obtained and measuring the maximum length of red and yellow pieces, the dimensions appear between 2,57 mm and 52,33 mm. No elements of dimensions lower than 2 mm were detected. Even in this case, the absence of pieces with dimensions between 0 mm and 2 mm could be the consequence of the sieving used for the recovery of the sediment.

In this sense, the dimensional classes used to evaluate the diachronic distribution of the elements in function to the maximum length also appear valid for the vestiges of La Garma A (Fig.IV.18).

The referenced histogram confirms the absence of dimensional 0-2 mm classes in all units studied. The dimensional class 2-10 mm appears to be the best attested, while the dimensional class >10 mm is underestimated.

By starting from the lower unit, the dimensional class 2-10 mm is well attested in unit G, but drastically falls in S.U. I. In unit J, it reaches a similar level to unit G while it undertakes a noticeable increase in unit L.

A new decrease is attested in unit N and later in unit O in which the dimensional class 2-10 mm goes back to the levels of units G and J.

In unit O, the dimensional class 2-10 mm experiences an increase.

As for the pieces with dimensions >10 mm, they are found in almost all units, except in unit I. Starting from S.U. G, this dimensional class is much lower than the 2-10 mm class.

In unit I this class disappears totally to then reappear in S.U. J even if poorly attested. On the contrary, the number of pieces with dimensions >10 mm in unit L is more abundant than any other unit. This dimensional class is well attested in S. U. L also in relation to the dimensional class 2-10 mm. A reduction of elements >10 mm is observed in unit N and additionally in unit O in which at least 3 pieces >10 mm was counted. A new increase is registered in unit Q where 16 pieces with dimensions >10 mm was counted. Generally, the evolutionary tendency of the pieces in function to the maximum length reflects that of mass. No discrepancies were found.

In regards yellow pieces, the total of 64 elements counted is distributed into two main dimensional classes 2-10 mm; > 10 mm (Fig.IV.19). The best represented class is the one of the pieces with dimensions between 2 and 10 mm. This class

is attested with 12 elements in S. U. G which is halved in S.U. J to then go back once again to 12 in S.U. L.

The situation for unit N is the same in which 10 pieces were counted of class 2-10 mm. Exactly half of the elements correspond to the following unit: S.U. O. It doubles once more in unit Q.

The dimensional class >10 mm on the other hand is rather underestimated. A total of 10 distributed elements between S. U. G (n. 1); S. U. J (n. 3); S.U. L (n.5); S.U. Q (n.1).

By calculating the correlation between the average values of the maximum lengths and the mass of the red and yellow pieces counted for each stratigraphic unit, it is possible to see a positive linear relation.

The correlation coefficient obtained for the red vestiges ($r^2=0,9$) attests a very high correlation and therefore confirms that with a dimensional increase, there is also an increase in weight.

For the yellow vestiges, the value ($r^2=0,5$) indicates a relation between the two variables. Nevertheless, the correlation ratio is mid on a reference scale between 0 and 1. In observing the graph, a strong correspondence between the dimensional increase and mass is seen in units O and L where the points perfectly intersect the regression line. Aligned in parallel to the line are the points of units G and J in which the relation is discrete, while the points of units N and Q are dispersed and get further away from the linear line.

Considering this result, an increase in the maximum length does not always correspond to an increase in mass (Fig.IV.20).

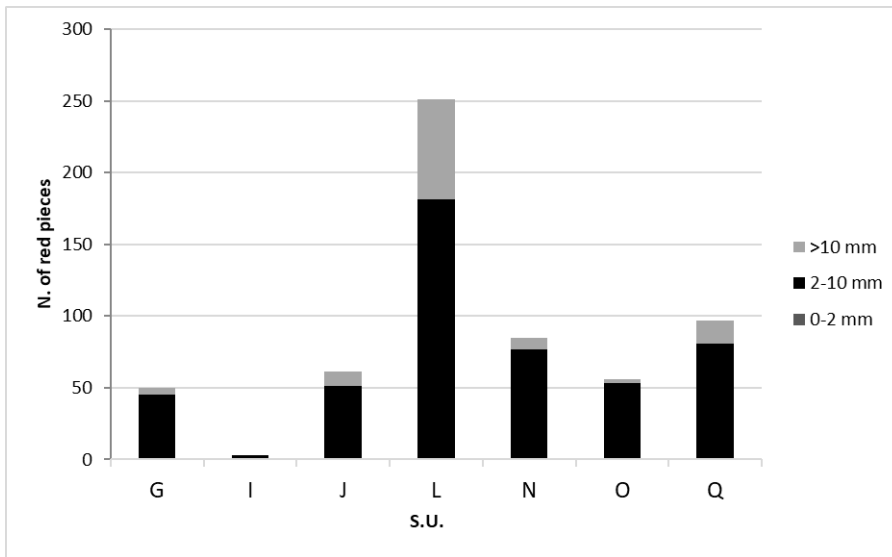


Fig.IV.18.: Dimensional distribution of red pieces from La Garma A.

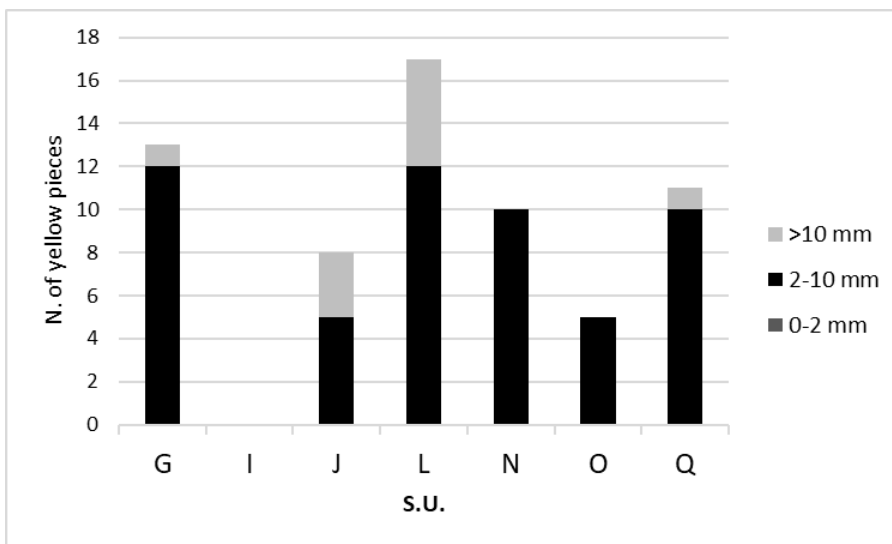


Fig.IV.19.: Dimensional distribution of yellow pieces from La Garma A.

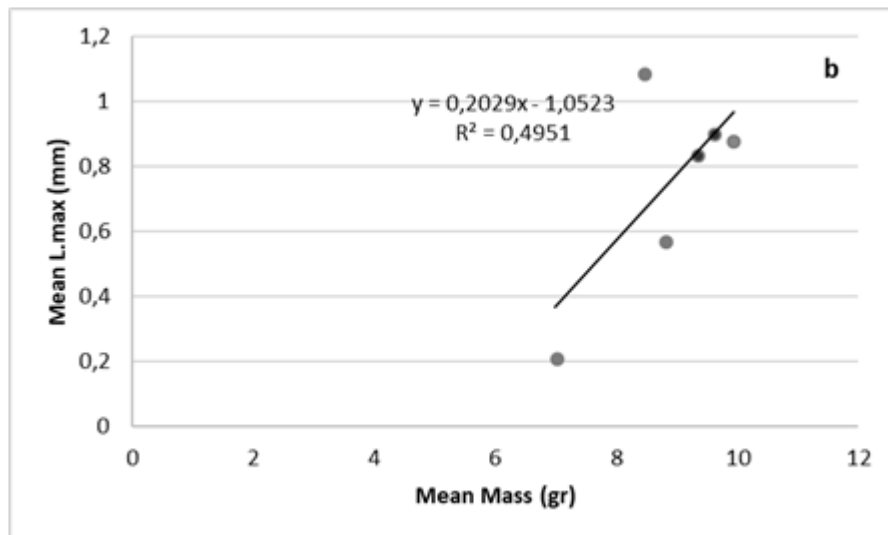
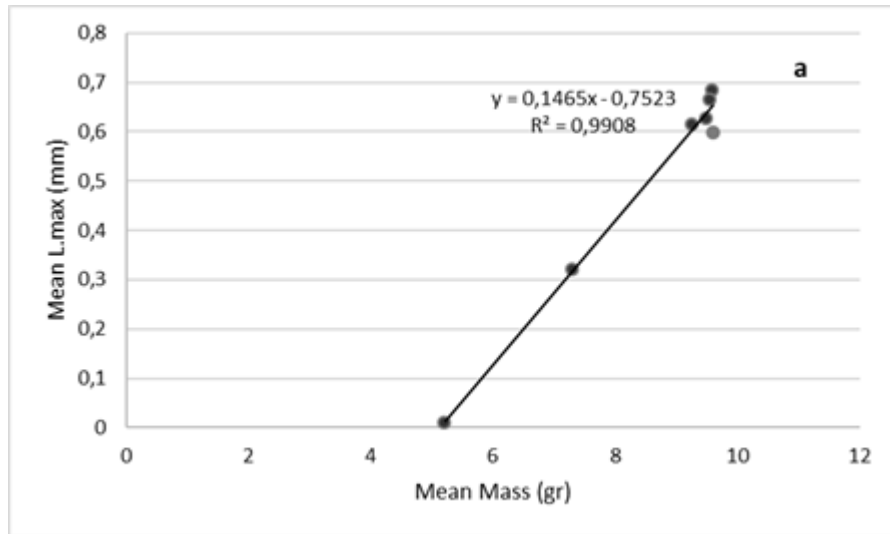


Fig.IV.20: La Garma A: correlation graph of mean values of Length max. (mm) and Mass(gr) of red (a) and yellow pieces.

IV.3.3. State of conservation

The state of conservation of both the red and yellow materials appear similar in all units of the archaeological deposit. Objects with traces and were attested in several units even if they represent only 4% (n. 26 pieces) of the total of the red and yellow vestiges.

A large part of the material sieving the sediment with water and drying it to open air. These operations also ensured the recovery of smaller pieces. Nevertheless, the passage of water sediment can alter the archaeological surfaces by removing past marks and traces especially in the presence of non-hard elements like ochre.

In the case of La Garma A, it is fundamental to keep in mind that almost 64% of the red vestiges and 94% of the yellow vestiges were tender and powdered upon touch. In this sense, it is necessary to point out that normally, the estimation of the hardness of the mineral is carried out using. Moss scale in which the values from 1 to 10 correspond to scratching of the surfaces with objects or minerals. In regards the archaeological material, it is not possible to perform this test without damaging the surfaces of the objects. To overcome this problem, during the general organization of the material, it is possible to verify some parameters like the level of powder of the object and its integrity upon touch.

This issue will be better dealt with later. For now, it is important to highlight that the high percentages of tender materials can explain the low percentages of elements with traces. The powdered vestiges upon touch have rather delicate surfaces in which it is plausible that the action of water eliminated use wear traces and other diagnostic signs of anthropic actions. Therefore, the estimation

of the diversity of the objects inside the archaeological assemblage and the degree of fragmentation provides useful data to investigate an anthropic origin of the materials.

Index of Shannon-Weaver (H) and Evenness (J)

The set of materials coming from the Palaeolithic and Mesolithic levels of the archaeological deposit of La Garma A shows a certain compositional variability which is expressed in the identification of four categories where it is possible to insert single objects. The probability that any red or yellow element can be included in one of these categories is verified through the Shannon-Weaver index (Tab.IV.9).

The evaluation of mass, dimensions and state of conservation allows us to divide the red pieces into four distinct categories: raw pieces 2-10 mm; raw pieces >10 mm; modified pieces 2-10 mm; modified pieces >10 mm. By calculating the relative abundance (P_i) of each category and multiplying it by its correspondent in \log_2 , it is possible to have a diversity index equal to 0,9 (H). When evaluated with the maximum possible diversity, or rather $H(\max)=2$, it indicates that there is a 50% possibility that each of the red objects falls in one of these categories.

The homogeneity index value of (J) obtained from the ratio between H and $H(\max)$ is 0,5, which, on a scale from 0 to 1, confirms the level of a middle homogeneity. It was possible to recognize the same categories also for yellow pieces. The index value is $H=0,8$. Considering that in this case the maximum diversity is equal to 2, the probability that each single element can fall in one of the categories is slightly lower than 50%. The pieces are distributed in the

various categories of the yellow group in a discretely homogeneous way ($J=0,4$).

Index of fragmentation

The evaluation of the distribution of objects by dimensional classes as well as the mass and the state of conservation, attests the presence of several fragments with dimensions between 2 and 10 mm and some fragments with dimensions higher than 10 mm. The presence of fragments is a consequence of the fragmentation of larger blocks of red and yellow raw materials for both anthropic and natural agents. Thus, it is worth evaluating the fragmentation level of the assemblage and the ratio between the modified pieces to evaluate the human intentionality.

The calculation of the index of fragmentation has been applied for both red elements and yellow ones despite the lack of statistical representativeness (Tab.IV.10). By plotting the values obtained for the various categories of red pieces, the modified pieces (2-10 mm) of unit L were extremely fragmented. Unit N had a much lower fragmentation index for the same class. The raw pieces (2-10 mm) show an average fragmentation level and quite similar to G, L and Q while it is lower in S. U. J. Lastly, the class of raw pieces with dimensions larger than 10 mm is attested with similarly low indexes of fragmentation as in units J, L and Q. The set of yellow pieces is highlighted only in two classes: raw pieces (2-10mm) and modified pieces (> 10 mm). By starting from the class of raw pieces with dimensions between 2 and 10 mm, the highest fragmentation index is in unit L followed by unit G and unit N, with the lowest being unit Q. For the class of modified pieces, it was possible to calculate the fragmentation index of unit L which is extremely low.

Red pieces				
Categories	Quantity	Relative abundance (Pi)	Log2(Pi)	Pi * Log2(Pi)
Raw pieces (2-10 mm)	471	0,785	-0,34923544088309	-0,274149821
Raw pieces (> 10 mm)	93	0,155	-2,68965987938785	-0,416897281
Modified pieces (2-10 mm)	17	0,028333333	-5,14135584924554	-0,145671749
Modified pieces (> 10 mm)	19	0,031666667	-4,9808911770523	-0,157728221
			H	0,994447072
			J	0,497223536
Yellow pieces				
Categories	Quantity	Relative abundance (Pi)	Log2(Pi)	Pi * Log2(Pi)
Raw pieces (2-10 mm)	50	0,793650794	-0,33342373372519	-0,264622011
Raw pieces (> 10 mm)	11	0,174603175	-2,51784830486262	-0,439624307
Modified pieces (2-10 mm)	1	0,015873016	-5,97727992349992	-0,094877459
Modified pieces (> 10 mm)	1	0,015873016	-5,97727992349992	-0,094877459
			H	0,894001236
			J	0,447000618

Tab.IV.9.: La Garma A: Index of Shannon-Weaver (H) and Evenness (J) of red and yellow pieces.

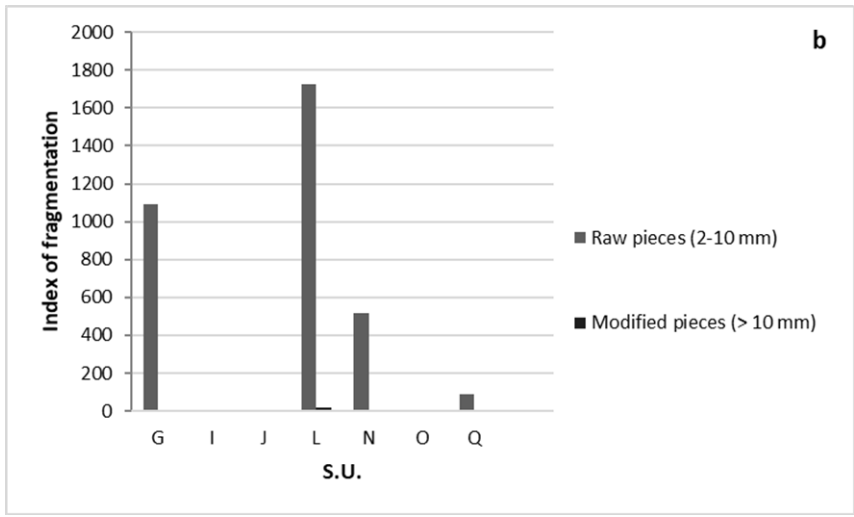
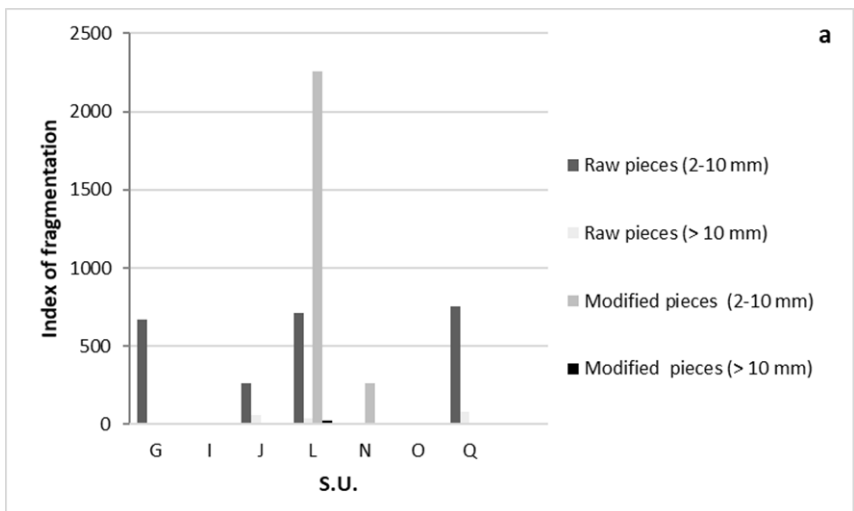


Fig.IV.19.: La Garma A: distribution of the fragmentation indices according to the established categories for the red (a) and yellow (b) pieces.

IV.4. Grotta di Pozzo

The site of Grotta di Pozzo is a cave of modest dimensions that opens in carbonate rocks of Mesozoic origin, in the heart of the Apennines in South-Central Italy. The archaeological deposit is characterized by levels originated between Late Glacial Maximum and Initial Holocene.

Red pieces				
	Raw pieces (2-10 mm)	Raw pieces (>10 mm)	Modified pieces (2-10 mm)	Modified pieces (>10 mm)
G	671,7	n.c.*	n.c.	n.c.
I	n.c.	n.c.	n.c.	n.c.
J	262	59,5	n.c.	n.c.
L	713,1	38,6	2,258	25,8
N	n.c.	n.c.	263,1	n.c.
O	n.c.	n.c.	n.c.	n.c.
Q	751,8	77,7	n.c.	n.c.
Yellow pieces				
	Raw pieces (2-10 mm)	Raw pieces (>10 mm)	Modified pieces (2-10 mm)	Modified pieces (>10 mm)
G	1090,9	n.c.*	n.c.	n.c.
I	n.c.	n.c.	n.c.	n.c.
J	n.c.	n.c.	n.c.	n.c.

L	1724,1	n.c.	n.c.	15
N	517,2	n.c.	n.c.	n.c.
O	n.c.	n.c.	n.c.	n.c.
Q	90	n.c.	n.c.	n.c.

**n.c. (not calculable)*

Tab.IV.10.: Values of Indices of fragmentation: red and yellow pieces from La Garma A.

From these levels were collected more than about hundred fragments of red and yellow pieces as well as lithic tools and shell ornaments in some cases with red ochre residues (Catelli *et al.*, 2016; Brunelli *et al.*, 2016). Accurate prospections inside the cave allowed us to verify the absence of ochre sources inside and in the immediate vicinity of the site. The anthropic use of ochre in Grotta di Pozzo is already confirmed thanks to the analysis of superficial residues on artefacts and ornaments from the Epigravettian and Sauveterrian levels of the site. Nevertheless, the absence of ochre processing tools in the archaeological deposit raises many doubts regarding the exploitation of ochre and the ways of treatment and transformation of raw materials. In this way, it is worth pointing out that a total of 138 elements were collected from stratigraphical units of Grotta di Pozzo. In some of these units there are few elements do not statistically significant. To overcome this problem, the stratigraphic units will be grouped to obtain an assemblage that is numerically consistent, in which it is possible to make rather reliable statistical considerations. For this reason, the stratigraphic units will be chrono-culturally grouped as follows:

- PS13-PS7 (PS α ; PS11; PS10; PS9; PS8) Ancient Epigravettian;
- InterPS6/PS7-PS1 (interPS6/PS7; PS6; PS6/PS5; PS4; PS3; PS2, PS1) Final Epigravettian ;
- Chiocciolaio3/2bis (Chiocciolaio3; Chiocciolaio2; Chiocciolaio2bis): Sauveterrian..

IV.4.1. Colour

The best represented colour is red followed by yellow. Both were attested with different tonalities and shades though the Munsell Soil Colour Charts. In the table below, the distinct colours are listed which have been included in two large colour classes: red and yellow (Tab.IV.11).

By evaluating the evolutionary tendency of the two-colour classes, the histogram allows us to notice a substantial difference between the two Palaeolithic blocks PS13/PS7 and interPS6/PS1. For the lower block (Ancient Epigravettian) only two pieces from PS13 and three red pieces from PS7 were counted while the units PS α , PS11, P10, PS8 did not return any materials.

A noticeable increase is registered in the block interPS6/PS7-PS1 in which the red elements are the most represented class. Also, the class of yellow elements were attested with many objects in comparison with other units in the deposit.

For the Mesolithic block (Chiocciolaio3, Chiocciolaio2; Chiocciolaio 2bis), both classes were poorly represented.

IV.4.2. Mass and dimensions

The estimation of mass and dimension is surely the most reliable way to evaluate the exact quantity of red and yellow raw materials in the deposit. A quantification in a diachronic sense shows a scarce quantity of red ochre for the lower levels (PS13/PS7) while yellow ochre is absent. Copious quantities of red ochre are observed in the block of interPS6/PS1 just above the mass of material collected from the upper Chiocciolaio3/Chiocciolaio2bis block.

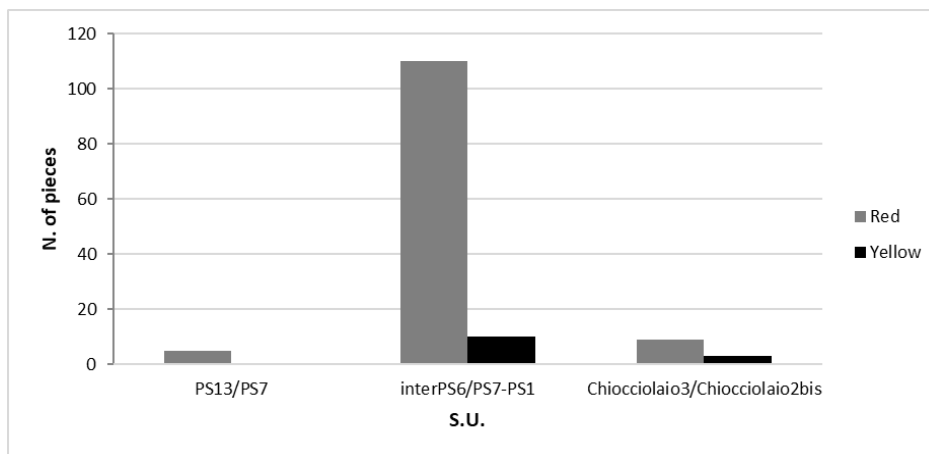


Fig.IV.20.: Grotta di Pozzo: distribution of number of red and yellow ochre pieces collected from each stratigraphic unit of the archaeological deposit.

By comparing the evolutionary tendency of the mass values (gr) with the number of objects by colour class, there is a net discrepancy between the number of red ochres quantified for the Mesolithic levels and the small number of pieces counted in them.

Comparatively, the objects counted in the units of block interPS6/PS1 are 110 and have a mass of around 15 gr like the quantifiable one for the units of block

Chiocciolaio3/Chiocciolaio2bis in which only 9 heavier pieces were counted. In regards the mass of the yellow materials, this corresponds to little more than 1gr divided between the block interPS6/PS7 and Chiocciolaio3/Chiocciolaio2bis (Fig.IV.21).

List of tints in the Munsell Soil Color Charts	
Red	Yellow
10R 3/4 dusky red	10YR 6/6 brownish yellow
10R 3/6 dark red	10YR 7/8 yellow
10R 4/6 red	7.5YR 5/6 strong brown
10R 4/8 red	7.5YR 5/8 strong brown
2.5YR 4/6 dark red	10YR 6/8 brownish yellow
2.5YR 4/8 dark red	
2.5YR 5/6 red	
2.5YR 5/8 red	
5YR 5/8 yellowish red	
5YR 6/8 reddish yellow	

Tab.IV.11.: *Grotta di Pozzo: list of tints in Munsell Soil Color Charts approximate in two set of colours: red and yellow.*

The dimensional distribution attests most pieces with dimensions between 2-10 mm. In the block of the lower units, only this dimensional class is attested with numbers which are rather low. A substantial increase is highlighted for the intermediary block with 99 class elements (2-10 mm) and 11 elements >10 mm.

For the higher block there are 5 pieces with dimensions between 2 and 10 mm and 4 pieces with dimensions >10 mm (Fig.IV.22). For the yellow elements, the maximum lengths fall in a dimensional range between 2 and 10 mm where there are 10 elements from the intermediary block and 3 elements from the higher block.

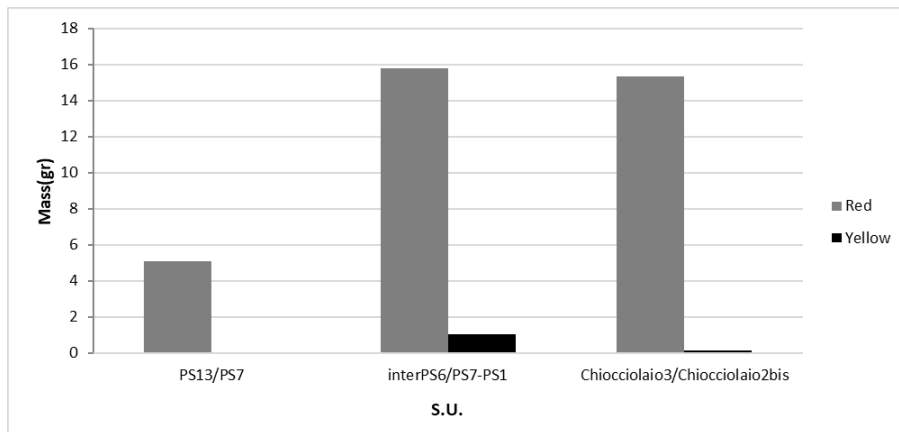


Fig.IV.21.: Grotta di Pozzo: distribution of red and yellow ochre specimens in function of the mass in grams.

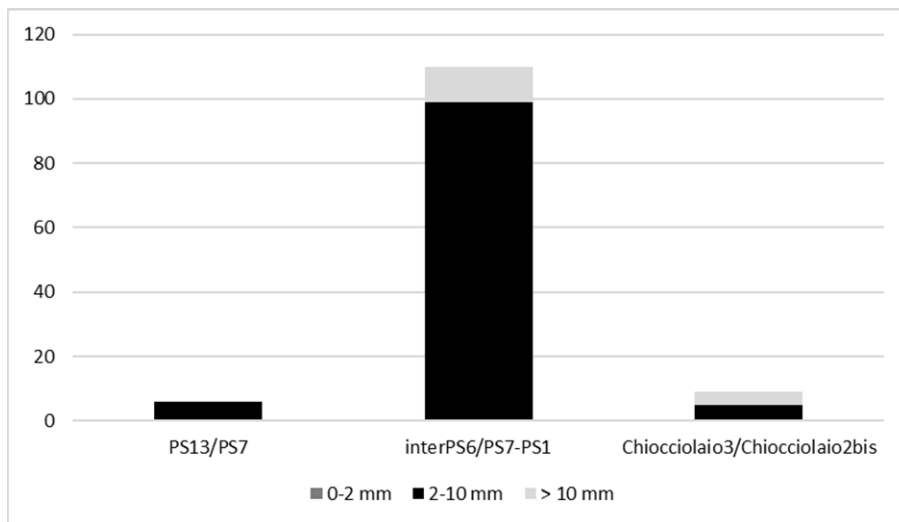


Fig.IV.22.: Dimensional distribution of yellow pieces from Grotta di Pozzo.

IV.4.3. State of conservation

The materials show a regular state of conservation in all the units of the archaeological deposit. It is possible to see greyish concretions like an external cortex in most of the red vestiges, in that the original colour is visible in fracture. This cortex is not observed on the yellow vestiges. From a preliminary observation by naked eye, this cortex was attributed to a post depositional contamination.

The microscopic observation allowed us to define this element as a physical peculiarity of the raw material. This consideration is supported by the fact that the cortex only appears on the red ochre. These red vestiges come from the same unit as the yellow vestiges which are without greyish cortex. Furthermore, this species of greyish cortex characterizes the pieces from different layers distinguished. This element allows us to disprove the hypothesis of a post depositional contamination and strengthen the idea of a natural origin in that if the presence of the cortex were linked to the amount of material in a contaminated layer, it should only have characterized those elements collected from the contaminated layer and not a large part of red pieces. The cortex therefore corresponds to a specific physical property of the material itself and its presence or absence on the pieces of ochre can help classify the raw materials. The greyish concretions cover a large part of the surface which does not show any diagnostic marks or traces. This absence is explained by analysing the hardness of materials. Both red and yellow vestiges are rather tender and powdered upon touch with breakable surfaces that could have easily favoured the elimination of traces despite the materials being recovered in an accurate way. The whole sediment taken from the squares of each stratigraphic unit was dry sieved and accurately selected to favour the

recovery of very small elements such as micromammal or fish remains which are abundant in the site. Even the ochre remains were recovered by sieving the previously dry sediment and covered in aluminium and then kept in plastic sterile bags to avoid contamination. By acknowledging the absence of modified pieces, it is worth calculating the diversity index of Shannon-Weaver to estimate the heterogeneity of the sample and to verify the incidence of the dimensional difference of each element in relation to the assemblage of the materials. Furthermore, to estimate the effective representativeness of raw materials of the site, besides the quantification of the mass of material collected, it is useful to estimate the level of fragmentation of the assemblage since it is in the presence of many small pieces with similar physical traits that could derive from the fragmentation of a similar and more voluminous block.

Index of Shannon-Weaver (H) and Evenness (J)

To calculate the Shannon-Weaver index, it is necessary to establish categories to enclose each element. In the case of Grotta di Pozzo, it was possible to divide the red pieces into three categories: raw pieces (2-10 mm); raw pieces (>10 mm); raw blocks. In regards the yellow pieces, the total of 19 elements were included in a single category: raw pieces (2-10 mm). For this reason, it was not possible to apply the diversity index. For the red elements, the Shannon-Weaver index had a value of 0,5, thus indicating a rather low diversity of the assembly in which the single objects tended to distribute themselves in a non-homogeneous way as indicated by the Evenness value ($J= 0,3$).

Index of fragmentation

Just like the Shannon-Weaver index, it was also possible to calculate the index of fragmentation just for red ochres. The class of pieces with dimensions between 2 and 10 mm is the one that refers to the highest indexes. For the lower levels, PS13/PS7, the index of fragmentation is rather low while it increases substantially in the intermediary levels interPS6/PS1 and in the lower levels Chiocciolaio3/Chiocciolio2bis. In regards the raw pieces >10mm, the intermediate levels with rather low indexes were attested when compared to raw pieces 2-10 mm.

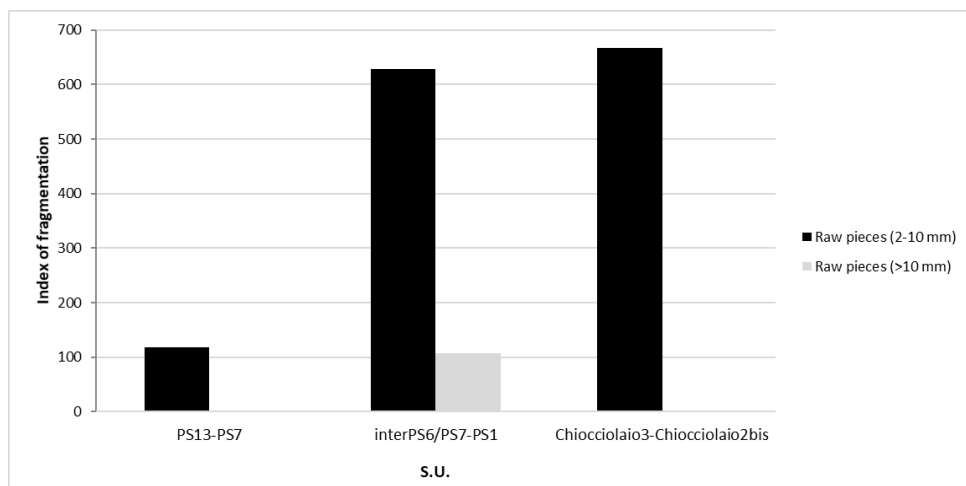


Fig.IV.23: Grotta di Pozzo: distribution of the fragmentation indices according to the established categories for the red pieces.

Red pieces				
Categories	Quantity	Relative abundance (Pi)	Log2(Pi)	Pi * Log2(Pi)
Raw pieces (2-10 mm)	112	0,896	-0,158429362604483	-0,141952709
Raw pieces (> 10 mm)	13	0,896	-0,158429362604483	-0,141952709
Raw blocks	3	0,024	-5,38082178394093	-0,129139723
				-0,542184863
			H	0,542184863
			J	0,342080562

Tab.IV.12: Grotta di Pozzo: Index of Shannon-Weaver (H) and Evenness (J) of red pieces.

Red pieces			
	Raw pieces	(2-10 mm)	Raw pieces (>10 mm)
PS13-PS7	117,6		n.c.*
interPS6/PS7-PS1	627,7		107
Chiocciolaio3-Chiocciolaio2bis	666,6		n.c.

**n.c. (not calculable)*

Tab.IV.13: Values of Indices of fragmentation: red pieces from Grotta di Pozzo

Chapter V.

Identification and characterization of raw materials

The identification and characterization of raw materials allows us to obtain reliable data to investigate human behaviors involved in ochre exploitation among Upper Palaeolithic and in south-western Europe. In order to orientate the reasoning in an organized way, the data will be presented in the same order as chapter IV.

The identification of raw materials and the estimation of their proportions inside the archaeological record will allow us to investigate the degree of human intention in the exploitation and use of colouring minerals. Furthermore, to outline a framework of human behaviors on a continental scale, some samples from the previously mentioned sites as Grotta del Romito, Grotta San Teodoro and S'Orku and S'Orku will be examined. The importance of these ochre samples for comparative studies is related to the archaeological contexts that offer essential comparisons for the presence of red ochre associated to human burials.

The characterization of ochre remains collected from funerary contexts is significant to search indexes of anthropic transformations of colouring materials in order to recognize intentional mixtures.

V.1. Classification criteria

The opportunity to macro-microscopically observe each single piece allows us to set a series of principles to identify raw materials based on visual criteria: external colour; presence of mineral inclusions.

The evaluation of ochre vestiges starting from these essential criteria allows us to recognize classes of raw materials. The external colour was detected as described in the previous chapter. The colour was coded with the Munsell Soil Color Charts as a point of reference to distinguish rocks, minerals and soils through colour.

Colour is one of the most immediate and simple visual criteria for identification. The oxides, oxy-hydroxides and hydroxides of iron play a key role in this sense for their strong pigmentation between red, orange and yellow. Several studies use connotations of colour to elaborate classification systems of ochre by starting from the presupposition that iron ores are the main responsables of their pigmentations (Salomon, 2009; Dayet, 2013).

By a naked eye observation, the iron ores have the following colours: *goethite* yellow-brown; *lepidocrocite* orange; *hematite* red; *feroxyhyte* and *ferrihydrate* dark reddish-brown colour (Cornell & Schwertmann, 2004).

Geochemical characterization and comparisons between soils and minerals (Schwertmann & Taylor, 1989; Barrera-Bassols & Zinck, 2000; Viscarra Rossel *et al.*, 2010) allows us to distinguish oxides, hydroxides and oxy-hydroxides of iron starting from their colours coded in the Munsell Soil Color Charts (Tab.V.1). The materials were evaluated based on these correspondences.

<i>Mineral</i>	<i>Munsell Soil Color Chart</i>	<i>Colour</i>	<i>Formula</i>
Hematite	10R 4/8	Red	(Fe ₂ O ₃)
Goethite	10YR 8/6	Yellow	(FeOOH)
Goethite	7.5YR 5/6	Strong Brown	(FeOOH)
Lepidocrocite	5YR 6/8	Reddish Yellow	(γ -FeO(OH))
Lepidocrocite	2.5YR 4/6	Orange	(γ -FeO(OH))
Ferrihydrite	2.5YR 3/6	Dark Reddish Brown	((Fe ³⁺) ₂ O ₃ •0.5H ₂ O)

TabV.1.: List of colours in Munsell Soil Color Charts of main iron ores forming red and yellow ochres.

The detection of mineral inclusions is another distinctive criterion. The observation by naked eye and binocular microscope allow to attest the presence of inclusions as quartz, limestone and micas which are often associated to ochres (Cornell & Schwertmann, 2004). The presence or absence of these inclusions not only permits to discriminate different typologies of raw materials but can give fundamental indications concerning genetic processes and provenance from specific geological sources. By starting from these criteria, a classification of raw materials that compose the ochre assemblages examined for this research, here is exposed.

V.1.1. Characterization of raw materials

The characterization of the raw materials was carried out through the geochemical investigation of ochres. Qualitative and quantitative analyses were done by starting from the chosen methods through the execution of preliminary

tests as described in chap. II of this work. The investigation of major and minor elements and chemical compounds is important to prove what was established through macro-microscopic observation and to search for anthropic selection and transformation indicators. Furthermore, the detection of mineral associations can give indications on the properties of iron ores related to specific uses.

V.2. Los Canes

V.2.1. Iron ores and colour

The observation of ochre samples attests the following colours: red, orange, dark reddish brown, yellow, strong brown, that according to the Munsell system can be related to the presence of *hematite* (10R 4/8 red); *lepidrocrocite* (2.5YR 4/6; 5YR 6/8); *ferrihydrite* (2.5YR 3/6); *goethite* (10YR 8/6; 7.5YR 5/6). By plotting a ternary graph, the colours detected on surface highlight clear groupings around the fixed points which represent the colour-coded guide by the Munsell Soil Color Charts (Cornell & Schwertmann, 2004). These tint-guides are represented by fixed points in the graph.

Regarding red ochres, it appears clear that there is a tendency to distribute them into two different groups defined by ellipses of confidence with an interval at 95%. The first group includes the points near colours 2.5YR 4/6 (*lepidrocrocite*) e 2.5YR 3/6 (*ferrihydrite*).

The second group includes the colours near 10R 4/8 (*hematite*). According to this distribution, the specimens between orange and dark reddish brown potentially contain iron oxides-hydroxides (*lepidrocrocite* and *ferrihydrite*). On

the other hand, the elements which have a deep reddish superficial colour may contain iron oxides (hematite). This distribution confirms the relation with oxides (hematite) and oxy-hydroxides (lepidocrocite, ferrihydrite) as potential primary constituents of red ochres.

For what concern the yellow vestiges, a large part of the elements except two points, are enclosed by the same confidence ellipse (interval at 95%) around *goethite* (10YR 8/6; 7.5YR 5/6).

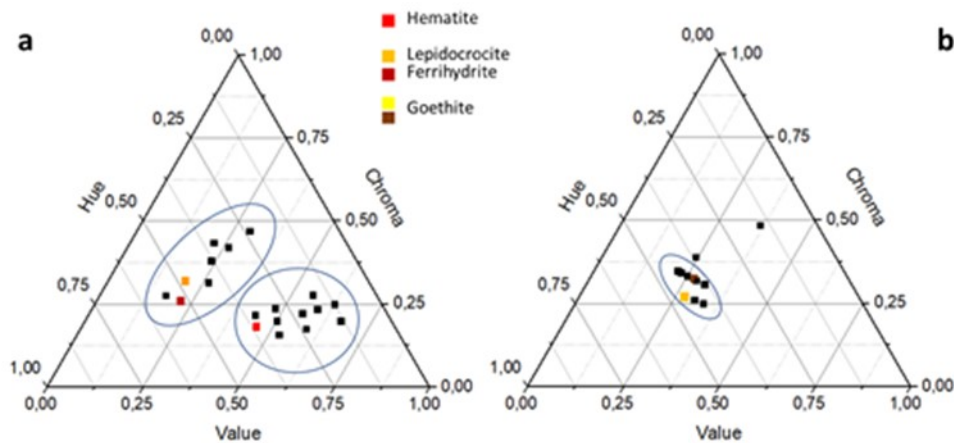


Fig.V.1.: Los Canes: ternary plot of ochres grouped for raw materials by colour in Munsell Soil Color Charts. Black points correspond to archaeological colours.

The identification by colour attests three main classes (Fig. V. 34) of raw materials: iron oxides (hematite); iron oxy-hydroxides (lepidocrocite; ferrihydrite); iron hydroxide (goethite).

Iron oxide (hematite): compact structure and very fine granulometry with a deep red colouring with black inclusions (magnetite). Particles of quartz and calcium are also frequent. Inside this class, it is possible to recognize two sub-classes: (I-

a) characterized by a homogeneous surface and a red colouring with a metallic aspect due to the presence of iron iridescent elements; (I-b) includes materials with an opaque-powdered, heterogeneous and porous surface with a deep red colour.

Iron oxy-hydroxide (lepidocrocite/ferrihydrite): (2) compact and massif structure characterized by red, brownish red, orange shades heterogeneously mixed on surface. Rare inclusions of quartz and calcium.

Iron hydroxide (goethite): (5) compact structure with a high porosity. The opaque and powdered surface has a heterogeneously distributed colouring. Compact structure with inclusions of white calcium and rare mica inclusions.

It should be noted that the microscopic observation, highlighted the presence of three specimens with a very light-yellow colour associated with a slightly compact structure and a glassy consistency with translucent surfaces. Due to these traits, it is almost certainly not goethite. Geochemical analyzes can clarify their chemical nature.

V.2.2. Geochemical composition

The geochemical analysis confirm what was hypothesized by the classification based on visual criteria. SEM-EDS analysis attests the presence of oxides, hydroxides and oxy-hydroxides of iron confirming the relation between colour and chemical traits.

Iron oxide (hematite): The crystalline structure is formed by rhomboidal and pseudo hexagonal crystals which are typical of hematite. The semi-quantitative characterization detects the presence of Fe, Si, Al as bigger elements that are

distributed according to the following percentages: Fe >50%; Si <5%; Al <3%. Ca (calcium) is also largely detected as suggested by the mineral inclusions observed in the samples. In one case, traces of K were detected while in another case, Cl was detected too. The presence of this element can suggest the genesis in a marine-coastal environment located at about 15-16 km far from the cave.

Iron oxy-hydroxide (lepidocrocite) the structure appears to be defined as lath-like or tabular crystals often aggregated in the typical flower structures of lepidocrocite. In regards the presence of other iron oxides and oxy-hydroxides, ferrihydrite can be recognized. This oxy-hydroxide is rather difficult to identify due to its low degree of structural order and in this case, it seems that it is characterized by small spheroidal crystals aggregated into lattice fringes. In any case, the high susceptibility of the transformation of iron ores among themselves can determine the presence of intermediary forms which at an external and superficial level seem to have the same colour and do not have any evident differences. The main constituents are Fe, Si, Al with different percentages (Fe 20-50%; Al <8%; Si <15%). There is also the presence of secondary elements like K (<2%) and rarely P-Mg-Mn (<1%). The presence of Ca is also attested with low percentages (<3%).

Iron hydroxide (goethite): the crystalline structure appears to be formed by acicular crystals which can vary in size. The acicular crystals are organized in botryoidal aggregates. The major elements are Fe 50-60% and Si <5%. In some cases also Al (<3%) and K(<1%) and Ca (<3%) are present.

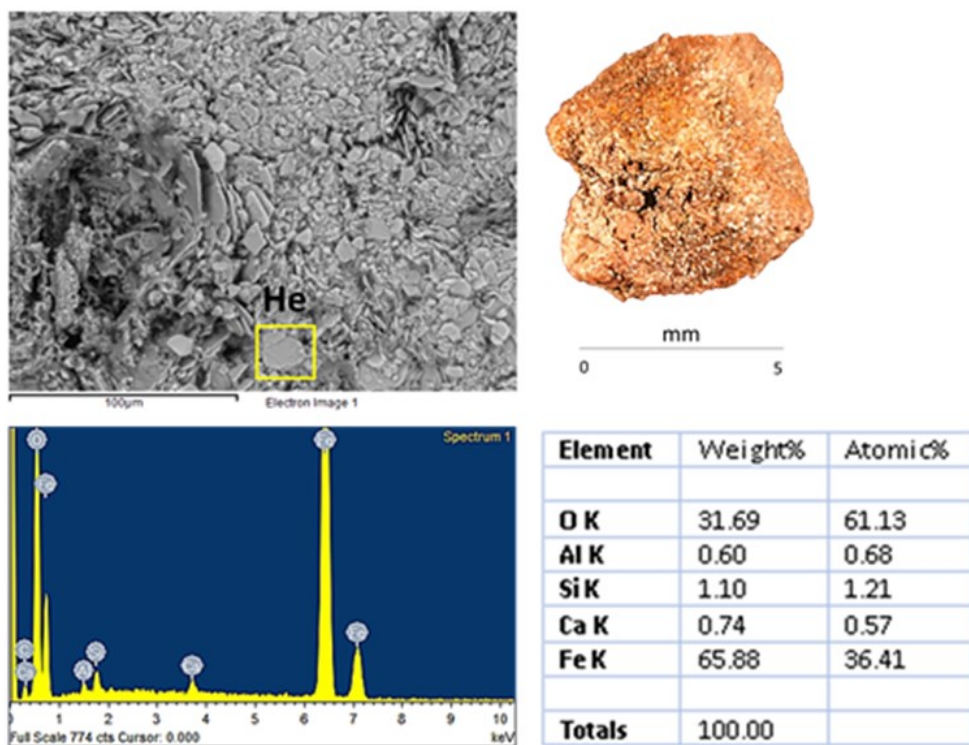


Fig.V.2.: Characterization by SEM-EDS of hematite sample from Los Canes

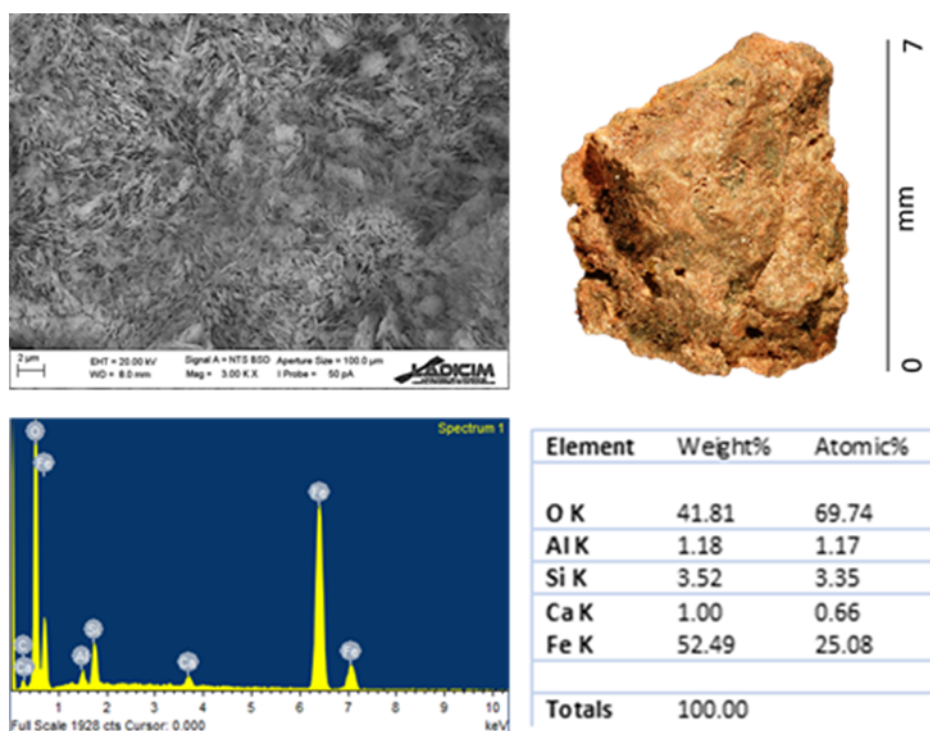


Fig.V.3.: Characterization by SEM-EDS of lepidocrocite sample from Los Canes.

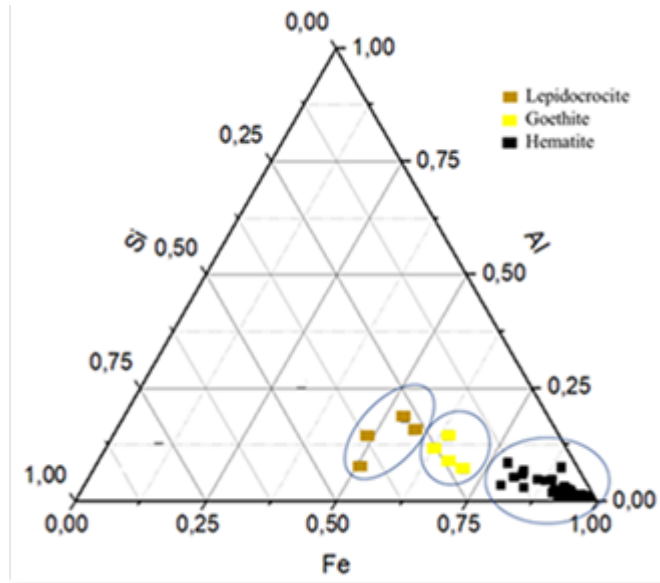


Fig.V.4.: Ternary plot of main iron raw materials from Los Canes based on the percentages of Fe-Al-Si.

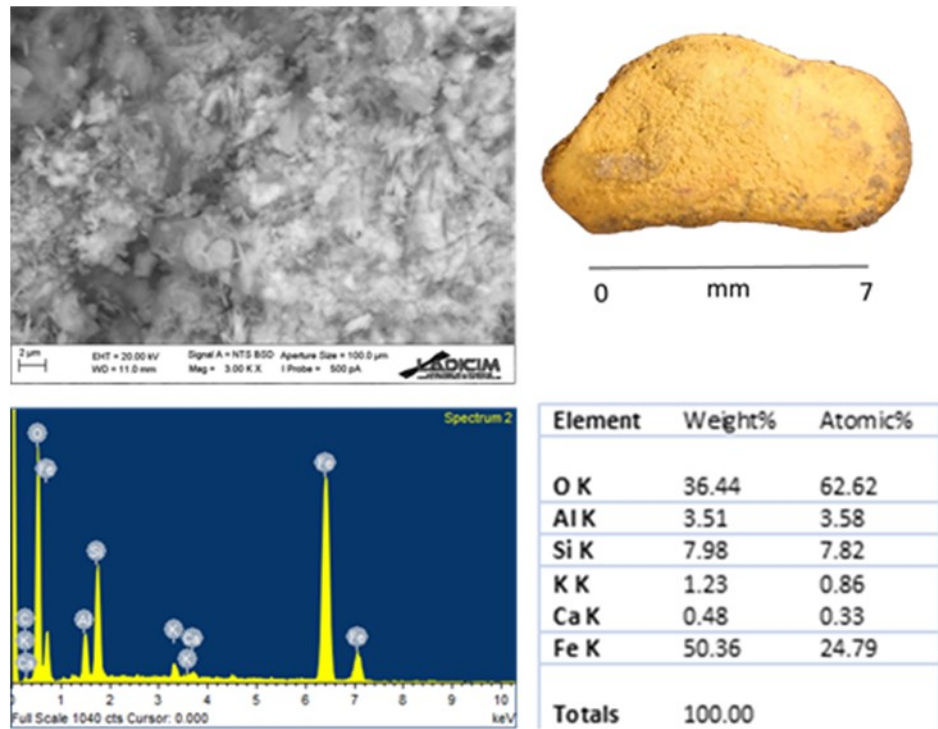


Fig.V.5.: Characterization by SEM-EDS of goethite sample from Los Canes.

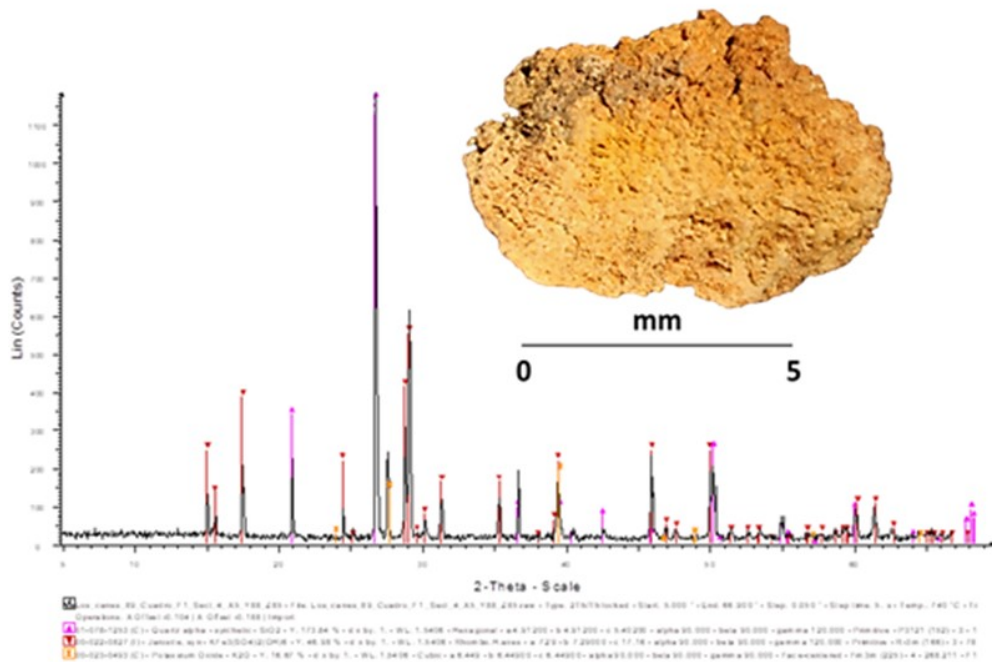


Fig.V.6.: XRD spectrum of jarosite archaeological sample from Los Canes.

Basic sulphate of potassium and iron (Jarosite): the presence of Fe (~30%); S (~10%), K (~6%); Si (<5%) and traces of Al (<1%) in yellow rocks is due to the presence of Jarosite. By observing the crystalline structure, pseudo-cubic and rhomboidal crystals can be distinguished. The diffraction analysis (XRD) confirm the presence of Jarosite as the main chemical compound. The spectrum of reference also highlights the association with quartz and potassium oxide.

V.2.3. Proportion of raw materials

The high degree of fragmentation, as established in the previous chapter, poses several problems of representativeness of the raw materials in relation to the total number of pieces collected at the site that could be overestimated. In this case, it is useful to evaluate the proportion of the raw materials in function of

mass, density, dimension and fragmentation. Regarding mass, hematite is the most abundant one. The total mass of materials is characterized by 96% red hematite, 3% of lepidocrocite/ferrihydrate and only 1% of goethite (Fig. V.7). By analyzing the representativeness of raw materials, there are substantial differences in the density per stratigraphic unit.

The density of hematite (Fig. V.8) is generally high in all the stratigraphic units of the archaeological deposit. Nevertheless, by analyzing the evolutionary tendency in a diachronic sense, the density of hematite is particularly low from Solutrean (2A) to Magdalenian (2B; 2C). The density of hematite increases notably in the Azilian units 3A and 3B. It reduces in unit 3C and once again goes back to increase in unit 4, but is appear to be low in unit 5 is low. In regards the units of structure 6III, the density of hematite is quite remarkable when compared to the other Mesolithic units 6III and 6I. It is necessary to consider that the realization of burial 6III largely affected the Solutrean and Magdalenian levels of the deposit and partly the Azilian ones by determining a redistribution of materials. For unit 6II, the density of hematite is rather low and increases slightly in unit 6I.

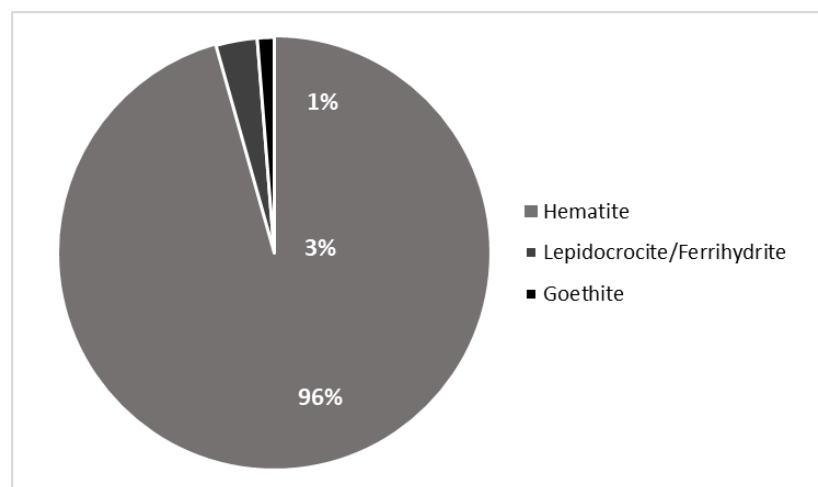


Fig.V.7.: Percentages of the total mass of raw materials at Los Canes.

As far as units 6A, 6B and 6C are concerned, these also correspond to the filling of less deep pits. Specifically, the excavation of the 6A structure affected Palaeolithic and Azilean levels, unlike structures 6B and 6C whose excavation cutted base unit 1. It is therefore advisable to highlight the differences that emerge between the density of hematite in unit 6A, greater than the units 6B and 6C characterized by a rather low density. The density of lepidocrocite/ferrihydrate and goethite is generally low for all units of the deposit. There are no differences even if lepidocrocite/ferrihydrate has a slightly higher density in unit 6III and 6I in accordance with goethite.

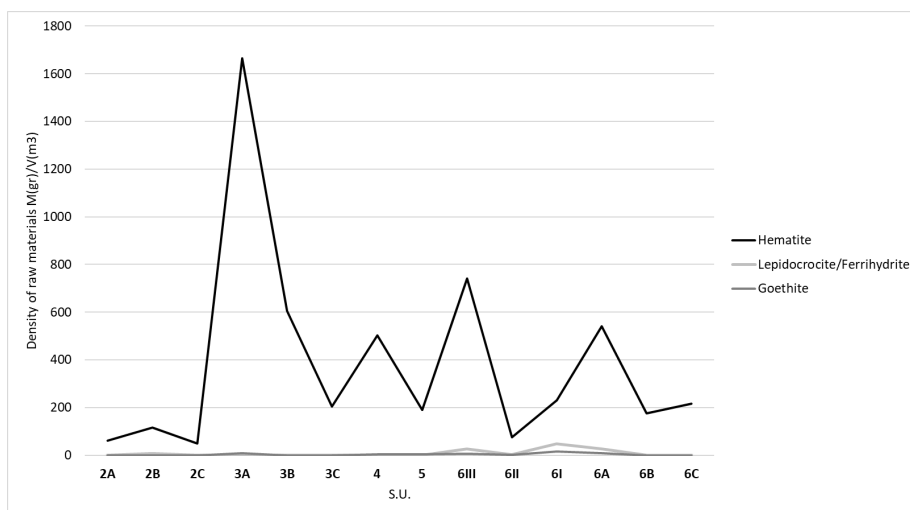


Fig.V.8.: Density distribution of raw materials at Los Canes.

In this calculation, it is necessary to consider that the realization of burial 6III largely affected the Solutrean and Magdalenian levels of the deposit and partly the Azilian ones by determining a redistribution of materials. For unit 6II, the density of hematite is rather low and increases slightly in unit 6I. As far as units 6A, 6B and 6C are concerned, these also correspond to the filling of less

deep pits. Specifically, the excavation of the 6A structure affected Palaeolithic and Azilean levels, unlike structures 6B and 6C whose excavation cutted base unit 1. It is therefore advisable to highlight the differences that emerge between the density of hematite in unit 6A, greater than the units 6B and 6C characterized by a rather low density. The density of lepidocrocite/ferrhydrite and goethite is generally low for all units of the deposit. There are no differences even if lepidocrocite/ferrhydrite has a slightly higher density in unit 6III and 6I in accordance with goethite. In fact, from the graph, there is a distributed density that is similar for both goethite and lepidocrocite/ferrhydrite of the funerary structures 6III and 6I.

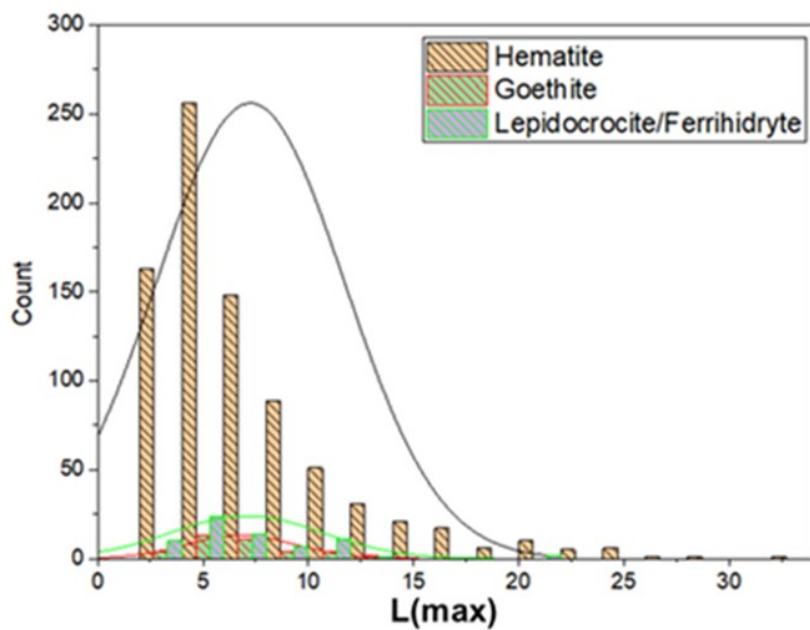


Fig.V.9.: Distribution of the maximum length values $L(max)$ in function to the raw materials of Los Canes: hematite; lepidocrocite/ferrhydrite; goethite.

By testing the maximum length values based on type of raw material, there is a non-normal distribution in all cases (Fig. V.9). By evaluating length, width and thickness, there are differences in sizes in function to the raw materials due to

the presence of few pieces of large sized hematite and lepidocrocite/ferrihydrite (Fig. V.10).

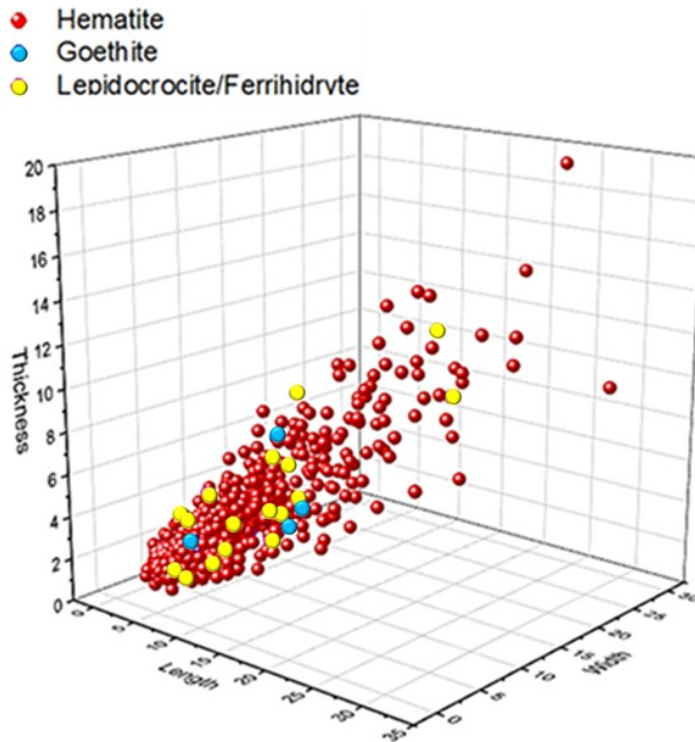


Fig.V.10.: Dimensional comparative evaluation (length, width and thickness) in function of the raw materials of Los Canes: hematite; lepidocrocite/ferrihydrite; goethite.

Most of the pieces are ranked in a dimensional range between 2 and 10 mm. The absence of large pieces of goethite and lepidocrocite/ferrihydrite can indicate an anthropic selection during the procurement of raw materials or a more intense fragmentation of the whole blocks brought into the site. This last hypothesis is confirmed by the values of fragmentation indices. Goethite shows the highest value followed by lepidocrocite/ferrihydrite. Hematite has a lower fragmentation index (Fig.V.11). By comparing the proportions of mass (gr) and number of pieces in function to the raw material, the proportion of hematite appears to be notable in accordance with the density values. Goethite and

lepidocrocite/ferrihydrate are slightly represented both for mass (gr) and for the number of pieces (Fig. V.12).

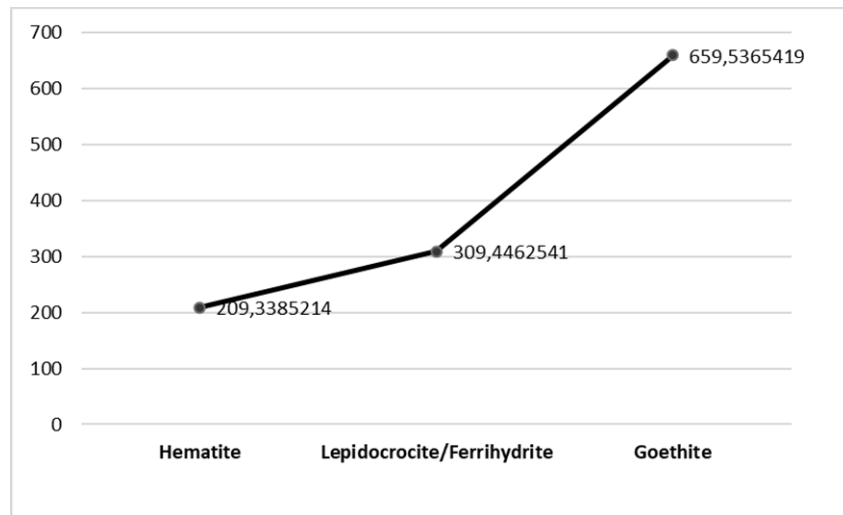


Fig.V.11.: Comparative evaluation of fragmentation indexes in function of the raw materials of Los Canes: hematite; lepidocrocite/ferrihydrate; goethite.

By evaluating the distribution of raw materials in function to the categories of objects, hematite is the largely attested one and characterizes every class. The second one in terms of quantity of objects is the class of iron oxy-hydroxides (ferrhydrite/lepidocrocite). Even this class is attested for each category. Goethite characterizes raw and modified fragments.



Fig.V.12.: Proportion of mass (gr) and number of pieces in function to the raw materials in the site of Los Canes.

V.2.4. Evaluation of identification and characterization factors of raw materials

The site of Los Canes returned a rich ochre collection. Hematite is the primary constituents of red vestiges followed by ferrhydrite/lepidocrocite. While goethite is the main constituent of yellow vestiges. Some samples (n.3) of light yellow colour that do not fall within the group of yellow ochres (10YR 8/6; 7.5YR 5/6) are composed by jarosite. The identification based on visual criteria (colour, mineral inclusions), the chemical characterization and the estimation of the representativeness of raw materials in the deposit confirm the presence of three main classes of raw materials: iron oxide (hematite); iron oxy-hydroxide (lepidocrocite/ferrhydrite); iron hydroxide (goethite).

Based on mass and number of pieces as well density in association with with the presence of both fragments and larger pieces that are morphologically non-standardized, it is presumable that the blocks of hematite have undergone a reduction in size due to gross fragmentation (*concessage grossier*) that would leave no diagnostic traces, but rather irregular fractures (Salomon, 2009; Dayet, 2013). An additional non-marginal feature which characterizes some pieces of hematite is the presence of black magnetite inclusions. These inclusions can be recognized in pieces coming from both Palaeolithic and Mesolithic layers giving valid indicators on the continuous use over time of the same raw materials.

Lepidocrocite and ferrhydrite which have a colour between orange and reddish-brown are the second most attested raw materials at the sites in terms of number of pieces and mass. These raw materials characterize rather heterogeneous pieces from a dimensional point of view and with a modest fragmentation, but higher than hematite. It must to consider that the value of

the fragmentation index is certainly influenced by the presence of larger sized pieces which tend to push the index towards the lowest.

In any case, by evaluating the ratio between mass and number of pieces in function to the “red” raw materials (oxides and iron oxy-hydroxides), a propensity for hematite associated to a red colour appears to be evident rather than lepidocrocite and ferrihydrite, with a less intense colour.

Goethite and jarosite are the constituents of yellow rocks. In particular, goethite is larger in number of pieces and mass compared to jarosite which characterizes only three objects. Substantially, the yellow materials have a low representativeness in the assemblage. As far as goethite is concerned, it is worth highlighting that the lack of large pieces and the low representativeness in the assemblage tend to push the fragmentation index values higher.

It is clear that the presence of goethite in the site is due to an anthropic contribution. Analyzing the density of raw material for each stratigraphic unit, it is possible to observe substantial variations. In the case of a non-anthropic contribution, similar density values in all units were desirable. As far as jarosite is concerned, the finding of only three samples in the whole collection suggests an accidental presence in the deposit.

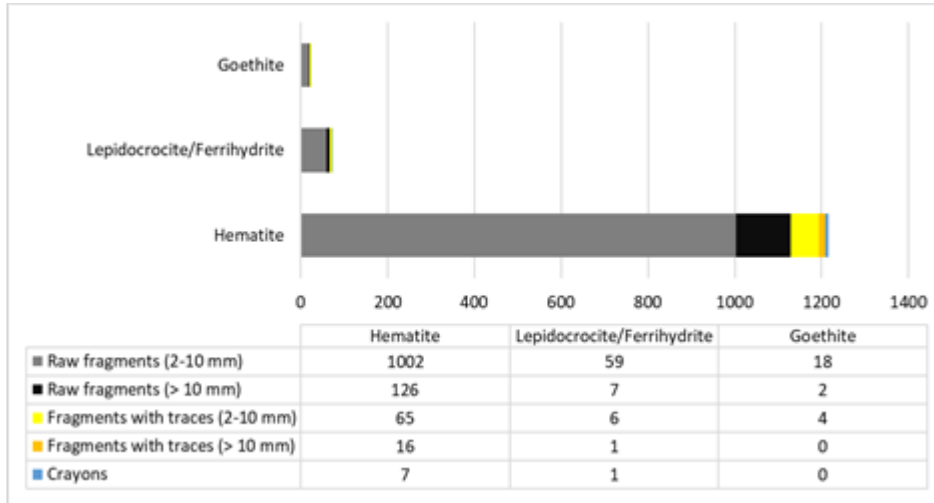


Fig.V.13.: Proportion of raw materials per category of objects from Los Canes.

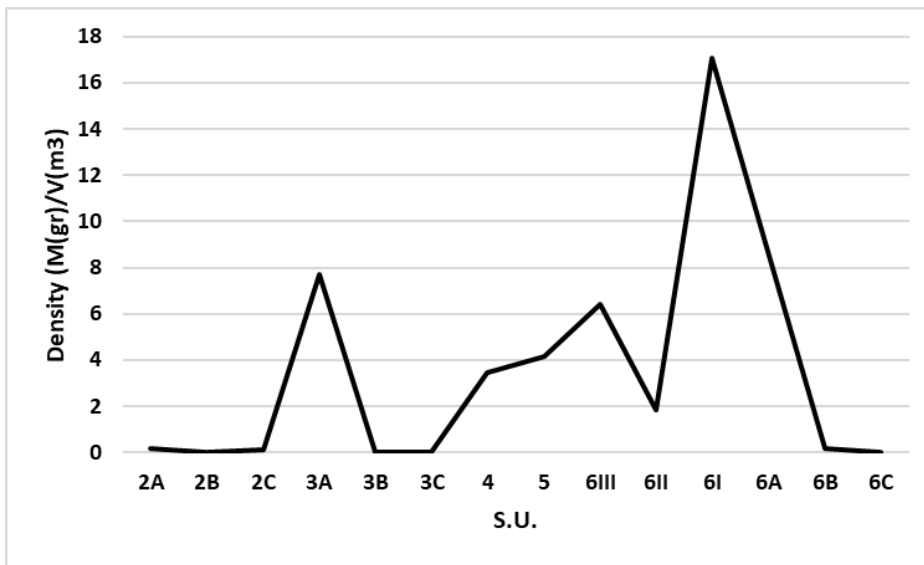


Fig.V.14.: Distribution of the density of goethite at Los Canes.

V.3. Arangas

V.3.1. Iron ores and colour

By observing the external colour, it is possible to recognize a set of colours between red and yellow as shown previously in chap IV. According to the coded colours in the ternary graph created from the fixed points corresponding to hematite (10R 4/8), lepidocrocite (2.5YR 4/6; 5YR 6/8), ferrihydrite (2.5YR 3/6), show a clear distribution of the archaeological specimens around the point of hematite. There are no archaeological points in the ellipse of lepidocrocite and ferrihydrite tints.

Iron oxide (hematite): the colour of hematite is associated to two sub-classes which are distinguishable by the colour and brightness of the surface.

The first sub-class (I-c) includes dark red elements with a rather low saturation. The surface appears heterogeneous and marked by the alternations of areas with higher concentrations of red and areas with a metallic aspect due to the presence of iridescent and shiny particles probably due to the presence of high concentrations of Fe.

The second sub-class (I-d) has a high saturation with a vivid and intense red. The surface is opaquer and the colour appears to be evenly distributed. There is the presence of groups of inclusions of black magnetite in four elements of this sub-class.

In both sub-classes, it is possible to observe rare inclusions of quartz and extremely rare white inclusions of calcium.

Iron oxy-hydroxide (lepidocrocite/ferrihydrite): this colour is associated to samples very similar for structure and composition to the samples of the first class. The

objects are distinguished by a more orange colour, but they have a homogeneous structural composition with inclusions of quartz and calcite (rare) and magnetite like in the case of iron oxide classes. Data could suggest a variation in the external colour which corresponds to a similar elemental composition. The geochemical characterization will be able to clarify this doubt. As far as yellow elements are concerned, the archaeological specimens fall within goethite with its colour between yellow and brown (10YR 8/6; 7.5YR 5/6).

Iron hydroxide (goethite): (6) elements with inclusions in this class have a yellow colour associated to the presence of goethite. The colour appears rather heterogeneous. The surface is characterized by intense yellow areas and areas which tend towards a beige tint. All the yellow samples have inclusions of quartz while inclusions of white calcium is observed in some elements. Three samples that are associated to pure yellow are excluded from the class of iron hydroxide (2.5Y 7/8 yellow; 5Y 7/8 yellow).

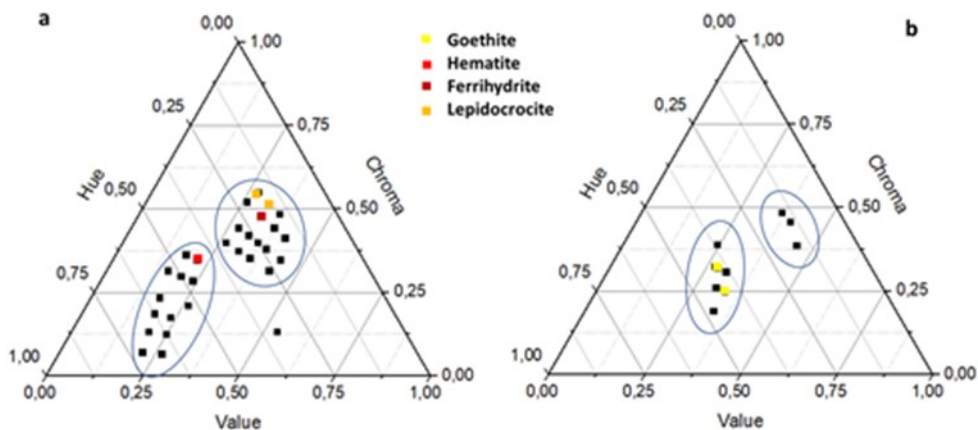


Fig.V.15.: Arangas: ternary plot of ochres grouped for raw materials by colour in Munsell Soil Color Charts. Black points correspond to archaeological colour.

V.3.2. Geochemical composition

The geochemical characterization with SEM-EDS confirms the presence of iron oxide (hematite) and iron hydroxide (goethite), by confirming the absence of iron oxy-hydroxide associated to an orange/dark reddish-brown colour. The compositional analysis highlights the presence of three types of raw materials: iron oxide (hematite); iron hydroxide (goethite); basic sulphate of potassium and iron (jarosite).

Nevertheless, it is interesting to ascertain the presence of lepidocrocite as the accessory mineral of goethite.

Iron oxide (hematite): the major elements characterizing this class are Fe (>40%) and Si, Al, C in varying percentages (0-10 %). The crystalline structure appears to be formed by pseudo-hexagonal crystals typical of hematite, in both the two sub-classes based on the visual criteria. Data is confirmed by the X-ray Diffractometry carried out on representative samples of the two classes. The XRD spectrum highlights the presence of hematite in both cases as the main mineral and thus confirming the data obtained with SEM-EDS.

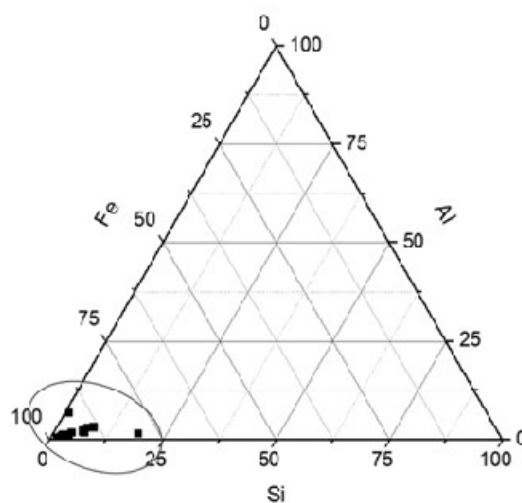


Fig.V.16: Ternary plot of hematite archaeological samples from Arangas.

Iron hydroxide (goethite): goethite is characterized by thin acicular crystals aggregated. The main chemical element is Fe (10-40%), followed by Si (<20%) and Al (<10%), K (<5%), Mg e Ti (<1%). The presence of these elements is due to the inclusion of muscovite (silicate), brucite (magnesium hydroxide) and quartz. The analyses with X-ray Diffractometry confirm the presence of goethite as the main chromophore of yellow ochres and accessory minerals like muscovite and brucite (Mg(OH)₂).

Basic sulphate of potassium and iron (jarosite): jarosite is the main mineral responsible for the pale yellow colour of some samples excluded by the goethite class. The main constituents are Fe (<30%); S (<10%); K (<6%) and Si (<5%).

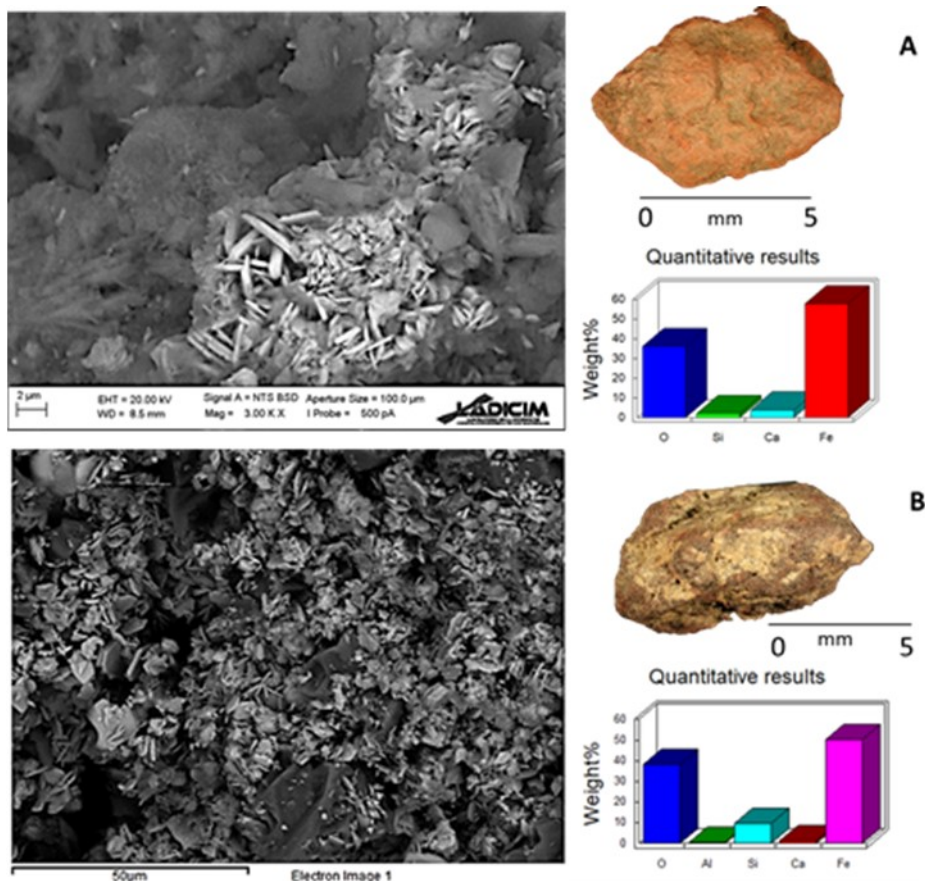


Fig.V.17.: Characterization by SEM-EDS of iron oxide (hematite) samples from Arangas: a) sub-class (1); b) sub-class (2).

V.3.3. Proportion of raw materials

Hematite is the most represented for both number of pieces (95%) and mass in grams (99%). The conspicuous presence of pieces with dimensions between 2-10 mm (hematite 84%; goethite 81%) and the value of fragmentation rates (hematite: $if=58$; goethite: $if=235$) imply a problem of representativeness of the effective number of pieces of hematite and goethite. The high fragmentation of goethite in relation to the effective number of pieces (no.16) determine an overestimation in the quantity of goethite at the site in comparison to hematite. By evaluating the proportions of mass (gr) of raw materials, it is possible to overcome the problem of representatives in number of pieces. According to this evaluation, the mass of hematite is distributed heterogeneously between the different units of the deposit. There is a large concentration in the Azilian units 5B and 5A, with substantial variations in the other units. A similar situation is highlighted for goethite which characterizes units 5B and 5A while it is not detected in other units. This heterogeneous distribution among the different units of the deposit together with a high fragmentation index in function to the quantity collected as well as the lack of large sized pieces (Fig. V.20) suggest an anthropic origin of red ochres.

The presence of just 3 pieces of jarosite in the whole of the assemblage raises doubts of a natural contamination. By evaluating the distribution of the maximum lengths in function to the classes of raw materials, the non-normal distribution of both hematite and goethite show notable dimensional variations.

The evaluation of the three dimensions (length, width, thickness) displays a large concentration of pieces with dimensions between 2-10 mm and the presence of big pieces enclosed in the hematite group. Nevertheless, by comparing this distribution to the number of pieces counted for each class,

goethite has rather high dimensions in function to the total number of objects in accordance to the fragmentation value.

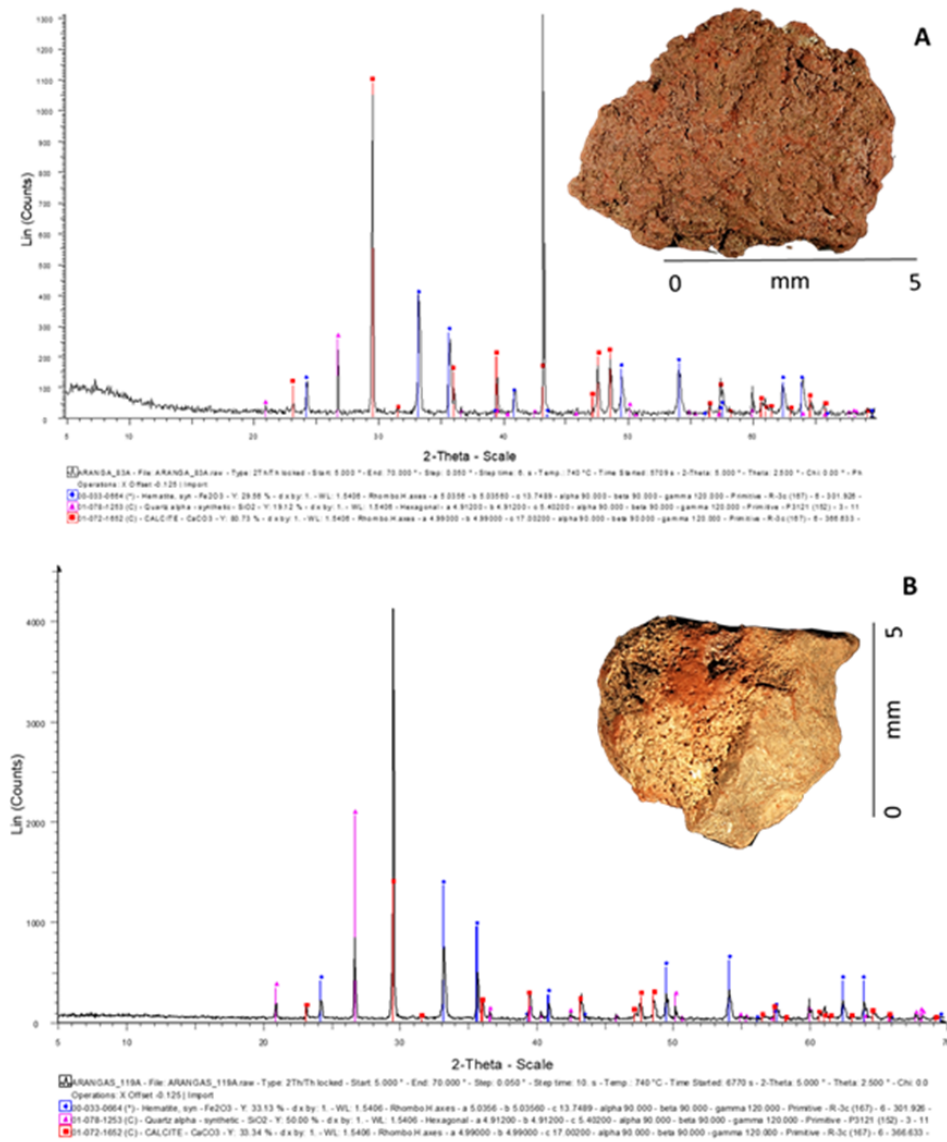


Fig.V.18.: XRD spectrum of hematite samples from Arangas: a) sub-class (1); b) sub-class(2).

Sample ID	Chromophore	Accessory mineral	Elemental Composition
1a	Hematite	Larnite	Fe, Si, Al, Ca, Mn, Mg
2	Hematite	-----	Fe, Si, Al, P, K, Ca
10e	Jarosite	Quartz	Fe, Si, S, K, Ca
20a	Hematite	Maghemite	Fe, Ca, Si
33a	Goethite	Brucite, Muscovite, Quartz, Lepidocrocite (traces)	Fe, Si, Al, K, Ca, Mg
83a	Hematite	Quartz, Calcite	Fe, Si, Al, K, Ca
119a	Hematite	Quartz, Calcite	Fe, Si, Al, Ca
130	Goethite	Brucite, Muscovite, Quartz	Fe, Si, Al, K, P, Mg, Ca, Ti
104a	Hematite	Calcite	Fe, Si, Al, Ca
104d	Jarosite	Quartz	Fe, Si, S, K, Ca

Tab.V.2.: Mineral compounds and elemental content of representative ochres for each class of raw materials from the assemblage of Arangas.

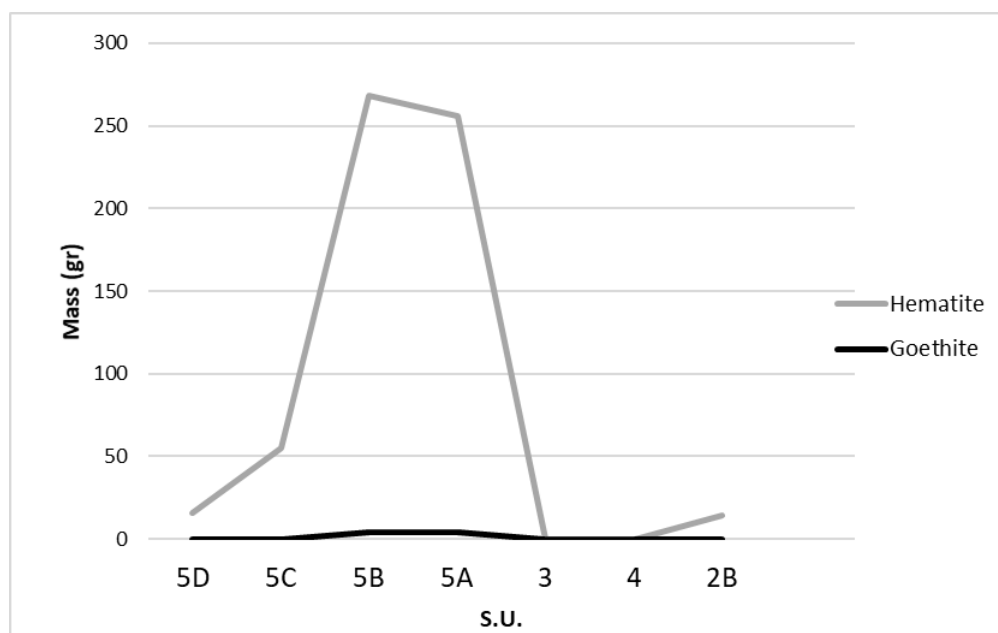


Fig.V.19.: Diachronic distribution of mass (gr) of raw materials in the site of Arangas: hematite and goethite.

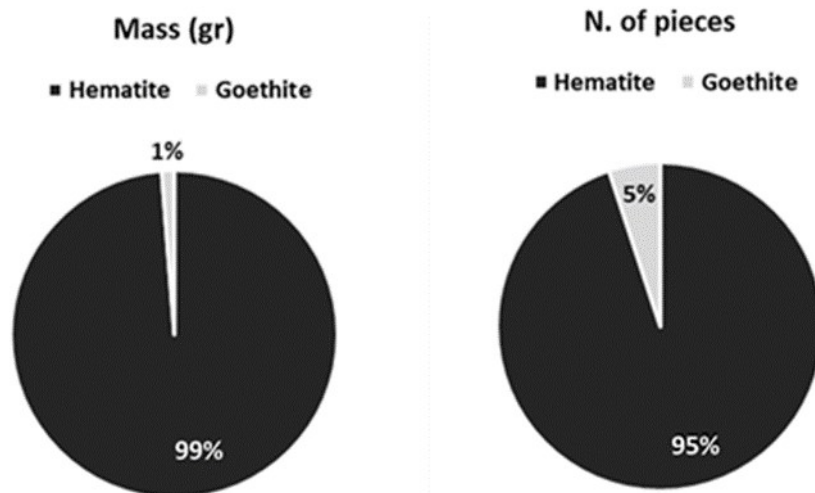


Fig.V.20.: Proportion of mass (gr) and number of pieces in function to the classes of raw materials in the Arangas site.

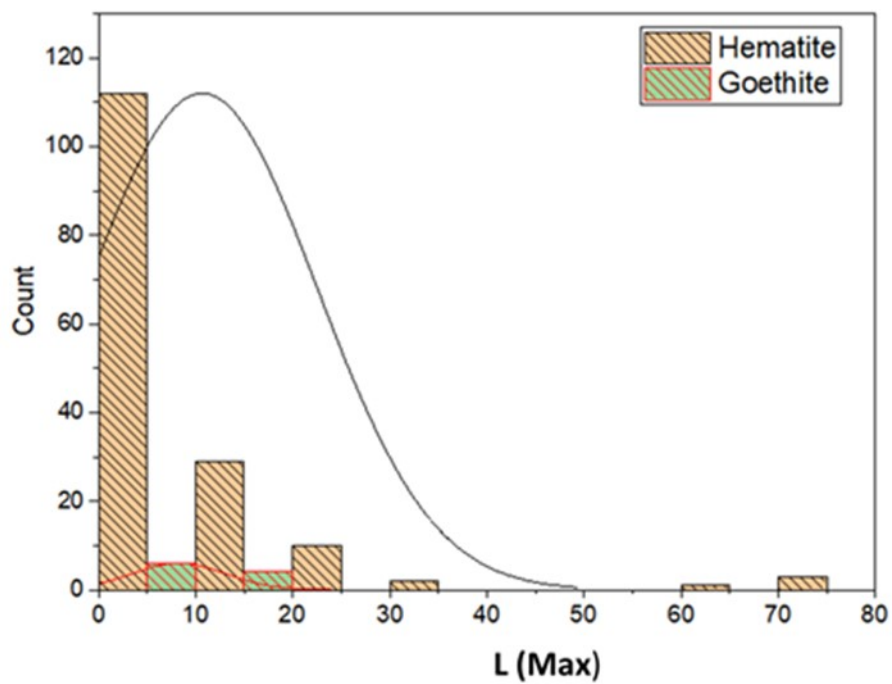


Fig.V.21.: Distribution of values of maximum lengths L(max) in function to the raw materials at Arangas: hematite; goethite.

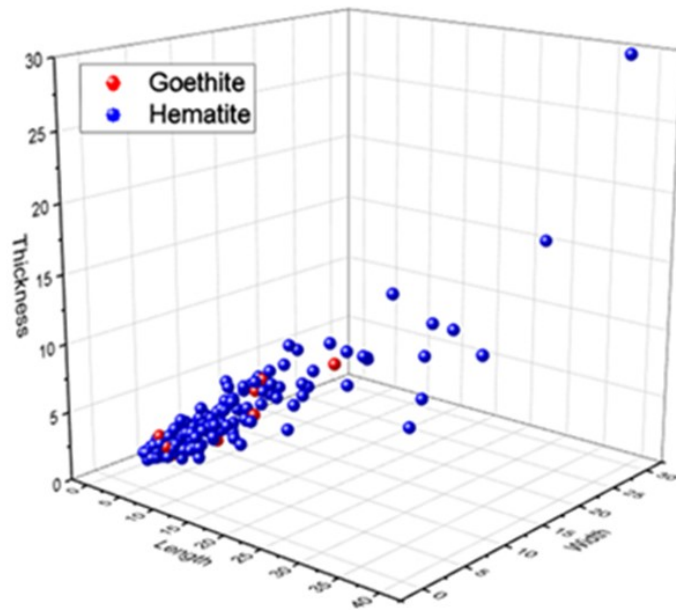


Fig.V.22.: Comparative dimensional evaluation (length, width and thickness) in function to the raw materials from Arangas: hematite; goethite.

V.3.4. Evaluation of identification and characterization factors of raw materials

The analysis of raw materials confirm the presence of two main different types of raw materials: iron oxide (hematite); iron hydroxide (goethite). The evaluation of visual parameters like the external colour and the presence of inclusions highlight the discrepancy between the results of the chemical characterization. The detection of colours associated to multiple iron ores (oxides and oxy-hydroxides) does not correspond with the geochemical characterization which shows the same crystalline structure with pseudo-hexagonal crystals which can be perfectly associated to hematite (Fe₂O₃). Furthermore, the percentages of major elements in the classes divided by colour

(hematite/ferrhydrite-lepidocrocite) confirm the same quantities of Fe, Si, Al as the main constituents. The variation of the percentages of elements like P, K, Mn and Mg in the hematite samples depend on the nature of the accessory minerals. .

In regards yellow materials, the colour identification is rather effective in that it preliminarily discriminates a more conspicuous group which falls within the colours associated to goethite where some elements grouped among them are excluded. Even in this case, the high percentages correspond to Fe, Si, Al, K, Ca with traces of Mg and Ti in the specimens associated to the colours of goethite. Iron and Sulphur followed by Si, K, Ca are the main constituents of specimens excluded from the grouping of goethite. The analysis of the crystalline structure highlights the crystals of jarosite which is clearly identifiable due to the presence of S, Fe, K. The XRD analysis confirms the data. The distribution of pieces by quantities (gr) in the units, the high fragmentation and the lack of large pieces indicate the anthropic origin in the site. As for Los Canes, jarosite is scarce in Arangas moving doubts regarding the anthropic introduction in the site.

V.4. La Garma A

V.4.1. Iron ores and colour

The most representative colours are red, orange, dark reddish brown, yellow, strong brown which according to what has been discussed until now and based on the preset visual criteria, are associated to the presence of iron ores. In particular, hematite (10R 4/8 red); lepidocrocite (2.5YR 4/6; 5YR 6/8); ferrihydrite (2.5YR 3/6); goethite (10YR 8/6; 7.5YR 5/6).

The ternary graph obtained from the coding coloursw by Munsell system highlights the presence of points in the group of iron oxides (hematite) and iron oxy-hydroxides (lepidocrocite/ferrhydrite) for the red vestiges. By enclosing the point in a confidence ellipse with an interval at 95%, the arrangement of the archaeological colours confirm the association with hematite, lepidocrocite and ferrihydrite identifiable as potential constituents of red ochre.

For what concern the yellow specimens, the disposition of the points highlight two groups: one around the colours of goethite (10YR 8/6; 7.5YR 5/6) and the other towards a lighter tonality of yellow which would suggest the presence of mineral pigments of bright yellow colour (jarosite) as confirmed in Los Canes and Arangas. Based on this distribution, it is possible to recognize three main classes (Fig.V.34) of iron ores: iron oxide (hematite); iron oxy-hydroxide (lepidocrocite/ferrihydrite) and iron hydroxide (goethite) with the potential presence of jarosite.

Iron oxide (hematite): two variants are distinguished inside this class. The first (I-f) is characterized by samples with pure red colour, intensely saturated and evenly distributed all over the surface. The structure is granular and compact with rare white inclusions of calcium, quartz and black reflecting mica. The second (I-e) variant includes the samples with a red colour which tends to a purplish colour with a metallic aspect. The colour appears to be well distributed on the whole surface. The structure is compact with rare calcium inclusions.

Iron oxy-hydroxide (lepidocrocite/ferrihydrite): (3-a; 3-b) this class includes a red brown colour with orange shades. The structure is compact and micro-granular. There are rare inclusions of calcium and very rare inclusions of quartz.

Iron hydroxide (goethite): (7) the class is distinguished by the presence of vestige of yellow colour distributed on the whole of the surface. The structure is

compact and massif. In one case, it is possible to observe a slightly microgranular structure with diffused deep red stains due to the post depositional contact with red material (hematite) and not from the raw material. Very few inclusions of calcium, but larger than the red materials. Rare quartz included.

V.4.2. Geochemical composition

It was not possible to chemically characterize the raw materials of La Garma A for logistical and timing issues of this research. The identification of raw materials was possible based on the visual criteria (colour, mineral inclusions) whose effectiveness has been validated on the results obtained for Los Canes and Arangas.. The comparisons based on the correspondance between physical traits and chemical composition attest the suitability of the visual classification principles. Starting from this assumption, it is possible to recognize the main classes of raw materials also for La Garma A.

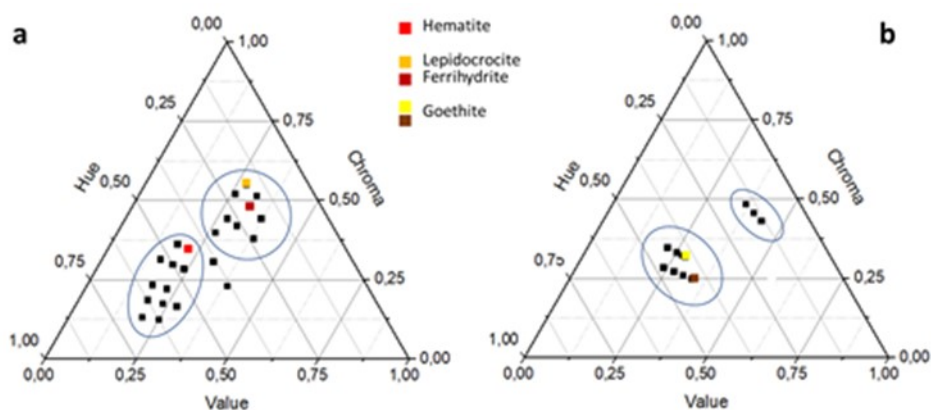


Fig.V.23.: La Garma A: ternary plot of ochres grouped into raw materials by colour in Munsell Soil Color Charts. Black points correspond to archaeological colours.

V.4.3. Proportion of raw materials

Among the ferruginous rocks, hematite is the most abundant. By evaluating the mass percentages, 78% of the total is represented by red ochres as hematite. Even yellow ochres potentially identifiable as goethite (13%) has a good percentage if compared with previously situations for Los Canes and Arangas. Lastly, there are reddish-brown/orange ochres as iron hydroxides (lepidocrocite/ferrihydrate) with around 8% of the total.

The percentages of the mass in grams of raw materials are well matched with the number of pieces counted for hematite (80%). Regarding lepidocrocite / ferrihydrate and goethite there are discrepancies between mass and number of pieces. This datum can be explained by evaluating the fragmentation indexes per classes of raw materials: hematite (163,6); lepidocrocite/ferrihydrate (188,3); goethite (124,4).

From these values, it appears clear that there is a greater fragmentation for the class of iron oxy-hydroxides which explains the higher number of pieces counted in relation to a lower mass. On the other hand, goethite has an inverse condition in which a lower fragmentation corresponds to a major mass of pieces.

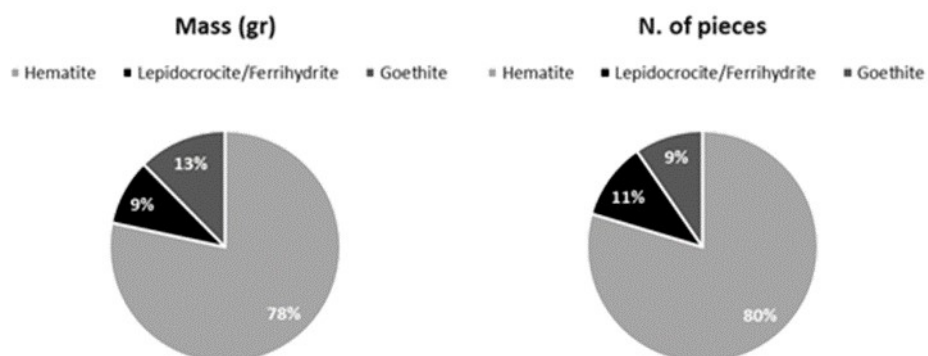


Fig.V.24.: Proportion of mass (gr) and number of pieces in function to the classes of raw materials in the site of La Garma A.

The percentages of mass are proportionally more reliable to the number of pieces per class of raw material, which, due to their fragmentation, have problems of representativeness. By starting from this presupposition, the evaluation of the distribution of raw materials mass in the deposit, shows a rather heterogeneous distribution for the hematite with high quantitative discrepancies between the different units. This data, in addition to demonstrating the anthropic origin of the iron oxide at the site, shows the high concentration peaks for the Middle Magdalenina layer (L).

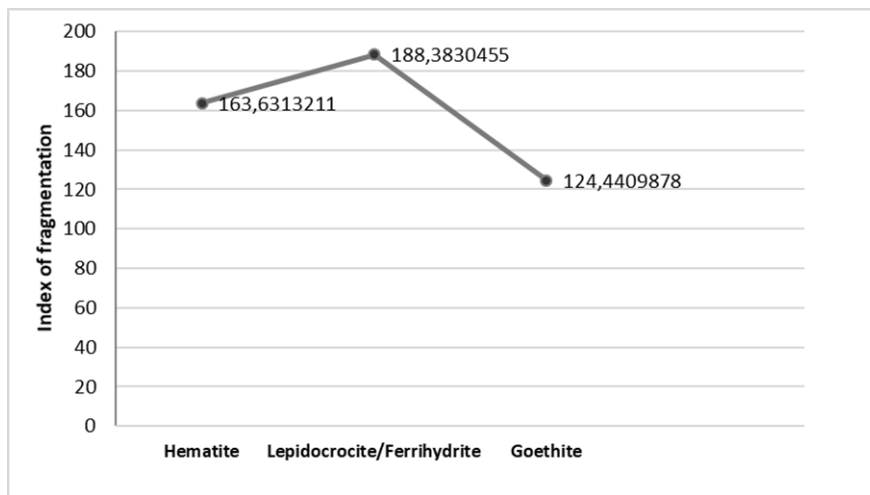


Fig.V.25.: *Index of fragmentation in function to the classes of raw materials in the site of La Garma A.*

In the lower units units associated to more ancient cultural phases, it is possible to observe a low concentration in the Solutrean unit (G) which increases at the beginning of the Magdalenian (J) to reach the maximum peak in the Middle Magdalenian and then fall once again in the units of Upper (N) and Final (O) Magdalenian. An increase is observed in the Mesolithic (Q) even if it has a lower concentration compared to the Middle Magdalenian (L).

As far as lepidocrocite/ferrihydrate and goethite is concerned, they are distributed in a heterogeneous way following the distribution line of hematite, but with lower concentrations. Also in this case, a natural contamination can be ruled out due to the heterogeneous distribution of hematite. A further parameter that should be evaluated is the distribution of the value of the maximum lengths of the objects of each class of raw materials. The distribution curve appears to be non-normal for all classes with higher values for hematite. As already discussed in the general evaluation of the material, the dimensional values depend on the indirect selection carried out on sieving with meshes of 0,2 mm. Nevertheless, it is possible to see a substantial variation in the maximum length in function to the raw material.

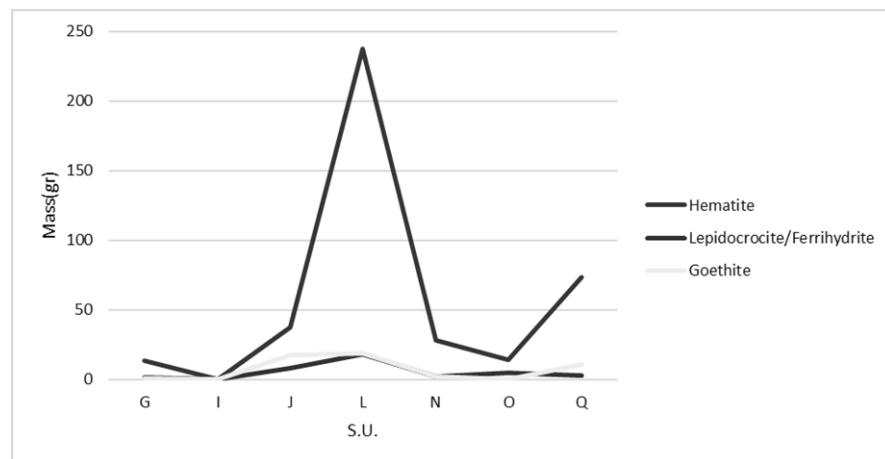


Fig.V.26.: Diachronic distribution of mass (gr) of raw materials in the site of La Garma A: hematite, lepidocrocite/ferrihydrite, goethite.

By plotting length, width and thickness values for each class, a higher concentration of pieces with dimensions between 2-10 mm are highlighted.

Nevertheless, it is interesting to notice a broad dispersion of the pieces with dimensions >10 mm which belong to both hematite and goethite. The presence

of large sized goethite pieces explains the values of the fragmentation indexes and shows the comparison between mass (gr) and number of pieces counted per class of raw material.

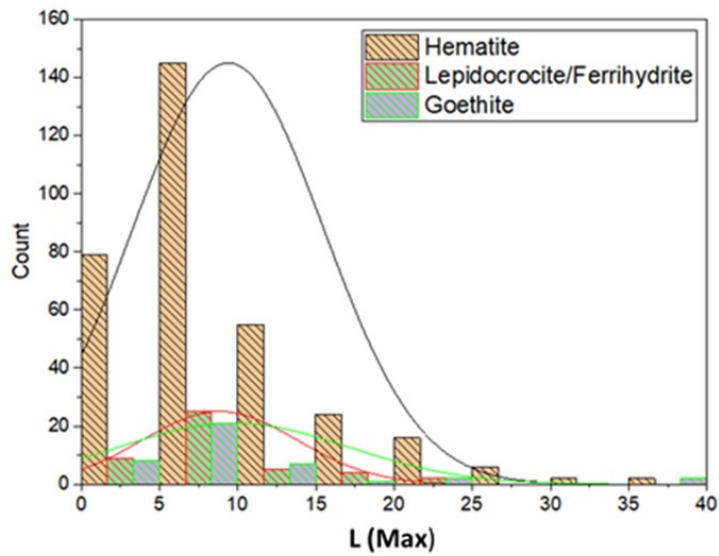


Fig.V.27.: Distribution of values of maximum lengths $L(max)$ in function to the raw materials of La Garma A: hematite; lepidocrocite/ferrihydrite; goethite.

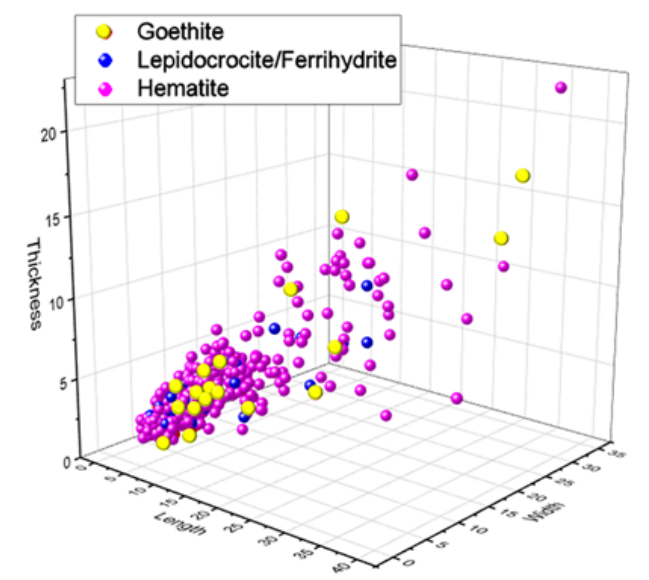


Fig.V.28.: Comparative dimensional evaluation (length, width and thickness) in function to the raw materials from Grotta di Pozzo: hematite; goethite.

V.4.4. Evaluation of identification and characterization factors of raw materials

The classification that was carried out based on visual criteria through macro-microscopic observation of the objects was fully acceptable in that it is justified by the comparisons with Los Canes and Arangas.

Red ochres are the most abundant in the assemblage with two variants: metallic purplish red and pure intense red.

The class of the yellow vestiges are well represented in that all the objects fall within the colour associated to iron hydroxide (goethite). Some yellow objects show a colour which does not fall in this group and which, based on the pale yellow detected to Los Canes and Arangas is presumably next to Jarosite. Moreover, the data obtained from the evaluation of the proportions confirm the abundance of hematite and attest rather similar quantities of goethite and lepidocrocite/ferrihydrate whose variations in mass percentages are to be related to the fragmentary nature of the objects. For each of these classes of raw materials, the heterogeneity of the diachronic distribution excludes the natural contamination of the deposit. The anthropic contribution is demonstrated by the different concentration of raw materials per stratigraphic unit with substantial diachronic dissimilarities. In an ideal natural contamination condition, the concentration should be rather similar in the different units of the deposit. The data obtained allows us to confirm that the geochemical gaps can be partly filled through the investigation protocol ascertained here.

V.5. Grotta di Pozzo

V.5.1. Iron ores and colour

The macro-microscopic observation of the archaeological vestiges highlights a set of colours from red to yellow. By coding these colours in the Munsell system, it is possible to recognize some association to iron oxide (hematite); iron oxy-hydroxide (lepidocrocite/ferrihydrite) and iron hydroxide (goethite).

From microscopical observation, a further data emerges: the classes of red-orange raw materials have shades with intense opacity, not so shiny and a rather powdered surface upon touching. These characteristics are not seen in the yellow objects (Fig. V.34).

So, it is possible to describe the main classes as here below:

Iron oxide (hematite): (4) this class includes all those objects with an intense red colour, from carmine red to intense fire red which mixes among themselves in a compact structure with a granular aspect. The black reflective mica inclusions are visible. Many white calcareous inclusions are added and rare microscopic inclusions of quartz.

Iron oxy-hydroxide (lepidocrocite/ferrihydrite): this class includes the objects which have a colour associated to the tonality of lepidocrocite and ferrihydrite. The red-orange is the predominant colour which is intensely saturated and homogeneously distributed. The structure appears compact and granular with abundant inclusions of calcium and frequent inclusions of quartz. Mica inclusions are rare.

Iron hydroxide (goethite): (8) this class includes the archaeological vestiges with a homogeneously distributed intense yellow colour. The structure appears to be

characterized by obvious grains compacted among them and interspersed by many mineral inclusions. There are abundant calcium inclusions among these and also reflecting black mica are frequent.

The ternary graph obtained from the distribution of archaeological colour shades in the Munsell system allows us to clearly distinguish two groups by classes of iron oxide (hematite) and iron oxy-hydroxide (lepidocrocite/ferrihydrite). The distribution of yellow colour is also well defined and are all associated to the colours of goethite (Fig. V.29).

V.5.2. Geochemical composition

The analysis of the chemical composition of Grotta di Pozzo ochres already occurred in the preliminary stage of the research on ochre carried out by the author of this thesis for her Master. The analyses were done through Raman spectroscopy. From the spectrum acquired from representative points of the surface of the archaeological vestige, the ferruginous nature was confirmed. The samples show a very similar spectrum among them with peaks positioned at 223-289-404-608 cm^{-1} due to the clear presence of hematite (Fe_2O_3) and peaks at 299-387 cm^{-1} due to goethite ($\text{FeO}(\text{OH})$). The analyzed and represented samples of the classes of raw materials distinguished by colour do not display an evident presence of iron oxy-hydroxides such as ferrihydrite and lepidocrocite.

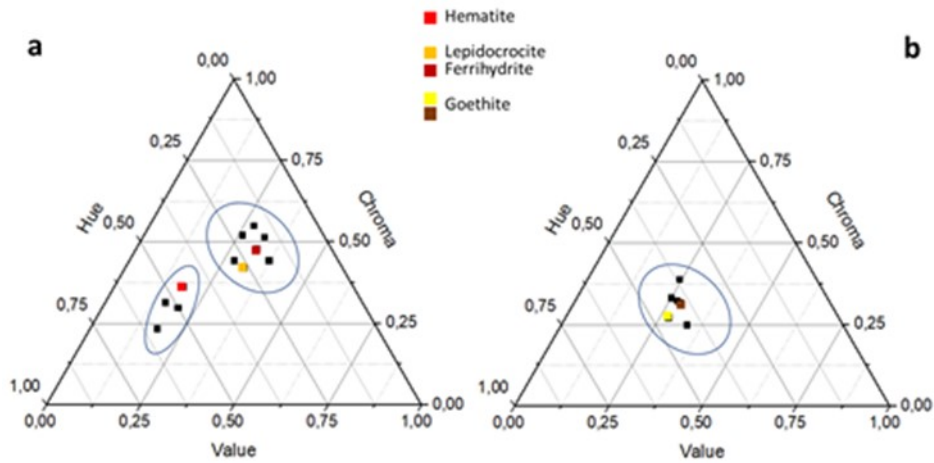


Fig.V.29.: Grotta di Pozzo: ternary plot of ochres grouped for raw materials by colour in Munsell Soil Colour Charts. Black points correspond to archaeological colours.

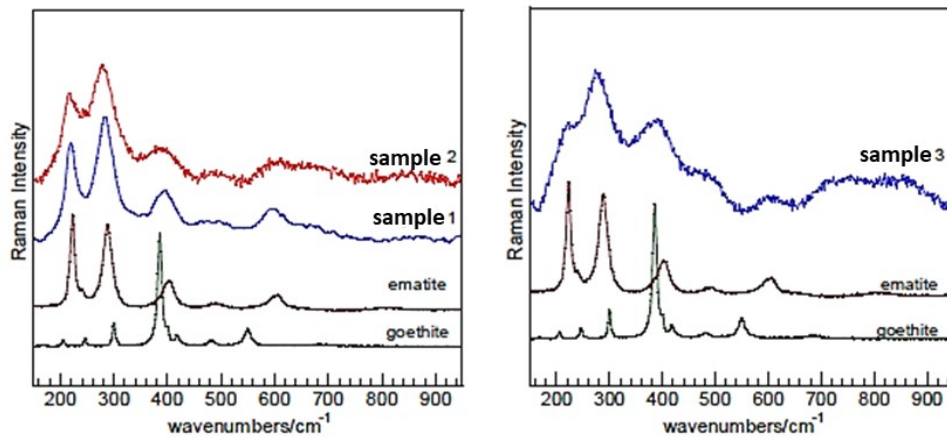


Fig.V.30.: Raman spectrum of some samples representing the classes of raw materials recognized at Grotta di Pozzo.

V.5.3. Proportion of raw materials

The best represented class in the site is hematite for both the number of pieces counted (91%) and the quantity of grams collected (97%). The class of goethite appears to be poorly represented in both number of pieces (9%) and in mass (3%). The fragmentation rate in function to the classes of raw materials appears

rather high in both cases, even though goethite is greater. This heterogeneity induces us to research an evaluation criteria which allows us to have a reliable evaluation concerning the proportions of raw materials in the deposit. For this reason, it is worth taking mass as an evaluation parameter into consideration.

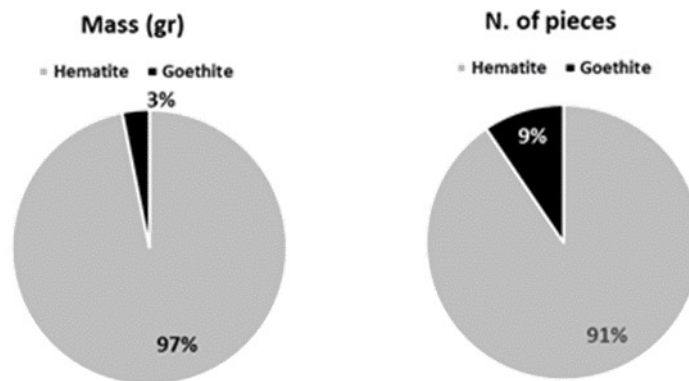


Fig.V.31.: Proportion of mass (gr) and number of pieces in function to the classes of raw materials in the site of Grotta di Pozzo.

The diachronic distribution highlights the substantial divergences between the two classes of raw materials. Hematite is the most abundant in all the units of the deposit but is lower in the most ancient phases of the site with a notable increase in the Final Epigravettian. The quantities of hematite remains similar in the Mesolithic units too. The distribution in function to mass suggests an anthropic contribution which is not possible to established for goethite due to its low quantities. Nevertheless, it is interesting to see that goethite is larger in quantity which corresponds to the Final Epigravettian unit. In the Mesolithic, it decreases once again (Fig.V.32). The non normal distribution of the maximum lengths highlights a greater dimensional width for the hematite (Fig.V.32). By evaluating the representativeness of the classes of raw materials in function to the length, width and thickness, the wide dimensional range highlighted by the

distribution curve shows a notable dispersion in the three dimensional space of the samples of hematite which also reach notable dimensions. On the other hand, goethite appears to be close and is in a range between 2 and 10 mm (Fig.V.33).

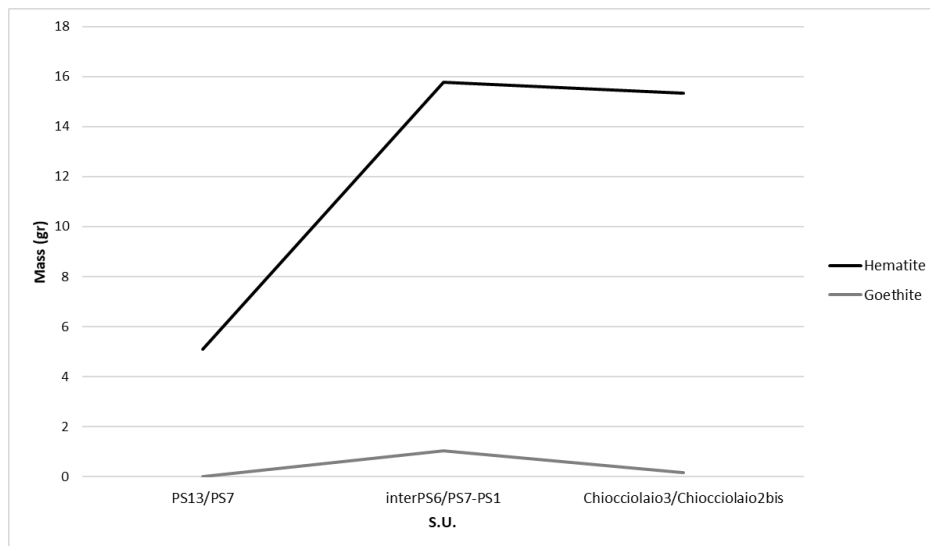


Fig.V.32.: Diachronic distribution of mass (gr) of raw materials in the site of Grotta di Pozzo: hematite and goethite.

V.5.4. Evaluation of identification and characterization factors of raw materials

Two main classes are identifiable: iron oxide (hematite) and iron hydroxide (goethite). The identification based on visula criteria (external colour and mineral inclusions) is partially acceptable. The results of the chemical characterization does not confirm the presence of iron oxy-hydroxides associated to the colours of lepidocrocite and ferrihydrite in the Munsell code. Identification based on colour does not seem completely irrelevant, since the

classes of iron oxide (haematite) and iron hydroxide (goethite) are well represented and find full correspondence on the basis of visual determination. The notable heterogeneity between the two classes of hematite and goethite is reflected in the dimensions too. Hematite is attested with a wide dimensional range and non standardized dimensions which follow a rather irregular logic. Goethite is characterized by the dimensions concentrated in a dimensional range between 2 and 10 mm. The data can not be statistically relevant due to the low quantities.

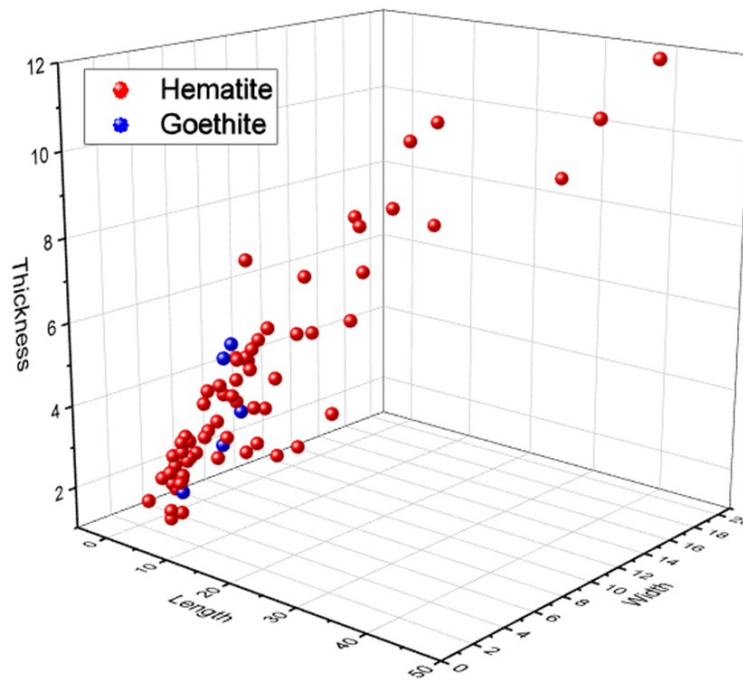


Fig.V.33.: Comparative dimensional evaluation (length, width, thickness) in function to the raw materials from Grotta di Pozzo: hematite; goethite.

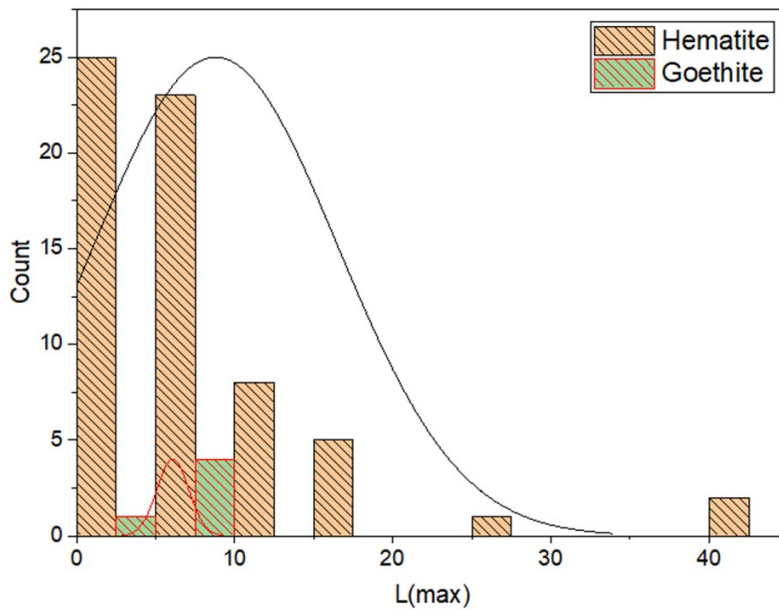


Fig.V.34.: Distribution of the values of maximum lengths $L(max)$ in function to the raw materials at Grotta di Pozzo: hematite; goethite.

V.6. Comparative analysis

At this point of the research, it is interesting to show the data obtained from the physical-chemical analysis of the vestiges associated to the Mesolithic burials of Los Canes with those obtained from Grotta del Romito, Grotta San Teodoro and S'Orku e S'Orku in a comparative perspective to better understand the role of ochre for paleolithic and mesolithic human groups of south-west Europe.

The results were obtained from the physical-chemical analysis according to the methodological protocol set up for this research (chap. II) of a set of samples of red ochre from Paleolithic and Mesolithic funerary contexts of South-Western Europe. The analyzed samples is made up of a total of 22 elements coming from the Mesolithic units of Los Canes (6III; 6II; 6I); 14 fragments and around 1 gr of powder from Epigravettian levels of Grotta del Romito; 6 elements from the

Epigravettian levels of the Grotta San Teodoro and 5 elements from the Mesolithic units of S'Ormu e S'Orku.

Site	Class	Chromophore	Mineral inclusions	Mineral Phase
Los Canes	Iron oxide	Hematite	Quartz, Calcium Carbonate, Magnetite	He+Qz+Ca+Mn
Los Canes	Iron oxide-hydroxide	Lepidocrocite/ Ferrihydrite	Quartz, Calcium Carbonate	Le+Qz+Ca
Los Canes	Iron hydroxide	Goethite	Calcium Carbonate, Micae	Go+Qz;
Los Canes	Sulphate of iron and potassium	Jarosite	Quartz	Ja+Qz+K(oxide)
Arangas	Iron oxide	Hematite	Hematite, Quartz, Calcium Carbonate, Larnite, Maghemite	He+La; He; He+Qz; He+Qz+Ca
Arangas	Iron hydroxide	Goethite	Brucite, Muscovite, Quartz, Lepidocrocite	Go+Br+Mu+Qz+Le
Arangas	Sulphate of iron and potassium	Jarosite	Quartz	Ja+Qz+K(oxide)
La Garma A	Iron oxide	Hematite	Quartz+Calcium Carbonate+Micae	-----
La Garma A	Iron oxide-hydroxide	Lepidocrocite/ Ferrihydrite	Quartz+Calcium Carbonate	-----
La Garma A	Iron hydroxide	Goethite	Quartz+Calcium Carbonate	-----
Grotta di Pozzo	Iron oxide	Hematite	Quartz+Calcium Carbonate+Micae	He+Qz+Ca
Grotta di Pozzo	Iron hydroxide	Goethite	Quartz+Calcium Carbonate+Micae	Go+Qz+Ca

Tab.V.3.: Summary table of main classes of raw materials and mineral content of each site: Los Canes, Arangas, La Garma A, Grotta di Pozzo.

V.6.1. Iron ores and colour

By observing the images representative of the comparative samples, it is possible to distinguish the raw materials into the following classes:

- a) This class includes those samples with a colour which is mixed with intense red (10R4/8) and orange (2.5YR 4/6) with a heterogeneous surface, friable and powdered consistency. The granular structure is characterized by evident quartz, calcium and shiny black mica grains within a finer matrix of granular iron minerals.
- b) This class includes those samples from a metallic aspect and a dark red colour (10R 3/6) homogeneously distributed on the whole surface. The structure is compact and characterized by a fine matrix in which large grains of quartz and black mica inclusions are inserted.
- c) Those elements with evident black inclusions of magnetite are part of this class and are grouped in some areas of the surface and alternated with large inclusions of quartz and calcite within a fine reddish brown matrix (2.5YR 3/6) and red orange ferruginous crusts (2.5YR 4/8)
- d) The class includes those elements with granular and porous structures formed by large grains of quartz with a fine pure red and intensely saturated red colour matrix (10R 5/8).

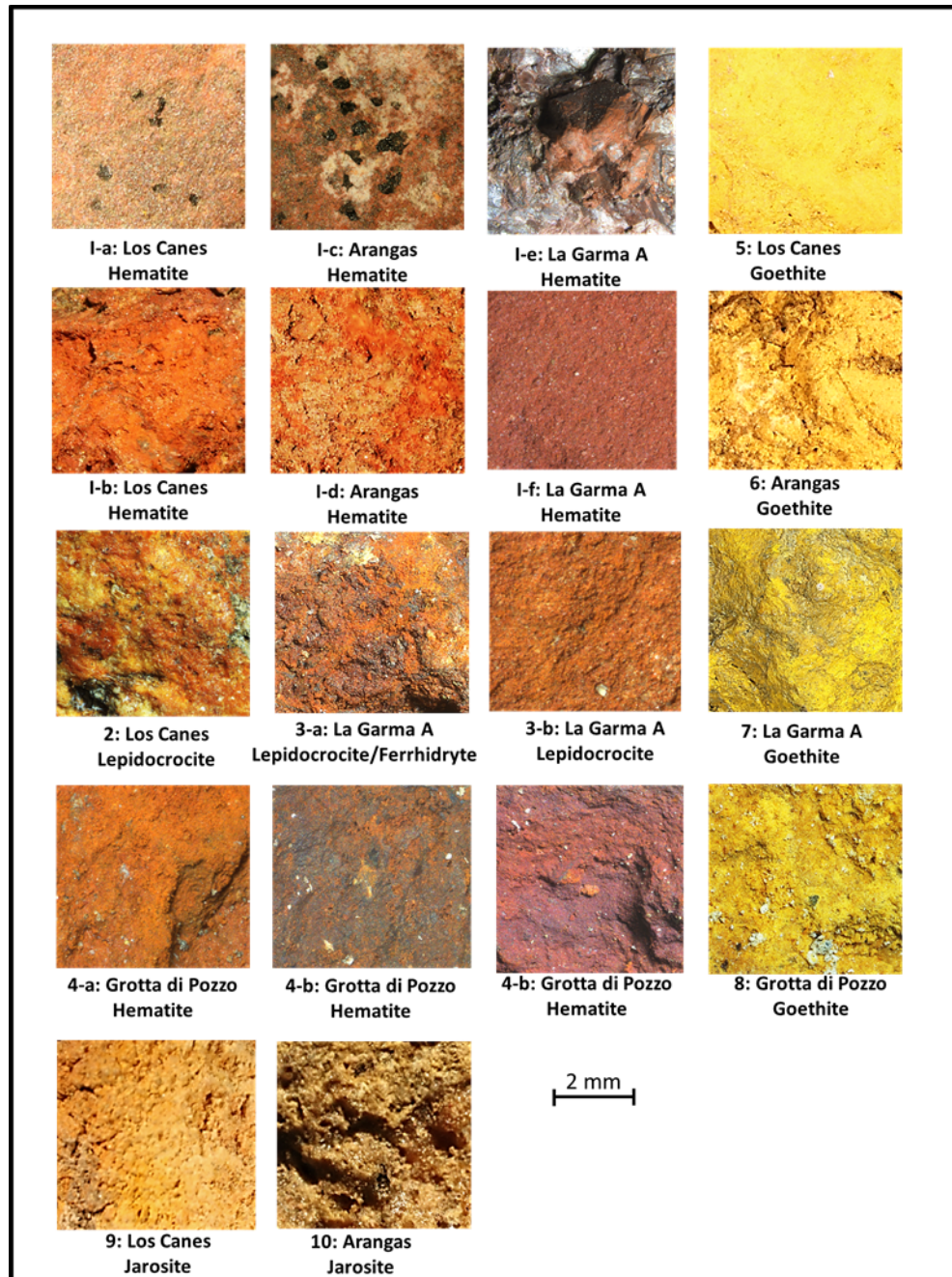


Fig.V.35.: Images of main classes of raw materials of ochre distinguished by visual criteria: samples from Los Canes, Arangas, La Garma A, Grotta di Pozzo.

Class	Colour	Surface	Structure	Inclusions	Site
a	(10R4/8) (2.5YR 4/6)	Heterogenous	Granular, crumbly and dusty	Quartz, Calcium, Micae	ROM ST
b	(10R 3/6)	Homogenous	Compact and fine granular	Quartz, Micae	SOMK
c	(2.5YR 3/6) (2.5YR 4/8)	Heterogenous	Granular	Quartz, Calcium, Magnetite	ROM
d	(10R 5/8)	Homogenous	Fine granular with ferruginous crusts	Quartz	ROM ST

Tab.V.4.: Summary table of main classes of raw materials of comparative samples: Grotta del Romito (ROM); Grotta San Teodoro (ST); S'Omu e S'Orku (SOMK).

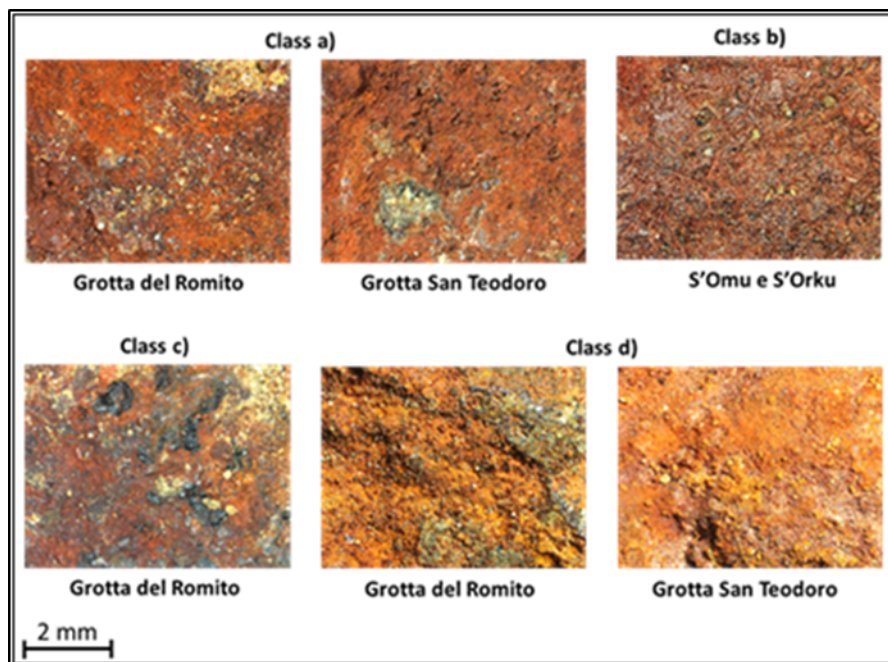


Fig.V.36.: Images of main classes of raw materials of ochre distinguished by visual criteria: comparative samples from Grotta del Romito, Grotta San Teodoro, S'Omu e S'Orku.

V.6.2. Geochemical composition

The semi-quantitative characterization with SEM-EDS shows a composition similar to ochres. By plotting the percentages of chemical elements in a ternary graph (Fe, Al, Si), the ferrous nature is confirmed. The enclosed samples in a broader ellipse contain Fe in variable percentages between 40-80%.

The enclosed samples in the more restricted second ellipse from the burial 6III of Los Canes contain percentages of Fe between 20-30%. The images representative of each class identify by visual criteria show the crystalline structure of the ochres:

Class **a)** is characterized by pseudo-prismatic crystals (Fe_2O_3) organized in granular agglomerates.

Class **b)** shows thin hexagonal crystals organized in typical “flower structures” of iron oxides.

Class **c)** has a crystalline structure formed by rhomboidal crystals (hematite) interspersed by polyhedral crystals (octahedral) of the magnetic and large prismatic crystals of quartz.

Class **d)** shows a matrix formed by thin aggregated pseudo-hexagonal crystals in which large prismatic crystal of quartz are inserted. It is possible to see pseudo-subica of Ca (calcium) also.

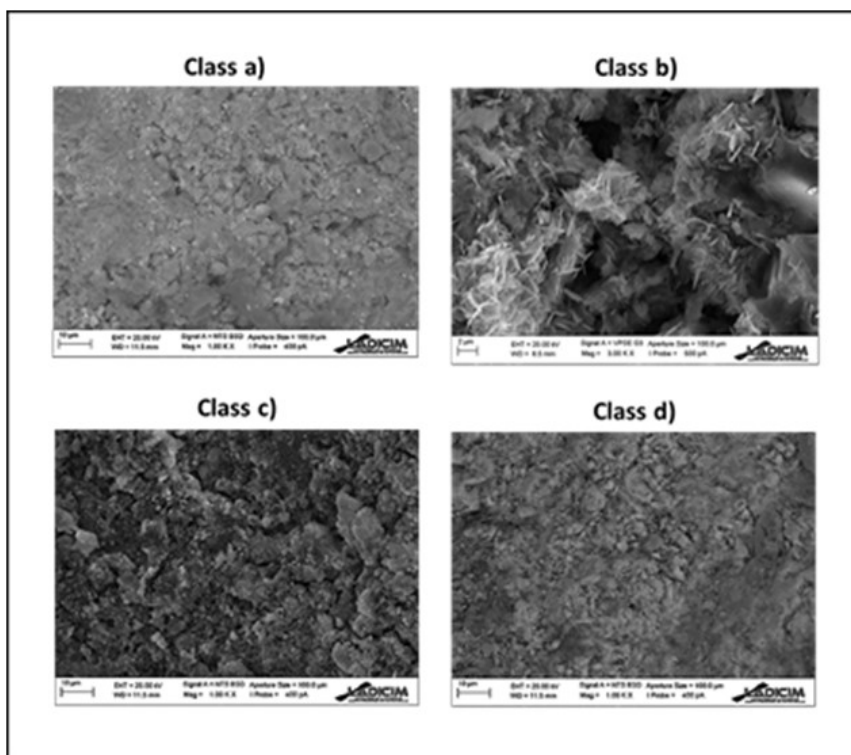


Fig.V.37.: SEM-EDS images of representative samples of the main classes of raw materials of comparative ochres.

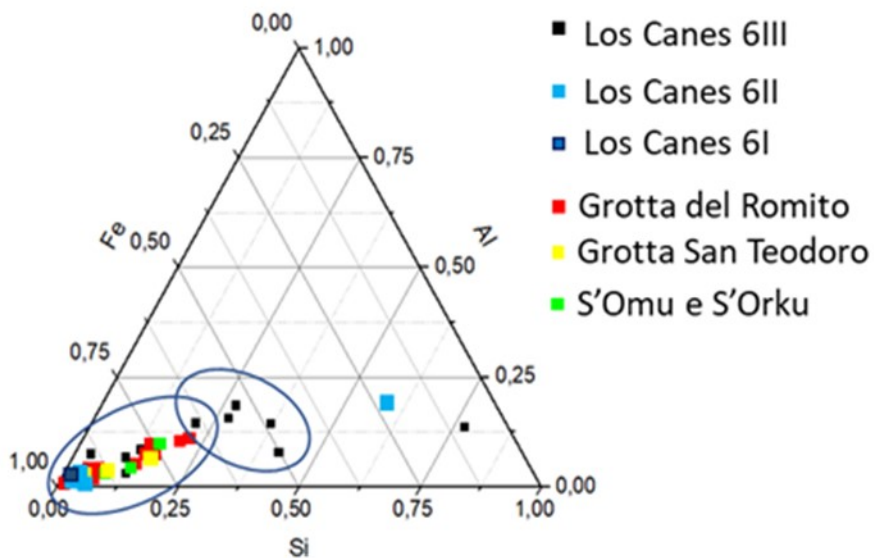


Fig.V.38.: Ternary plot of comparative samples by Fe-Al-Si content.

Site	Chromophore	Mineral compound	Mineral inclusions	Mineral Phase
Grotta del Romito	Hematite	Iron oxide	Quartz, Calcium Carbonate,	He+Qz+Ca
Grotta San Teodoro	Hematite	Iron oxide	Quartz, Calcium Carbonate	He+Qz+Ca
S'Orku e S'Orku	Hematite	Iron oxide	Calcium Carbonate, Cuprite, Margarite	He+Qz+Ca+Cu He+Qz+Ca+Marg

Tab.V.5.: Summary table with the qualitative chemical composition of comparative ochres.

The X-ray Diffractometry confirms the nature of the crystals by highlighting the presence of compounds of Fe in the shape of oxides (Fe₂O₃). The external colour of the samples is due to the presence of hematite, the main chromophore of the ochres. Furthermore, the XRD spectra attest the nature of accessory minerals: quartz, calcium carbonate, cuprite, margarite.

Data is summarized in the referenced tables (Tab.V.5). The Principal Component Analysis carried out with the percentages obtained by SEM-EDS highlights two main groups. The main elements (Fe-Al-Si) are not discriminating for classes of raw materials or the provenance site. In any case, a chemical affinity appears evident due to the percentages of Fe present in the samples based on iron oxide in the form Fe₂O₃.

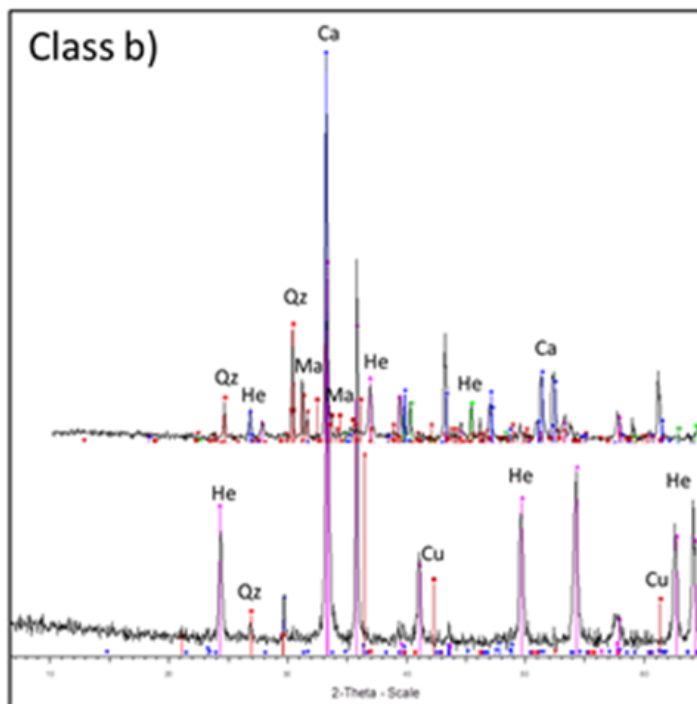
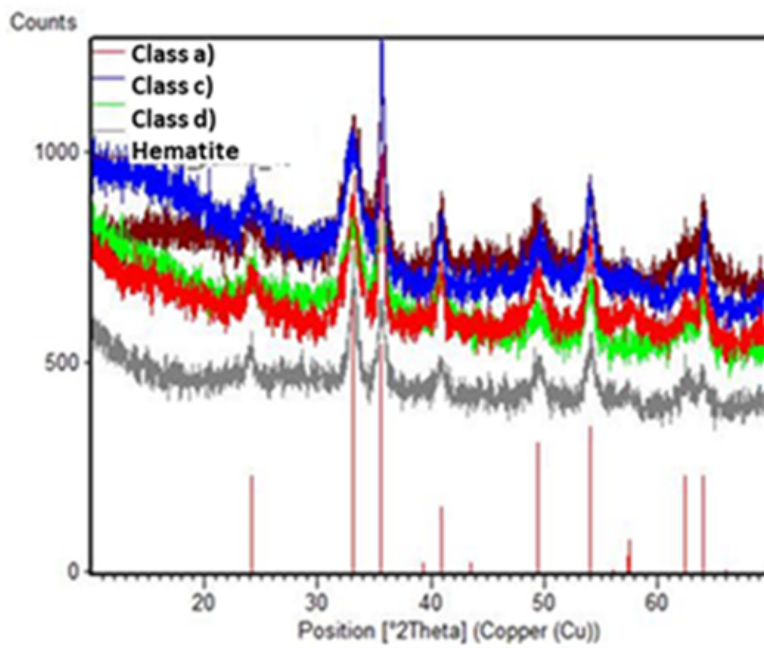


Fig.V.39.: XRD spectra of representative samples of comparative ochres: qualitative characterization of raw materials.

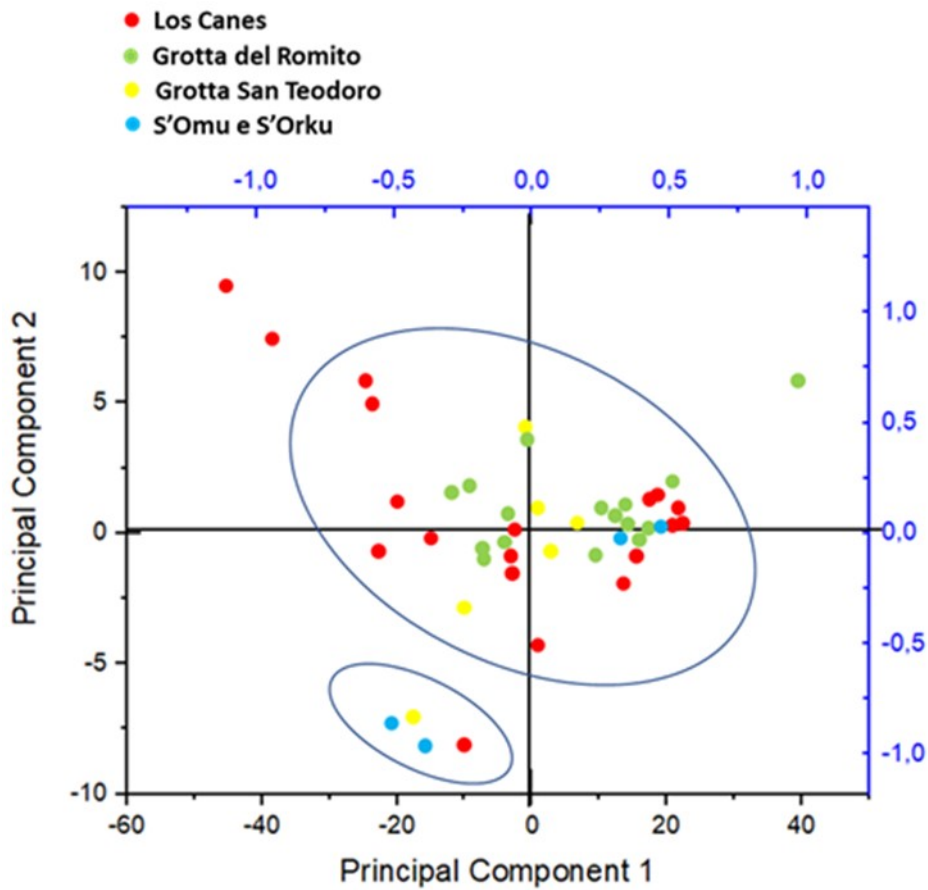
V.6.3. Evaluation of comparison factors

By evaluating the set of comparison factors, the samples of red ochre associated to human burials can be discriminated on the visual basis. By analyzing the samples representative of each class, the division of visual parameters does not correspond with the elemental composition. By plotting a ternary graph with the chemical content of major elements, it is possible to appreciate two groups: the largest contains samples from each of the sampled sites with the high percentages of Fe. The second contains samples (S.U. 6III of Los Canes) with lowest percentages of iron.

The analysis of the main components (PCA) reflects the chemical affinity and, at the same time, does not discriminate the ochres by classes of raw materials which were visually recognized.

From a quantitative analysis, iron oxide in the formula Fe_2O_3 is the main compound responsible for the external pigmentation. The X-ray Diffractometry confirms the presence of quartz and calcite identified through optic observation. Furthermore, XRD analysis demonstrates the presence of further accessory minerals which may indicate source of origin (S'Ormu e S'Orku): cuprite and margarite.

The comparative study allows us to establish the presence of red ochre based on hematite in Paleolithic and Mesolithic ochres from funerary contexts. In addition, the semi-quantitative and qualitative characterization confirm the absence of organic compounds. So, the nature of the ochres depend on the mixture of inorganic mineral compounds typically associated to ochres. External additives of any type are not detected.



Elements	N. analysis	N. missing	Mean	Standard Deviation
Si	40	1	6,72325	6,0728
Al	40	9	3,07475	2,21956
Fe	40	1	42,14575	16,98762

Fig.V.40.: Principal Component Analysis results showing the grouping by Fe-Si-Al in the comparative ochres with Los Canes ochres.

Chapter VI.

Ochre procurement strategies and supplying areas

The physical-chemical characterization of ochres and the identification of raw materials give us essential data to investigate potential ochre sources and selection criteria of Palaeolithic and Mesolithic hunter-gatherers.

Provenance research is fundamental to establish the link between geological sources and archaeological contexts. In this sense, the main starting point is to define the mineral richness of a territory surrounding archaeological sites and the accessibility to the geological formations in a well-defined moment in time as in this case the Late Pleistocene and the Initial Holocene.

The knowledge of geological context is important in order to make reflections on exploitation strategies of mineral resources in relation to human needs. Furthermore, this aspect plays a key role in the reconstruction of human mobility patterns and the geographical areas that were anthropically explored as well as on the economic resources that are presumable available. In fact, the discovery in the archaeological context of a raw material not locally available implies the possibility that it was obtained through exchanges or moves on short or long distances (Dixon *et al.*, 1968). So, communication among human groups and mobility are therefore further aspects that are related to the ochre supply.

Certainly, dealing with the issue of exchange and communication between individuals or human groups is rather complicated for colouring materials if it refers to very ancient phases. Compared to other categories, it is impossible to recognize specific cultural taxonomic entities for ochre vestiges as for lithic and bone industries or objects of art and ornaments whose peculiarities are identifying of a specific human culture. For this reason, it is important to investigate original geological sources also to reconstruct human movements.

From a Binfordian perspective (Binford, 1980), mobility of Palaeolithic and Mesolithic hunter-gatherers can be distinguished in *residential mobility* and *logistic mobility*. In the first case, the hunter-gatherers establish their settlements in proximity to the resources needed for their subsistence according to an opportunistic strategy perpetuated by small “familiar” groups with non-residential installations.

In the second case, it is possible to recognize big base-camps where groups of families live with mobile satellite camps where individuals who are responsible to procure the resources for group members lived and moved towards the presence of supply sources.

The use of space is directly related to the availability of resources which influences human behaviours. The model proposed by Binford is a reference point for the studies of human mobility and supply strategies.

Nevertheless, even the model proposed by Geneste (1988) is pertinent to the case study. In his work entitled “*Systèmes d’approvisionnement en matières premières au Paléolithique moyen et au Paléolithique supérieur en Aquitaine*”, the procurement of raw materials occurred over short, medium or large distance. The author proposes a model in which different situations are expected based on the localization of supply sources: short movements with the exploitation of

local sources within a range of approximately 5 km from the site and which can be reached in an hour on foot; long distance movements to reach supply sources beyond 20 km from the site which require more than four hours on foot and a break along the journey.

Based on these models, Djindjian (2012) proposed five different socio-economic strategies of hunter-gatherers in the European Upper Palaeolithic which potentially influenced the supply of raw materials.

The "*Local Opportunistic Strategy*" foresaw a reduced territorial availability ($\leq 1,000 \text{ Km}^2$) with low mobility and opportunistic exploitation of local resources up to their depletion. At this point, the group is forced to move themselves. The communications among the human groups were extremely reduced. According to the author, this strategy would have been adopted by Mousterian groups during the isotopic stage 4 (OIS 4) and abandoned during the Middle Palaeolithic/Upper Palaeolithic transition in Europe.

The "*Extended planned strategy*" is characterized by the movements over long distances within a larger territorial area (10,000-100,000 Km^2). The sources of raw materials are distant, and the resources exploitation occurs through specialized and organized expeditions. Contacts are established in several meeting points which favour the exchange and spread of standardized cultural forms. The human groups live in seasonal camp-sites. This strategy would have been adopted during the Upper Palaeolithic (Aurignacian, Gravettian, Magdalenian).

The "*Semi-sedentary strategy*" was implemented by human groups who lived in residential camp-sites for most of the year (8-10 months) and who moved within a vast territory over short periods (10,000-100,000 Km^2). This is the strategy implemented by the hunter-gatherers in North-Eastern Europe in three

moments of the Upper Palaeolithic: Pavlovian towards the 27,000 cal BP in Moravia, Eastern Gravettian (24,000 – 21,000 cal BP) in Central and Eastern Europe and Mezinian in the mid-upper Dnepr basin (15,000-14,000 cal BP).

The “*Seasonal mobility strategy*” was founded on seasonal movements during warm months of the year. The human groups migrated over hundreds of kilometres to follow the movement of the large herbivores (reindeers) and find excellent quality raw materials like flint, to then go back to “refuge areas”. This strategy would have been implemented in the Late Glacial Maximum by the groups of Late Solutrean and Late Badegoulian in Western Europe, Sagvarian in Central Europe and Moldovan in Eastern Europe.

Lastly, the “*Restricted Planned strategy*” where human groups moved within a territorial area between 1,000 e 10,000 Km² with seasonal camp-sites and with extremely diversified food and an intensive and opportunistic exploitation of the local raw materials in relation to the quality of the available mineral sources. The author attributes this strategy to the European Epipaleolithic/Mesolithic human groups.

In Djindjian’s theory, the territorial extension is directly proportional to the availability of resources and in turn conditions the movements of humans.

The highlighting of geological sources is therefore essential in order to understand the selection criteria of raw materials and the way in which these arrived at the site. In this study perspective, it is important to keep in mind some works which not only define the patterns of human mobility to procure ochre by identifying the original sources (Dayet, 2015), but it also suggests how the acquisition of colouring raw materials has a symbolic-ritual significance. Ochre is not researched for its physical-chemical peculiarity, but it is mainly for the symbolic value of specific sources. (MacDonald, 2016).

Surely, a further factor that presumably address human choices in the recovery of ochre is the function (utilitarian/symbolic). The procurement of raw materials therefore is inevitably linked to anthropic activities, technological skills of human group and its economic-social organization.

VI.1. Provenance research and archaeological contexts

Sourcing archaeological ochres establishing the original geological sources is significant, but at the same time too difficult to develop. The presence of various collections and diversified types of ochre vestiges from Palaeolithic and Mesolithic contexts on a continental scale, implies the definition of some essential aspects to define this study.

First, this kind of investigation must be conducted with the aim of satisfying the postulate of provenance according to this definition: *“Sourcing is possible as long as there exists some qualitative and quantitative chemical or mineralogical difference between natural sources that exceeds the qualitative or quantitative variation within each source”* (Weigand *et al.*, 1977; Neff, 2001).

Until this can be verified, it is necessary to circumscribe the research in a well-defined geographical area based on the potential range explorable by the inhabitants of the archaeological site. Moreover, a good knowledge of the geological setting is essential to identify the mining outcrops in order to collect geomaterials to be compared with the archaeological ones. Based on these assumptions, it has been possible to carry out geochemical sourcing studies for Los Canes and Arangas, the two sites in the same karstic complex, in the Asturian region (northern Spain).

The choice of beginning from the contexts of Los Canes and Arangas depends on the sampling feasibility. A careful analysis of study conditions in function to the available collections and to the possibility to explore the territory sampling geological materials, guided us towards the choice of the two adjacent Iberian contexts.

The setup of the investigation methodology was not immediate and required a meticulous planning of the exploration and sampling activities as well as carrying out a preliminary test (chap. II) for the validation of the analytical protocol by having to deal with some research limits.

First, the high variability intrinsic to iron ores formations can make the direct connection between the archaeological material and the geological source quite difficult. Moreover, these formations can have a substantial extension in space and a variable accessibility over time. These two aspects can affect the completeness and reliability of sampling and thus compromise the discrimination of original geological sources.

A further limiting aspect is the potential variation of the accessibility to the geological sources in time and space. In fact, it is presumed that from Pleistocene until now, the physical geography of the territory investigated has undergone changes and alternations due to natural and anthropic agents.

Lastly, limits in the provenance research derive from the unavailability of an assorted reference collection of Asturian ferruginous rocks from sources marked on a territorial distribution map.

Considering these limits, it is fundamental to research supporting factors to the provenance study.

VI.1.1. Geological setting

The current geological setting of the Asturian territory is characterized by a heterogeneous context where endogenous and exogenous geodynamic forces modelled different morphological units: coastal ridges, pre-littoral depression, Asturian reliefs, Picos de Europa Unit and central carboniferous basin.

The Coastal ridge is a series of raised beaches and steep cliffs on siliceous basements to the west, and littoral platform with complex karst forms such as sea caves, blowholes (*bufones*), *dolinas* and small sierras to the central-eastern part.

The Pre-littoral depression is a tectonic depression, filled by Meso-Cenozoic sediments, that extends for 80 km from the Narcea river (west of Oviedo) to the confluence of Piloña-Sella rivers (east of Cangas de Onis) with a width range between 3-30 km.

The Asturian Reliefs are organized into two main blocks, those of the *Cantabrian zone* formed by Precambrian-Palaeozoic carboniferous rocks (Sanchez De Posada, *et al.*, 2002) and those of the *West Asturian-Leonese zone* formed by Cambrian-Ordovician siliciclastic rocks (Pérez-Estaún *et al.*, 1990).

The unit of *Picos de Europa* is represented by a complex horst of carboniferous limestones (Cendrero & Saiz De Omenaca, 1979) crossed by Duje and Cares rivers. These mountain peaks extend for about 20 km in length and form part of the Cantabrian Mountains range, between Asturias, Cantabria and Castile-Lèon. This unit can be divided into three smaller units: Eastern Massif, Central Massif, Western Massif (Alonso, 2009).

Bordered by Picos de Europa, León and Palencia peaks and sierras de Peña Labra and Peña Sacra, there is the Liebana valley, a hydrographic basin in the

Cantabria region, but only accessible by the Desfiladero de la Hermida, a system of gorges between Asturias and Cantabria (Maas, 1974).

The Central Carboniferous Basin, in the middle of the Cantabrian Mountains range, is a thrust sheet made by carboniferous sediments of marine and continental origin (Piedad-Sanchez *et al.*, 2005). This main geological unit can be organized into three smaller units: unit of Riosa-El Viso, in the west, unit of Rio Aller, in the south, unit of Mieres-Sama de Langreo-Lieres, in the northeast (Perez Estaun & Bastida, 2012).

The Sierra de Cuera is a mountain chain located in the eastern part of the Cantabrian Mountains Range, in which Arangas and Los Canes caves are located. This mountain chain extends from east towards west parallel to the coast and the caves entrance are located on the southern slope. The chain, about 6 km Sierra de Cuera far away from the sea, geographically represents the north-eastern extension of the Ponga-Nappe Province. This geological structure is characterized by a set of imbricate thrust sheets subparallel to the layers, originating from the Cambrian to the Carboniferous, and developed along an east-west direction (Marquínez, 1989).

Sierra the Cuera is composed by carbonates rocks organized into two main lithostratigraphic units: Barcaliente-Valdeteja of Bashkirian age (323,2-315,2 Ma), and Picos de Europa of Moscovian age (315,2-307 Ma).

At the base levels of Barcaliente-Valdeteja formation, overlying Ordovician quartzites, it is possible to recognize formations of iron ores with accumulation of hematite and manganese, due to phenomena of mineralization and biomineralization (Adaro & Junquera, 1916; Della Porta *et al.*, 2006).

By keeping into account, the localization of the geological source used for the supply of lithic raw materials in the Upper Palaeolithic and Mesolithic, the geological perspectives were concentrated in a coastal area between Pimiango and La Franca and in the internal area around the archaeological sites of Los Canes and Arangas.

The intense climate variations which characterized the latter part of the Pleistocene and the progressive climate warming of the Holocene transformed the geomorphology of the territory by changing the accessibility to the iron ores deposits from the Upper Palaeolithic and Mesolithic until the current age. However, it is possible to appreciate ferruginous deposits in the explored areas and presumably accessible for Palaeolithic and Mesolithic hunter-gatherers.

During the investigations on the territory carried out with the aim of finding geomaterials to do a comparative analysis with archaeological samples, it was rather difficult to reach the coastal area due to the thick plant cover and the intense variations in the sea level in relation to the tides.

Nevertheless, it was possible to visit the rocky formations which outcrop on the sea cliff close to the small village of Pimiango. The geological units rich in ochre nodules are in the NW zone of the Regorgueru Beach and are accessible through a narrow path only available during low tide periods. In regards the formations in proximity of archaeological sites, these were easily accessible through the road cuts visible from the main road (AS-345) which leads to the village of Arangas, proceeding from Santander, which is the starting point for the geological expedition (Fig.VI.1).

VI.2. Iron ores sources

VI.2.1. Geological mapping

The first step towards the research of original sources of ochre was the one to define the geographical area which can be potentially explored by the Palaeolithic and Mesolithic human groups who occupied the caves of Los Canes and Arangas. By keeping the limits into account that might have conditioned the study, it was first necessary to define the territorial space where the provenance studies were concentrated by establishing the minimum and maximum distances passable between the Upper Palaeolithic and Mesolithic for reducing the uncertainty of discriminating ochre sources.

To calculate the “range” of Palaeolithic and Mesolithic hunter-gatherers, it was decided to start from the already known distances for the geological sources of lithic raw materials. It is presumed that the human groups also stocked up with ochre during their movements when supplying lithic resources. In the case of Los Canes and Arangas, previous studies provided us with potential geological formations of lithic raw materials.

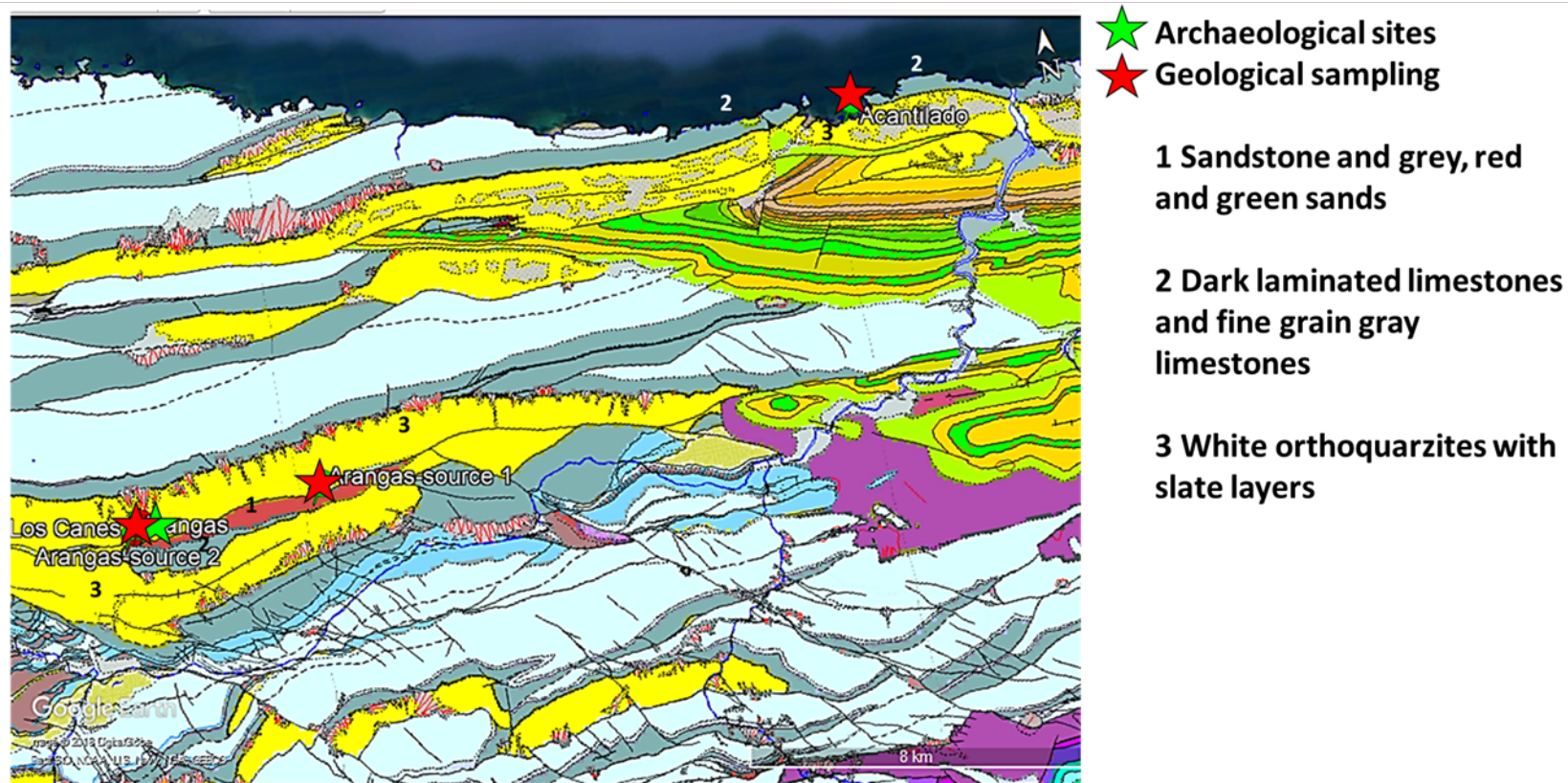


Fig.VI.1.: Simplified geological map of the area surrounding the archaeological sites of Los Canes and Arangas with the geological sampled sources (IGME maps 1: 50.000; n.56 and n.32).

The following formations were identified for Los Canes (Arias, 2002):

- *Local formations* of red radiolarite based on *griotte* limestone of Visense-Tournaisiensea around a hundred meters from the site (Lower Carboniferous); of black flint and quartz in the formation (Barcaliente-Valdeteja) in which the same cave is opened;
- *Puentellés formation* of grey flint to the east of the municipality of Arenas de Cabrales around 15 km from the site (Estefanian);
- *Allochthone formations* cretaceous flint probably localized in the central and western part of the Cantabrian region and in Mesozoic around 16 km distant from the site;
- In the case of Arangas, the lithic materials are localized in the following formations (Arias *et al.*, 2013):
- Radiolarite (red, black, green) from coastal formations (*Alba Formation*) and internal formations around the site (Tournaisiense-Visseens). The coastal formations were identified in Ballota, *Vidiago, Andrín, San Antolín*;
- Honey coloured flint from different formations of Estefanian stage of the Asturian interior such as *Mier, Cerebanes, Cavandi*;
- Grey Flysch from Namurian formations in the coastal areas between *Pendueles* (around 20 Km) and *Pimiango* (approximately 24 Km);
- Cretaceous flint from *Asiego* (approximately 2 Km) and *Colombres* (about 26 Km);
- Black flint from local formations (Namurian) around the cave;
- Quartzite of the *Oville* and *Barrios* formations located in *Oceño* (approximately 9km) surrounding the river Cares (around 25km).

By locating the geological sources in the map, the potential area explored by human groups is around 300 Km² within a range of 0,2-22 Km distant from the sites. By tracking ideal lines to calculate the distance between the archaeological sites and the geological sites and sources take on a radial arrangement walkable in a few minutes (*Arangas-source 1; Arangas-source 2*) to a maximum of around 10 hours (*Andrín*). The travel time was estimated based on the current paths which can be used. This estimation is random if it is considered the stochastic variables that can influence it such as the vegetation and physical geography. The vegetation coverage is variable in function to the intense climatic fluctuation of Pleistocene and the Holocene. As well as determining the environmental variations, the climatic oscillations could have changed the physical geography of the territory. In this sense, the human action should not be underestimated which represents one of the main transformations causes of the landscape. As evident from the distribution map (Fig.VI.2), the sites of Los Canes and Arangas are part of a geological context rich in mineral resources. The cartography established by the *Instituto Geológico y Minero de España* (IGME) in scale 1:50.000, n.32 of Llanes (Asturias) has dark limestone formations of Namurian origin suitable for the formation of ferruginous deposits at around 20 km distant from the sites and less than 200 m from the Pimiango formations. Namurian formations (limestones laminated of black colour and grey fine granular limestones) also characterize the geological context where the two caves are inserted. Furthermore, the cartography of reference (IGME, 1:50.000, no.50 of Carreña-Cabrales) also highlights the presence of feldspathic with gluconates microconglomerates of Late Devonian origin (Frasnian-Famennian) in the same area around the two caves.

- Archaeological sites
- Geological sources of lithic raw materials
- Geological sources of iron ores

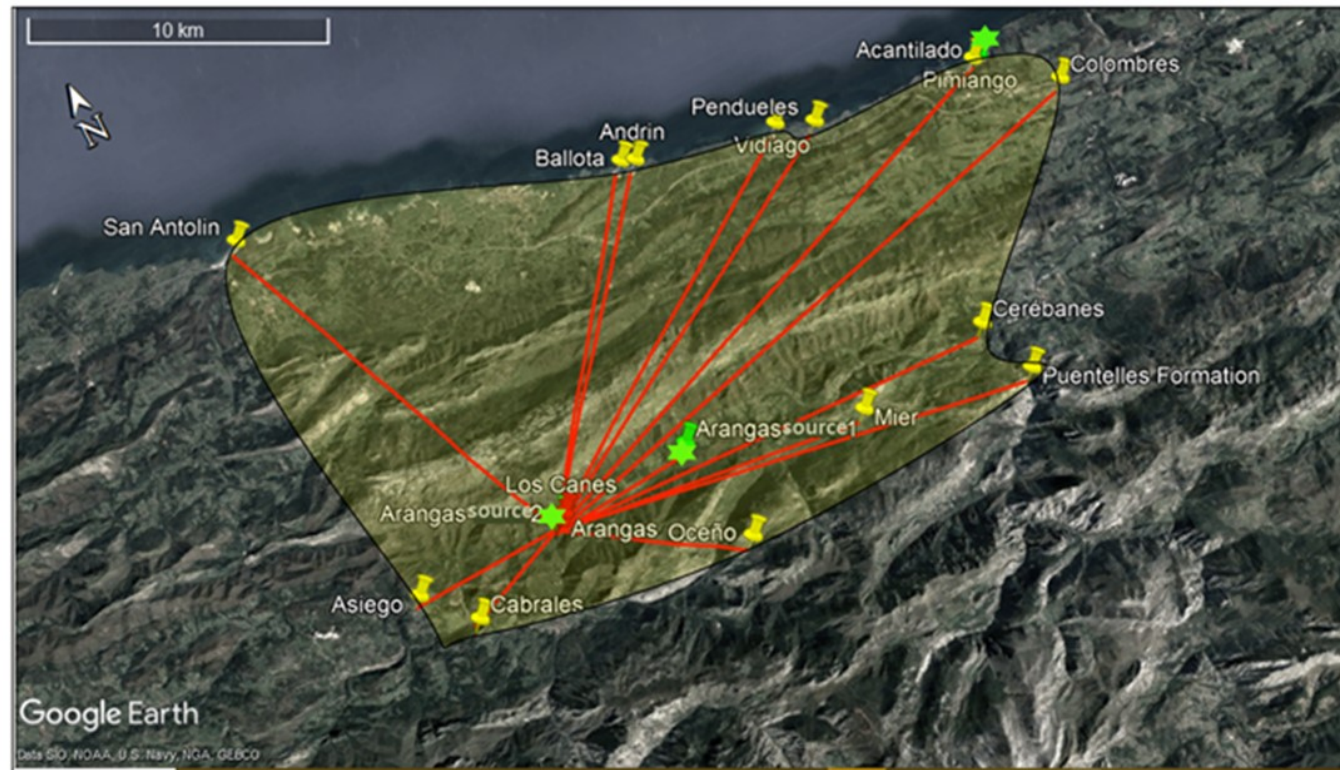


Fig.VI.2.: Map of the study area showing the localization of the archaeological sites with the geological sources of lithic raw materials and the potential sources of iron ores

VI.2.2. Geological survey

The geological survey was planned and carried out with the collaboration of Prof. Miguel Angel Sanchez-Carro, geologist and professor at the University of Santander (Cantabria, Spain). The exploration had the aim to search the potential deposits of ochre recognized on the maps. The first expedition carried out in the coastal areas allowed us to detect the presence of iron accumulations of spheroidal nodules which intercalate thin ferruginous laminae inside the Namurian dark laminated limestones. The nodules appear compact and massif with an intense red colour and metallic shine. The point has been marked on the map as *Acantilado* (Fig.VI.2).

The second expedition in the surrounding areas around the caves allowed us to detect ferruginous layers in two points overlapping the black laminated limestones. During the explorations, the feldspar microconglomerates with gluconates were not identified which could have been potentially offered by the deposits. The vegetation covering this area was particularly thick which made it possible to see the ferruginous formations in the road cuts. The points were marked on the map as *Arangas-source 1* and *Arangas-source 2* (Fig.VI.2). The geological survey allowed us to attest the richness of the Asturian formations of iron ores. But, at the same time, allow to establish the absence of yellow minerals as jarosite, goethite in the explored areas. The lack of a geological comparison for yellow ochres does not allow to carry out geochemical analyses to discriminate ochre geological sources.

Geological Sources	Distance as the crow flies from the sites (Km)	Walking time*
Arangas-source 2	0,2	15 min.
Arenas de Cabrales	3	30 min.
Arangas-source 1	5	50 min.
Oceño	6	3 h
Mier	11	4 h
Asiego	5,5	5 h
Cerébanes	15	5 h
San Antolin	14	6 h
Puentellés Formation	16	6 h
Acantilado	20	8 h
Pimiango	20	8 h
Bellota	12	9 h
Pendueles	15,5	9 h
Andrín	12	10 h
Vidiago	14,5	10 h

****Approximate estimation based on the current physical geography of the paths accessible by foot**

Tab.VI.1.: Summary table reporting the geological sources of raw materials with the distance in Km (as the crow flies) from the archaeological sites and valued walking time.

VI.2.3. Geological samples

The sample involved two types of ferruginous deposits: Iron-rich nodules and Ferruginous Crusts. Iron-rich nodules in laminated dark limestones of Namurian is localized in the coastal area.

The formation of these accumulations is due to weathering reactions which determined the removal of iron ores from the upper soils. The iron ores taken by the rainwater were re-deposited by filling the empty spaces between the

rocks and alternating the limestone laminae. The samples were collected from three distinct points in the same formation that preliminary indicated as *Acantilado I*, *Acantilado II* and *Acantilado III*.

The ferruginous crusts are common in the investigated geological context. It is possible to see these formations in both the coastal and interior areas due to supergenic enrichment phenomena. It is possible to also see the side cuts of the main road to the village of Arangas (Asturias), the ferruginous crusts overlap the Namurian limestones (Barcaliente and Valdeteja formations) in which the two caves are opened the microscopical observation of geological samples shows superficial and structural differences between the samples from the coastal formations (*Iron-rich nodules*) and the internal sources around the caves (*Ferruginous crust*). The *Iron-rich nodules* have a bright red colour which mixes with a deep red. The surface is glossy and has a metallic shine due to the richness of the Fe. The structure is compact and finely grained in which inclusions are not observed from a macro-microscopical observation.

The SEM-EDS analysis of thin sections of these samples allow to detect a crystalline structure typical of iron oxides with overlapped lamellar crystals in which it is possible to recognize inclusions that are well distinguished by the brightness and morphology of the crystals.

The quantitative characterization confirms the presence of a Fe-rich matrix in which inclusions of Ti are inserted (Fig.VI.5). The analyses confirm a similar nature for the samples collected from the three different points in the same formation. For this reason, the results shown below will include all in the same group *Acantilado*, without any distinction. The samples of *Ferruginous crust* have a red superficial colour less saturated with light shades which tends towards orange.

The surfaces in some points appear shiny and reflecting due to the presence of Fe. The compact and massif structure is rich of inclusions of quartz and calcite which can be clearly seen by naked eye. The SEM-EDS analysis of thin sections shows an iron matrix characterized by overlapped thin crystals which appear to be very light grey and rich in Cu, Ni, Fe, Zn (Fig.VI.6). The geochemical characterization confirms the ferruginous nature of the samples and distinguishes the samples based on the content of the major elements.



Fig.VI.3.: Iron-rich nodules in dark laminated limestones on the coastal area between Pimiango and La Franca (Asturias).

<i>Sample group</i>	<i>Source localization</i>	<i>UTM coordinates</i>	<i>Occurrence</i>
Iron-rich nodules	Acantilado	43°19'13.92"N/ 4°44'55.31"O	Namurian dark laminated limestones
Ferruginous crusts	Arangas-source 1; Arangas-source 2	43°19'13.92"N/ 4°44'55.31"O; 43°18'47.17"N/ 4°48'15.24"O	Namurian black laminated limestones
<i>Sample group</i>	<i>Source localization</i>	<i>UTM coordinates</i>	<i>Occurrence</i>
Iron-rich nodules	Acantilado	43°19'13.92"N/ 4°44'55.31"O	Namurian dark laminated limestones
Ferruginous crusts	Arangas-source 1; Arangas-source 2	43°19'13.92"N/ 4°44'55.31"O; 43°18'47.17"N/ 4°48'15.24"O	Namurian black laminated limestones
<i>Sample group</i>	<i>Source localization</i>	<i>UTM coordinates</i>	<i>Occurrence</i>

Tab.VI.2.: Summary table of geological iron ores deposit sampled for provenance purposes.

VI.3. Sourcing raw materials

The research of ochre sources exploited by Palaeolithic and Mesolithic hunter-gatherers is based on the comparison between the sampled geomaterials from the mineral sources on the coast and around the archaeological sites according to the methodology described in chapter II of this thesis. Hematite represents the most abundant colouring raw material in Los Canes and Arangas.

The presence of this material represents a circumstance in that both sites as the richness of the archaeological deposits does not depend on the presence of iron ores formations in the caves.



Fig.VI.4.: Ferruginous crust on laminated limestones near the caves at few meters from the village of Arangas (Asturias). The formations are clear visible from the road cuts.

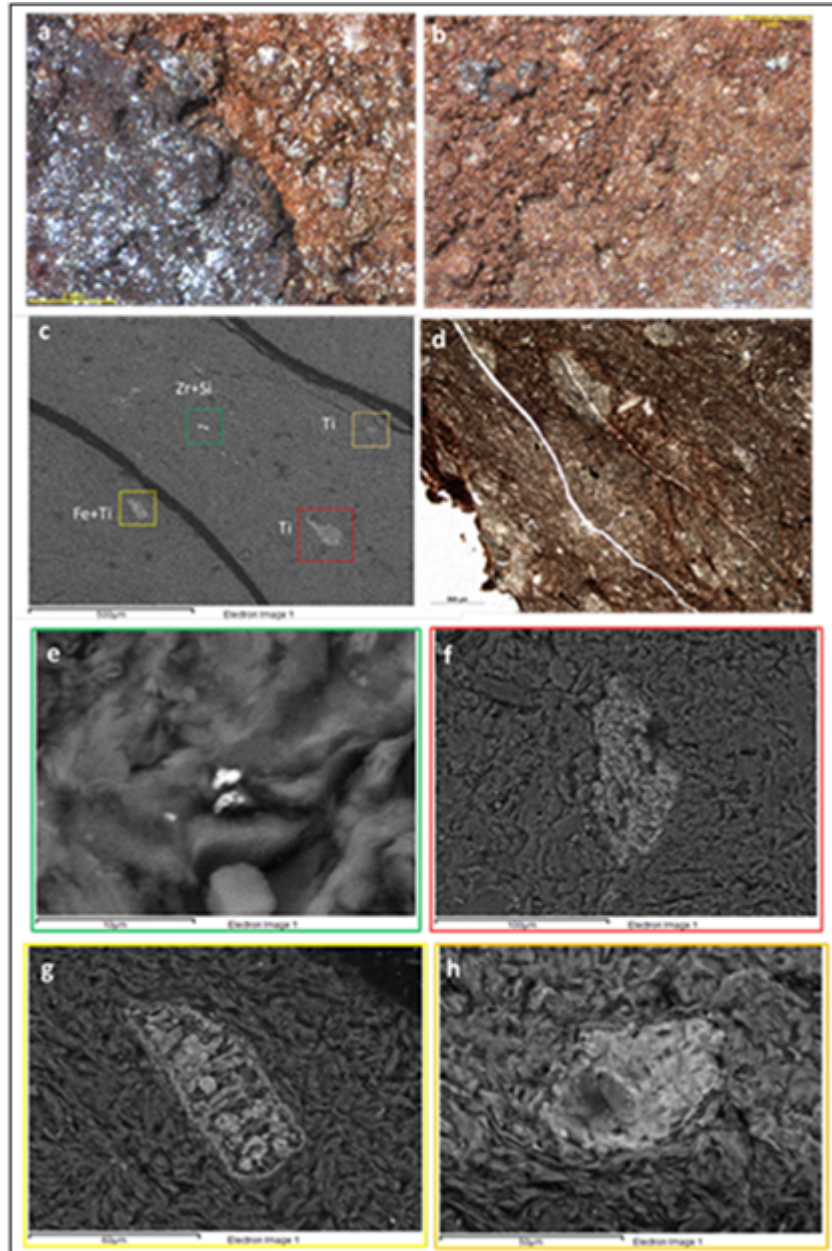


Fig.VI.5.: Iron rich- nodules images: a-b) images of samples obtained by optical microscope at x8.0 magnification; c) images of thin sections obtained by SEM-EDS; d) microphotography of thin sections. SEM-EDS images of mineral inclusions: e) Zr + Si; f-h) Ti; g) Zr + Si.

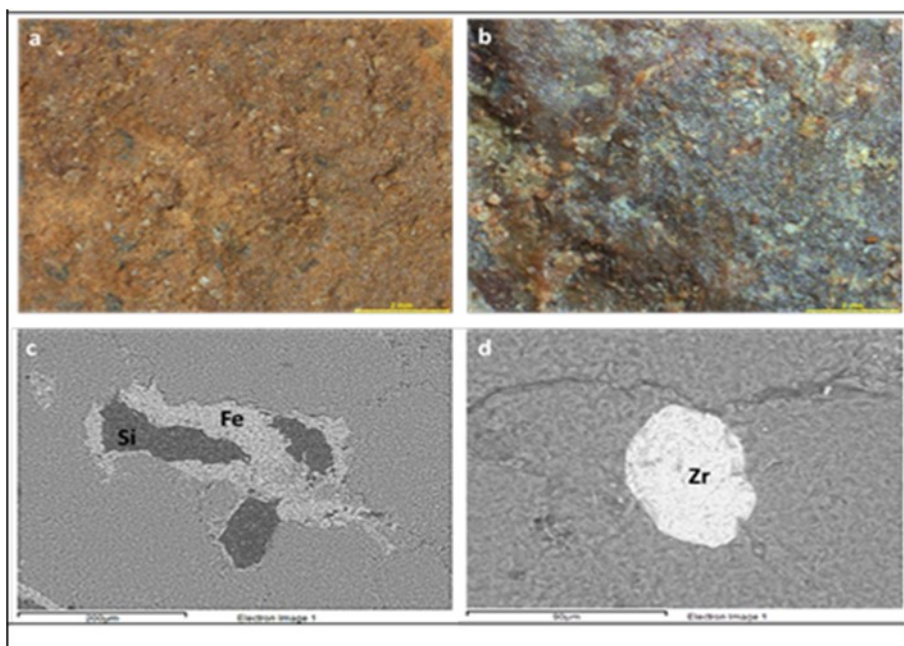


Fig.VI.6.: Ferruginous crust: a-b) images obtained by optical microscope at x8,0 magnification. SEM-EDS images of thin sections showing c) Fe and Si elements; d) inclusion of Zr.

The anthropic and exogenous origin of this raw material both in Los Canes and Arangas can therefore be confirmed.

As far as Los Canes is concerned, a microscopic observation of ochres belonging to this class show a certain external variability for colour and brightness with a heterogeneous surface. This variability does not appear discriminating to the level of the mineral composition (chap. V) and therefore is not related to a distinct provenance.

The presence of black inclusions (magnetite) represents a criterion which can be assessed in the research of the geological sources just as much as inclusions are observed in hematite elements coming from Arangas.

The external structure and the presence of inclusions represent important parameters to distinguish the geological sources of provenance.

From a macroscopic observation, the external surface of the geological samples from the *Acantilado* source is similar to hematite of subclass I-a however no black inclusions of magnetite in geological samples were observed.

The hematite in Arangas appear rather like those in Los Canes. The structural variability in this case also is reflected in the presence of two sub-classes in which one is characterized by grouping of black magnetite inclusions like Los Canes.

The affinity in the external structure and the similarity of inclusions correspond to the raw materials of Los Canes and Arangas and in this case also, is not reflected in the geological samples based on the visual parameters.

The analysis of the major and minor elements with XRF can give more essential information.

The samples enclosed in the ferrihydrite/lepidocrocite (Fe 20-50%) class at Los Canes, are more like the geological samples from Arangas-source 1 and Arangas-source 2 by the external pigmentation. Nevertheless, the correspondence does not appear direct when evaluating the hardness of the geological samples upon touch (soft) and the abundance of quartz inclusions.

At this point, an evaluation of the percentages of the powdered elements can help resolve the provenance question.

XRF and statistical data processing

In order to verify the geochemical affinity between the samples and confirm the ferruginous nature of archaeological and geological samples, a PCA on a total of 105 samples was carried out with 44 coming from Los Canes, 45 from Arangas and 16 geological (11 from the *Acantilado* formation, 5 from the

Arangas-source 1 and *Arangas-source 2*). A total of 13 variables were measured: Fe, Ca, K, Ti, P, Cu, Mn, V, Zn, Cl, Ar, Sn, Pb, As, Sb.

By starting from a group of broader variables (Si, Al, Ca, K, Ti, P, Cu, Mn, V, Zn, Cl, Ar, Sn, Pb, As, Sb), Si and Al were excluded from the measurements because they strongly correlated negatively with the Fe. Pearson's coefficient calculation allowed to verify the type of correlation (Fig.VI.7) and to determine the exclusion of the two variables as indicated in table.VI.3.

The score graph (Fig.VI.8) obtained from PCA carried out on the first two main components which respectively explain 100% and 99,88% (Tab.VI.4) allows to confirm the ferruginous nature of the samples. A total of 3 samples, 2 from Arangas and 1 from Los Canes, are outside the ellipse confidence with an interval at 95%.

		Si	Al	K	Ti	Ca	P	Cu	Mn	V	Zn	Cl	Ar	Sn	Pb	As	Sb	Fe
"Si"	Pearson Corr.	1	0,95	0,94	0,94	0,92	-0,03	0,92	0,94	0,93	0,93	0,93	0,93	0,93	0,93	0,03	0	-0,3
"Si"	p-value	---	0	0	0	0	0,8	0	0	0	0	0	0	0	0	0,77	0,98	0
"Al"	Pearson Corr.	0,95	1	0,96	0,95	0,94	0	0,94	0,94	0,94	0,94	0,94	0,95	0,94	0,95	-0,05	-0,02	-0,23
"Al"	p-value	0	---	0	0	0	0,97	0	0	0	0	0	0	0	0	0,66	0,83	0,02
"K"	Pearson Corr.	0,94	0,96	1	1	1	-0,02	1	1	1	1	1	1	1	1	0,44	0,01	-0,04
"K"	p-value	0	0	---	0	0	0,86	0	0	0	0	0	0	0	0	0	0,95	0,65
"Ti"	Pearson Corr.	0,94	0,95	1	1	1	-0,02	1	1	1	1	1	1	1	1	-0,03	-0,01	-0,03
"Ti"	p-value	0	0	0	---	0	0,86	0	0	0	0	0	0	0	0	0,79	0,91	0,75
"Ca"	Pearson Corr.	0,92	0,94	1	1	1	-0,01	1	1	1	1	1	1	1	1	-0,07	-0,01	-0,02
"Ca"	p-value	0	0	0	0	---	0,9	0	0	0	0	0	0	0	0	0,52	0,89	0,85
"P"	Pearson Corr.	-0,03	0	-0,02	-0,02	-0,01	1	-0,02	-0,02	-0,02	-0,02	-0,02	-0,02	-0,02	-0,02	-0,01	-0,01	-0,16
"P"	p-value	0,8	0,97	0,86	0,86	0,9	---	0,83	0,84	0,84	0,84	0,83	0,84	0,84	0,84	0,91	0,9	0,11
"Cu"	Pearson Corr.	0,92	0,94	1	1	1	-0,02	1	1	1	1	1	1	1	1	0,21	-0,01	0
"Cu"	p-value	0	0	0	0	0	0,83	---	0	0	0	0	0	0	0	0,07	0,93	1
"Mn"	Pearson Corr.	0,94	0,94	1	1	1	-0,02	1	1	1	1	1	1	1	1	0,04	0,01	-0,01
"Mn"	p-value	0	0	0	0	0	0,84	0	---	0	0	0	0	0	0	0,72	0,95	0,94
"V"	Pearson Corr.	0,93	0,94	1	1	1	-0,02	1	1	1	1	1	1	1	1	-0,08	0	-0,01
"V"	p-value	0	0	0	0	0	0,84	0	0	---	0	0	0	0	0	0,49	0,99	0,94
"Zn"	Pearson Corr.	0,93	0,94	1	1	1	-0,02	1	1	1	1	1	1	1	1	0,14	-0,01	0
"Zn"	p-value	0	0	0	0	0	0,84	0	0	0	---	0	0	0	0	0,22	0,91	0,98
"Cl"	Pearson	0,93	0,94	1	1	1	-0,02	1	1	1	1	1	1	1	1	-0,03	-0,01	0

	Corr.																	
"Cl"	p-value	0	0	0	0	0	0,83	0	0	0	0	---	0	0	0	0,81	0,91	0,99
"Ar"	Pearson Corr.	0,93	0,95	1	1	1	-0,02	1	1	1	1	1	1	1	1	0,51	-0,01	-0,01
"Ar"	p-value	0	0	0	0	0	0,84	0	0	0	0	0	---	0	0	0	0,91	0,96
"Sn"	Pearson Corr.	0,93	0,94	1	1	1	-0,02	1	1	1	1	1	1	1	1	0,23	-0,01	0
"Sn"	p-value	0	0	0	0	0	0,84	0	0	0	0	0	0	---	0	0,04	0,91	0,97
"Pb"	Pearson Corr.	0,93	0,95	1	1	1	-0,02	1	1	1	1	1	1	1	1	0,06	-0,01	0
"Pb"	p-value	0	0	0	0	0	0,84	0	0	0	0	0	0	0	---	0,57	0,91	0,97
"As"	Pearson Corr.	0,03	-0,05	0,44	-0,03	-0,07	-0,01	0,21	0,04	-0,08	0,14	-0,03	0,51	0,23	0,06	1	1	-0,12
"As"	p-value	0,77	0,66	0	0,79	0,52	0,91	0,07	0,72	0,49	0,22	0,81	0	0,04	0,57	---	0	0,28
"Sb"	Pearson Corr.	0	-0,02	0,01	-0,01	-0,01	-0,01	-0,01	0,01	0	-0,01	-0,01	-0,01	-0,01	-0,01	1	1	-0,12
"Sb"	p-value	0,98	0,83	0,95	0,91	0,89	0,9	0,93	0,95	0,99	0,91	0,91	0,91	0,91	0,91	0	---	0,29
"Fe"	Pearson Corr.	-0,3	-0,23	-0,04	-0,03	-0,02	-0,16	0	-0,01	-0,01	0	0	-0,01	0	0	-0,12	-0,12	1
"Fe"	p-value	0	0,02	0,65	0,75	0,85	0,11	1	0,94	0,94	0,98	0,99	0,96	0,97	0,97	0,28	0,29	---

Tab.VI.3.: Pearson Correlations of chemical elements in archaeological and geological samples

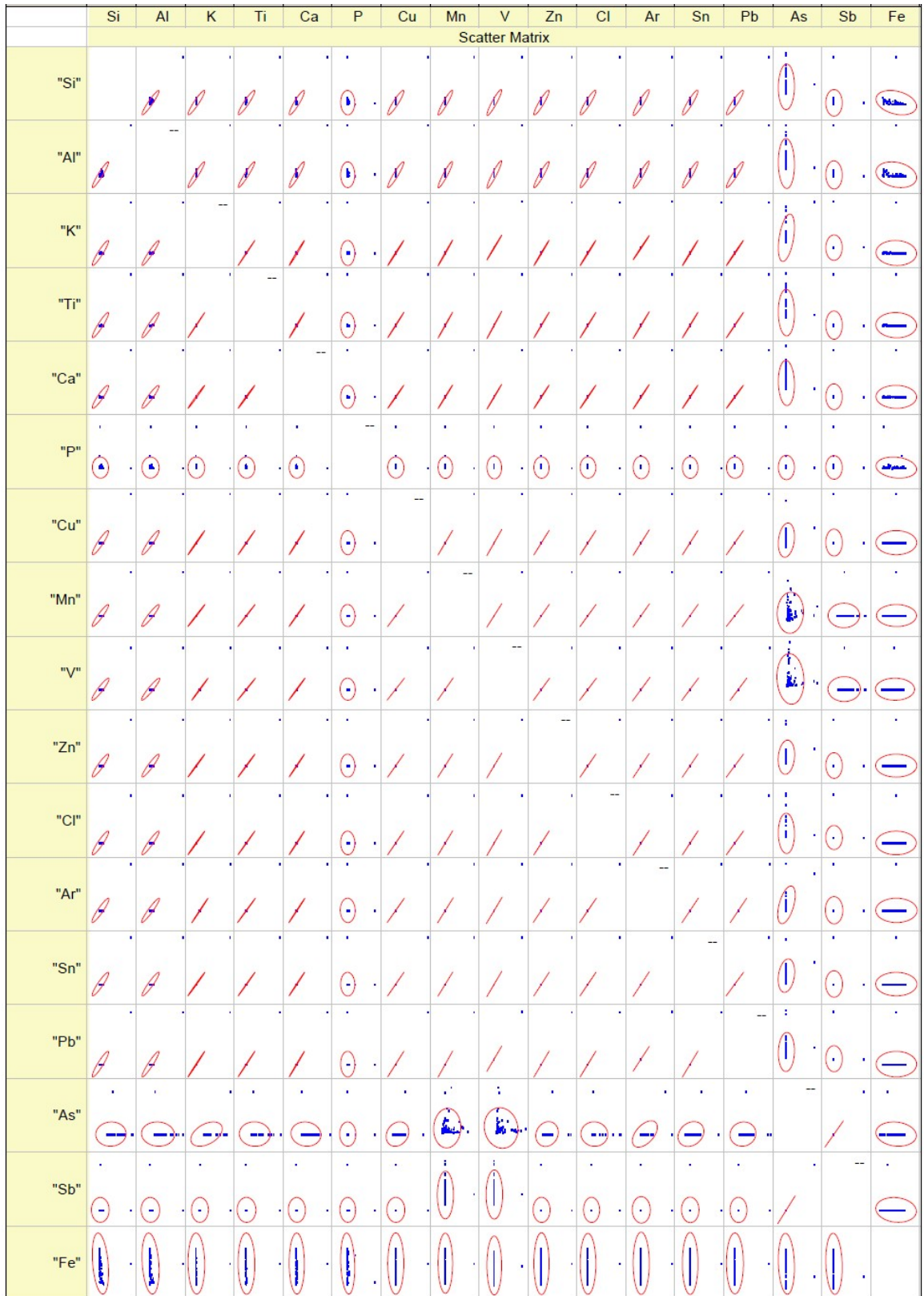


Fig.VI.7.: Scatter matrix of Pearson's correlation coefficient of the tested variables in the PCA of archaeological and geological samples.

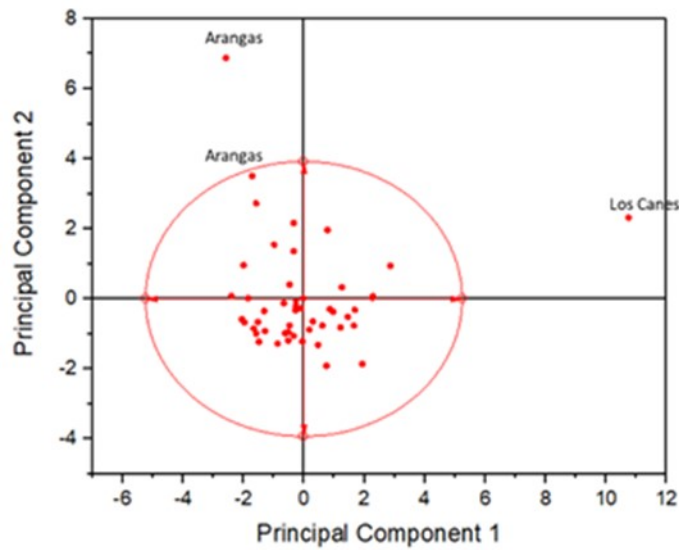


Fig.VI.8.: Score plot of PCA realized on archaeological and geological samples. The graph confirms the nature of samples as iron ores.

By analysing the biplot graph, it is possible to notice how the vectors which mainly guide the distribution of the samples are Pb and Sb on one hand, and Mn, As, Ti, K, P on the other. At this point, following the methodological protocol previously established, it is tried to isolate the geological sources to discriminate the provenance of the archaeological samples by plotting the elements which show the longest vectors in pairs with Fe, guiding the variance of the samples.

After several attempts and combinations, the ratio Mn/Fe-As/Fe was the most suitable one to distinguish the geological sources.

The scatter graph obtained from $\log\text{Mn/Fe}$ vs. $\log\text{As/Fe}$ differentiates the geological sources into two separate groups even though the analysis is limited to the availability of a single sample in some cases (*Arangas-source 2*).

	<i>Eigenvalue</i>	<i>Percentage of Variance</i>	<i>Cumulative</i>
1	4,1342	29,53%	29,53%
2	2,31601	16,54%	46,07%
3	1,65125	11,79%	57,87%
4	1,45784	10,41%	68,28%
5	1,11532	7,97%	76,25%
6	1,01996	7,29%	83,53%
7	0,63225	4,52%	88,05%
8	0,43093	3,08%	91,13%
9	0,42454	3,03%	94,16%
10	0,29951	2,14%	96,30%
11	0,23688	1,69%	97,99%
12	0,15983	1,14%	99,13%
13	0,10452	0,75%	99,88%
14	0,01698	0,12%	100,00%

Tab.VI.4.: Eigenvalues of variables that explain the variance in the samples.

Some examples are shown which confirm the dispersion of the samples obtained from the ratios of Sb, Ti, Pb, Mn with Fe. The situation also appears similar in the other experimented combinations. From the results obtained, non-discrimination of the geological sources is evident, which in this case are certain for the sampling carried out in controlled conditions.

After having distinguished the geological sources, the same ratio was used to verify the fitting of the archaeological samples. The biplot graph of reference shows that, by adding the archaeological samples, they fall in the ellipses expected and overlapped among themselves. The samples from *Acantilado* (Iron-

rich nodules) and the sample from *Arangas-source 1* and *Arangas-source 2* (*Ferruginous crusts*) are enclosed by two distinct ellipses. The distinction appears clear when adding the samples with Fe>50% from Los Canes and Arangas. The archaeological samples show a high level of geochemical affinity between themselves but not with geological sources. The geological referential that was found does not allow to geologically attribute the archaeological samples to the sampled iron ores deposits. In any case, the ratio between As and Mn with Fe confirms the geochemical attribution of the archaeological samples to the same groups of raw materials which show high percentages of Fe greater than 50%

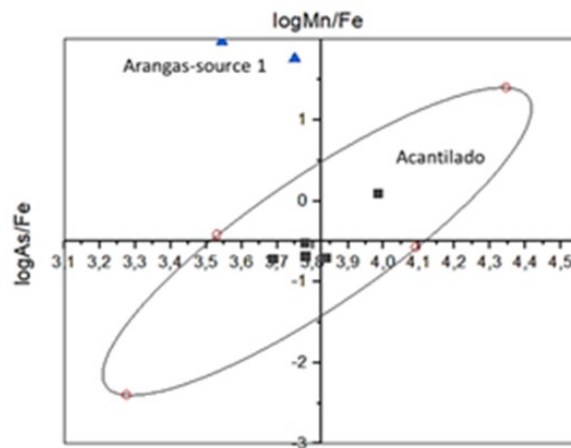


Fig.VI.9.: Biplot graph showing $\log\text{Mn}/\text{Fe}$ vs $\log\text{As}/\text{Fe}$ with confidential ellipse (95%).

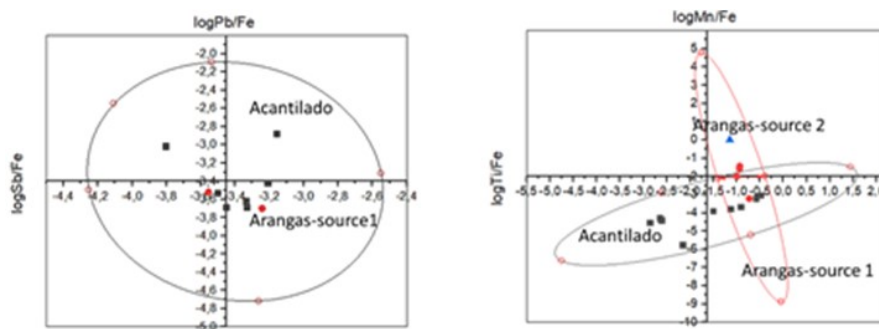


Fig.VI.10.: Biplot graphs showing the non-discrimination per sources of the samples using the ratios Sb/Fe vs. Pb/Fe and Ti/Fe vs. Mn/Fe .

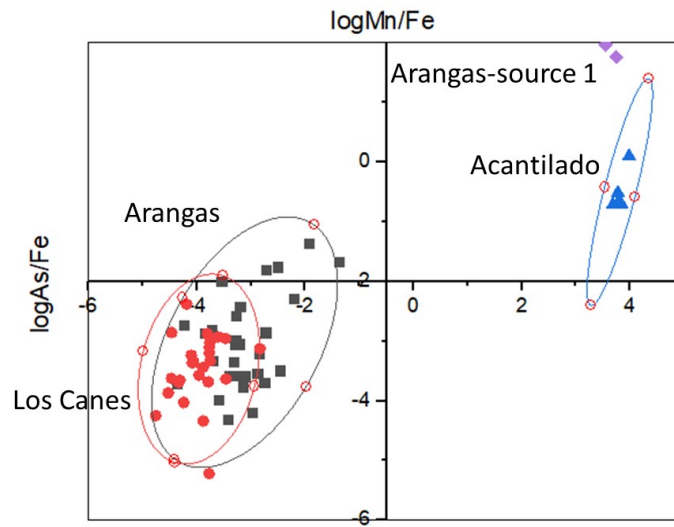


Fig.VI.11.: Biplot graphs showing the distribution of archaeological samples ($Fe > 50\%$) and geological samples by $\log As/Fe$ vs $\log Mn/Fe$.

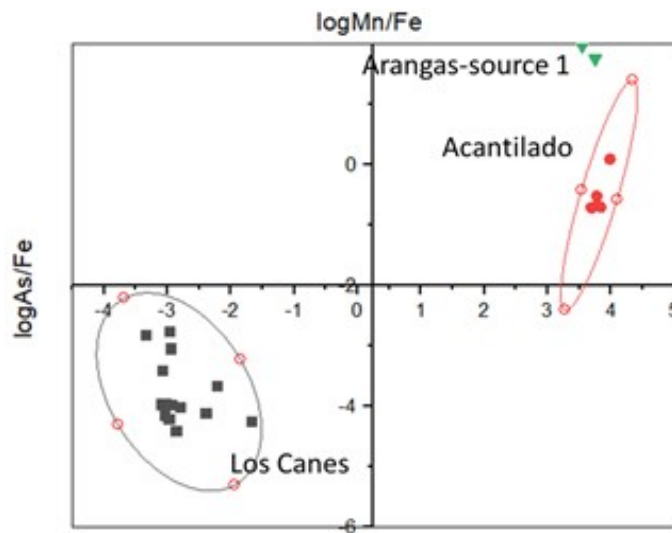


Fig.VI.12.: Biplot graphs showing the distribution of archaeological samples ($Fe < 50\%$) and geological samples by $\log As/Fe$ vs $\log Mn/Fe$.

The distinction persists when plotting the archaeological samples with percentages of Fe < 50% in the same combination. The archaeological samples do not intersect with the geological samples thus confirming the geochemical dissimilarity.

VI.3.1. Comparative analysis

To support the methodology adopted and to prove the results obtained for Los Canes and Arangas, a comparative analysis is developed using ochre samples from Grotta San Teodoro and S'Omu e S'Orku examined with XRF.

The calculation of the Pearson coefficient on geological samples from the *Acantilado* and *Arangas-source* formations (1-2) with some archaeological samples (hematite) from Los Canes and Arangas to which were added those collected from Grotta San Teodoro and S'Omu and S 'Orku, establishes the correlations between the elements tested (Si, Al, K, Ti, Ca, P, Cu, Mn, V, Zn, Sn, Cl, Ar, Pb, As, Sb) with Fe.

The elements that show a good positive correlation with Fe are Zn, Sn, Pb, Sb. While, other elements are strongly correlate negatively: Si, Al, K, Ti, Ca, P, Mn. By making a first PCA with two main components, with the elements positively correlated to Fe, a preliminary discrimination appears evident. From the main group, *Arangas-source 1* and S'Omu e S'Orku (1 sample) stand out well. The remaining samples appear indiscriminate.

The result does not meet the expectations, for this reason a second PCA was performed. This time, the PCA tested the negatively correlated variables to Fe: Si, Al, K, Ti, Ca, P, Mn.

Combining with each other (base log₁₀) the negatively correlate elements to the Fe, in various combinations, the Ca / Fe vs. P / Fe appears discriminating. (Fig.VI.14).

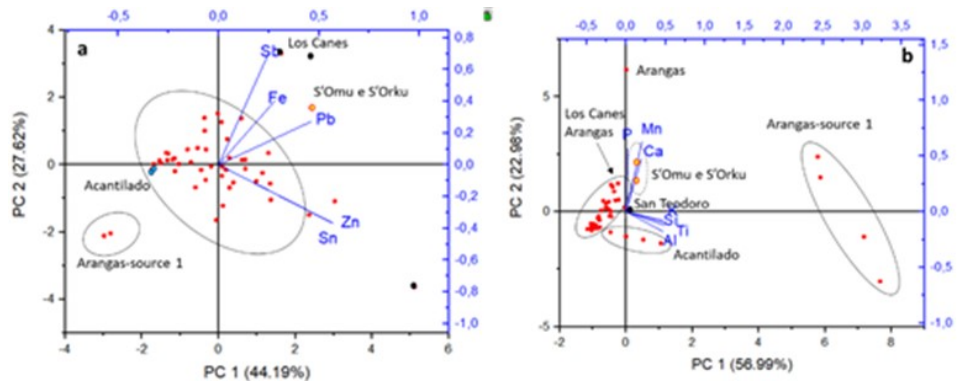


Fig.VI.13.: Biplot graphs of PCA for comparative analysis: a) positively correlated elements with Fe; b) negatively correlated elements with Fe.

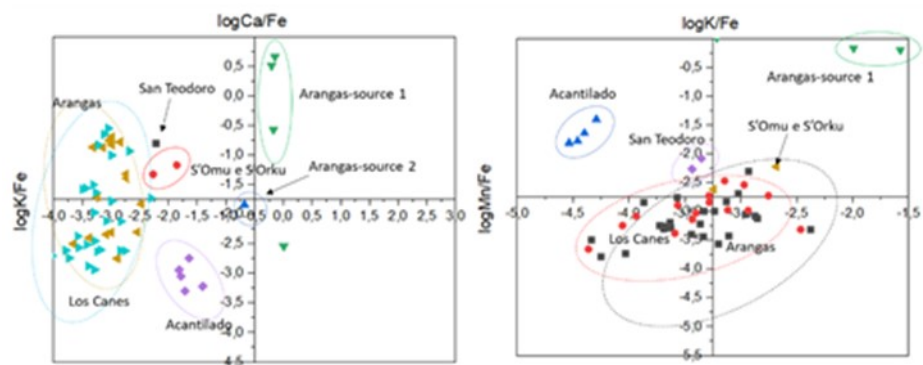


Fig.VI.14.: Scatter plot graph of $\log K/Fe$ vs. $\log Ca/Fe$ and $\log Mn/Fe$ vs. $\log K/Fe$.

PCA: positively correlated elements with FE			
	Eigenvalue	Percentage of Variance	Cumulative
1	2,20948	44,19%	44,19%
2	1,38086	27,62%	71,81%
3	0,8721	17,44%	89,25%
4	0,38187	7,64%	96,89%
5	0,15569	3,11%	100,00%
PCA: negatively correlated elements with FE			
	Eigenvalue	Percentage of Variance	Cumulative
1	3,98895	56,99%	56,99%
2	1,60833	22,98%	79,96%
3	0,82409	11,77%	91,73%
4	0,38092	5,44%	97,18%
5	0,14521	2,07%	99,25%
6	0,03213	0,46%	99,71%
7	0,02036	0,29%	100,00%

Tab.VI.5.: Eigenvalues of variables that explain the variance in the samples tested for comparative purposes.

VI.4. Summary of results

The data obtained from the comparison between the archaeological samples and the geological referential, does not satisfy the postulate of provenance. The question of the origin of red ochres in the sites of Los Canes and Arangas is still open.

Although the geological indices are well known and documented, the samples collected in the formations identified on the geological maps and considered potentially accessible in the past (Upper Palaeolithic/Mesolithic) as in the current epoch do not allow to establish a relationship with the archaeological materials.

This fact certainly does not exclude the anthropic contribution to the sites and the exogenous origin of the raw materials but attests the necessity to continue the geological sampling by exploring further geological formations.

The amplitude of the Asturian territory, in fact, is not an aspect to be underestimated especially if it reflects on the mineral richness of its formations as evident from the geological maps (Fig.VI.1).

Even though, in light of the available data, it is not possible to establish the origin of archaeological materials, this study is part of a preliminary research that opens the way to future research to investigate further geological formations. In any case, a non-marginal datum is the synchronic and diachronic geochemical affinity between the two sites which confirms the presence of the same colouring raw materials in Los Canes and Arangas.

Combining these data with those obtained from the provenance research, the mismatch with the sampled sources and the archaeological materials, and the geochemical correspondence between the ochres from the Palaeolithic and

Mesolithic units of the two sites, suggest the exploitation of the same geological source simultaneously and continuously over time, for the two sites. The presence of the same raw materials in chrono-culturally connectable units, leads us to discuss a double possibility: the same group moved between the two caves bringing with them the colouring raw materials; communication and exchange between two distinct groups that share the same geographical area.

These hypotheses appear acceptable just for the Upper Palaeolithic because both caves were used as domestic places. Starting from the Mesolithic, Los Canes was exploited as a funeral space, while for Arangas continued the domestic function. For this period, the first of the proposed hypotheses would seem acceptable. In this sense, the exploitation of local sources is likely to occur within a space surrounding the two sites that could not be accurately sampled. As previously reported, the thick covering vegetation and the current geography reduce the access to ferruginous deposits just visible from road cuts. It is necessary to intensify the research of ochre sources around the two sites by assessing the degree of accessibility between 21,000 and 8,000 cal BP.

		Si	Al	K	Ti	Ca	P	Cu	Mn	V	Zn	Cl	Ar	Sn	Pb	As	Sb	Fe
"Si"	Pearson Corr.	1	0,15	---	0,52	0,63	-0,27	0,02	-0,06	0,1	-0,09	-0,25	0,13	0,04	-0,38	-0,29	-0,01	-0,36
"Si"	p-value	---	0,1	0	0	0	0	0,81	0,55	0,29	0,38	0,01	0,16	0,66	0	0	0,96	0
"Al"	Pearson Corr.	0,15	1	---	0,23	0,27	0,04	0	0,94	0	-0,01	-0,08	-0,01	-0,05	-0,12	-0,1	0,04	-0,06
"Al"	p-value	0,1	---	0,02	0,01	0	0,67	0,97	0	0,97	0,92	0,37	0,95	0,6	0,22	0,3	0,68	0,55
"K"	Pearson Corr.	-0,76	-0,22	1	-0,61	-0,67	-0,33	-0,19	0	-0,36	0,12	0,2	0,02	0,03	0,39	0,31	-0,15	0,43
"K"	p-value	0	0,02	---	0	0	0	0,04	0,97	0	0,24	0,03	0,85	0,73	0	0	0,18	0
"Ti"	Pearson Corr.	0,52	0,23	---	1	0,81	-0,24	0,03	-0,05	0,03	0,08	-0,19	0,06	0,05	-0,26	-0,19	0,01	-0,19
"Ti"	p-value	0	0,01	0	---	0	0,01	0,73	0,57	0,72	0,44	0,04	0,56	0,61	0,01	0,05	0,96	0,07
"Ca"	Pearson Corr.	0,63	0,27	---	0,81	1	-0,17	0,08	-0,06	0,19	0,12	-0,22	0,06	-0,11	-0,39	-0,22	0,07	-0,28
"Ca"	p-value	0	0	0	0	---	0,07	0,37	0,52	0,05	0,23	0,02	0,54	0,26	0	0,02	0,49	0,01
"P"	Pearson Corr.	-0,27	0,04	---	-0,24	-0,17	1	0,14	0,11	0,36	-0,19	0,01	-0,23	-0,18	-0,05	-0,08	0,17	-0,16
"P"	p-value	0	0,67	0	0,01	0,07	---	0,15	0,25	0	0,05	0,94	0,02	0,08	0,6	0,4	0,1	0,14
"Cu"	Pearson Corr.	0,02	0	---	0,03	0,08	0,14	1	-0,03	0,19	-0,05	0,05	-0,07	0	-0,05	-0,04	0,36	-0,12
"Cu"	p-value	0,81	0,97	0,04	0,73	0,37	0,15	---	0,78	0,05	0,65	0,6	0,45	0,99	0,63	0,7	0	0,27
"Mn"	Pearson Corr.	-0,06	0,94	0	-0,05	-0,06	0,11	-0,03	1	-0,05	-0,06	-0,01	-0,04	-0,01	0,02	-0,03	-0,07	0,01
"Mn"	p-value	0,55	0	0,97	0,57	0,52	0,25	0,78	---	0,59	0,57	0,94	0,71	0,9	0,82	0,77	0,53	0,93
"V"	Pearson Corr.	0,1	0	---	0,03	0,19	0,36	0,19	-0,05	1	0,05	0,26	-0,19	0,01	-0,03	0,11	-0,06	-0,19
"V"	p-value	0,29	0,97	0	0,72	0,05	0	0,05	0,59	---	0,63	0,01	0,05	0,91	0,77	0,27	0,58	0,08
"Zn"	Pearson Corr.	-0,09	-0,01	0,12	0,08	0,12	-0,19	-0,05	-0,06	0,05	1	0,26	0,33	0,14	0,18	0,51	0	0,08
"Zn"	p-value	0,38	0,92	0,24	0,44	0,23	0,05	0,65	0,57	0,63	---	0,01	0	0,18	0,08	0	0,99	0,49
"Cl"	Pearson Corr.	-0,25	-0,08	---	-0,19	-0,22	0,01	0,05	-0,01	0,26	0,26	1	0,12	0,6	0,78	0,51	0,08	-0,01
"Cl"	p-value	0,01	0,37	0,03	0,04	0,02	0,94	0,6	0,94	0,01	0,01	---	0,2	0	0	0	0,45	0,96

"Ar"	Pearson Corr.	0,13	-0,01	0,02	0,06	0,06	-0,23	-0,07	-0,04	-0,19	0,33	0,12	1	0,09	0,05	0	-0,08	-0,04
"Ar"	p-value	0,16	0,95	0,85	0,56	0,54	0,02	0,45	0,71	0,05	0	0,2	---	0,36	0,64	0,98	0,44	0,74
"Sn"	Pearson Corr.	0,04	-0,05	0,03	0,05	-0,11	-0,18	0	-0,01	0,01	0,14	0,6	0,09	1	0,76	0,17	0	-0,16
"Sn"	p-value	0,66	0,6	0,73	0,61	0,26	0,08	0,99	0,9	0,91	0,18	0	0,36	---	0	0,08	0,97	0,15
"Pb"	Pearson Corr.	-0,38	-0,12	---	-0,26	-0,39	-0,05	-0,05	0,02	-0,03	0,18	0,78	0,05	0,76	1	0,42	-0,04	0,03
"Pb"	p-value	0	0,22	0	0,01	0	0,6	0,63	0,82	0,77	0,08	0	0,64	0	---	0	0,7	0,78
"As"	Pearson Corr.	-0,29	-0,1	---	-0,19	-0,22	-0,08	-0,04	-0,03	0,11	0,51	0,51	0	0,17	0,42	1	0,1	0,39
"As"	p-value	0	0,3	0	0,05	0,02	0,4	0,7	0,77	0,27	0	0	0,98	0,08	0	---	0,34	0
"Sb"	Pearson Corr.	-0,01	0,04	-0,15	0,01	0,07	0,17	0,36	-0,07	-0,06	0	0,08	-0,08	0	-0,04	0,1	1	-0,07
"Sb"	p-value	0,96	0,68	0,18	0,96	0,49	0,1	0	0,53	0,58	0,99	0,45	0,44	0,97	0,7	0,34	---	0,58
"Fe"	Pearson Corr.	-0,36	-0,06	---	-0,19	-0,28	-0,16	-0,12	0,01	-0,19	0,08	-0,01	-0,04	-0,16	0,03	0,39	-0,07	1
"Fe"	p-value	0	0,55	0	0,07	0,01	0,14	0,27	0,93	0,08	0,49	0,96	0,74	0,15	0,78	0	0,58	---

Tab.VI.6.: Pearson Correlations of chemical elements in samples tested for comparative analysis.

Chapter VII.

Ochre exploitation and mechanical transformations

As demonstrated in the previous chapters, the red ferruginous rocks represent the most abundant raw materials in Palaeolithic and Mesolithic deposits of the European contexts chosen for this research.

After having established the anthropic origin of these materials and recognized the nature of raw materials, it is necessary to found in what way these were processed. Investigating the transformations of raw materials is therefore fundamental to better understand the role of ochre played among the life of Palaeolithic and Mesolithic hunter-gatherers. In this sense, it is important to remember that the colouring raw materials can be subjected to two main types of transformations: *mechanical* and *chemical*, as previously mentioned (Chap. II).

The absence of intrinsic alterations of ochres due to anthropic actions as demonstrated by the chemical analysis (SEM-EDS and XRD) privileges the idea of processing for mechanical transformations. The presence of indices which support this hypothesis drives the research in this direction. The abundance of very small pieces as well as the frequency of modified pieces and, in some cases, with used surfaces, suggest a reduction of large volumes.

Nevertheless, the presence of products of *debitage*, faceted objects and *crayons* lets us to identify further processing stages. The presence of diagnostic traces also allows to formulate functional interpretations.

In order to verify these hypotheses, a comparison by the results of published experiments conducted on ochre represents a valid means, as it provides to the researcher several elements to corroborate the theories formulated during the work. Currently, experimental archaeology is an essential way of interpretation to verify an archaeological fact through the identical reproduction of objects and situations by using the same resources in the same conditions of the past. The experiments are not just limited to the interpretation of reproduced elements (gestures, situations, conditions, objects, facts...) but they can be supported by traceological studies. The analysis of use-wear traces requires well-defined criteria according to the availability of a well-matched experimental referential. The verification of experimental traces produced in controlled conditions supports the interpretation of signs of use that can mark the surface of archaeological objects.

Regarding this research, the materials were largely recovered by sieving the sediment excavated from the deposit, first in dry conditions and, then, with water. The treatment in water could have influenced the readability of superficial traces. However, the presence of diagnostic traces on the surface of the archaeological objects can be influenced by additional variables such as specific physical traits of raw materials, environment of sedimentation and post-depositional processes. In this case, the general state of assemblages appears to be as a trigger factor for the readability of the surfaces and the uniformity of data.

For this reason, the traces observed were cataloged and evaluated in light of valid references available in literature (Wadley, 2005; Hodgskiss, 2010; Hodgskiss & Wadley, 2017).

The data relating to red ochres collected from Palaeolithic and Mesolithic units of Los Canes, La Garma A, Arangas and Grotta di Pozzo are exposed below. The yellow vestiges will be excluded at this moment of the research due to the low representativeness in the archaeological deposits and for the lack of diagnostic traces.

VII.1. Mechanical transformations

For what concern the mechanical transformations of red ochres, it is possible to distinguish *initial* and *secondary* stages in the *chaîne opératoire* of ferruginous rocks. The initial transformations are those implemented in the first stage of working process of raw materials such as *roughing*, *crushing*, *debitage* (Salomon, 2009; Dayet, 2013). The secondary transformations however occur after the initial ones and imply an additional working of the product such as creating powder. (chap. I).

VII.1.1. Archaeological indices

A set of archaeological evidences allows us to reconstruct mechanical transformations in relation to the ochre vestiges: sizes and morphology of pieces, signs of *debitage* (negatives of detachments; bulbs of percussions, fractures), use-wear traces. The data obtained from the evaluation of these aspects on red ochres will be presented by an integrated perspective.

VII.1.1.1. Upper Palaeolithic

Dimension and morphology

Based on data exposed in chapter IV of this thesis, the net prevalence of small sized objects appears clear. The experiments carried out by Salomon (2009) demonstrates that pieces with dimensions above 1,5 cm and below 5 cm (*roughing*) are produced by *crushing*.

Crushing is related to the presence of fragments >1,5 cm which in *fine crushing* is associated to powder fractions.

In the collections examined, the minimum sizes start from 2 mm. By considering the indirect selection of sieving (meshes of 2 mm) and placing the maximum limit to 5 cm, according to Salomon (2009) for *roughing*, the graph (Fig.VII.1) shows that almost 99% of the pieces fall within the dimensional range of *crushing* (0,2-3 cm approx.). The intersection in the same confidence ellipse (interval at 95%) of fragments from Los Canes, Arangas, La Garma A and Grotta di Pozzo attests the dimensional affinity suggesting a similar origin.

The *crushing* produces fragments morphologically irregular (Dayet, 2013). By evaluating the distribution curve of length, width and thickness values, a non-normal distribution appears evident in each case. The data confirms the absence of standardized morphologies by taking on the hypothesis of *crushing*. However, the presence of peculiar objects such as unretouched flakes, indicates the shaping of raw blocks by *debitage*.

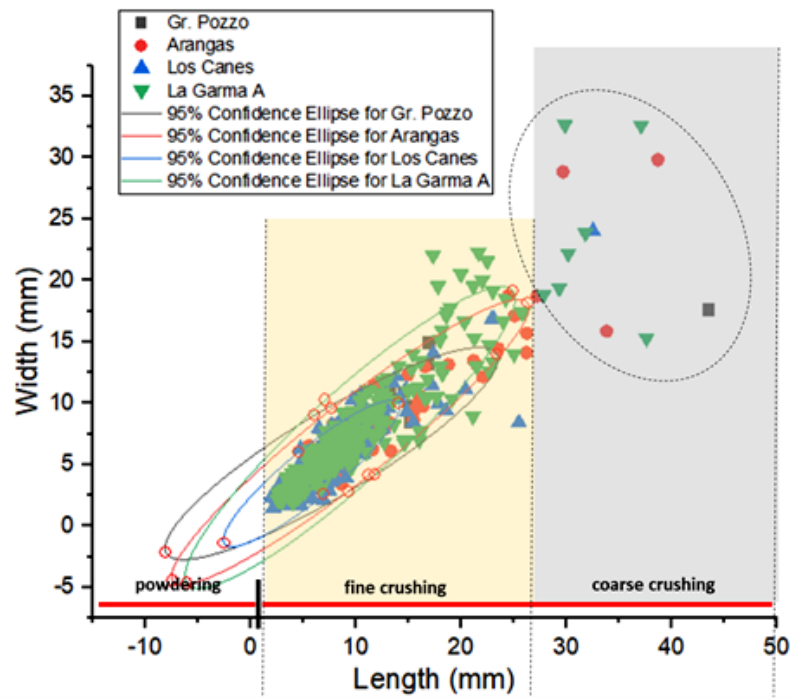


Fig.VII.1.: Dimensional distribution of red ochre from Upper Palaeolithic layers by the range of 2-50 mm fixed on the experiments conducted to test the hypothesis of mechanical transformation of ferruginous raw materials (Salomon, 2009).

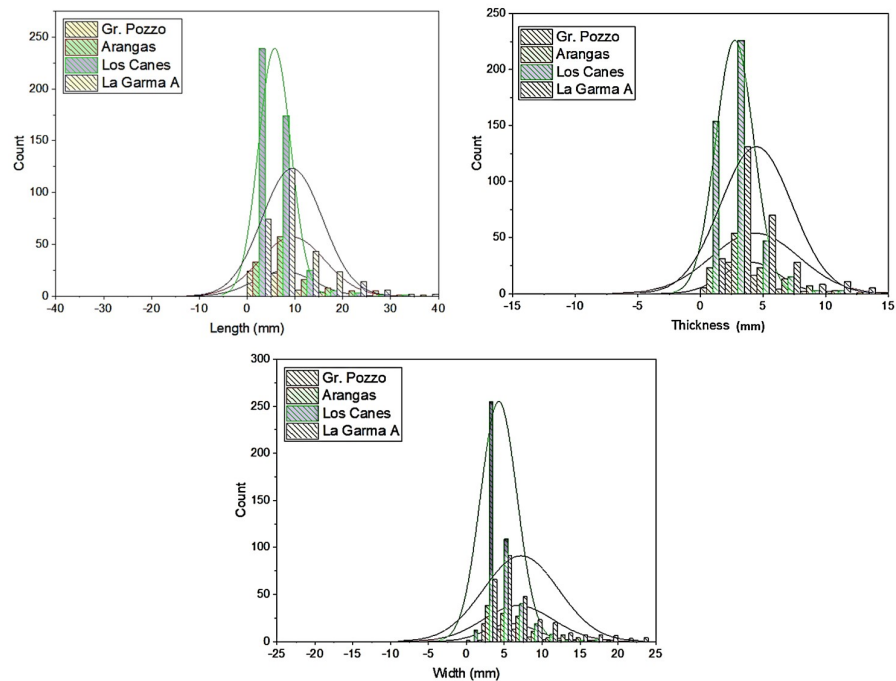


Fig.VII.2.: Non-normal distribution of morphological values (Length, Width, Thickness): red ochres Upper Palaeolithic

Debitage

The elements which are typically identified as products of *debitage* are extremely rare but significantly present. These objects represent less than 1% of the total number of materials analyzed (n. 2 from Arangas and n.1 from La Garma A). From a typological point of view, these objects are unretouched flakes.

ID sample-n. 22360 (ID*¹ sample-n.471a): unretouched flake of 14 x 25 x 5 mm and with a weight of 2,53 gr on hematite (10R 4/8 red) from La Garma A, S.U. J2c (19,230±239 cal BP), Lower Magdalenian.

ID sample-n. 31260 (ID* sample-n. 79a): unretouched flake of 33,81 x 15,86 x 10,47 mm with a weight of 9,99 gr on hematite (10R 4/6 red) from Arangas, S.U. 5C (14,806 ± 329 cal BP), Upper Magdalenian.

ID sample-n. 34180 (ID* sample-n.72): unretouched flake of 26,21 x 15,69 x 6,22 mm and with a weight of 3,09 gr on hematite (10R 4/4 weak red) from Arangas, S.U. 5B (12,137 ± 269 cal BP), Azilian.

The presence of *debitage* (unretouched flakes) products confirms the working of raw blocks by direct percussion. The absence of diagnostic traces like pressure waves or ripples, hackles, traces of preparation, impact points is related to the type of raw material. Usually, *debitage* signs appear visible in the hard rocks with well-defined fractures (Inizan *et al.*, 1999), whereas they are labile in the ferruginous rocks (Dayet, 2013). This aspect is confirmed evaluating the hardness in Moss scale: lithic hard rocks usually processed as quartz and flint have a hardness of 7, while hematite has a hardness between 5.5-6.5.

¹ * ID number of pieces in the database realized for this thesis.

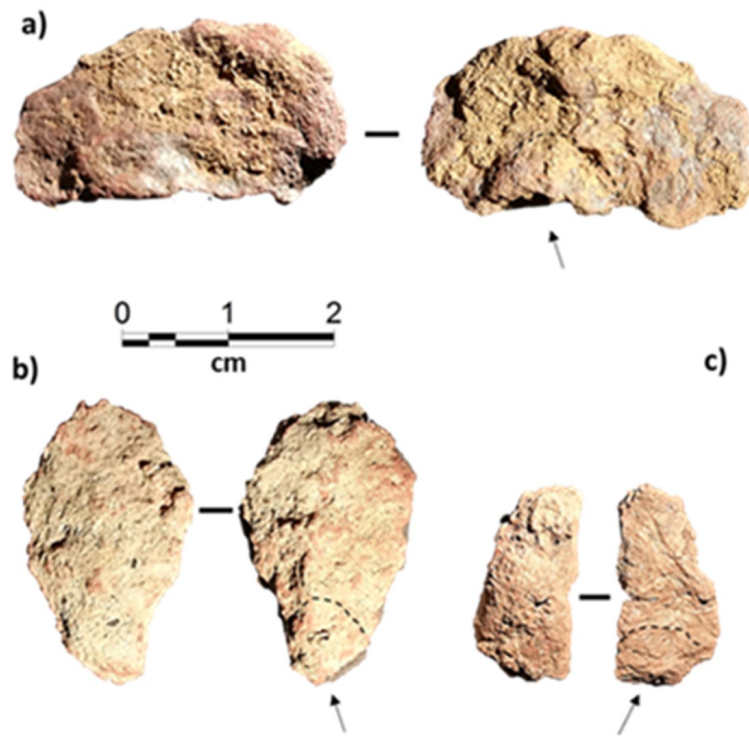


Fig.VII.3.: Unretouched ochre flakes: a) n. 22360 (La Garma A); b) n. 34180 and c) n.31260 (Arangas).

Use-wear traces

Use wear traces are observed on approximately 7% of the pieces on the total of Upper Palaeolithic elements examined for this study (tot. 1,440 elements). There are no traces on the materials from Grotta di Pozzo. This absence could be related to both sampling strategies (partial water sieving) and to the degree of hardness of raw materials, rather low. In the pieces with visible use-wear traces, it is possible to recognize a set of diagnostic traces like striations, metallic lusters, polishing, chipping (Fig.VII.4). As demonstrated from the experiments (Hodgskiss, 2010), these traces are diagnostic of mechanical activities which attest the processing of ochre for *grinding* and *scoring*. Furthermore, some of these traces attest the activity of *rubbing* as can be seen in figure VII.5.

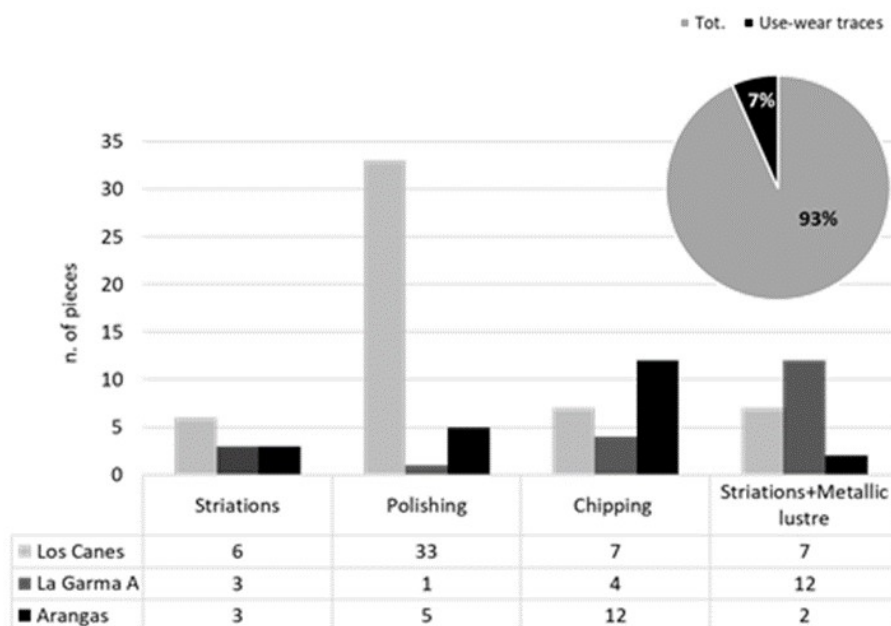


Fig.VII.4.: Number of red ochre pieces with use-wear traces from Los Canes, La Garma A, Arangas: Upper Palaeolithic.

Grinding: a total of 8 pieces have traces which are exclusive to this activity. For Los Canes and Arangas, the diagnostic traces consist of wide parallel and perpendicular striae on the surfaces with a U-shaped profile. The striae are unidirectional and thus demonstrates movements carried out in the same direction. The pieces of La Garma A reveal several striae near to each other parallel with a V section. The trend is multidirectional with overlapping oblique striae with perpendicular striae demonstrating a change of the movements carried out to grind the piece (Fig.VII.6).

Scoring: the traces of this activity appear on a total of 9 pieces. The traces are superficial and grouped with internal micro-striae. According to what was obtained by experiments (Hodgskiss, 2010), these striae are comparable to the ones created with organic materials (wood, bone). Only two pieces in La Garma A show single linear engravings with a precise and net trend related

to a controlled movement. The striae have a U profile. There are no internal or external micro-striae (Fig.VII.7).

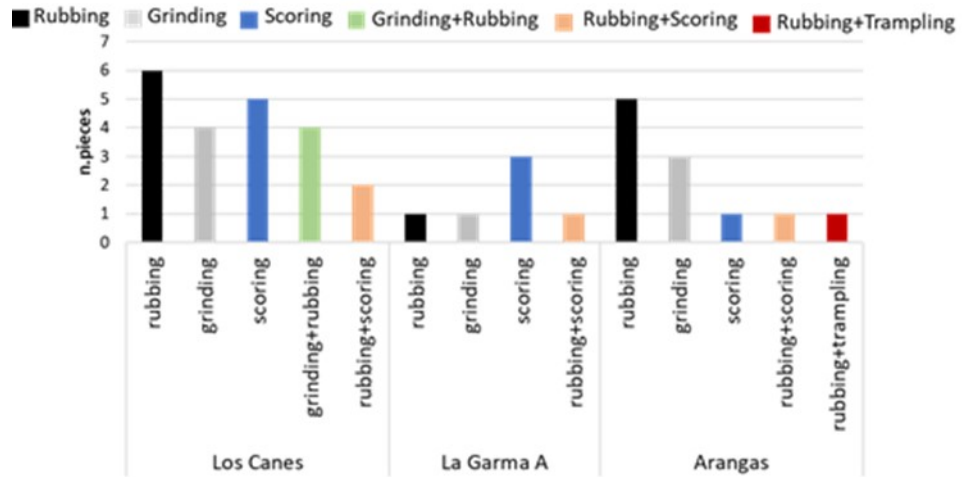


Fig.VII.5.: Frequency of red ochre pieces with diagnostic traces of each activities as referred by experiments (Hodgskiss, 2010): Upper Palaeolithic.

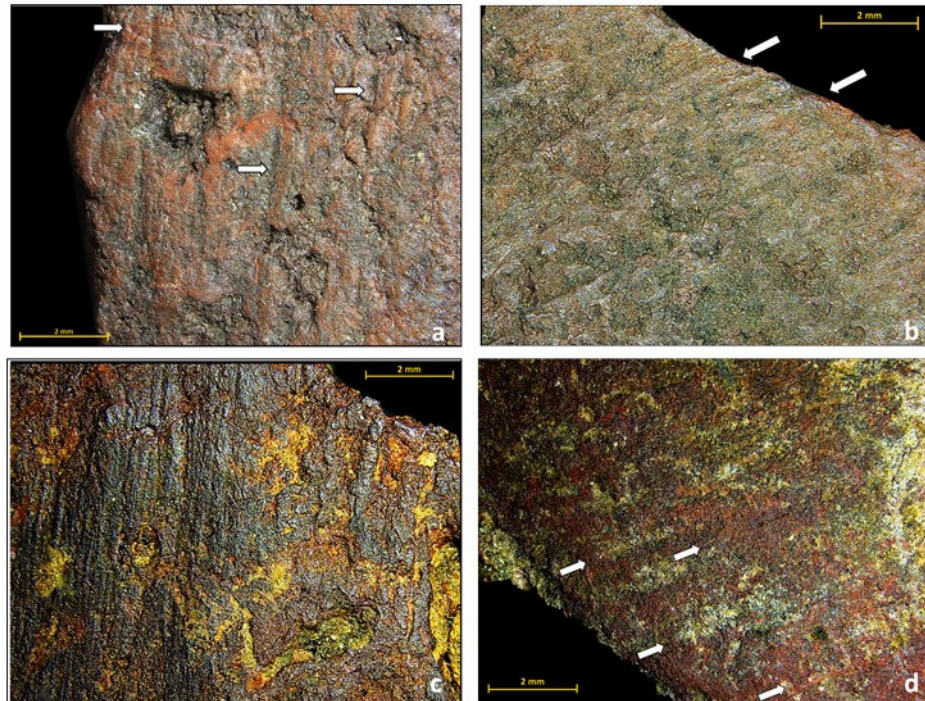


Fig.VII.6.: Use wear traces of grinding on Upper Palaeolithic pieces from a-b) Los Canes; c) La Garma A; d) Arangas.

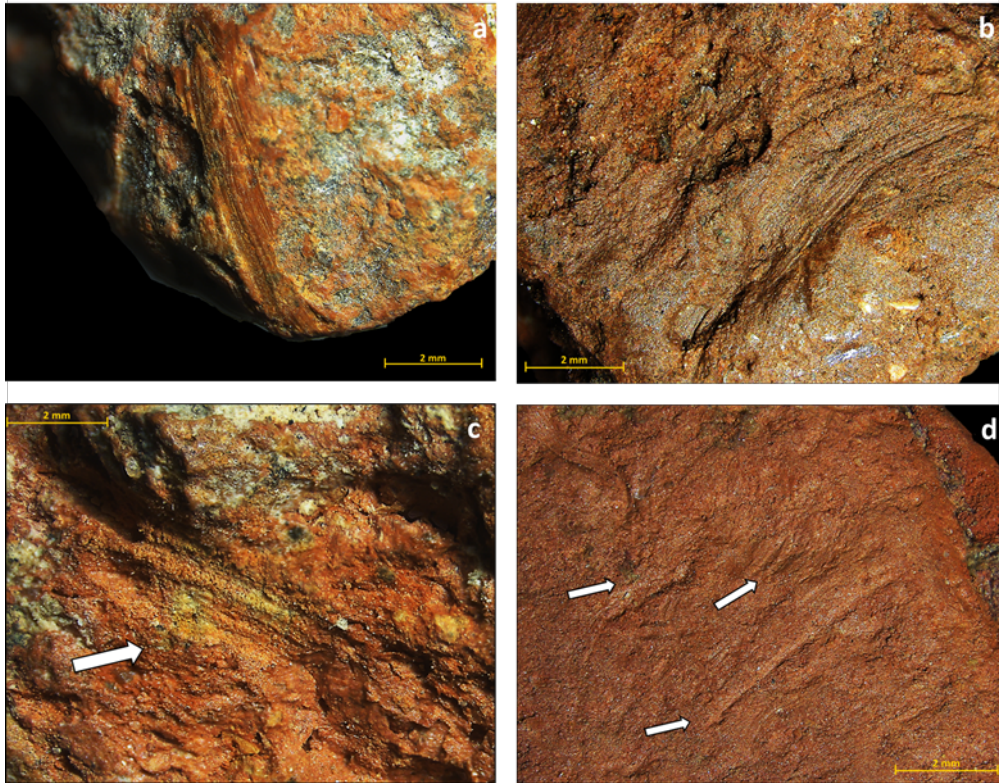


Fig.VII.7.: Use wear traces of scoring on Upper Palaeolithic pieces from a-b) Los Canes; c) Arangas; d) La Garma A.

Rubbing: a total of 12 pieces show traces of this activity. The main indicators are polishing on smoothed surfaces in some cases combined with slight micro-striations. Every piece has flattened surfaces in the area with diagnostic traces. In some cases, also are observed round edges (n.2-Los Canes; n.1-Arangas).

Combined grinding and rubbing: the combined traces of these two activities characterize the surfaces of 4 pieces from Los Canes. The unidirectional parallel striae are partially affected by metallic lustrations which overlap them.

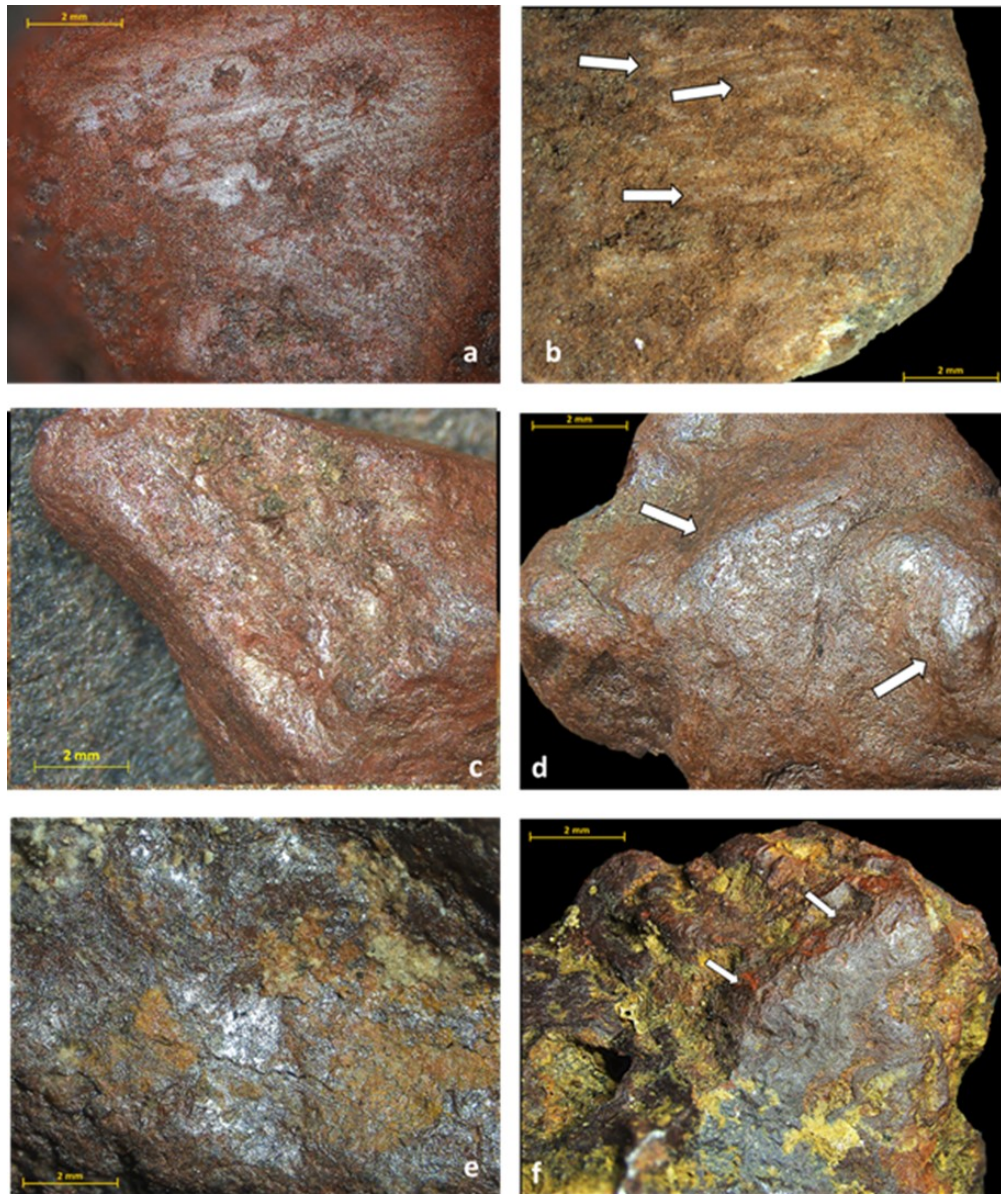


Fig.VII.8.: Use wear traces of rubbing on Upper Palaeolithic pieces from a-d) Los Canes; e) Arangas; f) La Garma A.

Combined scoring and rubbing: in some pieces, polishing and smoothed areas associated to *rubbing* are marked by single groups of well-defined and not too long striae which are located only in some areas of the surfaces. These signs are comparable to those produced for *scoring* experimentally (Hodgskiss, 2010).

Combined rubbing and trampling: in this case, it is possible to observe an overlapping of scuffmarks produced by post depositional trampling on a previously rubbed piece rather than a combination of traces.

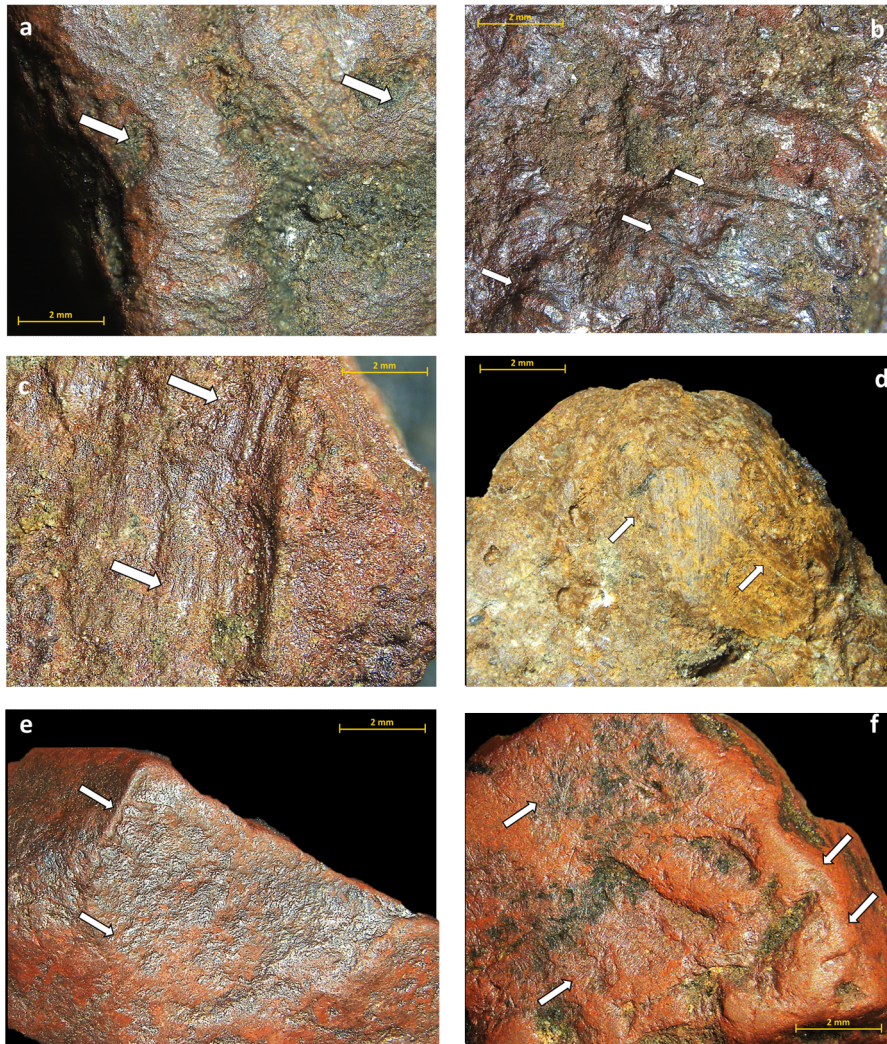


Fig.VII.9.: Combined use wear: a-c) grinding and rubbing (Los Canes); d) rubbing and scoring (Los Canes); e) rubbing and trampling from e) Arangas and f) La Garma A.

Crayons and abrasion facets

Crayons-like shaped pieces were found in Los Canes. A total of 3 objects come from the Palaeolithic units of the site. Morphologically, they are distinguished by two main types: triangular prism and rectangular. A set of use traces were observed on the surfaces.

ID sample-n. 4600 (ID* sample-n.27b): crayon (9,71 x 7,72 x 4,03 mm with a weight of 0.45 gr) with triangular prism morphology marked by a total of 3 lateral faces. The facets are particularly worn and not too much readable. The edges that characterize the joints at the top of the lateral facets appear round and polished. On one of the side facets, it is possible to see parallel and perpendicular micro-striae at the main axis of the piece. A hinge fracture (Shea, 1988) is visible on the top right part of the piece.

ID sample-n. 5797 (ID* sample-n.22): crayon with a volume enclosed in a rectangular shape (10,1 x 7,41 x 3,93 mm with a weight of 0,4 gr) formed by 4 lateral faces. The faces are largely smooth and homogeneous. Rounded edges with smoothed and polished areas were visible on proximal and distal parts confirming *rubbing* activity. Parallel striae with a V profile and polishing characterize one of the apical edges. The signs are related to the combined traces of *grinding* and *rubbing* (Hodgskiss, 2010). Polishing is also visible on one of the lateral faces.

ID sample-n. 5790 (ID* sample-n.23): crayon with a rectangular shape (22,92 x 16,85 x 5,96 mm with a weight of 2,5 gr). A total of 6 facets characterizes the piece. The surfaces appear powdered and friable which is an aspect that has

conditioned the low conservation of the traces. Use-wear traces of rubbing are also visible on rounded edges with micro-striae and polishing.

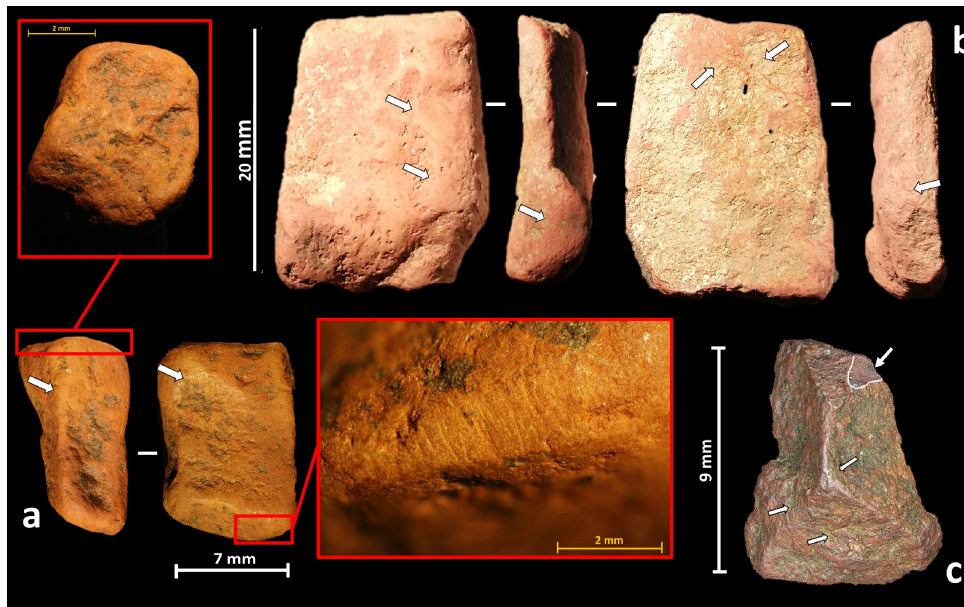


Fig.VII.10.: Crayons from Upper Palaeolithic units of Los Canes: a) n.22; b) n.23a; c) n.27b; d) n.61b.

The regular and well-defined morphologies induce to reflect on an intentional shaping of the supports. The triangular morphology develops within a triangular prism with faces organized in equilibrium in the three-dimensional plane. The wide triangular base would favor the grip of the object that would have been used as a real pencil. The tip, in fact, has a chipping presumably due to use. The rectangular morphology is perfectly engraved in a parallelepiped rectangle determined by right angles due to the joining of the rectangular facets. The recurring morphology in two elements with use-wear traces on the edges attests the intentions of the shape in function to the use of the objects like crayons. This intentional morphology appears evident also by the geometrical symmetry of the rectangular facets which define the parallelepiped.

An object morphologically crayon-like shape (**ID sample-n. 144548; ID* sample-n.61a**): was also found at La Garma A. Unlike the objects found at Los Canes recognizable as crayons *stricto sensu*, this object from Magdalenian layers (S.U. L3) of La Garma A (16,965±322 cal BP), revokes the waste products obtained grinding ochre nodules to have a powder product, experimentally (Wadley, 2005). The object is distinguished by a triangular morphology and a total of 2 abrasion facets – the main one on the ventral facet and the other on the top left. Striations and polishes due to *grinding* are clearly recognizable on the main abrasion facet.

The main striae are parallel and oblique on the main axis of the piece in the direction of the movement carried out to grind the piece. The evident and deep striae reach the rounded edges with polishing. Further groups of parallel striae transversely overlap the main striae and thus attest a change of direction in the *grinding* movement. Two large striae parallel between them obliquely cut the main striae in the central part of the ventral facet crossing almost entirely the entire length.

The second abrasion facet in the left apical position is particularly flat, regular and largely smooth. Labile micro-striae cross the whole facet up to the edges to the large axis of the facet and transversely to the main striae of the ventral facet.

The dorsal facet appears rugged and heterogeneous with rounded edges and polishing which indicates that the piece was probably rubbed on a softer surface compared to the ventral abrasion facet.

This is demonstrated by the net and deep striae that are clearly readable for the hardness of the raw material.

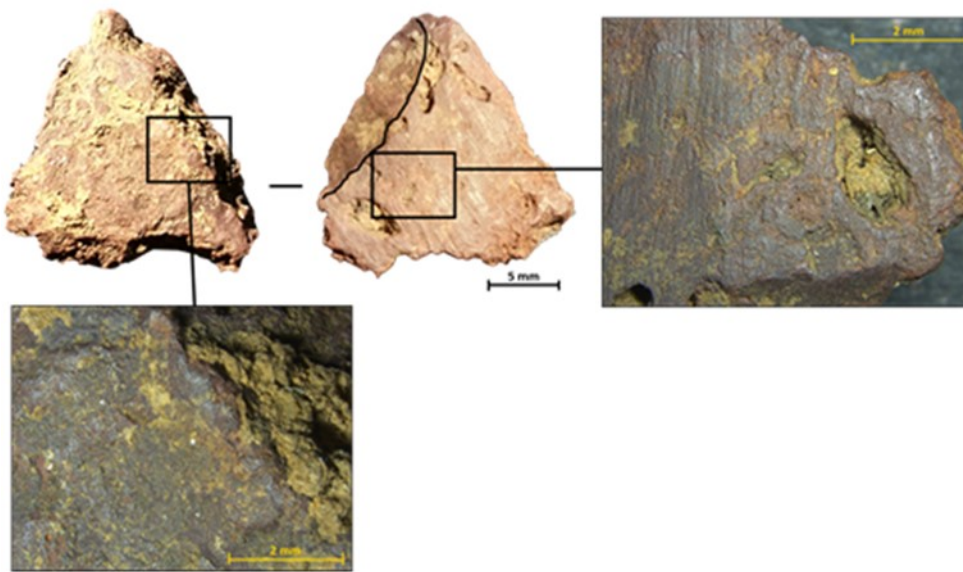


Fig.VII.11.: Faceted piece from La Garma A: n.61a (18,94 mm x 17,77 mm x 6,95 mm; weight 2,5 gr).

VII.1.1.2. Mesolithic

Dimension and morphology

A majority of small sized elements are also registered in the Mesolithic levels. The reference graph (Fig. VII) in which $X=L(\text{max})$ and $Y=W(\text{max})$, attests that all the pieces fall perfectly within the range of *crushing* (min.1,95 mm; max. 41,13 mm) enclosed by the same confidence ellipse (interval at 95%) which confirms the dimensional affinity (Fig. VII.12).

From a morphological point of view, even the elements from the Mesolithic levels do not show regular and repeated shapes. A non-normal distribution of the three dimensions (length, width, thickness) confirms the absence of standardized forms (Fig.VII.13).

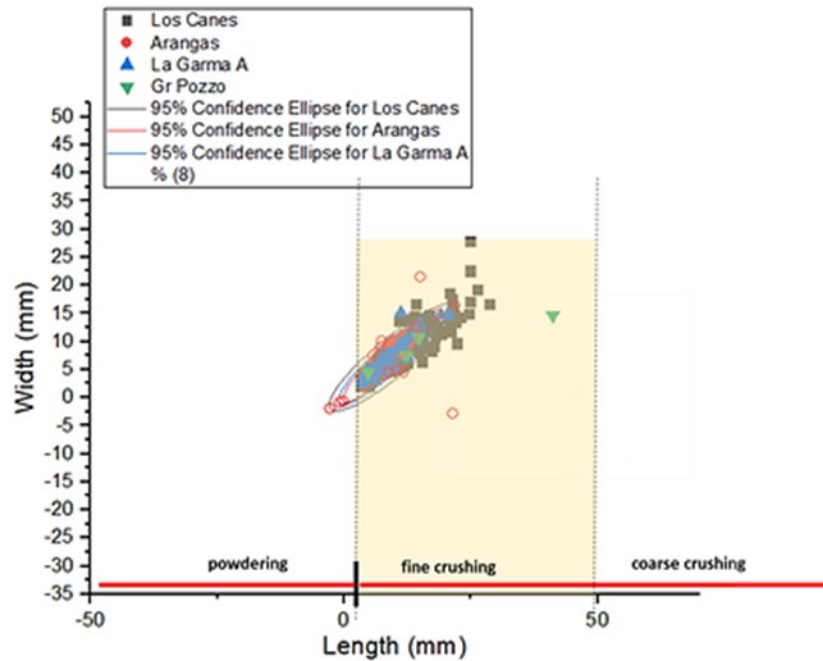


Fig.VII.12.: Dimensional distribution of red ochre from Mesolithic layers by the range of 2-50 mm fixed on the experiments conducted to test the hypothesis of mechanical transformation of ferruginous raw materials (Salomon, 2009).

Debitage

Regarding *debitage* products, there are no elements in the Mesolithic layers. Data is non-marginal when discussing the evolutionary tendencies of the technological size of the human groups.

The absence of *debitage* products suggest the lack of one of the initial phases of the operating sequences of ochre in Mesolithic.

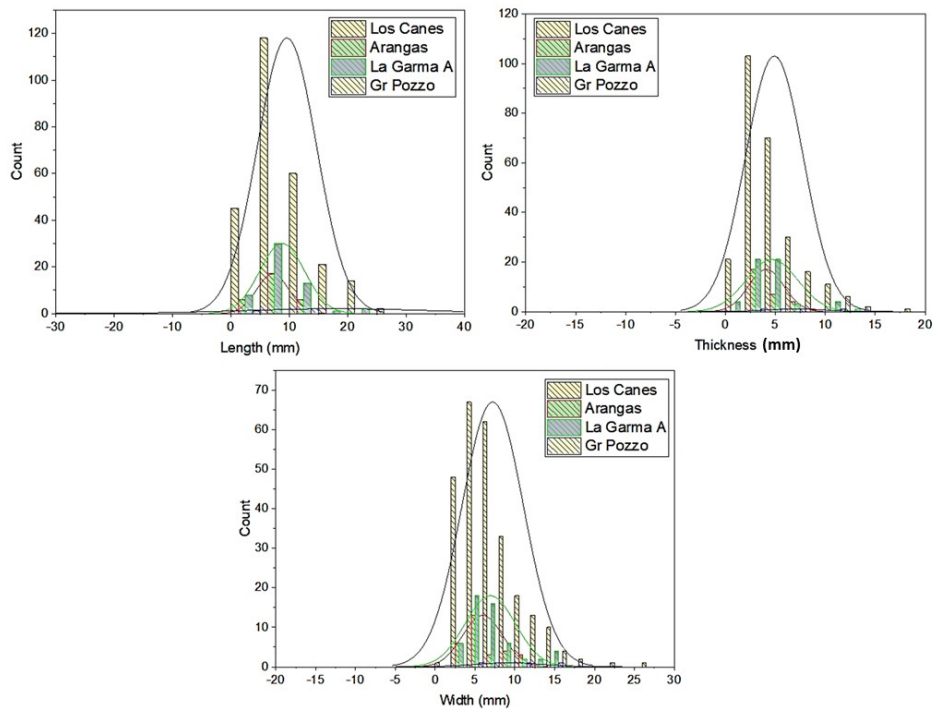


Fig.VII.13.: Non-normal distribution of morphological values (Length, Width, Thickness): red ochres Mesolithic.

Use-wear traces

Diagnostic traces were also observed on about 2% (n.17) of the total Mesolithic materials from the collections of Los Canes, La Garma A and Arangas (total n.805). As shown in the graph (Fig. VII.14) most of these elements come from the site of Los Canes. Even in this case, it is possible to confirm the absence of use-wear traces on ochres from Grotta di Pozzo.

The percentage of elements with use-wear traces is extremely reduced but, in any case, even if the scarcity, these objects give important information on the stages of operative sequences.

Diagnostic traces like striations, polishing, chipping, also in combination amongst themselves are important to recognize mechanical activities of

grinding, scoring, rubbing as demonstrated by the experiment (Hodgskiss, 2010).

From the graph (Fig.VII.15), it is evident that most elements with use-wear traces come from Mesolithic units of Los Canes. An element with polishing was found at La Garma A. Furthermore, an element with striations and metallic lustres from Arangas.

Grinding: a total of 11 pieces from Los Canes and 1 piece from Arangas shows parallel and perpendicular striae at the surfaces with a unidirectional trend recording this activity.

Rubbing: the indicators of this activity like polishing on a smoothed surface and micro-striae are observed on a total of 12 objects in which 11 from Los Cane and 1 from La Garma A.

Scoring: there are no traces of this activity for the Mesolithic levels.

Combined grinding and rubbing: traces of rubbing are observed on 2 previously grinded elements from Los Canes on a hard-abrasive surface due to the depth and definition of the striae.

At this point, it is worth making a distinction of the pieces of Los Canes with traces which come from S.U. 5 and those from the units of human burials to explore a relation between processing activities of ochre and funerary practices. For unit 5, *grinding* is well attested (n.4 pieces) followed by a piece with *scoring* traces and another one with *rubbing*. It is possible to recognize a combination of *grinding+rubbing* traces on a total of 2 pieces. In regards unit 6, traces which

attest the activities of *grinding* and *rubbing* appear on pieces that come from the fills of Mesolithic structures.

It is interesting to notice that 7 elements from S.U. 6III returned *rubbing* traces produced by the transfer of colour on a soft surface. The elements are followed by traces of *grinding* (n.3). *Rubbing* and *grinding* are documented also in burials 6II and 6I. In S.U. 6II, a total of 4 elements show traces of *grinding* and one of *rubbing*. In S.U. 6I two elements were grinded on an abrasion surface and 1 element was rubbed on a soft surface.

For unit 6A, there is a piece with traces of *grinding* and one with *rubbing*.

Unit 6B returned only one piece with evident parallel striae which attest *grinding* on abrasion surfaces.

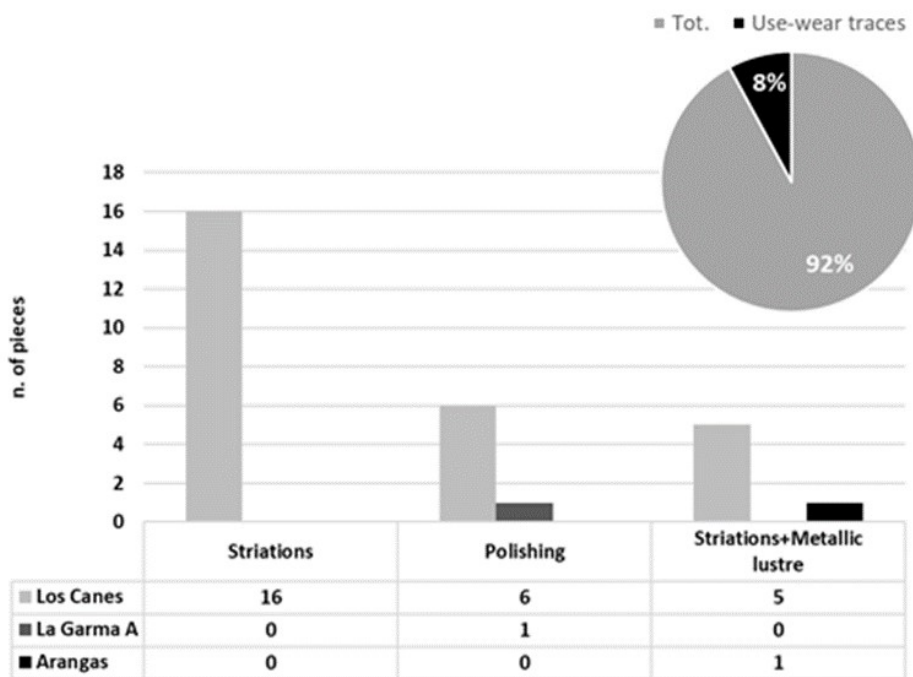


Fig.VII.14.: Number of red ochre pieces with use-wear traces from Los Canes, La Garma A, Arangas: Mesolithic.

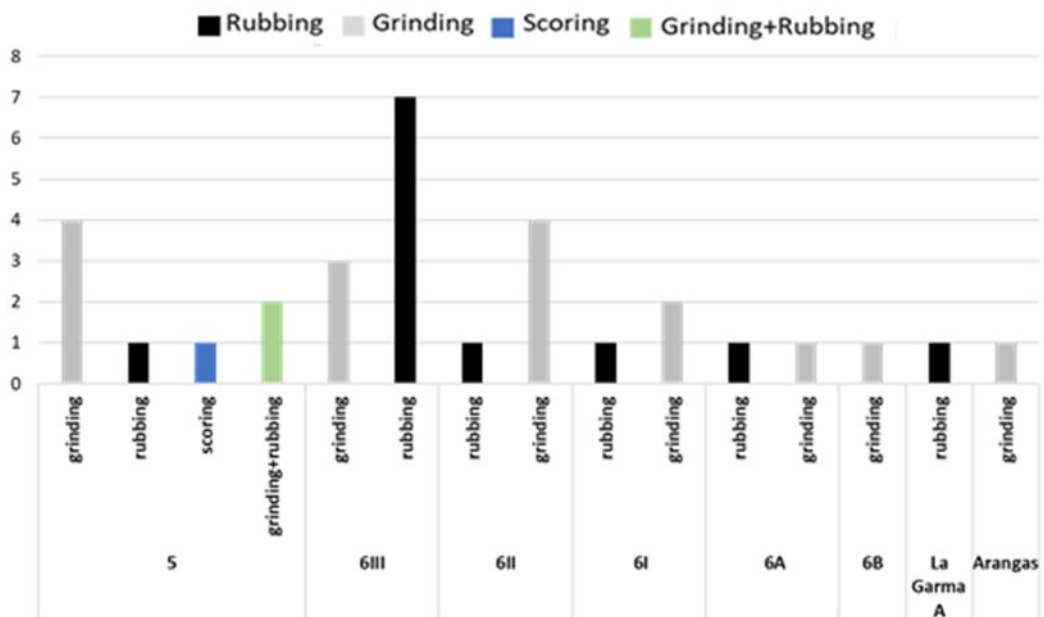


Fig.VII.15.: Frequency of red ochre pieces with diagnostic traces of each activities as referred by experiments (Hodgskiss, 2010): Mesolithic.

Crayons and abrasion facets

The category of crayons and faceted pieces appears numerically lower than the Mesolithic levels. Well defined morphologies from rather regular geometries exclusively characterize some pieces from Los Canes. Furthermore, a faceted nodule was found at Arangas.

A total of 4 crayons were found in the Holocene units:

ID sample-n. 5867 (ID* sample-n.61b): crayon with a conical morphology (8,97 x 7,86 x 7,92 mm and with a weight of 0,72gr). The volume is marked by a circular base and an apical part with a blunt and rounded tip. Micro-striae and polishing both on the top and the side portion attesting the use. The conical morphology is associated to a naturally rounded object in that no abrasion is observed on the surfaces of the objects which could be characterized by

intentional shaping. The flattening characterizes the apical portion which is clearly related to the use of the objects like crayons. The circular base attests an adaptation of natural holes to anthropic needs.

ID sample-n.11309 (ID* sample-n.121a): crayon in a rectangular shape (17,33 x 9,18 x 6,72, peso di 2,5 gr). The volume appears marked by (6) lateral facets which are not equal amongst them but, with parallel side edges up to the maximum height and perpendicular to the bases. The facets are flattened with parallel and oblique striae at the major axis of the facet itself resulting in the adaptation of the form in function to the natural morphology. By following the longest profile, it is possible to observe a lateral curve that is adapted to a set of small rounded protuberances due to the natural aggregation state of the mineral. The element comes from the unit 5.

ID sample-n. 10373 (ID* sample-n.214): this element classified as crayons consists of a grinded block on a hard surface due to the presence of deep parallel striae used also like a crayon. The object (15,47 x 8,74 x 7,96 with a weight of 1,4 gr) was collected from the bottom of burial 6III in unit 6IIIA, near the skeletal remains (chap.III-Fig.III.5). The morphology appears regular and geometrically inscribable in a prism with a pseudo-triangular section. A total of 3 facets form the volume of the piece obtained through *debitage* as the negative detachments attested on one of the non-abrasive flat facets. The other facets have unidirectional and transversal parallel striae at the major axis. In one case, the main striae were cut transversely by single deep engravings with a U section. About the edges, there are not striations on the facets. Traces associated to rubbing were observed on the rounded edges with polishing and slightly parallel, unidirectional and oblique micro-striae at the edge itself.

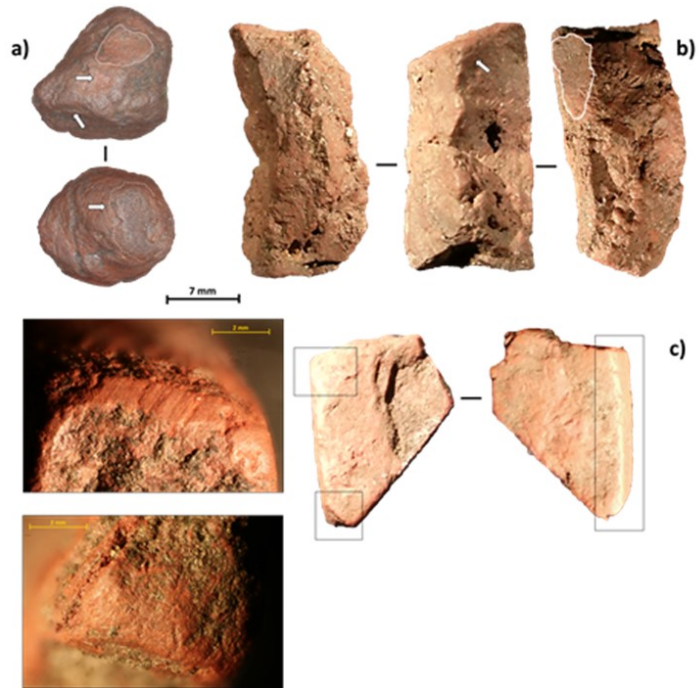


Fig.VII.16.: Mesolithic red ochre crayons from Los Canes: a) 61b; b) 121a; c) 241a.

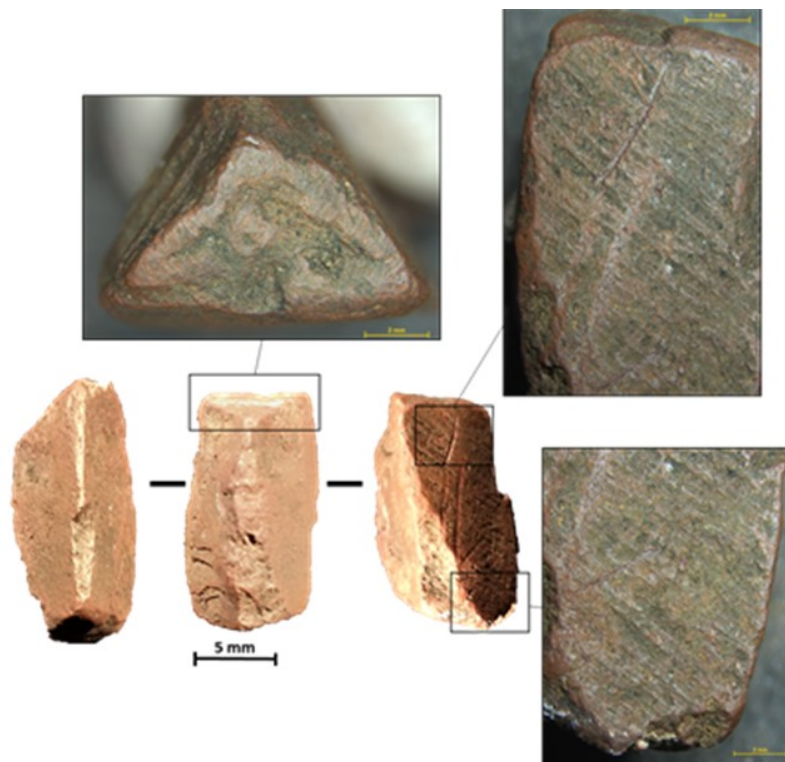


Fig.VII.17.: Mesolithic red ochre crayon from Los Canes (S.U.6IIIA): n.214.

ID sample-n. 10661 (ID* sample-n.241a): crayon with triangular morphology (16,12 x 7,24 x 3,15 mm, weight 0,42 gr). Even this is associated to the burial 6III (chap.III-Fig.III.5). This crayon has two main flat facets joined by a long narrow flat facet which creates thickness in the element. One of the two facets have a detachment which occupies half of the top right of the facet. Striae of *grinding* are absent on both facets. It is possible to observe irregular and deep signs attributable to trampling. The third flat, narrow and long facet that makes up the large edge of the piece has light and unidirectional parallel micro-striae and polishing. Traces that are associated to *rubbing* are localized towards the external portions while the central area appears heterogeneous and is characterized by a rough and irregular surface.

A nodule (25 mm x 17 mm x 15 mm) with abrasion facets (**ID sample-n. 144548; ID* sample-n.84a**) was also found in the Azilian levels of Arangas (S.U.5B-12,137±269 cal BP). The object has a globular morphology affected by the abrasion facets which use the nodule throughout its volume. This “opportunistic” use of the piece is directly proportional to the intensity of the exploitation. Nevertheless, the friability of the surfaces and the hardness of raw material (soft) does not allow to have a perfect reading of the use traces. The surfaces used are flattened and brightened by a more intense red colour. The initial morphology of the nodule appears to be different from the flattening of the used surfaces by abrasion that is confirmed by the presence of parallel and oblique micro-striae at the top of the piece on one of the facets. On the rounded edges, it is possible to see polishing regardless of the intense opacity of the raw material.

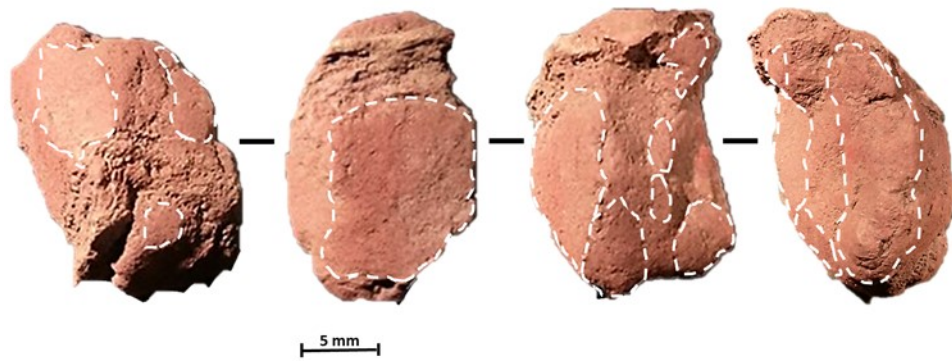


Fig.VII.18.: Ochre nodule with abrasions from Arangas-n.84a.

VII.2. Ochre processing from domestic contexts

In domestic contexts such as La Garma A, Arangas and Grotta di Pozzo, the *debitage* and *crushing* characterize an initial moment of ochre transformation. The archaeological evidence suggests a direct percussion by a hard object by oblique (*debitage*) and perpendicular (*crushing*) movements.

The abundance of fragments with dimensions $>1,5$ mm suggest a further fragmentation by *fine crushing*. As demonstrated by the experiments (Salomon, 2009), increasing the frequency of the impact and decreasing the amplitude of the launched percussion produces smaller fragments compared to those produced for *coarse crushing* with dimensions around 1,5 mm. Similar vestiges come from both the Palaeolithic and Mesolithic units of La Garma A, Arangas and Grotta di Pozzo.

In any case, fine fractions of ochre could be obtained by *grinding* or *scoring* ochre pieces. A set of traces which identify these activities were observed on some pieces from the Upper Palaeolithic of La Garma A and Arangas.

The transformation of ochre pieces by *scoring* appears to be the one most documented in La Garma A, followed by *grinding*. On the other hand, at Arangas, the percentages of the pieces with *grinding* traces overtake the *scoring* ones. So, the production of powder for *fine crushing*, as well as *grinding* and *scoring* appear to be a well-documented practice in the Upper Palaeolithic in La Garma A, Arangas and Grotta di Pozzo. The *fine crushing* continued in the Mesolithic while only evidence of *grinding* was found at Arangas.

As far as ochre processing is concerned, the interpretation of some traces suggests an additional activity from fragmentation or pulverization. This activity in a final moment of the operative sequence is associated not so much to an ochre processing *stricto sensu*, as to a use for colour transfer on a soft surface (human or animal skin). *Rubbing* was attested during Upper Palaeolithic in La Garma A and Arangas, and during Mesolithic also in La Garma A. Furthermore, *rubbing* in combination with *scoring* was documented in La Garma A.

The experiments (Hodgskiss, 2010) explain the combination of the traces as the consequence of a use of the same piece of ochre for both activities. The difficulty in registering the *rubbing* traces depends on the hardness of the material. In some cases, if the ochre is extremely hard, it would not transfer colour on the surface that is rubbed and consequently does not produce traces (polishing and micro-striae) on the piece. Traces of *rubbing* are easily readable on the ochre pieces used for previous activities as attested for La Garma A where signs of *scoring* are combined to traces of *rubbing*.

VII.3. Ochre processing from funerary contexts

The issue of ochre processing in Los Canes appears rather complex if analysed in function to the context type. By considering the fact that the cave begins to be used as a location for human burials during Mesolithic, in the Upper Palaeolithic, it does not appear to be correct to talk about funerary contexts. The human occupation of cave is attested right from the Solutrean and continued during the whole Upper Palaeolithic. By organizing the data, the *coarse crushing* followed by *fine crushing* appear to be well documented in the Upper Palaeolithic. Pulverization follows the fragmentation phase. The *grinding* of ochre has archaeological evidence for both the presence of traces of this activity on Palaeolithic materials and for the presence of ochre powder about 1-2 mm thick in the soil between S.U. 3A and S.U. 3B (chap. IV). The production of powder in the Upper Palaeolithic occurred by *grinding* ochre pieces on an abrasion surface and *scoring* with a cutting object as demonstrated by the traces. The cataloging of the traces and their comparison with experimental tests allow to also recognize the activity of *rubbing* ochre pieces on soft surfaces (Hodgskiss, 2010).

The combination of traces on some pieces from the Palaeolithic units assumes the combined exploitation of ochre pieces which were previously treated (*grinding/scoring*) and then rubbed on soft surfaces.

As far as Mesolithic is concerned, the unit 5 returned evidences of *coarse crushing* and *fine crushing*. In addition, the comparison of traces with experimental references presumes the pulverization of ochre by *grinding* and *scoring*. *Rubbing* is configured as a proxy of use on soft surfaces in this cultural period too.

It is certainly interesting to carry out an evaluation of the data available for funerary structures for Mesolithic. An abundance of pieces with *rubbing* traces were registered in unit 6III. At this point, the association between *rubbing* traces and the use on soft surfaces (human skin) may suggest a practice of bodies manipulation. Nevertheless, by keeping in mind the taphonomic issues previously analysed, it is worth supplying data in relation to the three stratigraphic units that were further recognized in the excavation of the structures. From the unit 6IIIA, there is only one element with diagnostic traces of *grinding*. The elements attesting *rubbing* come from units 6IIIB and 6IIIC which are presumably formed by the redistribution of Palaeolithic materials and therefore without a clear Holocenic attribution. However, the presence of Mesolithic industries (Arias, 2002) evidence that not all fragments with traces of *rubbing* come from the rearrangements of the Pleistocene sediments. For the other structures (6II, 6I, 6A, 6B) where the excavation has not affected the Palaeolithic levels as for the structure 6III, *grinding* and *rubbing* are the most documented activities with more incidences of *grinding* for burials 6II and 6I. Nevertheless, evidence of *rubbing* comes from these structures.

VII.4. Ochre processing tools

A series of objects used to work ochre was found at Arangas. A total of 6 pebbles and an abrasion tablet with use wear traces and pigment residues were collected from the S.U. 3 referable to an initial moment of the Mesolithic (9,051-9,322 cal BP).

Although these ochre processing tools come from a stratigraphic unit from which apparently no pieces of ochre were collected, they deserve to be reported

as they provide essential data for ochre processing. The objects are described below:

ID sample-n. 944 (ID* sample-n.120): retoucher-percussor on a limestone pebble that is 7,9 cm long, 6,5 cm wide and 4,5 cm thick and has a weight of about 3,20 kg. The spheroidal shaped pebble has use wear traces that overlap the red pigment which brings about its removal near the edges and in some points of the two convex and symmetric faces. A thin blackish patina covers the ochre (Fig.VII.20).

ID sample-n. 2169 (ID* sample-n.121): retoucher-percussor on a spheroidal limestone pebble with traces of ochre visible on both convex and symmetrical surfaces. A deep red colour almost totally characterizes one of the faces while the other face has a widespread reddish colour. The finding is 6,4 cm long, 7 cm wide and 3,6 cm thick with a total weight of 1,88 kg (Fig.VII.21).

ID sample-n. 8740 (ID* sample-n.122): retoucher-percussor on an ovoid limestone pebble with diffused residues of red ochre. The pebble (9 cm x 6,3 cm x 3,7 cm, weight approx. 3,19 Kg) reports use wear traces affecting the pigment in some points on the two ends and in the middle part of the two faces, symmetrically opposed (Fig.VII.22).

ID sample-n. 713 (ID* sample-n.123): retoucher-percussor on a semi-circular limestone pebble with a clear basal fracture (8 cm x 4,6 cm x 3,5 cm; 1,48 kg). The ochre uniformly covers both the faces of the finding, up to the area of the fracture. Dark concretions overlap the red ochre residues (Fig.VII.23).

ID sample-n. 8706 (ID* sample-n.124): limestone angular pebble covered by red-purplish pigment. The pebble is 7,2 cm long, 46 cm wide and 4,4 cm thick with a weight of about 2.50 gr (Fig.VII.23).

ID sample-n. 2401 (ID* sample-n.125): Retoucher-percussor on an ovoid limestone pebble (10 cm x 5,2 cm x 25 cm; 2,04 Kg) with irregular reddish pigmentations spread on both faces. Due to post-depositional processes, a thin dark film covers the pigment in some areas (Fig.VII.24).

ID sample-n. 8702 (ID* sample-n.127): Abrasion tablet in quartzite (14 cm x 22 cm x 5 cm) with ochre residues on one of the two surfaces. The red pigmentation almost entirely covers the face of the slab. The surface is affected by striations and streaks stained by a thin layer of ochre (Fig.VII.24).

The XRF analysis of the concretions cleaning the pebbles (n.944, n.2169, n.2401) confirms the presence of Fe. Plotting the major elements usually associated to iron oxides (Al, Fe, Si), a geochemical affinity is clearly visible in all samples. No elements referable to organic compounds were detected.

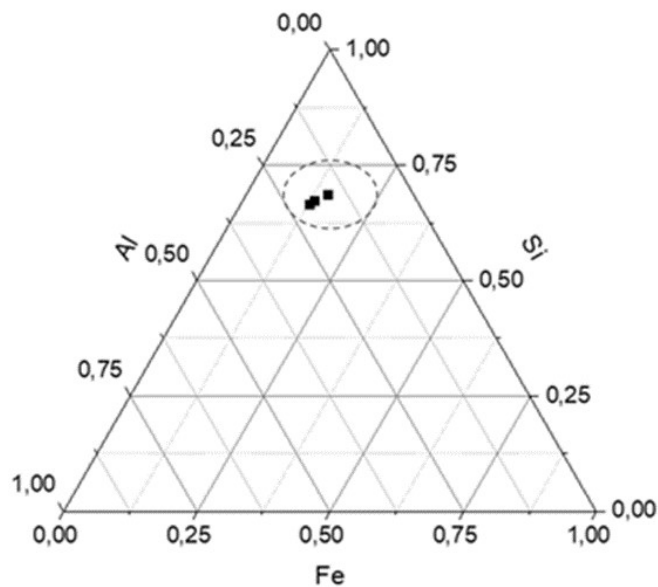


Fig.VII.19.: Ternary plot of major element Al, Si, Fe detected in the superficial concretions removed from the ochre processing tools (n.944, n.2169, n.2401).

The direct observation of objects allows to see that a thin layer of ochre covers most of the surfaces of some pebbles (n.2169; n.8706). The homogeneous covering appears to be in a well-defined portion of the object suggesting contact with a liquid substance.

In other cases (n.944; n.8740; n.2401), the colour appears heterogeneously diffused on the surface. Cups and stakes from the use of pebbles determine the removal of the sediment confirming the contact with the red ochre in a moment before the use as percussor/retoucher. It is presumed a pigmentation by accidental contact with ochre or by manipulation of the objects with hands painted by red pigment.

In the case of the abrasion table, a layer of red ochre covers the active face of the tablet on which unidirectional parallel strings filled with pigment appear clearly visible, attesting the use of the object as passive tool to grind ochre.

The presence of these ochre processing tools supports the identification of ochre transformation techniques. Combining the data obtained from the direct study of ochre pieces with those obtained from the observation of ochre processing tools, it is possible to appreciate the objectives behind the work of colouring raw materials providing a reconstruction of the operating sequences. The use-wear traces attest the use for direct and launched percussion. These data fit well with the *grinding* and *pulverizing* supposed by the study of physical features (dimension, morphology, use-wear traces). These objects are made of quartzite, a lithic raw material available at about 6 km away from the cave (chap.VI; Arias *et al.*, 2014) presuming a human effort to collect and bring to the site, peculiar types of lithic rocks functionally exploited. The presence of pebbles and a tablet with ochre residues in the same unit of the archaeological sequence implies that the transformation of colouring raw materials involved the use of two types of

instruments: one active (pestles) and one passive (tablets) as comparison (Salomon, 2009; Granato, 2011; Dayet, 2012; Altamura *et al.*, 2016; Rosso *et al.*, 2016).

The use of ochre processing tools of the same type of lithic raw material (quartzite) on the same type of colouring raw materials (iron oxide) could suggest a specific relationship between instrument and colorants. The presence of lithic tools in hard rocks such as quartzite would have played a fundamental role in the size of the powder together with the human force exerted in the practical gesture. However, by not having ochre pieces collected from the same unit as these objects, this is a plausible supposition based on the evidence in the other units of the archaeological sequence. In any case, the presence of Fe, as confirmed by the analysis of concretions on objects, and the colour of the residues confirm the processing of ferruginous red rocks which are the most abundant raw materials in the whole sequence of Arangas and which are the same found in Los Canes.

The evidence of the exploitation of a specific variety of ferruginous rocks with these tools reveals the use of quartzite objects to obtain fragments of red ochre which have morphology, dimensions and similar traces in both the contexts of which one domestic (Arangas), the other funerary (Los Canes) further corroborating the correspondence between the two sites already documented by the direct study of the ochre vestiges and provenance researches.

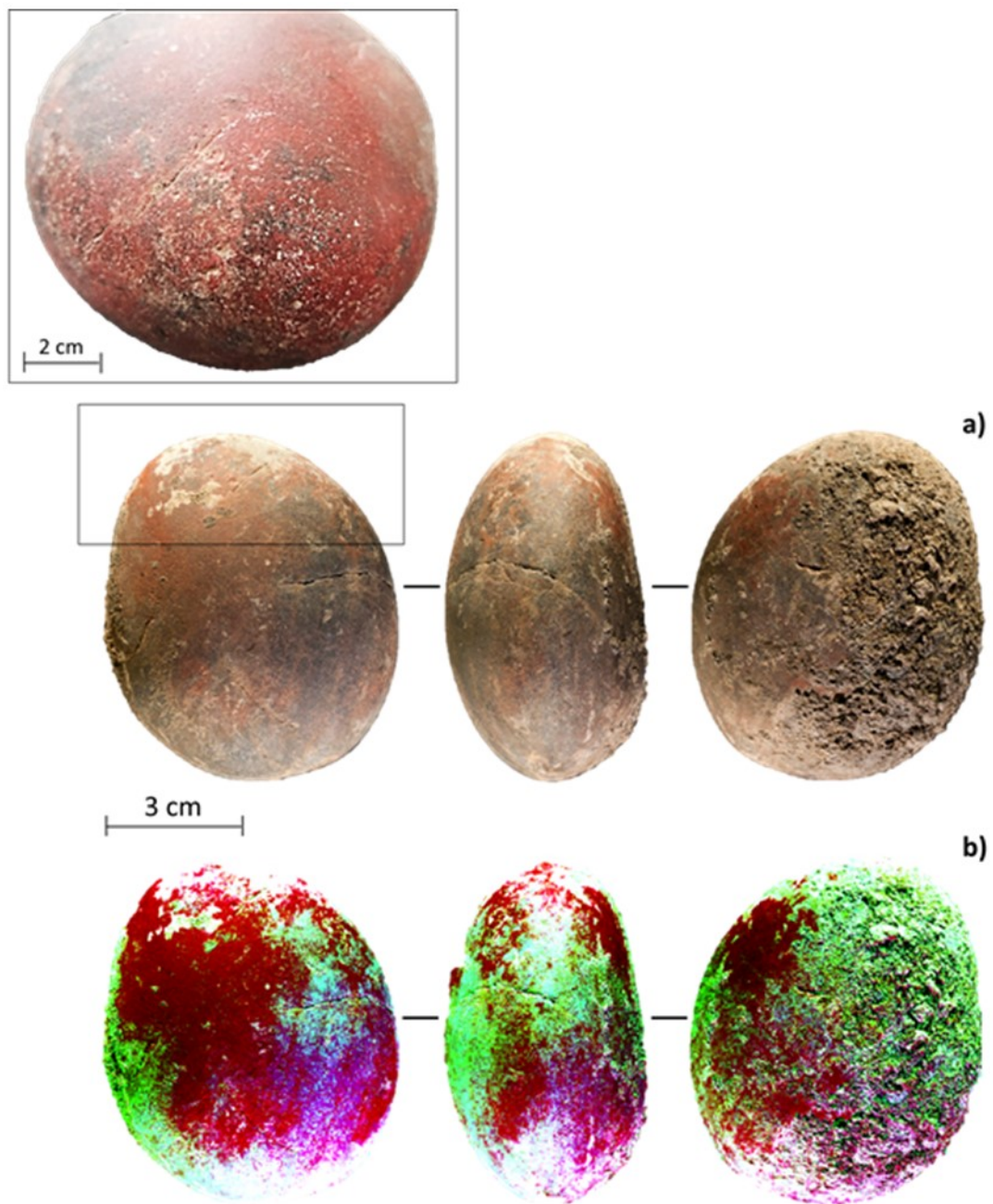


Fig.VII.20.: Ochre processing tool (n.944) from Arangas: a) original image; b) elaborated image by D-stretch to highlight the contrast between the areas covered by red ochre and the diagnostic traces.

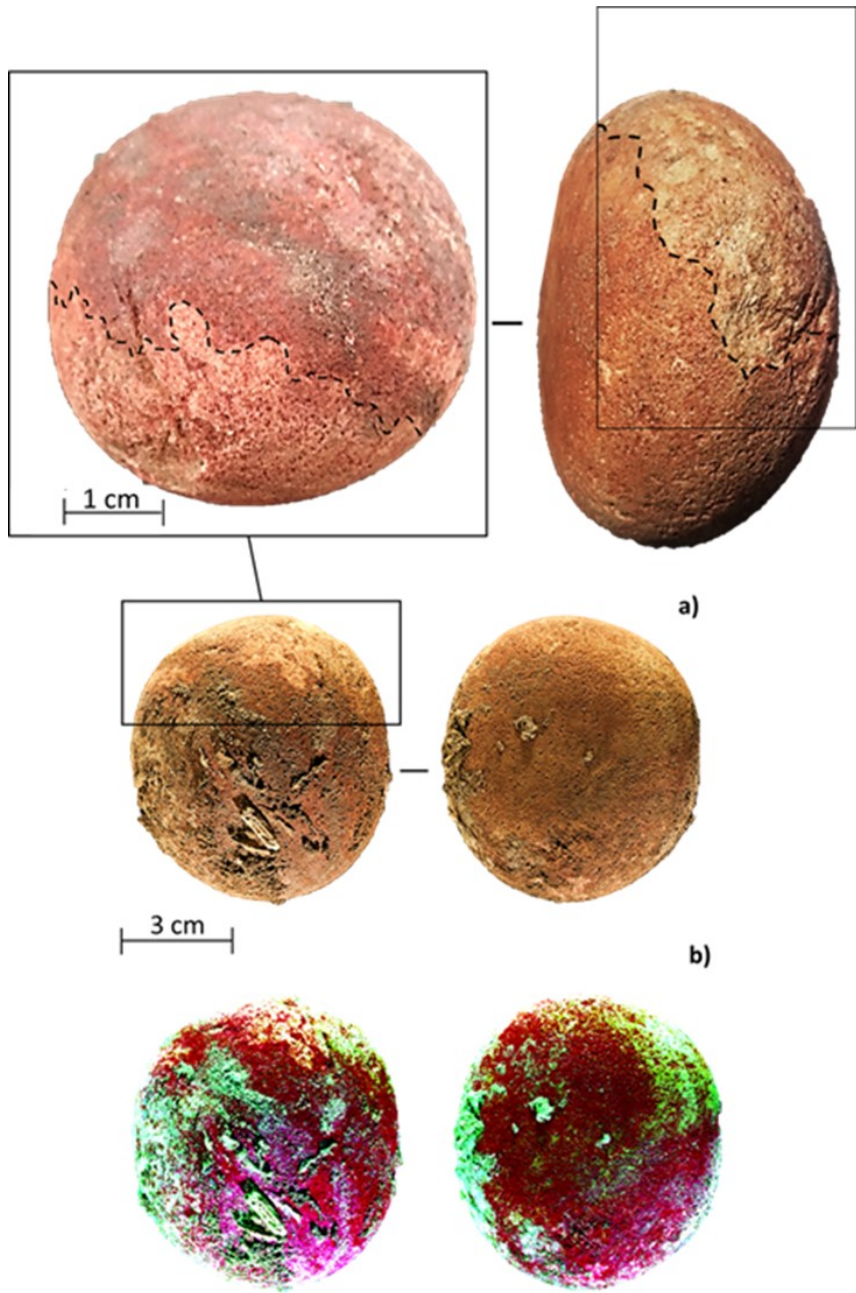


Fig.VII.21.: Ochre processing tool (n.2169) from Arangas: a) original image; b) elaborated image by D-stretch to highlight the contrast between the areas covered by red ochre and the diagnostic traces. In the top-left magnification image, the point of separation between the liquid substance and the lithic surface is evidenced.

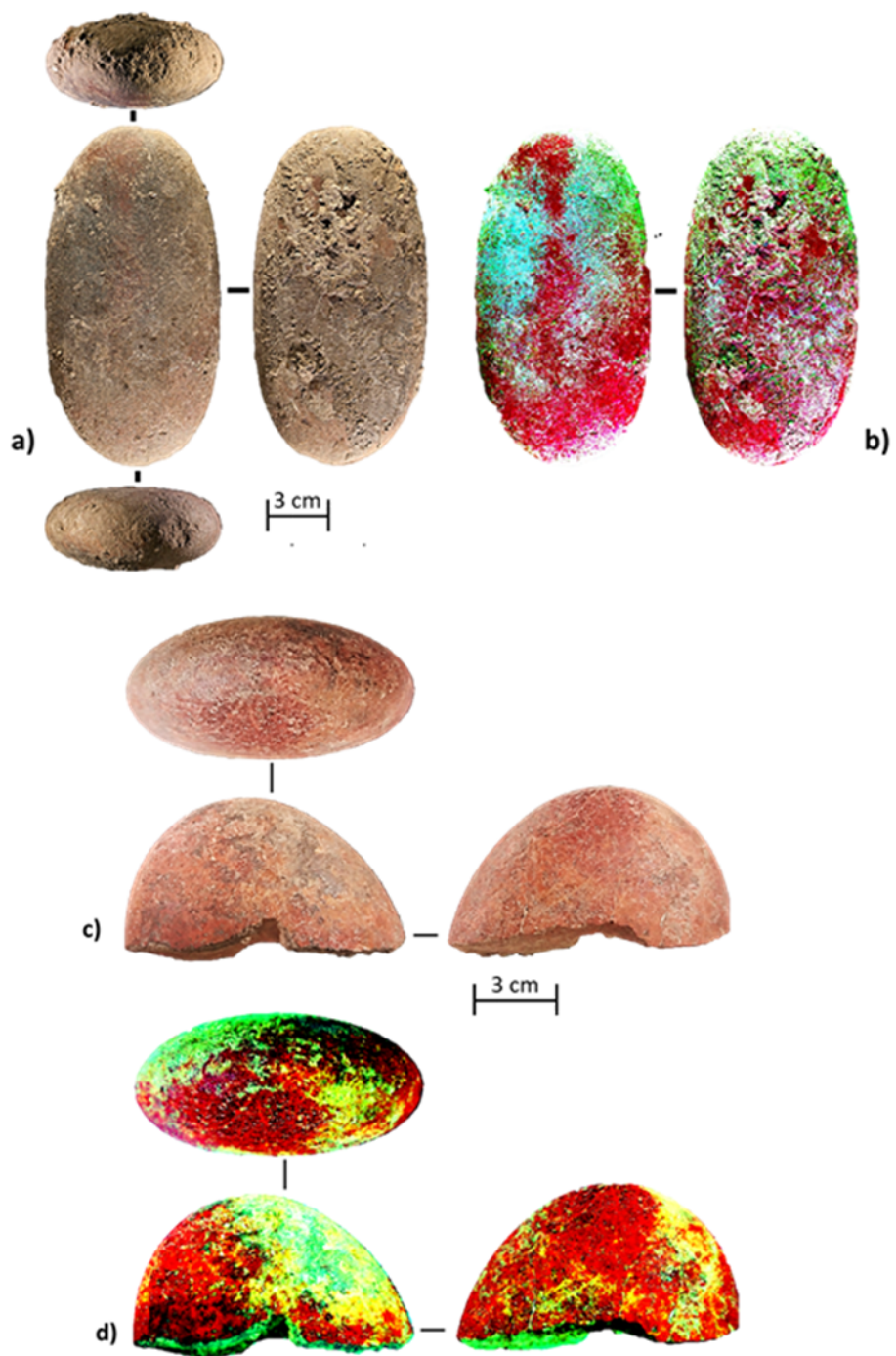


Fig.VII.22.: Ochre processing tools from Arangas: original images a)n.8740, c) n.713; elaborated image by D-stretch to highlight the contrast between the areas covered by red ochre b) n.8740, d) n.713.

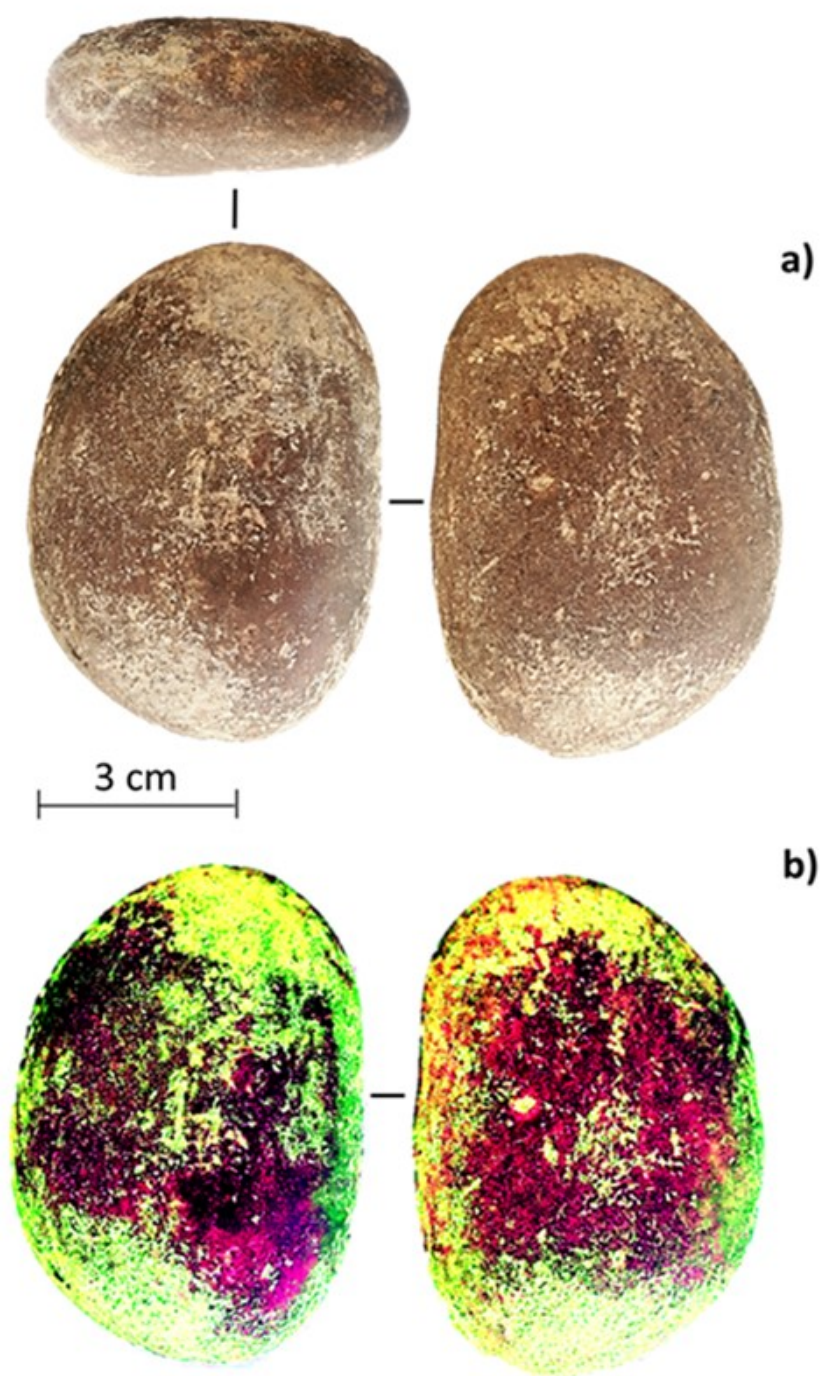


Fig.VII.23.: Ochre processing tool (n.8706) from Arangas: original images a) n.8740; b) elaborated image by D-stretch to highlight the contrast between the areas covered by red ochre.

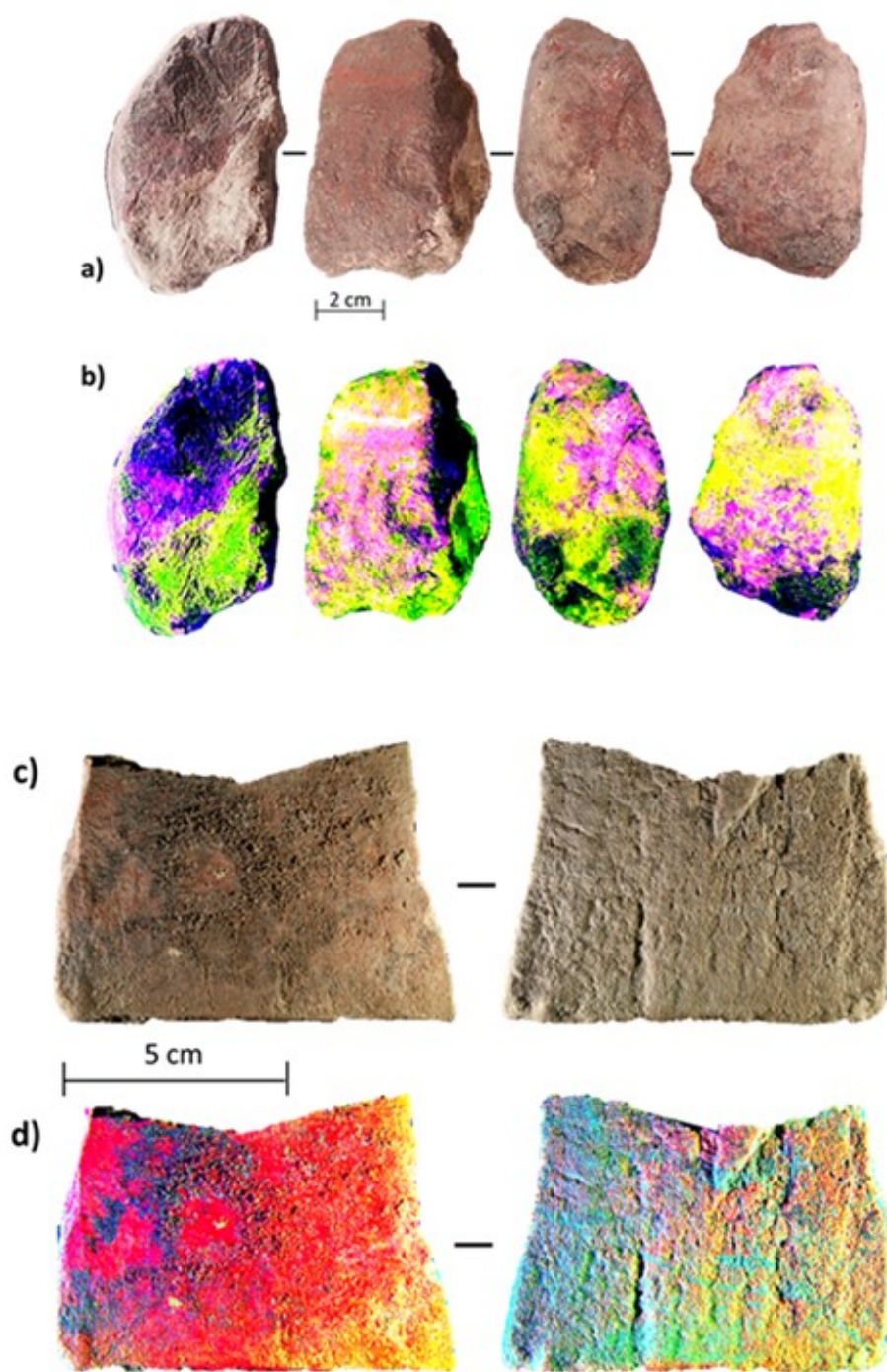


Fig.VII.24.: Original image and elaborated image by D-stretch of a-b) ochre processing tool n.2401 and c-d) an abrasion tablet n.8702.

VII.5. Reconstructing the *chaîne opératoire*

The dimensional and morphological data associated to the cataloguing of the use-wear traces allow to reconstruct ochre processing by mechanical transformations during Upper Palaeolithic and Mesolithic periods. The steps here recognized are oriented towards the production of ochre powder or more coarse fragments for a direct transfer of colour on soft surfaces (*rubbing*). An initial moment in this process is characterized by the shaping of blocks of raw materials by *coarse crushing* or *debitage*. Following these phases, the products obtained could be further fragmented by *fine crushing* or *grinded* on abrasion surfaces to obtain ochre powder or scored with a cutting/pointed tool. Nevertheless, *scoring* appears to be marginally used being attested by single rare deep incisions. It is presumable that *crushing* and *grinding* could be simultaneously executed, in the same moment of the *chaîne opératoire*.

A second stage of this process was characterized by ochre *rubbing* directly on soft (organic) surfaces. *Rubbing* occupies a final place in the *chaîne opératoire* of ochre. The pieces could be directly rubbed on surfaces or previously transformed for *grinding* or *scoring*.

Chapter VIII.

Spatial distribution

The methods used for the excavation of the archaeological surfaces allowed to analyse the spatial distribution of ochre remains in the sites of Los Canes, Arangas, La Garma A and Grotta di Pozzo for both the Palaeolithic and Mesolithic layers.

It was possible to evaluate the distribution of ochre for each sector in each square of the archaeological surface, for the Iberian sites. As far as Grotta di Pozzo is concerned, the spatial distribution was carried out according to the excavation's methodology applied in this site (chap.III, par.III.4.3.2.).

This type of analysis is useful to investigate the link between the ochre vestiges and the site in function to the context and anthropic structures existing in it. In this case, by having available both domestic and funerary contexts, the spatial analysis is fundamental to understand the degree of interaction between colouring materials and anthropic structures, as well as to reconstruct the organization of space occupied by human groups. Additionally, the evaluation of ochre distribution in relation to the stratigraphic units of the deposit, it allows to place the objects along the archaeological sequence in relation to the cultural content.

The stratigraphic sequences of the sites here presented, are long and made up of several units, some of which deposited during same cultural facies and, for this

reason, grouped in a unique block for the spatial analysis. A further problem is the representativeness of the effective quantity of colouring materials due to the high level of fragmentation of non-modified pieces. This aspect was resolved by carrying out an evaluation of the distribution by the mass (gr). With the aim of recognizing the specific areas related to ochre processing and gather more information on the management of colorants in the site, the concentrations of modified objects have been adequately reported to distinguish them from those of the unmodified objects. Although red ochre is the most abundant colouring material in the sites, it is also interesting to evaluate the distribution of yellow materials to better understand the association with both red vestiges and archaeological space anthropically exploited.

VIII.1. Los Canes

Solutrean

Unit 2A is the first unit of the Palaeolithic sequence of the cave testifying the most ancient anthropic occupation during the Late Solutrean (Arias, 2002). Discrete concentrations of red ochre can be seen towards the central part of the back cave. The ochre mass does not exceed 10 gr appearing well localized in a rather restricted area. A small concentration of yellow ochre (<1 gr) is localized in the South-Eastern section of square G1 (Fig.VIII.1).

Lower Magdalenian

Unit 2B attests the sporadic Magdalenian occupation of the cave as for the Solutrean period. A greatest concentration persists in the back cave with an expansion towards the northern wall. The ochre accumulations are localized in a well-defined area between the squares G1-G2-H1. The modified pieces

thicken in the contact band between G1 and G2 towards the South-East. The quantities in the north-western section of the squares G1 is above 10 gr. In square H1 behind G1 the quantities do not exceed 1 gr per sector. No yellow ochre pieces were present (Fig.VIII.1).

Upper Magdalenian

A significant change is observed in the stratigraphic unit 2C, even if the excavated volume is much lower for this unit than the previous ones. A sedimentary hiatus separates this unit from the S.U. 2B by marking the beginning of human occupation and directly referable to the Upper Magdalenian (Arias, 2002). Conspicuous quantities of ochre are observed in the back part of the cave. An expansion towards south-east is perceived for the non-modified pieces in squares G1 and G2 with notable quantities in the north-western section of square G1. Small quantities were collected in the western portion of F1 next to G1. Less than a gram of yellow ochre comes from square G2, the south-eastern section in association to red ochre.

The modified pieces get thicker in the layer between G1 and G2 giving the possibility to recognize a well-defined area where these objects are accumulated. Furthermore, in the same area of modified pieces (n.26), three *crayons* were also localized: two in G1 and one in F2. The thickening therefore appears significant and could correspond to an area of intense ochre exploitation. A small concentration of yellow ochre is localized in G2 in the south-eastern section (Fig.VIII.2).

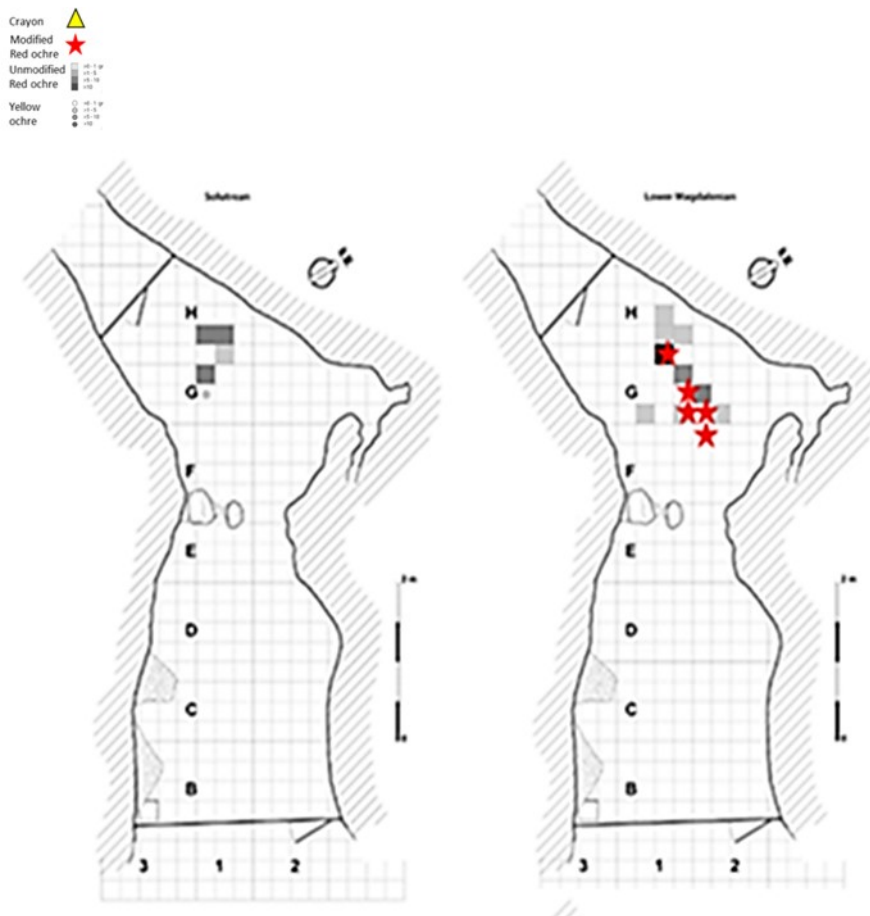


Fig.VIII.1.: Spatial distribution of ochre remains at Los Canes: Solutrean, Lower Magdalenian.

Azilian

The first unit which marks the transition from Upper Magdalenian to Azilian is S.U. 3. Although an extremely thin level is conserved at this unit, only in some areas was it possible to recognize the sub levels: 3A-3B-3C. S.U. 3A and S.U. 3B are distinguished by the presence of a red ochre separating them. Large concentrations are observed in squares G1-G2 in a continued way between S.U. 3A and S.U. 3B. An expansion is visible in S.U. 3C towards the square F2.

Additionally, two yellow ochre lumps of less than a gram in weight were localized in the front part of the cave towards the entrance in square B1.

Further ahead on the surface, in the southern section of the square E1, less than 1 gram of red ochre was distributed. The concentration of red ochre increases towards the bottom's cave. In the western section of the square F2, it also goes above 10 gr per sector. In G1 also, high concentrations of red ochre were distinguished in almost all the squares. An increase in this area of the cave is also recorded for the yellow vestiges with a greater expansion in square G2 where the north-eastern square is occupied.

It was possible to excavate only some evidence in squares E1-F1-F2-G2 for unit 4 (Azilian). The content of ochre was not particularly abundant, but overall it remained concentrated in the same areas of the previous Azilian units thus attesting a diachronic correspondence to the internal space of the cave.

As far as the modified pieces are concerned, the distribution appears quite spread in the same area where the non-modified pieces are concentrated. Among these objects, also a conic shaped *crayon* was localized (Fig.VIII.2).

Mesolithic (S.U. 5)

Stratigraphic unit 5 is probably the one which has the most taphonomical problems compared to the whole archaeological sequence. The association of the totality of the material at this unit remains doubtful due to the partial removal of deposits in the lower units. As already reported in the previous chapters of this thesis, the Holocene origin of this unit is confirmed, although there are some Pleistocenic inclusions.

In any case, an important accumulation is observed towards the bottom of the cave with a substantial variation for the lower levels with a clear shift towards the north wall.



Fig.VIII.2.: *Spatial distribution of ochre remains at Los Canes: Upper Magdalenian; Azilian*

Substantially, the back of the cave remains the most exploited, however, in this phase a well-defined accumulation is noted which takes the sectors of the squares H1 and G2 adjacent to the northern wall with an extension up to the north square of the square G1. An area with a greater concentration of modified pieces appears clear visible near the northern wall of the cave, in H1. The distribution of yellow ochre that never exceeds 1 gr of mass appears different. The concentrations are in the outer band that joins the two squares G1 and G2. Sporadic concentrations appear in the north-west section of G2 and in the south-west section of G1. Further concentrations are localized in sectors of H1 near the northern wall of the cave.

Two concentrations of pieces with use-wear traces are highlighted in the squares G2 and H1. In G2, a part of these objects is associated to a rather high concentration in the central part of the square in which small quantities of yellow ochre are found too.

The other accumulation of modified objects is localized in the part between the two H1-H2, near the northern wall in combination with a conspicuous quantity of non-modified red ochre fragments. Sporadic concentrations of yellow ochre appear in this same area. Moreover, the localization of a *crayon* from the northeaster extremity of H1, in the middle of this combination of modified and unmodified pieces of red ochre, in high quantities, highlights an area of intense exploitation (Fig.VIII.3).

Mesolithic (S.U. 6).

In regards the archaeological context of Los Canes, this unit surely appears the most interesting due to the presence of funerary structures. As already shown in the previous chapters, many pieces of ochre have been gathered at this unit and from the filling of the funerary pits.

The problems relating to the attribution of materials to Holocene units also arises in this case like in unit 5. The excavation of the burials, and especially burial 6III affected the lower Pleistocene levels and thus determining a removal of most ancient materials. The sediments of the lower layers were firstly exported to obtain funerary pits and later re-deposited to fill the pits.

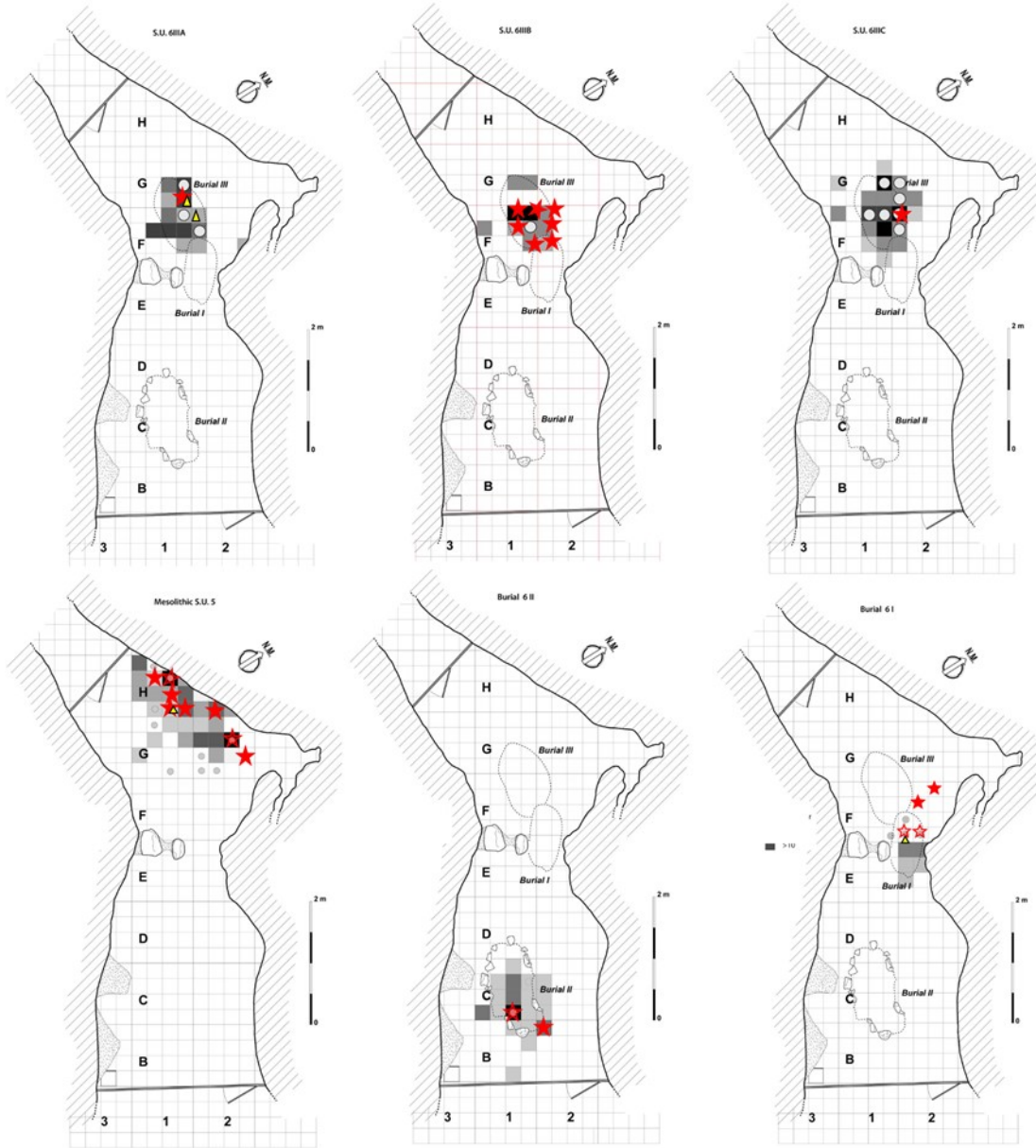
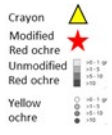


Fig.VIII.3.: Spatial distribution of ochre remains at Los Canes in Mesolithic units (S.U.5; S.U.6III, S.U. 6II, S.U. 6I).

By starting from burial 6III (Fig.VIII.3), it is worth observing the distribution of materials into three different filling units of the pit.

Unit 6IIIA, where most of the body was placed (head, upper limbs, chest, hip) and which presumably contained materials in direct relation with the burial, is characterized by good concentrations of ochre. Important concentrations appear under the left shoulder in the left section of the chest at the height of the upper ribs, hips and feet. The lower limbs were flexed and for this reason, they came out of this level in that only the feet were rested. In the higher portion near the head, the concentration of red ochre drops. From this unit, two *crayons* (n.214; n.241A; chapter VII, par.VII.1.1.2) were localized at the height of the left elbow beside the body. Additionally, concentrations <1 gr of yellow ochre were localized on the left of the occipital portion of the skull (3 fragments) in the hip area (1 fragment) and in the lower section on the left of the lower limbs. Of importance is the localization of some fragments with striae at the height of the left shoulder blade of the corpse. Combined with these objects are two *crayons* which were placed alongside the body.

In unit 6IIIB the distribution appears inhomogeneous compared to S.U. 6IIIA. This unit represent the first level of sediments used to cover the cadaver. The distribution of the materials appears rather considerable in function to the position of the body. The combination of modified and non-modified pieces indicates a sort of blanket of red vestiges for the coverage of the lower portion of the body from the hip to the feet. It is interesting to notice that in the point where the concentration of red ochre is low and there are no modified pieces, it is possible to see an accumulation of pieces of yellow ochre at the height of the head of the left femoral.

Unit 6IIIC constitute the closing layer of the burial. Red ochre fragments together with small quantities of yellow ochre are disposed homogeneously on the whole area of the pit. Large concentrations are observed in correspondence of the skull, hip and lower limbs, with shades towards the edges of the structure. The yellow vestiges seem to have a specific disposition in proximity to the head, on the left of the skull; in the direction of the low back area of the body and on the left at the height of the hip. Three fragments with striae are localized on the left side of the corpse at the height of the hip. As reported in chapter IV of this thesis (par.IV.1.2), these are mostly pieces with dimensions between 2 and 10 mm. The distribution would seem to indicate a systematic relationship between fragments obtained by *crushing* and the cover of the deceased.

Unit 6II (Fig.VIII.3) corresponds to a second funerary structure in which the body was placed in the south-western direction with the head towards the entrance of the cave. The distribution of ochre shows the burial area. A large concentration appears evident near the head with quantities which are greater than 10 gr and along the spinal cord with quantities between 5 and 10 gr. Ochre is reduced towards the lower limbs and disappears near the feet. A yellow ochre lump is localized in the area where the head of the corpse rests. The distribution of materials, non-modified fragments with dimensions between 2 and 10 mm (chap. IV, par.IV.1.2.) cover the body. Some fragments with striae are localized in the areas with large concentrations of material but they are quite sporadic.

Unit 6I (Fig.VIII.3) fills a similar oval pit which intersects those of structure 6III. Just like III, the burial of the corpse is placed with the head in the north-west and the lower limbs facing towards the entrance. The accumulations of red

ochre appear heterogeneous and localized on the left of the lower limbs of the corpse. A *crayon* is localized near the chest of the body. As far as the modified pieces are concerned, it is possible to observe two distinct concentrations: one inside the burial near the same area from where the *crayon* and small concentrations of yellow ochre came from, another one is outside, between burial III and burial II. The distribution highlights a sort of homogeneous blanket of fragments which cover the lower portion of the skeleton. There appears to be a non-casual distribution of fragments for yellow ochre. Yellow vestiges are placed according to the shape of the higher portion of the body: head, neck, shoulders.

Other structures open inside unit 6, some of which are presumably of funerary use due to the presence of human remains. A large part of these structures is localized between tombs III and I with a depth of around 10-20 cm (Arias, 2002). The excavation of semi-circular pits highlighted a sediment with a chaotic and reworked orientation. Ochre fragments inserted themselves inside these sediments. The chaotic orientation of the materials and their redeposition let us hypothesize a non-intentional disposition of ochre in these structures. Nevertheless, it is worth noticing how the distribution of ochre follows the area of the pits.

Unit 6A (Fig.VIII.4) presumably corresponds to the filling of a funerary structure since human remains were collected inside it. Ochre is concentrated in correspondence with the pit. The concentrations are rather high, and the modified pieces are associated to large concentrations of non-modified pieces. A similar situation can be observed in the following burial III at the first level in which the body was placed. At this point, the distribution could suggest a

systemic relation between the concentrations of red ochre and the human remains as recurrent data in Mesolithic funerary practices.

A completely different situation is highlighted for unit 6B (Fig.VIII.4). In this case it is the filling level of an oval structure whose conservation is not optimal, and the funeral attribution is doubtful. The ochre follows an extremely inhomogeneous distribution and only one modified fragment appears isolated and outside the accumulation area. Good concentrations are observed in the central band (west-east) of square F2 together with low concentrations horizontal to the concentrations of the central band. Further accumulations are localized higher towards the bottom of the cave in square G1. The South-Eastern squares show slight concentrations of red ochre. Less than a gram of yellow ochre was localized in the south-eastern corner of square G1.

Unit 6C (Fig.VIII.4) characterizes the last of the structures highlighted towards the bottom of the cave on unit 6. The distribution of ochre marks an area which intersects the burials underlying 6III and 6I. The distribution does not appear to be localized in a well-defined area. Low concentrations are observed in the north-western section of F2 with sporadic accumulations at the centre of F1 and in the south-western corner of E2. An important concentration of yellow ochre characterizes a part of G1. Yellow ochre appears homogeneously distributed in the southern section of square G1. The quantities are low but there are recurrent accumulations in each sector on this section.

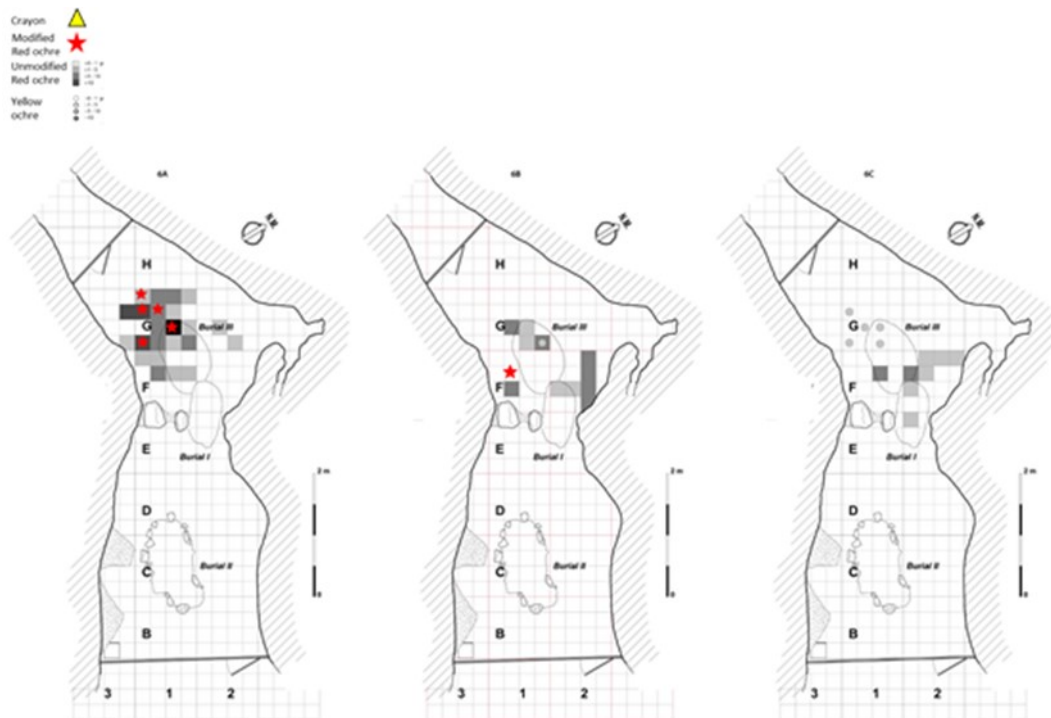


Fig.VIII.4.: Spatial distribution of ochre remains at Los Canes in Mesolithic units (S.U.6A; S.U.6B, S.U. 6C).

VIII.1.1. Evaluation of results

The analysis of the spatial distribution of the materials on the archaeological surfaces allows a series of general reflections on the management of the space occupied (inhabited/sepulchral) by the Palaeolithic and Mesolithic human groups.

The evaluation of the distribution of colouring materials (unmodified pieces, modified pieces) in each of the stratigraphic units highlights some significant trends.

For the Upper Palaeolithic levels the distribution of colouring materials appears rather poor for the Solutrean phase, while a progressive quantitative increase is recorded, with a markedly wider expansion towards the cave bottom, parallel

to the northern wall. This increase is even more evident in the Azilian occupation phase of the site. Observing the general state of the materials (chap. IV), most of them are very small pieces (<10 mm), highly fragmented. However, a substantial difference emerges between the Solutrean and the Magdalenian. During the first anthropic occupation of the cave (Solutrean) there are no modified pieces that, instead, characterize the following occupation phase (Magdalenian).

A marked difference emerges in the Azilian in which the abundance of red ochre compared to the previous phases is associated with a horizontal expansion to the anthropic occupation plan. The high fragmentation of the materials, the conspicuous presence of modified pieces and the presence of red ochre lenses (S.U. 3A-S.U. 3B) in the ground bears witness to an intense reduction of raw materials at the site.

The location of the materials towards the cave bottom, in the same area already highlighted for the previous phases, support the idea of the presence of a specific area of the site related to the ochre processing. Although, on this site the Palaeolithic levels do not appear to be conspicuous in the front part of the vestibule and for this reason they do not allow definitive reflections on the management of the colouring materials exclusively in this part of the cave.

The comparison of the spatial distribution with the unit ascribable to the Mesolithic phase that precedes the funeral use of the site (S.U. 5) reveals some significant trends. The accumulation of modified objects to the north wall suggest the idea of the presence of a specialized area on the site (Fig.VIII.5).

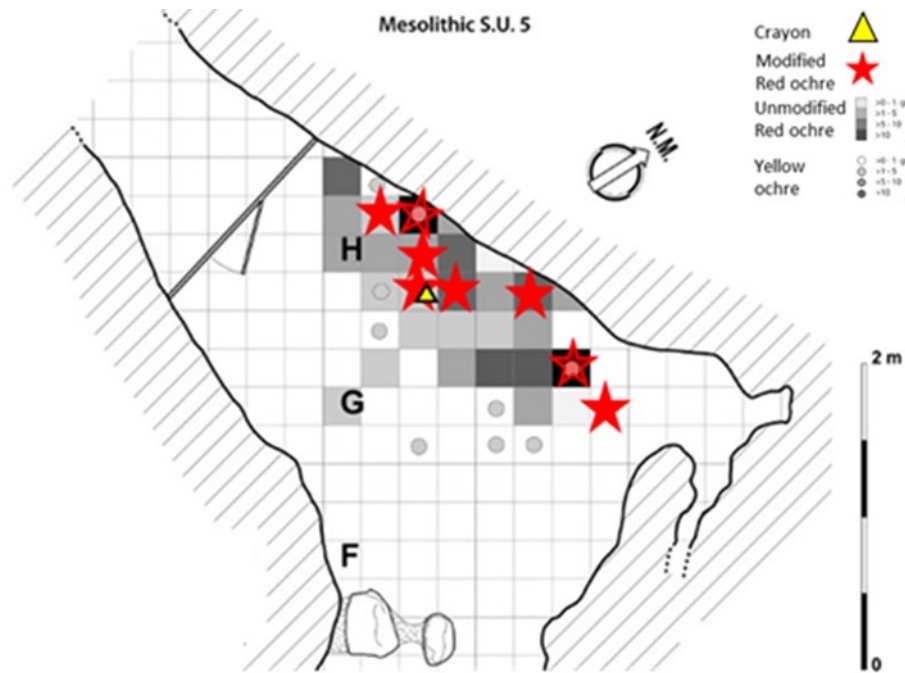


Fig.VIII.5.: Spatial distribution of ochre remains during the Azilian at Los Canes.

Regarding the Mesolithic structures, the ochre is distributed in areas occupied by human bodies. Comparative observation with the underlying layers highlights a radical transformation of space in the cave. If during the previous phases of occupation, the distribution of ochre makes it possible to recognize well-defined areas towards the cave bottom, at the time to which the burials refer, the distribution appears to be bound to funerary structures.

Among the funerary structures, the 6 III appears the richest in materials (Fig.VIII.6). A relevant element is the conspicuous presence of modified fragments, as well as the presence of two crayons beside the deceased. The situation of this burial is very complex due to the presence of infantile bones at the base of level 6-IIIc, in association with faunal remains (chap.III). The hypothesis of a reopening of the tomb to deposit the infant is the most probable (Arias, 2002).

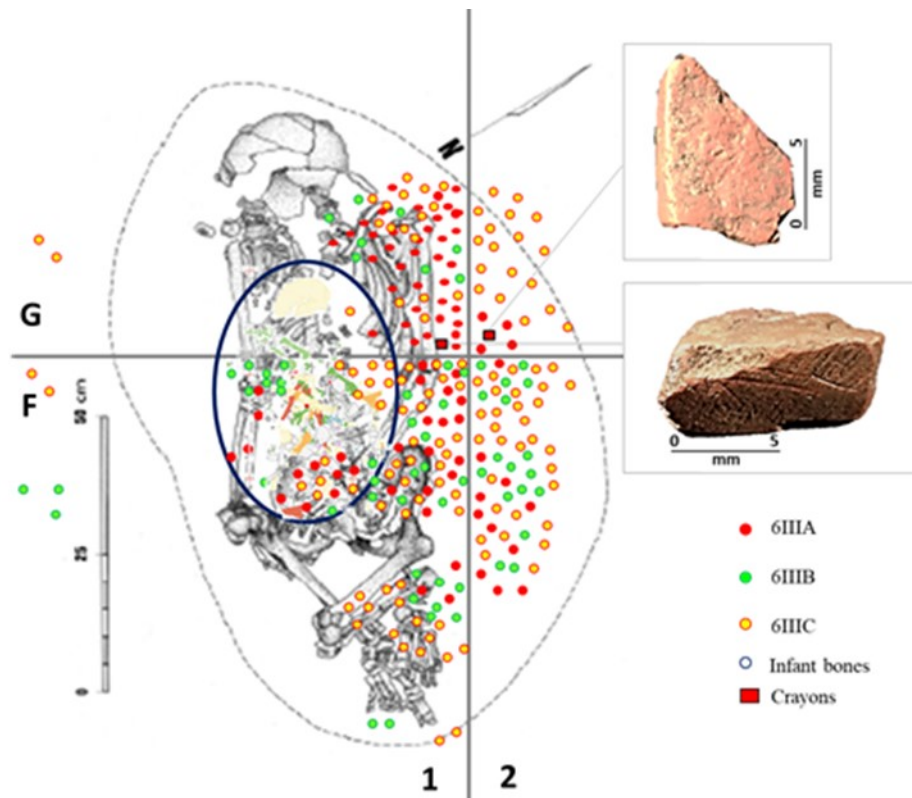


Fig.VIII.6.: Ochre distribution in the burial 6III. The circle indicates the infant bones.

In this sense, the 6-III C and 6-III B levels appear to be the most removed. At this point a significant aspect emerges from the spatial distribution, that is the material of the 6-III A unit associated with the burial of the adult skeleton. Assuming that no element of grave goods appears to be highlighted (Arias, 2002), the analysis made here clearly shows that the two crayons are located at the side of the adult male. The existence of two burial phases in a tomb appears to be a well-documented case for the Mesolithic (Teviec, Hoedic) as reported by Arias (2002). Even the presence of ochre blocks as grave goods remains a practice witnessed both in the Upper Palaeolithic (Arene Candide, Cardini,

1980) and in the Mesolithic (Moita Do Sebastiao, Roche, 1960, Roche, Veiga, 1967).

For this reason, the idea of an intentional association of these objects (crayons) with the burial is acceptable. As far as other burials are concerned, they are generally less rich in ochre than in tomb III.

However, also for these other structures the association with ochre is evident. The distribution appears linked to the burial pits in which highly fragmented, largely unmodified materials are concentrated (Fig.VIII.7; Fig.VIII.8).

From this distribution analysis it is possible to state that the ochre on the Los Canes site can make significant considerations. First of all, the ochre is an indicator of human activity in the site. Secondly, this material relates to the type of activity carried out in the cave, highlighting the radical transformation in the use of space that occurs between the Upper Palaeolithic (residential) and the Mesolithic (funeral). Finally, the relationship between the colouring materials and the funeral sphere is well clear.

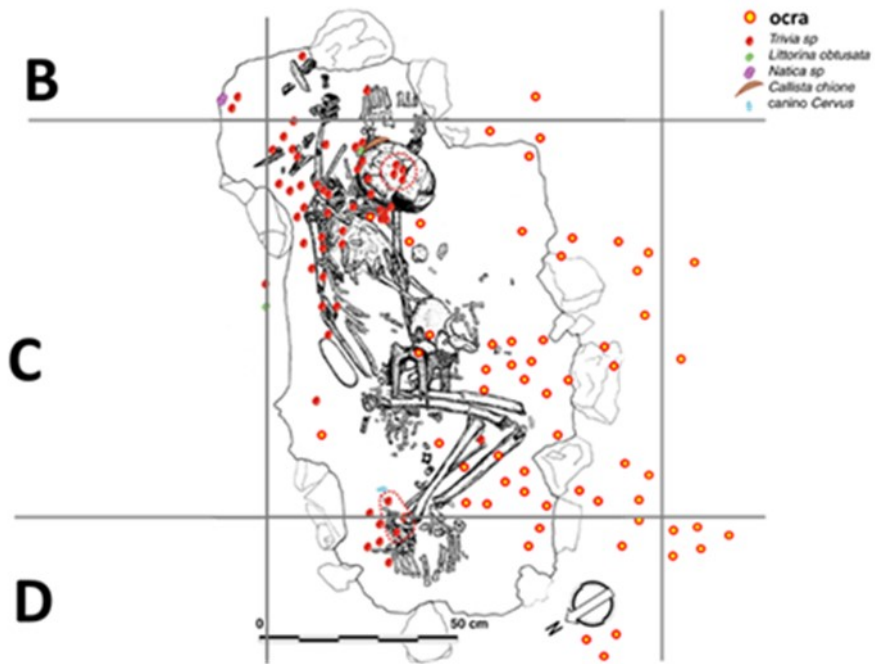


Fig.VIII.7.: Ochre distribution in the burial 6II.

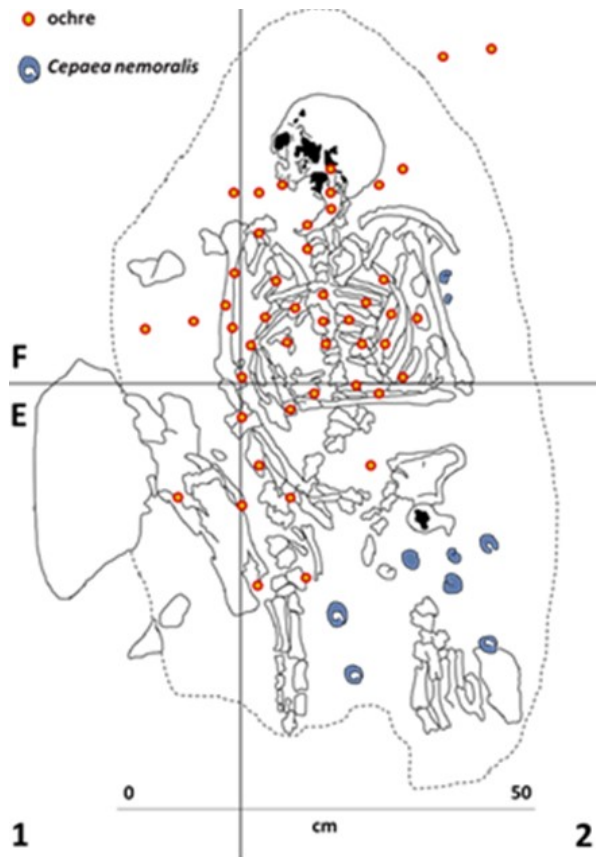


Fig.VIII.8.: Ochre distribution in the burial 6I.

VIII.2. Arangas

Lower Magdalenian

Unit 5D was formed during the first part of the Magdalenian period. The low density of archaeological evidence for this unit attests a sporadic anthropic occupation of the cave. Even the concentrations of ochre appear quite poor and localized in squares D9 and I12 (Fig.VIII.9).

Upper Magdalenian

An increase is noticed in unit 5C compared to the lower unit even though the anthropic evidence for these phases is still lacking. Considerable accumulations with quantities higher than 10 gr are localized in the central area and would indicate an ochre exploitation area. Small quantities are localized in F7. It is not possible to distinguish associations with anthropic structures which can add information to the exploitation of ochre *in situ* for this unit just like in the lower one. This unit still testify a reduced anthropic occupation of the cave (Fig.VIII.9).

Azilian

The Azilian occupation of the cave appears to be well documented in the stratigraphic units 5C and 5B which have the same date (12,137±269 cal BP) and for this reason grouped in the spatial analysis. During the Azilian phase of the site, ochre concentrations appear more consistent and significant in relation to the anthropic exploitation of space. A broad and consistent accumulation of red ochre is highlighted in the northern part of the cave in area B. In squares F9 and

F8, quantitatively important accumulations of non-modified pieces in association to modified pieces are shown. Furthermore, the association between red and yellow materials are well represented even if the latter are in lower concentrations in the same areas. The horizontal position of ochre in the plane would seem to indicate an area in the north of the cave connected to the management of colouring materials (Fig.VIII.10).

Mesolithic

For unit 2B (Mesolithic), it is possible to observe a substantial reduction in the concentrations of coloured materials. The thickest area always remains the northern part of the wall. The mass, by sector, does not go beyond 5 gr. Two yellow ochre fragments with a weight >1 gr is localized in E11. A single modified fragment appears in the north-eastern corner in square F10 (Fig.VIII.10).

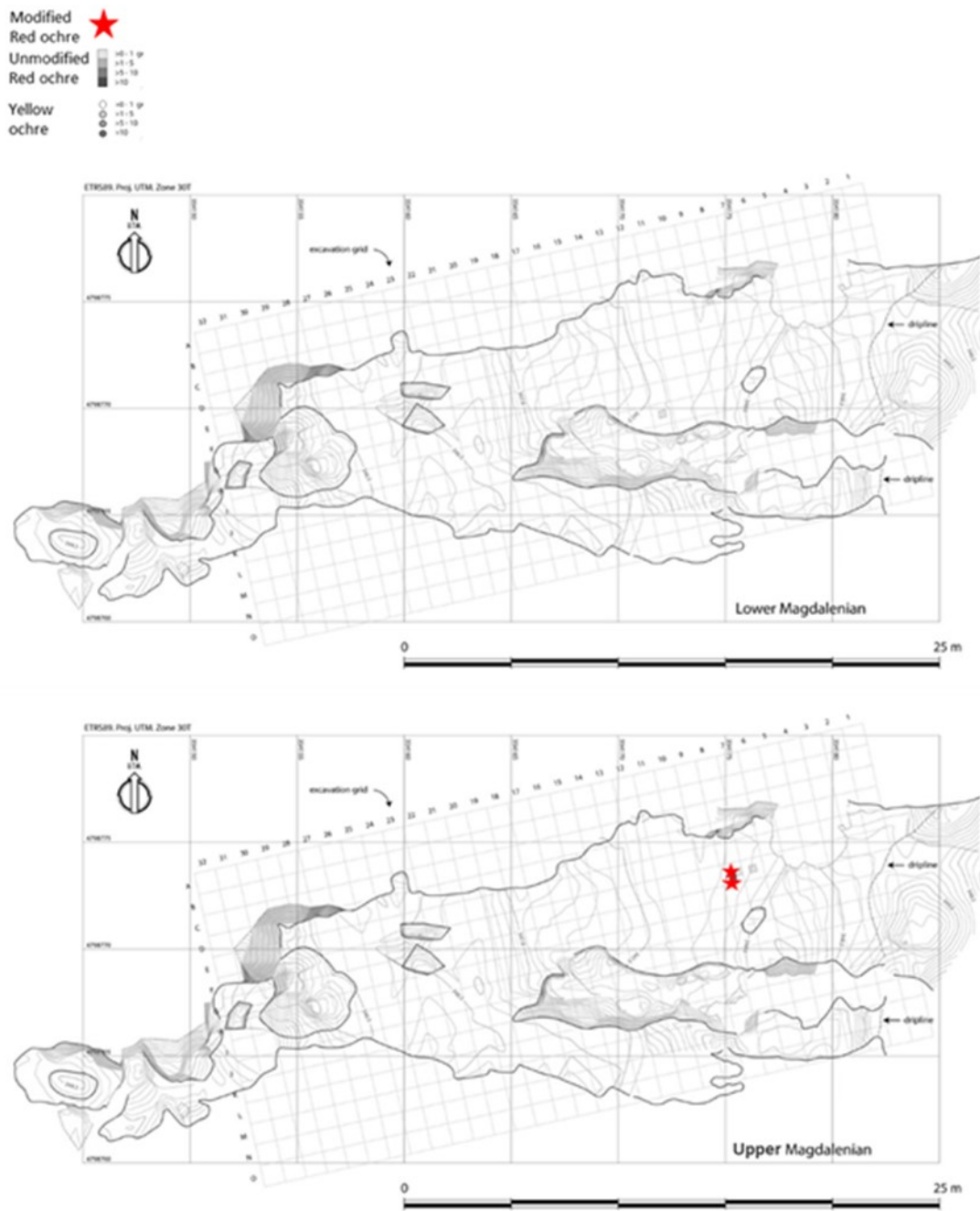


Fig.VIII.9.: Spatial distribution of ochre remains at Arangas: Lower Magdalenian, Upper Magdalenian

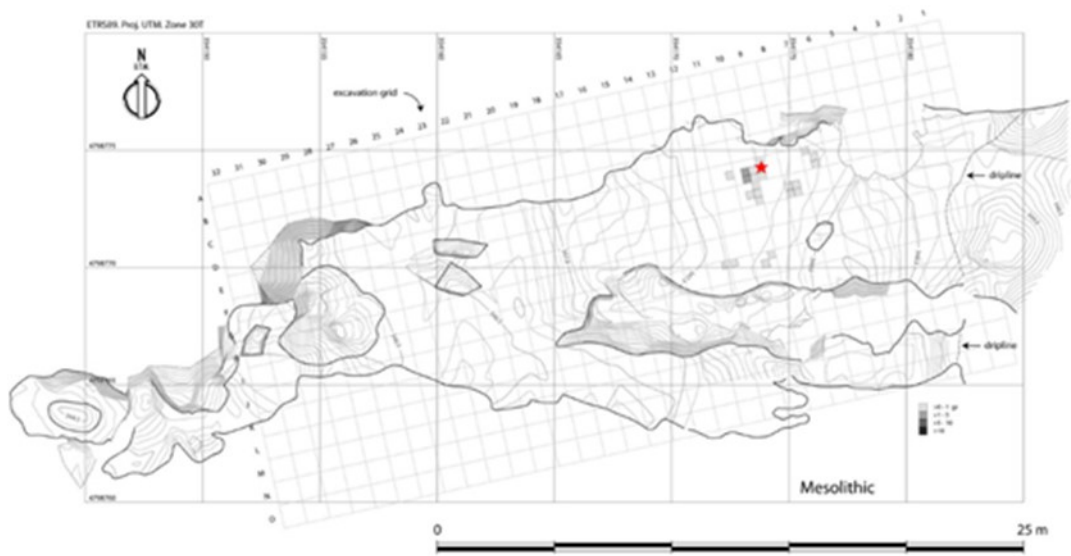
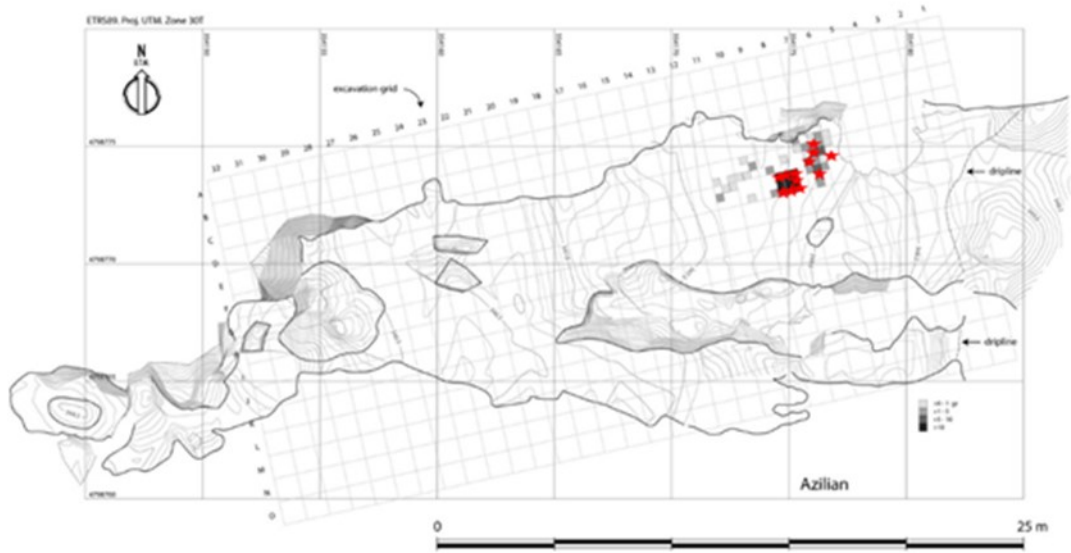


Fig.VIII.10.: Spatial distribution of ochre remains at Arangas: Azilian, Mesolithic.

VIII.2.1. Evaluation of results

The analysis of the spatial distribution shows significant aspects for the management of colouring materials in the site according to the different phases of occupation. The ochre concentrations appear quite different between the Palaeolithic and the Mesolithic levels.

By observing the spatial distribution to the site, in the Lower Magdalenian the concentrations of highly fragmented pieces (chap. IV) appear to be rather scarce and not significant in the management of space. The considerable increase recorded in the Upper Magdalenian displays a concentration of unmodified and modified fragments in a well-circumscribed and rather reduced area.

A significant trend emerges in the Azilian phase. During this period an important increase both quantitative and qualitative (modified and not modified) is observed towards the northern part of the cave. Near a recess of the rock wall, highly fragmented modified and unmodified pieces are concentrated, indicating a well-defined area. In functional terms, it could be an area reserved for the management of colouring materials. An area where human activities could be intense (Fig.VIII.11)

The distribution appears to be significant with respect to this phase of occupation of the site as a similar condition is not evident in the other units. In fact, in the Mesolithic, a contraction of the horizontal ochre distribution and a reduction of the modified pieces appears clear. This situation leads us to reflect on the high fragmentation of the Azilian materials which, combined with the conspicuous presence of pieces with traces of transformation, suggest an intense anthropic activity in the reduction of raw materials in fine fraction. The nodule with abrasion facets (chap. VII) comes precisely from these levels

indicating a production of powder product. Certainly, the element that makes us reflect most is the presence of ochre processing tools (chap. VII) from levels referring to an ancient phase of the Mesolithic that, although not directly related to ochre remains. However, these objects attest the transformation of red ochre at Arangas.



Fig.VIII.11.: *Spatial distribution of ochre remains in the Azilian unit of Arangas.*

VIII.3. La Garma A

Solutrean

Unit G refers to the anthropic occupation of the cave during Solutrean period. In regards this phase, red ochre is distributed in three areas of the cave: the vestibule, the central room and the back part. At the entrance of the cave, ochre vestiges are low concentrated. Towards the middle of the cave, the concentrations appear more consistent with the accumulation of modified pieces in G10 to the north. At the back of the cave, it is possible to appreciate another area with sporadic concentrations which do not go over 1 gr in mass.

Yellow ochre spots can be seen in a point, in the vestibule and in several points in the central part in association with red ochre. Even to the back, in the northern section of H12 already occupied by red ochre, it is possible to notice a small concentration of yellow ochre in the middle of this band (Fig.VIII.12).

Lower Magdalenian

Large concentrations characterize the stratigraphic unit J. In the vestibule area it is possible to see conspicuous accumulations of red ochre in band D. In association with red ochre in D6, appear high concentrations of yellow ochre. The distribution is thinned towards the centre of the cave and to the bottom. A band of red ochre with small concentrations of yellow ochre can be observed at the curve of the northern wall to the central area of the cave. In this level, modified pieces are not present (Fig.VIII.12).

Middle Magdalenian

A substantial increase characterizes S.U. L formed during the Middle Magdalenian occupation of the site. The ochre specimens are distributed almost entirely on the whole surface of the cave with notable accumulations (>10 gr) just outside the vestibule. The area of the vestibule is densely occupied by a large concentration of red ochre which follows on continuously to the central area of the cave where accumulations are intense. In the recess of the northern wall, where slight concentrations were already observed in the previous phase, during the Magdalenian the concentrations appear conspicuous and enclosed within an area well bounded by a circle of rocky blocks that close the semi-circle recess. The concentrations inside this structure appear less conspicuous

compared to the vestibule and the centre of the cave where they are over 10 gr in association to small accumulations of yellow ochre. For modified pieces, there is no homogeneous distribution with specific concentrations. These objects appear scattered in the different areas of the cave, in association with unmodified fragments and yellow ochre. Spatial analysis confirms the results of previous analysis: an intense presence of ochre in the Middle Magdalenian. Additionally, the horizontal distribution of these materials allows to appreciate an intense exploitation of colouring materials in relation to the internal surface of the cave. Another significant data is the association between the faceted piece with striae (chap. VII, par.VII.1.1) with considerable accumulations of red ochre and about 1 gr of yellow ochre (Fig.VIII.13).

Upper/Final Magdalenian

A significant change is observed in units (N-O) deposited during the final stage of Magdalenian. The ochre disappears from the vestibule area where reduced accumulations appear in the northern and adjacent squares of D7 and D8 along with a small concentration of yellow ochre and some modified fragments. The sporadic and rather low concentrations characterize the central area in a heterogeneous way. Nevertheless, near the blocks which delimit the semi-circular space in the entrance of the northern wall, it is possible to notice an important accumulation of well localized modified pieces in association with notable quantities of unmodified red ochre pieces and yellow ochre. Inside the structure appear modest concentrations of red ochre with yellow spots (Fig.VIII.13).

Mesolithic

Unit Q (Mesolithic) shows a new increase in comparison to the previous phase. The distribution appears considerable towards the final portion of the vestibule by progressively settling to the beginning of the central room. A modified fragment is also localized next to the vestibule.

As it moves towards inside of the cave, the concentrations increase with considerable accumulations in G10. In this square it can also observe a notable concentration of yellow ochre in the south-western corner together with slight concentrations of red ochre. There are small concentrations of red ochre in G13 inside the structure. Therefore, the vestibule and the central area appear as two areas with large concentrations of ochre (Fig.VIII.14).



Fig.VIII.12.: Spatial distribution of ochre remains at La Garma A: Solutrean, Early Magdalenian.

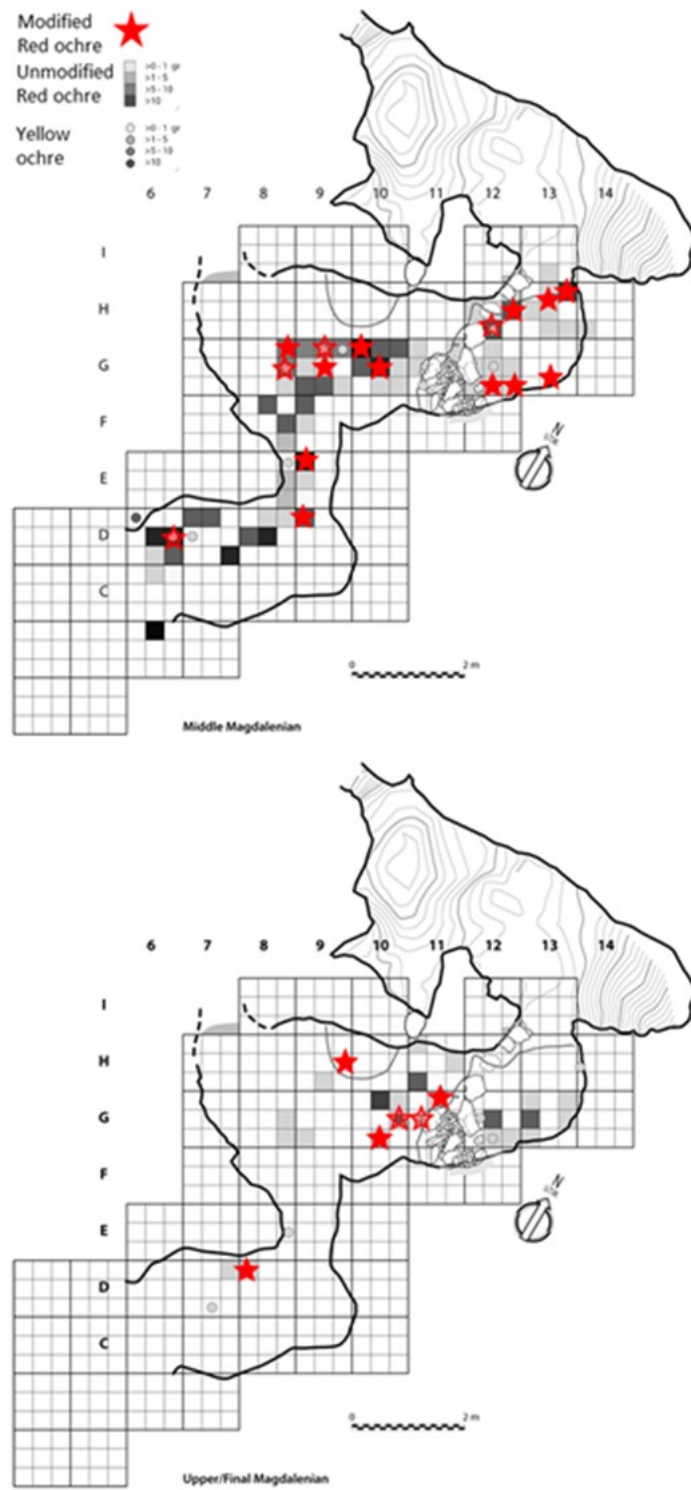


Fig.VIII.13.: Spatial distribution of ochre remains at La Garma A: Middle Magdalenian, Upper/Final Magdalenian.

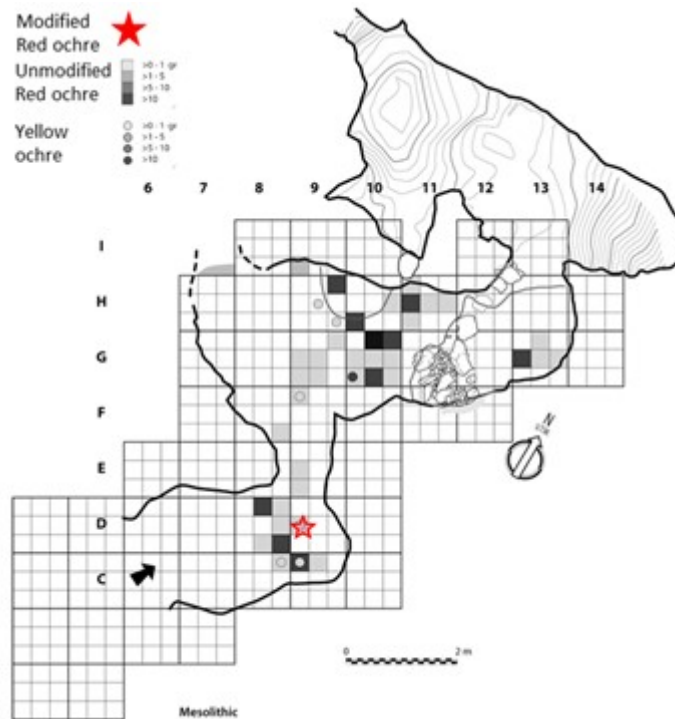


Fig.VIII.14.: Spatial distribution of ochre remains at La Garma A: Mesolithic.

VIII.3.1. Evaluation of results

From the global distribution of colouring materials at La Garma A, it is possible to present some reflections on the management of ochre in the site and on the organization of the space inside the cave. Spatial analysis shows a marked difference between the Solutrean and the Magdalenian. The concentrations of ochre on the Solutrean surfaces are quantitatively scarce in all the space.

A change is already observed in the Early Magdalenian. During this phase, a marked disparity emerges between the elevated concentrations in the vestibule area and those still rather scarce towards the central hall and the bottom of the cave. The major concentrations are located towards that area of the cave open to the outside, an area of access to the site. Considering the mass in relation of the

fragmentation index (chap. IV), the information that this data provide is quite significant. The number of pieces is approximately the same (S.U. G: n.50, S.U.J: n.61), however in the Lower Magdalenian the pieces appear larger and less fragmented than in the previous phase (Solutrean).

Certainly, the most significant tendencies emerge for the Middle Magdalenian. During this phase, a structure of lithic blocks is created with a semi-circular arrangement to delimit a recess in the northern wall of the cave. In this case, the spatial distribution shows a significant change compared to the previous phases (Solutrean, Lower Magdalenian).

The colouring materials are distributed in three areas of the cavity: the vestibule, the central hall and the interior of the structure. A larger concentration of modified pieces appears inside the structure, near ochre-coloured blocks of sandstone. Evaluating the results obtained considering the available data on the structure of the Middle Magdalenian (Arias *et al.*, 2005), it is possible to add some new considerations. First, it is from this plane that most of the pieces of ochre come from. In addition, the large concentration of unmodified and modified pieces in the central area of the cave is associated with the abundance of remains of mammals and transformation of lithic materials. In this part of the cave there was the processing and consumption of prey, as well as the transformation of lithic raw materials. In the vestibule area, largely unmodified pieces with dimensions >10 mm and little fragments are concentrated. This area is interpreted as a transit area and reserved for the retouching of lithic artefacts (Arias *et al.*, 2005).

Regarding the structure, it is a sort of semi-circle of stones that closes a corner in the central wall of the cave where the lower density of lithic and bony remains, very fragmented, allowed to be interpreted as a space reserved for activities in

the residential context. The observation of the distribution of ochre pieces allows, however, to highlight a concentration of modified pieces (chap. VII) within this space. The association, (Fig.VIII.15) between an accumulation of sandstone blocks with red ochre residues and grinded ochre pieces in the same point supports the idea of an area intentionally delimited by a construction bound to domestic uses within the hypogeal space (Arias *et al.*, 2005).

This organization of the interior space with a fractionation of the surface does not appear less clear over time. The progressive decrease in ochre concentrations and the absence of modified pieces within the structure highlight a change in the anthropic exploitation of the space. The density of ochre pieces in the central part of the cave reflects an intense occupation of this area also towards the end of the Magdalenian. At the same time, slight concentrations of ochre in the structure still attest the use of this space, but with a lower intensity compared to the previous phase. The vestibule area is almost ochre-free. The spatial distribution shows a contraction in the distribution of colorants, with a concentration in the central hall.

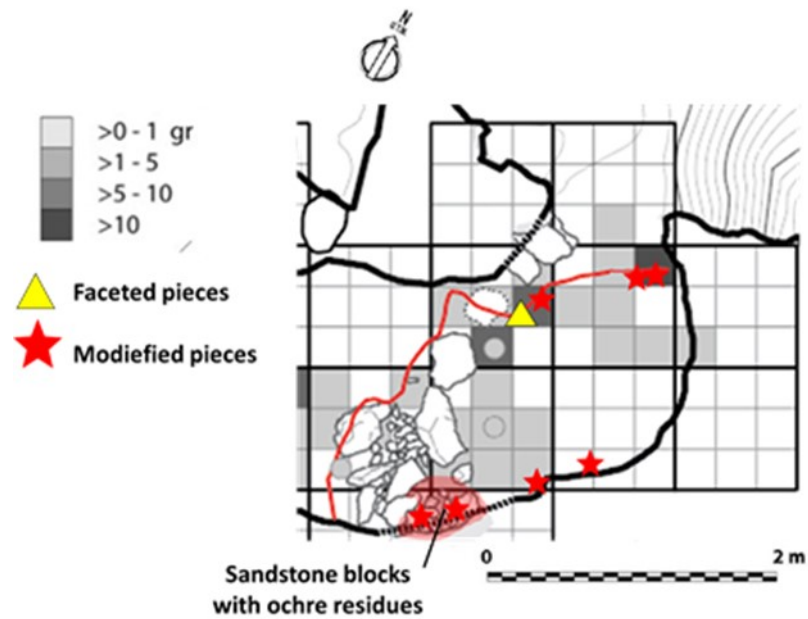


Fig.VIII.15.: Spatial distribution of materials inside the Middle Magdalenian structure.

A similar situation can be observed in the Mesolithic. The difference with the Middle Magdalenian is evident. The space most occupied by the ochre is the central hall, although good concentrations are observed near the vestibule. The presence of fragments within the structure testifies the diachronic exploitation of this space.

Although, even in the Mesolithic there are not modified pieces inside the structure. This aspect could favour the idea of a change in the use of the internal area of the structure starting from the Final Magdalenian and throughout the Mesolithic.

VIII.4. Grotta di Pozzo

Ancient Epigravettian

In regards the layers deposited during the first part of the Epigravettian (PS13-PS8), the concentrations of ochre appear quite reduced and sporadic. In both J10 and L7 the quantities do not go beyond 1 gr. Other types of colouring are not attested. A combination of ochred artefacts with small amounts of ochre in H9 is highlighted (Fig.VIII.16).

Final Epigravettian

The second part of the Epigravettian (interPS6/PS7-PS1) is characterized by a substantial increase. The distribution appears rather diffused with large concentrations that move from the centre towards the north-western part with large concentrations in H10 and H9. By evaluating this distribution in function to some ochred lithic industries found at the site (Catelli, 2014) the association between artefacts and ochre fragments appear systematic. As for the yellow ochres, concentrations not exceeding 1 gr characterize the central band. Mild concentrations characterize K7, on the cave bottom, and H9 where ochre remains are associated with conspicuous accumulations of lithic industries with residues of red pigment (Fig.VIII.17).

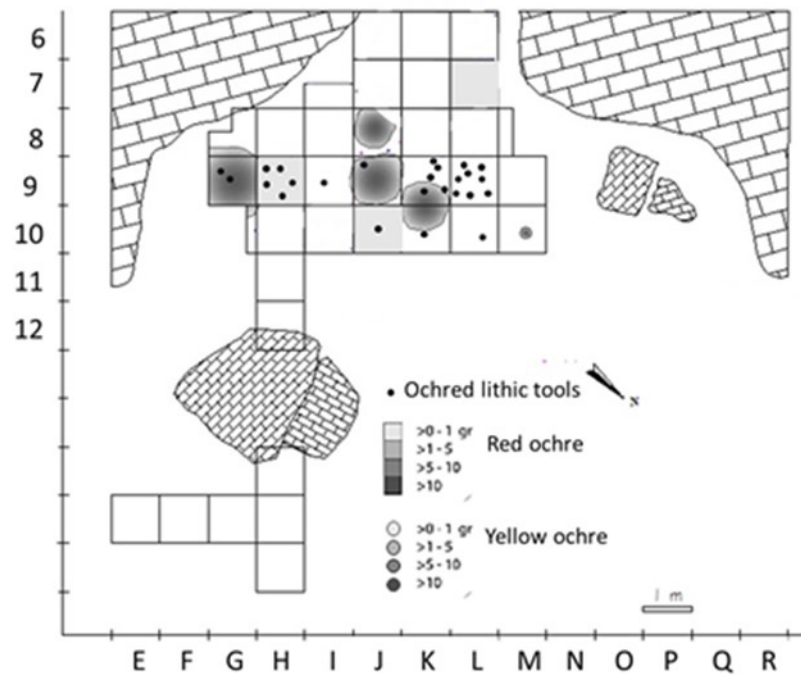


Fig.VIII.16.: Spatial distribution of ochre remains at Grotta di Pozzo: Ancient Epigravettian.

Mesolithic

The concentrations appear reduced during Mesolithic (Chiocciolaio1-2bis) when compared to the lower levels of the previous Epigravettian phase. Accumulations of red ochre are observed in the north-eastern part of the cave and towards the central part. A concentration of yellow ochre appears in one of the Holocenic pits which affects the Mesolithic levels. In any case the representativeness remains rather dubious. Regarding the association with ochred artefacts, there are clearly visible relations between lithic tools and ochre pieces in the central part of the cave in combination with shell-middens remains highlighting a processing area (Fig.VIII.18).

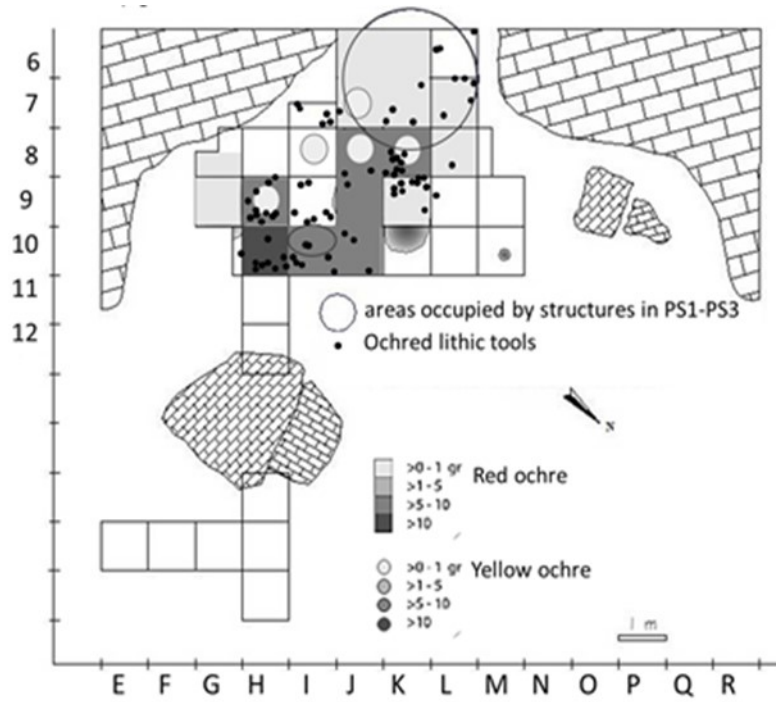


Fig.VIII.17.: Spatial distribution of ochre remains at Grotta di Pozzo: Final Epigravettian.



Fig.VIII.18.: Spatial distribution of ochre remains at Grotta di Pozzo: Mesolithic.

VIII.4.1. Evaluation of results

Observing the ochre concentrations in relation to some ochred artefacts (Catelli, 2014) already in the Ancient Epigravettian it is possible to appreciate a marked association between the ochre fragments and the lithic industries. Comparison of spatial distribution highlights the rather poor concentrations of very fragmented ochre pieces. Towards the north-western extremity there is an association of ochre artefacts and some ochre fragments.

A change is highlighted in the next phase. During the second half of the Epigravettian emerge marked differences with the previous phase. The central-western area of the shelter is characterized by conspicuous concentrations of ochre to which ochre artefacts are associated. It must be considered that during the Epigravettian (14,500 cal BP approx.) the back cave was occupied by fireplaces and *vidange de foyer* (Piarulli *et al.*, 2015). Furthermore, the deposition of the layers according to the plan with a slope towards the west, could have favoured the accumulation of the materials in the -west corner of the site.

A significant change occurs during the Mesolithic. First, the concentrations of ochre in the site and ochred artefacts are minor. The latter data could be a consequence of the lower quantities of colorants available in the cave. In any case, the spatial distribution shows a concentration of materials in the central area of the shelter with a contraction of the space. The search for a continuity with the lower levels in the occupation of spaces appears complicated because the surface was excavated by Holocene pits that disturbed the deposition of the layers and removed part of the materials. (chap. III) An interesting element emerges from the evaluation of the previous studies, the conspicuous presence of ochred lithic instruments (Catelli, 2014) and ochred shell ornaments respect

to the previous phases. This element can provide clues to the destination of ochre use in the Upper Palaeolithic and in the Mesolithic at the site.

VIII.5. Synthesis of data analysis

The evaluation of spatial distribution in the horizontal surface allowed to reflect on ochre as an indicator of the anthropic exploitation of spaces both in residential and funerary contexts. The results obtained allow us to recognize areas for the management of colorants in domestic sites (Arangas, La Garma A, Grotta di Pozzo). The presence of modified and unmodified fragments and the association with other categories of materials (La Garma A, Grotta di Pozzo) would identify spaces reserved for specific activities which comparisons exist in other European regions (Bosinski 1979; Baffier *et al.*, 1991; Gaudzinski *et al.*, 2003; Salomon *et al.*, 2009). Moreover, the presence of ochre in funeral pits and the association of colouring objects (*crayons*) with human remains support the key role of this material in prehistoric funerary rituals.

This practice is widely documented in the Upper Palaeolithic and in the Mesolithic of the European continent. Direct comparisons that contextualize this practice in south-western Europe between the Late Glacial and the Early and Middle Holocene are represented by Grotta del Romito, Grotta San Teodoro and S'Omu and S'Ormu.

Furthermore, spatial analysis highlighted diachronic tendencies in the management of anthropic space. During the more ancient phases (Solutrean, Ancient Epigravettian) the space occupied by ochres is still reduced, in the following phases (La Garma A: Middle Magdalenian, Final Epigravettian:

Grotta di Pozzo, Azilian: Arangas) a better expansion of ochre in relation to the site emerges This suggests a continuous use of colouring materials from the Upper Palaeolithic to the Mesolithic.

Chapter IX.

Final considerations

This research allowed us to collect a considerable amount of data to formulate valid hypotheses on the exploitation of ochre by hunter-gatherers who occupied south-west Europe between Late Glacial and Early and Middle Holocene. In the light of the results obtained, it is possible to formulate significant reflections on several aspects related to these issues: supply strategies, treatment and transformation of raw materials, management of ochre in the site, uses. These final reflections are essential to better understand what the role played by ochre in the life of human groups of the Upper Palaeolithic and Mesolithic was.

IX.1. Procurement strategies and exploitation of raw materials

The study of archaeological remains allowed us to obtain useful information to reconstruct the strategies of ochre procurement and to better understand the criteria of raw materials selection.

First of all, a fundamental aspect that emerges from the initial phases of this study is the tendential predilection of red ochre obtained from rocks rich in iron (hematite), both in the Iberian and in the Italian region. The abundance of hematite characterizes both the residential and funerary spaces where this

mineral was intentionally introduced by the hunter-gatherers who occupied them. Other colouring minerals were also collected, such as lepidocrocite and ferrihydrite with orange-red-brown colours, and yellow goethite. However, the hematite persisted as the most exploited ferruginous rock. The high presence of iron can be conferred a metallic aspect and nuances from deep red to violet-red. The blocks or nodules of raw materials would be selected for their colouring properties and chosen based on specific tints.

The scarce presence of other orange, red-brown and yellow minerals documents this human choice. Moreover, the absence of large pieces in each of the studied contexts could indicate a privileged selection of pieces of not very large size, with a hardness that would allow the fragmentation and reduction in powder.

Analysing the question of supply in a diachronic sense, some interesting elements emerge. In the Iberian Peninsula, the procurement of red ochre is more intense at La Garma A, in the Upper Palaeolithic. This element is in direct comparison with the Galería Inferior, in the lower level of same karstic complex. This site returns extraordinary correspondences with the upper level (La Garma A) allowing the contextualization of several evidences as artificial structures, accumulations of faunal remains and lithic tools referable to an intense phase of occupation during the Middle Magdalenian. A change is observed towards the end of the Upper Palaeolithic that becomes more marked in the Mesolithic where the ochre accumulation in La Garma A decrease recording the epilogue of that golden phase experienced by the site in the Middle Magdalenian.

Regarding the Asturian sites as Los Canes and Arangas, it is possible to observe an inverse situation to that recorded in La Garma A. The ochre accumulations are rather scarce for the more ancient phases while there is a substantial

increase in the Mesolithic in correspondence with assiduous anthropic frequentation of the caves. Furthermore, in the two nearby sites of Los Canes and Arangas, the colouring raw materials are the same. This aspect allows significative reflections. The human groups that occupy these two cavities sporadically in the Upper Palaeolithic and assiduously in the Mesolithic were supplied from the same geological sources by selecting the same raw materials. In one case the raw materials arrived in an area of every-day activity (Arangas) and in a second case (Los Canes), in a space used to bury the defuncts. The supply of the same colouring materials favours a double reflection: the presence of different human groups in contact with each other and culturally similar, or a complementary occupation of the two environments by the same group (Arias, 2002) that buries the defuncts out of the living space.

Also, for the Italian Peninsula it is possible to observe a situation similar to the Cantabrian region. The human groups prefer highly ferric rocks (haematite) with bright red hues. A practice that persists in time and that reaches its peak during the Late Pleistocene (Final Epigravettian) drawing attention to what happens at La Garma A in the Middle Magdalenian. However, at Grotta di Pozzo the general question of the intensification of human activities could be depend directly from the climatic conditions. The rock-shelter, along with other caves, bordered a big lake (Lake Fucino) whose variations in level influenced human accessibility to the territory. At about 16,000-13,000 cal BP the highest temperatures testified by the low presence of eolian deposits in the caves of this area (Giraudi, 1997, 1998; Giraudi & Frezzotti, 1995), favoured the expansion of the prairie. In correspondence of this changes a substantial increase in colouring matters at the site is recorded. As shown by geological sampling in the Cantabrian region for studies of provenance (chap VI), dense vegetation can cover ferruginous deposits. The expansion of the prairie would have favoured a

greater visibility of the territory in general, and of the mineral sources. The hunter-gatherers could have easier access to the ochre deposits collecting more quantities. On the other hand, the supply of red ochre is a widespread practice among the Epigravettian groups that occupied the other caves around the Lake Fucino as Grotta Continenza, Grotta di Ortucchio, Grotta Maritza, Grotta Tronci (Radmilli, 1977, Serradimigni & Colombo, 2015). Comparisons that reveal the intentional selection of iron-rich red minerals also in these sites (Serradimigni & Colombo, 2015).

Although the study conducted involved numerous contexts with evidence of ochre in the archaeological record, the search for provenance was only possible in the Asturian territory in relation to the sites of Los Canes and Arangas. The simultaneous occupation of the sites (about 18,000-8,000 cal BP), as well as belonging to the same geological context, allowed a comparative study.

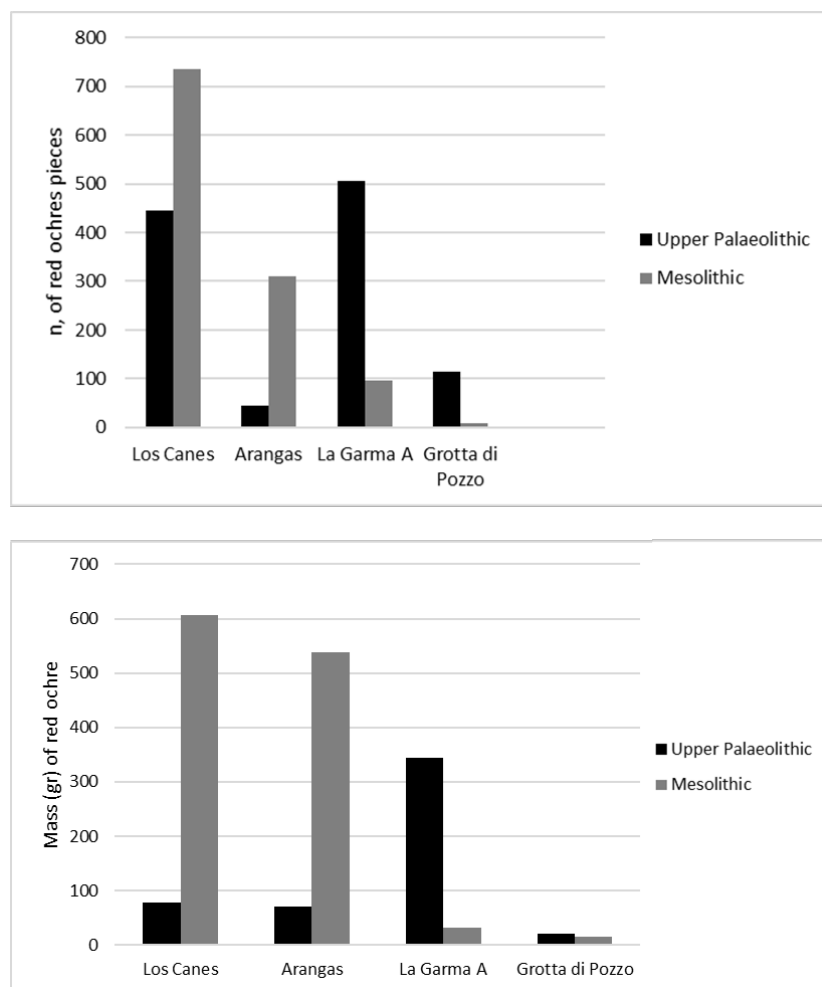


Fig.IX.1.: Comparison of the quantities (number and mass) of red ochre distribution in the sites analysed in this work among the Upper Palaeolithic and the Mesolithic.

As already reported, the raw materials found in the archaeological deposit of Los Canes and Arangas are the same. This geochemical affinity has led to the search for geological sources more or less distant from the sites to investigate which were the places in which the Palaeolithic and Mesolithic human groups supplied colorant resources. The geological survey carried out in the Asturian territory allowed to detect mineral richness of the formations surrounding the two cavities and the easy availability of red-coloured rocks compared to the yellow ones (goethite). At this point a question arises spontaneously: how can

we be sure that the abundance of red ochre depends directly on human subjective preferences and not on an objective availability of natural resources? Of course, establishing the degree of subjectivity in human choices is rather complex. In this case, it would be a matter of understanding the perceptive dimension of the Palaeolithic and Mesolithic hunter-gatherers in relation to the landscape in which they moved, reconstructing the cognitive processes underlying their decisions. The archaeological remains are the only positive evidences of the forms of human thought and on the basis of these testimonies, the hypothesis of a selection of raw materials for factors that disregard the ease of access to geological sources appears plausible. Especially if it takes into account some situations in which even the necessity of red colouring materials led to the heat treatment of goethite (yellow) as Riparo Dalmeri (Gialanella *et al.*, 2011) and Riparo Tagliente (Cavallo *et al.*, 2015). Therefore, about the criteria for selecting raw materials, the available data testify the high propensity towards hematite.

The reflections so far carried out, allow more 'extensive considerations. Regarding the selective criteria, it is possible to observe a change in relation to the dimension of red ochre pieces depending on the degree of anthropic occupation of the sites. The presence of bigger pieces in Palaeolithic units and of smaller pieces in Mesolithic units supporting the hypothesis of a selection of raw materials by sizes, as well as by colour (red). At La Garma A, for example, a lower concentration of ochre in the more recent units corresponds to a fragmentation increase and a progressive decrease of the larger pieces. This variation recorded in several units chrono-culturally differentiated, would draw the attention to a change in supply strategies according to cultural variations. However, the paleoenvironmental variations according to the paleoclimatic ones could modified the landscape and, consequently, the accessibility to the

geological sources. This aspect appears plausible also by considering the variations of the marine shells exploited in La Garma A probably related to climatic changes between the Late Glacial and Early Holocene (Álvarez-Fernández *et al.*, 2011).

IX.2. The *chaîne opératoire*

A dominant *chaîne opératoire* has been highlighted (Fig. IX. II) for the ochre processing. The sequence of gestures was implemented with the objective of obtaining a powder product, fragments or objects that can be used directly to transfer colour to another surface (e.g. *crayons*).

The sites where the operating sequences are best documented are the Iberian ones due to the presence of pieces with a diversified dimensional range (about 2-30 mm) and to the presence of pieces with use-wear traces and ochre processing tools (Arangas). A preliminary *roughing* of the raw material blocks would have preceded the *debitage* and the *crushing*. The reduced volume blocks would have been more or less crushed, by direct percussion with a hard tool, according to the final objective: *coarse crushing*-more coarse fragments; *fine crushing*-powder. The powder could also be obtained by abrading an ochre piece on an abrasive surface (tablet) or scored with a pointed instrument (chap. VII).

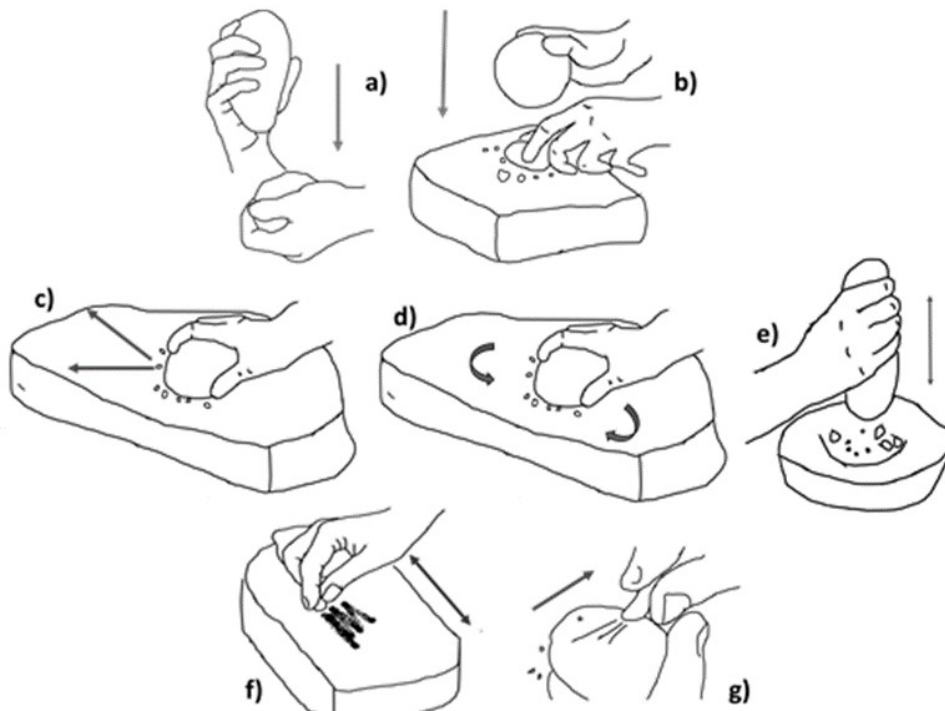


Fig.IX.2.: Reconstruction of the principal stages of the chaînes opératoire: a) *debitage*; b) *roughing*; c) *coarse crushing*; d-e) *fine crushing*; f) *abrasion*; g) *scoring*. The scheme includes all the phases identified for the processing of ochre. All phases are well attested in the Upper Palaeolithic units. In the Mesolithic units there is no evidence of *debitage*. In Los Canes the *scoring* is attested in the Mesolithic unit that precedes the burials (S.U.5). At La Garma A *scoring* and *grinding* have left no traces in the Mesolithic record. In Arangas there is no evidence of *scoring* for the recent phases.

This series of gestures appear well documented in the Upper Palaeolithic, whereas the lack of evidence of *debitage* products in the later stages do not allow to identify this operation in the Mesolithic. This diachronic difference draws the attention to the variation attested in the procurement strategies of raw materials. In the Mesolithic levels of sites such as La Garma A and Grotta di Pozzo, the mass of ochre is much lower than in the Upper Palaeolithic. The pieces are smaller and lighter. One could therefore raise the idea of a *debitage* related to the shaping of larger blocks that well characterized the levels of the Upper Palaeolithic. Even *scoring* is poorly documented in the Mesolithic

compared to other processing steps. If it considers the evidences of this operation (chap. VII), it is possible to make significant reflections. The materials associated with the burials of Los Canes show evident traces of *grinding* and *rubbing*, but there are no traces of *scoring*. Ultimately, the obtaining of a dusty *scoring* product suggests that this operation related to human activities carried out in domestic contexts, in a daily dimension.

Another issue is the presence of faceted objects (*crayons*) both in the Upper Palaeolithic and the Mesolithic. The different morphologies brought to light highlight human intentionality in realizing pre-determined forms, adapting also natural forms to the functionality of the object. Certainly, the preparation of these objects presupposes a specific use of the ochre for transfer of colour on a surface.

About the presence of ochre processing tools in Arangas, it is not possible to relate these objects with ochre vestiges. In any case, this finding provides indications on the general processing of ochre. The instruments show the traces of the reduction in red ochre powder. Some of them show direct contact with an intense red liquid substance, raising the idea of making ochre-based liquids.

In fact, all these elements that converge towards the mechanical transformation of ochre add up the accumulations in the ground and the residues on objects (Los Canes and Grotta di Pozzo) that attest to the presence of a powder product.

Considering the above, it is possible to make a greater reflection: the variations highlighted in the transformation of ochre would not seem to concern *crushing* and *grinding* operations. For this reason, the main objective is to obtain a powder product.

To conclude, the comparative observation of the Iberian and Italian contexts allows a final reflection. The technical correspondences highlighted on a continental scale could be related to the diachronic exploitation of the same type of raw materials.

IX.3. Management of ochre in the archaeological sites

From the analysis of ochre spatial distribution on the archaeological surface, it is possible to deduce an organization of the space in relation to the anthropic activities carried out on the sites. The distribution of colouring materials highlights a subdivision of living space into functional areas obtained both by exploiting the natural physical characteristics of the habitat, e.g.: depressions in the rocky wall (Los Canes, Arangas) and by building artificial structures (La Garma A). The available evidences would indicate the presence of spaces reserved for the management of colouring materials. In some cases, these areas coincided with spaces also used for other activities essential for the life of the group such as the processing of hunted animals or the chipping of the stone (La Garma A). However, the correspondences emerged with this research allow to make an interesting consideration. In the Iberian cavities such as La Garma, and Arangas, the significant concentrations of ochre are located towards the bottom of the cave, far from the access area that was the best illuminated part, but also more exposed to external factors such as atmospheric agents, etc ...

The comparison with the Italian region highlights a variation in the management of the space at Grotta di Pozzo where the greatest concentration of ochres and ochred artefacts (Final Epigravettian) can be observed in the front

part of the cave, facing north. It must be specified that the site has a different conformation from the Iberian cavities. It is a medium-sized rock-shelter with a wide opening well radiated by natural light in the early part of the day and in autumn. These aspects determine the creation of an internal microclimate and would have favoured the seasonal occupation of the site (Mussi *et al.*, 2008). As observed by the spatial distribution (chap. VIII) of the materials, the most significant concentrations are appreciated in the central part of the cave. Considering the presence of hearths and *vidange de foyer* on the back cave during the Final Epigravettian occupation, the wide central part was reserved for functional activities such as the management of colourants; while the back space, which offered greater protection against atmospheric agents, was suitable for the furnishing of hearths. This subdivision of the space is maintained over time. In the Mesolithic, despite the numerous disturbing elements such as the excavation of pits, the combination of ochred artefacts and ochre remains persist towards the centre of the cave attesting a continuity in the use of space.

In a synchronic-spatial perspective, it is possible to make some significant considerations: while on the one hand, some sites preserve this division of the space according to their use as a domestic site (Arangas, La Garma A, Grotta di Pozzo), on the other some contexts such as Los Canes show a radical transformation of the interior space over time. Although, on this site the Palaeolithic levels are well conserved in the back part of the vestibule and for this reason they do not allow to carry out conclusive reflections on the management of the colouring materials exclusively in this part of the cave. Certainly, the conspicuous presence of objects modified close to the north wall, in a well-defined area (chap. VIII), would support the idea of an area reserved for the management of the colorants on the site. During the Mesolithic, the site

was used as a place of burial. The available evidence attests the close relationship between ochres and human burials which is part of the symbolic dimension typical of prehistoric funeral rituality. This aspect permits more significant reflections on the connection between red ochre and the funeral sphere that could derive both from a specific practical ochre function and from a symbolic role of this material. The fact is that variations in the accumulation of ochre on the site mark the transition of the cave from a living place (Upper Palaeolithic) to a funerary place (Mesolithic).

These reflections, therefore, highlight the importance of colouring minerals in the life of Palaeolithic and Mesolithic hunter-gatherers and identify this category of materials as a valid support for the framing of the cultural trends of the human groups that exploited it.

IX.4. Hypotheses on ochre functions

So far, the study of archaeological remains highlighted three main aspects: the intense red colour of the most selected rocks, the mechanical transformation (shaping, fragmentation and powder reduction) and the ubiquity in domestic and funerary contexts of the Upper Palaeolithic and of the Mesolithic. It is well known that iron ores (oxides, hydroxides and oxyhydroxides) are widespread in nature and present in each of the components of the planet Earth: atmosphere, pedosphere, biosphere, hydrosphere and lithosphere (Cornell & Schwertmann, 2004). Therefore, the wide availability of these mineral resources could have triggered chain mechanisms in which the abundance of iron ores in anthropic contexts would have been favoured by the wide diffusion in nature. The conspicuous availability of these minerals would have attracted the human

groups who, after discovering their properties, would have widely used them in different ranges of their lives.

The data obtained from this research document the use of ochre in both domestic contexts, where the group's daily activities took place, and funerary contexts where the daily dimension was interrupted by the rituality of death. This aspect makes it possible significant considerations on the role of ochre in the life of Palaeolithic and Mesolithic hunter-gatherers and its value both utilitarian and symbolic. The archaeological evidences discussed in this work support the hypotheses of multiple uses of ochre: use on soft organic surfaces (animal skin and human skin), use as pigment, use as grave goods. These uses can also be added to the adhesive agent, hypothesized in previous research conducted at the Grotta di Pozzo (Catelli *et al.*, 2016).

The use on soft surfaces such as animal or human skin is a privileged hypothesis in contexts where some pieces of ochre show diagnostic traces of *rubbing*. The interpretation of these traces based on experimental references (Hodgskiss, 2010) and archaeological comparisons (Hodgskiss, 2013) would seem a sustainable thesis for the domestic contexts of La Garma A, Arangas and Los Canes. In this sense, ochre would assume a utilitarian value in the context of daily activities. A condition that finds both archaeological (Dubreuil & Grosman, 2009) and ethnographic (Bleek & Lloyd 1911; Couraud, 1991; Wadley *et al.*, 2004b) comparisons, furthermore assessed by experiments (Aoudin & Plisson, 1982; Rifkin, 2011).

The examination of materials revealed traces of this use on pieces from both Palaeolithic and Mesolithic units, also in association to burials. The information that these elements provide leads us to reflect on the continuity of this practice from the Late Glacial to the Holocene, supporting the thesis of a transmission of

knowledge. This idea is supported by the continuity over time of the main activities performed to process ochre (*roughing, crushing and grinding*). Furthermore, the discovery of these elements in human burials implies a symbolic value. The combination of data leads us to reflect on the possible application of ochre on the defunct skin, even if no residues are found on skeletal remains (Arias, pers.comm.). However, ethnographic comparisons support the hypothesis of a use of ochre to manage defunct during funerary practices both with a utilitarian (Berndt & Berndt, 1964) and symbolic value (Galton, 1853; Tönjes, 1911).

The discovery of ochre remains in other funerary contexts of the Upper Palaeolithic (Grotta del Romito and Grotta San Todoro) and of the Mesolithic (S'Omu and S'Orku), as shown by the comparative analyses (chap. V), is a not occasional aspect, which supports the hypothesis of the existence of a ritual system in which the use of red ochre becomes a formalized behaviour in the burial of the individuals.

The involvement of iron ores in the funeral sphere could favour a double interpretation: ochre as a symbol of cultural identity or as a reflection of a practical need based on the antiseptic, antibacterial and desiccant properties of iron oxides (chap. I).

In the first case, ochre would have a symbolic value as an expression of behaviour derived within the human group's ideological system. This theory would explain the synchronic variations on a continental scale between the Asturian Mesolithic (Los Canes: fragments of ochre mixed with the sediment that fills the burials and, in some cases, *crayons* used as grave goods) and the Italian Mesolithic (S'Omu and S'Orku: ochre powder impregnates the bones of the deceased, while fragments appear scattered in the deposit).

In the second case, ochre would have a functional role based on a utilitarian use for its physical-chemical properties that could have interacted with the inhumation practice (chap. I). A further aspect places the ochre at the centre of prehistoric funeral ritual. As previously discussed, *crayons* (faceted objects with traces of rubbing on a surface to transfer the colour) were found next to the inhumate of the tomb III of Los Canes. This aspect leads us to question the relationship of these objects with the deceased. First of all, it is necessary to specify that the combination of the diagnostic traces with the faceted morphology documents the presence of these objects also in the Upper Palaeolithic units of the site rejecting the hypothesis of an exclusive use of *crayons* as grave goods. So, it is possible to make a dual consideration: the use of ochre pieces to transfer colour on a surface and the maintenance of this technology over time.

The exploitation of ochre pieces as *crayons* is a widely documented practice in prehistory (Couraud, 1983; San Juan, 1990; Henshilwood *et al.*, 2001; Watts, 1998; Henshilwood *et al.*, 2001; Wadley, 2005). Furthermore, the presence of *crayons* suggests the use of ochre as a colorant as these objects were used to transfer colour onto surfaces (chap. VII). This aspect implies an ochre use as pigment. This use could be associated with a symbolic value (Deacon, 1995; Knight *et al.*, 1995; Power, 1999; 2009; Power & Aiello, 1997; Power *et al.*, 2013; McBrearty & Brooks, 2000; Henshilwood & Marean, 2003; Henshilwood *et al.*, 2009; Watts, 2002; 2009; 2010).

Ochre can be used to draw abstract or concrete concepts with symbolic value, on an object or a surface. In this case the sign is a bearer of meaning.

Or the pigment identifies an object or an individual as part of a cultural system. In this sense, the function of ochre as element of grave goods fits well with the symbolic value, suggesting its role as a marker of cultural identity.

The use of ochre as pigment is also attested by residues on shell-ornaments such as in Los Canes (two specimens of *Trivia* sp. and a *Littorina obtusata*) and in Grotta di Pozzo. On this last site, a detailed study of the materials (Brunelli *et al.*, 2016) highlighted the presence of red ochre on 1 *Cyclope neritea*, 1 *Glycimeris* sp. and 1 *Columbella rustica* from the levels of the Final Epigravettian and 14 specimens of *Columbella rustica* and 26 specimens of *Antalis dentalis* from the Sauveterrian levels. Concerning La Garma A, the use of ochre as pigment is suggested by the conspicuous quantities of ochre processed in the Middle Magdalenian coeval with some parietal red paintings in the Galería Inferior (Arias *et al.*, 2011; Gay *et al.*, 2015) from which could directly access from La Garma A.

The colouring power of ochre is certainly the best-known property of iron oxides (Cornell & Schwertmann, 2004; Triat, 2011) which induces almost immediate deductions. However, as shown by this research, the exploitation of ochre to obtain colouring substances is only one of the uses hypothesise for this material.

Regarding the use of ochre as an adhesive agent, the data collected during previous investigations carried out at Grotta di Pozzo document this function. The examination of lithic artefacts from Epigravettian and Sauveterrian levels (Catelli, 2014) highlighted the presence of red ochre residues on potentially hafted objects. The geochemical characterization of these residues confirmed the presence of iron oxides (hematite) supporting this thesis. This function does not appear documented in the other sites object of this research.

The available data point the attention to the link between use and function (utilitarian/symbolic) in relation to the context. This research shows that the utilitarian/symbolic opposition, in the Upper Palaeolithic and Mesolithic does not appear so clear. In domestic contexts and funerary contexts, the utilitarian and symbolic function of ochre can interlace, preventing a direct discussion of the two functions separately. At this point, it is more appropriate to discuss a daily use (domestic context) and a ritual use (funerary context).

Ultimately, according to the reflections carried out so far, on a regional scale, the use of ochre would allow a consideration on the affinity between Palaeolithic and Mesolithic technical traditions in which ochre assume a certain value depending on the place occupied in the life of human groups. The variations brought to light depend on the satisfaction of different human needs according to the context of use (domestic/funerary).

Conclusions

The role of ochre in south-western Europe

Considering what has been exposed so far, significant elements emerge to reflect on the role of ochre in south-western Europe during the Upper Palaeolithic and the Mesolithic. First of all, it is clear the preferential procurement of red rocks rich in iron on a continental scale, both in dwelling areas and sepulchral places. Moreover, ochre processing is highlighted through a series of steps aimed to obtain a product in fine fraction or, in some cases, modelling blocks or nodules of raw materials to obtain objects suitable to transfer colour on a surface (*crayons*). The different transformations could have been carried out simultaneously during the processing of raw materials.

In any case, the abundant quantities of red ochre and the evidence of its anthropic exploitation in the Upper Palaeolithic as well as in the Mesolithic emphasize a significant investment of time and human energy, from the procurement to the mechanical transformation. Thus, the not secondary role of ochre in the life of hunter-gatherer is clear highlighting a cultural common *substratum* to geographically distant human groups.

The ochre is used to satisfy human needs by charging both a utilitarian and a symbolic meaning. The exploitation of this material crosses the significant socio-economic changes that involve human cultures in the transition from the Pleistocene to the Holocene. This continuity is evident in the processing techniques that would indicate a transmission of skills in relation to the

exploitation of the same types of natural resources. Even in the ochre uses, it would recognize an element of connection between the Upper Palaeolithic and the Mesolithic, moderating the idea of a separation between the cultural traditions raised in the Pleistocenic environment and those of the Early-Middle Holocene.

The ochre appears as an extremely versatile material that, for its physical-chemical properties, occupies a significant place in the prehistoric human dimension. Its ubiquity in domestic and funerary contexts, in which it is widely used, documents this non-marginal role. The ochre could identify itself as a useful resource for the life of the hunter-gatherers, also as an element of contact between the "living" and the "dead".

In conclusion, from the analysis of the archaeological evidence it is not possible to establish fixed parameters to clearly separate functional use and symbolic use of ochre. This material plays a key role in the human cultures of the Upper Palaeolithic and Mesolithic as *signifier* and *signified*. The material itself, the ferruginous rock, corresponds to the *signifier* as a "tangible and visible element" that bears a meaning depending on its mental representation, the idea that the sight of this material evokes in the human mind. The correlation between *signifier* and *signified* is expressed in the sign. When this sign is recognized and shared by the members of a group becomes a symbol. In this sense, ochre does not have a fixed meaning, its value is relative and depends not on its function, but on the place occupied in human life.

Conclusiones

El papel del ocre en el suroeste de Europa

Teniendo en cuenta lo que se ha expuesto hasta ahora, emergen elementos significativos para reflexionar sobre el papel del ocre en el suroeste de Europa durante el Paleolítico Superior y el Mesolítico. En primer lugar, está claro el aprovisionamiento preferencial de rocas rojas ricas de hierro a una escala continental, tanto en contextos domésticos como en contextos funerarios. Además, el procesamiento del ocre se destaca a través de una serie de pasos para obtener un producto en fracción fina o, en algunos casos, modelar bloques o nódulos de materias primas para obtener objetos adecuados para transferir color sobre una superficie (*lápices*). Las diferentes transformaciones podrían haberse llevado a cabo simultáneamente durante el procesamiento de las materias primas.

En cualquier caso, las abundantes cantidades de ocre rojo y la evidencia de su explotación antrópica tanto en el Paleolítico Superior como en el Mesolítico desvelan una importante inversión de tiempo y energía humana, desde el aprovechamiento hasta la transformación mecánica. Por lo tanto, el papel no secundario del ocre en la vida de los cazadores-recolectores es claro, destacando un sustrato cultural común a grupos humanos geográficamente distantes.

El ocre ha sido utilizado para satisfacer las necesidades humanas cargándose de un significado tanto utilitario como simbólico. La explotación de este material atraviesa los cambios socio-económicos significativos que involucran a las

culturas humanas en la transición del Pleistoceno al Holoceno. Esta continuidad es evidente en las técnicas de procesamiento que indicarían una transmisión de habilidades en relación con la explotación de los mismos recursos naturales. Incluso en los usos del ocre, se podría reconocer un elemento de conexión entre el Paleolítico Superior y el Mesolítico, moderando la idea de una separación entre las tradiciones culturales del Pleistocénico y del Holoceno Temprano-Medio.

El ocre se presenta como un material muy versátil que, por sus propiedades físico-químicas, ocupa una posición significativa en la dimensión humana prehistórica. Su ubicuidad en contextos domésticos y funerarios, en los que se usa ampliamente, documenta este papel no marginal. El ocre podría identificarse como un recurso útil para la vida de los cazadores-recolectores, también como un elemento de contacto entre los "vivos" y los "muertos".

En conclusión, a partir del análisis de las evidencias arqueológicas, no es posible establecer parámetros fijos para separar claramente el uso funcional y el uso simbólico del ocre. Este material desempeña un papel clave en la cultura humana del Paleolítico Superior y del Mesolítico como *significante* y *significado*. El material en sí, la roca ferruginosa, corresponde al *significante* como un "elemento tangible y visible" que tiene sentido según su representación mental, la idea que la vista de este material evoca en la mente humana. La correlación entre el *significante* y el *significado* se expresa en el signo. Cuando este signo es reconocido y compartido por los miembros de un grupo se convierte en un símbolo. En este sentido, el ocre no tiene un significado fijo, su valor es relativo y no depende de su función, sino del lugar ocupado en la vida humana.

Conclusioni

Il ruolo dell'ocra nell'Europa sud-occidentale

Alla luce di quanto esposto sino ad ora, emergono degli elementi significativi per riflettere sul ruolo dell'ocra nell'Europa sudoccidentale durante il Paleolitico Superiore ed il Mesolitico. Prima di tutto, è chiaro l'approvvigionamento preferenziale di rocce rosse ricche di ferro su scala continentale, sia in contesti abitativi che in luoghi sepolcrali. Inoltre, si evidenzia un processamento dell'ocra una serie di passaggi volti ad ottenere un prodotto in frazione fine o, in alcuni casi, al modellamento di blocchetti o noduli di materie prime per ottenere oggetti adatti al trasferimento di colore su una superficie (*crayon*). Le diverse trasformazioni sarebbero state eseguite contemporaneamente durante la lavorazione delle materie prime.

In ogni caso, le abbondanti quantità di ocra rossa e l'evidenza del suo sfruttamento antropico nel Paleolitico Superiore e nel Mesolitico sottolineano un significativo investimento di tempo e di energie umane, dall'approvvigionamento alla trasformazione meccanica. Quindi, il ruolo non secondario dell'ocra nella vita dei cacciatori-raccoglitori appare chiaro evidenziando un substrato culturale comune a gruppi umani geograficamente distanti.

L'ocra è usata per soddisfare i bisogni umani caricandosi di un significato sia utilitario che simbolico. Lo sfruttamento di questo materiale attraversa i cambiamenti socio-economici che coinvolgono le culture umane nella

transizione dal Pleistocene all'Olocene. Questa continuità è evidente nelle tecniche di elaborazione che indicherebbero una trasmissione di competenze in relazione allo sfruttamento degli stessi tipi di risorse naturali. . Anche nei potenziali usi dell'ocra si riconoscerebbe un elemento di connessione tra il Paleolitico Superiore e il Mesolitico riducendo l'idea di una cesura netta tra le tradizioni culturali maturate nell'ambiente pleistocenico e quelle dell'Olocene Medio-Iniziale.

L'ocra appare come un materiale estremamente versatile che, per le sue proprietà fisico-chimiche, occupa un posto significativo nella dimensione umana preistorica. La sua ubiquità nei contesti domestici e funerari, in cui è ampiamente utilizzata, documenta questo ruolo non marginale. L'ocra potrebbe identificarsi come una risorsa utile per la vita dei cacciatori-raccoglitori, anche come elemento di contatto tra i "vivi" e i "morti".

In conclusione, dall'analisi delle evidenze archeologiche non è possibile stabilire parametri fissi per scindere nettamente uso funzionale e uso simbolico dell'ocra. Essa gioca un ruolo chiave nelle culture umane del Paleolitico Superiore e del Mesolitico in quanto *significante* e *significato*. Il materiale in se', la roccia ferruginosa, corrisponde al *significante* in quanto "forma tangibile e visibile" portatrice di un *significato* ovvero la sua rappresentazione mentale, l'idea che la vista di questo materiale evoca nella mente umana dei cacciatori-raccoglitori. La correlazione tra *significante* e *significato* si esprime nel *segno*. Nel momento in cui questo *segno* viene riconosciuto e condiviso dai membri di un gruppo diventa un *simbolo*. In questo senso, l'ocra non ha un significato invariabile, il suo valore e' relativo e dipende non dalla sua funzione, ma dal posto che va ad occupare nella vita umana.

References

Adaro, L. De, Y Junquera, G., 1916. Criaderos de hierro de España; tomo 11, Hierros de Asturias, Memorias del Instituto Geológico y Minero de España, Criaderos de hierro de España, 2: 610.

Allain, J., Rigaud, A., 1989. Colles et mastics au Magdalénien., in: Olive, M., Taborin, Y. (Eds.), Nature et fonction des foyers préhistoriques. Actes du Colloque international de Nemours (12-14 mai 1987), Association pour la Promotion de la Recherche Archéologique en Ile-de-France, Nemours, pp. 221-223.

Allard, M., Drieux, M., Jarry, M., Pomiès, M.-P., Rodière, J., 1997. Perles en bois de renne du niveau 18 des Peyrugues, Orniac (Lot): hypothèse sur l'origine du Protomagdalénien. *Paléo*, 9: 355-369.

Alarashi, H., 2014. La parure épipaléolithique et néolithique de la Syrie (XIIe au VIIe millénaire avant J.-C.): techniques et usages, échanges et identités. Université Lumière-Lyon 2, Lyon. PHD thesis.

Alonso, J.L., Marcos, A., y Suárez, A. (2009): Paleogeographic inversion resulting from large out of sequence breaching thrusts: The León Fault

(Cantabrian Zone, NW Iberia). A new picture of the external Variscan Thrust Belt in the Ibero-Armorican Arc. *Geologica Acta*, 4: 451-473.

Altamura, F., Catelli, E., Gazzoli, D., Mussi, M. "Caracterización superficial de pigmentos sobre artefactos Paleolíticos de la zona de los Montes Albanos (Roma, IT) por microscopia óptica y espectroscopia Raman", 2016. *digitAR*, 3: 7-13.

Álvarez-Fernández, E., Chauvin, A., Cubas, M., Arias Cabal, P., Ontañón R., 2011. Mollusc Shell Sizes in Archaeological Contexts in Northern Spain (13 200 to 2600 Cal Bc): New Data From La Garma A And Los Gitanos (Cantabria). *Archaeometry*, 53, 5: 963-985.

Anand, R.R., Gilkes, R.J., Roach, G.I.D., 1991. Geochemical and mineralogical characteristics of bauxites, Darling Range, Western Australia. *Applied Geochemistry*, 6 (3): 233-248.

Anca F., 1860. Note sur deux nouvelles grottes ossifères découvertes en Sicile en 1859. *Bulletin de la Société géologique de France*, 17: 684-695.

Anthony, J.W., Bideaux, R.A., Bladh, K.W., and Nicois, M.C., 1997. Handbook of Mineralogy. Volume III: Halides, Hydroxides, Oxides. Tucson (Mineral Data Publishing), <http://www.handbookofmineralogy.org/>.

Aranguren B., Revedin A. 1996. Problemi relativi all'insorgenza del Mesolitico in Sicilia. In: Early Societies in Sicily, a cura di Leighton R: Londra.

Aranzadi, T., Barandiaran, J.M., 1935. Exploraciones en la caverna de Santimamiñe (Basondo:Cortézubi). Tercera memoria, yacimientos Azilienses y Paleolíticos. Exploraciones de la caverna de Lumentxa (Lekeitio). Excma. Diputación de Vizcaya. Bilbao.

Arias Cabal, P. 1999. Antes de los cántabros. Panorama del Neolítico y las Edades de los Metales en Cantabria. En AAVV. 1999. I Encuentro de Historia de Cantabria, Vol. I, Universidad de Cantabria, Gobierno de Cantabria, Santander.

Arias Cabal, P., 2002. La cueva de Los Canes (Asturias): Los últimos cazadores de la Península Ibérica ante la muerte. Universidad de Cantabria.

Arias Cabal, P., 2013. Los últimos cazadores. El mesolítico asturiano visto desde la cueva de Los Canes. In: De Blas Cortina M. Á.. 2013. De neandertales a albigones: cuatro lugares esenciales en la Prehistoria de Asturias. Real Instituto De Estudios Asturianos Principado De Asturias.

Arias Cabal, P., Gil Álvarez, G., Martínez Villa, A., Pérez Suárez, C., 1981. Nota sobre los grabados digitales de la cueva de Los Canes (Arangas, Cabrales). *Boletín del Instituto de Estudios Asturianos*, 104: 937-956.

Arias Cabal, P., Pérez Suarez, C., 1990. Las sepulturas de la cueva de los Canes (Asturias) y la neolitización de la región Cantábrica. *Trabajos de Prehistoria*, 47: 39-62.

Arias Cabal, P. Y Pérez Suárez, C., 1995. Excavaciones arqueológicas en Arangas, Cabrales (1991-1994). Las cuevas de los Canes, el Tiu Llines y Arangas.

Excavaciones arqueológicas en Asturias 1991-94: 79-92. Oviedo: Servicio de Publicaciones del Principado de Asturias.

Arias Cabal, P., Garralda, M.D., 1996a. Les sépultures épipaléolithiques de la Cueva de los Canes (Asturies, Espagne). In : Otte, M. (dir.), *Nature et Culture. Actes du colloque international de Liège. 13-17 décembre 1993*, vol II: 871-897. Liège: Université de Liège (Études et Recherches Archéologiques de l'Université de Liège 68).

Arias Cabal, P., Garralda, M.D., 1996b. Mesolithic burials in Los Canes cave (Asturias, Spain). *Human Evolution*, 11, (2): 129-138.

Arias Cabal, P., Ontañón, R., Alvarez, E., Aparicio, M.T., Chauvin, A., Conte, I., Cueto, M., González, J.E., Ibañez, J.J., Tapia, J., Teira, L., 2005. La estructura magdaleniense de La Garma A. In: Bicho, N. (Ed.), *O Paleolítico. Actas do IV Congresso de Arqueologia Peninsular, Promontoria Monográfica 2*, Faro, pp. 123-141.

Arias Cabal, P., Cerrillo-Cuenca, E., Álvarez Fernández, E., Gómez Pellón, E., González Cordero, A., 2009. A view from the edges: the Mesolithic settlement of the interior areas of the Iberian Peninsula reconsidered. In: McCartan, S., Schulting, R., Warren, G., Woodman, P., (eds), *Mesolithic Horizons*, 303-311. Oxford Books.

Arias Cabal, P., Armendariz, A., de Balbín, R., Fano, M.A., Fernández-Tresguerres, J., González Morales, M.R., Iriarte, M.J., Ontañón, R., Alcolea, J., Álvarez-Fernández, E., Etxeberria, F., Garralda, M.D., Jackes, M., Arrizabalaga,

Á., 2009. Burials in the cave: new evidence on mortuary practices during the Mesolithic of Cantabrian Spain. In: Mc Cartan, S. *et al.* (eds). Mesolithic Horizons. Papers presented at the Seventh International Conference on the Mesolithic in Europe, Belfast 2005. Oxbow Books. Oxford: 650-656.

Arias Cabal, P., Laval, E., Menu, M., González Sainz, C., Ontañón, R., 2011. Les colorants dans l'art pariétal et mobilier paléolithique de La Garma (Cantabrie, Espagne). *L'Anthropologie*, 115: 425-445.

Arias Cabal, P., Ontañón, R., 2012. La Garma (Spain): Long-term human activity in a karst system. In: 422 Skeates, K.A.B.a.R. (Ed.), *Caves in Context. The Cultural Significance of Caves and 423 Rockshelters in Europe*. Oxbow, Oxford pp. 101-117.

Arias Cabal, P., Álvarez-Fernández, E., Cubas, M., Teira, L., Tapia, J., Cueto, M., Fernández Sánchez, P., López-Dóriga, I., 2014. Intervención arqueológica en el sistema cárstico de Arangas (Cabrales). Campaña de 2007. *Excavaciones Arqueológicas En Asturias 2007-2012*, 7: 121-133.

Attard Montalto, N., Shortland, A., and Rogers, K., 2012, The provenancing of ochres from the Neolithic Temple Period in Malta, *Journal of Archaeological Science*, 39 (4), 1094–102.

Aubert, M., Brumm, A., Huntley, J., 2018. Early dates for “Neanderthal cave art” may be wrong. *Journal of Human Evolution*, in press.

Audouin, F., Plisson, H., 1982. Les ocres et leurs témoins au Paléolithique en France: enquête et expériences sur leur validité archéologique. Cahiers du Centre de Recherches Préhistoriques, 8: 33-80.

Aura, J.E., Tiffagom, M., Jordá Pardo, J.F., Duarte Matías, E., Fernández de la Vega Medina, J., Santamaría Álvarez, D., Rasilla Vives, M. de la, Vadillo, M., Pérez Ripoll, M., 2012. The Solutrean–Magdalenian transition: a view from Iberia. *Quaternary International*, 272, (3): 75–87.

Baffier, D., Girard, M., Menu, M., Vignaud, C., 1999. La couleur à la grande grotte d'Arcy-sur-Cure (Yonne). *L'Anthropologie* 103: 1–21.

Balbín Behramm, R de., Alcolea González, J. J., 2005. Espace d'habitation, espace d'enterrement, espace graphique. Les coïncidences et les divergences dans l'art paléolithique de la corniche cantabrique. In: Vialou, D., Renault-Miskowsky, J.; Pathou-Mathis, M. Ed. 2005. Comportements des hommes du Paléolithique moyen et supérieur en Europe: territoires et milieux. Actes du colloque du G. D. R. 1945 du CNRS. Paris. 8-10 Janvier 2003. ERAUL. N° 111. Liège: 193-206.

Bar-Yosef, O., Vandermeersch, B., Arensburg, B., Belfer Cohen, A., Goldberg, P., Laville, H., Meignen, L., Rak, Y., Speth, J. D., Tchernov, E., Tillier, A-M., Weiner, S., 1992. The Excavations in Kebara Cave, Mt. Carmel. *Current Anthropology*, 33 (5): 497.

Barrera-Bassols N, Zinck J.A., 2000. Ethnopedology in a worldwide perspective. Enschede, The Netherlands.

Bailleau, J.-G. 1869. Grotte des Fées de Chatelperron. Desrosiers, Moulins.

Barham, L., 1998. Possible early pigment use in south-central Africa. *Current Anthropology*, 39: 703-710.

Barham, L., 2002. Systematic pigment use in the Middle Pleistocene of south-central Africa. *Current Anthropology*, 43: 181-190.

Barham, L., Mitchell, P., 2008. *The First Africans: African Archaeology from the Earliest Toolmakers to Most Recent Foragers*. Cambridge World Archaeology.

Basedow, H., 1925. *The Australian Aboriginal*. Preece and Sons, Adelaide.

Beaumont, P., Vogel, J., 2006. On a timescale for the past million years of human history in central South Africa. *South African Journal of Science*, 102: 217-228.

Beck, L., Lebon, M., Pichon, L., Menu, M., Chiotti, L., Nespoulet, R., Paillet, P., 2011. PIXE characterization of prehistoric pigments from Abri Pataud (Dordogne, France). *X-Ray Spectrometry*, 40: 219-223.

Beck, L., Rousselière, H., Castaing, J., Duran, A., Lebon, M., Moignard, B., Plassard, F., 2014. First use of portable system coupling X-ray diffraction and X-ray fluorescence for in-situ analysis of prehistoric rock art, *Talanta*, 129: 459-464.

Becker, M., Wendorf, F., 1993. A micro wear study of a late Pleistocene Qadan assemblage from Egypt. *Journal of Field Archaeology*, 20: 389-398.

Beyries, S., Inizan, M.L., 1982. Typologie, ochre, fonction. In: Cahen, D. (Ed.), *Tailler! Pour quoi faire*. Muséum de l'Afrique centrale, Tervuren, pp. 313-322.

Beyries, S., 1983. Fonction et mode d'utilisation d'une série de lames ocrées capsienes. In: Cauvin MC (ed) *Traces d'Utilisation Sur Les Outils Néolithiques Du Proche Orient*. Maison de L'Orient, Lyon, pp 135–142

Beyries, S., Walter, P., 1996. Raclours et colorants à Combe-Grenal: le problème de la retouche Quina. *Quaternaria Nova*, 6, 167-185.

Bicho, N., Carvalho, A.F., González Sainz, C., Sanchidrián, J.L., Villaverde, V., Straus, L.G., 2007. The Upper Paleolithic Rock Art of Iberia. *Journal of Archaeological Method and theory*, 14, (1): 81–151.

Binford, L. R. 1980. Willow Smoke and Dogs' Tails: Hunter-Gatherer Settlement Systems and Archaeological Site Formation. *American Antiquity*, 45, (1): 4-20.

Bisconti, M., Mallegni, F., Martini, F., Ricci, S., 2005. Le sepolture Romito 7 e Romito 8: paleobiologia dei resti umani. XV Congresso dell'Associazione Antropologica Italiana, Variabilità umana e storia del popolamento in Italia, Chieti, I: 101-109.

Bisegna A., D'angelo E., Gioia P., Mussi M., 2011. Raccolta e cottura delle lumache in Abruzzo: preistoria e attualità in Lugli F., Stoppiello A. A., Biagetti S. (a cura di) *Atti del 4° Convegno Nazionale di Etnoarcheologia*, BAR International Series 2235, Roma, pp. 95-101.

Bleek, W.H.I. & Lloyd, L.C., 1911. *Specimens of Bushman folklore*. London: George Allen & Company.

Blockley, S., Pellegrini, M., Colonese, A.C., Lo Vetro, D., Albert, P.G., Brauer, A., Di Giuseppe, Z., Evans, A., Harding, P., Lee-Thorp, J., Lincoln, P., Martini, F., Pollard, M., Smith, V., Donahue, R., 2017. Dating human occupation and adaptation in the southern European last glacial refuge: The chronostratigraphy of Grotta del Romito (Italy). *Quaternary Science Reviews*, XXX: 1-21.

Bonfiglio, L., 1983. Prima campagna di scavo dei depositi a Mammiferi pleistocenici dell'area della grotta di S.Teodoro (Acquedolci, Messina, Sicilia). (1983), *Geologica Romana*, 22: 271-285.

Bonfiglio, L., Mangano, G., Martinelli, M.C., 2005. I tesori della preistoria siciliana ad Acquedolci e alla Grotta di S. Teodoro. Università degli Studi di Messina, Dipartimento di Scienze della Terra. Guida alla mostra perenne.

Bonneau, A., Pearce, D.G., Pollard, A.M., 2012. A multi-technique characterization and provenance study of the pigments used in San rock art, South Africa. *Journal of Archaeological Science*, 39, 287-294.

Bordes, F., 1952. Sur l'usage probable de la peinture corporelle dans certaines tribus moustériennes. *Bulletin de la Société préhistorique française*, 49, 169-17.

Boucquetin, F., Bar-Yosuf, O., 2004. Early Natufian remains: evidence for physical conflict from Mt. Carmel, Israel. *Journal of Human Evolution*, 47: 19-23.

Bouyssonie, J., 1923. Station préhistorique aurignacienne de Bos- del-Ser (Corrèze). In: Association Française pour l'Avancement des Sciences, pp. 617-622, 47^e session.

Bouzouggar, A., Barton, N., Vanhaeren, M., d'Errico, F., Collcutt, S., Higham, T., Hodge, E., Parfitt, S., Rhodes, E., Schwenninger, J.-L., Stringer, C., Turner, E., Ward, S., Moutmir, A., Stambouli, A., 2007. 82,000-year-old shell beads from North Africa and implications for the origins of modern human behavior. *PNAS*, 104 (24): 9964-9969.

Breuil, H., 1912. Les Subdivisions du Paléolithique Supérieur et Leur Signification. XIV Congrès International d'Anthropologie et d'Archéologie Préhistoriques, I : 165-238.

Breuil, H., 1940. Découverte d'une remarquable grotte ornée, au domaine de Lascaux, Montignac (Dordogne). *Comptes rendus des séances de l'Académie des Inscriptions et Belles-Lettres*, 84^e année, 5 : 387-390.

Broglio, A., 1997. Considérations sur l'Epigravettien italique. In J.M.Fullola & N. Soler eds., *El mon mediterrani després del Pleniglacial (18.000 - 12.000 B.P.)*. Girona, pp. 147-157.

Broglio, A., 1998. *Introduzione al Paleolitico*. Ed. Laterza.

Broglio A. & Lanzinger M., 1990. Considerazioni sulla distribuzione dei siti tra la fine del Paleolitico Superiore e l'inizio del Neolitico nell'Italia Nord-orientale. In: Paolo Biagi (a cura di), *The Neolithisation of the Alpine Region*. *Natura Bresciana*, 13: 53-69.

Brunelli, E., Catelli, E., Gargani E., Gazzoli, D., Mussi, M., 2016. Ornamenti e Pigmenti a Grotta di Pozzo (AQ): livelli epigravettiani e livelli sauveterriani. In:

Il Fucino e le aree limitrofe nell'antichità, Atti del IV Convegno di Archeologia. Avezzano, maggio 2015.

Byers, A. M., 1994. Symboling and the Middle-Upper Paleolithic transition: a theoretical and methodological critique. *Current Anthropology*, 35, 369–399.

Cabrera Garrido, J.M., 1978. Les matériaux de peinture de la caverne d'Altamira. Actes de la 5e réunion triennale du comité de conservation de l'ICOM, Zagreb. pp. 1–9.

Capitan, L. & Peyrony, D., 1921. Les origines de l'art à l'Aurignacien moyen-nouvelles fouilles à La Ferrassie. *Rev. Anthropol*, pp. 92–112.

Cârciumaru M., Țuțuianu-Cârciumaru M., 2009, L'ocre et les récipients pour ocre de la grotte Cioarei, village Boroșteni, commune Peștișani, dép. de Gorj, Roumanie, Annales d'Université Valahia Targoviste, Section d'Archéologie et d'Histoire, XI, 1 :7-19.

Cardini L., 1942. Nuovi documenti sull'antichità dell'uomo in Italia: reperto umano del Paleolitico Superiore nella Grotta delle Arene Candide. *Razza e Civiltà*, 3: 5-25.

Cardini L., 1980. La necropoli mesolitica delle Arene Candide (Liguria). *Memorie dell'Istituto Italiano di Paleontologia Umana*, 3: 9-31.

Caron, F., d'Errico, F., Del Moral, P., Santos, F., Zilhão, J., 2011. The reality of Neandertal symbolic behavior at the Grotte du Renne, Arcy-sur-Cure. *PLoS ONE* 6, e21545.

Cartailhac, E. & Breuil, H., 1906. La caverne d'Altamira à Santillane, près Santander (Espagne). Monaco.

Cavalcante, L. C. D., Luz, M. F., Guidon, N., Fabris, J. D., Ardisson, J. D., 2011. Ochres from rituals of prehistoric human funerals at the Toca do Enoque site, Piauí, Brazil. *Hyperfine Interactions* 203/1-3: 39-45.

Catelli, E., 2014. *Ler industrie litiche ocrate di Grotta di Pozzo (AQ): livelli epigravettiani e livelli sauveterriani*. Sapienza-Università di Roma. PHD thesis.

Catelli, E., De Angelis, G., Ruta, G., Fiore, I., Gazzoli, D., Mussi, M., 2016. La caccia a Grotta di Pozzo (AQ): armi e prede". In: *Il Fucino e le aree limitrofe nell'antichità*, Atti del IV Convegno di Archeologia. Avezzano, maggio 2015.

Cattelain P., Bozet N., Di Stazio, G., 2012. La parure de Cro-Magnon à Clovis. In: *Les Parures 417 au Paléolithique et au Mésolithique : coquillages, dents, os, ivoire et pierres*.

Cavallo G., Fontana F., Gonzato F., Guerreschi A., Riccardi M. P., Sardelli G., Zorzin R., 2015. Sourcing and processing of ochre during the late upper Palaeolithic at Tagliente Rock-shelter (NE Italy) based on conventional X-ray powder diffraction analysis. *Journal of Archaeological and Anthropological Sciences*, 9, (5): 763–775.

Ceccarini, 2014. Antropologia del paesaggio: il landscape come processo culturale.

Cendrero, A., Saiz de Omenaca, J., 1979. Geology of the Picos de Europa; a brief outline. *Memoire de la Société Botanique de Genève*, 1: 23-29.

Česnys G. Butrimas A., 2009. Reinventing Mesolithic skulls in Lithuania: Donkalis and Spiginas sites. *Acta Medica Lituanica*, 16, (1-2); 1-8.

Chalmin, E., Menu, M., Altuna, J., 2002. Les matières picturales de la grotte d'Ekain (Pays Basque). *Munibe*, 54, 35-51.

Chauchat, C., 1968. Les industries préhistoriques de la région de Bayonne, du Périgordien ancien à l'Asturien, vol. 2. Université de Bordeaux I. PHD thesis.

Chavaillon, J. & Berthelet, A., 2004. The archaeological sites of Melka Kunture, in: J. Chavaillon, M. Piperno (Eds.), *Studies on the Early Paleolithic Site of Melka Kunture, Ethiopia*, Florence, Istituto Italiano di Preistoria e Protostoria, pp. 25-80.

Clottes, J., Menu, M., Walter, P., 1990. La préparation des peintures magdaléniennes des cavernes ariégeoises. *Bulletin de la Société Préhistorique Française*, 87, 170-192.

Cooper, J.M., 1946. The Patagonian and Pampean Hunters, in: Steward, J.H. (Ed.), *Handbook of South American Indians*, vol. 1, The Marginal Tribes. Smithsonian Institution, Bureau of American Ethnology, Bulletin 143, Government Printing Office, Washington, D.C., pp. 127-168.

Combiér, F., 1989. Soyons, Grotte de Néron (Ardèche). Archéologie de la France, 30 Ans de la découverte. Editions de la Réunion des Musées Nationaux. Paris. 65.

Corchón Rodríguez, M.S., 1971. El Solutrense en Santander. Institución Cultural de Cantabria. Santander.

Corchón Rodríguez, M.S., 1981. Cueva de las Caldas. San Juan de Priorio (Oviedo). Excavaciones Arqueológicas en España, liS. Ministerio de Cultura. Madrid.

Cornell, R. M., & Schwertmann, U., 2004. The Iron Oxides: Structure, Properties, Reactions, Occurrences and Uses, Second Edition. Wiley-VCH Verlag GmbH & Co. KGaA.

Correnti, V., 1967. Risultati di uno studio perigrafico sui crani di S. Teodoro (Sicilia). *Rivista di Antropologia*, 54: 1-16.

Coulonges, L., 1930. Le Gisement Préhistorique du Martinet à Sauveterre-la-Lémance (Lot-et-Garonne). *Bulletin de la Société préhistorique française Année, 27*, (3) : 174-179.

Couraud, C., 1983. Pour une étude méthodologique des colorants préhistoriques. *Bulletin de la Société préhistorique française*, 80 (4): 104-110.

Couraud, C., 1991. Les pigments des grottes D'Arcy-sur-Cure (Yonne). *Gallia Préhistoire*, 33, 17-52.

Cremaschi M., Peretto C., 1988. Les sols d'habitat du site Paleolitique d'Isernia La Pineta (Molise, Italie Centrale). *L'Anthropologie*, 92 (4): 1017-1040.

Cristiani, E., Živaljević, I., Borić, D., 2014. Residue analysis and ornament suspension techniques in prehistory: Cyprinid pharyngeal teeth beads from Late Mesolithic burials at Vlasac (Serbia). *Journal of Archaeological Science*, 46: 292–310.

Cruz-Uribe, K., Klein, R. G., Avery, G., Avery, M., Halkett, D., Hart, T., Milo, R. G., Garth Sampson, C., Volman, T. P., 2003. Excavation of Buried Late Acheulean (Mid-Quaternary) Land Surfaces at Duinefontein 2, Western Cape Province, South Africa. *Journal of Archaeological Science*, 30 (5): 559-575.

Cuenca-Solana, D., Gutiérrez-Zugasti, F.I., González-Morales, M.R., Setién-Marquinez, J., Ruiz-Martinez, E., García-Moreno, A., Clemente-Conte, I., 2013. Shell Technology, Rock Art, and the Role of Marine Resources during the Upper Paleolithic. *Current Anthropology*, 54:3, 370-380.

Cuenca-Solana, D., Gutiérrez-Zugasti, I., Ruiz-Redondo, A., González-Morales, M.R., Setién, J., Ruiz-Martínez, E., Palacio-Pérez, E., de las Heras-Martín, C., Prada-Freixedo, A., Lasheras-Corruchaga, J.A., 2016. Painting Altamira Cave? Shell tools for ochre-processing in the Upper Palaeolithic in northern Iberia. *Journal of Archaeological Science*, 74: 135-151.

d'Errico, F., Henshilwood, C., Vanhaeren, M., van Niekerk, K., 2005. Nassarius kraussianus shell beads from Blombos Cave: evidence for symbolic behaviour in the Middle Stone Age. *Journal of Human Evolution*, 48, (1), 3-24.

d'Errico, F., 2008. Le rouge et le noir: implications of early pigment use in Africa, the near East and Europe for the origin of cultural modernity. *South African Archaeological Society Goodwin Series* 10, 168–174.

d'Errico, F., Vanhaeren, M., Wadley, L., 2008. Possible shell beads from the Middle Stone Age layers of Sibudu Cave, South Africa. *Journal of Archaeological Science*, 35 (10): 2675-2685.

d'Errico, F., Vanhaeren, M., 2009. Earliest personal ornaments and their significance for the origin of language debate, in: Botha, R., Knight, C. (Eds.), *The Cradle of Language*, Oxford. University Press, Oxford, pp. 16-40.

d'Errico, F., Salomon, H., Vignaud, C., Stringer, C., 2010. Pigments from the Middle Paleolithic levels of Es-Skhul (Mount Carmel, Israel). *Journal of Archaeological Science*, 37 (12): 3099-3110.

d'Errico, F., Henshilwood, C., 2011. The origin of symbolically mediated behaviour, in: Henshilwood, C., d'Errico, F. (Eds.), *Homo symbolicus: The Dawn of Language, Imagination and Spirituality*, John Benjamins Publishing Company, Amsterdam.

Dalmeri G. & Lanzinger M., 2002. L'evoluzione dell'ambiente e del popolamento umano del bacino dell'Adige alla fine del Tardiglaciale e nell'Olocene antico. In: *Preistoria e Protostoria del Trentino Alto Adige/Südtirol. Atti IIPP XXXIII, Trento 1997*: 25-32.

d'Errico, F., García Moreno, R. & Rifkin, R. F., 2012. Technological, elemental and colorimetric analysis of an engraved ochre fragment from the Middle Stone

Age levels of Klasies River Cave 1, South Africa. *Journal of Archaeological Science*, 39: 942–952.

de Faria, D. L. A.; Lopes, F. N., 2007. Heated goethite and natural hematite: Can Raman spectroscopy be used to differentiate them? *Vibrational Spectroscopy*, 45: 117-121.

Dayet, L., 2012. Matériaux, transformations et fonctions de l'ocre au Middle Stone Age. Le cas de Diepkloof Rock Shelter dans le contexte de l'Afrique austral. Université Michel de Montaigne Bordeaux 3. PHD thesis.

Dayet, L., Texier, P.-J., Daniel, F., Porraz, G., 2013. Ochre resources from the Middle Stone Age sequence of Diepkloof Rock Shelter, Western Cape, South Africa. *Journal of Archaeological Science*, 40: 3492-3505.

Dayet, L., d'Errico, F., Garcia-Moreno, F., 2014. Searching for consistencies in Châtelperronian pigment use. *Journal of Archaeological Science*, 44: 180-193.

Dayet, L., Le Bourdonnec, F.X., Daniel F., Porraz, G., Texier, P.J., 2015. Ochre provenance and procurement strategies during the middle stone age at Diepkloof rock shelter, South Africa. *Archaeometry*, 58: 807–829.

David, F., Connet, N., Girard, M., Miskovsky, J.-Cl, Mourer-Chauvire, C., Roblin Jouve, A., 2005. Les niveaux du Paléolithique supérieur de la grotte du Bison (Arcy-sur-Cure, Yonne): couches A à D. *Rev. Archéologique l'Est*, 54: 5-50.

de Sonnevile-Bordes, D., 2002. Les industries du Roc-de-Combe (Lot) : Périgordien et Aurignacien. *Préhistoire du sud-ouest* 9, (2): 121-161

de Mortillet, G., 1873. Classification des diverses périodes de l'Age de la Pierre. C.I.A.A.P., C.R. 6th session, Brussels (1872).

Deacon, H.J., 1995. Two Late Pleistocene-Holocene Archaeological Depositories from the Southern Cape, South Africa. *The South African Archaeological Bulletin*, 50 (162): 121-131.

Deer, W.A., Howie, R.A. and Zussman, J., 2013. An Introduction to the Rock-Forming Minerals, 3 ed. The Mineralogical Society, London.

Dei F. 2004. Tavola rotonda sul libro "Patrie elettive. I segni dell'appartenenza. In: I riti del fuoco e dell'acqua, Edup, Roma.

Della Porta G, Mamet A, Préat A., 2006. Bacterial mediation in the formation of red limestones, Upper Carboniferous, Cantabrian Mountains, Spain. In: Wong ThE (ed) Proceedings of the 15th International Congress on Carboniferous and Permian Stratigraphy. Utrecht, Royal Dutch Academy of Arts and Sciences, Amsterdam, pp 243–250

Delporte, H., Surmely, F., Urgal, A., 1999. Châtelperron: Un grand gisement préhistorique de l'Allier. Conseil Gene de l'Allier, Moulins

Demars, P.Y., 1992. Les colorants dans le Mousterien du Périgord L'apport des fouilles de F. Bordes. *Préhistoire Ariégeoise* 47: 185-194.

Desaulty, A.-M., Mariet, C., Dillmann, P., Joron, J. L., Fluzin, P., 2008, A provenance study of iron archaeological artefacts by inductively coupled plasma– mass spectrometry multi-elemental analysis, *Spectrochimica Acta Part B: Atomic Spectroscopy*, 63 (11): 1253–62.

Didon, L., 1911. L'Abri Blanchard des Roches. *Bulletin de la Société Historique et Archéologique du Périgord*, 87 : 246-241 et 321-345.

Dixon, J.E., Cann, J. R., Renfrew, C., 1968. Obsidian and the Origins of Trade. *Scientific American*, 218, (3): 38-47.

Djindjian F., 2012. Contacts et déplacements des groupes humains dans le Paléolithique supérieur européen : les adaptations aux variations climatiques des stratégies de gestion des ressources dans le territoire et dans le cycle annuel. In : Modes de contacts et de déplacements au Paléolithique eurasiatique. Colloque international dans le cadre de la commission 8 (Paléolithique supérieur) de l'UISPP, Programme et résumés, Liège, 47–48

Drak, L., Garralda, M.D., Balbín Behramm, R de., Alcolea González, J. J., 2008. Restos humanos Mesolíticos de la cueva de Tito Bustillo (Ribadesella, Asturias). In: Nieto Amada, J. L., Obón Nogués, J. A., Baena Pinilla, S. (eds). Genes, ambiente y enfermedades en poblaciones humanas. Prensas Universitarias de Zaragoza: 113-125.

Drak, L., Garralda, M.D., Arias Cabal, P., 2010. Arqueotematología de las sepulturas mesolíticas de la cueva de Los Canes (Asturias). En: Gutiérrez-

Redomero, E., Sánchez Andrés, Á., Galera, V., eds, *Diversidad Humana y Antropología Aplicada*. Alcalá de Henares: Universidad de Alcalá, pp. 455-465.

Dubreuil, L. & Grosman, L., 2009. Ochre and hide-working at a Natufian burial place. *Antiquity*, 83: 935–954.

Duday H., Courtaud P. 1998 - La nécropole mésolithique de La Vergne (Charente- Maritime). In: J. Guilaine (Ed.) *Sépultures d'Occident et genèse des mégalithismes (9000- 3500 avant notre ère)*. Séminaire du Collège de France 1997. Paris: Errance, p. 27- 37.

Erdogu, B., & Ulubey, A., 2011. Colour symbolism in the prehistoric architecture of central Anatolia and Raman spectroscopic investigation of ochre in Chalcolithic Çatalhöyük. *Journal of Archaeology*, 30(1): 1–11.

Erlandson, J. M., J. D. Robertson, And C. Descantes. 1999. Geochemical analysis of eight red ochres from western North America. *American Antiquity*, 64:517–26.

Escalon de Fonton M., 1966. Du Paléolithique supérieur su Mésolithique dans le Midi Méditerranéen. *BSPF LXIII-1*: 66-180.

Escalon de Fonton M., 1967. Tardenoisien et Castelnovien. *BSPF LXIV*: 219-224.

Escalon de Fonton M., 1968. *Préhistoire de la Basse Provence occidentale. Les Martigues*.

Esu, D., Mangano, G., Bonfiglio, L., 2007. The molluscan fauna from the Upper Pleistocene vertebrate-bearing deposits of S. Teodoro Cave (north-eastern Sicily). *Rivista Italiana di Paleontologia e Stratigrafia*, 113, 127–138.

Fano, M.A., 2004. Un nuevo tiempo: el Mesolítico en la región cantábrica. In: Fano, M., Martínez, M.A. (Ed.), *Las Sociedades del Paleolítico en la Región Cantábrica*. *Kobie*, 8: 337-401.

Fano, M.A., 2018. The Mesolithic “Asturian” culture (North Iberia), one century on. *Quaternary International*, In Press.

Fabbri, P.F., Mallegni, F., 1988. Dental anthropology of the Upper Palaeolithic remains from Romito cave at Papisidero (Cosenza, Italy). *Bulletin et Memoires de la Societe d'Anthropologie de Paris*, 5, XIV: 163- 178.

Fabbri, P.F., 1995. Dental anthropology of the Upper Palaeolithic sample from San Teodoro and influence on the peopling of Sicily. *Zeitschrift für Morphologie und Anthropologie*, Bd. 80, H. 3: 311-327.

Fernández Sánchez, P., 2016. La gestión de recursos líticos en el Oriente de Asturias (8000-1500 cal BC). Universidad de Cantabria. PHD tesis.

Fernández-Tresguerres Velasco, J. A., 1976. Enterramiento Aziliense de la cueva de Los Azules I (Cangas de Onís, Oviedo). *Boletín del Instituto de Estudios Asturianos*, n.87. Diputación Provincial de Oviedo. Oviedo: 273-288. *ArqueoWeb. Revista sobre Arqueología en Internet*, 14, 2012-2013: 227-267.

Fernández-Tresguerres Velasco, J. A., 1979. L'Azilien de la grotte de Los Azules I, Asturias (Espagne). La fin des temps glaciaires en Europe. *Colloques Internationaux du Centre National de la Recherche Scientifique*. N° 271. París: 746-752.

Fernández-Tresguerres, J., 2006. El Aziliense de la región cantábrica. *Zephyrus*, 59,163-180.

Flood, J., 1983. *Archaeology of the dreamtime*, University of Hawaii Press.

Floris, R., Melis, R.T., Mussi, M., Palombo, M.R., Iacumin, P., Usai, A., Mascia, F., 2009. La presenza umana nella Sardegna centro occidentale durante l'Olocene antico: il sito di S'Orku e S'Orku (Arbus, VS). In: Atti XLIV Riunione Scientifica: La preistoria e la protostoria della Sardegna- Cagliari 22-28 novembre 2009.

Fontana, F., Guerreschi, A., Bertola, S., Briois, F., Ziggiotti, S., 2016. The Castelnovian burial of Mondeval de Sora (San Vito di Cadore, Belluno, Italy): evidence for changes in the social organisation of Late Mesolithic hunter-gatherers in north-eastern Italy. In: *Mesolithic burials – Rites, symbols and social organisation of early postglacial communities. Mesolithische Bestattungen – Riten, Symbole und soziale Organisation früher postglazialer Gemeinschaften.*

Frankel, R.B., Blakemore, R. P., 1991. *Iron biominerals*. New York: Plenum Press.

Fridrich, J., 1976. Příspěvek k problematice počátků uměleckého a estetického citění u paleantropů: Ein Beitrag zur Frage nach den Anfängen des künstlerischen und ästhetischen Sinns der Urmenschens (Vor-Neandertaler, Neandertaler). *Pamatky Archeogicke*, 68: 5-27.

Gagnière, S., de Lanfranchi, F., Miskovsky, J.C., Prost, M., Renault-Miskovsky J., Weiss M.C., 1969. L'abri d'Araguina-Sennola à Bonifacio (Corse). *Bulletin de la Société préhistorique française. Études et travaux*, 66, (1), 385-418.

Galton, F., 1853. *The Narrative of an Explorer in Tropical South Africa*. London: John Murray.

García-Borja, P., Domingo, I., Roldán, C., Verdasco, C., Ferrero, J., Jardón, P., Bernabeu, J., 2004, Aproximación al uso de la materia colorante en la Cova de l'Or, *Recerques del Museu d'Alcoi*, 13: 35–52.

García Díez, M., 2001. Estudio de la materia colorante de las pinturas del Friso de las Pinturas. In: Montes, R., Sanguino, J. (Eds.), *La cueva de El Pendo. Actuaciones arqueológicas 1994–2000*. Ayuntamiento de Camargo.

Gazzoni, V., 2011. Contributo alla ricostruzione delle identità regionali e della differenziazione sociale presso i gruppi di cacciatori-raccoglitori paleo-mesolitici. Studio della ritualità funeraria in Italia e Francia e analisi degli isotopi stabili sul campione umano del versante alpino sud-orientale. Università degli Studi di Ferrara. PHD thesis.

Gázquez, F., Calaforra, J.M., Forti, P., 2011. Black Mn-Fe crusts as markers of abrupt palaeoenvironmental changes in El Soplao Cave (Cantabria, Spain). *International Journal of Speleology*, 40, 163–169.

Gay, M., Alfeld, M., Menu, M., Laval, E., Arias, P., Ontañón, R., Reiche, I., 2015. Palaeolithic paint palettes used at La Garma Cave (Cantabria, Spain) investigated by means of combined in situ and synchrotron X-ray analytical

Methods. *J. Anal. At. Spectrom.*; 30: 767–776.

Gay, M., Müller, K., Plassard, F., Cleyet-Merle, J.-J., Arias, P., Ontañón, R., Reiche, I., 2016. Efficient quantification procedures for data evaluation of portable X-ray fluorescence – Potential improvements for Palaeolithic cave art knowledge. *Journal of Archaeological Science: Reports* xxx (2016) xxx–xxx.

Geneste, J.M., 1989. Systèmes d’approvisionnement en matières premières au paléolithique supérieur en Aquitaine. In (M. Otte, Ed.) *L’Homme de Neandertal, 8 : La Mutation*, pp. 61–70. Liège : Etudes et Recherches Archéologiques de l’Université de Liège.

Geupel, V., 1977. Das Rötelgrab von Dürrenberg, Kr. Merseburg. In J. Herrmann (ed.) *Archäologie als Geschichtswissenschaft. Studien und Untersuchungen*. Öhringen. 101-110.

Gialanella, S., Belli, R., Dalmeri, G., Lonardelli, I., Mattarelli, M., Montagna, M., Toniutti, L., 2011. Artificial or natural origin of hematite-based red pigments in archaeological contexts: the case of Riparo Dalmeri (Trento, Italy). *Archaeometry*, 53, 5: 950-962.

Gibson, N.E., Wadley, L., Williamson, B.S., 2004. Residue analysis of backed tools from the 60 000 to 68 000-year-old Howiesons Poort layers of Rose Cottage Cave, South Africa. *Southern African Humanities*, 16: 1-11.

Giraudi, C., Frezzotti, M., 1995. Palaeoseismicity in the Gran Sasso Massif (Abruzzo, Central Italy). *Quaternary International* 25: 81-93.

Giraudi, C., Frezzotti, M., 1997. Late Pleistocene glacial events in the Central Apennine, Italy. *Quaternary Research* 48: 280-290.

Giraudi, C., 1997. Prima segnalazione dell'apparato glaciale del M. Breccioso (Val Roveto- Abruzzo): un contributo all'inquadramento cronologico delle fasi glaciali tardo-pleistoceniche. *Il Quaternario*, 10:201-206.

Giraudi, C., 1998. Late Pleistocene and Holocene lake level variations in Fucino lake (Abruzzo-central Italy) inferred from geological, archaeological and historical data. ESF "Workshop Paleohydrology as reflected in lake-level changes as climatic evidence for Holocene times". *Palaoklimaforschung-Paleoclimate Research* 25:1-18.

Giraudi, C. & Mussi, M., 1999. The central and southern Apennine (Italy) during OIS 3 and OIS 2: the colonisation of a changing environment. *Préhistoire Européenne*, 15: 113-121.

Giusti, F., 1971. *Notulae Malacologicae XVI. I molluschi terrestri e di acqua dolce viventi sul massiccio dei Monti Reatini (Appennino centrale)*. Lavori della società Italiana di Biogeografia, Nuova Serie II, pp.423-576.

Glascok, M., Neff, H., 2003. Neutron activation analysis and provenance research in archaeology *Measurement Science and Technology*, 14 (9): 1516-1526.

Goemaere, É., Salomon H., Billard C., Querré G., Mathis, F., Golitko, M., Dubrulle-Brunaud, C., Savary, X., Dreesen, R., 2016. Les hématites oolithiques

du Néolithique ancien et du Mésolithique de Basse-Normandie (France) : caractérisation physico-chimique et recherche des provenances. *Anthropologica et Præhistorica*, 125/2014: 89-119.

González Echegaray, J., Freeman, L. G., 1971. Cueva Morín: Excavaciones 1966-1968. Publicaciones del Patronato de las Cuevas Prehistóricas de la Provincia de Santander. Santander.

González Echegaray, J., Freeman, L. G., 1973. Cueva Morín: Excavaciones 1969. Publicaciones del Patronato de las Cuevas Prehistóricas de la Provincia de Santander. Santander.

González Echegaray, J., Freeman, L. G., 1978. Vida y muerte en cueva Morín. Institución Cultural de Cantabria, Diputación Provincial. Santander.

González Sainz, C., Cacho Toca, R., Fukazawa, T., 2003. Arte paleolítico en la región cantábrica. Universidad De Cantabria.

González Sainz, C., Utrilla, P., 2005. Problemas actuales en la organización y datación del Magdaleniense de la Región Cantábrica. In: Bicho, N. (Ed.), *O Paleolítico. Actas do IV Congreso de Arqueología Peninsular*, Promontoria Monográfica 2, Faro, pp. 39-47.

González Sampérez, P., Leroy, S.A.G., Carrión, J.S., Fernández, S., García, M., Gil, MaJ., Uzquiano, P., Valero, B., Figueiral, I., 2010. Steppes, savannahs, forests and phytodiversity reservoirs during the Pleistocene in the Iberian Peninsula. *Review of Palaeobotany and Palynology*, 162, (3): 427-457.

Goodall, R.A., David, B., Kershaw, P., Fredericks, P.M., 2009. Prehistoric hand stencils at Fern Cave, North Queensland (Australia): environmental and

chronological implications of Raman spectroscopy and FT-IR imaging results. *Journal of Archaeological Science*, 36, 2617-2624.

Granato, D., 2011. Le arene candide, i livelli epigravettiani: macine ed altri strumenti per la lavorazione dell' ocra. *Origini: Preistoria e Protostoria delle Civiltà Antiche*, 33: 39-60.

Graziosi, P., 1943. Gli scavi dell'Istituto Italiano di Paleontologia Umana nella Grotta di San Teodoro (Messina), *Memorie della società toscana di Scienze Naturali*, 52: 82-99.

Graziosi, P., 1947. Gli uomini paleolitici della Grotta di San Teodoro (Messina), *Antropologia*, Firenze, Spinelli, pp. 3-105.

Graziosi, P., 1961. Papasidero (prov. di Cosenza). *Rivista di Scienze Preistoriche, Notiziario*, XVI: 259.

Graziosi, P., 1962. Papasidero (prov. di Cosenza). *Rivista di Scienze Preistoriche, Notiziario*, XVIII: 315.

Graziosi, P., 1964. Papasidero (prov. di Cosenza). *Rivista di Scienze Preistoriche, Notiziario*, XIX: 301-302.

Graziosi, P., 1965. Papasidero (prov. di Cosenza). *Rivista di Scienze Preistoriche, Notiziario*, XX: 367-368.

Graziosi, P., 1968. Grotta del Romito (Papasidero, prov. di Cosenza). *Rivista di Scienze Preistoriche, Notiziario*, XXIII: 399.

Graziosi P., Maviglia C. (1946): La grotta di S. Teodoro (Messina). *Rivista di Scienze Preistoriche*, I (4): 227-283.

Grün, R. and P. Beaumont, 2001. Border Cave Revisited: a Revised ESR Chronology. *Journal of Human Evolution*, 40 (6):467-482.

Guérin, G., Frouin, M., Talamo, S., Aldeias, V., Bruxelles, L., Chiotti, L., Dibble Harold L., Goldberg, P., Hublin, J.J., Jain, M., Lahaye, C., Madelaine, S., Maureille, B., McPherron, S.J.P., Mercier, N., Murray A.S., Sandgathe D., Steele, T.E., Thomsen K.J., Turq, A., 2015. A multi-method luminescence dating of the Palaeolithic sequence of La Ferrassie based on new excavations adjacent to the La Ferrassie 1 and 2 skeletons. *Journal of Archaeological Science*, 58: 147-166.

Gurina, N. N., 1956. Oleneostrovski mogil'nik. Materialy i issledovania po arkheologii SSSR, 47. Moskva & Leningrad.

Harrison, S.P., Digerfeldt, G., 1991. European lakes as palaeohydrological And palaeoclimatic indicators. *Quaternary Science Reviews*, 12, 233–248.

Hayes, E.H., Cnuts, D., Lepers, C., Rots, V., 2017. Learning from blind tests: Determining the function of experimental grinding stones through use-wear and residue analysis. *Journal of Archaeological Science: Reports*, 11: 245-260.

Helwig, K., Monahan, V., Poulin, J., Andrews, T.D., 2014. Ancient projectile weapons from ice patches in northwestern Canada: identification of resin and compound resin-ochre hafting adhesives. *Journal of Archaeological Science*, 41, 655-665.

Henshilwood, C.S., Sealy, J.C., Yates, R., Cruz-Uribe, K., Goldberg, P., Grine, F.E., Klein, R.G., Poggenpoel, C., van Niekerk, K., Watts, I., 2001. Blombos Cave, Southern Cape, South Africa: preliminary report on the 1992–1999 excavations of the Middle Stone Age levels. *Journal of Archaeological Science*, 28:421–448.

Henshilwood, C., Marean, C., 2003. The Origin of Modern Human Behavior: Critique of the Models and Their Test Implications. *Current Anthropology*, 44 (5): 627-651.

Henshilwood, C., d'Errico, F., Vanhaeren, M., van Niekerk, K., Jacobs, Z., 2004. Middle Stone Age Shell Beads from South Africa. *Science*, 304 (5669): 404.

Henshilwood, C.S., d'Errico, F., Watts, I., 2009. Engraved ochres from the Middle Stone Age levels at Blombos Cave, South Africa. *Journal of Human Evolution*, 57 (1): 27-47.

Heyes, P., K. Anastasakis, W. de Jong, A. van Hoesel, W. Roebroeks, and M. Soressi. 2016. Selection and use of manganese dioxide by Neanderthals. *Scientific Reports* 6. Art. n. 22159.

Hernanz, A., Gavira-Vallejo, J., Ruiz-López, J.F., Edwards, H.G.M., 2008. A comprehensive micro-Raman spectroscopic study of prehistoric rock paintings from the Sierra de las Cuerdas, Cuenca, Spain. *Journal of Raman Spectroscopy*, 39, 972-984.

Hernanz, A., Ruiz-López, J.F., Gavira-Vallejo, J.M., Martin, S., Gavrilenko, E., 2010. Raman microscopy of prehistoric rock paintings from the Hoz de Vicente, Minglanilla, Cuenca, Spain. *Journal of Raman Spectroscopy*, 41 (11): 1394-1399.

Hodgskiss, T., 2010. Identifying grinding, scoring and rubbing use-wear on experimental ochre pieces. *Journal of Archaeological Science*, 37 (12): 3344-3358.

Hodgskiss, T., 2012. An investigation into the properties of the ochre from Sibudu, KwaZulu-Natal, South Africa. *Southern African Humanities*, 24: 99-120.

Hodgskiss, T., 2013. Ochre use in the Middle Stone Age at Sibudu, South Africa: grinding, rubbing, scoring and engraving. *Journal of African Archaeology*, 11:75-95.

Hodgskiss, T., Wadley, L., 2017. How people used ochre at Rose Cottage Cave, South Africa: Sixty thousand years of evidence from the Middle Stone Age. *PLoS ONE*, 12, (4): e0176317.

Hoffmann, D. L., Standish, C. D., García-Diez, M., Pettitt, P. B., Milton, J. A., Zilhão, J., Alcolea-González, J. J., Cantalejo-Duarte, P., Collado, H., De Balbín, R., Lorblanchet, M., Ramos-Muñoz, J., Weniger, G.-Ch., Pike, A. W. G., 2018. U-Th dating of carbonate crusts reveals Neandertal origin of Iberian cave art. *Science*, 912-915.

How, M.W., 1962. The mountain Bushmen of Basutoland, J. L. van Schaik, Pretoria.

Inizan, M-L, Gaillard, J.M., 1978. Coquillages de Ksar-'Aqil: éléments de parure? *Paléorient*, 4: 295–306.

Inizan, M.L., Reduron, M., Roche, H., Tixier, J., 1995. Technologie de la pierre taillée, Meudon, éd. du Cercle de Recherches et d'Études préhistoriques.

Inizan, M.-L., Reduron-Ballinger, M., Roche, H. & Tixier, J., 1999. Technology and Terminology of Knapped Stone. Nanterre: CREP. Kaplan, J. (1990). The Umhlatuzana rock shelter sequence: 100,000 years of Stone Age history. *Natal Museum Journal of Humanities*, 2: 1–94.

Iriarte, E., Foyo, A., Sanchez, M.A., Tomillo, C., Setién, J., 2009. The origin and geochemical characterization of red ochres from the Tito Bustillo and Monte Castillo caves (northern Spain). *Archaeometry*, 51 (2): 231-251.

Jaanits, L., 1965. Über die Ergebnisse der Steinzeitforschung in Sowjetestland. *Finskt Museum LXXII*: 5-46.

Jacobs, Z., Roberts, R.G., 2008. Testing times: old and new chronologies for the Howieson's Poort and Still Bay industries in environmental context. *South African Archaeological Society. Goodwin Series*, 10, 8-33.

Jercher, M., Pring, A., Jones, P.G., Raven, M.D., 1998. Rietveld X-ray diffraction and X-ray fluorescence analysis of Australian Aboriginal ochres. *Archaeometry*, 40: 383-401.

Jezequel, P., Wille, G., Beny, C., Delorme, F., Jean-Prost, V., Cottier R., Breton, J., Dure, F., Desprie, J., 2011. Characterization and origin of black and red Magdalenian pigments from Grottes de la Garenne (Vallée moyenne de la

Creuse-France): a mineralogical and geochemical approach of the study of prehistorical paintings. *Journal of Archaeological Science*, 38, (6): 1165-1172.

Johansson, T. B., Akselsson, R., Johansson, S. A. G., 1970. Choice of physical parameters in charged particle induced X-ray fluorescence analysis.

Nuclear Instruments and Methods in Physics Research Section B: Beam Interactions with Materials and Atoms, 84, 141.

Jordá Cerdá, F., 1960. El complejo Solutrense/Magdalenense en la Región Cantábrica. I Symposium de Prehistoria Peninsular. Pamplona. 1959.

Jordá Cerdá, F., 1963. El Paleolítico Superior Cantábrico y sus industrias. *Saitabi*, 13:3-22.

Jordá Cerdá, F., 1970. Lledías, Cueva de. En: Gran Enciclopedia Asturiana. Gijón: Silverio, Cañada, 9: 183-185.

Knight, C., 1991. Blood relations. Menstruation and the origins of culture. New Haven and London: Yale University Press.

Knight, C., Powers, C., Watts, I., 1995. The human symbolic revolution: a Darwinian account. *Cambridge Archaeological Journal*, 5: 75-114.

Labeau, M., 1993. New analysis of the Cougnac are pigments. In: Lorblanchet, M., Bahn, P. (Eds.), *Rock art studies: the post-stylistic era or where do we go from here?* 35, pp. 72-73 (Dir.), Oxbow monograph, Oxford.

Laloy, L., 1906. Rapport de G. Steinmann. *L'Anthropologie* 17, 153.

Lalanne, G., 1913. La Venus de Laussel. *Congres international d'anthropologie et d'archéologie préhistorique, Genève, 1912,14.*

Langley, M.C., Augier, D., Delage, C., Pauthier, A., 2015. A Magdalenian decorated baguette demi-ronde from Grotte de l'Abbé (Charente, France). *Comptes Rendus Palevol*, 14, (4): 321-330.

Lartet, L., 1868. Une sépulture des troglodytes du Périgord. *Bulletin de la Société d'Anthropologie de Paris*, 2ème série, 3 : 335-349.

Leakey, L., 1958. Recent discoveries at Olduvai Gorge, Tanganyika. *Nature*, 181: 1099-1103.

Leroi-Gourhan, A., 1964. *Le Geste et la Parole*. 2 Vols., Albin Michel, Paris.

Leroi-Gourhan, A., 1976. Sur les aspects socio-économiques de l'art paléolithique. *L'autre et l'ailleurs ; Hommages à Roger Bastide*, 1: 164-168.

Leroi-Gourhan, A., Brezillon, M., 1966. L'habitation magdalénienne no. 1 de Pincevent près Montereau (Seine-et-Marne). *Gallia Préhistoire*, 11: 263-385.

Lombard, M., 2005. The Howeisons Poort of South Africa: what we know, what we think we know, what we need to know. *Southern African Humanities*, 17: 33-55.

Lombard, M., 2006. Direct evidence for the use of ochre in the hafting technology of Middle Stone Age tools from Sibudu Cave. *Southern African Humanities*, 18 (1): 57-67.

Lombard, M., Wadley, L., 2007. The morphological identification of microresidues on stone tools using light microscopy: progress and difficulties based on blind tests. *Journal of Archaeological Sciences*, 34, 155-165.

López López-Dóriga, I., 2016. La explotación de los recursos vegetales en el sur de la Fachada Atlántica Europea durante el Mesolítico y el Neolítico. Estudio carpológico. Universidad de Cantabria. PHD tesis.

Lorblanchet, M., 1996. Quercy. Pigments des grottes ornées. *Bilan Scientifique de la Région Midi-Pyrénées*, 152–155.

Lotter, A. F., B. Ammann & M. Sturm, 1992. Rates of change and chronological problems during the late-glacial period. *Climate Dynamics*, 6: 233–239.

Maas, K., 1974. The geology of Liebana, Cantabrian Mountains, Spain; deposition and deformation on a flysch area. *Leidse Geol. Meded.*, 49 (3): 379-465.

Madariaga, B., 1976. Consideraciones acerca de la utilización del pico marisquero del Asturiense. XL Aniversario del Centro de Estudios Montañeses, Institución Cultural de Cantabria. Santander, pp. 437–451.

Mallegni, F., Fabbri, P.F., 1995. The human skeletal remains from the Upper Palaeolithic Burials found in Romito Cave (Papasidero, Cosenza, Italy). *Bulletin et Memoires de la Societe d'Anthropologie de Paris* 7: 88-137.

Mandl, I., 1961. Collagenesis and elastases. *Adv. Enzymol.* 23, 164-264.

Mangano, G., Bonfiglio, L., 2005. New stratigraphic and taphonomic data from the late Pleistocene deposits of the S. Teodoro Cave (North-Eastern Sicily, Italy). *Annali dell'Università degli Studi di Ferrara, Museologia Scientifica e Naturalistica*, pp. 89–97 (volume speciale).

Marean, C. W., Bar-Matthews, M., Bernatchez, J., Fisher, E., Goldberg, P., Herries, A. I. R., Jacobs, Z., Jerardino, A., Karkanas, P., Minichillo, T., Nilssen, P. J., Thompson, E., Watts, I., Williams, H. M., 2007. Early Human Use of Marine Resources and Pigment in South Africa During the Middle Pleistocene. *Nature*, 449 (7164): 905-908.

Marquínez, J., 1989. Mapa geológico de la región del Cuera y los Picos de Europa. *Trabajos de Geología*, 18: 137-144.

Marshack, A., 1981. On paleolithic ochre and the early uses of colour and symbol. *Current Anthropology*, 22: 188–191.

Marshack, A. (1989). Evolution of the human capacity: the symbolic evidence. *Yearbook Of Physical Anthropology*, 32: 1-34.

Marshack, A., 1991. The female image: A “time-factored” symbol (A study in style and aspects of image use in the Upper Palaeolithic). *Proceedings of the Prehistoric Society* 57(1): 17–31.

Martini, F., 1993. Grotta della Serratura a Marina di Camerota. Culture e ambienti dei complessi olocenici. Garlatti e Razzai, Firenze.

Martini, F., 2000-2001. Grotta del Romito (Papasidero, Prov. di Cosenza). *Rivista di Scienze Preistoriche*, Notiziario, LI: 496.

Martini, F., 2002. Grotta del Romito (Papasidero, Prov. di Cosenza). *Rivista di Scienze Preistoriche*, Notiziario, LII: 371-372.

Martini, F., 2006a. Le evidenze funerarie nella grotta e nel Riparo del Romito (Papasidero, Cosenza). In: Martini, F. (Ed.), *La cultura del Morire nelle società preistoriche e protostoriche italiane. Studio interdisciplinare dei dati e loro trattamento informatico. Origines*, vol. 1. Museo e Istituto Fiorentino di Preistoria, Firenze, pp. 46-57.

Martini, F., 2006. *La cultura del morire nelle società preistoriche e protostoriche. Studio interdisciplinare dei dati e del loro trattamento informatico. Dal paleolitico all'Età del Rame. Origines*, Firenze.

Martini, F., 2008. *Archeologia del Paleolitico. Storia e culture dei popoli cacciatori-raccoglitori*. Carocci, Roma.

Martini F., 2016. *L'Arte paleolitica e mesolitica in Italia*, Firenze.

Martini F. & Tozzi C., 1996 - *Il Mesolitico in Italia centromeridionale*.

In: Kozłowski S.K. & Tozzi C. (eds), *The Mesolithic. XIII International Congress of Prehistoric and Protohistoric Sciences, Forlì - Italia - 8/14 september 1996*, Colloquium XIII: 47-58.

Martini, F., Cattani, L., Colamussi, V., Colonese, A., Martino, G., Mallegni, F., Noto, F., Ricciardi, S., Rickards, O., Rolle, R., 2004. I primi risultati delle nuove ricerche nei livelli epigravettiani di Grotta del Romito a Papasidero (scavi 2000-2002). *Atti XXXVII Riunione Scientifica Preistoria e Protostoria della Calabria*, pp. 85-89.

Martini, F., Lo Vetro, D., 2005. Grotta del Romito (Papasidero, Cosenza): recenti risultati degli scavi e degli studi. In: Ambrogio, B., Tiné, V. (Eds.), *Atti delle giornate di studio sulla Preistoria e Protostoria della Calabria: Scavi e Ricerche 2003*, Atti delle giornate di studio, Pellaro (RC), pp. 5e15.

Martini, F., Lo Vetro, D. (Eds.), 2011. *Grotta del Romito a Papasidero: uomo, ambiente e cultura nel Paleolitico della Calabria: ricerche 1961-2011*. Guide del Museo e Istituto fiorentino di Preistoria, Firenze. Editoriale Progetto 2000, Cosenza, 43-53.

Mathis F., Bodu P., Dubreuil O., Salomon H., 2014. Pixe identification of the provenance of ferruginous rocks used by Neanderthals. *Nuclear Instruments and Methods. Physics Research, Section B*, 331: 275–279.

Maviglia, C., 1941. Scheletri umani del Paleolitico superiore rinvenuti nella grotta di S. Teodoro. *Arch. Antrop. Etnol.* 70: 94-104.

Maviglia, C., 1942. I microbulini nell'industria litica della Grotta di S. Teodoro (Messina). *Arch. Antrop. Etnol.* 71: 90-97.

Mc Brearty, S., 2001. The Middle Pleistocene of east Africa. In Barham, L.H., & Robson-Brown, K., (eds) *Human Roots: Africa and Asia in the Middle Pleistocene*. Bristol: Western Academic and Specialist Press, pp.81-98.

Mc Brearty, S. & Brooks, A.S., 2000. The Revolution that wasn't: a new interpretation of the origin of modern human behavior. *Journal of Human Evolution*, 39:453-563.

Mc Brearty, S. & Tryon, C., 2006. From the Acheulean to Middle Stone Age in the Kapturin Formation, Kenya. In: *Transition Before the Transition: Evolution and Stability in the Middle Paleolithic and Middle Stone Age*. Hoovers, H. & Kuhn, S., (eds) Springer, pp. 257-277.

MacDonald, B.L., 2016. Methodological developments for the geochemical analysis of ochre from archaeological contexts: case studies from British Columbia and Ontario, Canada. McMaster University. PHD thesis.

McPherron, S. P., Soressi, M., Dibble, H., 2001. Deux nouveaux projets de recherche á Pech-de-l'Azé (Dordogne, France). *Préhistoire du Sud-Ouest*, 8 : 11-30.

Melis, R.T., Mussi, M., R. Floris, Lamothe, M., Palombo, M. R., Usai, A., 2012. Popolamento e ambiente nella Sardegna centro occidentale durante l'Olocene antico: primi risultati. In: *Atti XLIV Riunione Scientifica: La preistoria e la protostoria della Sardegna-Cagliari 22-28 Novembre 2009*.

Melis, R.T. & Mussi, M., 2016. Mesolithic burials at S'Orku e S'Orku (SOMK) on the south-western coast of Sardinia. Mesolithic burials – Rites, symbols and social organisation of early postglacial communities. Mesolithische Bestattungen – Riten, Symbole und soziale Organisation früher postglazialer Gemeinschaften.

Mellars, P. A., 1989. Major issues in the origin of modern humans. *Current Anthropology*, 30, 349–385.

Menu, M., Walter, P., Vigears, D., Clottes, J., 1993. Façons de peindre au Magdalénien : Niaux (Ariège). *Bulletin Société Préhistorique Française*, 90 (6): 426–432.

Menu, M., Walter, P., 1996. Les rythmes de l'art préhistorique. *Techné, Arts préhistoriques* 3, 11–23.

Menu, M., 2009. The analysis of prehistoric art. *L'Anthropologie*, 113, (3–4): 547–558.

Messeri, P., 1966. Note paleontologiche sul materiale scheletrico umano rinvenuto nella Grotta del Romito a Papasidero in Calabria (Cosenza). *Atti X Riunione Scientifica dell'Istituto Italiano di Preistoria e Protostoria*, Verona, 1965, pp. 301-307.

Moissan, H., 1902. Sur les matières colorantes des figures de la grotte de Font-de-Gaume. *Compte-rendu de l'académie des sciences*, 134 : 1536-1540.

Moyo, S., Mphuthi, D., Cukrowska, E., Henshilwood, C. S., Niekerk, K. V., Chimuka, L., 2016. Blombos Cave: Middle Stone Age ochre differentiation through FTIR, ICP OES, ED XRF and XRD. *Quaternary International*, 404: 20-29.

Mussi M., 1986. Italian Palaeolithic and Mesolithic Burials. *Human Evolution*, 1 (6): 545-546.

Mussi, M., 1996. Problèmes récents et découvertes anciennes : la statuette de Savignano (Modène, Italie). Préhistoire ariégeoise. *Bulletin de la Société Préhistorique Ariège-Pyrénées*, LI : 55-79.

Mussi, M., 2002. Earliest Italy: an Overview of the Italian Paleolithic and Mesolithic, dans *Interdisciplinary Contributions to Archaeology*, XVIII, New York, 2002.

Mussi, M. 2005. La Venere di Savignano: scoperta, polemiche, descrizione e prospettive. *Origini*, XXVII, pp. 219-246.

Mussi, M., 2009. Chi e dove seppellire?. Un bilancio per il Paleolitico Superiore. In *Atti del convegno internazionale: Sepolti tra i vivi. Evidenza ed interpretazione di contesti funerari in abitato*, pp.17-47.

Mussi, M., Melis, R.T., Mazzella, G., 2003. Grotta di Pozzo (prov. L'Aquila): oscillazioni climatiche e presenza umana tra Tardiglaciale e Olocene. *Atti della XXXVI° Riunione scientifica dell' Istituto italiano di Preistoria e Protostoria*: 65-79.

Mussi, M., Cocca, E., D'Angelo E., Fiore, I., Melis, R.T., Russ, H., 2008. Tempi e modi del ripopolamento dell'Appennino centrale nel Tardiglaciale: nuove evidenze da Grotta di Pozzo (AQ). In: Mussi M., *Il Tardiglaciale in Italia – Lavori in corso*, Oxford, British Archaeological Reports Int. Ser. 1859: 111-132.

Mussi, M., Cancellieri, E., D'Angelo, E., Fiore, I., Melis, R.T., Russ, H., Salvadei, L., 2011. Ricerche a Grotta di Pozzo (AQ): 1992-2009. In: *Atti del III Convegno di archeologia "Il Fucino e le aree limitrofe nell'antichità"*, 2009.

Navarro Gascón, J.V., 2002. Resultados analíticos obtenidos en el estudio de muestras de pigmentos y posibles materiales colorantes de las pinturas de la cueva de Tito Bustillo. In: Balbín Behrmann, R., Alcolea González, J. (Eds.), *I Symposium Internacional de Arte Prehistórico*, 54. Ribadesella, 1-3 Octubre (Dir.), pre-Actas.

Neff, H., 2001. Production and distribution of Plumbate pottery: Evidence from a provenance study of the paste and slip clay used in a famous Mesoamerican Tradeware. FAMSI. Foundation for the advancement of Mesoamerican Studies, Los Angeles.

Noetling, F., 1909. Red ochre and its use by the Aborigines of Tasmania. *Papers and Proceedings of the Royal Society of Tasmania*, pp. 30-39

Olivares, M., Castro, K., M. Corchon, S., Garate, D., Murelaga, X., Sarmiento, A., Etxebarria, N., 2013. Non-invasive portable instrumentation to study Palaeolithic rock paintings: the case of La Peña Cave in San Roman de Candamo (Asturias, Spain). *Journal of Archaeological Science*, 40, (2): 1354-1360.

Palma Di Cesnola A., Bietti A., 1983. Le Gravettien et l'Épigravettien ancien in Italie. *Rivista di Scienze Preistoriche*, XXXVIII, 1-2: 181-228.

Pardini, E., 1975. Su di un cranio frammentario paleolitico trovato nella Grotta S. Teodoro (Messina). *Rivista di Scienze Preistoriche*, XXX (1-2): 347-351.

Pargeter, J., 2007. Howiesons Poort segments as hunting weapons: experiments with replicated projectiles. *South African Archaeological Bulletin*, 62, (186): 147–153.

Peñalver, E., Álvarez-Fernández, E., Arias, P., Delclòs, X., Ontañón, R., 2007. Local amber in a Palaeolithic context in Cantabrian Spain: the case of La Garma A. *Journal of Archaeological Science*, 34 (6): 843-849.

Pepe, C., Clottes, J., Menu, M., Walter, P., 1991. Le liant des peintures paléolithiques ariégeoises. *Académie des Sciences*, 312 (2) : 929–934.

Péquart, M., Péquart, S.J., 1929. La nécropole mésolithique de Téviac. *L'Anthropologie*, 39.

Péquart, M., Péquart, S.J., 1934. La nécropole mésolithique de l'île d'Hoedic. *L'Anthropologie*, 44.

Pérez Pérez, M., 1999. Aproximación a la traceología del pico asturiense. *Revista del Instituto de Prehistoria y Arqueología Sautuola*, 6: 211-217.

Pérez Estaún, A., Bastida, F., Martínez-Catalan, J.R., Gutierrez, Marco J.C., Marcos, A., Pulgar, J.A. 1990. Chapter 2: Stratigraphy. In: Dallmeyer, R.D., Martínez-García, E. (Eds.), *Pre-Mesozoic Geology of Iberia*. Springer-Verlag, Berlin, pp. 92-102.

Pérez Iglesias, J.M., 2013-2014. Las prácticas funerarias en la Península Ibérica Durante el Paleolítico Superior y Epipaleolítico. *ArqueoWeb. Revista sobre Arqueología en Internet*, 14: 227-267.

Peterson, N. & Lampert, R. 1985. A Central Australian ochre mine. *Record of the Australian Museum*, 37: 1-9.

Pettitt, P., Richards, M., Maggi, R., and Formicola, V., 2003. The Gravettian burial known as the Prince (Il Principe): new evidence for his age and diet. *Antiquity* 77(295): 15–19.

Pettitt, P., 2010. *The Palaeolithic origins of human burial*. Milton Park, Abingdon, Oxon: Routledge.

Pettitt, P.B., 2011. The living as symbols, the dead as symbols: problematising the scale and pace of hominin symbolic evolution, Henshilwood, C., d'Errico, F. (Eds.), *Homo symbolicus: The Dawn of Language, Imagination and Spirituality*, John Benjamins Publishing Company, Amsterdam, pp. 141–61.

Petru, S. (2010). The power of colour. *Préhistoire, art et sociétés : bulletin de la Société Préhistorique de l'Ariège*, (65) : 296-297.

Peyrony, D., 1930. Le Moustier, ses gisements, ses industries, ses couches. *Revue Anthropologique*, 40, p. 48–76.

Peyrony, D., 1934. La Ferrassie : Moustérien-Périgordien-Aurignacien. *Préhistoire I*, 1-92.

Piarulli, F., D'Angelo, E., Mussi, M., 2015. Strutture di combustione e tecniche di cottura a Grotta di 13. Pozzo (AQ) (23.000-9.000 cal BP). Comunicazione in: PREISTORIA DEL CIBO, 50° Riunione Scientifica dell'Istituto Italiano di Preistoria e Protostoria Roma 5-9 ottobre 2015.

Piedad-Sánchez, N., Martínez, L., Izart, A., Suárez-Ruiz, I., Elie, M., Menetrier, C., Lannuzel, F., 2005. Artificial maturation of a high volatile bituminous coal from Asturias (NW Spain) in a confined pyrolysis system Part II. Gas production during pyrolysis and numerical simulation. *Journal of Analytical and Applied Pyrolysis* 74: 77–87.

Pierce, D.G. & Bonneau, A., 2018. Trouble on the dating scene. *Nature Ecology & Evolution*, 2: 925–926.

Piette, E., 1889. Les subdivisions de l'époque magdalénienne et de l'époque néolithique. In : Burdin, A. et C.

Piette, E., 1894. Sur de nouvelles figurines d'ivoire provenant de la station de Brassempouy. *Comptes rendus des séances de l'Académie des Sciences*, 19: 927–929.

Pike, A. W. G., Hoffmann, D. L., García-Diez, M., Pettitt, P. B., Alcolea, J., De Balbín, R., González-Sainz, C., de las Heras, C., Lasheras, J. A., Montes R., Zilhão, J., 2012. U-Series Dating of Paleolithic Art in 11 Caves in Spain. *Science*, 336, (6087): 1409-1413.

Plinio Il Vecchio. Storia naturale. Libro XXXV. I colori minerali. A cura di Sillabe, 2014. Volume 7 di Arte e memoria.

Pomiès, M.P., 1997. Pigments rouges préhistoriques : goethite chauffée ou hématite nanocristalline naturelle ? Université de Paris VI, Paris, France, PHD thesis.

Pomiès, M.P., Morin, G., Vignaud, C., 1998. XRD study of the goethite-hematite transformation: Application to the identification of heated prehistoric pigments. *European Journal of Solid State and Inorganic Chemistry*, 35 (1), 9-25.

Pomiès, M.P., Barbaza, M., Menu, M., Vignaud, C., 1999. Préparation des pigments rouges préhistoriques par chauffage. *L'Anthropologie*, 103, 503–518.

Pomiès, M.P., Menu, M., Vignaud, C., 2000. Lascaux, pigments préhistoriques à base d'oxydes de fer : hématite naturelle collectée ou goethite chauffée? In: Goupy, J., Mohen, J.-P. (Eds.), Art et chimie, la couleur : actes du Congrès, Editions du CNRS, Paris, pp. 18-23.

Popelka-Filcoff, R. S., Miksa, E. J., Robertson, J. D., Glascock, M. D., and Wallace, H., 2007, Elemental analysis and characterization of ochre sources from southern Arizona, *Journal of Archaeological Science*, 35, (3): 752-762.

Power, C., 1999. Beauty magic: The origins of art. In: Dunbar R.I.M., Knight, C., Power. C., (eds), *The Evolution of Culture*. Edinburgh University Press, Edinburgh, 92-112.

Power, C., 2009. Sexual selection models for the emergence of symbolic communication: Why they should be reversed. In: Botha R, Knight C (eds), *The Cradle of Language*. Oxford University Press, Oxford, 257-280.

Power, C., 2004. Women in Prehistoric Art. In *New Perspectives on Prehistoric Art*, edited by G. Berghaus, pp. 75-103. Westport, London.

Ravdonikas, V. I., 1956. Neoliticheski mogil'nik na Yuzhnom Olen'em ostrove Onezhskogo ozera. *Materialy i issledovania po arkheologii SSSR*, 47, pp. 7-24. Moskva-Leningrad.

Power, C., Aiello, L.C., 1997. Female proto-symbolic strategies. In: Hager LD (ed), *Women in Human Evolution*. Routledge, New York and London, 153-171.

Power, C., V. Sommer, and I. Watts. 2013. The seasonality thermostat: female reproductive synchrony and male behaviour in monkeys, Neanderthals and modern humans. *PaleoAnthropology* 2013: 33-60.

Pradeau, J.V., 2015. Les matières colorantes au sein des systèmes techniques et symboliques au Néolithique (VIe et Ve millénaires BCE) dans l'arc liguro-provençal. *Sociologie*. Université Nice Sophia Antipolis.

Renfrew C., Bahn P., 1995. *Archeologia: teorie, metodi, pratica*, Bologna, Zanichelli.

Rifkin, R.F., 2011. Assessing the efficacy of red ochre as a prehistoric hide-tanning ingredient. *Journal of African Archaeology*, 9 (2), 131–158.

Rifkin, R.F., 2012/a. Processing ochre in the Middle Stone Age: Testing the inference of prehistoric behaviours from actualistically derived experimental data. *Journal of Anthropological Archaeology*, 31 (2): 174-195.

Rifkin, F. R., 2015. Ethnographic and experimental perspectives on the efficacy of ochre as a mosquito repellent. *South African Archaeological Bulletin*, 70 (201): 64–75.

Rifkin, F. R., d’Errico, F., Dayet-Boulliot, L., Summers, B., 2015. Assessing the photoprotective effects of red ochre on human skin by in vitro laboratory experiments. *South African Archaeological Bulletin*, 111(3/4): 1-8.

Rios-Garaizar, J., 2008. Nivel IX (Chatelperroniense) de Labeko Koba: gestión de la industria lítica y función del sitio. *Munibe*, 59, 25-46.

Rios-Garaizar, J., Libano Silvente, I., Garate Maidagan, D., 2012. El yacimiento chatelperroniense al aire libre de Aranbaltza (Barrika, Euskadi). *Munibe*, 63, 81-92.

Rivière, E., 1887. De l’antiquité de l’homme dans les Alpes-Maritimes. *Paléoethnologie*.

Roche, L'Abbé J. 1956. Récentes découvertes au gisement de Moita do Sebastião – Muge (Portugal). In: Congresos Internacionales de Ciencias Prehistoricas y Protohistoricas, Actas de la IV Sesion, Madrid 1954, 155–161.

Rodríguez Asensio, J. A., Barrera Logares, J. M., Aguilar Huergo, E., 2012. Cueva de La Lluera I (San Juan de Priorio, Oviedo, Asturias, España): Estratigrafía solutrense. *Espacio, Tiempo y Forma, Nueva época*, 5: 235-248.

Roebroeks, W., Sier, M.J., Nielsen, T.K., De Loecker, D., Parés, J.M., Arps, C.E.S., Mücher, H.J., 2012. Use of red ochre by early Neandertals. *PNAS*, 109 (6): 1889-1894.

Rosso, D. E., d'Errico, F., & Zilhao, J., 2014. Stratigraphic and spatial distribution of ochre and ochre processing tools at Porc-Epic Cave, Dire Dawa, Ethiopia. *Quaternary International*, 343, 85–99.

Russ, H., 2008. Taphonomic processes and human accumulations of fish remains at Palaeolithic sites in Europe. Grotto di Pozzo: a case study, in P. Béarez, S. Grouard, B. Clavel (a cura di), *Archéologie du Poisson. 30 Ans d'Archéo-ichtyologie au CNRS, Hommage aux Travaux de Jean Desse et Nathalie Desse-Berset*, Antibes : Editions APCDA: 295–300.

Russ, H., Jones, A.K.G., 2009. Late Upper Palaeolithic fishing in the Fucino Basin, central Italy, a detailed analysis of the remains from Grotta di Pozzo, *Environmental Archaeology* 14: 155-162.

Sagona, A., Webb, J., 1994. Toolumbunner in perspective. In Sagona, A. (ed.) *Bruising the red earth: ochre mining and ritual in Aboriginal Tasmania. Melbourne University Press*, 133-151.

Šajnerová-Dušková, A., Fridrich, J. & Fridrichová-Sýkorová, I., 2009. Pitted and grinding stones from Middle Palaeolithic settlements in Bohemia: a functional study. In: Sternke, F., Costa, L.J. & Eigeland, L. (eds.), *Non-flint Raw Material Use in Prehistory: Old Prejudices and New Directions. Proceedings of the XV Congress of the U.I.S.P.P. Archaeopress, Oxford*, pp. 1–10.

Salomon, H., 2009. *Les matières colorantes au début du Paléolithique supérieur : sources transformations et fonctions. Université de Bordeaux 1, Bordeaux, PHD thesis.*

Salomon, H., Vignaud, C., Coquinot, Y., Pagès-Camagna, S., Pomiès, M.-P., Geneste, J.-M., Menu, M., Julien, M., David, F., 2008. Les matières colorantes au début du Paléolithique supérieur. In: *Caractérisation chimique et structurale, transformation et valeur symbolique*, pp. 17-23. *Technè Hors-série.*

San-Juan, C. 1990. Les matières colorantes dans les collections du Musée National de Préhistoire des Eyzies. *Paléo*, 2: 229–242.

Sanchez De Posada, L. C., Martínez-Chacón, M. L., Villa, E. & Mendez, C. A., 2002. The Carboniferous succession of the Asturian-Leonese Domain. An overview. In *Palaeozoic conodont from northern Spain* (eds S. García-Lopez and F. Bastida), pp. 61–92. *Cuadernos del Museo Geominero 1. Instituto Geologico y Minero de Espana, Madrid.*

Scandiuzzi, R., 2008. Les Tambourets: un gisement châtelperronien de plein air au seuil des Petites Pyrénées. Université Toulouse II, Toulouse (Mémoire de master).

Schwarcz, H.P., Grun, R., Vandermeersch, B., Valladas, H., Tchernov, E., 1988. ESR dates for the hominid burial site of Qafzeh in Israel. *Journal of Human Evolution*, 17 : 733–737.

Schwertmann, U., Taylor, R.M., 1989. Iron oxides. In: Dixon, J.B., Weed S.B., (Eds.), *Minerals in Soil Environments*, second ed., Soil Sci. Soc. Am. J. Madison, Wisconsin, USA, pp. 379-428.

Seawright, C., 2014. Ochre and the African middle stone age record. <http://www.thekeep.org/~kunoichi/kunoichi/themestream/ARC3PAL.htm>.

Sineo L., Bigazzi R., D'amore G., Tartarelli G., Di Patti C., Berzero A., Caramella Crespi, V., 2002. I resti umani della Grotta di S. Teodoro (Messina): datazione assoluta con il metodo della spettrometria gamma diretta (U/Pa). *Antropo*, 2: 9-16. www.didac.ehu.es/antropo .

Smith, P.E.L., 1966: *Le Solutréen en France*. Imp. Delmas. Bordeaux.

Smith, M.A., Fankhauser, B., & Jercher, M., 1998. The changing provenance of red ochre at Puritjarra Rock Shelter, central Australia: Late Pleistocene to present. *Proceedings of the Prehistoric Society*, 64: 276-292.

Smith, D.C., Bouchard, M., Lorblanchet, M., 2001. Analyse de pigments par Microscopie Raman. In: Lorblanchet, M. (Ed.), *La grotte ornée de Pergouset (Saint-Géry, Lot). Un sanctuaire secret paléolithique. Documents d'Archéologie Française*, 85. Maison des Sciences de l'Homme, Paris, pp. 174–180 (Dir.).

Solecki, R., 1960. Three adult Neanderthal skeletons from Shanidar Cave, northern Iraq. *Smithsonian Institution Annual Report for 1959*, 603–625.

Solecki, R., 1961. New anthropological discoveries at Shanidar, northern Iraq. *Trans. N.Y. Acad. Sci.* 23, 690–699.

Soressi, M., D'Errico, F., 2007. Pigments, gravures, parures : les comportements symboliques controversés des Néandertaliens. In: Vandermeersch, B., Maureille, B. (Eds.), *Les Néandertaliens, biologie et cultures, C.T.H.S., Documents préhistoriques*, Paris, pp. 297-309.

Soressi, M., Rendu, W., Texier, J.-P., Claud, E., Daulny, L., d'Errico, F., Laroulandie, V., Maureille, B., Niclot, M. & Tillier, A.-M. 2008. Pech-de-l'Azé I (Dordogne, France): nouveau regard sur un gisement moustérien de tradition acheuléenne connu depuis le XIXe siècle. In: J. Jaubert, J.-G. Bordes & I. Ortega (eds), *Les sociétés Paléolithiques d'un grand Sud-Ouest: nouveaux gisements, nouvelles méthodes, nouveaux résultats. Paris: Bulletin de la Société Préhistorique française*, 95–132.

Schmidt, R.R., 1909. Die spätpaläolithischen Bestattungen der Ofnet. *Mannus* (1912) I (suppl. vol.I): 56-62.

Seva-Román, R., Biete-Banon, C., Landete-Ruiz, M.D., 2015. Analysis of the red ochre of the El Miron burial (Ramales de la Victoria, Cantabria, Spain). *Journal of Archaeological Science*, 60 : 84-98.

Sims, L., Otero, X., 2016. Praileaitz I: a Magdalenian lunar-solar cave at 15,500 bp in the Basque country. *Mediterranean Archaeology and Archaeometry*, 16 (4), 275-282.

Soriano, S., Villa, P., Wadley, L., 2009. Ochre for the toolmaker: shaping the Still Bay points at Sibudu (Kwazulu-Natal, South Africa). *Journal of African Archaeology*, 7, (1), 41-54.

Stewart, T. D., 1977. The Neanderthal Skeletal Remains from Shanidar Cave, Iraq: A Summary of Findings to Date. *Proceedings of the American Philosophical Society*, 121 (2): 121-165.

Straus, L.S., 1975. ¿Solutrense o Magdalenense Inferior Cantábrico? Significado de las diferencias. *Boletín del Instituto de Estudios Asturianos*. 86:781-790.

Straus, L.S., 1983. El Solutrense Vasco-Cantábrico. Una nueva perspectiva. Centro de Investigaciones y Museo de Altamira. Monografías. 10. Ministerio de Cultura. Madrid.

Straus, L.S., 2000. A quarter-century of research on the Solutrean of Vasco-Cantabria, Iberia and beyond. *Journal of Anthropological Research*, 56 (1):39– 58.

Straus, L.S., 2005. Chronostratigraphy of the Pleistocene/Holocene boundary: the Azilian problem in the Franco-Cantabrian region. *Paleohistoria*, 27: 89-122.

Straus, L.G., Gonzalez Morales, M.R., 2012. The Magdalenian settlement of the Cantabrian region (Northern Spain): the view from El Miron Cave. *Quaternary International*, 272–273: 111-124.

Straus, L.G., González Morales, M. R., Carretero, J. M., Marín-Arroyo, A.B., 2015. The Red Lady of El Mirón. Lower Magdalenian life and death in Oldest Dryas Cantabrian Spain: an overview. *Journal of Archaeological Science*, xxx: 1-4.

Stringer, C. B. & Gamble, C., 1996. In search of the Neanderthals: solving the puzzle of human origins. London: Thames and Hudson.

Taborin, Y., 2003. La mer et les premiers hommes modernes. In: Vandermeersch, B. (Ed.), *Echanges et diffusion dans la préhistoire méditerranéenne*. CTHS, Paris, pp. 113-122.

Tönjes, H., 1911. Ovamboland: Country People Mission with Particular Reference to the Largest Tribe, the Kwanyama. Windhoek: Namibia Scientific Society.

Tournié, A., Prinsloo, L.C., Paris, C., Colomban, Ph., Smith, B., 2010. The first *in situ* Raman spectroscopic study of San rock art in South Africa: procedures and preliminary results. *Journal of Raman Spectroscopy*, 42: 399-406.

Turq, A., Dibble, H., Goldberg, P., McPherron, S.J.-P., Sandgathe, D., Mercier, N., Bruxelles, L., Laville, D., Madelaine, S., 2012. Reprise des fouilles dans la partie ouest du gisement de la Ferrassie, Savignac-de-Miremont, Dordogne : problématique et premiers résultats. *Quaternaire continental d'Aquitaine* : un

point sur les travaux récents. In: Bertran, P., Lenoble, A. (Eds.), Quaternaire Continental d'Aquitaine, Excursion AFEQ e ASF 2012, pp. 78-87.

Onoratini, G., Perinet, G., 1985. Données minéralogiques sur les colorants rouges préhistoriques de Provence : démonstration que certains d'entre eux ont été obtenus par calcination de goethite. *Comptes rendus de l'Académie des sciences, Série 2* 301, 119-124.

Taborin, Y., 1993. La parure en coquillage au Paléolithique. *XXIX suppl. à Gallia Préhistoire*. Editions du CNRS, Paris.

Trendall, A.F. & Morris, R.C., 1983. *Iron-Formation: Facts and problems*. Elsevier, Amsterdam.

Triat, J.-M., 2010. *Les ocre*, Editions du CNRS, Paris.

Tributsch, H. 2016. Ochre bathing of the bearded vulture: a biomimetic model for early humans towards smell prevention and health. *Animals* 6.

Tryon, C. A. & McBrearty, S., 2002. Tephrostratigraphy and the Acheulian to Middle Stone Age transition in the Kapthurin Formation, Kenya. *Journal of Human Evolution*, 42(1-2): 211-235.

Valladas, H., Joron, J.L, Valladas, G., Arensberg, P., Bar Yosef, O., Belfer Cohen A., Goldberg, P., Laville, H., Meignen, L., Rak, Y., Tchernov, E., Tillier, A.-M., Vandermeersch, B., 1987. Thermoluminescence dates for the Neanderthal burial site at Kebara (Mount Carmel, Israel). *Nature*, 330: 159–160.

Utrilla, P., 1996. La sistematización del Magdaleniense cantábrico: una revisión histórica de los datos. In: Moure Romanillo, A (ed.), "El Hombre Fósil" , 80 años después, Universidad de Cantabria, Santander, pp. 211-247.

Van Peer, P. & Vroomans, J. M., 2004. A Story of Colourful Diggers and Grinders: the Sangoan and Lupemban at Site 8-B-11, Sai Island, Northern Sudan. *Before Farming*, 3: 1-28.

Vanhaeren, M., d'Errico, F., Stringer, C., James, S.L., Todd, J.A., Mienis, H.K., 2006. Middle Paleolithic Shell Beads in Israel and Algeria, *Science*, 312: 1785-1788.

Vega del Sella, Conde de la, 1923. El Asturiense. Nueva Industria Preneolítica. Comisión de Investigaciones Paleontológicas y Prehistóricas, vol. 32. Museo Nacional de Ciencias Naturales, Madrid.

Velo, J., 1984. Ochre as Medicine: A Suggestion for the Interpretation of the Archaeological Record. *Current Anthropology*, 25 (5): 674.

Venditti, V., Lemorini, C., Bordigoni, M., Zampetti, D., Amore, M., Tagliacozzo, T., 2017. The role of burins and their relationship with art through trace analysis at the Upper Palaeolithic site of Polesini Cave (Latium, Italy). *Origini*, XXXIX: 7-29.

Vidal Encinas, J.M. Fernández Rodríguez, C., Prada Marcos, M.E., Fuertes Prieto, M.N., 2008. Los hombres mesolíticos de la Braña- Arintero (Valdelugeros, León): Un hallazgo excepcional en la vertiente meridional de la cordillera Cantábrica. In: RAMIL REGO, E. (Ed.). Actas I Congreso

Internacional de Arqueología de Vilalba (Lugo) 11-14 Junio 2008. Vilalba. Lugo: 153-164.

Vidal Encinas, J.M.; Prada Marcos, M.E. (Coord.), 2010. Los hombres mesolíticos de la cueva de la Braña- Arintero (Valdelugeros, León). Museo de León. Estudios y Catálogos 18. Junta de Castilla y León. Consejería de Cultura y Turismo.

Vigliardi A. (1968): L'industria litica della Grotta di S. Teodoro, in provincia di Messina. *Rivista di Scienze Preistoriche*, 23: 33-144.

Vigliardi A. (1989): L'industria litica della Grotta di S. Teodoro. In Catalogo della Mostra "Ippopotami di Sicilia", EDAS, Messina, pp. 62-69.

Villa, P., Delagnes, A., Wadley, L., 2005. A late Middle Stone Age artefact assemblage from Sibudu (KwaZulu-Natal): comparisons with the European Middle Palaeolithic. *Journal of Archaeological Science*, 32: 399-422.

Viscarra Rossel, R. A., Rizzo, R., Demattê, J. A. M., Behrens, T., 2010. Spatial modelling of a soil fertility index using vis-NIR spectra and terrain attributes. *Soil Science Society of America Journal*, 74: 1293-1300.

Wadley, L., Williamson, B.S., Lombard, M., 2004/b. Ochre in hafting in Middle Stone Age southern Africa: a practical role. *Antiquity*, 78: 661-675.

Wadley, L., 2005. Putting ochre to the test: replication studies of adhesives that may have been used for hafting tools in the Middle Stone Age. *Journal of Human Evolution*, 49 (5): 587-601.

Wadley, L., 2009. Post-depositional heating may cause over-representation of red-coloured ochre in stone age sites. *South African Archaeological Bulletin*, 64 (190): 166-171.

Wadley, L., 2013. Recognizing Complex Cognition through Innovative Technology in Stone Age and Palaeolithic Sites. *Cambridge Archaeological Journal*, 23,163-183.

Walter, P., 1995. La peinture des femmes préhistoriques. In: Delporte, H. (ed.), *La Dame de Brassempouy: Ses ancêtres, ses contemporaines, ses héritières*, ERAUL, 74, Liège, pp. 221–238.

Watts, I., 1998. The origin of symbolic culture: The Middle Stone Age of southern Africa and Khoisan ethnography. University of London. PhD thesis.

Watts, I., 1999. The origin of symbolic culture. In: Dunbar, R., Knight, C. & Power, C. (eds) *The evolution of culture*, 113-146. Edinburgh: Edinburgh University Press.

Watts, I., 2002. Ochre in the Middle Stone Age of Southern Africa: Ritualised Display or Hide Preservative? *The South African Archaeological Bulletin*, 57 (175): 1-14.

Watts, I., 2009. Red ochre, Body Painting, and Language: Interpreting the Blombos Ochre, in: Botha, R., Knight, C., (Eds), *The Cradle of Language*, Oxford University Press, pp. 62-92.

Watts, I., 2010. The pigments from Pinnacle Point Cave 13B, Western Cape, South Africa. *Journal of Human Evolution*, 59 (3-4), 392-411.

Weigand, P.C., Harbottle, G., Sayre, E.V., 1977. *Turquoise Sources and Source Analysis: Mesoamerica and the Southwestern USA*. Academic Press, New York.

Wernert, P., 1957. Stratigraphie paléontologique et préhistorique des sédiments quaternaires d'Alsace. Achenheim. Mémoire du service de la carte géologique de l'Alsace-Lorraine, Université de Strasbourg, 262: 24.

White R., 1992. Ivory personal ornaments of Aurignacian age: technological, social and symbolic perspectives, J. Hahn, M. Menu, Y. Taborin (eds.), *Le travail et l'usage de l'ivoire au Paléolithique supérieur*, Ravello, p. 29-62.

White R., Bisson, M.S., 1998 Imagerie féminine du Paléolithique. L'apport des nouvelles statuettes de Grimaldi. *Gallia Préhistoire*, 40: 95–132.

White, R., 2006. The women of Brassempouy: A century of research and interpretation. *Journal of Archaeological Method and Theory*, 13 : 251–304.

Wierer U. & Boscato P., 2006. Lo sfruttamento delle risorse animali nel sito mesolitico di Galgenbühel/Dos de la Forca (Salorno e BZ): la macrofauna. In: Tecchiati, U., Sala, B. (Eds.), *Studi di archeozoologia in onore di Alfredo Riedel*. Ripartizione Beni Culturali,, Bolzano: 85-98.

Wreschner, E.E., 1980. Red ochre and human evolution: a case for discussion. *Current Anthropology*, 21: 631--44.

Young, T., 2000. The Paviland ochres: characterisation and sourcing. In: Aldhouse-Green, S. (Ed.), *Paviland Cave and the 'Red Lady'*. Western Academic & Specialist Press Limited, Bristol, UK, pp. 205-226.

Zagorskis, F., 2004. *Zvajniek (N Latvia) Stone Age Cemetery*. BAR International Series 1292. Oxford.

Zilhão, J., Trinkaus, E., 2002. Portrait of the Artist as a Child. The Gravettian Human Skeleton from the abrigo do Lagar Velho and its archeological context. Instituto Português de Arqueologia. Lisboa. *Trabajos de Arqueología*, 22.

Zilhão, J., Angelucci, D.E., Badal-Garcia, E., d'Errico, F., Daniel, F., Dayet, L., Douka, K., Higham, T.F.G., Martinez-Sanchez, M.J., Montes-Bernardez, R., Murcia-Mascaros, S., Perez-Sirvent, C., Roldan-Garcia, C., Vanhaeren, M., Villaverde, V., Wood, R., Zapata, J., 2010. Symbolic use of marine shells and mineral pigments by Iberian Neandertals. *Proceedings of the National Academy of Sciences of the United States of America*, 107: 1023–1028.

Zipkin, A.M., Wagner, M., McGrath, K., Brooks, A.S., Lucas, P.W., 2014. An experimental study of hafting adhesives and the implications for compound tool technology. *PLoS One*, 9, e112560.

List of figures

Fig.II.1.: Geographical position of geological samples (b) near the coast (a) and near the archaeological sites (c). **p.60**

Fig.II.2.: Image of mineral inclusions in Arangas ochre samples: a) n.119a-grain quartz; b) n.133b-mica. **p.65**

Fig.II.3.: Backscattered images of ochre from Los Canes and Arangas obtained by SEM-EDS: the collected spectra on more intense light grey areas report Fe high concentrations **p.67**

Fig.II.4.: Red ochre a) and yellow ochre b) samples from Los Canes analysed by SEM-EDS showing the crystalline structure and quantitative composition with major elements **p.69**

Fig.II.5.: Overlapped XRD spectra of red ochres from Arangas (n.1a-n.20a) H (hematite); L (larnite); M (magnetite). **p.70**

Fig.II.6.: XRD spectra of Los Canes yellow ochres reporting the main chemical compounds: Q (quartz); G (goethite); J (jarosite); P (potassium oxide). **p.70**

Fig.II.7.: FT-IR spectra of yellow ochres (a) and red ochres (b) from Arangas. **p.71**

Fig.II.8.: Bivariate loading plots of Principal Component Analysis performed with sample of Los Canes, Arangas, Acantilado (I-II-III) and Arangas source (1-2). **p.76**

Fig.II.9.: Log10 (Sb/Fe) vs. log10 (As/Fe) with confidence ellipse of 95%. **p.78**

Fig.II.10.: Log10 (Mn/Fe) vs.log10 (As/Fe) with confidence ellipse of 95%. **p.78**

Fig.II.11.: Log10 (As/Fe) vs.log10 (Al/Fe) with confidence ellipse of 95%. **p.79**

Fig.II.12.: Log10 (K/Fe) vs.log10 (As/Fe) with confidence ellipse of 95%. **p.80**

Fig.II.13.: Log10 (V/Fe) vs. Log10 (Al/Fe) with confidence ellipse of 95%. **p.80**

Fig.III.1.: Geographical localization of the Iberian sites: La Garma A; Los Canes; Arangas (map elaborated from Google Earth) **p.101**

Fig.III.2.: La Garma A: (a) archaeological surface and (b) section of the hill (Peñalver *et al.*, 2007). **p.102**

Fig.III.3.: La Garma A: a) stratigraphic sequence visible on the Southern profile (quadrants 9 and 10); b) photogrammetric return of the stratigraphic sequence from the Northern profile of the vestibule (quadrants F and G). **p.105**

Fig.III.4.: Planimetry of the archaeological surface (elaborated from Arias, 2002). **p.110**

Fig.III.5.: Los Canes: image of funerary structure 6-III with the skeletal of the male adult individual. In the circle are enclosed the faunal remains and the infant bones (adapted from Arias, 2002). **p.111**

Fig.III.6.: Los Canes: image of funerary structure 6-II (adapted from Arias, 2002). **p.112**

Fig.III.7.: Los Canes: image of funerary structure 6-I (adapted from Arias, 2002). **p.113**

Fig.III.8.: Transversal section of the central portion of the funerary structure 6-III (Arias, 2002). **p.117**

Fig.III.9.: Transversal profile of the entrance to the cave with the view of the section of the funerary structure 6-II (Arias, 2002). **p.118**

Fig.III.10.: Planimetry of the archaeological surfaces of Arangas. **p.123**

Fig.III.11.: Geographical position of Italian sites: Grotta del Romito, Grotta San Teodoro, Grotta di Pozzo, S'Ormu e S'Orku. **p.129**

Fig.III.12.: Geographical localization of Grotta del Romito (1) and the cave entrance (2-3). Planimetry of the archaeological surface showing the distribution of trenches and burials (4). Cross-section of the site and of the excavated area along the axis a-a' indicated in the plan (5) (Martini & Lo Vetro, 2011; Blockley *et al.*, 2017). **p.131**

- Fig.III.13.:** Image of human burial Romito 7 (Martini, 2002). **p.132**
- Fig.III.14.:** Stratigraphical sequence of Grotta del Romito (Bockley *et al.*, 2017). **p.135**
- Fig.III.15.:** Image of the cave's vestibule and planimetry of the archaeological surface of San Teodoro (Mangano & Bonfiglio, 2005). **p.139**
- Fig.III.16.:** Planimetry of archaeological surface with human remains from Grotta San Teodoro (da Palma di Cesnola, 1993 in Gazzoni, 2011). **p.141**
- Fig.III.17.:** Stratigraphy of Grotta San Teodoro (da Graziosi in Bonfiglio *et al.*, 2005) with the highlighted area from which two of the ochre samples used for this research were collected. **p.142**
- Fig. III.18.:** Planimetry of the archaeological excavated surface and picture of the interior cave of Grotta di Pozzo (Catelli, 2014). **p.147**
- Fig.III.19.:** Panoramic view of S'Orku e S'Orku and localization of the archaeological deposit (Melis & Mussi, 2016) **p.150**
- Fig.III.20.:** Human skeletal remains with red ochre residues of burial SOMK 1 (Melis & Mussi, 2016). **p.152**
- Fig.III.21.:** Lithostratigraphic sequence of S'Orku e S'Orku: a) Pleistocenic aeolianites; b) aeolian deposits; c) rock fall; d) debris slope with sand matrix and ashes; e) sandy loam slope deposits with metamorphic and aeolianite debris and blocks; f) sandy gravel deposit rich in charcoal fragments (Melis & Mussi, 2016). **p.154**

Fig.IV.1.: Los Canes: distribution of number of red and yellow ochre pieces collected from each stratigraphic unit of the archaeological deposit. **p.164**

Fig.IV.2.: Los Canes: distribution of red and yellow ochre specimens in function of the mass in grams. **p.168**

Fig.IV.3.: Los Canes: distribution of ochre specimens in function of the density $M(\text{gr})/V(\text{m}^3)$. **p.168**

Fig.IV.4.: Dimensional distribution of red pieces from Los Canes. **p.170**

Fig.IV.5.: Dimensional distribution of yellow pieces from Los Canes. **p.170**

Fig.IV.6: Los Canes: correlation graph of mean values of Length max. (mm) and Mass(gr) of red (a) and yellow (b) pieces. **p.171**

Fig.IV.7.: Los Canes: distribution of the fragmentation indices according to the established categories for the red (a) and yellow (b) pieces. **p.175**

Fig.IV.8.: Main identifying morphologies of crayons by inscribing the forms in a two-dimensional plane. **p.178**

Fig.IV.9.: Arangas: distribution of red and yellow ochre specimens in each stratigraphic unit of the archaeological deposit. **p.181**

Fig.IV.10.: Arangas: distribution of red and yellow ochre specimens in function of the mass(gr). **p.185**

- Fig.IV.11.:** Dimensional distribution of red pieces from Arangas. **p.186**
- Fig.IV.12.:** Dimensional distribution of yellow pieces from Arangas. **p.186**
- Fig.IV.13:** Arangas: correlation graph of mean values of Length max. (mm) and mass(gr) of red (a) pieces and correlation graph of values of Length max. (mm) and mass(gr) (b) of individual yellow pieces. **p.188**
- Fig.IV.14.:** Arangas: distribution of the fragmentation indices according to the established categories for the red pieces. **p.192**
- Fig.IV.15.:** La Garma A: distribution of number of red and yellow ochre pieces collected from each stratigraphic unit of the archaeological deposit. **p.195**
- Fig.IV.17.:** La Garma A: distribution of red and yellow ochre specimens in function of the mass in grams **p.197**
- Fig.IV.18.:** Dimensional distribution of red pieces from La Garma A. **p.200**
- Fig.IV.19.:** Dimensional distribution of yellow pieces from La Garma A. **p.200**
- Fig.IV.20:** La Garma A: correlation graph of mean values of Length max. (mm) and Mass(gr) of red (a) and yellow pieces. **p.201**

- Fig.IV.19.:** La Garma A: distribution of the fragmentation indices according to the established categories for the red (a) and yellow (b) pieces. p.206
- Fig.IV.20.:** Grotta di Pozzo: distribution of number of red and yellow ochre pieces collected from each stratigraphic unit of the archaeological deposit. p.210
- Fig.IV.21.:** Grotta di Pozzo: distribution of red and yellow ochre specimens in function of the mass in grams. p.212
- Fig.IV.22.:** Dimensional distribution of yellow pieces from Grotta di Pozzo. p.212
- Fig.IV.23:** Grotta di Pozzo: distribution of the fragmentation indices according to the established categories for the red pieces. p.215
- Fig.V.1.:** Los Canes: ternary plot of ochres grouped for raw materials by colour in Munsell Soil Color Charts. Black points correspond to archaeological colours. p.221
- Fig.V.2.:** Characterization by SEM-EDS of hematite sample from Los Canes. p.224
- Fig.V.3.:** Characterization by SEM-EDS of lepidocrocite sample from Los Canes. p.224
- Fig.V.4.:** Ternary plot of main iron raw materials from Los Canes based on the percentages of Fe-Al-Si. p.225

Fig.V.5.: Characterization by SEM-EDS of goethite sample from Los Canes. **p. 225**

Fig.V.6.: XRD spectrum of jarosite archaeological sample from Los Canes. **p.226**

Fig.V.7.: Percentages of the total mass of raw materials at Los Canes. **p.227**

Fig.V.8.: Density distribution of raw materials at Los Canes **p. 228**

Fig.V.9.: Distribution of the maximum length values L(max) in function to the raw materials of Los Canes: hematite; lepidocrocite/ferrihydrite; goethite. **p.229**

Fig.V.10.: Dimensional comparative evaluation (length, width and thickness) in function of the raw materials of Los Canes: hematite; lepidocrocite/ferrihydrite; goethite. **p.230**

Fig.V.11.: Comparative evaluation of fragmentation indexes in function of the raw materials of Los Canes: hematite; lepidocrocite/ferrihydrite; goethite. **p.231**

Fig.V.12.: Proportion of mass (gr) and number of pieces in function to the raw materials in the site of Los Canes. **p.231**

Fig.V.13.: Proportion of raw materials per category of objects from Los Canes. **p.234**

Fig.V.14.: Distribution of the density of goethite at Los Canes. **p. 234**

Fig.V.15.: Arangas: ternary plot of ochres grouped for raw materials by colour in Munsell Soil Colour Charts. Black points correspond to archaeological colour. **p.236**

Fig.V.16: Ternary plot of hematite archaeological samples from Arangas. **p.237**

Fig.V.17.: Characterization by SEM-EDS of iron oxide (hematite) samples from Arangas: a) sub-class (1); b) sub-class (2). **p.238**

Fig.V.18.: XRD spectrum of hematite samples from Arangas: a) sub-class (1); b) sub-class(2). **p.240**

Fig.V.19.: Diachronic distribution of mass (gr) of raw materials in the site of Arangas: hematite and goethite. **p.241**

Fig.V.20.: Proportion of mass (gr) and number of pieces in function to the classes of raw materials in the Arangas site. **p.242**

Fig.V.21.: Distribution of values of maximum lengths L(max) in function to the raw materials at Arangas: hematite; goethite. **p. 242**

Fig.V.22.: Comparative dimensional evaluation (length, width and thickness) in function to the raw materials from Arangas: hematite; goethite. **p.243**

Fig.V.23.: La Garma A: ternary plot of ochres grouped into raw materials by colour in Munsell Soil Colour Charts. Black points correspond to archaeological colours. **p.246**

Fig.V.24.: Proportion of mass (gr) and number of pieces in function to the classes of raw materials in the site of La Garma A. **p.247**

Fig.V.25.: Index of fragmentation in function to the classes of raw materials in the site of La Garma A. **p.248**

Fig.V.26.: Diachronic distribution of mass (gr) of raw materials in the site of La Garma A: hematite, lepidocrocite/ferrihydrate, goethite. **p.249**

Fig.V.27.: Distribution of values of maximum lengths L(max) in function to the raw materials of La Garma A: hematite; lepidocrocite/ferrihydrate; goethite. **p.268**

Fig.V.28.: Comparative dimensional evaluation (length, width and thickness) in function to the raw materials from Grotta di Pozzo: hematite; goethite. **p.250**

Fig.V.29.: Grotta di Pozzo: ternary plot of ochres grouped for raw materials by colour in Munsell Soil Colour Charts. Black points correspond to archaeological colours. **p.254**

Fig.V.30.: Raman spectrum of some samples representing the classes of raw materials recognized at Grotta di Pozzo. **p.254**

Fig.V.31.: Proportion of mass (gr) and number of pieces in function to the classes of raw materials in the site of Grotta di Pozzo. **p.255**

Fig.V.32.: Diachronic distribution of mass (gr) of raw materials in the site of Grotta di Pozzo: hematite and goethite. **p.256**

Fig.V.33.: Comparative dimensional evaluation (length, width, thickness) in function to the raw materials from Grotta di Pozzo: hematite; goethite. **p.257**

Fig.V.34.: Distribution of the values of maximum lengths L(max) in function to the raw materials at Grotta di Pozzo: hematite; goethite. **p.258**

Fig.V.35.: Images of main classes of raw materials of ochre distinguished by visual criteria: samples from Los Canes, Arangas, La Garma A, Grotta di Pozzo. **p.261**

Fig.V.36.: Images of main classes of raw materials of ochre distinguished by visual criteria: comparative samples from Grotta del Romito, Grotta San Teodoro, S'Ormu e S'Orku. **p.262**

Fig.V.37.: SEM-EDS images of representative samples of the main classes of raw materials of comparative ochres. **p.264**

Fig.V.38.: Ternary plot of comparative samples by Fe-Al-Si content. **p. 264**

Fig.V.39.: XRD spectra of representative samples of comparative ochres: qualitative characterization of raw materials. **p.266**

Fig.V.40.: Principal Component Analysis results showing the grouping by Fe-Si-Al in the comparative ochres with Los Canes ochres. **p.268**

Fig.VI.1.: Simplified geological map of the area surrounding the archaeological sites of Los Canes and Arangas with the geological sampled sources (IGME maps 1: 50.000; n.56 and n.32). **p.279**

Fig.VI.2.: Map of the study area showing the localization of the archaeological sites with the geological sources of lithic raw materials and the potential sources of iron ores. **p.282**

Fig.VI.3.: Iron-rich nodules in dark laminated limestones on the coastal area between Pimiango and La Franca (Asturias). **p.286**

Fig.VI.4.: Ferruginous crust on laminated limestones near the caves at few meters from the village of Arangas (Asturias). The formations are clear visible from the road cuts. **p.288**

Fig.VI.5.: Iron rich- nodules images: a-b) images of samples obtained by optical microscope at x8.0 magnification; c) images of thin sections obtained by SEM-EDS; d) microphotography of thin sections. SEM-EDS images of mineral inclusions: e) Zr + Si; f-h) Ti; g) Zr + Si. **p.289**

Fig.VI.6.: Ferruginous crust: a-b) images obtained by optical microscope at x8,0 magnification. SEM-EDS images of thin sections showing c) Fe and Si elements; d) inclusion of Zr. **p.290**

Fig.VI.7.: Scatter matrix of Pearson's correlation coefficient of the tested variables in the PCA of archaeological and geological samples. **p.295**

Fig.VI.8.: Score plot of PCA realized on archaeological and geological samples. The graph confirms the nature of samples as iron ores. **p.296**

Fig.VI.9.: Biplot graph showing $\log\text{Mn}/\text{Fe}$ vs $\log\text{As}/\text{Fe}$ with confidential ellipse (95%). **p.298**

Fig.VI.10.: Biplot graphs showing the non-discrimination per sources of the samples using the ratios Sb/Fe vs. Pb/Fe and Ti/Fe vs. Mn/Fe . **p. 298**

Fig.VI.11.: Biplot graphs showing the distribution of archaeological samples ($\text{Fe}>50\%$) and geological samples by $\log\text{As}/\text{Fe}$ vs $\log\text{Mn}/\text{Fe}$. **p.299**

Fig.VI.12.: Biplot graphs showing the distribution of archaeological samples ($\text{Fe}<50\%$) and geological samples by $\log\text{As}/\text{Fe}$ vs $\log\text{Mn}/\text{Fe}$. **p. 299**

Fig.VI.13.: Biplot graphs of PCA for comparative analysis: a) positively correlated elements with Fe; b) negatively correlated with Fe. **p.301**

Fig.VI.14.: Scatter plot graph of $\log\text{K}/\text{Fe}$ vs. $\log \text{Ca}/\text{Fe}$ and $\log\text{Mn}/\text{Fe}$ vs. $\log.\text{K}/\text{Fe}$. **p. 301**

Fig.VII.1.: Dimensional distribution of red ochre from Upper Palaeolithic layers by the range of 2-50 mm fixed on the experiments conducted to test the hypothesis of mechanical transformation of ferruginous raw materials (Salomon, 2009). **p.311**

Fig.VII.2.: Non-normal distribution of morphological values (Length, Width, Thickness): red ochres Upper Palaeolithic. **p.311**

Fig.VII.3.: Unretouched ochre flakes: a) n. 22360 (La Garma A); b) n. 34180 and c) n.31260 (Arangas). **p.313**

Fig.VII.4.: Number of red ochre pieces with use-wear traces from Los Canes, La Garma A, Arangas: Upper Palaeolithic. **p.314**

Fig.VII.5.: Frequency of red ochre pieces with diagnostic traces of each activities as referred by experiments (Hodgskiss, 2010): Upper Palaeolithic. **p.315**

Fig.VII.6.: Use wear traces of grinding on Upper Palaeolithic pieces from a-b) Los Canes; c) La Garma A; d) Arangas. **p. 315**

Fig.VII.7.: Use wear traces of scoring on Upper Palaeolithic pieces from a-b) Los Canes; c) Arangas; d) La Garma A. **p.316**

Fig.VII.8.: Use wear traces of rubbing on Upper Palaeolithic pieces from a-d) Los Canes; e) Arangas; f) La Garma A. **p.317**

Fig.VII.9.: Combined use wear: a-c) grinding and rubbing (Los Canes); d) rubbing and scoring (Los Canes); e) rubbing and trampling from e) Arangas and f) La Garma A. **p.318**

Fig.VII.10.: Crayons from Upper Palaeolithic units of Los Canes: a) n.22; b) n.23a; c) n.27b; d) n.61b. **p.320**

Fig.VII.11.: Faceted piece from La Garma A: n.61a (18,94 mm x 17,77 mm x 6,95 mm; weight 2,5 gr). **p.322**

Fig.VII.12.: Dimensional distribution of red ochre from Mesolithic layers by the range of 2-50 mm fixed on the experiments conducted to test the hypothesis of mechanical transformation of ferruginous raw materials (Salomon, 2009). **p.323**

Fig.VII.13.: Non-normal distribution of morphological values (Length, Width, Thickness): red ochres Mesolithic. **p.324**

Fig.VII.14.: Number of red ochre pieces with use-wear traces from Los Canes, La Garma A, Arangas: Mesolithic. **p.326**

Fig.VII.15.: Frequency of red ochre pieces with diagnostic traces of each activities as referred by experiments (Hodgskiss, 2010): Mesolithic. **p.327**

Fig.VII.16.: Mesolithic red ochre crayons from Los Canes: a) 61b; b) 121a; c) 241a. **p.329**

Fig.VII.17.: Mesolithic red ochre crayon from Los Canes (S.U.6III A): n.214. **p. 329**

Fig.VII.18.: Ochre nodule with abrasions from Arangas-n.84a. **p.331**

Fig.VII.19.: Ternary plot of major element Al, Si, Fe detected in the superficial concretions removed from the ochre processing tools (n.944, n.2169, n.2401). **p.336**

Fig.VII.20.: Ochre processing tool (n.944) from Arangas: a) original image; b) elaborated image by D-stretch to highlight the contrast between the areas covered by red ochre and the diagnostic traces. **p.339**

Fig.VII.21.: Ochre processing tool (n.2169) from Arangas: a) original image; b) elaborated image by D-stretch to highlight the contrast between the areas covered by red ochre and the diagnostic traces. In the top-left magnification image, the point of separation between the liquid substance and the lithic surface is evidenced. . **p.340**

Fig.VII.22.: Ochre processing tools from Arangas: original images a) n.8740, c) n.713; elaborated image by D-stretch to highlight the contrast between the areas covered by red ochre b) n.8740, d) n.713. **p.341**

Fig.VII.23.: Ochre processing tool (n.8706) from Arangas: original images a) n.8740; b) elaborated image by D-stretch to highlight the contrast between the areas covered by red ochre. **p.342**

Fig.VII.24.: Original image and elaborated image by D-stretch of a-b) ochre processing tool n.2401 and c-d) an abrasion tablet n.8702. **pag343**

Fig.VIII.1.: Spatial distribution of ochre remains at Los Canes: Solutrean, Lower Magdalenian. **p.348**

Fig.VIII.2.: Spatial distribution of ochre remains at Los Canes: Upper Magdalenian;Azilian. **p.350**

Fig.VIII.3.: Spatial distribution of ochre remains at Los Canes in Mesolithic units (S.U.5; S.U.6III, S.U. 6II, S.U. 6I).. **p.352**

Fig.VIII.4.: Spatial distribution of ochre remains at Los Canes in Mesolithic units (S.U.6A; S.U.6B, S.U. 6C). **p.357**

Fig.VIII.5.: Spatial distribution of ochre remains during the Azilian at Los Canes. **p.359**

Fig.VIII.6.: Ochre distribution in the burial 6III. The circle indicates the infant bones. **p.360**

Fig.VIII.7.: Ochre distribution in the burial 6II. **p.362**

Fig.VIII.8.: Ochre distribution in the burial 6I. **p.362**

Fig.VIII.9.: Spatial distribution of ochre remains at Arangas: Lower Magdalenian, Upper Magdalenian. **p.365**

Fig.VIII.10.: Spatial distribution of ochre remains at Arangas: Azilian, Mesolithic. **p.366**

Fig.VIII.11.: Spatial distribution of ochre remains in the Azilian unit of Arangas. **p.368**

Fig.VIII.12.: Spatial distribution of ochre remains at La Garma A: Solutrean, Early Magdalenian. **p.372**

Fig.VIII.13.: Spatial distribution of ochre remains at La Garma A: Middle Magdalenian, Upper/Final Magdalenian. . **p.373**

Fig.VIII.14.: Spatial distribution of ochre remains at La Garma A: Mesolithic **p.374**

Fig.VIII.15.: Spatial distribution of materials inside the Middle Magdalenian structure. **p.377**

Fig.VIII.16.: Spatial distribution of ochre remains at Grotta di Pozzo: Ancient Epigravettian. **p.379**

Fig.VIII.17.: Spatial distribution of ochre remains at Grotta di Pozzo: Final Epigravettian. **p.380**

Fig.VIII.18.: Spatial distribution of ochre remains at Grotta di Pozzo: Mesolithic. **p.380**

Fig.IX.1.: Comparison of the quantities (number and mass) of red ochre distribution in the sites analysed in this work among the Upper Palaeolithic and the Mesolithic **p.389**

Fig.IX.2.: Reconstruction of the principal stages of the *chaînes opératoire*: a) debitage; b) roughing; c) coarse crushing; d-e) fine crushing; f) abrasion; g) scoring. The scheme includes all the phases identified for the processing of ochre. All phases are well attested in the Upper Palaeolithic units. In the Mesolithic units there is no evidence of debitage. In Los Canes the scoring is attested in the Mesolithic unit that precedes the burials (S.U.5). At La Garma A scoring and grinding have left no traces in the Mesolithic record. In Arangas there is no evidence of scoring for the recent phases **p.392**

List of tables

- Tab.II.1.:** List of archaeological samples from Palaeolithic and Mesolithic units of Los Canes and Arangas used for the preliminary test. **p.61**
- Tab.II.2.:** Pearson correlation coefficients calculated on the samples selected to perform a preliminary test (correlation is significant at the 0,05 level). **p.73**
- Tab.III.1.:** Radiocarbon dates of La Garma A (Arias Cabal, pers.comm.). **p.108**
- Tab.III.2.:** Radiocarbon dates of Los Canes re-calibrated from re-calibrated from raw dates in Arias (2002). **p.120**
- Tab.III.3.:** Radiocarbon dates of Arangas calibrated from raw dates unpublished (standard error not received). **p.126**
- Tab.III.4.:** Radiocarbon dates of Grotta del Romito re-calibrated from raw dates in Bockley *et al.* (2017). **p.137**
- Tab.III.5.:** Radiocarbon dates of Grotta di Pozzo. **p.149**
- Tab.III.6.:** Radiocarbon dates of S'Orku e S'Orku (Melis & Mussi, 2016). **p.155**
- Tab.III.7.:** Summary table of total of ochre samples and sampling conditions. **p.156**

Tab.IV.1.: Los Canes: list of tints in Munsell Soil Color Charts approximate in two set of colours red and yellow. **p.166**

Tab.IV.2.: Los Canes: Index of Shannon-Weaver (H) and Evenness (J) of red and yellow pieces. **p.173**

Tab.IV.3a.: Values of Indices of fragmentation: red pieces from Los Canes. **p.176**

Tab.IV.3b.: Values of Indices of fragmentation: yellow pieces from Los Canes. **p.177**

Tab.IV.4.: Summary table of main physical traits of crayons. **p.179**

Tab.IV.5.: Arangas: list of tints in Munsell Soil Color Charts approximate in two set of colours red and yellow. **p.183**

Tab.IV.6.: Arangas: Index of Shannon-Weaver (H) and Evenness (J) of red and yellow pieces. **p.190**

Tab.IV.7.: Values of Indices of fragmentation: red pieces and yellow pieces from Arangas. **p.192**

Tab.IV.8.: La Garma A: list of tints in Munsell Soil Color Charts approximate in two set of colours: red and yellow. **p.196**

Tab.IV.9.: La Garma A: Index of Shannon-Weaver (H) and Evenness (J) of red and yellow pieces. **p.205**

Tab.IV.10.: Values of Indices of fragmentation: red and yellow pieces from La Garma A. **p.208**

- Tab.IV.11.:** Grotta di Pozzo: list of tints in Munsell Soil Color Charts approximate in two set of colours: red and yellow. **p.211**
- Tab.IV.12:** Grotta di Pozzo: Index of Shannon-Weaver (H) and Evenness (J) of red pieces. **p.216**
- Tab.IV.13:** Values of Indices of fragmentation: red pieces from Grotta di Pozzo **p.216**
- Tab.V.1.:** List of colours in Munsell Soil Color Charts of main iron ores forming red and yellow ochres **p.235**
- Tab.V.2.:** Mineral compounds and elemental content of representative ochres for each class of raw materials from the assemblage of Arangas. **p.241**
- Tab.V.3.:** Summary table of main classes of raw materials and mineral content of each site: Los Canes, Arangas, La Garma A, Grotta di Pozzo. **p.259**
- Tab.V.4.:** Summary table of main classes of raw materials of comparative samples: Grotta del Romito (ROM); Grotta San Teodoro (ST); S'Orku e S'Orku (SOMK). **p.262**
- Tab.V.5.:** Summary table with the qualitative chemical composition of comparative ochres. **p.265**
- Tab.VI.1.:** Summary table reporting the geological sources of raw materials with the distance in Km (as the crow flies) from the archaeological sites and valued walking time. **p.284**
- Tab.VI.2.:** Summary table of geological iron ores deposit sampled for provenance purposes. **p.287**

Tab.VI.3.: Pearson Correlations of chemical elements in archaeological and geological samples. **p.294**

Tab.VI.4.: Eigenvalues of variables that explain the variance in the samples. **p.297**

Tab.VI.5.: Eigenvalues of variables that explain the variance in the samples tested for comparative purposes. **p.301**

Tab.VI.6.: Pearson Correlations of chemical elements in samples tested for comparative analysis **p.305**

ANNEX I

List of archaeological samples: chemical analysis (SEM-EDS; XRF)¹

¹ Percentages of elements detected by SEM-EDS: 0=0-5%; 1=5-10%; 2=10-20%; 3=20-30%; 4=20-40%; 5=40-60%; 6=>60%.

*(ppm): elements detected by XRF.

SITE	CULTURAL ATTRIBUTION	ID sample	S.U.	Si%	Al%	Fe%	*Si ppm	*Al ppm	*Fe ppm	*K ppm	*Ti ppm	*Ca ppm	*P ppm	*Cu ppm	*Mn ppm	*V ppm	*Zn ppm	*Cl ppm	*Ar ppm	*Sn ppm	*Pb ppm	*As ppm	*Sb ppm
Los Canes	Solutrean	3873	2A	0		5	1,23	0,232	31,97	0,0221	0,0109	35,33	0,217	0,527	0,128	0,0024	0,0582	0,0111	0,035	0,0284	0,0318	0,0025	0,0329
Los Canes	Solutrean	11959	2A	0	0	5	0,542	0,339	38,93	0,0315	0,0125	29,37	0,167	0,502	0,0612		0,0558	0,0088	0,0163	0,0251	0,0173	0,0039	0,0043
Los Canes	Solutrean	11959	2A	0	0	5	10,54	6,26	42,32	0,976	0,139	0,823	0,446	0,652	0,0575	0,0081	0,0863	0,0101	0,0494	0,0291	0,0261	0,0017	
Los Canes	Solutrean	12224	2A	0	0	5	12,04	0,426	45,07	0,0641	0,0262	4,58	0,233	0,0082	0,0402	0,0011	0,0043	0,0059	0,0023		0,0125	0,0033	0,0112
Los Canes	Solutrean	12224	2A	0	0	5	7,48	0,204	46,61	0,0217	0,0062	8,64	0,0439	0,256	0,0533		0,0386	0,0106	0,0086	0,0174	0,014	0,0051	0,0301
Los Canes	Solutrean	12224	2A	0		5	3,4	2,7	57,09	0,454	0,0547	0,434	0,181	1,85	0,0654	0,0064	0,411	0,0222	0,188	0,0847	0,111	0,0557	0,0168
Los Canes	Solutrean	12224	2A	0	0	6	2,48	0,932	57,75	0,12	0,0344	6,66	0,155	0,167	0,0544	0,0028	0,0315	0,0001		0,0088	0,015	0,0101	0,0306
Los Canes	Solutrean	12224	2A	0	0	5	0,695	0,32	58,81	0,0355	0,0086	8,62	0,203	0,706	0,0255	0,0016	0,0833	0,006	0,0283	0,0284	0,0375	0,0049	0,0447
Los Canes	Solutrean	12336	2A	0		6	2,42	0,23	63,1	0,0202	0,0098	1,65	0,0395	1,05	0,0029	0,0021	0,126	0,0154	0,0346	0,0454	0,0442	0,0083	0,0532
Los Canes	Solutrean	12336	2A	0	0	5	1,76	0,687	64	0,0368	0,0293	0,148	0,0355	1,95	0,012	0,0027	0,195	0,0207	0,121	0,066	0,084		0,0191
Los Canes	Solutrean	12354	2A	0	0	5	1,71	0,387	66,29	0,0267	0,0116	0,0874	0,017	0,268	0,0238	0,0018	0,0423	0,0032	0,0239	0,0128	0,0219	0,0086	0,0809
Los Canes	Solutrean	12354	2A	0	0	6	1,04	0,553	66,45	0,0062	0,0105	0,131	0,0401	0,815	0,0004	0,0484	0,104	0,0166	0,0264	0,0325	0,0433	0,0113	0,017
Los Canes	Solutrean	12354	2A	0	0	6	0,75	0,252	67,13	0,0176	0,0185	0,283	0,0225	0,851		0,0042	0,103	0,0102	0,0439	0,0382	0,0347	0,0044	0,0426
Los Canes	Magdalenian	11714	2C	0	0	6																	
Los Canes	Magdalenian	4911	2C	1	0	5																	
Los Canes	Magdalenian	4442	2C	0	0	5	0,89	0,395	67,03	0,0351	0,01	0,234	0,0363	0,62	0,0159	0,0001	0,0778	0,0103	0,0154	0,0326	0,0257	0,0023	0,032
Los Canes	Magdalenian	4442	2C	0	0	6	0,791	0,861	67,08	0,0975	0,0246	0,162	0,049	0,126	0,009	0,0067	0,0138	0,0089	0,0081	0,0065	0,0088	0,002	0,0188
Los Canes	Magdalenian	4600	2C	0	0	6																	
Los Canes	Magdalenian	10559	2C	0		6	21,19	0,16	36,65	0,0206	0,009	0,101	0,0293	1,03	0,0386	0,0008	0,107	0,0313	0,0711	0,0379	0,0407	0,0023	0,02
Los Canes	Magdalenian	10414	2C	1	0	5	13,34	4,83	39,7	0,725	0,299	0,522	0,23	1,34	0,108	0,0159	0,211	0,0324	0,181	0,061	0,0497		0,0102
Los Canes	Magdalenian	5797	2C	2	2	4																	

Los Canes	Magdalenian	10511	2C	0	0	5	2,36	1,56	61,91	0,092	0,0402	0,465	0,16	0,763	0,0459	0,0067	0,373	0,0064	0,0251	0,0356	0,0956	0,0908	0,0514
Los Canes	Magdalenian	10474	2C	0	0	5																	
Los Canes	Magdalenian	10511	2C	2	0	4																	
Los Canes	Magdalenian	10474	2C	0	0	6	0,554	0,175	67,68	0,0127	0,0256	0,122	0,0216	0,86	0,0063	0,0123	0,0868	0,0165	0,0407	0,0381	0,0421	0,0039	0,0493
Los Canes	Magdalenian	12432	2C	0		6	0,964	0,253	66,05	0,0361	0,0085	1,52	0,0325	0,417	0,0137	0,0016	0,0517	0,0122	0,0199	0,0201	0,024	0,0108	0,045
Los Canes	Magdalenian	10699	2C	0	0	5	0,925	0,267	49,51	0,0323	0,0146	18,5	0,0407	0,123	0,055	0,0017	0,0213	0,0127	0,0076	0,0159	0,0136	0,046	0,139
Los Canes	Magdalenian	10699	2C	0	0	5																	
Los Canes	Magdalenian	4600	2C	0		5	0,612	0,258	61,99	0,0638	0,021	6,08	0,0352	0,338	0,0288	0,0139	0,0393	0,0973	0,0213	0,0242	0,0131	0,0111	0,106
Los Canes	Azilian	10389	4				4,58	3,63	54,45	0,714	0,0936	0,972	0,388	0,646	0,0727	0,0022	0,203	0,0411	0,0694	0,0276	0,0345	0,0204	0,0065
Los Canes	Azilian	10404	3A				1,28	0,341	54,53	0,0491	0,0188	15,23	0,0377	0,925	0,0601	0,0062	0,102	0,0141	0,0321	0,037	0,0381	0,0186	0,0734
Los Canes	Azilian	10420	3A				3,22	2,29	56,39	0,281	0,0854	1,04	0,279	2,82	0,0663	0,0902	0,404	0,044	0,224	0,107	0,106	0,014	0,0109
Los Canes	Azilian	10478	3A				8,22	0,197	56,96	0,0093	0,0066	0,138	0,021	0,175	0,0032	0,0018	0,0175	0,0008	0,0046	0,0094	0,0123	0,001	0,0288
Los Canes	Azilian	10501	3B				5,93	0,324	58,26	0,0284	0,0147	1,82	0,0653	0,105	0,243	0,0038	0,0141	0,0043	0,0084	0,0076	0,0089	0,0038	0,0352
Los Canes	Azilian	10642	3B				2,02	0,35	63,84	0,0233	0,0169	1,74	0,0271	0,629	0,0294	0,0057	0,0576	0,0133	0,0472	0,0373	0,028	0,0055	0,0533
Los Canes	Azilian	11538	3C				1,23	0,758	65,7	0,018	0,0083	0,178	0,0478	0,653	0,0415	0,0482	0,0927	0,0079	0,015	0,0246	0,227	0,0113	0,148
Los Canes	Azilian	11771	3C				0,857	0,184	66,95	0,0341	0,0115	0,709	0,0174	0,567	0,0136	0,006	0,066	0,0106	0,011	0,0277	0,0266	0,0031	0,0681
Los Canes	Azilian	7701	3C				0,798	0,244	67,5	0,0348	0,0081	0,0774	0,0194	0,58	0,0149	0,0043	0,0615	0,0137	0,046	0,0328	0,0256	0,0033	0,101
Los Canes	Mesolithic	164a	5	0	0	6	1,46	0,835	64,73	0,0539	0,0248	0,494	0,0253	1,03	0,0867	0,0276	0,127	0,013	0,0708	0,0413	0,0532	0,0102	0,0332
Los Canes	Mesolithic	9969	6 IIIA	2	2	3	1,12	0,781	66,36	0,116	0,0568	0,158	0,0255	0,357	0,0177	0,0061	0,0431	0,0198	0,0257	0,0167	0,0195	0,0073	0,0669
Los Canes	Mesolithic	8502	6 IIIA	1	2	3																	
Los Canes	Mesolithic	8365	6 IIIA	1	0	5																	
Los Canes	Mesolithic	8751	6 IIIA	2	0	3																	

Arangas	Magdalenian	25768	5D	0	2	6	6,01	1,54	35,54	0,393	0,0775	21,73	0,414	0,446	0,0556	0,0038	0,0616	0,0117	0,0176	0,023	0,0235	
Arangas	Magdalenian	2840	5D	0	0	5	4,71	0,325	51,58	0,0541	0,0097	10,37	0,0471	0,29	0,0394	0,0097	0,0419	0,0117	0,0074	0,0208	0,0196	
Arangas	Magdalenian	2732	5D	0	0	5	0,546	0,124	56,2	0,0271	0,0106	7,57	3,02	0,0388	0,193	0,0051	0,0226	0,0126	0,0037	0,0128	0,0125	0,0368
Arangas	Magdalenian	2732	5D	0	0	6	0,471	0,213	67,97	0,0281	0,0075	0,268	0,0782	0,429	0,0175	0,0044	0,0467	0,0092	0,0178	0,0242	0,017	0,017
Arangas	Magdalenian	1174	5D	0	0	6																
Arangas	Magdalenian	25768	5C	0		5	24,74	13,16	7,69	5,9	0,625	0,395	0,082	0,0613	0,0395	0,0168	0,0158	0,0196	0,0073	0,0049	0,004	
Arangas	Magdalenian	2840	5C	0	2	5	0,902	0,387	17,16	0,0553	0,0265	50,64	0,183	0,387	0,133		0,0546	0,0097	0,0191	0,0199	0,0188	0,0013
Arangas	Magdalenian	2732	5C	0	0	4	18	6,38	30,43	2,03	0,558	0,165	0,101	0,779	0,0186	0,036	0,0776	0,0227	0,0504	0,0254	0,0569	0,0764
Arangas	Magdalenian	2732	5C	0	2	4	13,4	0,416	41,71	0,0646	0,0221	6,91	0,166	0,272	0,0371	0,002	0,0305	0,004	0,0101	0,0139	0,0137	0,0185
Arangas	Magdalenian	34901	5C	0	0	5	0,835	0,389	66,79	0,192	0,132	0,33	0,0661	0,225	0,0716	0,0626	0,0391	0,0107	0,0117	0,0169	0,0225	0,0403
Arangas	Magdalenian	37152	5C	0		6	0,396	0,149	68,52	0,0877	0,0411	0,121	0,0398	0,214	0,0187		0,0276	0,0074	0,0061	0,0161	0,0278	
Arangas	Azilian	2757	5A	0	0	6	18	9,04	19,01	3,18	0,443	6,33	0,903	0,0157	0,146	0,0311	0,0153	0,0129			0,0135	0,0027
Arangas	Azilian	3435	5A	0	0	6	8,35	1,8	24,63	7,13	0,0894	1,05	0,681	0,75	0,0196		0,0917	0,0259	0,0777	0,0367	0,0376	0,0538
Arangas	Azilian	3435	5A	0	0	4	4,92	0,41	37,87	0,0661	0,0225	24,24	0,105		0,017	0,0024	0,0031	0,002			0,008	0,0348
Arangas	Azilian	6124	5A	0	0	4	3,59	0,109	38,82	0,0301	0,0048	25,28	0,0689	0,314	0,0183		0,0359	0,009	0,014	0,0191	0,0179	0,0513
Arangas	Azilian	6124	5A	0	0	4	2,92	0,138	39,54	0,0349	0,0063	25,67	0,034	0,368	0,0209	0,0040	0,0504	0,0163	0,0222	0,0225	0,0177	0,0349
Arangas	Azilian	12533	5A	0	0	5	1,68	0,253	43,99	0,0793	0,0365	23,02	0,0442	0,0106	0,0614	0,0034		0,0124		0,0098	0,0084	
Arangas	Azilian	12533	5A	0		5	3,13	0,119	45,06	0,0285	0,0051	20,14	0,0442	0,0065	0,0397			0,0045			0,007	0,0359
Arangas	Azilian	14664	5A	0	0	5	0,869	0,382	47,88	0,0681	0,0202	19,95	0,0755	0,304	0,0225	0,0027	0,0335	0,0129	0,0157	0,0167	0,0201	
Arangas	Azilian	17536	5A	0	0	5	8,5	0,471	54,99	0,0555	0,0492	0,268	0,0429	0,787			0,105	0,017	0,0313	0,0362	0,0349	0,0081
Arangas	Azilian	25715	5A	0	0	5	0,788	0,566	57,75	0,0827	0,0347	9,49	0,1	0,405	0,0302	0,0096	0,0552	0,0202	0,0295	0,0228	0,0705	0,0084
Arangas	Azilian	25719	5A	0		5	0,829	0,359	57,83	0,054	0,0146	10,14	0,048	0,0297	0,023	0,0029	0,0065	0,0091	0,0049	0,0043	0,0081	0,0084

Arangas	Azilian	28915	5B	0	0	5	1,64	0,364	66,28	0,0546	0,0174	0,3	0,0474	0,163	0,0077	0,003	0,0192		0,0099	0,0142	0,0136	0,0028	
Arangas	Mesolithic	3311	2B	0	0	5	0,46	0,252	30,08	0,0382	0,0067	38,69	0,124	0,309	0,0416		0,0341	0,0052	0,0088	0,0172	0,015	0,0205	
Arangas	Mesolithic	3378	2B	0		5	9,92	0,168	51,82	0,096	0,0069	2,47	0,18	0,0046	0,027	0,0028		0,0051		0,0022	0,0063	0,0219	
Arangas	Mesolithic	3378	2B	0		6	0,788	0,566	57,75	0,0827	0,0347	9,49	0,1	0,405	0,0302	0,0096	0,0552	0,0202	0,0295	0,0228	0,0705	0,0277	
Arangas	Mesolithic	3560	2B	0		6	0,563	0,381	58,19	0,0601	0,0379	8,61	0,364	0,848	0,0677	0,0059	0,105	0,0147	0,021	0,044	0,147	0,0181	
Arangas	Mesolithic	3576	2B	0	0	5	0,681	0,265	59,9	0,0431	0,0592	7,93	0,0481	0,492	0,0221	0,0069	0,0536	0,0128	0,0267	0,0239	0,0303	0,0035	
Arangas	Mesolithic	3619	2B	0	0	6	2	1,3	62,02	0,209	0,0405	0,915	0,33	1,13	0,0445	0,0188	0,135	0,0183	0,0392	0,0498	0,089	0,0134	
Arangas	Mesolithic	24730	2B	0		6	1,33	0,635	62,84	0,117	0,0496	2,53	0,198	0,661	0,111	0,0579	0,0921	0,0252	0,0336	0,0355	0,0414	0,0162	
Arangas	Mesolithic	24730	2B	0	0	6	0,769	0,178	66,12	0,0374	0,0081	1,27	0,0505	0,685	0,0058	0,0058	0,0781	0,0114	0,0348	0,0313	0,0287	0,023	
Arangas	Mesolithic	25780	2B	0	0	5	0,165	0,186	68,94	0,0152	0,0043	0,216	0,0291	0,163	0,003	0,0028	0,0223			0,0132	0,0141	0,0084	
Los Canes	Mesolithic	3747	6 IIIC				2,22	0,813	39,31	0,246	0,0337	24,59	0,11	0,695	0,0479	0,0092	0,0911	0,0128	0,0527	0,0272	0,0274	0,0024	
Los Canes	Mesolithic	8264	6 IIIC				10,24	3,54	47,14	0,211	0,101	0,837	0,306	0,661	0,0371	0,0057	0,124	0,0143	0,0246	0,0278	0,0384	0,005	0,002
Grotta del Romito	Epigravettian		D31	0	0	5																	
Grotta del Romito	Epigravettian		D32	0	0	5																	
Grotta del Romito	Epigravettian		D25 A	2	0	5																	
Grotta del Romito	Epigravettian		D29 A	2	0	40.81																	
Grotta del Romito	Epigravettian		E2	0		64.71																	
Grotta del Romito	Epigravettian		D29	2	0	4																	
Grotta del Romito	Epigravettian		D27	0	0	6																	

Grotta del Romito	Epigravettian	D33	0	0	5
Grotta del Romito	Epigravettian	D26	0	0	5
Grotta del Romito	Epigravettian	E4	0	0	5
Grotta del Romito	Epigravettian	G2	0	0	5
Grotta del Romito	Epigravettian	D32	0	0	5
Grotta del Romito	Epigravettian	D28	2	0	4
Grotta del Romito	Epigravettian	F2	2	0	5
Grotta S. Teodoro	Epigravettian		0		6
Grotta S. Teodoro	Epigravettian	taglio I-II	0	0	5
Grotta S. Teodoro	Epigravettian		2	2	5
Grotta S. Teodoro	Epigravettian	strato 10	1	0	4
Grotta S. Teodoro	Epigravettian	strato 10	0	0	4
Grotta S. Teodoro	Epigravettian		1		5
S'Orku e S'Orku	Mesolithic	C1	0	0	5
S'Orku e S'Orku	Mesolithic	B2	0	0	4
S'Orku e S'Orku	Mesolithic	C2			

S'Ormu e S'Orku	Mesolithic	B2 (Lo)	0	0	4
------------------------	------------	------------	---	---	---

S'Ormu e S'Orku	Mesolithic	B1	0	0	5
------------------------	------------	----	---	---	---

S'Ormu e S'Orku	Mesolithic	C1	0	0	5
------------------------	------------	----	---	---	---

ANNEX II

List of geological samples: chemical analysis (XRF)¹

¹*(ppm): elements detected by XRF.

Source	ID sample	*Si ppm	*Al ppm	*Fe ppm	*K ppm	*Ti ppm	*Ca ppm	*P ppm	*Cu ppm	*Mn ppm	*V ppm	*Zn ppm	*Cl ppm	*Ar ppm	*Sn ppm	*Pb ppm	*As ppm	*Sb ppm
Acantilado	1A	18,26	1,83	38,82	0,755	0,269	0,0194	0,0305	0,0205	0,00007	0,05	0,0041	0,0158	0,0017	0,0074	0,008		0,018
Acantilado	2B	42,97	2,53	0,904	0,881	0,219	0,0109	0,0363	0,0217		0,0031	0,0029	0,0048	0,0021	0,0032	0,0015		
Acantilado	3C	20,98	15,56	11,54	6,05	0,363	0,0195	0,0169	0,033	0,0015	0,0196	0,0063	0,0068		0,0064	0,0112	0,0012	0,0018
Acantilado	A	4,71	4,86	54,67	0,908		0,0485	0,0565	0,0533	0,0019	0,0683	0,0281	0,277	0,0042	0,0036	0,0132	0,0091	0,0252
Acantilado	B	4,77	3,99	54,93	1,25	0,134	0,0987	0,0257	0,0246	0,0022	0,0459	0,0144	0,758	0,0031	0,0025	0,0114	0,0113	0,0194
Acantilado	C	6,08	5,28	50,88	2,01	0,114	0,0306	0,0212	0,0407	0,0026	0,0553	0,0097	0,49		0,0044	0,015	0,0085	0,016
Acantilado	D	3,44	2,95	58,26	0,896	0,0798	0,0659	0,0426	0,3	0,0017	0,0752	0,046	0,982	0,0044	0,0174	0,0221	0,0085	0,0359
Acantilado	1	42,23	2,42	2,02	0,84	0,249	0,0142	0,0338	0,0227	0,00043	0,0027	0,0055	0,184	0,0168	0,0053	0,0027		0,0014
Acantilado	2	19,01	15,62	12,15	7,19	0,901	0,0403	0,0546	0,0563	0,002	0,0259	0,0089	0,378	0,003	0,0067			0,0037
Acantilado	3	23,05	17,03	3,27	8,25	1,07	0,0208	0,0422	0,0077	0,0031	0,0228	0,0049	0,316	0,0065	0,0036	0,0005		
Acantilado	4	22,09	17,8	3,67	8,44	0,959	0,0152	0,0284	0,0395	0,0023	0,0204	0,0076	0,129	0,0055	0,0037	0,0014		
Arangas-source 1	A1	18,79	8,87	5,95	3,72	0,681	19,1	0,112	0,0878	0,159	0,0112	0,0178	0,0058	0,0038	0,0056	0,0034	0,0017	
Arangas-source 1	B2	22,94	11,95	8,99	6,03	0,905	2,39	0,285	0,0145	0,0916	0,0198	0,023	0,0082		0,0055	0,0025	0,0016	0,0018
Arangas-source 1	C3	16,53	8,31	5,3	3,78	0,621	23,96	0,0817	0,0127	0,195	0,016	0,0162	0,0062	0,0034	0,0045	0,0032		0,0016
Arangas-source 1	D4	22,19	18,67	5,4	5,48	1,01	0,0154	0,0287	0,0157	0,0033	0,0223	0,0058	0,0048	0,0046	0,0028	0,0019		
Arangas-source 2	I	43,24	1,1	2,02	0,424	0,144	0,029	0,0252	0,132		0,0035	0,0147	1,04	0,0345	0,0077	0,0059	0,0003	

